Vol. 120 November 1 1980
Complete in one issue

ISSN 0003-2670

ANALYTICA CHIMICA ACTA

International journal devoted to all branches of analytical chemistry

ELSEVIER SCIENTIFIC PUBLISHING COMPANY

ANALYTICA CHIMICA ACTA

International journal devoted to all branches of analytical chemistry
Revue internationale consacrée à tous les domaines de la chimie analytique
Internationale Zeitschrift für alle Gebiete der analytischen Chemie

PUBLICATION SCHEDULE FOR 1980 (incorporating the section on Computer Techniques and Optimization).

	J	F	M	A	M	J	J	A	S	O	N	D
Analytica Chimica Acta	113/1 113/2	114	115	116/1	116/2	117	118/1	118/2	119/1	119/2	120	121
Section on Computer Techniques and Optimization			122/1			122/2			122/3			122/4

Scope. *Analytica Chimica Acta* publishes original papers, short communications, and reviews dealing with every aspect of modern chemical analysis, both fundamental and applied. The section on *Computer Techniques and Optimization* is devoted to new developments in chemical analysis by the application of computer techniques and by interdisciplinary approaches, including statistics, systems theory and operation research. The section deals with the following topics: Computerized acquisition, processing and evaluation of data. Computerized methods for the interpretation of analytical data including chemometrics, cluster analysis, and pattern recognition. Storage and retrieval systems. Optimization procedures and their application. Automated analysis for industrial processes and quality control. Organizational problems.

Submission of Papers. Manuscripts (three copies) should be submitted as designated below for rapid and efficient handling:

Papers from the Americas to: Professor Harry L. Pardue, Department of Chemistry, Purdue University, West Lafayette, IN 47907, U.S.A.

Papers from all other countries to: Dr. A. M. G. Macdonald, Department of Chemistry, The University, P.O. Box 363, Birmingham B15 2TT, England.

For the section on *Computer Techniques and Optimization:* Dr. J. T. Clerc, Universität Bern, Pharmazeutisches Institut, Sahlistrasse 10, CH-3012 Bern, Switzerland.

American authors are recommended to send manuscripts and proofs by INTERNATIONAL AIRMAIL.

Information for Authors. Papers in English, French and German are published. There are no page charges. Manuscripts should conform in layout and style to the papers published in this Volume. Authors should consult Vol. 111, p. 343 for detailed information. Reprints of this information are available from the Editors or from: Elsevier Editorial Services Ltd., Mayfield House, 256 Banbury Road, Oxford OX2 7DE (Great Britain).

Reprints. Fifty reprints will be supplied free of charge. Additional reprints (minimum 100) can be ordered. An order form containing price quotations will be sent to the authors together with the proofs of their article.

Advertisements. Advertisement rates are available from the publisher.

Subscriptions. Subscriptions should be sent to: Elsevier Scientific Publishing Company, P.O. Box 211, 1000 AE Amsterdam, The Netherlands. The section on *Computer Techniques and Optimization* can be subscribed to separately.

Publication. *Analytica Chimica Acta* (including the section on *Computer Techniques and Optimization*) appears in 10 volumes in 1980. The subscription for 1980 (Vols. 113–122) is Dfl. 1390.00 plus Dfl. 160.00 (postage) (total approx. U.S. $795.00). The subscription for the *Computer Techniques and Optimization* section only (Vol. 122) is Dfl. 139.00 plus Dfl. 16.00 (postage) (total approx. U.S. $79.50). Journals are sent automatically by airmail to the U.S.A. and Canada at no extra cost and to Japan, Australia and New Zealand for a small additional postal charge. All earlier volumes (Vols. 1–112) except Vols. 23 and 28 are available at Dfl. 153.00 (U.S. $78.50), plus Dfl. 11.00 (U.S. $5.50) postage and handling, per volume.

Claims for issues not received should be made within three months of publication of the issue, otherwise they cannot be honoured free of charge.

Customers in the U.S.A. and Canada who wish to obtain additional bibliographic information on this and other Elsevier journals should contact Elsevier/North Holland Inc., Journal Information Center, 52 Vanderbilt Avenue, New York, NY 10017. Tel: (212) 867-9040.

ANALYTICA CHIMICA ACTA
VOL. 120 (1980)

ANALYTICA CHIMICA ACTA

International journal devoted to all branches of analytical chemistry

ELSEVIER SCIENTIFIC PUBLISHING COMPANY

Anal. Chim. Acta, Vol. 120 (1980)

Printed in The Netherlands.

Analytica Chimica Acta, 120 (1980) 1—17

Review

THE DEVELOPMENT OF ROOM TEMPERATURE PHOSPHORESCENCE INTO A NEW TECHNIQUE FOR CHEMICAL DETERMINATIONS
Part 2. Analytical Considerations of Room Temperature Phosphorimetry

R. T. PARKER,[a] RICHARD S. FREEDLANDER[b] and R. BRUCE DUNLAP*
Department of Chemistry, University of South Carolina, Columbia, SC 29208 (U.S.A.)
(Received 29th February 1980)

SUMMARY

The rapidly developing technique of room temperature phosphorimetry is discussed from a practical analytical standpoint in this second part of the review. Basic factors concerning the technique such as methods of sample preparation, special instrumentation employed, and quantitative capability are presented, together with a listing of the variety of organic compounds reported to display room temperature phosphorescence. Potential applications of room temperature phosphorimetry and the advantages of sensitivity and selectivity afforded by this technique are discussed.

Room temperature phosphorimetry (r.t.p.) has added new dimensions to the area of luminescence spectroscopy of organic compounds [1—36]. Until the recent development of this new technique, the determination of organic compounds by phosphorimetric methods found limited use because of the general restriction that the determination be carried out at extremely low temperatures [37—40]. The simplicity and sensitivity offered by room temperature phosphorimetry has provoked new investigations into the area of phosphorimetry; and this technique promises to provide a powerful new tool for the trace determination of compounds important to the areas of biochemistry, clinical chemistry, and environmental chemistry. Room temperature phosphorimetry affords much greater selectivity than other luminescence techniques (either fluorimetry or low temperature phosphorimetry). Further, conventional luminescence spectroscopy usually provides higher selectivity than molecular absorption techniques of spectrometry. These features combine to make room temperature phosphorimetry highly attractive to the analyst.

In Part 1 of this series [1], the origins of room temperature phosphorescence (r.t.p.) and various aspects associated with the physical nature of the phenomenon were introduced. This second and concluding part of the article concentrates on the practical aspects of r.t.p. directly associated with its analytical utility. The analytical developments reported in the literature thus

[a]Present address: Monsanto Industrial Chemicals Company, Nitro, WV 25143, U.S.A.
[b]Present address: ICI Americas, Inc., Biological Research Center, P.O. Box 208, Goldsboro, NC 27530, U.S.A.

TABLE 1

Room temperature phosphorescence characteristics of a selection of organic and biological compounds[a]

Compound	Peak maxima (nm)			
	Excitation	Emission	Support[b]	Ref.
7-(Acetylamino)-1-ethyl-1,4-dihydro-4-oxy-1,8-naphthyridine-3-carboxylic acid	346	456	Paper [NaOH]	21
5-Acetyluracil	305	421	Paper [NaOH]	6
Acridine	360	660	Paper [$Pb(CH_3COO)_2$]	34
Adenine	290	470	Paper [NaI:NaOH]	9
Adenosine	300	469	Paper [NaOH]	6
m-Aminobenzoic acid	290	430	CH_3COONa	18
p-Aminobenzoic acid	273	426	Paper [NaOH]	6
	280	430	Paper [NaI:NaOH]	9
	300	430	Paper [$Pb(CH_3COO)_4$]	16
	290	426	CH_3COONa	18
	287	432	Silica gel	25
4-Amino-2,6-dihydroxylpyrimidine	310	421	Paper [NaOH]	6
p-Aminohippuric acid	328	448	CH_3COONa	18
2-Amino-6-methylmercaptopurine	331	487	Paper [NaOH]	5
1-Aminonaphthalene-4-sulfonic acid	345	535	Paper [NaOH]	4
2-Amino-1-naphthalene sulfonic acid	352	526	Paper [NaOH]	5
4-Amino-3,5,6-trichloropicolinic acid	310	490	Paper	35
Anthracene	375	500	Paper [$AgNO_3$]	13
Antrenyl	280	490	Paper [NaI:NaOH]	22
Anturane	285	460	Paper [NaI:NaOH]	22
Apresoline	280	440	Paper [NaOH]	22
	280	440	Paper [NaI:NaOH]	22
Auramine O (hydrochloride)	460	520	Paper	4
4-Azafluorene	330	465	Silica gel	26
Barbituric acid	290	455	Paper [NaI:NaOH]	9
Benomyl	308	480	Paper	35
1,2-Benzanthracene	290	515	Paper [$AgNO_3$]	23
2,3-Benzofluorene	343	505	Paper [NaI]	34
Benzo[a]pyrene	360	680	Paper[$AgNO_3$]	13
	395	698	Paper [$Pb(CH_3COO)_2$]	34
1,2-Benzpyrene (Benzo[e]pyrene)	348	548	Paper [$AgNO_3$]	23
	335	543	Paper [CsI]	34
Benzo[f]quinoline	370	510	Silica gel	26
2-Biphenylcarboxylic acid	280	475	Paper [NaOH]	4
4-Biphenylcarboxylic acid	290	480	Paper [NaOH]	4
	300	490	Paper [$Pb(CH_3COO)_4$]	16
Carbazole	323	435	Paper [NaI:NaOH]	13
	296	415	Paper [CsI]	34
Chloroneb	307	490	Paper	35
6-Chloropurine	280	463	Paper [NaOH]	6
	290	460	Paper [NaI:NaOH]	9
Chrysene	272	515	Paper [$AgNO_3$]	23
	325	515	Paper [$Pb(CH_3COO)_2$]	24

Table 1—*continued*

Compound	Peak maxima (nm)			
	Excitation	Emission	Support[b]	Ref.
Chrysene—*continued*	280	505	CH_3COONa [$AgNO_3$]	23
	330	518	Paper [NaI]	34
Cinoxacin	370	515	Paper [$Pb(CH_3COO)_4$]	16
Cocaine hydrochloride	285	460	Paper [NaI:NaOH]	9
Coproporphyrin III	410	625	Paper	4
Coronene	310	525	Paper [$AgNO_3$]	23
	300	515	CH_3COONa [$AgNO_3$]	23
Cytosine	301	405	Paper [NaOH]	6
2,6-Diaminopurine	286	451	Paper [NaOH]	6
4,5-Diaminouracil	357	524	Paper [NaOH]	6
1,2,3,4-Dibenzanthracene	295	567	Paper [CsI]	34
1,2,5,6-Dibenzanthracene	300	555	Paper [$AgNO_3$]	23
	305	555	Paper [NaI]	34
	300	565	CH_3COONa [$AgNO_3$]	23
1,2,7,8-Dibenzaphenanthrene	290	510	Paper [$AgNO_3$]	23
Dibenzocarbazole	295	475	Paper [NaI]	34
Dichlone	310	489	Paper	35
Dichlorophen	309	489	Paper	35
Dicloran	310	494	Paper	35
N,N-Dimethyl-4-aminobenzoic acid	290	430	CH_3COONa	18
2,9-Dimethyl-4,7-diphenyl-1,10-phenanthroline	330	518	Silica gel	26
Diphenic acid	275	490	Paper [NaOH]	4
Diphenyl	275	470	Paper [$Pb(CH_3COO)_4$]	16
Diphenylacetic acid	320	500	Paper [$Pb(CH_3COO)_4$]	16
4,4'-Diphenyldisulfonic acid	290	485	Paper [$Pb(CH_3COO)_4$]	16
4,7-Diphenyl-1,10-phenanthroline	310	518	Silica gel	26
2,4-Dithiopyrimidine	374	464	Paper [NaOH]	6
Eosin Y	530	680	Paper	4
Esidrex	275	440	Paper [NaOH]	22
	275	440	Paper [NaI:NaOH]	22
1-Ethyl-1,4-dihydro-7-hydroxy-4-oxy-1,8-naphthyridine-3-carboxylic acid	320	468	Paper [NaOH]	21
1-Ethyl-1,4-dihydro-4-oxy-1,8-naphthyridine-3,7-dicarboxylic acid	357	470	Paper [NaOH]	21
Ethyl violet (chloride)	590	655	Paper	4
Fenaminosulf	310	498	Paper	35
Fluoranthene	284	555	Paper [$AgNO_3$]	23
	365	545	Paper [$Pb(CH_3COO)_2$]	34
	363	560	CH_3COONa [$AgNO_3$]	23
Fluorene	270	428	Paper [CsI]	34
2-Fluorobiphenyl	280	460	Paper [$Pb(CH_3COO)_4$]	16
Folic acid	320	465	CH_3COONa	18
	380	520	Paper [CH_3COONa]	30
Folpet	305	489	Paper	35
Guanine	280	450	Paper [NaI:NaOH]	9
Hydroquinone	285	435	CH_3COONa	18
p-Hydroxybenzoic acid	285	420	CH_3COONa	18

Table 1—*continued*

Compound	Peak maxima (nm)			
	Excitation	Emission	Support[b]	Rel
5-Hydroxyindole-acetic acid	312	510	CH_3COONa	18
p-Hydroxymandelic acid	290	420	CH_3COONa	18
4-Hydroxy-3-methoxy benzaldehyde (vanillin)	332	519	Paper [NaOH]	6
6-Hydroxymethylpterin	375	515	Paper [CH_3COONa]	30
4-Hydroxypteridine	350	490	Paper [CH_3COONa]	30
5-Hydroxytryptophan	355	500	CH_3COONa	18
Indole	288	436	Paper [NaI]	33
Isoquinoline	330	520	Silica gel	26
Isoxanthopterin	345	495	Paper [CH_3COONa]	30
Lumazine	370	510	Paper [CH_3COONa]	30
3-Methyl-4-aminobenzoic acid	290	430	CH_3COONa	18
6-Methylmercaptopurine	292	466	Paper [NaOH]	6
	290	458	Paper [NaI:NaOH]	9
Methyl-1-naphthaleneacetate	306	494	Paper	35
7-Methyl-1,8-naphthyridin-4-ol	353	474	Paper [NaOH]	21
6-Methylpurine	268	449	Paper [NaOH]	6
Metopirone	285	460	Paper [NaI:NaOH]	22
Nalidixic acid	338	472	Paper [NaOH]	21
Naphthalene	275	472	Paper [$Pb(CH_3COO)_2$]	24
	289	510	Paper [NaI]	28
1-Naphthaleneacetamide	300	490	Paper	35
1-Naphthaleneacetic acid	299	494	Paper	35
Naphthalene-1-sulfonic acid	293	513	Paper [NaOH]	5
	290	515	Paper [$Pb(CH_3COO)_4$]	16
Naphthalene-β-sulfonic acid	310	525	Paper [NaOH]	4
Naphthalic acid	310	535	Paper [NaOH]	4
1-Naphthoic acid	300	530	Paper [NaOH]	4
2-Naphthoic acid	290	525	Paper [NaOH]	4
	300	515	Paper [$Pb(CH_3COO)_4$]	16
1-Naphthol	310	530	Paper [NaI]	34
1-Naphthol-5-sulfonate (disodium salt)	385	575	Paper [NaOH]	4
2-Naphthol-6-sulfonate (disodium salt)	350	535	Paper [NaOH]	4
2-Naphthol-6-sulfonate (monosodium salt)	300	520	Paper	4
2-Naphthol-7-sulfonate (disodium salt)	360	555	Paper [NaOH]	4
2-Naphthol-7-sulfonate (monosodium salt)	335	530	Paper	4
2-Naphthoxyacetic acid	310	504	Paper	35
Nupercaine hydrochloride	295	445	Paper	22
	295	445	Paper [NaI]	22
	295	515	Paper [$AgNO_3$]	22
Pentachlorophenol	311	492	Paper	35
Phenanthrene	260	505	Paper [$AgNO_3$]	23
	295	474	Paper [NaBr]	34

Table 1—*continued*

Compound	Peak maxima (nm)			
	Excitation	Emission	Support[b]	Ref.
Phenanthrene—*continued*	290	505	CH_3COONa [$AgNO_3$]	23
Phenanthridine	360	510	Silica gel	26
1,10-Phenanthroline·H_2O	325	520	Silica gel	26
Phenylmercuric benzoate	244	439	Paper	35
Phthalic acid	289	432	Silica gel	25
Plantvax	309	487	Paper	35
Priscoline hydrochloride	280	500	Paper [NaI:NaOH]	22
Privine hydrochloride	280	510	Paper	22
	280	520	Paper [NaOH]	22
	280	520	Paper [NaI:NaOH]	22
	280	520	Paper [NaI]	22
	280	515	Paper [$AgNO_3$]	22
Procaine hydrochloride	305	445	Paper	22
	275	430	Paper [NaOH]	22
	275	430	Paper [NaI:NaOH]	22
	300	460	Paper [$AgNO_3$]	22
Pterin	370	505	Paper [CH_3COONa]	30
Pterin-6-carboxylic acid	375	505	Paper [CH_3COONa]	30
Pyrene	322	590	Paper [$AgNO_3$]	23
	343	595	Paper [$Pb(CH_3COO)_2$]	34
	346	597	Paper [NaI]	28
2,5-Pyridinedicarboxylic acid	289	435	Silica gel	26
Quinine sulfate	335	510	Paper [$Pb(CH_3COO)_4$]	16
Quinoline	320	510	Silica gel	26
	305	505	Paper [$AgNO_3$]	34
Ritalin hydrochloride	332	515	Paper [NaOH]	22
	282	525	Paper [NaI:NaOH]	22
Salicylic acid	320	470	Paper [NaI:NaOH]	9
Serpasil (Reserpine)	280	520	Paper [NaI:NaOH]	22
Sulfanilamide	267	426	Paper [NaOH]	6
	280	427	Paper [NaI:NaOH]	9
Sulfguanidine	267	426	Paper [NaOH]	6
Terephthalamide	283	410	Silica gel	25
Terephthalic acid	292	418	Silica gel	25
2,3,4,6-Tetrachlorophenol	310	494	Paper	35
2-Thio-6-aminouracil	307	441	Paper [NaOH]	6
2-Thio-4,6-dioxypyrimidine	342	467	Paper [NaOH]	6
Thiopropozate dihydrochloride	300	520	Paper [NaOH]	22
	275	515	Paper [NaI:NaOH]	22
	280	510	Paper [$AgNO_3$]	22
Trasentine hydrochloride	275	520	Paper [NaI:NaOH]	22
	300	520	Paper [NaI]	22
2,4,5-Trichlorophenol	308	489	Paper	35
2,4,6-Trichlorophenol	310	494	Paper	35
Triphenylene	268	465	Paper [$AgNO_3$]	23
L-Tryptophan	280	448	Paper [NaOH]	6
	296	445	Paper [NaI]	33
	299	448	Paper [NaI:NaOH]	33

Table 1—*continued*

Compound	Peak maxima (nm)			
	Excitation	Emission	Support[b]	Ref.
L-Tryptophan methyl ester	298	444	Paper [NaI]	33
L-Tryptophyl-L-tyrosine	295	442	Paper [NaI]	33
L-Tyrosine	285	444	Paper [NaI]	33
L-Tyrosine methyl ester	286	434	Paper [NaI]	33
Vinblastine sulfate	278	515	Paper [NaOH]	22
	278	515	Paper [NaI]	22
Vioform	300	510	Paper [NaI:NaOH]	22

[a]This Table is composed only of compounds for which excitation and emission maxima have been given in the literature. The listed compound may actually be present in the form of a salt depending on other agents which have been added to the analyte solution or the r.t.p. support.

[b]The support also contained the substance given in brackets. This substance was introduced to the sample matrix by spotting a solution of the agent on the support prior to analyte application or by dissolving the agent in the analyte solution to be applied to the support.

far are reviewed, and potential means of improving r.t.p. analyses drawn from these developments are proposed. Future directions and potential applications of this evolving technique are also presented.

SELECTION OF COMPOUNDS AND SUPPORT MATERIALS

As described in detail in Part 1, room temperature phosphorescence can be observed from a variety of compounds when the substance is adsorbed on a suitable substrate (support material) such as cellulose, silica or sodium acetate [4, 10, 25]. The key factor in observing r.t.p. from these compounds is that moisture be thoroughly excluded from the sample matrix. This can be accomplished by drying samples prepared with aqueous solvents in anhydrous atmospheres [5, 11] or, in some cases, by utilizing anhydrous solvents in sample preparation [10, 20]. Examination of Table 1 illustrates the diverse nature and number of compounds thus far shown to display r.t.p. The specific support material employed and other crystalline agents present in the sample matrix are given for each compound cited in Table 1. Among the compounds listed are substances of considerable biological, clinical, pharmaceutical and environmental importance. Since r.t.p. is in the early stages of development, this already sizeable list is expected to increase considerably in the future.

Several criteria appear to be important in selecting a potential room temperature phosphor. Firstly, the compound should have a reasonable phosphorescence quantum yield at low temperature. Most compounds meeting this criterion are highly conjugated and contain one or more aromatic rings [37]. Secondly, compounds containing highly polar or ionic functional groups usually have the highest probability of showing r.t.p. R.t.p. can be

observed from certain nonpolar compounds (polynuclear aromatic hydrocarbons); however, the presence of a heavy atom perturber is necessary in order to obtain reasonable r.t.p. emission [12, 13, 23, 24, 27, 34]. Examination of the r.t.p. from 2-naphthol illustrates the importance of either highly polar character or the presence of heavy atoms in observing strong r.t.p. Virtually no r.t.p. is observed from 2-naphthol adsorbed on paper even though the compound contains a polar hydroxyl group. The ionic form (sodium 2-naphthoxide) displays intense r.t.p. [41]. Intense r.t.p. is also observed from 2-naphthol on addition of a heavy atom (sodium iodide) [7, 41].

A variety of materials function successfully as substrates (or supports) for r.t.p. as illustrated in Table 2. Most suitable supports either contain an abundance of hydroxyl groups [11] or possess a number of ionic sites [18]. By far, the most widely employed support is paper [2—9, 11—16]. This material seems to produce excellent r.t.p. intensities from a wide spectrum of compounds. Silica gel [25, 26] and sodium acetate [18] have also been used quite successfully and may prove to be superior to paper in certain applications. The exploration of different support materials in quantitative analysis is still in the early stages. So far, only paper [5, 6, 11—13, 21—23, 27, 30, 33—35] (which sometimes contains added agents to enhance the

TABLE 2

Support materials employed in room temperature phosphorescence

Support	Ref.	Support	Ref.	Support	Ref.
Paper (various types)	4,5	Paper treated with:		Paper treated with:	
Alumina	4	Lead subacetate	16	Thorium nitrate	16
Silica gel	4,25	Lead borate	16	Sodium fluoride	19
Asbestos	4	Lead chloride	16	Calcium chloride	19
Sodium acetate	10,23	Beryllium acetate	16	Strontium chloride	19
Sucrose	11	Sodium acetate	16,30	Barium chloride	19
Starch	11	Magnesium acetate	16	Ammonium chloride	19
Paper lint-crushed		Calcium acetate	16	Ammonium carbonate	19
quartz mixture	20	Scandium chloride	16	Potassium hydroxide	19
Paper treated with:[a]		Zinc acetate	16	Boric acid	19
Sodium hydroxide	4,5	Strontium acetate	16	Glycine	19
Sodium iodide	7,9	Cadmium acetate	16	Alanine	19
Potassium iodide	16	Indium acetate	16	Glucose	19
Thallium(III) acetate	16	Tin chloride	16	Sucrose	19
Thallium(I) acetate	16	Antimony chloride	16	Silver nitrate	23
Thallium(I) fluoride	16	Cesium acetate	16	Sodium malonate	23
Thallium(I) sulfate	16	Barium acetate	16	Sodium citrate	23
Lead tetraacetate	16	Cerium(III) acetate	16		

[a]The reagents listed were added to paper either by spotting the paper with solutions of the agent before application of the analyte or by applying an analyte solution containing the dissolved agent. Paper treated with these reagents generally provides more intense r.t.p. from certain compounds compared to untreated paper; however, this effect may be specific for the compound of interest. Also, some of the reagents listed may serve as suitable r.t.p. supports when used alone.

r.t.p.), silica gel [25, 26], sodium acetate [10, 17], and a mixture of paper lint and quartz [20] have been used for quantitative work.

The choice of the support material can be critical in the successful observation of r.t.p. A compound might prove to be an intense phosphor with one support material and yet yield very poor r.t.p. with another support. An excellent example of this is seen with sodium 4-biphenylcarboxylate. This compound is one of the most intense room temperature phosphors when adsorbed on paper; however, practically no r.t.p. is observed from sodium 4-biphenylcarboxylate adsorbed on sodium acetate [30]. In a similar fashion, terephthalic acid displays excellent r.t.p. when adsorbed on silica gel [25], but no emission is reported for the compound adsorbed on sodium acetate [18]. It is sometimes necessary to employ a combination of two different support materials in order to obtain strong r.t.p. emission. Pterin-6-carboxylate (sodium salt) shows an r.t.p. intensity arbitrarily set at 100 when adsorbed on paper impregnated with sodium acetate. This compound gives intensities of only 1.4 and 4.5 when adsorbed on paper and sodium acetate, respectively [30]. The selection of an optimum support material for r.t.p. seems to be largely trial and error at this stage of development; however, several parameters which may be adjusted in an attempt to maximize r.t.p. intensities will be discussed in a later section.

QUANTITATIVE ABILITY

The analytical potential of phosphorimetry was first demonstrated by Keirs et al. for samples at low temperature [42]. A theoretical relationship was derived from the Beer—Lambert law which predicted a linear correlation between the intensity of phosphorescence and the analyte concentration for sufficiently dilute solutions. This prediction was verified by constructing calibration plots (working curves) for benzaldehyde, benzophenone and other compounds in transparent glasses at 77 K.

A modified form of the equation developed by Keirs et al. for the expression of phosphorescence intensity is given [43] by

$$I_p = Q_p I_0(1 - 10^{-\epsilon bC}) \quad (1)$$

where I_p is the intensity of the phosphorescence, Q_p is the phosphorescence quantum yield (the fraction of the molecules which emit out of the total number of molecules directly excited by the incident light), I_0 is the intensity of the incident light, ϵ is the molar absorptivity (in units of $1\ mol^{-1}\ cm^{-1}$), b is the thickness of the solution in cm, and C is the concentration in mol l^{-1}. At low analyte concentration, eqn. (1) reduces to the simple linear relationship given by

$$I_p = Q_p I_0\ 2.3\ \epsilon bC \text{ or } I_p = kC \quad (2)$$

where k is a constant which can be determined by constructing a calibration plot of I_p versus C. Equation (1) relies on the assumption that the solvent or

support medium is completely transparent; however, the support materials employed in r.t.p. are obviously not transparent and do not meet this criterion. Zweidinger and Winefordner [14, 44] have developed an equation for the intensity of phosphorescence in nontransparent media:

$$I_p = 2\,Q_p\,\beta\,I_0\,[(1+\beta)\exp(K\bar{b}) + (1-\beta)\exp(-K\bar{b}) - 2]/[(1+\beta)^2\exp(K\bar{b}) - (1-\beta)^2\exp(-K\bar{b})] \quad (3)$$

where: β is $[2.3\,\epsilon C/(2.3\,\epsilon C + 2s)]^{1/2}$, s is the fraction of exciting radiation scattered per average path length and has no units, $\bar{b}$ is the average cell path length for diffuse reflectance in cm, and K is $[2.3\,\epsilon C\,(2.3\,\epsilon C + 2s)]^{1/2}$. Although eqn. (3) is considerably more complex than eqn. (1), this expression also reduces to a simple linear relationship between phosphorescence intensity and concentration for sufficiently dilute samples and is given by

$$I_p = 2\,Q_p I_0\,(1 + 2s\bar{b})^{-1}\,2.3\,\epsilon\,\bar{b}C \text{ or } I_p = k'C \quad (4)$$

where k' is a constant dependent on the compound and the properties of the support material and can be determined by constructing a calibration plot. Both eqns. (1) and (3) depart from linearity at higher analyte concentrations (plots of I_p versus C give slopes approaching 0). In practice, these effects can occur at lower concentrations than predicted because of the inner filter effect, self-quenching, and other factors [43]. A negative slope in the analytical calibration curve can even be encountered at high concentrations of analyte.

Winefordner et al. [5] first illustrated the quantitative capability of r.t.p. by measuring the working curves of a selection of compounds adsorbed on paper. These plots displayed a range of linearity at low concentrations as predicted by eqns. (3) and (4). Subsequent studies have expanded the quantitative potential of r.t.p. to a larger number of compounds adsorbed on paper and other materials [6, 10—13, 17, 20—23, 25—27, 30, 33—35]. For example, a simple determination of *p*-aminobenzoic acid in vitamin tablets has been reported by von Wandruszka and Hurtubise [10]. Several suspected carcinogens have been successfully quantified by r.t.p. [13, 23]. Recently, Winefordner et al. demonstrated the applicability of r.t.p. in determining a number of pesticides [35].

SAMPLE PREPARATION AND INSTRUMENTAL CONSIDERATIONS

The preparation of r.t.p. samples simply involves applying a solution containing the desired analyte to the support material much in the same fashion as one would spot paper or a t.l.c. plate for chromatography. After analyte application, the sample is dried and introduced to the spectrophosphorimeter for phosphorescence spectral and/or intensity measurements. For qualitative spectral measurements or spot tests for potential room temperature phosphors, samples can be prepared quite crudely and rapidly by dispensing the analyte solution onto a filter paper circle or other material using a medicine

dropper or disposable Pasteur pipet. Sample drying can be accomplished in a few minutes by using a hand-held blow drier or a lab oven [4] (most samples display r.t.p. after two or three minutes of drying in this manner; however, some compounds may require extensive drying times in a desiccator before r.t.p. is observed [30]). At this point, phosphorescence can be observed visually by exciting the sample with a convenient u.v. source.

Quantitative measurements in r.t.p. require more stringent control of the sample preparation technique. The amount of analyte solution applied to the support should be precisely measured using analytical syringes [5] or precision disposable micropipets [30]. It is also necessary to control the amount and surface area of the support material [5, 10] unless integrating techniques are applied to scan and quantify an analyte spot spread over a relatively undetermined area of the support surface [12] (i.e., spots on paper chromatograms or t.l.c. plates). One popular and convenient method of preparing consistent r.t.p. samples involves applying a specific volume of analyte solution to precut filter paper sections [5, 6, 11, 30]. Uniform paper supports can be made easily by punching 0.64-cm diameter circles from filter paper sheets with a paper-hole puncher [5]. Only 5 μl of analyte solution is required to cover a support of this size completely, and solutions in the 10^{-6}—10^{-3} M range typically provide excellent r.t.p. signals. Drying may be accomplished with heat, in a desiccator or in an instrument cell compartment flushed with a dry gas [5, 11]. The sample may be precisely aligned in the instrument by mounting it on a specially constructed holder such as the one shown in Fig. 1 (designed for the Aminco-Bowman spectrofluorimeter containing a phosphoroscope attachment).

R.t.p. samples are somewhat more difficult to prepare on crystalline supports such as sodium acetate or sucrose than they are on paper supports [10, 11]. For example, von Wandruszka and Hurtubise [10] have described a procedure where a measured amount of sodium acetate was added to the analyte solution. Before analysis, the solvent was evaporated and the resultant dry solid had to be quantitatively transferred to a mortar and pestle where it was ground to a fine powder. The powder then had to be carefully transferred to circular depressions on a brass plate which served as the sample holder. We are currently using a simpler procedure than that of von Wandruszka and Hurtubise for preparing r.t.p. samples on crystalline supports. This involves applying concentrated solutions of the desired crystalline substance (sodium acetate, sucrose, sodium tartrate, etc.) to precut circles of glass-fiber filter paper (0.64-diameter circles of Whatman GF/C are typically loaded with 1—10 mg of crystalline material depending on the analyte to be used with the support). After drying, these supports are handled as easily as paper and analyte samples are prepared in a similar fashion.

Several systems have been described for making quantitative measurements of r.t.p. from analyte spots which do not cover the entire surface of the support [12, 16, 21, 25, 26]. In general, a specific volume of analyte must be very carefully spotted on a paper sheet or t.l.c. plate such that the spots

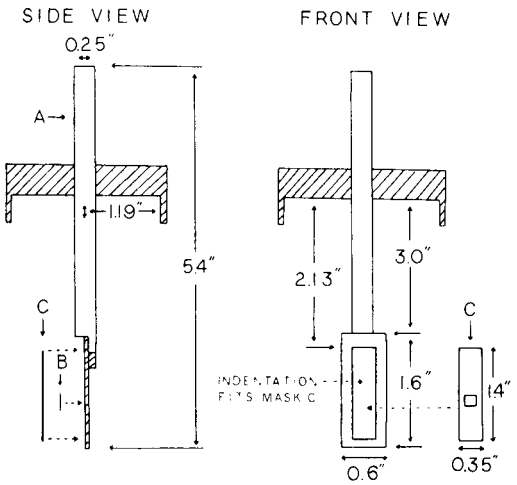

Fig. 1. Holder for r.t.p. samples adsorbed on precut paper supports or other thin materials. The holder allows mounting of paper supports with optimum geometry for excitation/emission measurements and replaces the standard quartz Dewar assembly used with the phosphoroscope accessory of the Aminco-Bowman spectrofluorimeter. Note the hollow tube (A) that allows passage of a desired gas directly over the face of the sample (B) which is held in place by a mask (C) exposing a 5 × 5 mm surface. The mask is simply a cell slit from the Aminco-Bowman instrument.

are of fairly uniform size. The sample is mounted on a device capable of positioning the spot in the excitation beam of the spectrophosphorimeter. Ford and Hurtubise [26] have described a modified version of a Schoeffel spectrodensitometer which works well for this purpose and allows viewing of 8 or 9 sample spots on one paper sheet or t.l.c. plate. A "continuous filter paper device" has also been developed for viewing multiple analyte spots applied in series along a continuous strip of paper [12, 27]. This system, described by Winefordner et al., offers the potential of automated determination by r.t.p. A Technicon continuous filter (a module of the Technicon Auto-Analyzer) was employed to feed a paper tape first under a syringe for sample spotting, then through a drying oven, and finally into a modified cell compartment of a spectrophosphorimeter for r.t.p. analysis. The paper tape moved at a constant speed across the aperture of the sample compartment, and the emission intensity from the analyte spot was integrated as the spot moved over the aperture. This system allowed measurement of 7 to 8 sample spots per minute. Lloyd [20] has described a rather unique sampling system which might also lend itself to automation. Methanolic solutions of the analyte (1-μl volume) were injected into a packed flow-through cell containing a mixture of paper lint and crushed quartz as the adsorbent. Traces of moisture were removed by flushing anhydrous diethyl ether through the cell. Afterwards, r.t.p. measurements were made, and the sample was washed out of the cell with aqueous media.

Several factors affect the precision of r.t.p. measurements. Care should be

taken to maintain an exact routine in sample spotting and in mounting and positioning the sample in the instrument [5]. The drying technique used is of primary importance [6, 9, 11, 12]. Regardless of the drying method (i.e., ovens, i.r. lamps or desiccators), sufficient time should be allowed for the r.t.p. intensity to stabilize or reach its maximum intensity. A wise practice is to maintain a set drying time. The optimum drying time can be determined by observing the time required for the r.t.p. sample to provide a maximum and constant emission intensity as a function of the drying period [5, 6]. In most cases, the instrument cell must be flushed with a dry gas to exclude moisture. If samples are exposed to a humid atmosphere upon removal of the sample from the drying device and subsequent introduction of the sample to the instrument cell, a period of time should be allowed for the sample to equilibrate in the dry atmosphere of the cell [5]. If the instrument cell is heated to facilitate drying, the temperature should be held constant [9, 12]. Schulman and Parker [11] have demonstrated that r.t.p. intensities can be temperature-dependent. Also, the presence of oxygen in the drying atmosphere has been implicated in reducing the precision of r.t.p. measurements [11], thus drying in nitrogen or argon atmospheres is recommended to maximize precision. With close control of the sample preparation technique, r.t.p. measurements with relative standard deviations in the 1—5% range can be realized [11, 12, 26, 30].

Several recent reviews have dealt with advances in instrumentation and techniques in low temperature phosphorimetry [45, 46]. Most of these developments such as pulsed source-gated detector systems, photon counting, and time-resolved and phase-resolved techniques are of direct use in r.t.p. Although no commercial attachments are currently available for r.t.p. analysis, most spectrophosphorimeters may be readily adapted for r.t.p. measurements by constructing a special sample holder and/or by minor modification of the instrument cell compartment [5, 10, 11, 12, 16, 20, 21, 26]. R.t.p. procedures are completely analogous to those used at low temperature with the exceptions of the sample preparation methods and the omission of the cryogenic equipment required for low temperature phosphorimetry.

OPTIMIZING CONDITIONS FOR DETERMINATIONS

Of primary importance in devising an r.t.p. analysis is that of optimizing the sample matrix conditions to provide the strongest possible r.t.p. signal from the analyte without unduly increasing the phosphorescence background emission. As mentioned earlier, trial and error may play a major role in arriving at an appropriate support material; however, certain other steps may be taken to enhance the r.t.p. emission from the analyte. One important factor, which has received little attention to date, is control of the pH of the sample matrix or more specifically the pH of the analyte solution applied to the support material. Von Wandruszka and Hurtubise [18] first noted that the r.t.p. intensity of *p*-aminobenzoic acid adsorbed on sodium acetate

declined sharply with either strongly acidic or alkaline conditions. A study by de Lima and de M. Nicola [21] involving a series of 1,8-naphthyridine derivatives has revealed that each particular compound has an optimum pH associated with the maximum r.t.p. intensity obtained from the compound. This study involved measuring the r.t.p. intensities of the compounds adsorbed on paper as a function of the pH of the analyte solutions applied to the paper initially. Current investigations along these lines in this laboratory have verified that pH can have a dramatic effect on the r.t.p. intensities from certain compounds [41].

In Part 1 of this review [1], it was mentioned that certain salts or crystalline compounds added to a paper sample matrix can provide considerable enhancements of the r.t.p. intensity from the analyte. Several of these agents used in conjunction with the paper sample matrix are listed in Table 2. Although addition of these agents to the same matrix may not always provide beneficial results, enhancement of the r.t.p. emission can be spectacular in some cases. For example, the r.t.p. intensity from pterin-6-carboxylate (sodium salt) can be enhanced 70-fold by employing a paper matrix treated with sodium acetate as compared to untreated paper [30]. Bower and Winefordner [23] have advised caution in the use of some of these agents since the enhancement in the phosphorescence background emission from the sample matrix sometimes may overshadow the enhancement of the analyte signal and thus adversely affect the detection limit. Generally, background emission problems in r.t.p. are much less severe than in low temperature phosphorimetry; however, the background emission remains an important factor in determining the r.t.p. detection limit.

Recently, the external heavy-atom effect (described thoroughly in Part 1 [1]) has been exploited selectively to enhance the r.t.p. emission of a desired compound present in a complex mixture [34]. Specific heavy atom salts such as $Pb(COOCH_3)_2$, NaBr and CsI were found to enhance preferentially the r.t.p. emission from individual components in a multicomponent mixture. This effect, termed selective external heavy-atom perturbation (SEHAP), was employed to determine each component of a seven-component mixture without the aid of any physical or chemical separation technique. Manipulating the sample pH and/or adding specific non-heavy-atom salts to the sample matrix might also be used to enhance selectivity even more in r.t.p. analyses.

Several means of improving r.t.p. analyses involving instrumental techniques have been reported [24, 28, 31, 32]. Walden and Winefordner [32] have utilized ellipsoidal and parabolic mirrors to increase the collection efficiency of sample luminescence for small volume samples such as those encountered in r.t.p. Other workers have taken advantage of both the second-derivative method [28] and synchronous scanning of the excitation and emission monochromators [24, 31] to enhance the selectivity of the technique.

ADVANTAGES OF ROOM TEMPERATURE PHOSPHORIMETRY

Phosphorescence spectrometry is an extremely sensitive and selective analytical tool, and these factors make its use highly desirable in situations

where trace amounts of analyte must be determined in complex sample matrices [45, 46]. Phosphorimetric methods have not been widely used because of the experimental difficulties associated with traditional low temperature techniques; however, the advent of room temperature phosphorimetry promises to change this picture. R.t.p. techniques provide a number of advantages over low temperature phosphorescence (l.t.p.) methods. The cryogenic techniques, which make l.t.p. analyses cumbersome and time-consuming, are eliminated with r.t.p. methods [5, 11]. Expensive quartz Dewars and sample tubes required in l.t.p. are replaced by inexpensive solid adsorbents such as paper, sodium acetate or silica gel. R.t.p. samples are simply discarded after use; therefore tedious cleaning of small sample tubes such as are employed in l.t.p. is avoided. Virtually any solvent which dissolves the analyte, is suitable for preparing r.t.p. samples. Aqueous solutions are readily employed [4, 5], whereas the expansion of aqueous media on freezing presents the problem of shattering the quartz sample tube in low temperature phosphorimetry [47, 48]. Solvents which do not form clear glasses at low temperature (i.e., solvents which crack upon freezing) can also present difficulties in making quantitative measurements in l.t.p. [49, 50] unless special spinning sample cells are used [51].

The r.t.p. method offers exceptional selectivity since relatively few compounds display this luminescence compared to fluorescence or l.t.p. The potential of avoiding tedious separations with r.t.p. analysis is apparent. Von Wandruszka and Hurtubise [10] demonstrated this by determining *p*-aminobenzoic acid in vitamin tablets without the aid of complex separation procedures. As mentioned earlier, enhanced selectivity among a mixture of potential room temperature phosphors might also be realized by choosing an approximate support material and optimizing the sample matrix for the compound of interest.

The sensitivity afforded by r.t.p. is excellent. Nanogram quantities of material are easily detected by r.t.p., as illustrated by some typical detection limits given in Table 3. The linear dynamic range of r.t.p. working curves is also quite good. Ranges spanning three to four orders of magnitude have been reported [6]. With careful sample preparation, very precise r.t.p. measurements may be made. Schulman and Parker [11] have reported typical relative standard deviations of 2.5% from making only four replicate measurements of sodium 4-biphenylcarboxylate samples [11]. R.t.p. also offers the advantage of requiring very small amounts of sample. Conventional fluorescence and phosphorescence techniques require 0.1—2 ml of analyte solution as compared to 3—5 μl volumes needed for r.t.p. measurements [14].

Promising applications of r.t.p. in the direct detection and quantification of separated components on paper chromatograms and t.l.c. plates can be foreseen. L.t.p. techniques have already been utilized for this purpose [52, 53]. The use of r.t.p. in this area could greatly simplify the t.l.c. procedures. R.t.p. analysis could be carried out simply by cutting out the analyte spot, drying it, and mounting it on a suitable holder for placement in a spectro-

TABLE 3

Typical detection limits in room temperature phosphorescence

Compound	Detection limit[a] (ng)	Compound	Detection limit[a] (ng)
Analyte adsorbed on paper support [6]		*Analyte adsorbed on silica gel* [26]	
p-Aminobenzoic acid	0.1	Benzo[f]quinoline	3
2,4-Dithiopyrimidine	7	Phenanthridine	6
4-Amino-2,6-dihydroxylpyrimidine	10	4-Azafluorene	10
2-Amino-6-methylmercaptopurine	4	1,10-Phenanthroline·H_2O	25
2,6-Diaminopurine	2	4,7-Diphenyl-1,10-phenanthroline	12
6-Methylpurine	5	2,9-Dimethyl-4,7-diphenyl-1,10-phenanthroline	20
6-Chloropurine	15	Quinoline	25
6-Methylmercaptopurine	0.3	Isoquinoline	22
Sulfanilamide	3	*p*-Aminobenzoic acid	10
Sulfguanidine	0.9	2,5-Pyridinedicarboxylic acid	15
Tryptophan	4		
5-Acetyluracil	1.5		
2-Thio-6-aminouracil	0.5		
Vanillin	0.1		

[a]Detection limit is reported for the amount of sample in ng applied to the support material.

photophosphorimeter. De Lima and de M. Nicola [21] have described a device that accepts entire paper chromatograms for r.t.p. analysis, and a system accepting t.l.c. plates has been developed by Ford and Hurtubise [26]. R.t.p. also adds another nondestructive means of visualizing certain separated components on chromatograms. Methylvinylmaleimide was located and tentatively identified on paper chromatograms by the visual observation of r.t.p. [54]. This compound was isolated from the photooxidation products of bilirubin and was the only component in the mixture to show r.t.p. Since methylvinylmaleimide did not show fluorescence, phosphorescence was the only luminescent means of viewing this compound.

In conclusion, room temperature phosphorimetry offers an exceptionally sensitive and selective means of detecting a variety of compounds important in real-life situations. The potential for determining drugs, carcinogens, pesticides and other important compounds is apparent (Table 1). Also, the technique is very economical from the commercial standpoint and is simple enough to be used without extensive training or expertise.

These investigations were supported by NIH grant CA12842 from the National Cancer Institute. R. Bruce Dunlap is the recipient of a Faculty Research Award (FRA-144) from the American Cancer Society.

REFERENCES

1 R. T. Parker, R. S. Freedlander and R. B. Dunlap, Anal. Chim. Acta, 119 (1980) 1.
2 M. Roth, J. Chromatogr., 30 (1967) 276.
3 E. M. Schulman and C. Walling, Science, 178 (1972) 53.
4 E. M. Schulman and C. Walling, J. Phys. Chem., 77 (1973) 902.
5 R. A. Paynther, S. L. Wellons and J. D. Winefordner, Anal. Chem., 46 (1974) 736.
6 S. L. Wellons, R. A. Paynther and J. D. Winefordner, Spectrochim. Acta, Part A, 30 (1974) 2133.
7 P. G. Seybold and W. White, Anal. Chem., 47 (1975) 1199.
8 E. M. Schulman, J. Chem. Educ., 53 (1976) 522.
9 T. Vo-Dinh, E. Lue Yen and J. D. Winefordner, Anal. Chem., 48 (1976) 1186.
10 R. M. A. von Wandruszka and R. J. Hurtubise, Anal. Chem., 48 (1976) 1784.
11 E. M. Schulman and R. T. Parker, J. Phys. Chem., 81 (1977) 1932.
12 T. Vo-Dinh, G. L. Walden and J. D. Winefordner, Anal. Chem., 49 (1977) 1126.
13 T. Vo-Dinh, E. Lue Yen and J. D. Winefordner, Talanta, 24 (1977) 146.
14 T. Vo-Dinh and J. D. Winefordner, Appl. Spectrosc. Rev., 13 (1977) 261.
15 W. White and P. G. Seybold, J. Phys. Chem., 81 (1977) 2035.
16 I. M. Jakovljevic, Anal. Chem., 49 (1977) 2048.
17 R. M. A. von Wandruszka and R. J. Hurtubise, Anal. Chim. Acta, 93 (1977) 331.
18 R. M. A. von Wandruszka and R. J. Hurtubise, Anal. Chem., 49 (1977) 2164.
19 G. J. Niday and P. G. Seybold, Anal. Chem., 50 (1978) 1577.
20 J. B. F. Lloyd, Analyst, 103 (1978) 775.
21 C. G. de Lima and E. M. de M. Nicola, Anal. Chem., 50 (1978) 1658.
22 E. L. Y. Bower and J. D. Winefordner, Anal. Chim. Acta, 101 (1978) 319.
23 E. L. Y. Bower and J. D. Winefordner, Anal. Chim. Acta, 102 (1978) 1.
24 T. Vo-Dinh and R. B. Gammage, Anal. Chem., 50 (1978) 2054.
25 C. D. Ford and R. J. Hurtubise, Anal. Chem., 50 (1978) 610.
26 C. D. Ford and R. J. Hurtubise, Anal. Chem., 51 (1979) 659.
27 E. L. Y. Bower and J. D. Winefordner, Appl. Spectrosc., 33 (1979) 9.
28 T. Vo-Dinh and R. B. Gammage, Anal. Chim. Acta, 107 (1979) 261.
29 R. T. Parker, R. S. Freedlander, E. M. Schulman and R. B. Dunlap, in R. L. Kisliuk and G. M. Brown (Eds.), Chemistry and Biology of Pteridines, Elsevier North Holland, New York, 1979, p. 61.
30 R. T. Parker, R. S. Freedlander, E. M. Schulman and R. B. Dunlap, Anal. Chem., 51 (1979) 1921.
31 T. Vo-Dinh, R. B. Gammage, A. R. Hawthorne and J. H. Thorngate, Environ. Sci. Technol., 12 (1978) 1297.
32 G. L. Walden and J. D. Winefordner, Appl. Spectrosc., 33 (1979) 166.
33 M. L. Meyers and P. G. Seybold, Anal. Chem., 51 (1979) 1609.
34 T. Vo-Dinh and J. R. Hooyman, Anal. Chem., 51 (1979) 1915.
35 J. J. Aaron, E. M. Kaleel and J. D. Winefordner, J. Agric. Food Chem., 27 (1979) 1233.
36 J. B. F. Lloyd and J. N. Miller, Talanta, 26 (1979) 180.
37 S. K. Lower and M. A. El-Sayed, Chem. Rev., 66 (1966) 199.
38 C. A. Parker and C. G. Hatchard, Analyst, 87 (1962) 664.
39 J. J. Aaron and J. D. Winefordner, Talanta, 22 (1975) 707.
40 C. M. O'Donnell and J. D. Winefordner, Clin. Chem., (Winston Salem, NC), 21 (1975) 285.
41 R. T. Parker, R. S. Freedlander and R. B. Dunlap, 1978, unpublished results.
42 R. J. Kiers, R. D. Britt, Jr. and W. E. Wentworth, Anal. Chem., 29 (1957) 203.
43 D. G. Peters, J. M. Hayes and G. M. Hieftje, Chemical Separations and Measurements, W. B. Saunders, Philadelphia, 1974.
44 R. A. Zweidinger and J. D. Winefordner, Anal. Chem., 42 (1970) 639.

45 J. J. Aaron and J. D. Winefordner, Talanta, 22 (1975) 707.
46 C. M. O'Donnell and J. D. Winefordner, Clin. Chem., (Winston-Salem, NC), 21 (1975) 285.
47 R. J. Lukasiewiez, P. A. Rozynes, L. B. Sanders and J. D. Winefordner, Anal. Chem., 44 (1972) 237.
48 R. J. Lukasiewiez, J. J. Mousa and J. D. Winefordner, Anal. Chem., 44 (1972) 1339.
49 E. L. Wehry, Fluoresc. News, 8 (1974) 21.
50 J. D. Winefordner and P. A. St. John, Anal. Chem., 35 (1963) 2211.
51 H. C. Hollifield and J. D. Winefordner, Anal. Chem., 40 (1968) 1759.
52 E. Sawicki and P. Johnson, Microchem. J., 8 (1964) 85.
53 E. Sawicki and J. D. Pfuff, Anal. Chim. Acta, 32 (1965) 521.
54 W. E. Kurtin, Photochem. Photobiol., 27 (1978) 503.

Analytica Chimica Acta, 120 (1980) 19—30

DIFFERENTIAL POTENTIOMETRIC STRIPPING ANALYSIS

LARS KRYGER

Department of Chemistry, Aarhus University, Langelandsgade 140, 8000 Aarhus C (Denmark)

(Received 25th March 1980)

SUMMARY

Differential potentiometric stripping analysis, a sensitive instrumental modification of potentiometric stripping analysis, is described. For trace elements like cadmium and lead, which exhibit transport-controlled potentiometric stripping, signal enhancement is possible by employing a scheme involving multiple stripping and re-reduction of the preconcentrated analytes. For such elements the detection limit is below 5×10^{-10} M with 60-s plating. The accuracy of the technique is tested on a biological reference material. Like potentiometric stripping analysis, the technique presented is not sensitive to reversible redox couples in solution.

Although potentiometric stripping analysis (p.s.a.) is a relatively new electrochemical technique for the determination of trace elements [1, 2], it appears to be as widely applicable as stripping voltammetry and differential pulse stripping voltammetry [3—6]. Moreover, the resolution of the technique compares well with that of differential pulse stripping voltammetry [7]. Stripping analysis, potentiometric as well as voltammetric, is particularly well suited for the determination of heavy metals in liquid samples, since often no pretreatment of such samples is necessary. The time-consuming part of the analysis in such cases is often the plating time.

This paper introduces a new instrumental mode of potentiometric stripping analysis: differential potentiometric stripping analysis (d.p.s.a.). D.p.s.a. is characterized by high sensitivity even for short plating times, and it corresponds to p.s.a. in much the same manner as does differential pulse voltammetric stripping to linear sweep stripping voltammetry.

PRINCIPLE

In d.p.s.a., as in p.s.a., redissolution of the preconcentrated analytes is brought about by some oxidizing agent in the sample solution being transported towards the working electrode, and the redissolution process is recorded potentiometrically. If the rate of the redissolution process is high compared with the rate at which the newly stripped material can escape, by diffusion or convection, from the vicinity of the working electrode, then a

high concentration region of analyte is created around the working electrode during the stripping step. D.p.s.a. exploits the formation of this region: after the plating has been accomplished, potentiostatic control is abandoned and the potential versus time behaviour of the working electrode is recorded by using a microcomputer. The electrode potential is, however, allowed to undergo only a small change of the order of 10—50 mV, and as soon as a preselected potential limit has been reached, potentiostatic conditions are resumed for a short period at a plating potential slightly anodic of the previous one. In this manner, a considerable amount of newly oxidized material can be replated and reoxidized in a subsequent stripping step going from the new plating potential across the potential window selected. The procedure is repeated until the entire potential range of interest has been covered. With a suitable choice of potential windows, the stripping signal at any potential interval is recorded several times and the results are accumulated in the computer memory. Hence, for a given plating period, a signal enhancement is likely to result. The process is analogous to the multiple scanning effect which provides the increased sensitivity of differential pulse stripping voltammetry compared to the linear sweep technique.

During any stripping phase in d.p.s.a., the potential distribution is recorded by the computer in the following manner: a word in the computer memory is associated with a particular potential interval; whenever a potential value has been observed, the corresponding word in the computer memory is incremented. The resulting function will then exhibit maxima at the stripping potentials, and the area of these maxima will be a measure of concentration.

This mode of data acquisition, which has previously been denoted as "multichannel potentiometry" [7, 8], produces an analytical signal which bears the same relationship to the conventional stripping potentiogram as does the differential pulse stripping voltammogram to a linear sweep stripping voltammogram. In differential pulse stripping voltammetry, the analytical signal is taken as the difference of the average currents over a short period towards the end of the pulse and immediately before the application of the pulse. This essentially means that the differential potentiogram exhibits a peak when the applied pulse passes through a stripping potential of a component. In voltammetry and polarography, the analytical signal is the faradaic current, whereas in p.s.a. the signal of interest is the total time elapsed since potentiostatic control was abandoned. Hence, to obtain a "differential" potentiogram, the entire potential region covered could first be divided into small intervals and the primary analytical signal assigned to any such interval would be the total time elapsed at that potential. The differential potentiogram could then be obtained by assigning to the nth potential interval the difference between the primary signals in the nth and $(n-1)$th intervals. The proposed scheme of monitoring the potential distribution is, however, better suited to rapid real-time data acquisition since it involves less arithmetic and the potentiograms obtained by the two techniques are identical.

The principle of d.p.s.a. is illustrated in Fig. 1. Curve (a) shows a normal

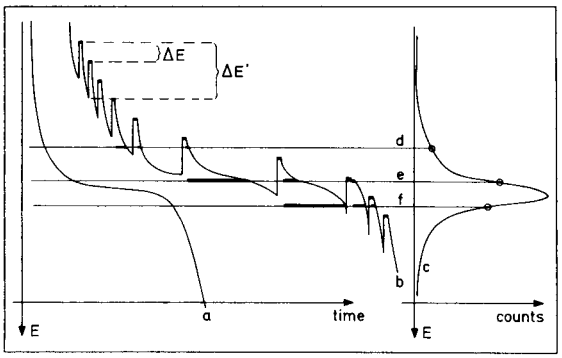

Fig. 1. Principle of differential potentiometric stripping analysis. Curve a, normal potential vs. time behaviour during stripping of a plated component; curve b, potential vs. time behaviour during differential potentiometric stripping; curve c, differential stripping potentiogram.

stripping potentiogram, i.e. the potential vs. time behaviour of the working electrode during redissolution of a preconcentrated analyte; the length of the plateau is a measure of the analyte bulk concentration. Curve b shows the potential vs. time behaviour of the working electrode during stripping in the d.p.s.a. mode. The fat horizontal parts of the curve indicate the short periods of potentiostatic control between the scans. After each short plating period (of the order of 1 ms) the electrode potential is allowed to change by the amount $\Delta E'$ mV. After the stripping across this interval is accomplished, the short-term plating at a new potential, ΔE mV more anodic than the previous one, is started, and so on. By using this scheme and values of $\Delta E'$ and ΔE such that $\Delta E'/\Delta E = n$ (where n is an integer larger than 1), each potential interval is scanned n times. The total times spent at three selected potentials are indicated as the fat parts of the lines, d, e and f. When, for each potential, these times are added, the differential stripping potentiogram (curve c) is formed. The differential potentiogram is essentially the derivative of time with respect to potential, and where the stripping potentiogram exhibits a plateau signalling the stripping of a component, the differential potentiogram shows a maximum.

The technique is related to the multiple-scanning potentiometric stripping technique previously reported [8]. The multiple scanning technique, however, employs one plating potential only, and the potential interval studied in each scan is of the order of several hundred mV, so that cadmium and lead, for example, may be stripped in the same scan. This leads to an unwanted correlation of the cadmium recovery with the lead concentration: a large concentration of lead forces the working electrode to stay at the stripping potential of lead for a long time. At this potential the newly stripped cadmium can escape from the working electrode by diffusion/convection and so there is a poor recovery of cadmium between scans. In d.p.s.a., if the magnitude of

$\Delta E'$ is kept sufficiently small, cadmium and lead are not stripped in the same scan, and the correlation vanishes. The correlation problem in multiple-scanning potentiometric stripping has been overcome by allowing the magnitude of the stripping interval to increase gradually. Thus, first the component with the most cathodic stripping potential is determined by multiple scanning, then another component is included in the scan and so on. This "interrupted stripping" can be considered a crude type of d.p.s.a., but requires prior knowledge of stripping potentials. Moreover, to achieve any significant recovery of analytes with multiple-scanning potentiometric stripping analysis, the stripping must be carried out in a quiet solution. This is not necessary with d.p.s.a.

EXPERIMENTAL

Electrochemical cell and electrode preparation

The electrochemical cell comprised a Radiometer M22 rotating electrode assembly with a 50-ml polyethylene beaker. The rotating electrode was made from a 2-mm thick glassy carbon rod fitted in glass tubing. The reference electrode was a Radiometer K401 saturated calomel electrode. The counter electrode was a platinum wire (0.5 mm thick and 1 cm long). Prior to analysis, the cell was cleaned with (1 + 1) hydrochloric acid. The working electrode was preplated by rotating it in a solution of 1.25×10^{-4} M mercury(II) acetate in 0.1 M acetate buffer (pH 4.8) for 2 min at a potential of −400 mV vs. SCE followed by 30 s at 0 mV vs. SCE. During all preliminary studies, the solutions were not deaerated and dissolved oxygen was used as the oxidizing agent. However, for the determinations of trace metals in biological material, sample solutions were deaerated with argon for 10 min prior to analysis.

Chemicals

Triply distilled water and analytical-grade chemicals were mostly used. The mineral acids and the sodium acetate were of Suprapur (Merck) grade. Stock solutions were prepared from cadmium sulphate (3.40×10^{-4} M with respect to Cd(II)), lead acetate (2.64×10^{-4} M) and mercury(II) acetate (1.25×10^{-2} M). The certified reference material, Bowen's Kale [9], was obtained from Dr. H. J. M. Bowen, Reading University, U.K.

Computer and interface

The computer employed was an Alpha LSI-3/05 (Computer Automation) microcomputer (4K 16-bit words of memory). The computer was interfaced to a general I/O module for electroanalytical work. The hardware and software have previously been described [7]. To obtain maximum sensitivity with the data acquisition scheme described, the data acquisition rate and real-time data processing rate should be maximized [7]. The maximum rate possible with the system is 6 kHz, because of the software overhead for the d.p.s.a. mode.

RESULTS AND DISCUSSION

Signal dependence on ΔE and $\Delta E'$

To evaluate the dependence of the stripping potentiogram on the potential intervals, ΔE and $\Delta E'$, a sample which was 3.90×10^{-8} M in cadmium(II) and 2.64×10^{-8} M in lead(II) in 0.1 M acetate buffer pH 4.80 was electrolysed at −1300 mV vs. SCE for 60 s using the rotating mercury film electrode (at about 600 rpm). After the electrolysis, the differential stripping potentiograms were recorded without interrupting the electrode rotation. The experiment was run a total of eight times with different values of ΔE and $\Delta E'$. The results are shown in Fig. 2. The potentiograms in column A were obtained with a constant $\Delta E' = 80$ mV. As the value of ΔE is decreased from 40 mV to 2 mV, the signal amplitudes increase. This effect can be attributed to the simultaneous increment of the number of times (n) each potential interval is scanned. As ΔE is decreased, the time used to obtain the differential potentiogram increases. The total number of seconds (including the 60 s of electrolysis) is indicated below each of the potentiograms in Fig. 2. The ratio between the signal amplitudes and the total time spent increases when ΔE is decreased from 40 mV to 20 mV and further to 10 mV. For $\Delta E = 2$ mV, this ratio is lower than for $\Delta E = 10$ mV. Hence, with the d.p.s.a. technique, for a

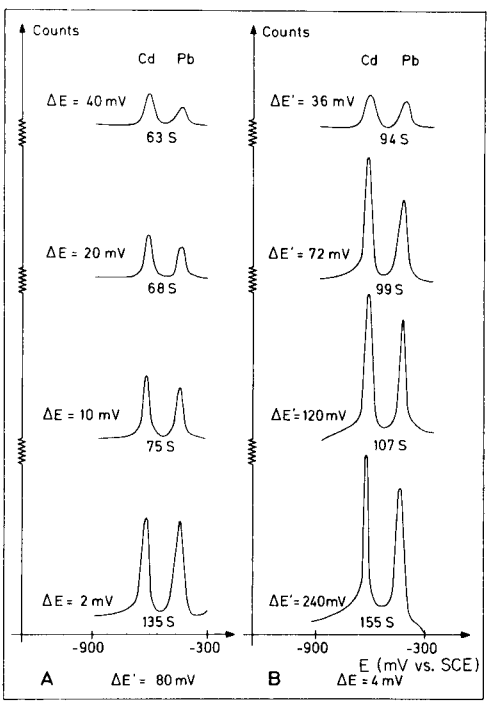

Fig. 2. Dependence of the magnitudes and interference of stripping signals on the magnitudes of the potential windows ΔE and $\Delta E'$.

given electrolysis time, the analytical signal can be enhanced by employing smaller potential steps. That the signal amplitude per time unit cannot be infinitely high is due to the fact that even for small values of $\Delta E'$, some of the oxidized material escapes from the working electrode and is not replated.

Going from top to bottom in column A of Fig. 2, the ratio of peak heights for cadmium and lead is seen to decrease gradually. This can be attributed to the fact that with $\Delta E' = 80$ mV the stripping of cadmium and lead takes place partly within the same scan interval; hence, as in multiple-scanning potentiometric stripping, the time spent during the stripping of lead is available for oxidized cadmium to escape the working electrode.

The effect of varying the window width $\Delta E'$ is shown in Fig. 2, column B: clearly, increasing the magnitude of $\Delta E'$ results in increased amplitudes of the analytical signals, but also in increasing overlap of peaks. The overlap vanishes only if $\Delta E'$ is kept sufficiently small to avoid stripping of both cadmium and lead, i.e. less than, say, 30% of the peak separation. In this manner, the peak correlation previously mentioned disappears, and experience has shown that although the peak area is proportional to the sought concentrations, the peak heights are then just as good a measure. During the remaining investigations, the values $\Delta E = 10$ mV and $\Delta E' = 50$ mV were employed. With these values cadmium and lead are stripped independently.

The potentiograms of Fig. 2 (and Fig. 4) are smoothed. However, the signal/noise ratio at the 3×10^{-8} M concentration level with 60 s plating can be estimated from the lower potentiogram of Fig. 3 which is unsmoothed.

Signal enhancement by d.p.s.a.

In order to evaluate further the performance of d.p.s.a., the solution previously used was electrolysed for 60 s at the rotating electrode and the differential stripping potentiogram was recorded without interrupting the electrode rotation. The total time used to obtain the potentiogram (shown in Fig. 3 — lower trace) was (60 + 29) s. The upper trace is the single-scan potentiogram obtained by electrolysing the same solution for a total of 89 s. Obviously, the procedure results in an appreciable signal improvement. It has previously been pointed out that the "counting statistics" obtained in computerized stripping potentiometry can be improved by increasing the data-acquisition rate [7]. Thus the sensitivity of d.p.s.a. can be improved either by going to a faster computer and an A/D converter, or, probably better, by replacing as much as possible of the software overhead by analog circuits. The limiting factor is then likely to be the rate at which the potentiostat is able to re-establish plating conditions at the electrode/solution interface at the end of any stripping step.

Effect of electrode rotation rate

The results previously reported were all obtained with an electrode rotation rate of about 600 rpm. This rate provides the best reproducibility. At high rates, mercury droplets are likely to be shaken off the glassy carbon surface

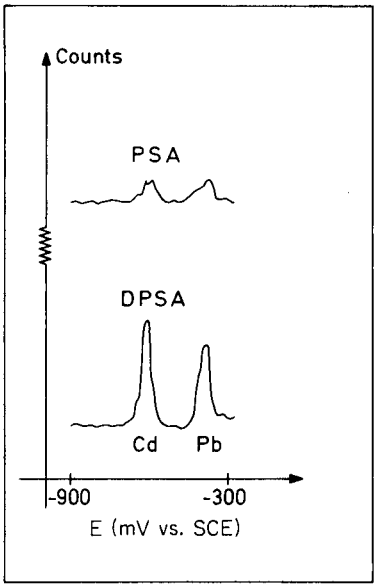

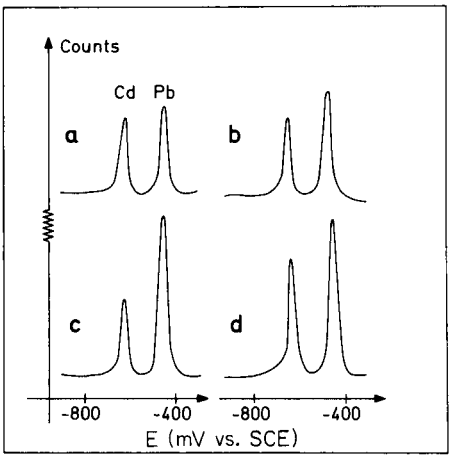

Fig. 3. Signal enhancement by the differential potentiometric stripping technique. Upper trace: normal potentiogram. Lower trace: differential stripping potentiogram.

Fig. 4. Standard additions to a 0.1 M acetate buffer (pH 4.80) solution containing cadmium(II) and lead(II): (a) spiked with 3.9×10^{-8} M cadmium(II) and 2.6×10^{-8} M, lead(II); (b) spiked with 3.9×10^{-8} M cadmium(II) and 5.2×10^{-8} M lead(II); (c) spiked with 3.9×10^{-8} M cadmium(II) and 10.4×10^{-8} M lead(II); (d) spiked with 7.8×10^{-8} M cadmium(II) and 10.4×10^{-8} M lead(II).

in an unpredictable manner and convection may fluctuate. The signal amplitude decreases slightly when the rotation rate is doubled. This can be attributed to a decreased recovery of newly oxidized material between the scans.

A more accurate investigation of the influence of the rotation rate requires a rotating electrode assembly with better mechanical properties than the one available for this study.

Effect of time delay between individual scans

The effect of varying the time delay between the individual scans was investigated. If delays, as short as the time resolution of the computerized system permits, are used, i.e. about 100 μs, a significant recovery of heavy metals is observed between the individual scans. However, the recovery and thus the signal amplitudes increase when the delays are prolonged to 1—2 ms (depending on the electrode rotation rate). Any further delay has no effect or even a negative effect on the ratio of signal to the total time of analysis. With ΔE = 10 mV and a total potential range of 1000 mV, these short plating periods, therefore, contribute less than one second to the total time.

Quantitative analysis by d.p.s.a.

When $\Delta E' \leqslant 50$ mV is employed, the cadmium and lead signals are independent. This is illustrated in Fig. 4, which shows the differential stripping potentiograms of a solution containing cadmium(II) and lead(II) when the lead(II) content is gradually increased (curves a, b and c). Clearly, the cadmium signal remains constant. When the cadmium(II) concentration is increased (curves c and d), the lead signal is unaffected.

Standard addition procedures were carried out for both cadmium and lead over the range 10^{-8}—5×10^{-7} M and resulted in linear plots. The detection limit of the technique depends on the plating time used. With 60-s plating times, 5×10^{-10} M cadmium(II) produces a clearly significant signal. Figure 5(A) shows the result of d.p.s.a. of an acetate buffer solution (pH 4.8) containing impurities of zinc(II) and lead(II), for a plating time of 60 s. Figure 5(B) shows the effect of repeating the experiment after the addition of 5×10^{-10} M cadmium(II). The detection limit can probably be improved by going to higher data handling rates.

The precision was estimated by obtaining ten consecutive differential stripping potentiograms on a solution containing 5×10^{-10} M cadmium(II); the relative standard deviation was 0.10. Since the blank concentration for lead(II) is somewhat above 5×10^{-10} M even when Suprapur (Merck) chemicals are employed, the standard deviation for lead cannot be stated at this concentration level. At 5×10^{-9} M, however, the standard deviations for cadmium and lead are similar and are about 0.05 with 1-min plating times.

To estimate the accuracy for routine work, two determinations of cadmium

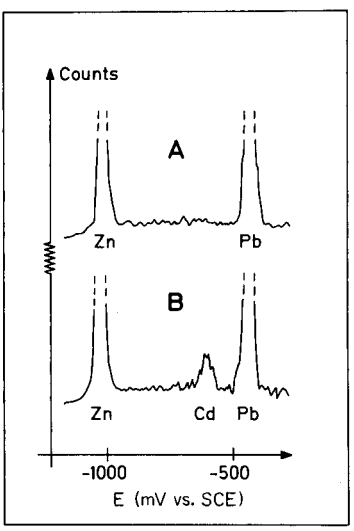

Fig. 5. Differential stripping potentiograms of acetate buffer solution containing impurities of zinc(II) and lead(II): (A) after 60-s plating, and (B) after the addition of 5×10^{-10} M cadmium(II) with 60-s plating.

and lead in a standard reference material (Bowen's Kale [9]) were carried out. For decomposition, 0.2-g samples of the kale were digested with 3 ml of concentrated nitric acid at 100°C in a PTFE-lined pressure bomb overnight. Next a blank solution containing 35 ml of acetate buffer and 2 ml of mercury(II) acetate stock solution was prepared, and the total concentrations of cadmium(II) and lead(II) in this solution were determined by standard addition. Then the kale digest (3 ml) was added to this spiked blank solution and the total concentrations of cadmium(II) and lead(II) were determined by further standard additions to this solution (containing the blank concentrations, the concentrations arising from the previous standard addition and the sought concentrations). The sought concentrations were then found by subtraction and appropriate corrections for dilution effects. This two-step procedure is necessary since the amount of oxidizing agent changes drastically when the digest is added to the spiked blank; digests of biological materials often contain large amounts of oxidizing agents, e.g. iron(III). In potentiometric stripping analysis, the sensitivity, defined as the analytical signal per unit of analyte, decreases with increasing concentration of the oxidizing agent, thus the stripping signals for given amounts of analytes diminish when the oxidizing digest is added to the spiked blank. Despite the acetate content, the diluted digest was acidic and the plating potential was therefore kept at a value of −900 mV vs. SCE. The results of the procedure are given in Table 1.

Possible applications of d.p.s.a.

Since d.p.s.a. is characterized by high sensitivity, even for short plating times, and since the stripping signals are obtained in a non-quiet solution, the technique is well suited for determination of trace elements in a continuously flowing stream. An important condition to be fulfilled is, however, that the redissolution process be sufficiently rapid to ensure the formation of a high concentration region of redissolved analytes in the vicinity of the working electrode. This means that activation-controlled redissolution of the analyte, such as is observed, for example, for the stripping of anodically preconcentrated manganese (as manganese dioxide), prohibits signal enhancement by d.p.s.a. and the multiple-scanning procedure [4]. In favourable cases, however, increased temperature may raise the redissolution rate sufficiently to compete with the processes which counteract the formation of a high concentration region, i.e. diffusion and convection in the sample.

TABLE 1

Cadmium and lead in Bowen's Kale determined by d.p.s.a.

	Sample 1	Sample 2	Certified best mean value (and range) [9]
Cd ($\mu g\ g^{-1}$)	0.73	0.87	0.80 (0.38—1.06)
Pb ($\mu g\ g^{-1}$)	2.87	2.44	2.645 (1.6—3.8)

COMPARISON OF DIFFERENTIAL POTENTIOMETRIC STRIPPING ANALYSIS AND DIFFERENTIAL PULSE ANODIC STRIPPING VOLTAMMETRY

The advantage of d.p.s.a. over conventional potentiometric stripping analysis is essentially the increased sensitivity, i.e. the possibility of lowering the total time per determination. This situation is also encountered when going from linear-sweep stripping voltammetry to differential pulse stripping voltammetry. It could be argued that the price paid for the increased sensitivity with d.p.s.a. is high, since the simplicity of the instrumental design is abandoned and that differential pulse stripping voltammetry might just as well be used. There is, however, an important difference between the voltammetric and potentiometric techniques [6]: while the pulsed voltammetric technique is sensitive to dissolved reversible redox couples, this is not true for potentiometric stripping analysis.

With voltammetric techniques, soluble reversible redox couples may cause interference problems. The equilibrium concentrations at the working electrode of such couples are determined by the controlled electrode potential according to the Nernst equation. When the electrode potential passes the characteristic potential of the couple, a rapid, transport-controlled redox conversion takes place and a faradaic signal results. Reversible couples may often exist as intermediate products when natural samples containing organic traces are subjected to voltammetric analysis. With pulsed voltammetric techniques where rapid potential steps are employed, the effect is more pronounced than with slow potential sweeps.

In potentiometric stripping analysis, where the sample contains excess of oxidizing agent, dissolved reversible couples exist only while potentiostatic control is maintained, i.e. during the plating period. During the stripping, when potentiostatic control is abandoned, only the oxidized species can exist, the reduced species being converted so quickly that no characteristic plateau/peak is observable. The transport rate of oxidizing agent towards the working electrode is of little importance here, since the reduced species is not preplated on the electrode and is therefore of low concentration compared with the concentration of oxidizing agent immediately available at the electrode.

To illustrate this difference between the voltammetric and potentiometric techniques, the two types of stripping experiments were carried out with an unstirred solution of (2:1) 0.1 M hydrochloric acid/methanol spiked with 3.9×10^{-7} M cadmium(II) and 2.6×10^{-7} M lead(II), and the effect of adding nitrobenzene to this solution was studied. Although the overall reduction of nitrobenzene is irreversible and consists of several electron-transfer and chemical steps, the intermediate existence of reversible couples in acidified aqueous methanol medium has previously been observed [10].

Figure 6 (curve A) shows the cyclic differential pulse voltammogram of the heavy metal solution. The cyclic potential scan was interrupted at the switching potential (−1200 mV) for 30 s to allow for plating of heavy metals.

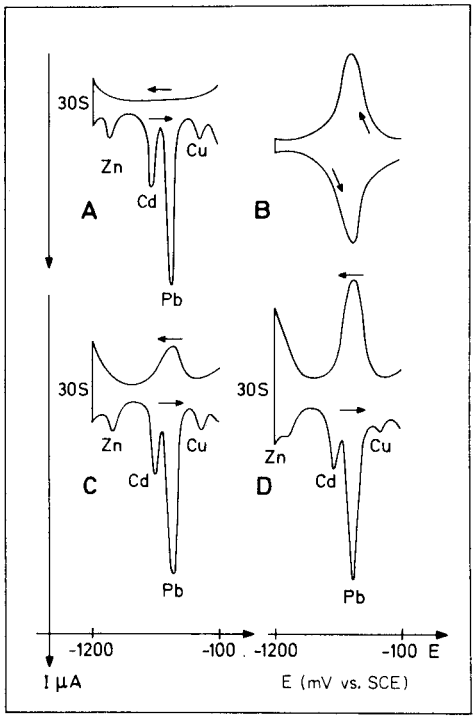

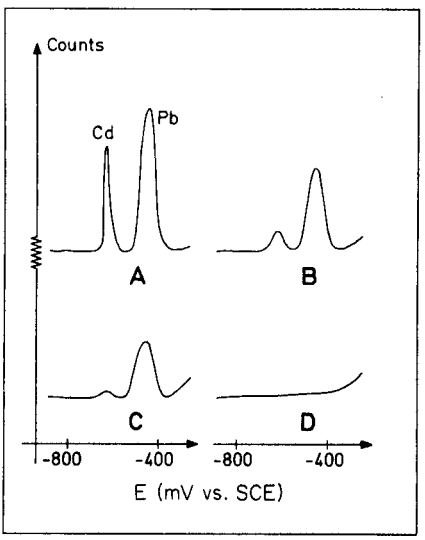

Fig. 6. Effect on cyclic differential pulse voltammograms of the addition of nitrobenzene to a solution of trace metals. (A) Voltammogram of metal solution; (B) voltammogram of nitrobenzene; (C and D) voltammograms of trace metal solution after the addition of nitrobenzene (10^{-4} M and 2×10^{-4} M, respectively). Pulse amplitude 30 mV; pulse width 30 ms; pulse spacing 100 ms; integrations over 20 ms; scan rate 50 mV s^{-1}.

Fig. 7. Effect on differential stripping potentiogram of the addition of nitrobenzene to a solution of trace metals. (A) Differential stripping potentiogram of metal solution; (B and C) differential stripping potentiograms of metal solution spiked with nitrobenzene (10^{-4} M and 2×10^{-4} M, respectively); (D) as for (C) but with zero plating time.

The cadmium and lead signals are almost resolved; traces of zinc and copper are also visible. Figure 6 (curve B) shows the cyclic differential pulse voltammogram of 2×10^{-4} M nitrobenzene. The effects of adding nitrobenzene (10^{-4} M and 2×10^{-4} M) to the heavy metal solution are shown by curves C and D: the anodic branch of the nitrobenzene voltammogram seriously overlaps the cadmium and lead peaks. The interference is worse in a stirred solution.

The experiment was then repeated with the d.p.s. technique. Figure 7 (curve A) shows the d.p.s. curve of the metal solution. Curves B and C show the effects of adding nitrobenzene (10^{-4} M and 2×10^{-4} M). Curve D was obtained in the same solution as curve C, but with zero plating time. Obviously, the nitrobenzene produces no visible signal. The addition of

nitrobenzene is here equivalent to the addition of a mild oxidizing agent with a reduction potential close to the oxidation potential of lead, hence the magnitudes of the cadmium and lead signals decrease. These decreases are of no importance if standard addition is used for quantitative work.

The support of the Danish Natural Science Research Council, grant no. 511-8032, for the computerized instrument is gratefully acknowledged.

REFERENCES

1 D. Jagner and A. Graneli, Anal. Chim. Acta, 83 (1976) 19.
2 D. Jagner, Anal. Chem., 50 (1978) 1924.
3 D. Jagner, Anal. Chim. Acta, 105 (1979) 33.
4 J. K. Christensen and L. Kryger, Anal. Chim. Acta, 118 (1980) 53.
5 D. Jagner, L. G. Danielsson and K. Årén, Anal. Chim. Acta, 106 (1979) 15.
6 D. Jagner and S. Westerlund, Anal. Chim. Acta, 117 (1980) 159.
7 H. J. Skov and L. Kryger, Anal. Chim. Acta, 122 (1980) 179.
8 J. Mortensen, E. Ouziel, H. J. Skov and L. Kryger, Anal. Chim. Acta, 112 (1979) 297.
9 H. J. M. Bowen, J. Radioanal. Chem., 19 (1974) 215.
10 L. Meites and P. Zuman, Electrochemical Data, Part 1, Vol. A, J. Wiley, New York, 1974.

Analytica Chimica Acta, 120 (1980) 31—39

POLAROGRAPHIC ANALYSIS FOR CORTICOSTEROIDS
Part 5. Reduction Mechanism of Halogen-containing Corticosteroids and Analysis of some Preparations

H. S. DE BOER and W. J. VAN OORT*

Department of Analytical Pharmacy, Faculty of Pharmacy, State University of Utrecht, Catharijnesingel 60, 3511 GH Utrecht (The Netherlands)

P. ZUMAN

Clarkson College of Technology, Department of Chemistry, Potsdam, NY 13676 (U.S.A.)

(Received 9th June 1980)

SUMMARY

In fluprednisolone and chloroprednisone acetate, the polarographic reduction of the carbon—halogen bond in position 6 occurs first. The carbanion—enolate formed is reduced at the dropping mercury electrode at more negative potentials than the conjugate acid. Controlled potential electrolysis at a mercury pool electrode where the carbanion—enolate can be protonated, yields the unsaturated ketone. Polarographic reduction of clobetasol-17-propionate and of clobetasone-17-butyrate results in cleavage of the C—Cl bond in the side-chain. This process is followed by reduction of the α,β-unsaturated ketone in the A-ring. Analytical methods for the determination of these compounds in ointments, creams and eye/ear drops gave results with standard deviations of 1—2%.

Investigations [1] of polarographic reduction of corticosteroids bearing a fluorine atom in position 9 of the steroid ring indicated that the carbon—fluorine bond in such molecules does not undergo protolytic cleavage. Consequently, current—voltage curves of dexamethasone, betamethasone and triamcinolone resemble closely those of prednisolone in all media studied. In contrast, corticosteroids bearing a halogen atom in position 6 or 21 show waves corresponding to reductive hydrolysis of the carbon—halogen bond.

Polarographic reduction of the C—F bond in fluprednisolone (I) and of the C—Cl bond in chlorprednisone acetate (II) in position 6 as well as the cleavage of the C—Cl bond in clobetasol propionate (III) and clobetasone butyrate (IV) is discussed in this paper. In position 6, the halogen atom is in a position adjacent to a —CH=CH—CO—CH=CH— conjugated system; in position 21, it is in the α-position to a carbonyl group.

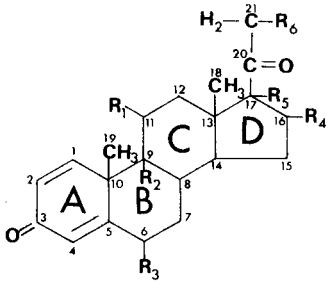

	R_1	R_2	R_3	R_4	R_5	R_6
I Fluprednisolone	HOH	H	F	H	OH	OH
II Chlorprednisone acetate	O	H	Cl	H	OH	OCOCH$_3$
III Clobetasol propionate	HOH	F	H	CH_3	$OCOC_3H_7$	Cl
IV Clobetasone butyrate	O	F	H	CH_3	$OCOC_4H_9$	Cl
V Prednisolone	HOH	H	H	H	OH	OH
VI Prednisone	O	H	H	H	OH	OH

In organic compounds bearing a halogen atom on an sp^3 carbon, aliphatic or alicyclic, in the majority of cases a 2-e process takes place; this has been likened to an S_{N^2} displacement reaction from the rear of the carbon—halogen bond by the electron-rich mercury surface [2—6]. In α-haloketones the reduction of the C—X bond is facilitated when compared with that of the corresponding α-halohydrocarbons and occurs at potentials more positive than that of the carbonyl group [7—14]. It had been realized rather early [15, 16] that whereas a vinylic C—X bond is more difficult to reduce than an aliphatic bond, the reduction of an allylic C—X bond is facilitated. In compounds bearing both vinylic (Br^1) and allylic (Br^2) halogen atoms, such as $Br^1CH{=}CH{-}CH_2Br^2$, the allylic is reduced first, at more positive potentials [17]. No systematic study on the role of the extension of the conjugated allylic system on the reducibility of the C—X bond in straight-chain compounds has been reported.

In the steroid series, most of the reductions of α-haloketones studied were those of α-bromoketones [18—21]. Whereas several compounds bearing chlorine or fluorine and the carbonyl group in the steroid skeleton have been studied [19, 22], only a single reduction of a 21-chloro-20-ketosteroid [19] has been reported.

The reduction of a carbon—halogen bond of the allylic type has been reported for some 6-fluoro-, 6-chloro- and 6-bromo-Δ^4-3-ketosteroids [19—24]. In some instances [22, 24], the possibility of the reduction of the carbon—halogen bonds (including those involving fluorine) occurring prior to the reduction of the —CO—CH=CH— group has been proposed.

In none of these cases has the proposed mechanism actually been proved experimentally. It is the aim of this paper to offer such an approach. Moreover, none of the individual compounds I—IV has been investigated before by means of polarography.

EXPERIMENTAL

Apparatus

The polarographic curves were recorded on a Bruker E 310 modular electrochemical system and a PAR 174 polarograph, both of which were equipped with a drop timer and a Houston Model 2000 X—Y recorder.

For voltammetric curves at the HMDE, the PAR polarograph was equipped with a model 303 SMDE (static mercury drop electrode). A water-jacketed 10-ml polarographic cell (Metrohm EA 880-T-5) was employed with a dropping mercury electrode (t = 6.7 s, m = 0.92 mg s^{-1}), a Metrohm EA 436 Ag/AgCl/saturated KCl reference electrode and a platinum wire auxiliary electrode. The potential of the reference electrode was −52 mV vs. SCE when the bridge was filled with 0.03 M $(CH_3)_4$ NOH in methanol. The cell was kept at a temperature of 20 ± 0.2°C. Controlled potential electrolysis was carried out with a Metrohm E524 coulostat and a Metrohm E525 integrator. Oxford P7000 micropipets (50 and 100 μl) were used for additions of small volumes of sample or standard to the supporting electrolyte. An Orion fluoride-selective electrode (model 94-09A) and an Orion chloride-selective electrode (model 94−17A) were used for fluoride and chloride determinations. An $Hg/HgSO_4$/saturated K_2SO_4 reference electrode (Metrohm EA 441/2) was used for chloride measurements to prevent diffusion of chloride from the reference electrode compartment. The potential of this reference electrode was −470 mV vs. SCE when the bridge was filled with 0.03 M $(CH_3)_4$NOH in methanol. The mercury pool electrode used had an area of 7.1 cm^2.

Chemicals

The steroids were used as supplied by the manufacturers: prednisolone and prednisone (Nogepha); fluprednisolone (Upjohn); chloroprednisone acetate (Organon); clobetasol-17-propionate and clobetasone-17-butyrate (Glaxo). The solvents and materials for the supporting electrolytes were: methanol (Nanograde, Mallinckrodt); dimethylformamide (DMF-Uvasol); tetramethylammonium hydroxide ($(CH_3)_4$NOH; 10% zur Polarographie; Merck); toluene (Baker analyzed reagent). The toluene was distilled twice before use; all other reagents were used without further purification.

Procedures

Polarographic curves. The methanolic solution of 0.03 M $(CH_3)_4$NOH (10 ml) was deaerated by a stream of nitrogen for about 10 min and the curve of the supporting electrode was recorded in the differential pulse polarographic mode with a scan rate of 2 mV s^{-1}, pulse amplitude of 100 mV and a controlled drop-time of 2 s. Then 100 μl of the freshly-prepared 0.02 M solution of the corticosteroid in methanol was added, resulting in a 2×10^{-4} M solution. After an additional deaeration for 1 min, the differential pulse polarographic curve was recorded.

Controlled potential electrolysis. A portion (20 ml) of a 10^{-3} M solution of corticosteroid in a methanolic solution of 0.1 M $(CH_3)_4$NOH was deaerated for 15 min. Then a potential was applied which was about 50 mV more negative than the peak potential of the first peak in the differential pulse polarogram until complete electrolysis was achieved; this took about 6 h. Deaeration by a stream of nitrogen was continued during the electrolysis for stirring and to prevent invasion of oxygen.

After complete electrolysis the fluoride or chloride concentration was measured with the appropriate selective electrode and the content was computed with the aid of a calibration curve, which was obtained under similar conditions. Then the solution was diluted 5 times and the differential pulse polarographic curve was recorded. These curves were compared with the curves of 2×10^{-4} M solutions of the original steroids and with those of 2×10^{-4} M prednisolone (V) and prednisone (VI).

Analysis of ointments. A sample (1 g) of the ointment was dissolved in 5.0 ml of toluene. Then 10 ml of 0.02 M $(CH_3)_4NOH$ in a mixture of DMF and water (8:1, v/v) was deaerated by purging by nitrogen for 10 min, and a differential pulse polarographic curve of the supporting electrolyte was recorded. An aliquot (1 ml) of the toluene solution of the ointment was then added, so that the final concentration of the steroid was between 1×10^{-5} and 1×10^{-3} M, the solution was deaerated for 1 min, and the differential pulse polarogram was recorded. A small volume of a 0.02 M solution of the corticosteroid in DMF was added, the solution was deaerated again for 1 min and the polarographic curve was again recorded. The volume was chosen so that the concentration of the steroid after the standard addition would approximately double. If this resulted in a change in the total volume of more than 1%, a correction for the volume change was introduced into the calculation of the sample concentration using the standard addition method. The height of the most positive peak was measured.

Analysis of creams. Treatment of 1 g of the creams with 5.0 ml of methanol resulted in disintegration of the creams and complete dissolution of the active constituents. The supporting electrolyte consisted of 0.03 M $(CH_3)_4NOH$ in methanol. The curve of 10 ml of the supporting electrolyte was recorded as above and 1 ml of the methanolic solution of the cream was added. The differential pulse polarogram was recorded and evaluated by standard addition as above.

RESULTS AND DISCUSSION

Fluprednisolone (I)

The differential pulse polarographic curve of a methanolic 2×10^{-4} M solution of fluprednisolone containing 0.03 M tetramethylammonium hydroxide, shows a reduction peak at $E_p = -1.34$ V, a second reduction peak at $E_p = -1.67$ V and a third peak at -2.00 V (Fig. 1a). Of these three peaks, only the third peak corresponding to the reduction of the side-chain in position 17 [1] was identical to the one observed for prednisolone. Peaks at -1.55 and -1.75 V corresponding to two 1-e reduction waves of prednisolone (V) were absent from the curves obtained for fluprednisolone.

Under the assumption that the carbon—halogen bond is reduced first [22, 24], waves of prednisolone would be expected to follow the first reduction step. To interpret the absence of such waves, it was first necessary

to determine if the C—F bond in 6-position is actually cleaved in the first reduction step and then to find an explanation for the absence of peaks at −1.55 and −1.75 V.

Controlled-potential electrolysis was used to prove the nature of the process occurring in the first wave. Because the first reduction peak on the voltammogram of fluprednisolone recorded for a hanging mercury drop electrode occurred in the same potential range as the first peak on the differential pulse polarographic curves, it was assumed that the product formed in controlled-potential electrolysis at a mercury pool electrode will be identical [25] to that formed at the dropping mercury electrode.

Electrolysis performed at the potential corresponding to the limiting current of the first reduction step at a mercury pool electrode gave a linear plot of log i vs. time. From the slope of this dependence, a value n = 1.96 was found. In the solution after completed electrolysis, fluoride ion concentration was determined by a fluoride-selective electrode. The concentration of fluoride produced was equal to the initial molar concentration of fluprednisolone. Furthermore, comparison of wave-heights of fluprednisolone with benzophenone and naphthoquinone obtained by d.c. polarography indicated a 2-e process. Thus the reduction peak of fluprednisolone (I) at −1.34 V corresponds to a carbon-fluorine bond fission involving the transfer of two electrons.

When the differential pulse polarographic curve of the solution was recorded after complete electrolysis of the fluprednisolone (I) at the pool electrode (Fig. 1a, broken line), the resulting curve showed peaks at −1.55, −1.75 and −2.00 V. These peak potentials and the relative heights of these three peaks were identical to those obtained in the same supporting electrolyte for prednisolone (V). Thus, prednisolone is the final electrolysis product of fluprednisolone, but is not formed as the primary product, and so is not shown on the polarographic curve of fluprednisolone, but in a relatively slow reaction which can take place during the hours needed for exhaustive electrolysis.

Study of the simple α-substituted ketones and related compounds by Lund [26] has indicated that reductive cleavage of the carbon—halogen bond results in the formation of a carbanion—enolate. Such a process can be assumed to occur in the reduction of fluprednisolone (I) (X = F):

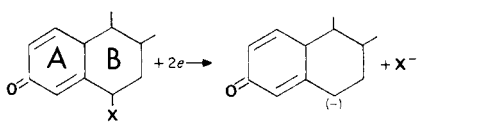

(1)

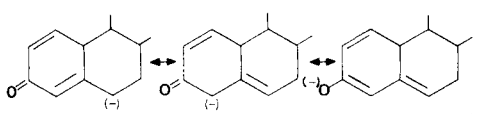

(2)

The rate of protonation of the carbanion—enolate, stabilized by conjugation (2), as indicated, is slow when compared with the "time window" of

about 60 ms in differential pulse polarography. Hence, the carbanion—enolate remains unprotonated in the course of polarographic measurement and is reduced at −1.67 V. The more negative potential of this reduction when compared with the first reduction step of prednisolone (at −1.55 V) is in agreement with the generally observed more negative reduction of the conjugate base than that of the corresponding acid.

A possibility of the formation of a carbanion—enolate has been mentioned in the case of reduction of α-haloketones [14, 18, 20, 23], but here (e.g. for Δ^4-2-bromo-3-ketosteroids [13]) no reduction wave was observed for the carbanion formed in the available potential range.

At the mercury pool electrode the carbanion—enolate formed has sufficient time to be protonated to form prednisolone (V), the presence of which was confirmed. The system represents another interesting example of differences between reduction processes at electrodes with renewable surface and at a pool electrode [25].

Reduction of the side-chain in position 17 is practically unaffected by changes occurring in rings A and B. Thus, the third reduction peak of fluprednisolone at −2.0 V (Fig. 1a, full line) occurs at the same potential and has the same shape as the corresponding peak of prednisolone, either added to the same supporting electrolyte or formed by exhaustive electrolysis (Fig. 1a, broken line).

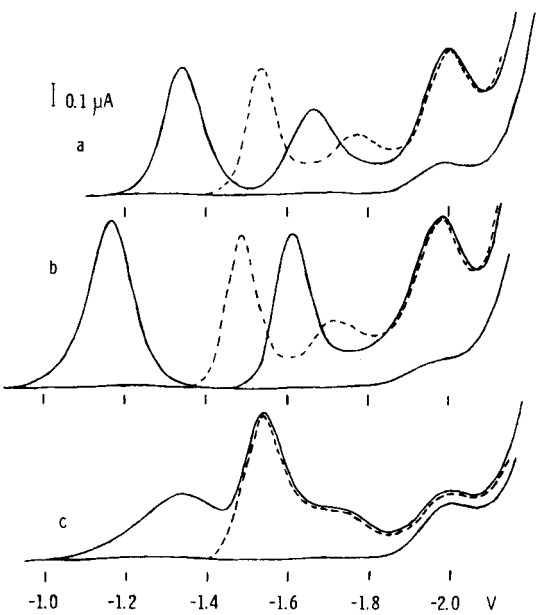

Fig. 1. Differential pulse polarographic curves of 2×10^{-4} M fluprednisolone (a), chlorprednisone acetate (b) and clobetasol propionate (c) in 0.03 M tetramethylammonium hydroxide in methanol before and after (broken line) complete electrolysis performed at 50 mV more negative than the peak potential of the most positive peak.

Chlorprednisone acetate (II)

Differential pulse polarographic curves, and the behaviour of the product of an exhaustive electrolysis at the mercury pool at the potential corresponding to the limiting current of the first reduction peak of solutions of clorprednisone acetate (II), resembled closely the patterns observed for fluprednisolone (I).

The reduction with $E_p = -1.17$ V (Fig. 1b, full line) thus corresponds to fission of the carbon—chlorine bond, resulting in formation of the corresponding carbanion—enolate according to reaction (I) (X = Cl). Reduction of the carbon—chlorine bond in position 6 occurs at more positive potentials than that of the carbon—fluorine bond in fluprednisolone. This follows the generally observed [20] sequence in which the reduction potential of the carbon—halogen bond becomes gradually more negative C—I > C—Br > C—Cl > C—F. Reduction of the carbanion—enolate derived from chlorprednisone acetate at −1.61 V occurs at more positive potentials than that of the carbanion—enolate of fluprednisolone, similarly as for the observed difference in peak potentials for prednisone/prenisolone and cortisone/hydrocortisone [1].

Values of n determined coulometrically at the mercury pool ($n = 1.98$) and by comparison of wave-heights of the first reduction step of chlorprednisone acetate with wave-heights of benzophenone and naphthoquinone obtained by d.c. polarography indicated a 2-e reduction step for the carbon—chlorine bond fission. Furthermore, electrolysis at potentials corresponding to the limiting current of the first reduction peak with the mercury pool electrode, yielded a concentration of chloride ions equimolar with the initial chlorprednisone acetate concentration, as was determined with the chloride-selective electrode.

The current—voltage curve after exhaustive electrolysis (Fig. 1b, broken line) is identical with that of prednisone (VI). The peak at −2.00 V, corresponding to the reduction of the side-chain in position 17, remains again practically unaffected by the presence and reduction of groups in rings A and B.

Clobetasol-17-propionate (III) and clobetasone-17-butyrate (IV)

In both these compounds the initial reduction involves the carbon—chlorine bond fission in position 21, *vicinal* to the electron-withdrawing keto group in position 20 (Fig. 1c, full line). This reduction occurs in a broad peak at −1.3 V, preceding the reduction peaks of the carbonyl group in position 3 at −1.55 V and −1.75 V for clobetasol (III) and −1.52 V and −1.72 V for clobetasone (IV) similarly to the first two reduction peaks of prednisolone (V) and prednisone (VI), respectively. Reduction in the side-chain does not affect reduction in ring A and thus both peaks of the reduction of the carbonyl group in position 3 are observed also in the solution, resulting in exhaustive electrolysis at a mercury pool (Fig. 1c, broken line).

Further evidence for the nature of the process at −1.3 V was obtained from coulometric data and comparison of d.c. polarographic wave-heights,

indicating $n = 2$. Hence, the smaller height of this peak in differential pulse polarography is due to a slow electrode process rather than to a lower number of electrons transferred. Moreover, determination of concentration of chloride ions in the solution after electrolysis indicated formation of one equivalent of chloride per clobetasol (III) or clobetasone (IV) molecule.

The adjacent conjugated system in ring A facilitates reduction of the carbon—chlorine bond in position 6 ($E_p = -1.17$ V) evidently more than the presence of a single carbonyl group in position 20 facilitates reduction of such a bond in position 21 (−1.3 V).

Reduction of the carbonyl group in the side-chain in position 17 does not occur, even after prolonged electrolysis. This can be attributed to the fact that the fission of the carbon—chlorine bond in position 21 yields a compound with a single —OR group adjacent to the carbonyl group. Such compounds, if reduced at all, undergo reduction at such negative potentials that their waves cannot be observed in methanolic media.

Applications

Some pharmaceutical preparations containing one of the examined corticosteroids were analyzed by the methods described in Experimental. Results are summarized in Table 1. For calculations, the most positive peak in the differential pulse polarographic curves was used. The contents were determined by the standard addition method. In solutions which were 10^{-5} M or less in steroid, a slight deviation from linearity of peak height with concentration occurred. At such low concentrations it was necessary to use a calibration curve. In the analysis of ointments, the electro-inactive constituents did not affect the polarographic behaviour of the corticosteroids to be determined.

Adremycine eye/ear drops were analyzed in the same way as ointments, using DMF—water mixture. Instead of dissolving in toluene, nevertheless, 0.5 ml of the liquid was directly used for analysis. This sample contains

TABLE 1

Assays of the dosage forms and standard deviations based on 5 determinations with separate sampling

Constituents	Content (mg g^{-1})	Name	Source	Found (mg g^{-1})	R.s.d. (%)
Clobetasol propionate	0.5	Dermovate ointment	Glaxo	0.50	1.2
Clobetasone butyrate	0.5	Eumovate ointment	Glaxo	0.50	1.3
Chlorprednisone acetate	1[a]	Adremycine eye/ear drops	Organon	1.03[a]	1.8
Neomycin sulphate	5[a]				
Paraffin					
Clobetasol propionate	0.5	Dermovate cream	Glaxo	0.50	1.2
Clobetasone butyrate	0.5	Eumovate cream	Glaxo	0.50	1.1

[a]Content in mg ml^{-1}.

liquid paraffin, which has been shown [27] to complicate the determination of $\Delta^{1,4}$-3-ketosteroids by an increase of the base line. Because, however, the reduction peak of the chlorine in position 6 occurs at potentials about 350 mV more positive than that of the reduction peak of the $\Delta^{1,4}$-3-keto group, the presence of paraffin does not affect the reduction peak of the C—Cl bond in chlorprednisone.

Inspection of Table 1 indicates that the content found follows closely the declared values. Standard deviations are in the range 1—2%; analysis takes about 15 min to carry out.

The authors thank Dr. C. Burgess (Glaxo Operations U.K.) for kindly supplying some of the examined preparations and pure compounds.

REFERENCES

1 H. S. de Boer, J. den Hartigh, H. H. J. L. Ploegmakers and W. J. van Oort, Anal. Chim. Acta, 102 (1978) 141.
2 P. J. Elving and B. Pullman, Adv. Chem. Phys., 3 (1961) 1.
3 F. L. Lambert and K. Kobayashi, J. Am. Chem. Soc., 82 (1960) 5324.
4 P. Zuman, Substituent Effects in Organic Polarography, Plenum Press, New York, 1967, p. 184.
5 P. J. Elving, Record Chem. Progr. (Kresge—Hooker Sci. Lib.), 14 (1953) 99.
6 C. L. Perrin, Progr. Phys. Org. Chem., 3 (1965) 165 (256).
7 P. J. Elving and C. E. Bennett, J. Electrochem. Soc., 101 (1954) 520.
8 P. J. Elving and R. Vanatta, Anal. Chem., 27 (1955) 1908.
9 P. J. Elving and J. T. Leone, J. Am. Chem. Soc., 79 (1957) 1546.
10 M. Hall and E. Harris, Anal. Chem., 41 (1969) 1130.
11 M. M. Romer and P. Zuman, J. Electroanal. Chem., 64 (1975) 258.
12 W. A. Szafranski and P. Zuman, J. Electroanal. Chem., 64 (1975) 255.
13 P. Zuman and S. Wawzonek, Prog. Polarogr., 1 (1962) 303.
14 A. M. Wilson and N. L. Allinger, J. Am. Chem. Soc., 83 (1961) 1999.
15 M. v. Stackelberg and W. Stracke, Z. Elektrochem., 53 (1949) 118.
16 P. Zuman, Chem. List., 48 (1954) 94.
17 P. Zuman, Substituent Effects in Organic Polarography, Plenum Press, New York, 1967, p. 185.
18 V. Delaroff, M. Bolla and M. Legrand, Bull. Soc. Chim. Fr., (1961) 1912.
19 P. Kabasakalian and J. McGlotten, Anal. Chem., 34 (1962) 1440.
20 P. Zuman, Talanta, 12 (1965) 1337.
21 P. Zuman, Substituent Effects in Organic Polarography, Plenum Press, New York, 1967, p. 332.
22 A. J. Cohen, Anal. Chem., 35 (1963) 128.
23 O. Hrdý, Collect. Czech. Chem. Commun., 27 (1962) 2447.
24 M. J. Heasman and A. J. Wood, J. Pharm. Pharmacol., 23 (1971) 176.
25 P. Zuman, in M. M. Baizer (Ed.), Organic Electrochemistry, M. Dekker, New York, 1973, p. 153.
26 H. Lund, Acta Chem. Scand., 13 (1959) 192.
27 H. S. de Boer, P. H. Lansaat and W. J. van Oort, Anal. Chim. Acta, 116 (1980) 69.

Analytica Chimica Acta, 120 (1980) 41—53

THE DIFFERENTIAL PULSE ANODIC STRIPPING VOLTAMMETRY OF COPPER AND LEAD AND THEIR DETERMINATION IN EDTA EXTRACTS OF SOILS WITH THE MERCURY FILM GLASSY CARBON ELECTRODE

T. E. EDMONDS, PU GUOGANG** and T. S. WEST*

The Macaulay Institute for Soil Research, Craigiebuckler, Aberdeen, AB9 2QJ (Gt. Britain)

(Received 9th June 1980)

SUMMARY

The differential pulse anodic stripping voltammetry of copper and lead at the mercury film glassy carbon electrode is discussed. The mercury film prevents the occurrence of a monolayer stripping peak for copper. The influence of antimony and bismuth on the anodic stripping voltammetric behaviour of copper and lead is discussed. An interaction between copper and antimony distorts the copper stripping peak and gives rise to an intermediate peak. The method described is suitable for determining copper and lead simultaneously in EDTA extracts of soils.

The biological significance and analysis of trace elements in soils has been reviewed recently [1]. Copper occurs in plant leaves as a constituent of the chloroplast protein, and is also present as part of several enzymes. It appears to function in the metabolism of proteins and carbohydrates in plants. Copper deficiency in a soil gives rise to visible deficiency symptoms in plants, such as white leaf tips, twisted leaves, poorly developed ears in cereals, summer-die-back in fruit trees, etc. It is, therefore, important to determine copper in soils, especially that fraction which is available to plants. A suitable extractant is 0.05 M EDTA at pH 7, which, when shaken with air-dried soil, removes a quantity of copper that correlates well with plant uptake [2].

For the determination of copper, spectrochemical methods, particularly atomic absorption spectrometry, are widely used [2—7]. Differential pulse anodic stripping voltammetry (d.p.a.s.v.) is also an attractive technique because of its excellent sensitivity and the possibility of simultaneous determinations of two or more trace metals [8—32]. For example, simultaneous determinations of Cd, Pb, Cu, Sb and Bi in chloride-containing solutions have been reported [9, 10, 17, 22, 24, 28, 29, 31]. Antimony and bismuth are the major interferences in the determination of copper by anodic stripping voltammetry. This interference may be removed by preconcentration and

**On leave from Department of Chemistry, University of Science and Technology of China, Hofei, People's Republic of China.

stripping in two separate media [24]; or copper may be separated by extraction into an organic solvent [21, 30] prior to voltammetry. This paper describes the differential pulse anodic stripping voltammetric behaviour of copper and lead with special reference to the monolayer stripping peak of copper at a glassy carbon electrode (GCE) and the interaction between antimony and copper deposited on a mercury film glassy carbon electrode (MFE). A method is also reported for determining copper and lead simultaneously in EDTA extracts of soils.

EXPERIMENTAL

Apparatus and reagents

A model 174A Polarographic Analyzer (Princeton Applied Research) and a Metrohm EA 1102 microcell (2-ml capacity) were used. A Metrohm EA 286/1 glassy carbon electrode was chosen as the working electrode. A platinum counter-electrode and an Ag/AgCl reference electrode (Metrohm EA 442) completed the cell. Oxygen-free nitrogen was used to deoxygenate the electrolyte and distilled, deionized water was used to prepare all solutions. EDTA, citric acid, acetic acid, sodium acetate and hydrochloric acid were all of analytical-reagent grade, but the hydrochloric acid and nitric acid used in the analysis of soil samples were Aristar grade. The stock solution for copper was made from pure copper (99.999%), and for lead from lead acetate (analytical-reagent grade), each in a mixed acid solution which was 1.0 M in hydrochloric acid and 0.1 M in citric acid. Stock solutions for antimony and bismuth were made from antimony(III) chloride and bismuth nitrate pentahydrate with 5 M HCl—0.1 M citric acid. All stock solutions were serially diluted to prepare 10 μg ml^{-1} working standards with 5 M HCl—0.1 M citric acid.

General procedures

The MFE was prepared as follows: 1 ml of the selected electrolyte solution was put into the cathode compartment of the Metrohm microcell, with 2—50 μg of mercury(II) iodide in 0.1 M nitric acid. The solution was de-aerated, and, whilst an inert atmosphere was maintained over the stirred solution, the glassy carbon electrode was polarized to —1.0 V for 1—3 min. This ensured a reasonably homogeneous distribution of active sites for the deposition of mercury. The potential was shifted to +1.0 V for 1—3 min to strip off the mercury and other metals. The treatment was repeated twice or three times. This procedure generally ensured that the electrode surface was in an active condition ready for use. Subsequently, mercury films for the deposition of analyte species were deposited during the preconcentration step. When the test solution in the cell was changed, the electrode was stored in distilled water to protect it from contact with the air.

It was found that the background current was much smaller when 0.5 M acetic acid—0.5 M sodium acetate was used instead of 5 M HCl—0.1 M citric

acid in the reference electrode compartment. A 0.6-ml aliquot of acetic acid—sodium acetate (pH 2.9) was, therefore, used as the electrolyte in the reference compartment. All voltages are given with respect to the Ag/AgCl reference electrode.

For a simultaneous determination of copper and lead, preconcentration was carried out at −1.0 V for 1—5 min. The stirring was stopped for 30—60 s, and the potential was scanned from −1.0 V to 0.2 V at 2—10 mV s^{-1} to record the differential pulse anodic stripping voltammogram. The potential was then stepped back to +1.0 V to strip off the mercury film. When the mercury film was not completely removed, the stripping peaks were greater in subsequent scans [33].

Procedure for EDTA extracts of soils

Air-dried soil (15 g) was shaken for 1 h at 20°C with 75 ml of 0.05 M diammonium EDTA at pH 7.0. The filtrate was collected and 5—10 ml were evaporated to dryness. The residue was digested with nitric and hydrochloric acids (1:1) 2—3 times and with hydrogen peroxide (30%) and hydrochloric acid, twice. The residue was dissolved, transferred to a 50-ml volumetric flask and made up with 5 M HCl—0.1 M citric acid solution. An aliquot (1 ml) of this solution was put into the Metrohm microcell, where copper and lead were determined by the method of standard additions.

RESULTS AND DISCUSSION

Working electrode

Initially, a GCE was selected as the working electrode. The GCE exhibits several useful features, such as a high overvoltage for hydrogen and an easily renewed active surface. However, it was found that the anodic stripping peak of copper was split into two at the GCE whenever the scan rate exceeded 2 mV s^{-1} (Fig. 1). Three dissolution peaks for copper on a pyrolytic graphite electrode and double stripping peaks on a graphite paste electrode have also been observed [34, 35]. This phenomenon could be due to underpotential deposition, i.e., the formation of a metal monolayer on the substrate electrode surface at potentials more positive than that predicted by Nernstian behaviour. This effect has been reviewed by Kolb [36]. The chemical potential of the first monolayer is markedly different from that of the bulk metal which is deposited subsequently, and this gives rise to two distinct stripping peaks, corresponding to the removal of the bulk metal, followed by the monolayer.

From the present experiments, it appeared that the monolayer stripping peak potential was shifted in the anodic direction with increasing voltage scan rate, but overlapped the bulk copper peak when the scan rate was less than 2 mV s^{-1}. Clearly, the stripping process of copper at the GCE is controlled not only by the electrochemical step, but also by the interaction between the deposited metal and carbon atoms or oxide forms [37], such

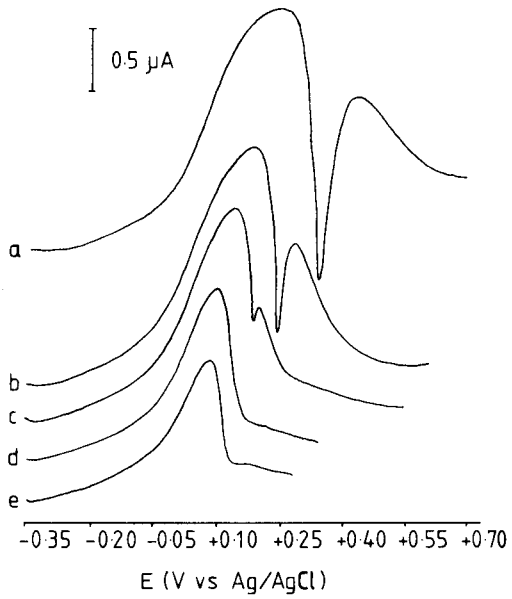

Fig. 1. Effect of stripping rate on the d.p.a.s.v. signal for copper (3 mg l^{-1}) in 0.5 M acetic acid—sodium acetate at the GCE. Pre-electrolysis at —0.8 V vs. Ag/AgCl for 1 min, stripping with 5-mV pulse at (a) 20, (b) 10, (c) 5, (d) 2, (e) 1 mV s^{-1}.

as hydroxyl, carbonyl or carboxyl. For analytical purposes, the glassy carbon electrode with a mercury film plated in situ [13, 14] was chosen as the working electrode. In the presence of this mercury film, the interaction between the metals and electrode substrate was minimized and the monolayer stripping peak of copper was generally eliminated. In addition, the difficulties that arise from intermetallic compounds in the simultaneous determination of several metals may be considerably reduced, though not completely eliminated.

Supporting electrolyte

The anodic stripping peak potential (E_p) of copper is located close to the potential of the anodic dissolution of mercury. Thus the base electrolyte must be such that separation between these two processes is adequate. Preliminary work in acetic acid—sodium acetate showed that there were strong interferences from antimony and bismuth, their peaks overlapping with that of copper even in acidic media. In this electrolyte, the background current of the GCE or MFE was rather large and the sensitivity for copper was insufficient, although it could be improved by reducing the pH, as shown in Table 1.

In hydrochloric acid media, the behaviour of copper, bismuth and antimony was markedly influenced by the chloride concentration, as observed by others [38]. The peak potentials of all three cations showed a progressive

TABLE 1

The influence of pH on the peak height of copper (in arbitrary units) for d.p.a.s.v. at the MFE in 0.5 M sodium acetate—acetic acid

pH	2.0	2.2	2.6	2.9	3.2	3.7	4.0
Peak height	16.3	10.5	9.2	7.8	7.6	3.6	0.9

cathodic shift as the chloride concentration was raised, and the shift for copper was greater than those for antimony and bismuth. The E_p values for copper, antimony and bismuth when each cation was present alone in solution were —0.28 V, —0.13 V and —0.14 V in 1 M HCl but —0.49 V, —0.27 V and —0.30 V in 5 M HCl. Interference from iron(III) occurred in the latter medium, and this required the addition of citric acid to suppress it. The E_p values for copper, antimony and bismuth in a mixed acid medium, 5 M HCl—0.1 M citric acid, were —0.41 V, —0.22 V and —0.25 V, respectively. Hence 5 M HCl—0.1 M citric acid was chosen as the base electrolyte for determining copper and lead. Cadmium, whose peak potential is —0.84 V, may be determined as well. The stripping peak of bismuth, however, overlaps that for antimony in this medium. A differential pulse anodic stripping voltammogram of Cd, Pb, Cu and Sb in 5 M HCl—0.1 M citric acid is shown in Fig. 2. The E_p for copper under these conditions is —0.34 V, because of the presence of antimony (see below).

The influence of antimony and bismuth

Bismuth did not interfere with the stripping of copper in this medium which is in accord with work reported by Brainina [28], but antimony interfered even though the stripping peaks of antimony and copper are separated adequately. In Fig. 3 the interference appears as a distortion on the anodic side of the stripping wave of copper (50 μg l^{-1}) and can be seen clearly even when only 5 μg Sb l^{-1} is added. A fresh peak appeared when 10 μg Sb l^{-1} was added. The peak potential of —0.34 V is more positive than that of copper (—0.41 V) in the absence of antimony. As the concentration of antimony was increased, the peak at —0.34 V was raised, and the copper peak at —0.41 V was reduced, disappearing completely when 50 μg Sb l^{-1} was present. When the copper concentration in the solution was progressively increased at this point, the peak at —0.41 V reappeared and increased (see Fig. 3B) while the antimony peak remained at —0.22 V, though its height decreased slightly with each fresh increment of copper.

The appearance of an intermediate peak at a potential midway between the anodic stripping peak potentials of the two metals could be attributed to the formation of a solid solution between the two. Such solutions can arise on the electrode surface when metals are of similar atomic radii [28]. However, in the case of antimony and copper, the difference in atomic radii seems significant (r_{Cu} = 2.56 Å and r_{Sb} = 3.22 Å). It is also noted that the

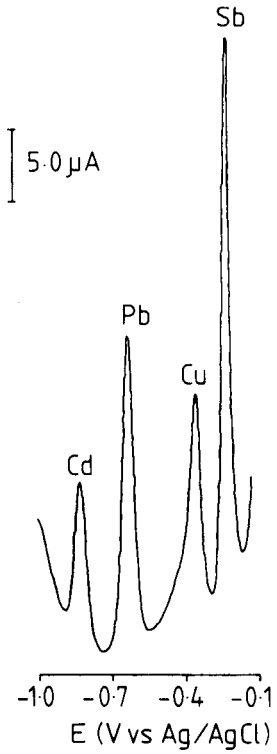

Fig. 2. D.p.a.s.v. of Cd, Pb, Cu and Sb (50 $\mu g\ l^{-1}$) at the MFE, in 5 M HCl—0.1 M citric acid. Pre-electrolysis at —1.0 V vs. Ag/AgCl for 2 min, stripping at 5 $mV\ s^{-1}$ with 25-mV pulse.

peak height for antimony is influenced by copper. In addition, there is no obvious improvement on the wave shape for copper even for a tenfold increase in the mercury(II) ion concentration. However, the influence of preconcentration potential on the stripping wave shape of copper was marked (Fig. 4). When the preconcentration potential was changed from —1.0 V to —0.70 V, the intermediate peak diminished, and disappeared completely as did that of antimony at potentials more positive than —0.70 V. Under these conditions a single copper stripping peak was obtained at —0.41 V. The copper peak shown in Fig. 4, curve d, was obtained with 2-min preconcentration. Preconcentration for 5 min yielded a larger peak that was still free from the distortion caused by antimony. Thus it appears that there is no deposition of antimony or formation of a solid solution between copper and antimony at the electrode surface at these more positive potentials. The behaviour of antimony in these experiments differs from previously reported work [28], which indicated that antimony deposition in a 1 M hydrochloric acid electrolyte is independent of the electrode potential from —0.3 to —0.8 V and decreases abruptly at a more negative potential. This interaction between

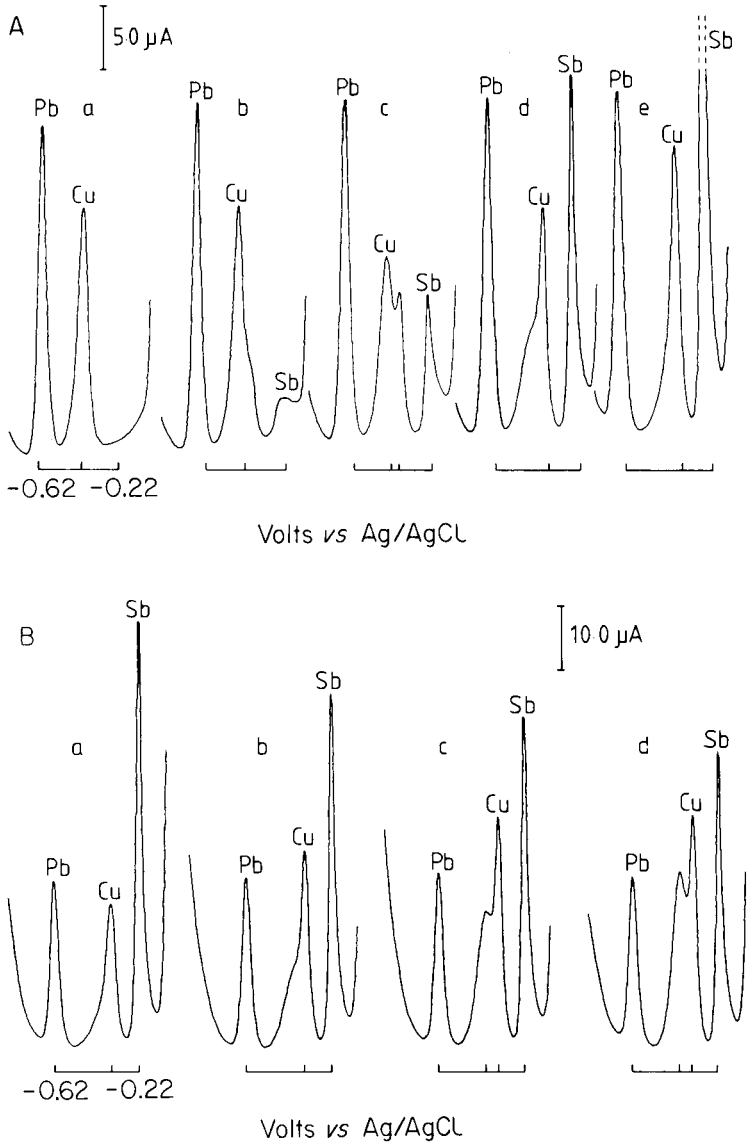

Fig. 3. (A) Effect of antimony at concentrations of (a) 0, (b) 5, (c) 10, (d) 20, (e) 50 $\mu g\ l^{-1}$, on the d.p.a.s.v. at the MFE of Cu and Pb (50 $\mu g\ l^{-1}$) in 5 M HCl—0.1 M citric acid. See Fig. 2 for other conditions. (B) Effect of copper at concentrations of (a) 50, (b) 70, (c) 100, (d) 120 $\mu g\ l^{-1}$, on the d.p.a.s.v. at the MFE of Pb and Sb (50 $\mu g\ l^{-1}$) in 5 M HCl—0.1 M citric acid. See Fig. 2 for other conditions.

antimony and copper clearly deserves further study. The interaction between copper and antimony at the MFE was also exhibited in 0.1 M HCl—2 M NaCl and in 0.1 M HCl—2 M NaCl—0.1 M citric acid. No interference was observed between antimony and lead in these media.

Fortunately, the antimony content of most soils is very low [39] and even when present, its interference can be reduced or eliminated by choosing an appropriate preconcentration potential (see Figs. 4 and 5). Hence, 5 M HCl—0.1 M citric acid is a suitable electrolyte for the simultaneous determination of copper and lead in EDTA extracts of soils by d.p.a.s.v. using a mercury film glassy carbon electrode.

Effects of mercury(II) concentration, amplitude and scan rate

The deposition process for a metal on a mercury film may be supposed to take place in two steps: $M^{n+} + ne^- \rightarrow M$ and $M + Hg \rightarrow M_xHg_y$. Obviously, within limits, if more mercury is deposited on the electrode surface, the deposition of copper and lead will be favoured, but if the mercury film is

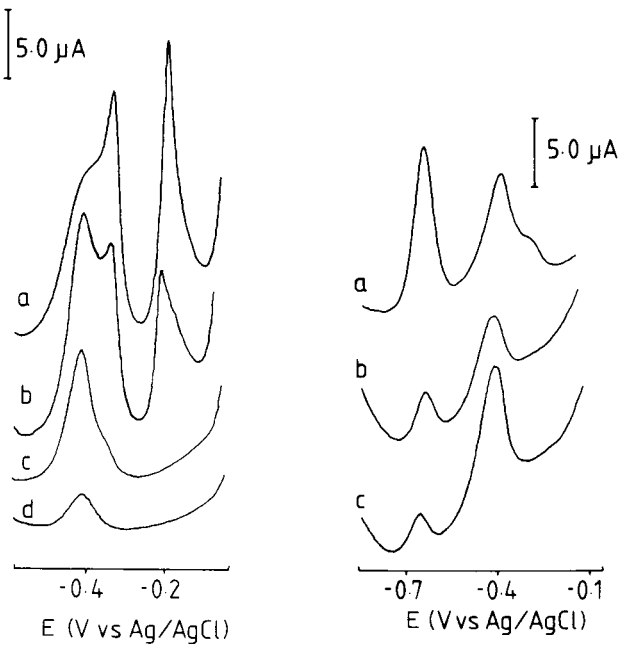

Fig. 4. Effect of pre-electrolysis potentials of (a) —1.0, (b) —0.8, (c) —0.7, (d) —0.6 V vs. Ag/AgCl on the d.p.a.s.v. of Cu and Sb (50 $\mu g\ l^{-1}$) at the MFE in 5 M HCl—0.1 M citric acid. See Fig. 2 for other conditions.

Fig. 5. Effect of pre-electrolysis potentials of (a) —1.0, (b) —0.8, (c) —0.8 V vs. Ag/AgCl on the d.p.a.s.v. of (a) and (b) EDTA extract of soil and (c) EDTA extract of soil + 30 μg Cu l^{-1}, at the MFE in 5 M HCl—0.1 M citric acid. Pre-electrolysis for 3 min. See Fig. 2 for other conditions.

too thick, the stripping process will be influenced to a greater extent by diffusion within the film. In practice, as Fig. 6A shows, the peak heights of both copper and lead increased with increasing concentration of mercury(II). In this work, 2—50 mg Hg(II) l^{-1} in nitric acid were used, depending on the range of copper concentrations to be measured.

As has generally been observed, there was a direct linear relationship between the peak heights of copper and lead, and the amplitude of the applied pulse.

The dependence of peak heights on scan rate is shown in Fig. 6B. The width at half-height of the stripping peaks also became larger, as the scan rate was increased, whilst the peaks shifted to slightly more anodic potentials for both copper and lead. A scan rate of 5 mV s^{-1} is a suitable compromise condition.

Preconcentration time and potential

The dependence of peak heights on the deposition time of the metals at the MFE was similar to that at the hanging mercury drop electrode, as shown in Fig. 7A.

The influence of the potential chosen for preconcentration of metals on the peak heights is shown in Fig. 7B. Because of the hydrogen ion discharge at potentials more negative than —1.1 V, a substantial amount of hydrogen was evolved at the electrode surface, and this hampered the deposition of metal. When the working electrode is exposed to a large amount of hydrogen discharge, its behaviour becomes poorly reproducible and repolishing with diamond paste is necessary. In order to decrease interference on the copper peak from traces of antimony, it was necessary to preconcentrate at a potential more positive than —0.8 V. In the absence of antimony a preconcentration potential of —1.0 V is preferred.

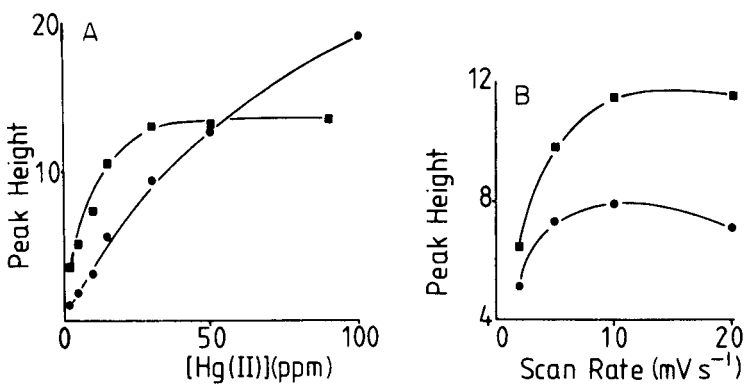

Fig. 6. Effect of (A) concentration of Hg(II) and (B) stripping scan rate, on the peak heights (arbitrary units) for 0.1 mg l^{-1} solutions of copper (▪) and lead (•). See Fig. 2 for the experimental conditions.

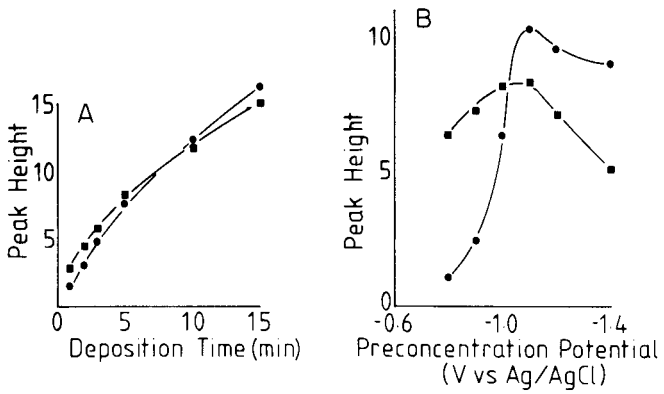

Fig. 7. Effect of (A) deposition time and (B) pre-electrolysis potential, on the peak height (arbitrary units) for 0.1 mg l^{-1} solutions of copper (▪) and lead (•). See Fig. 2 for the experimental conditions.

Determination of copper and lead in EDTA extracts of soils

In the procedure recommended in the Experimental section for the analysis of soils, the repeated digestion of the evaporated EDTA extract is necessary to remove micro-organisms and surface-active substances, which generally interfere with electrochemical determinations, as well as tin that could specifically interfere with the determination of lead [40—42]. The EDTA which would otherwise have affected the copper wave was also destroyed.

The results of these determinations were in broad agreement with those obtained by atomic absorption spectrometry (a.a.s.) within the error range for d.p.a.s.v. and microcell analysis (Table 2). The standard deviation obtained in repetitive experiments was normal for a.s.v., being less than ±20%.

The d.p.a.s.v. results for lead were systematically lower than those obtained by a.a.s. This could have been caused by imprecision in the a.a.s. determin-

TABLE 2

Comparison of d.p.a.s.v. and a.a.s. results for the determination of copper and lead in EDTA extracts of soil

Sample no.	Cu (mg l^{-1})		Pb (mg l^{-1})		Sample no.	Cu (mg l^{-1})		Pb (mg l^{-1})	
	D.p.a.s.v.	A.a.s.	D.p.a.s.v.	A.a.s.		D.p.a.s.v.	A.a.s.	D.p.a.s.v.	A.a.s.
1	1.01	0.87	5.89	—	8	0.23	0.13	0.19	0.12
2	0.79	0.78	0.27	—	9	0.07	0.09	0.19	—
3	0.25	0.25	0.38	0.52	10	0.22	0.42	0.38	0.78
4	0.39	0.32	0.91	1.32	11	0.22	0.23	0.32	0.39
5	0.24	0.30	0.20	0.39	12	0.16	0.12	0.18	0.25
6	0.26	0.24	0.28	—	13	0.69	0.54	1.71	—
7	0.32	0.21	0.45	0.52	14	0.66	0.75	0.40	—

ations which were carried out near the a.a.s. detection limit. Alternatively, lead might have been lost in the digestion procedure. Recovery studies for both copper and lead were, therefore, carried out on four samples. Soil extracts were spiked with 0—0.6 mg l^{-1} copper or lead. A 10-ml aliquot of the spiked extract was taken through the digestion procedure and made up to 50 ml with 5 M HCl—0.1 M citric acid solution, and the copper or lead was determined by d.p.a.s.v. at the MFE. The results (Table 3) show a normal distribution pattern for the d.p.a.s.v. of both metals.

In all the analytical determinations the variability of the blank value was a major source of error. This variability probably reflected contamination from the environment during the sample preparation procedures, rather than contributions from the reagents.

Conclusion

The determination of copper and lead by d.p.a.s.v. at the MFE is a relatively simple and sensitive technique. The GCE without a mercury film did not prove suitable for analytical use because of the occurrence of a monolayer stripping peak for copper. The major problems in the analysis arose from the influence of antimony and bismuth on the stripping of copper and lead, especially the interaction between copper and antimony at the MFE. The latter may have arisen from the formation of a solid solution between copper and antimony, which caused an additional anodic stripping peak to appear on the voltammogram at a potential midway between the potentials of the anodic stripping peaks of copper and antimony. Care should be taken when determining copper in a soil extract in which the presence of antimony is suspected, but preconcentration at potentials more positive than —0.8 V vs. Ag/AgCl avoids this problem. Interference from tin and surface-active materials can be eliminated by digesting the extracts with nitric and

TABLE 3

D.p.a.s.v. recovery of copper and lead added to soil extracts

Sample no.	Cu added ($\mu g\ l^{-1}$)	Cu measured ($\mu g\ l^{-1}$)	Recovery (%)	Pb added ($\mu g\ l^{-1}$)	Pb measured ($\mu g\ l^{-1}$)	Recovery (%)
1	0	24	—	0	70	—
	20	46	110	40	113	107
	20	44	100	80	160	113
2	0	38	—	0	59	—
	40	74	90	40	102	107
	80	125	109	40	98	98
3	0	21	—	0	65	—
	40	66	112	40	115	125
	80	97	95	80	159	117
4	0	33	—	0	58	—
	40	70	93	40	126	85
	80	111	98	120	155	81

hydrochloric acids. D.p.a.s.v. at the MFE in 5 M HCl—0.1 M citric acid can be used to determine copper and lead simultaneously in EDTA extracts of soil.

The authors thank M. L. Berrow of the Department of Spectrochemistry for carrying out the atomic absorption spectrometric determination of copper and lead in EDTA extracts of soil. We are also grateful to the Chinese Academy of Sciences and The Royal Society for granting leave of absence and providing funds to P. G.

REFERENCES

1 T. S. West, Biosignificance and Analysis of Trace Elements in Agricultural Soil, The Tom Miller Memorial Lecture, 3rd May 1979, Special publication, North of Scotland College of Agriculture, Aberdeen.
2 R. O. Scott, R. I. Mitchell, D. Purves and R. C. Voss, Spectrochemical Methods for the Analysis of Soil and Other Agricultural Material, Consultative Committee for Development of Spectrochemical Work, Bulletin 2, Macaulay Institute for Soil Research, Aberdeen, 1971.
3 R. M. Dagnall, G. F. Kirkbright, T. S. West and R.Wood, Anal. Chem., 43 (1971) 1765.
4 A. Mehlich and S. S. Bowling, Commun. Soil Sci. Plant Anal., 6 (1975) 113.
5 B. Pedersen, M. Willems and S. S. Jorgensen, Analyst, 105 (1980) 119.
6 A. M. Ure and M. L. Berrow, Anal. Chim. Acta, 52 (1970) 247.
7 K. L. Iu, I. D. Pulford and H. J. Duncan, Anal. Chim. Acta, 106 (1979) 319.
8 J. Golimowski, P. Valenta, M. Stoeppler and H. W. Nürnberg, Talanta, 26 (1979) 649.
9 D. Jagner, Anal. Chem., 50 (1978) 1924.
10 G. Gillain, G. Duyckaerts and A. Disteche, Anal. Chim. Acta, 106 (1979) 23.
11 M. I. Abdullah, B. Reuschberg and R. Klimek, Anal. Chim. Acta, 84 (1976) 307.
12 A. W. Mann and R. L. Deutscher, Analyst, 101 (1976) 652.
13 T. M. Florence, J. Electroanal. Chem., 27 (1970) 273.
14 T. M. Florence, J. Electroanal. Chem., 35 (1972) 237.
15 E. A. Zakharova and L. A. Ghernova, Zh. Anal. Khim., 29 (1974) 881.
16 A. I. Kamenev, E. N. Vinogradova and V. N. Khryatschevski, Zh. Anal. Khim., 29 (1974) 40.
17 A. H. Miguell and C. M. Jankowski, Anal. Chem., 46 (1974) 1832.
18 J. Dieker and W. E. van der Linden, Fresenius Z. Anal. Chem., 274 (1975) 97.
19 W. Lund and D. Onshus, Anal. Chim. Acta, 86 (1976) 109.
20 E. Ya. Nieman and M. F. Sumenkova, Zh. Anal. Khim., 30 (1975) 1625.
21 F. Vydra, K. Štulik and E. Julaková, Electrochemical Stripping Analysis, Ellis Horwood, Chichester, 1976.
22 D. Jagner and K. Åren, Anal. Chim. Acta, 100 (1978) 375.
23 H. W.Nürnberg, P. Valenta, L. Mart, B. Raspor and L. Sipos, Fresenius Z. Anal.Chem., 282 (1976) 357.
24 A. Mizuiki, T. Miwa and Y. Fujii, Mikrochim. Acta, 1 (1975) 125.
25 W. Lund and M. Salberg, Anal. Chim. Acta, 76 (1975) 131.
26 Y. Yukiharu, Jpn. Anal., 22 (1973) 763.
27 M. J. Pinchin and J. Newham, Anal. Chim. Acta, 90 (1977) 91.
28 Kh. Z. Brainina, Stripping Voltammetry in Chemical Analysis, Halsted Press, New York, 1974, pp. 47, 66—71.
29 V. D. Rudin and V. V. Shipotovskii, Tr. Stavropul. Sel'sokokhoz. Inst., 2 (33) (1970) 83.
30 N. A. Ulakhovich, G. K. Budnikov and C. G. Fomina, Zh. Anal. Khim., 34 (1979) 241.

31 E. S. Pilkington, C. Weeks and A. M. Bond, Anal. Chem., 48 (1976) 1665.
32 R. B. Smart and J. H. Weber, Anal. Chim. Acta, 115 (1980) 331.
33 Pu Guogang and Wang Er-kang, Acta Univ. Sci. Technol. China, 5 (1975) 121. China, 5 (1975) 121.
34 B. H. Vassos and H. B. Mark, J. Electroanal. Chem., 13 (1967) 1.
35 G. N. Popov, V. V. Pnev and M. S. Zakharov, Zh. Anal. Khim, 27 (1972) 1760.
36 D. M. Kolb, in H. Gerischer and C. W. Tobias (Eds.), Adv. Electrochem. Electrochem. Eng., 11 (1978) 125.
37 W. J. Blaedel and R. A. Jenkins, Anal. Chem., 46 (1974) 1952.
38 E. A. Schonberger and W. F. Pickering, Talanta, 27 (1980) 11.
39 A. M. Ure, J. R. Bacon, M. L. Berrow and J. J. Watt, Geoderma, 22 (1979) 1.
40 I. M. Kolthoff and P. J. Elving, Treatise on Analytical Chemistry, Vol. 3, Part II, J. Wiley, New York, 1961, p. 331.
41 I. M. Kolthoff and P. J. Elving, Treatise on Analytical Chemistry, Vol. 6, Part II, p. 118.
42 S. Kallmann, Anal. Chem., 23 (1951) 1291.

Analytica Chimica Acta, 120 (1980) 55—64

ANODIC STRIPPING VOLTAMMETRY OF GERMANIUM AT THE HANGING MERCURY DROP ELECTRODE

ZENON J. KARPIŃSKI, ANDRZEJ POŁOSAK and ZENON KUBLIK*

Department of Chemistry, University of Warsaw, Pasteura 1, 02093 Warsaw (Poland)

(Received 30th April 1980)

SUMMARY

The Ge(IV)—Ge(0) system was investigated by cyclic and stripping voltammetry at HMDE in acidic pyrogallol medium and in phosphate, borate and carbonate buffers. It was found that germanium electrodeposited from dilute Ge(IV) solutions dissolved anodically forming two peaks corresponding to the oxidation of the unstable homogeneous and stable heterogeneous amalgams. Both peaks can be exploited analytically for the determination of traces of germanium but due to the complex nature of the germanium amalgam the sensitivity and reproducibility of the determinations are lower compared to the results obtained for metals well-soluble in mercury.

Anodic stripping voltammetry with a hanging mercury drop electrode (HMDE) has become very widely used in trace analysis. However, this technique has rarely been used for the determination of traces of substances which form heterogeneous amalgams. The anodic stripping curves obtained for such amalgams are very complicated [1—4] and elucidation of their oxidation mechanisms remains an unsolved problem [5]. Recently, it has been shown [6, 7] that germanium is one of the elements that readily form heterogeneous amalgams. This finding is, however, in contrast with the opinion given by Stepanova et al. [8—10], according to whom the anodic stripping peak obtained after deposition of germanium in mercury corresponds to the oxidation of germanium from the homogeneous amalgam. A re-investigation of the problems in the determination of traces of germanium by anodic stripping voltammetry at the HMDE is reported in this paper.

EXPERIMENTAL

The voltammetric curves were recorded with a conventional Radelkis OH-102 polarograph with a three-electrode cell. The reference electrode was a saturated calomel electrode and all the potentials reported in this paper pertain to this reference electrode. The counter electrode was a platinum foil with ca. 1 cm^2 surface area. As indicating electrodes, two types of HMDE were used: an electrode of the type described by Kemula and Kublik [11] and an electrode with the mercury drop suspended on a

small silver contact sealed into a glass capillary by epoxy resin [12]. The latter electrode was more convenient for work in the negative potential range but replacement of the mercury drop was more cumbersome for this electrode.

Stock solutions (0.01 mol l^{-1} Ge(IV)) were prepared by dissolution of the appropriate weighed quantity of GeO_2 (Fluka 99.99%) in triply distilled water. To avoid the possible oxidation of dissolved pyrogallol by air, an appropriate mass of solid pyrogallol (Mallinckrodt) was introduced directly into the deaerated solution in a cell. The remaining solutions were prepared from reagent grade-chemicals and triply distilled water. Some portions of supporting electrolyte were purified by electrolysis at a large mercury cathode; the potential of the cathode was maintained at −1.3 V by means of a Radelkis OH-404/A potentiostat.

A water-jacketed cell was used. In most experiments the water temperature in the jacket was controlled at 25 ± 0.2°C. The results obtained at other temperatures are indicated elsewhere in the text. Prior to measurements, all the solutions were deaerated with argon.

RESULTS

Cyclic voltammetric experiments

In order to establish the most convenient medium for the determination of germanium(IV) by anodic stripping voltammetry, the behaviour of the system Ge(IV)—Ge/Hg was investigated under cyclic conditions in different solutions. According to the literature, germanium(IV) can be electroreduced in an acidic medium prior to hydrogen evolution if the solution contains a moderate amount of *o*-diphenols [13, 14] or a significant concentration of halide or thiocyanate ions [15—17]. However, it was found here that the reduction peaks of germanium(IV) obtained in the presence of halide or thiocyanate ions were drawn-out and merged markedly with the hydrogen evolution current.

The curves obtained in an acidic pyrogallol solution and in the phosphate and carbonate buffers are presented in Fig. 1. Curve 1 recorded for acidic solutions containing pyrogallol shows that the Ge(IV) reduction peak is well separated from the final rise of the cathodic current. The anodic portion of the curve shows two anodic peaks designated as a_1 and a_2. Peak a_2, corresponding to the dissolution of germanium from the heterogeneous amalgam, is high and sharp but is situated very close to the mercury dissolution current. Peak a_1, appearing at a reversible potential, corresponds to the dissolution of germanium from the homogeneous amalgam [6, 7]. This peak is hardly seen on curve 1 obtained for higher Ge(IV) concentrations but is very distinct on curve 1′ obtained for low Ge(IV) concentrations. The disappearance of peak a_1 at higher Ge(IV) concentrations is caused [6, 7] by transformation of the supersaturated homogeneous germanium amalgam into the heterogeneous amalgam which is oxidized in another potential range.

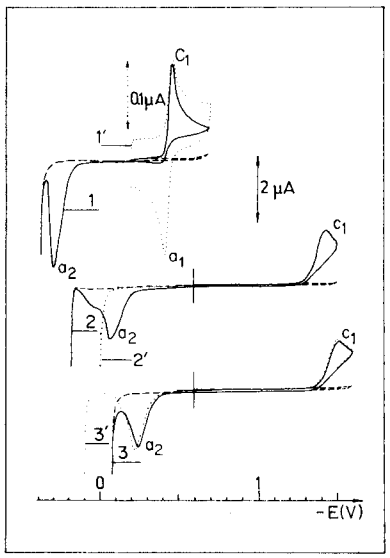

Fig. 1. Effect of supporting electrolyte composition on the cyclic voltammetric curves. (1 and 1') 1 mol l^{-1} $HClO_4$ + 0.05 mol l^{-1} pyrogallol; (2) phosphate buffer pH 8; (2') as (2) + 0.1 mol l^{-1} NaCl; (3) 0.2 mol l^{-1} Na_2CO_3 + 0.025 mol l^{-1} EDTA, pH 10.3; (3') carbonate buffer pH 10.3 Concentration of Ge(IV): (1,2,3,3') 1 × 10^{-4} mol l^{-1}; (1') 5 × 10^{-6} mol l^{-1}. Voltage scan rate 0.025 V s^{-1}.

The peaks obtained for Ge(IV) in the presence of pyrogallol depended on the acidity of the solution and on the pyrogallol concentration. The best defined cathodic and anodic peaks were obtained in 1 mol l^{-1} perchloric acid supporting electrolyte containing 0.05 mol l^{-1} pyrogallol. Both decrease and increase in the perchloric acid concentration led to a decrease of the height of peak c_1 and, in turn, to a decrease of the height of peaks a_1 and a_2. The replacement of perchloric acid by sulphuric acid did not lead to any essential changes. In a hydrochloric acid supporting electrolyte, the peak a_2 overlapped with the mercury dissolution current. Behaviour similar to that shown in curve 1 was observed also in the presence of catechol, gallic acid and tiron.

In neutral solutions in the absence of complexing agents, peak c_1 shifted significantly towards negative potentials. Addition of an excess of pyrogallol to such solutions led to the complete disappearance of this peak. The reproducibility of the peaks obtained in neutral and basic solutions improved markedly when the supporting electrolyte solutions were well buffered. The peaks obtained in the phosphate buffer solution are shown on curve 2. Under these conditions peak a_2 is better separated from the final rise of the anodic current but it is lower and broader. A decrease in the Ge(IV) concentration led to the appearance of the peak a_1 but the shape of this peak deviated markedly from a reversible behaviour.

Addition of chloride ions to the neutral, phosphate buffer solution

exerted no essential influence on the position of peak a_2 but, as is seen on curve 2', it shifted markedly the final rise of the anodic current towards negative potentials. Because of the significant overlap of peak a_2 with the final rise of the anodic current, neutral solutions containing chloride ion are of little value for investigations of the properties of heterogeneous germanium amalgams.

In borate and carbonate buffer solutions in the pH range 8—10, the general shape of the cyclic voltammetric curves varied only slightly. On curve 3', obtained in the carbonate supporting electrolyte at pH 10.3, peak a_2 is well separated from the final rise of the anodic current. On the curve 3, obtained as recommended by Stepanova et al. [9, 10] in the presence of EDTA, the separation of peak a_2 and the mercury dissolution current becomes poorer.

In solutions with a pH higher than 10.5, electroreduction of Ge(IV) becomes more complex. It has been shown [6] that under such conditions electroreduction of Ge(IV) leads to several products; one of these products is soluble in the aqueous phase and so the efficiency of the accumulation step decreases. It is, therefore, evident that solutions with high pH are inconvenient for the determination of Ge(IV) by the anodic stripping technique.

The results presented above indicate that there are some possibilities for the determination of traces of germanium(IV) by anodic stripping based on either the first or the second anodic peak.

Investigation of the properties of the more negative anodic peak under stripping conditions

It has been shown [6] that at 25°C the true solubility of germanium in mercury is 2×10^{-7} mol l^{-1}. The height of the dissolution peak obtained for such a concentration of germanium(IV) would be very low, and this fact excludes the successful use of the true homogeneous germanium amalgam in anodic stripping voltammetry. Further efforts were devoted to checking if the unstable supersaturated germanium amalgam could be exploited for the determination of germanium and if the solubility of germanium in mercury could be enhanced by increase in temperature. Figure 2 shows the effect of the increase in deposition time on the anodic stripping curves obtained at 25°C for 1×10^{-6} mol l^{-1} Ge(IV) in two supporting electrolytes. After deposition lasting 1 min in a quiet solution, only peak a_1 appeared on the anodic portion of the curves although the concentration of germanium in mercury was over 10 times higher than the concentration of germanium dissolved in a saturated amalgam (2×10^{-7} mol l^{-1}).

A comparison of curves 1 and 2 in Fig. 2 shows that the anodic stripping peak a_1 obtained in acidic pyrogallol medium is significantly better defined than peak a_1 obtained in the phosphate solution. As curves 1' and 2' show, increase in the deposition time leads in both cases to a decrease in peak a_1 and to the appearance of the second anodic peak a_2. The same effect was observed when after a 1-min deposition time a recording of the anodic

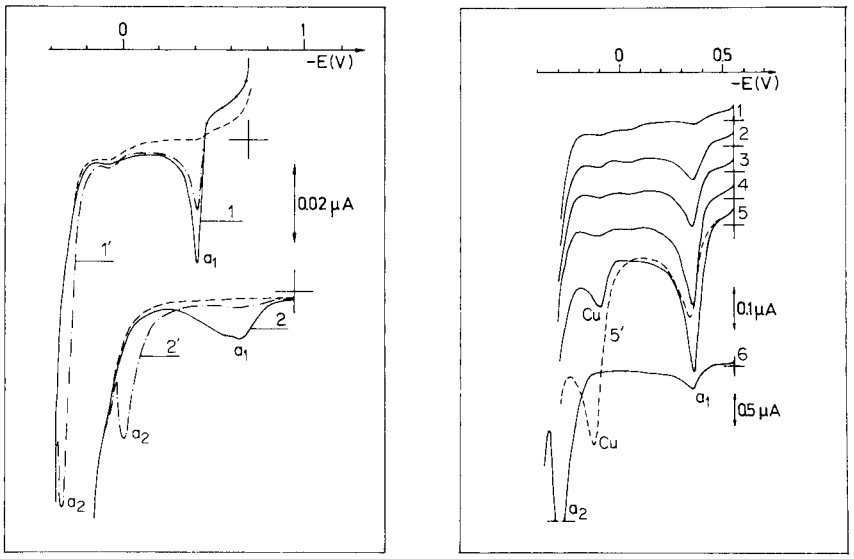

Fig. 2. Effect of variation in the deposition time on the germanium amalgam oxidation peaks. Deposition time: (1 and 2) 1 min; (1′ and 2′) 3 min. Solutions: (1 and 1′) 1 mol l^{-1} $HClO_4$ + 0.05 mol l^{-1} pyrogallol; (2 and 2′) phosphate buffer pH 8. Concentration of Ge(IV), 1×10^{-6} mol l^{-1}. Voltage scan rate, 0.008 V s^{-1}.

Fig. 3. Effect of changes in Ge(IV) concentration on the height of the stripping peaks obtained after a 10-min deposition time at −0.55 V in solutions containing 1 mol l^{-1} $HClO_4$ and 0.05 mol l^{-1} pyrogallol. Concentrations of Ge(IV); (1) 0; (2) 0.5; (3) 1; (4) 2; (5 and 5′) 3; (6) 20×10^{-7} mol l^{-1}. Concentration of Cu(II): (1—4 and 6) 0; (5 and 5′) 2×10^{-7} mol l^{-1}. (1—6) Deposition in quiet solutions; (5′) deposition in stirred solution. Temperature of the solution 80°C. Voltage scan rate 0.008 V s^{-1}.

curve was started after a delay of several minutes. Such behaviour is due to the transformation of the supersaturated germanium amalgam to the heterogeneous germanium amalgam. It is evident that acidic pyrogallol medium offers a better possibility than the phosphate solutions for the determination of traces of germanium(IV) by the anodic stripping technique. Hence, in further experiments only the former medium was investigated. It was found that in this medium the height of the peak a_1 was proportional to the germanium(IV) concentration in the range 2×10^{-7}—1×10^{-6} mol l^{-1} provided that the deposition step was performed in a quiet solution and the deposition time was not longer than 1 min.

Increase in temperature had only a small effect on the true solubility of germanium in mercury but it enhanced markedly the stability of the supersaturated germanium amalgam. In some experiments at 80°C in solutions with Ge(IV) concentrations below 1×10^{-6} mol l^{-1}, even an increase in the deposition time to 10 min did not lead to the appearance of peak a_2. Several curves obtained at 80°C for small concentrations of germanium(IV) are

presented in Fig. 3. The blank test (curve 1) shows that the supporting electrolyte contained only a very small concentration of lead(II) and copper(II). In the stripping cycle obtained after a 10-min deposition time in a quiet germanium(IV) solution, only peak a_1 was recorded. The height of this peak increased proportionally with germanium(IV) concentration in the range 5×10^{-8}—8×10^{-7} mol l^{-1} and this relation is shown in Fig. 4. Above this range, the height of peak a_1 began to decrease and simultaneously peak a_2 appeared. As can be seen by comparison of curves 5 and 5′ (Fig. 3), stirring of the solution during the deposition step leads to the expected increase in the copper stripping peak. In contrast to such behaviour, the height of the stripping peak of germanium decreases markedly under these conditions. The decrease of peak a_1 is not caused by transformation of a homogeneous germanium amalgam to a heterogeneous amalgam since peak a_2 does not appear simultaneously with any decrease in peak a_1.

In a search for the causes of such curious behaviour, several experiments were performed with electrodes aged for several minutes at open circuit in

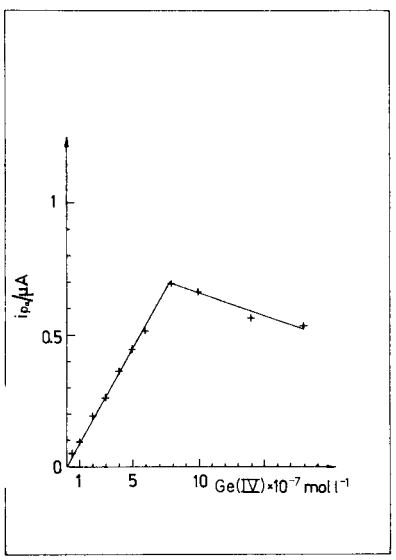

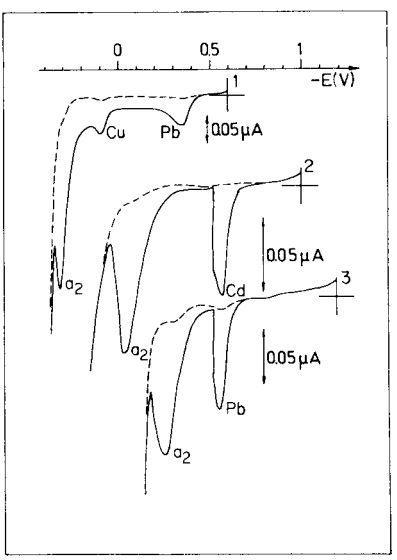

Fig. 4. Dependence of the height of the germanium dissolution peak from homogeneous germanium amalgam on Ge(IV) concentration. Deposition for 10 min at —0.55 V in quiet solution containing 1 mol l^{-1} $HClO_4$ + 0.05 mol l^{-1} pyrogallol plus increasing concentrations of Ge(IV). Temperature of the solution 80°C. Voltage scan rate 0.008 V s^{-1}.

Fig. 5. Effect of supporting electrolyte composition on the stripping curves recorded after a 5-min deposition time in stirred solutions containing 5×10^{-7} mol l^{-1} Ge(IV) and 2×10^{-7} mol l^{-1} Cd^{2+} or Pb^{2+} ions. (1) 1 mol l^{-1} $HClO_4$ and 0.05 mol l^{-1} pyrogallol; (2) phosphate buffer pH 8; (3) 0.2 mol l^{-1} Na_2CO_3 + 0.025 mol l^{-1} EDTA, pH 10.3. Voltage scan rate 0.008 V s^{-1}. Deposition potentials: (1) —0.6 V; (2) —1.5 V; (3) —1.7 V.

stirred solution prior to the deposition step which was done as previously in quiet solution. It was found that an ageing process of this type exerted the same effect as stirring the solution during the deposition step. The harmful action of stirring is highly specific. Under conditions where the germanium stripping peak decreased markedly, the lead stripping peak was unaffected and the copper stripping peak almost unaffected by ageing of the electrode prior to the deposition step.

In further experiments, the efficiency of the deposition process was investigated by recording the i—t curves in stirred solutions. The current obtained for lead(II) reduction in acidic solution containing pyrogallol was practically independent of the electrolysis time. In contrast, the current obtained under the same conditions for the reduction of germanium(IV) decreased with electrolysis time. After 3 min of electrolysis, the reduction current of 1×10^{-4} mol l^{-1} Ge(IV) was only 20% of the initial value. It should be noted that the harmful action of stirring on the germanium stripping peak was more distinct at elevated temperature.

The experiments described above show that despite some difficulties the dissolution peak of the homogeneous germanium amalgam can be exploited for the determination of traces of germanium provided that the experiments are performed in a quiet solution at elevated temperature.

Investigation of the properties of the more positive anodic peak under stripping conditions

There are several disadvantages associated with the use of peak a_2 in stripping analysis for germanium. One of these disadvantages, which is characteristic only for neutral or alkaline supporting electrolytes, results from the position of the reduction peak close to the final rise of the cathodic current. At low concentrations of germanium(IV), its electroreduction peak forms only a shoulder on the final rise of the cathodic current and at very low germanium(IV) concentrations, the reduction current becomes entirely hidden by this rise. Under such conditions, an increase in the negative value of the deposition potential leads not only to an increase of germanium deposition but also to an increase of hydrogen evolution. Hence, the deposition potential should not be too negative and its constancy must be carefully controlled.

A further problem arises from the fact that peak a_2 occurs in the potential range where the background current changes its slope (Fig. 5). This effect makes the measurement of peak height difficult particularly for acidic pyrogallol medium; in the latter case, peak a_2 does not appear when the concentration of germanium(IV) is less than 5×10^{-7} mol l^{-1}. Similarly, for such low concentrations, the anodic stripping peak was not observed in carbonate buffer solution in the absence of EDTA, although the cyclic curve obtained in this solution (Fig. 1, curve 3′) exhibited good separation of peak a_2 and the mercury dissolution current; yet stripping peak a_2 was observed at significantly lower germanium(IV) concentrations when some EDTA

was added. An essential advantage of the carbonate-EDTA solution over the acidic *o*-diphenol medium is a normal dependence of the height of peak a_2 on deposition time and stirring.

Figure 6 presents the stripping curves obtained for increasing concentrations of germanium(IV) in the supporting electrolyte recommended by Stepanova et al. [9, 10], i.e. sodium carbonate solution with EDTA; the detection limit seems to be about 5×10^{-8} mol l^{-1}. Peak a_2 may be obtained at lower concentrations if longer deposition times are used but the reproducibility of the results obtained under such conditions is very low.

Figure 7 presents the relation between log i_p for peak a_2 and log [Ge(IV)] obtained in different supporting electrolytes. These relationships are linear but the slopes are in the range 0.85—0.95. For measurements performed for 5×10^{-7} mol l^{-1} Ge(IV) in 0.2 mol l^{-1} sodium carbonate containing 0.025 mol l^{-1} EDTA, the relative standard deviation was 25% whereas under the same conditions the relative standard deviation obtained for copper was 4%.

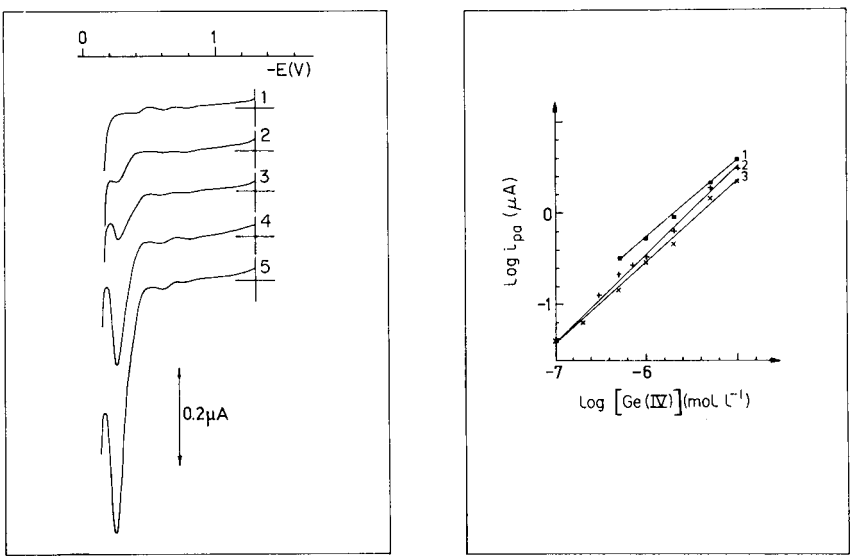

Fig. 6. Effect of increasing Ge(IV) concentration on the germanium dissolution peak from heterogeneous amalgam with a 10-min deposition time at —1.8 V in stirred solutions containing 0.2 mol l^{-1} Na_2CO_3 and 0.025 mol l^{-1} EDTA. Concentration of Ge(IV): (1) 0; (2) 1; (3) 2; (4) 4; (5) 8 × 10^{-7} mol l^{-1}. Voltage scan rate 0.008 V s^{-1}.

Fig. 7. Dependences of log $i_p^{a_2}$ on log [Ge(IV)] for germanium dissolution from heterogeneous amalgam. Solutions: (1) 1 mol l^{-1} $HClO_4$ + 0.05 mol l^{-1} pyrogallol; (2) phosphate buffer pH 8; (3) 0.2 mol l^{-1} Na_2CO_3 + 0.025 mol l^{-1} EDTA, pH 10.3. Deposition for 5 min in stirred solution at potentials of (1) —0.6 V; (2) —1.5 V; (3) —1.7 V. Voltage scan rate 0.008 V s^{-1}.

Interferences

Interferences occur in anodic stripping voltammetry either because the stripping peak of the metal to be determined overlaps with other peaks or because intermetallic compounds are formed in the mercury phase. The germanium stripping peak a_1 observed in acidic *o*-diphenol solutions overlaps strongly with the stripping peak of lead whereas peak a_2 observed in carbonate buffer solution merges significantly with the stripping peak of copper. Both Cu^{2+} and Pb^{2+} ions are common contaminants of many supporting electrolytes and therefore particular care must be taken to remove them from the supporting electrolyte used in the determination of traces of germanium(IV).

There is little information in the literature on the formation of intermetallic compounds between germanium and other metals in mercury. Stepanova et al. [18] found a $GeCu_3$ compound and determined its solubility product (8.4×10^{-13}). This value is fairly high, thus formation of $GeCu_3$ should not be harmful in the determination of traces of germanium by anodic stripping voltammetry.

The position of peak a_2 (Fig. 1) close to the mercury dissolution current means that all substances which shift the dissolution potential of mercury towards more negative potentials, cause severe interferences. Thus, peak a_2 obtained in acidic pyrogallol medium disappears completely in the presence of 1×10^{-5} mol l^{-1} of chloride ions. Chloride ions also interfere in the proper development of peak a_2 in neutral phosphate buffer solutions.

DISCUSSION

The experiments described above undoubtedly show that germanium electrodeposited into the HMDE may be anodically oxidized, forming two distinct peaks corresponding to the dissolution of supersaturated homogeneous germanium amalgam (more negative peak) and to the dissolution of heterogeneous germanium amalgam (more positive peak). These results do not confirm, therefore, the opinion given by Stepanova et al. [9, 10] who observed only the more positive peak and attributed it to the dissolution of a homogeneous germanium amalgam. The stripping peak of the homogeneous germanium amalgam is particularly well defined in acidic solutions containing *o*-diphenols. This peak was observed previously by authors who investigated the properties of germanium(IV) by cyclic oscillopolarography [15, 19, 20] but its nature was not explained. Odobesku et al. [21], investigating the solution of germanium(IV) in the presence of pyrogallol by cyclic voltammetry, did not observe this peak, and therefore suggested that the cathodic reduction peak does not correspond to a faradaic process.

The wider use of *o*-diphenol media for the stripping determination of traces of germanium(IV) is, however, limited by the anomalous dependence of the deposition current on the stirring of the solution. Similar anomalous dependence was observed previously for electroreduction of tin(IV) in the presence of pyrogallol [22]. It is known that in the electroreduction of

germanium(IV) and tin(IV) in *o*-diphenol media, the adsorption of *o*-diphenol plays an essential role [23, 24]. Głodowski and Kublik [22] suggested that the anomalous dependence of the deposition efficiency on stirring might be explained by competitive adsorption between *o*-diphenol and some surface-active agents which are usually present in many electrolytes as ultratraces. This suggestion may also be valid for the phenomenon observed here.

In comparison with the behaviour of other heterogeneous amalgams, e.g., iron [1—3] and cobalt [4] amalgams, the dissolution peak of a heterogeneous germanium amalgam behaves more reproducibly. Such a property provides a basis for the analytical exploitation of this peak, but the heterogeneous nature of this amalgam causes the anodic stripping peak of germanium to be poorly defined. Also the reproducibility of the results is not so good as for those obtained for metals readily soluble in mercury. In the light of these results it is evident that the germanium detection limit proposed by Stepanova et al. [9, 10] as 1×10^{-10} mol l^{-1} is exaggerated.

REFERENCES

1 W. Kemula and Z. Galus, Bull. Acad. Pol. Sci. Cl. 3, 7 (1959) 729.
2 V. F. Ivanov and Z. A. Yofa, Dokl. Akad. Nauk SSSR, 140 (1961) 1368.
3 Z. Stojek and Z. Kublik, J. Electroanal. Chem., 70 (1976) 317.
4 L. Janiszewska and Z. Galus, Rocz. Chem., 49 (1975) 249.
5 Z. Galus, CRC Crit. Rev. Anal. Chem., (1975) 370.
6 Z. Karpiński and Z. Kublik, J. Electroanal. Chem., 81 (1977) 53.
7 Z. Karpiński and Z. Kublik, J. Electroanal. Chem., 106 (1980) 47.
8 M. S. Zakharov, A. G. Stromberg, O. S. Stepanova and S. F. Gurskaya, Meth. Anal. Khim. Reakt., 5—6, IREA, Moscow, 1963, p. 95.
9 O. S. Stepanova, M. S. Zakharov and L. F. Trushina, Zavod. Lab., 30 (1964) 1180.
10 O. S. Stepanova, M. S. Zakharov and L. F. Trushina, Zh. Anal. Khim., 20 (1965) 153.
11 W. Kemula and Z. Kublik, Anal. Chim. Acta, 18 (1958) 104.
12 J. W. Ross, R. D. DeMars and I. Shain, Anal. Chem., 28 (1956) 1768.
13 N. Konopik, Monatsh. Chem., 91 (1969) 717.
14 Z. Karpiński and Z. Kublik, in preparation.
15 H. Alfaro, N. D. Guillermo and V. O. Platteau, Anal. Chim. Acta, 45 (1969) 360.
16 Ja. I. Turyan and T. E. Rozhkova, Elektrokhimiya, 12 (1976) 1592, 1629.
17 Ja. I. Turyan, T. E. Rozhkova, P. I. Kudinov and I. I. Moskatov, Zh. Obshch. Khim., 46 (1976) 2098.
18 O. S. Stepanova, M. S. Zakharov, L. F. Trushina and V. I. Aparina, Izv. Vyssh. Uchebn. Zaved. Khim. Khim. Tekhnol., 7 (1964) 184.
19 H. Vanderbroek and F. Verbeek, Anal. Lett., 5 (1972) 317.
20 R, Kaldova and N. Konopik, Fresenius Z. Anal. Chem., 244 (1969) 30.
21 N. S. Odobesku, L. S. Kopanskaya and S. I. Zhdanov, Zh. Anal. Khim., 28 (1973) 2171.
22 S. Głodowski and Z. Kublik, Anal. Chim. Acta, 104 (1979) 55.
23 Ja. I. Turyan, L. F. Ilina and P. I. Kudinov, Elektrokhimiya, 9 (1973) 1219.
24 A. J. Bard, Anal. Chem., 34 (1962) 266.

Analytica Chimica Acta, 120 (1980) 65—74

DOSAGE POLAROGRAPHIQUE DU BROME A L'ECHELLE DU NANOGRAMME
Application à la determination du brome sanguin et urinaire

J. J. VALLON*, Y. PEGON et M. ACCOMINOTTI

**Département de Chimie Analytique, Faculté de Pharmacie; Laboratoire de Biochimie, Toxicologie et Analyse des Traces, Hôpital Edouard Herriot, 69373 Lyon (France)*

(Reçu le 21 avril 1980)

SUMMARY

Polarographic determination of bromide at nanomolar levels. Application to the determination of bromide in blood and urine.

Colorimetric methods for bromide determination lack adequate sensitivity for normal levels in biological fluids. A sensitive amplification process is recommended: bromide is oxidized to bromate with hypochlorite; after reaction between bromate and excess of bromide, the bromine formed is extracted into chloroform and then reduced to bromide by ammonia; these different steps can be repeated. Alternating current polarography of bromate allows selective evaluation in biological fluids. The detection limit is 10^{-6} M and can be reduced to 10^{-9} M with further amplification steps. The effects of iodide and of instrumental parameters are discussed.

RESUME

Les méthodes colorimétriques de dosage du brome manquent de sensibilité pour apprécier des taux normaux dans les milieux biologiques. Les auteurs proposent un procédé multiplicateur de sensibilité: oxydation de Br^- en BrO_3^- par l'hypochlorite; réaction de BrO_3^- avec Br^- en excès; extraction de Br_2 formé dans le chloroforme; l'extrait chloroformique, en présence de l'ammoniaque, donne Br^- qui peut subir d'autres étapes d'oxydation identiques. La réduction de l'ion BrO_3^- en polarographie sinusoïdale surimposée permet le dosage sélectif dans les milieux biologiques. La limite de détection est 10^{-6} M pouvant aller jusqu'à 10^{-9} M avec le procédé multiplicateur.

Le dosage du brome minéral dans les milieux biologiques a donné lieu à peu de travaux depuis la diminution importante des thérapeutiques par les bromures au profit d'autres hypnosédatifs plus actifs. Il n'est cependant pas rare d'observer des manifestations de bromisme chez des sujets souvent en automédication, et nous avons recensé encore actuellement une centaine de spécialités à base de bromure, en France. Les dérivés organiques du brome à usages industriels dont l'absorption est, pour beaucoup, pulmonaire et l'élimination en partie urinaire, après transformation en bromure, donnent aussi un regain d'intérêt à ce dosage. Les taux trouvés dans les milieux

biologiques sont plus faibles que lors des traitements par les bromures; ils nécessitent des méthodes sensibles de dosage.

Les méthodes colorimétriques, les plus anciennes, faisaient appel à la formation, avec l'ion Br^-, de bromure d'or après addition de chlorure d'or [1, 2]. Beaucoup plus spécifiques sont les méthodes par oxydation en brome suivie de la bromation de molécules organiques; la colorimétrie de la bromorosaniline [3] permet d'avoir une limite de détection de l'ordre du $\mu g\ ml^{-1}$ et utilise l'oxydation en bromate par l'hypochlorite à pH 6,3 suivie d'acidification et libération de brome par addition de bromure [4, 5]. La réaction peut être catalysée par du molybdate et l'addition de t-butanol prévient la précipitation de la tétrabromorosaniline [6]; on peut alors détecter des concentrations de l'ordre de 50 $\mu g\ l^{-1}$ dans les milieux biologiques. La coloration rose de l'éosine (tétrabromofluorescéine) a été utilisée selon le même principe [7, 8] ainsi que la réaction de Deniges et Schelle [9] avec la fuchsine: les deux méthodes ont une sensibilité voisine mais qui reste assez faible. La spectrophotométrie dans l'ultra-violet a plus récemment [10] servi au dosage du brome minéral dans l'eau: elle est fondée sur l'absorptivité du complexe I_2Br^-. Notons enfin que les bromures sont souvent à l'origine d'interférences dans le dosage des chlorures [11]. Ainsi la méthode au thiocyanate de mercure(II) utilisée pour le dosage en flux continu des chlorures des milieux biologiques, donne des valeurs élevées en présence de bromures par suite de la plus grande stabilité du tétrabromo mercure(II). La méthode a été proposée pour un screening d'intoxication bromée [12].

La polarographie a aussi servi à doser les bromures; dans une première étape l'ion Br^- est oxydé en BrO_3^- dont la vague polarographique est mesurée après élimination de l'excès d'oxydant. C'est généralement l'hypochlorite qui sert d'agent oxydant [13, 14]. La méthode polarographique classique utilise la réduction de l'ion BrO_3^- [15], où la vague correspond au processus $BrO_3^- + 6H^+ + 6e^- \rightarrow Br^- + 3H_2O$, qui confère une grande sensibilité au dosage. La réduction est irréversible; elle a lieu à $-1{,}65$ V (vs. ECS) dans KCl 0.1 M et à $-1{,}32$ V dans les solutions 0,1 M de cations divalents ($CaCl_2$, $BaCl_2$, $SrCl_2$). Avec ces diverses conditions, les iodates montrent un comportement polarographique voisin mais toujours une vague distincte de celle des bromates. La polarographie des bromures en courant alternatif a été étudiée par Breyer et Hacobian [16] qui montrèrent l'existence d'une vague anodique asymétrique due à la formation de bromure de mercure(I); ce dernier s'adsorbe partiellement à la surface du mercure et crée un courant capacitif parasite rendant inutilisable la méthode pour un dosage des bromures.

Plus récemment, la potentiométrie par électrode sélective à membrane de bromure d'argent a fait son apparition [17]. Mais la méthode est inapplicable dans les milieux riches en chlorures du fait de l'interférence qu'ils produisent [11].

Le travail que nous présentons avait pour but d'augmenter la sensibilité des méthodes existantes pour atteindre les faibles niveaux de concentration

des milieux biologiques de sujets normaux ou faiblement imprégnés en brome. Deux principes nous ont guidés: tout d'abord rechercher un procédé de sensibilisation par génération quantitative de brome en grande quantité; nous avons ensuite étudié un des modes de dosage possible, la polarographie sinusoïdale.

Recherche d'un procédé multiplicateur de sensibilité

De nombreuses méthodes de dosage réalisent une première étape d'oxydation quantitative des bromures en bromate par l'hypochlorite à pH 6,5. La mécanisme de l'oxydation a été étudié par Szabo et Csanyi [5]: entre pH 6,5 et 7,5, l'oxydation donne de l'acide hypobromeux et du monochlorure de brome; la seconde étape, favorisée par un pH un peu supérieur, consiste en l'oxydation en bromate. La concentration d'hypochlorite doit être molaire dans la soude 0,1 M et l'hypochlorite doit être exempt de bromate. Pour cela, il est possible d'utiliser la méthode de Wright et al. [18] pour fabriquer l'hypochlorite. Après l'oxydation, il est nécessaire d'eliminer l'excès d'hypochlorite en chauffant la solution en présence de formiate de sodium. La deuxième étape, qui est catalysée par l'ion molybdate [19], consiste en une acidification avec addition d'un excès de bromure: $BrO_3^- + 5Br^- + 6H^+ \rightarrow 3Br_2 + 3H_2O$. Le brome sert alors à l'halogénation de molécules organiques diverses (rosaniline, fluorescéine, fuchsine, etc.).

Afin d'augmenter la sensibilité du dosage, nous avons pensé accroître la quantité de brome formé en soumettant celui-ci aux deux étapes suivantes: (1) extraction de l'halogène par le chloroforme suivie d'un contact avec une solution d'ammoniaque qui provoque sa réduction en bromure selon $3Br_2 + 8NH_4OH \rightarrow 6NH_4\,Br + N_2 + 8H_2O$; et (2) renouvellement de l'étape d'oxydation par l'hypochlorite suivie de la réaction $Br(V)Br^-$. La sensibilité du dosage doit théoriquement augmenter d'un facteur multiplicateur égal à 6 selon le bilan suivant

$$Br^- \xrightarrow{+\,3ClO^-} Br(V) \xrightarrow{+\,5Br^-} 6Br(0)\ (eau) \rightarrow 6Br(0)\ (Cl_3CH) \xrightarrow{NH_3} 6Br^- \xrightarrow{+\,18\,ClO^-} 6Br(V) \xrightarrow{Br^-} 36\,Br(0)$$

Ainsi, selon le nombre d'étapes choisi, on accroît chaque fois la quantité de bromure à doser d'un facteur 6, puis 36, puis 216, puis 1296, etc... Les essais que nous avons réalisés seront exposés plus loin: ils montrent la parfaite reproductibilité de ces opérations et le gain de sensibilité obtenu.

ETUDE DE LA VAGUE DE REDUCTION DU BROMATE

Influence du pH

Comme l'ont montré Kolthoff et Lingane [20], la vague est irréversible et la réduction nécessite une surtension de 1,3 V environ sur le mercure en milieu acide; la surtension est plus importante encore en milieu alcalin.

Nous avons recherché l'influence du pH sur le potentiel de réduction,

sur l'intensité et sur la largeur du pic polarographique des bromates et des iodates dont l'interférence est possible si le milieu biologique étudié renferme des iodures. L'étude a été faite dans l'acide perchlorique dilué pour les pH entre 0 et 2, et le tampon de Britton et Robinson (acides phosphorique, acétique et borique en solution aqueuse 0,03 M) pour les autres pH. Les réglages du polarographe sont donnés dans le Partie Experimentale. Les solutions de bromate et d'iodate de potassium étaient à la concentration de 2×10^{-3} M dans le tampon. Le Tableau 1 montre que les comportements polarographiques des deux anions diffèrent. La variation des potentiels de pics est linéaire pour les bromates qui passent de—0,45 V (vs. ECS) à pH 0 à une valeur presque constante (—1,07 V) à partir de pH 3. La variation du potentiel des iodates est linéaire mais plus lente (0 V vs. ECS pour pH 0 à —0,60 V pour pH 5); entre pH 5 et 6 le pic disparait puis le potentiel passe brusquement vers —1,20 V et garde pratiquement cette valeur. Les deux vagues de réduction des deux anions sont donc séparées de 50 mV environ en milieu acide; elles sont confondues à pH 6,5; au delà, la vague des iodates est plus négative de 0,10 V.

L'intensité du courant de pic montre de très grandes variations avec le pH (Tableau 1). En ce qui concerne la largeur de bande à mi-hauteur ($\Delta E_{Ip/2}$), le Tableau 1 montre qu'elle est maximum à pH 2 pour le bromate et pH 3 pour l'iodate. A pH 0, elle est minimum (plus grande réversibilité de la réduction) pour les deux ions.

Influence des réglages du polarographe

Les meilleures sensibilités étant obtenues à pH 0, nous avons étudié l'influence de l'angle de phase de détection dans l'acide perchlorique 1 M. Le Tableau 2 montre que la meilleure sensibilité est obtenue entre 0 et

TABLEAU 1

Influence du pH sur les paramètres polarographiques pour les ions BrO_3^- et IO_3^-[a]

pH	BrO_3^-			IO_3^-		
	E_p	$\Delta E_{Ip/2}$ (mV)	I_p (nA)	E_p	$\Delta E_{Ip/2}$	I_p (nA)
0	—0,45	270	530	0,00	120	1700
1	—0,65	370	360	—0.14	160	1200
2	—0,85	530	195	—0,34	210	540
3	—1,03	430	60	—0,43	285	70
4	—1,07	390	6	—0,51	260	20
5	—1,07	360	6	—0,60	230	1,6
6	—1,07	350	6	—0,70	220	0
7	—1,07	330	5,5	—1,10	200	450
8	—1,07	330	4	—1,22	180	540
9	—1,10	330	3,5	—1,26	160	650
10	—1,10	330	3	—1,26	130	980

[a] E_p (vs. ECS), potentiel de pic; $\Delta E_{Ip/2}$, largeur de pic à mi-hauteur; I_p, intensité du pic.

+ 25 grades. Le Tableau 3 indique que l'intensité due au pic de bromate reste constante quelle que soit la fréquence de la tension surimposée allant de 3 à 150 Hz. Par contre l'intensité résiduelle (I_r) augmente linéairement avec la fréquence.

L'étude de l'amplitude de la tension alternative entre 1 et 200 mV montre que, conformément à la théorie, l'intensité du pic n'augmente pas linéairement avec l'amplitude de la tension surimposée (Tableau 4). L'intensité est cependant multipliée par un facteur voisin de 100 entre 1 et 100 mV.

Interprétation et conséquences pratiques

Les résultats montrent qu'un pH très bas ($HClO_4$ 1M) permet à la fois d'avoir la meilleure sensibilité et de ne pas risquer l'interférence éventuelle de l'iodate, réductible à des potentiels supérieurs de 50 mV. La largeur des pics à mi-hauteur, assez grande (Tableau 1) traduit bien l'irréversibilité de la réduction qui est maximum vers pH 2 (vers pH 3 pour l'iodate) et minimum à pH 0. Un calcul approximatif selon Breyer et Bauer [21] indique un coefficient de transfert ($\alpha > 0{,}9$) pour la réduction de bromate qui traduit une irréversibilité importante.

TABLEAU 2

Influence de l'angle de phase de détection (ϕ) sur l'intensité de pic (I_p)[a]

ϕ (grades)	−50	−25	0	+25	+50	+75	+100	+125	+150
I_p (nA)	360	475	600	600	475	315	200	205	250

[a] ω = 90 Hz; ΔE = 5 mV; pH = 0 (1 M $HClO_4$); 2 × 10^{-3} M BrO_3^-.

TABLEAU 3

Influence de la fréquence (ω) sur les intensitiés du courant total (I_t), residuel (I_r) et du courant de pic (I_p)[a]

ω (Hz)	3	7	10	14	30	50	70	80	90	100	150
I_t (nA)	13	19	25	31	57	91	119	134	150	166	245
I_r (nA)	7	12	18	24	49	82	112	126	142	158	238
I_p (nA)	6	7	7	7	8	9	7	8	8	8	7

[a]Pour les autres conditions, voir Tableau 2.

TABLEAU 4

Influence de l'amplitude (ΔE) de la tension alternative sur l'intensité du pic (I_p) et sa largeur à mi-hauteur ($\Delta E_{Ip/2}$)

ΔE (mV)	1	2	5	10	20	50	100	200
I_p (nA)	104	224	610	1240	2500	5900	9600	14000
$\Delta E_{Ip/2}$ (mV)	290	285	265	265	270	270	330	455

La fréquence du signal surimposé a peu d'influence sur l'intensité mais, comme elle augmente linéairement le courant résiduel, les mesures les plus favorables sont obtenues à basse fréquence (3 Hz).

L'intensité maximum observée pour un angle de phase de 0° confirme l'irréversibilité de la réduction. L'accroissement de 0 à 100 mV de l'amplitude de la tension alternative ne modifie pas sensiblement la largeur des pics mais accroît la sensibilité d'un facteur 100.

En pratique les conditions les plus favorables à un dosage de bromate sont donc les suivantes: pH de mesure voisin de zéro ($HClO_4$ 1 M), tension alternative de 3 Hz avec une amplitude pouvant aller jusqu'à 100 mV, angle de phase de détection de 0°, frequénce de chute du mercure de 1 goutte s^{-1}.

Limite de détection et sensibilité du dosage polarographique du bromate

La limite de détection ou concentration donnant un signal égal à deux fois le bruit de fond a été recherchée en opérant avec la sensibilité maximum de l'appareil (12,5 nA pour 25 cm) et une amplitude de 20 mV pour la tension alternative. La Fig. 1 montre les enregistrements obtenus avec une solution de concentration égale à 2×10^{-6} M: le signal obtenu est de 0,78 nA (3,9 cm) et se distingue parfaitement du bruit de fond. On peut donc considérer la limite de détection à environ $0{,}5 \times 10^{-6}$ M. Le Tableau 5

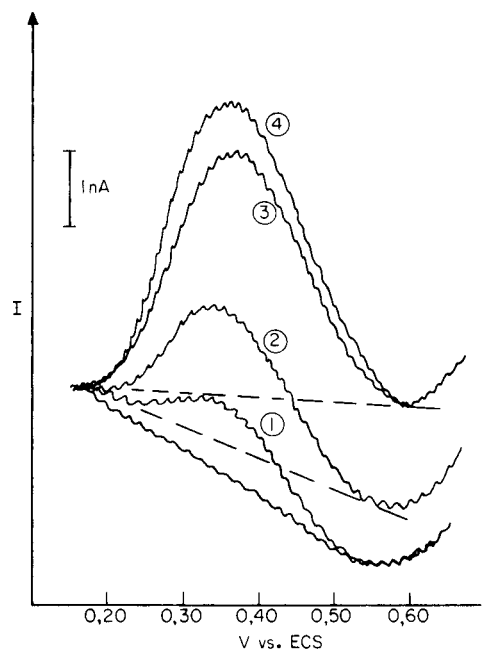

Fig. 1. Recherche de la sensibilité et de la limite de détection. Concentration en BrO_3^-: (1) 1×10^{-6} M; (2) 2×10^{-6} M; (3) 3×10^{-6} M; (4) 4×10^{-6} M.

TABLEAU 5

Limites de détection expérimentale (10^{-6} M) et théoriques (avec 1 à 4 étapes du procédé multiplicateur)

Limites de détection (L.D.)	
Procédé Multiplicateur	L.D. (M)
Aucun	10^{-6}
1 étape	$0{,}2 \times 10^{-6}$
2 étapes	$2{,}8 \times 10^{-8}$
3 étapes	$4{,}6 \times 10^{-9}$
4 étapes	$0{,}8 \times 10^{-9}$

donne les limites de détection réelles obtenues lors de la mise en oeuvre du procédé chimique multiplicateur de sensibilité: on atteint une limite de détection de l'ordre du nanogramme de brome en effectuant quatre étapes d'oxydation. La polarographie sinusoïdale est donc cent fois plus sensible (10^{-6} M) que la colorimétrie de la bromorosaniline (10^{-4} M) [4] et sa limite de détection peut facilement être abaissée d'un facteur mille. La sensibilité du dosage polarographique, etudiée entre 1×10^{-5} et 4×10^{-5} M, a été trouvée à 7,75 nA/10^{-5} M.

PARTIE EXPERIMENTALE

Les réglages de l'appareil (polarographe Tacussel PRG 3) étaient les suivants: fréquence de la tension alternative surimposée (ω) 90 Hz; amplitude de la tension alternative surimposée (ΔE) 5 mV; angle de phase de détection (ϕ) = 0°; vitesse de balayage des potentials (v) = 120 mV min^{-1}; hauteur du mercure (h) 60 cm; fréquence de chute du mercure (f) = 1 goutte s^{-1}.

Les enregistrements étaient réalisés après désoxygénation des solutions par barbotage d'azote.

Application au dosage du brome sanguin et urinaire

Extraction du brome sanguin. Le sérum (1 ml) est déféqué par addition de 2 ml d'acide perchlorique à 10%. Après centrifugation, 1 ml de filtrat est additionné de 1 ml de tampon phosphate pH 6,5 en concentration molaire et de 1 ml de solution d'hypochlorite de sodium titrant 0,4 degré chlorométrique. Après 5 min d'oxydation, on porte 30 s à l'ébullition pour éliminer l'hypochlorite et on complète à 3 ml avec de l'eau distillée: on obtient la solution A, contenant l'ion bromate.

Dans l'étape (1), le brome libéré par 2 ml de solution A, additionnés de 2 ml de NaBr 2 M, est ensuite extrait par 2 ml de chloroforme. La phase chloroformique est agitée avec 0,05 ml d'ammoniaque pure. On ajoute 1 ml de tampon phosphate pH 6,5 et 2 ml d'hypochlorite à 0,4 degré

chlorometrique et après 5 min de contact et 30 s d'ébullition, on complète à 3 ml avec de l'eau distillée; on obtient la solution B de bromate.

Dans l'étape (2), sur la solution B, on répète une fois le procédé énoncé (étape 1) afin d'obtenir une solution C renfermant une concentration de bromate égale à 36 fois celle du sérum (solution A). Ce procédé chimique multiplicateur de sensibilité peut d'ailleurs être répété si l'on désire sensibiliser le dosage.

Extraction du brome urinaire. Une prise d'essai de 2 ml d'urine diluée dans 1 ml de solution tampon de phosphate pH 6,5 molaire est oxydée par 1 ml d'hypochlorite à 0,4 degré chlorométrique. Après 5 min d'oxydation et quelques secondes d'ebullition, on complète au volume de 5 ml avec de l'eau distillée (solution A de bromate). En répétant les opérations d'oxydation indiquées (étapes 1 et 2) pour le sang, on peut obtenir, si nécessaire, les solutions B et C.

Dosages polarographiques. Des aliquotes de 0,5 ml des solutions A, B ou C précédentes sont diluées dans 7,5 ml d'acide perchlorique à 15% (solution voisine de 1 M) et l'enregistrement polarographique est effectué entre —0,10 et —0,60 V (vs. ECS). On répète l'enregistrement après addition à la solution précédente d'un ajout de bromate sensiblement égal à la quantité trouvée dans l'essai et sous un volume de 0,1 ml.

Enfin, un troisième polarogramme est enregistré après addition à la solution de 0,1 ml de NaBr 1 M. On détruit ainsi le bromate présent et l'enregistrement permet d'établir la ligne de base (blanc essai) et de vérifier l'identité du pic de bromate enregistré.

RESULTATS ET DISCUSSION

Nous avons réalisé une série de dosages sur 10 sérums provenant de malades hospitalisés pris au hasard. Dans tous les cas, trois étapes d'oxydation ont été utilisées (facteur multiplicateur de sensibilité égal à 36), et chaque dosage a été pratiqué sur deux échantillons (sérum pur et sérum chargé avec 0,60 mmol de NaBr). Enfin chaque détermination a été faite en traçant un polarogramme après addition d'un ajout dosé de bromate. Nous avons pu ainsi calculer le pourcentage de récupération de brome ajouté au départ dans le sérum. Le Tableau 6 indique des taux sériques compris entre 0,038 et 0,695 mmol l^{-1} (moyenne 0,136 mmol l^{-1}) et un pourcentage du récupération du brome ajouté au sérum allant de 90 à 101% (moyenne 95,1%).

Nous avons testé la reproductibilité de la méthode en répétant 10 fois le dosage sur un pool de sérums contenant 0,095 mmol l^{-1} du brome selon la même méthode que ci-dessus. La reproductibilité est excellente (C.V. = 0,75%), et la récupération du brome ajouté est 99,3—100%.

Chez 10 malades nous avons dosé l'halogène dans le sérum et les urines de 24 h. Le Tableau 7 montre que les dosages ont lieu avec un bon rendement (98,7% sur les sérums et 99,8% sur les urines). Les rapports

TABLEAU 6

Etude du brome sérique et du taux de récupération

Sérum no.	Taux sériques (mmol l^{-1})		Récupération de la charge (%)
	Sérum	Sérum chargé	
1	0,057	0,610	93
2	0,000	0,500	90
3	0,695	1,260	97
4	0,076	0,643	95
5	0,038	0,572	90
6	0,191	0,872	101
7	0,057	0,620	94
8	0,076	0,649	96
9	0,076	0,649	96
10	0,095	0,690	99,3
Moyennes	0,136	/	95,1

TABLEAU 7

Comparaison des taux sériques et urinaires du brome chez dix malades pris au hasard

Malade no.	Sérum (mmol l^{-1})			Urine (mmol l^{-1})			Rapport sérum/urine
	Direct	Chargé avec 0,60 mmol l^{-1}	Récupération (%)	Direct	Chargée avec 0,60 mmol l^{-1}	Récupération (%)	
1	0,228	0,808	97,6	0,040	0,635	99,22	5,7
2	0,217	0,800	97,7	0,038	0,638	100,00	5,7
3	0,448	1,047	99,9	0,076	0,675	99,85	5,9
4	0,218	0,808	98,8	0,039	0,637	99,69	5,6
5	0,336	0,916	97,9	0,058	0,657	99,85	5,8
6	0,115	0,700	97,9	0,020	0,621	100,16	5,7
7	0,106	0,703	99,6	0,019	0,617	99,68	5,6
8	0,228	0,827	99,9	0,040	0,639	99,84	5,7
9	0,173	0,763	98,7	0,030	0,627	99,52	5,8
10	0,058	0,647	98,3	0,010	0,609	99,84	5,8
$\bar{x}$	0,213		98,7	0,037		99,80	5,73

entre les taux sériques et urinaires se situent entre 5,7 et 5,9 (moyenne 5,73). Il semble donc que ce rapport soit remarquablement constant d'un individu à l'autre.

La méthode que nous proposons s'est avérée d'une parfaite sélectivité (même en présence de grandes quantités de chlorures) et d'une grande fiabilité. Les taux généralement trouvés dans le sérum et les urines, de l'ordre de 10^{-4} M, sont aisément dosés, alors qu'ils se situent au seuil de détection de la plupart des autres méthodes.

Le procédé chimique multiplicateur de sensibilité permet de repousser les limites de détection dans la zone 10^{-9} M (79,9 ng) par le procédé polarographique. Il est bien entendu applicable à toutes les autres tech-

niques de dosage et en particulier permet de sensibiliser les méthodes colorimétriques habituelles ce qui devrait les rendre plus fiables pour la mesure des taux biologiques.

Nous remercions Monsieur Jolivet, Pharmacien des Hôpitaux, d'avoir bien voulu nous communiquer la liste des spécialités pharmaceutiques françaises à base de bromures, et Mlle. Ch. Bichon pour la collaboration technique.

BIBLIOGRAPHIE

1 R. F. Barbour, F. Pilkington et W. Sargent, Br. Med. J., 2 (1936) 957.
2 S. Natelson et M. K. Clark, Proc. Soc. Exp. Biol. Med., 90 (1955) 723.
3 G. Hunter et A. Goldspink, Analyst, 79 (1954) 467.
4 J. F. Goodwin, Clin. Chem., 17 (1971) 544.
5 Z. G. Szabo et L. Csanyi, Anal. Chim. Acta, 6 (1952) 208.
6 G. Hunter, Biochem. J., 60 (1955) 261.
7 H. Baubigny, C. R. Acad. Sci., 125 (1897) 654.
8 F. Hahn, C. R. Acad. Sci., 197 (1933) 245.
9 G. Deniges et G. Schelle, C. R. Acad. Sci., 155 (1912) 721.
10 A. Hussain et R. Bawarshi, J. Pharm. Sci., 68 (1979) 513.
11 R. E. Wenk, J. A. Lustgarten, N. Johnpappas, R. I. Levy et R. Jackson, Am. J. Clin. Pathol., 65 (1976) 49.
12 S. S. Levinson et S. V. Reider, Clin. Chim. Acta, 52 (1974) 249.
13 E. F. Orlemann et I. M. Kolthoff, J. Am. Chem. Soc., 64 (1942) 1970.
14 M. Hemala, Chem. Listy, 47 (1953) 1323.
15 A. Rylich, Collect. Czech. Chem. Commun., 7 (1935) 288.
16 B. Breyer et S. Hacobian, Aust. J. Sci., Res., A4 (1951) 610.
17 G. A. Rechnitz et M. R. Kresz, Anal. Chem., 38 (1966) 1786.
18 E. R. Wright, R. A. Smith et S. Blach, in D. F. Boltz (Ed.), Colorimetric Determination of Nonmetals, Interscience, New York, 1958, p. 181.
19 I. M. Kolthoff et H. Yutzy, Ind. Eng. Chem., Anal. Ed., 9 (1937) 75.
20 I. M. Kolthoff et J. J. Lingane, Polarography, 2ème édn., Vol. 2, Interscience, New York, 1952, p. 574.
21 B. Breyer et H. H. Bauer, Alternating Current Polarography and Tensammetry, Interscience, New York, Vol.13 (1952) 51.

Analytica Chimica Acta, 120 (1980) 75—80

DETERMINATION OF ETHANOL BY AIR-STREAM SEPARATION WITH FLOW INJECTION AND ELECTROCHEMICAL DETECTION AT A NICKEL OXIDE ELECTRODE

T. N. MORRISON, K. G. SCHICK and C. O. HUBER*

Department of Chemistry, University of Wisconsin-Milwaukee, Milwaukee, WI 53201 (U.S.A.)

(Received 14th April 1980)

SUMMARY

Ethanol is separated by an air stream from a 1-ml sample with collection in 1 ml of 0.2 mol l^{-1} sodium hydroxide. Measurement is by voltammetry at a tubular, catalytic nickel oxide electrode with 30-μl sample injected into a continuous flow stream. Relative standard deviation for repetitive measurements is 1.8% for synthetic samples. Serum samples extracted for 100 s and then measured yielded linear results for concentrations of 2×10^{-4}—5×10^{-2} mol l^{-1} ethanol (0.001—0.23%), with relative standard deviation of 2.0%. The time per determination was about 2 min.

The determination of alcohols in solution has been reviewed by Jain and Cravey [1]. Current developments in such determinations appear to continue to depend largely upon gas chromatography or enzyme-based reactions [2]. The technique presented here involves separation of the alcohol by an air stream purge and trap method followed by electrochemical measurement at a nickel oxide electrode with a flow injection technique.

The nickel oxide anodic electrode process used here provides some selectivity, but not enough for all samples. Therefore, a separation procedure preceding the electrochemical step is needed. Separation based on volatility is the choice in this case. Methods involving equilibration between ethanol in the liquid and vapor phases (i.e., head-space equilibrium techniques) are, however, too slow even at elevated temperatures. In contrast, a dynamic purge and trap technique based on the rate of vapor transfer is suitably rapid.

The measurement step involves electrochemical oxidation at a nickel electrode. This electrode reaction has been studied by Fleischman and others [3—5] and has found analytical application for glucose [6]. The suggested mechanism is of the catalytic type, i.e.,

$$Ni(OH)_2 + OH^- \rightarrow NiO(OH) + H_2O + e^-$$
$$NiO(OH) + RCH_2OH \xrightarrow{r.d.s.} Ni(OH)_2 + \dot{R}CHOH$$
$$\dot{R}CHOH \rightarrow \text{products}$$

The electrolyte solution consists of 0.2 mol l^{-1} sodium hydroxide with trace amounts of nickel in solution, probably as $(NiOH^+)_4$. The soluble nickel ensures long-term stability of the electrode process.

The flow-through electrode in conjunction with the flow injection technique is used in order to reproduce convection effects conveniently at the electrode. Since the electrode reaction involves oxidation of an oxide layer, the current level increases with increasing pH. Thus, any pH shift of the sample from that of the electrolyte will impose a corresponding effect on the analytical signal. For this reason, the procedure uses electrolyte solution in the collection trap during the separation step. Advantages of the flow injection technique have been reviewed [7]. In the application reported here, the additional advantage of ready maintenance of an active electrode surface is significant.

The analytical procedure reported here appears to offer advantages of inexpensive reagents, easily maintained apparatus, and measurement times of about 2 min per sample. It is applicable to several low-molecular-weight alcohols in solution and to ethanol in serum samples without previous deproteinization.

EXPERIMENTAL

Reagents

All chemicals were reagent grade unless indicated otherwise. The background electrolyte consisted of 0.20 mol l^{-1} sodium hydroxide to which 0.1 mmol l^{-1} $NiSO_4$ was added. Although nickel(II) is thermodynamically soluble in 0.2 mol l^{-1} sodium hydroxide as its hydroxide complex, it is difficult to prevent partial formation of insoluble nickel hydroxide. When some insoluble hydroxide is present, use of the supernatant solution above the settled precipitate proved to be satisfactory.

A stock solution in distilled water of 0.514 mol l^{-1} ethanol was prepared using absolute ethanol, and standard solutions in distilled water were prepared from this stock solution. A second stock solution of ethanol in background electrolyte was 0.685 mol l^{-1}. Serum samples containing 0.92—230 mg dl^{-1} were prepared by additions of ethanol standard solutions to 1.00 ml of pooled blood serum. Three drops of light hydrocarbon oil were added to the sample solution in the separator to prevent foaming during extraction. The collector solution for the extraction consisted of background electrolyte.

Apparatus

The simple extraction system is shown in Fig. 1. It consists of two 13 mm × 5 cm test tubes connected by 0.5 mm i.d. fluorinated polyethylene tubing to a small diaphragm pump. The air flow rate was 150 ml min^{-1}.

The continuous-stream flow-injection system is depicted in Fig. 2. It consists of a gravity-feed electrolyte reservoir, a sample injection valve (Rheodyne Model 50-41) fitted with a 30-μl sample loop, and a flow-through electrochemical detector cell. The channel diameter for the continuous stream is 0.8 mm. Fluorinated polyethylene tubing was used for connections. The tubing length from injector to detector was 20 cm. The electrolyte flow rate was 2 ml min^{-1}.

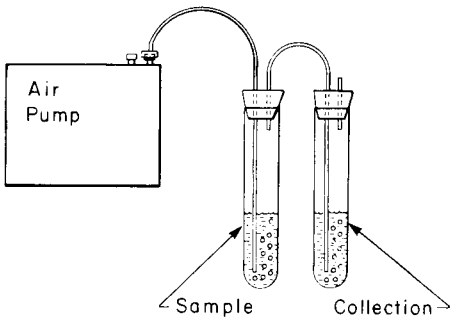

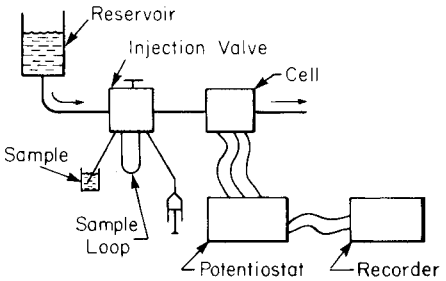

Fig. 1. Ethanol extraction apparatus.

Fig. 2. Flow injection system.

The electrochemical cell design is shown in Fig. 3. The cell housing is constructed of molded epoxy resin (Buehler Ltd., Evanston, IL) which was machined to provide the channels and to accommodate the fittings. The nickel working electrode was molded into the cell block before the sample channel was drilled. Thus the working electrode is a short tubular electrode of length 1.3 mm. The applied potential to the working electrode is 0.55 V vs. the mercury/mercury(II) oxide reference electrode. (0.47 V vs. SCE). Between uses the cell is stored with electrolyte in place and open circuit.

The mercury/mercury(II) oxide reference electrode was fashioned using a 6 mm × 3 cm polyethylene tube with epoxy resin seals for the platinum electrical contact. The auxiliary electrode was a 1 × 20 mm platinum wire fastened into the exit port using epoxy resin.

The potentiostat-current follower circuit was constructed using conventional analog operational amplifier circuit design [8]. The two operational amplifiers used were Motorola 356. The ±15 V d.c. power supply was Polytron P31, Paterson, NJ. The circuit is rather easily and inexpensively constructed or complete units are commercially available. Readout is by means of a potentiometric strip-chart recorder.

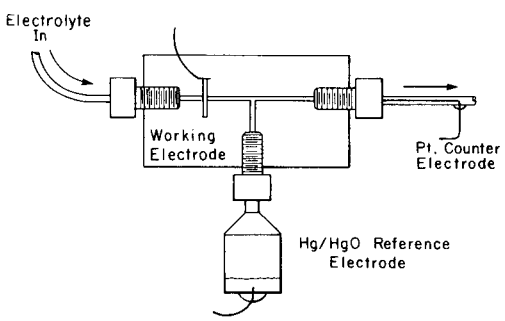

Fig. 3. Electrolyte cell.

Procedure

A sample determination consists of placing 1.00 ml of sample in the extractor sample tube and passing the air stream for 100 s. The collector tube solution is drawn into the sample loop and then injected into the flowing electrolyte stream. The signal consists of a peak current superimposed upon the background current. Peak height or peak area can be linearly related to alcohol concentration.

RESULTS AND DISCUSSION

Measurement characteristics

The analytical signal is a peak with a sharp initial rise and a somewhat slower decay with some tailing as the baseline is approached. Under the conditions used in this study, full recovery of the baseline is achieved in less than 15 s. The apex is obtained in 2—3 s. The extrapolated peak width at the base line is 5—10 s.

When 30-μl samples of ethanol in electrolyte are injected, the analytical current is linear in the concentration range from 0.005—4 mmol l^{-1}. The regression equation had a slope of 1.91 μA $mmol^{-1}$ l^{-1}, an intercept of 0.0001 μA, and a standard error of the estimate of 0.02 μA. The lower determination limit on the linear range is due to the signal noise. The upper limit is probably due to saturation of the surface-active sites of the working electrode by the analyte [3]. The response characteristics for three separate cells were in quantitative agreement.

Separation characteristics

The liquid volumes used in the extractor sample and collector tubes determine the contact times of bubbles with the solution. The analytical current obtained varies linearly with the sample tube solution volume but has a non-zero intercept. The analytical current is also linearly related to the collector tube solution volume with a non-zero intercept. Further, the current eventually levels as the collector volume is increased. The non-zero intercept may indicate that a substantial amount of transfer takes place at the surface of the solution. This suggestion is further supported by the fact that the collection efficiency was distinctly improved by decreasing the size of the air exit orifice of the collector vessel in order to minimize mixing with outside air. The analytical current varies linearly with purging time with a zero intercept. The above observations indicate that both the solution—vapor transfer in the sample tube, and the vapor—solution transfer in the collector tube are rate-controlled and therefore depend upon reproducible physical dimensions and purging time. Determining ethanol-in-water samples ranging from 0.25 to 48 mmol l^{-1} using a 1.00-ml sample solution and a 1.00-ml electrolyte collector solution with a 100-s purging time resulted in a calibration plot with a slope of 1.02 μA $mmol^{-1}$ l^{-1}. Comparing this linear range to that stated earlier for the isolated measurement step suggests that the extraction efficiency, although more than adequate, is less than 10%.

The sensitivity of the method exceeds that usually required for serum samples (a typical legal limit is 20 mmol l^{-1}); therefore, extraction parameters were not optimized. The larger the sample used, the more ethanol will be removed. The specific amount, however, is also dependent on the size and shape of the container. A reasonable measurement could readily be made with a much smaller volume and a shorter collection time than used here. With the apparatus described here, a satisfactory signal was obtained after as little as 25-s purge time. Extractor vessel size and shape as well as purge time can readily be adjusted in order to place the analytical current for a sample within the linear range. The needs of the individual user must dictate the final parameters of the separation system.

Temperature effects

Both the air stream extraction step and the electrochemical measurement step have a temperature-dependence. The extraction temperature effect is measured by simply immersing the apparatus in a controlled temperature bath. Over the range 23—31°C a positive linear dependence of 5%/°C is observed. The electrochemical measurement temperature effect is observed by immersing a 1-m coil for background electrolyte, the sample loop, and the electrochemical cell with reference electrode in a controlled temperature water bath. The mercury/mercury(II) oxide reference electrode potential temperature effect is −0.25 mV/°C [9] and so is relatively negligible. (The dependence of analytical current on applied potential of the working electrode is typically less than 0.05% mV^{-1}.) The experimental temperature dependence of analytical signal is positive: 7%/°C over a temperature range of 23°—33°C. The overall temperature dependence for the method can thus be estimated as 12%/°C. The background current temperature effect is 0.2 μA/°C with a typical room temperature background current of about 2 μA (i.e., ca. 10%). Practical laboratory apparatus considerations favor using the ambient laboratory atmosphere conditions for temperature control. This practice was adopted for the work reported here. Obviously, temperature shifts of more than approximately 0.5°C between samples and standards must be avoided.

Analytical results

A linear calibration plot passing through the origin was obtained for samples of pooled serum to which ethanol had been added, in the concentration range 0.2—50 mmol l^{-1} ethanol (0.001—0.23%). The regression equation for the analytical current has a slope of 0.16 μA $mmol^{-1}$ l^{-1}, an intercept of 0.03 μA, and standard error of the estimate of 0.02 μA. The extraction was found to be somewhat more efficient for ethanol in serum than for ethanol in distilled water. This may be attributed to a "salting-out" effect arising from the higher ionic strength of the serum. This ionic strength effect is relatively slight. It should, for example, not cause significant errors in measuring different serum samples. When standard ethanol solutions were

prepared in a physiological normal saline solution, the results matched those for serum.

Selectivity

Other low-molecular-weight alcohols as well as aldehydes and amines react at the nickel oxide electrode and thus are possible interferences. Under normal conditions, these other compounds are present in such low concentrations that the error is negligible [10]. When ethanol is metabolized, acetaldehyde is an intermediate. Although it is volatile and electroactive, concentrations are very much lower than for the ethanol [11] and measurement errors are negligible. Acetone, which for certain pathological conditions can be present in serum up to levels of 13 mmol l^{-1}, was experimentally shown to be both inactive and noninterfering at the electrode for concentrations exceeding 14 mmol l^{-1}. Furthermore, vapor extractions of 15 mmol l^{-1} ethanol from solutions with and without 14 mmol l^{-1} acetone yielded identical results.

Although acetone does not interfere in the method, its solvent properties require that plastics other than fluorinated polyethylene be avoided for the flow-stream apparatus. Acetyl acetate, sometimes present in serum, is the anion of a strong acid and thus would not be vapor-extracted. Its enzymatic conversion product, β hydroxy butyrate, is not sufficiently volatile to interfere (b.p. 130°C at 12—14 torr). Alcohols other than ethanol may at times be ingested and thus be present in measurable amounts. Methanol and n-propanol give the same response as ethanol within experimental error. The isopropanol response is approximately one-third that of ethanol.

Instrumentation Laboratory, Inc. provided support for a portion of the work reported here.

REFERENCES

1 N. C. Jain and R. H. Cravey, J. Chromatogr. Sci., 10 (1972) 257.
2 F. S. Cheng and G. D. Christian, Clin. Chem., 24 (1978) 621.
3 M. Fleischman, K. Kovinek and D. Pletcher, J. Electroanal. Chem., 31 (1971) 39.
4 M. V. George and K. S. Balachandran, Chem. Rev., 75 (1975) 491.
5 M. Amjad, D. Pletcher and C. Smith, J. Electrochem. Soc., 124 (1977) 203.
6 K. G. Schick, V. G. Magearu and C. O. Huber, Clin. Chem., 24 (1978) 448.
7 J. Růžička and E. H. Hansen, Anal. Chim. Acta, 114 (1980) 19.
8 P. T. Kissinger, C. Refshauge, R. Dreiling and R. N. Adams, Anal. Lett., 6 (1973) 465.
9 A. J. Bethone and N. A. S. Loud, Standard Aqueous Electrode Potentials and Temperature Coefficients, Clifford A. Hampel, Slokie, Il., 1964, p. 15.
10 H. H. Liebich and J. Wöll, J. Chromatogr., 142 (1977) 505.
11 J. F. Brien and C. W. Loomis, Clin. Chim. Acta, 87 (1978) 175.

Analytica Chimica Acta, 120 (1980) 81—92

DIFFERENTIAL POTENTIOMETRIC TITRATIONS OF BINARY MIXTURES OF HALIDES WITH TWO ION-SELECTIVE INDICATOR ELECTRODES

LJILJANA S. JOVANOVIĆ, JULIJA D. FIŠL[a] and FERENC F. GAÁL*

Institute of Chemistry, Faculty of Sciences, University of Novi Sad (Yugoslavia)

(Received 2nd January 1980)

SUMMARY

Differential potentiometric titrations with two different ion-selective indicator electrodes are described. Ion-selective electrodes for Cl^-, Br^-, I^-, F^-, S^{2-}, as well as glass and silver billet electrodes were used. The method was tested in the determination of binary mixtures of halides (Cl^-, Br^-, I^-, and F^-) by titration with solutions of silver nitrate, alone and mixed with lanthanum or thorium nitrate as required. Various factors influencing the determination were investigated. Results of simultaneous determinations of mixtures were in good agreement with the results of separate determinations within certain concentration limits. The method was successfully applied to the determination of a four-component halide mixture. Titrations of mixtures of fluoride with thiocyanate or hexacyanoferrate(III), and some other possibilities, are also reported.

The common potentiometric cell consisting of one ion-selective indicating electrode coupled with a reference double-junction electrode is inconvenient for measurements in which elimination of the liquid-junction potential is required. But, if one membrane electrode is kept in a solution with constant activity of the ion for which it is selective, a reference electrode without liquid-junction potential can be obtained. For this purpose, fluoride-selective [1, 2] and perchlorate-selective [2] electrodes have already been applied to the estimation of complexes of silver with acetonitrile and allyl alcohol. A thorough study on differential potentiometry with ion-selective electrodes, theory and instrumentation, with an original construction of a differential amplifier has been reported by Brand and Rechnitz [3]. They used a glass electrode as the reference in several complexim etric titrations. However, the introduction of a second ion-selective electrode to the electrode pair, in the role of the indicating electrode, offers further possibilities for their application to determinations of ion mixtures. In connection with this, differential potentiometry with electrodes of similar selectivity can improve the titrations of mixtures of ions with similar chemical behaviour. One such possibility was used by Popescu et al. [4] who applied two membrane electrodes, Ag_2S/-

[a]Permanent address: Institute for Productional Engineering, Faculty of Technical Sciences, University of Novi Sad, Yugoslavia.

AgI and Ag_2S, to follow the course of discontinuous argentimetric titrations of potassium cyanide alone and in mixtures with potassium bromide or iodide. At the end-points, they obtained either the usual potential jumps, or potential changes similar to the first or second derivative.

The determination of chloride, bromide, and iodide in various mixtures by different methods has been widely investigated. The most frequently applied are, surely, titrations with silver(I) ions, which can be quite successfully followed by potentiometry with silver halide electrodes. However, the fourth halide, fluoride, because of its different chemical nature, cannot be titrated with the same reagent as the other halides, and must be determined in a separate titration, for example with thorium(IV) or lanthanum(III). With the intention of determining all four halides in one titration, Chou and Sams [5] used a mixed titrant containing silver and thorium nitrates. The end-points of the derivative titration curves were determined by means of a platinum billet electrode with recording of the peaks for all four halides. In an attempt to reproduce these results, Selig [6] found that the peak for fluoride did not appear, because the platinum electrode did not respond to the fluoride concentration change.

In order to solve this analytical problem, it is shown here that a silver halide electrode can be coupled with the lanthanum(III) fluoride electrode and that this pair of indicating membrane electrodes can be used to follow the course of successive titrations of all four halides in a mixture. Since the problem normally reduces to the titration of binary mixtures of fluoride with some other halide, investigations were directed to a detailed analysis of such cases. Some theoretical aspects of the application of two different ion-selective electrodes in potentiometric titrations of binary mixtures, the choice of experimental conditions, and the results of determination of halide mixtures are described in the subsequent text.

THEORY

In a solution of ions A and B, two membrane electrodes, ISE_A and ISE_B, selective to the corresponding ion, are immersed. With regard to the interferences which may arise from the other ion at each electrode, three possible cases can be distinguished: (a) each electrode is sufficiently selective for only one ion; (b) only one electrode is selective for both ions, but the selectivities are different; (c) both electrodes are selective for both ions, but the selectivities are different.

In the first case, the potential E of each electrode is given by the following simplified Nernst equations

$$E_A = E_A^0 + f_1 \log a_A \tag{1}$$

$$E_B = E_B^0 + f_2 \log a_B \tag{2}$$

where E_A^0 and E_B^0 are constants characteristic of the corresponding electrode, f_1 and f_2 are the fractions of the Nernstian response of the electrode, and

a_A and a_B are the activities of ions A and B in the solution. The e. m. f. of the cell is then

$$\text{e.m.f.} = E_A - E_B = E_A^0 - E_B^0 + f_1 \log a_A - f_2 \log a_B \quad (3)$$

For case (b), electrode ISE_A is considered to be sufficiently selective for ion A, but to a lesser extent for ion B. The potential of this electrode will be the logarithmic function of activities of both ions, as in the Nikolski equation

$$E_A = E_A^0 + f_1 \log[a_A + K_{A,B}^{pot} (a_B)^{z_A/z_B}] \quad (4)$$

where $K_{A,B}^{pot}$ denotes the selectivity coefficient and z_A and z_B are integers with the value and sign of the valencies of ions A and B. The potential difference between such an electrode and ISE_B (eqn. 2) is

$$\text{e. m. f.} = E_A - E_B = E_A^0 - E_B^0 + f_1 \log[a_A + K_{A,B}^{pot} (a_B)^{z_A/z_B}] - f_2 \log a_B \quad (5)$$

In case (c), the potentials of the two electrodes ISE_A and ISE_B are given by the appropriate version of eqn. (4), and the e. m. f. of the cell can be written

$$\text{e. m. f.} = E_A - E_B = E_A^0 - E_B^0 + f_1 \log[a_A + K_{A,B}^{pot}(a_B)^{z_A/z_B}]$$
$$- f_2 \log[a_B + K_{B,A}^{pot} (a_A)^{z_B/z_A}] \quad (6)$$

Since in all three cases (3), (5), and (6), the potential difference $E_A^0 - E_B^0$ is constant, the change in e. m. f. of the cell depends only on the logarithmic terms. Obviously, the e. m. f. of a particular cell may suffer multiple interferences, depending on the composition of the solution. This complicated influence can lead to poorer definition of the established potential when variable concentrations of ions are present in the solution. Since the linear relationship between the potential of the electrode, i.e. the e. m. f. of the cell, and the logarithm of the activity of one ion is lost, the method becomes inconvenient for direct potentiometric determinations. However, under suitably selected conditions, two different ion-selective electrodes can behave as the indicating electrodes in titrimetric determinations of ion mixtures. Primarily, this means that the titrant concentration must be chosen so that the locations of the equivalence points in the titration of each ion are sufficiently far apart. For example, in titrations with the electrode couple whose e. m. f. is formed according to eqn. (3), the concentration of one ion is appreciably changed (which is monitored by the corresponding ion-selective electrode), but the concentration of the second ion must remain relatively constant; here the second electrode plays the role of "reference" electrode. However, if the e. m. f. is formed on the basis of eqn. (6), then during the titration both electrodes are to an appreciable extent indicating, and this creates a much more complicated pattern of the potential change at the end-points.

In the present paper, differential potentiometric titrations of binary halide mixtures with various electrode pairs are reported. In mixtures without fluoride, the e. m. f. of the corresponding cells I^-/Br^-, Br^-/Cl^-, I^-/Cl^-,

S^{2-}/I^-, S^{2-}/Br^-, and S^{2-}/Cl^- follows eqn. (6), i.e. case (c). With all these electrodes, the titration curve of a mixture of two halides (without fluoride) usually shows a peak in the form of a first derivative, instead of a second potential jump. The appearance of such a signal is due to insufficient difference between the selectivity coefficients of the two electrodes, which is especially pronounced near the equivalence point of the more soluble salt.

In contrast, in mixtures containing fluoride, the activity of which is followed by the fluoride-selective electrode, regardless of whether the silver halide or silver sulphide electrode is coupled, the e. m. f. of the cell follows eqn. (3), i.e. case (a). The reason for this is, of course, the high selectivities of the fluoride-electrode with respect to other halides, and of the silver halide or silver sulphide electrodes to fluoride. Similar considerations hold when the fluoride-selective electrode is replaced by a glass electrode, in order to determine the end-point of a fluoride titration by monitoring the pH change [7—9] (see Discussion). In these titrations under suitable chosen conditions, one electrode behaves as the indicating electrode up to the first end-point while the other is almost a reference. After the first equivalence point, the electrodes reverse their roles, resulting in a potential jump at the second end-point in the direction opposite to the previous one.

EXPERIMENTAL

Chemicals and solutions

All chemicals used were of p. a. purity. The solutions were made by dissolving the appropriate exact weight of the solid substances in triply distilled water.

The stock solutions were of the following concentrations: 0.0250 M KI, KBr, KCl or KSCN; 0.0500 M NaF; 0.00833 M $K_3[Fe(CN)_6]$.

The titrants used were: 0.0250 M $AgNO_3$, 0.0250 M $AgNO_3$ + 0.00833 M $La(NO_3)_3$, 0.0250 M $AgNO_3$ + 0.04160 M $La(NO_3)_3$, 0.0500 M $AgNO_3$ + 0.0156 M $La(NO_3)_3$, 0.0250 M $AgNO_3$ + 0.00625 M $Th(NO_3)_4$.

Apparatus

Radiometer electrodes were used. The ion-selective electrodes were as follows: S^{2-} (Ag_2S), Cl^- (AgCl), Br^- (AgBr), I^- (AgI) and F^- (LaF_3). A glass electrode (G-202 C) was also used. In order to compare the results obtained with ion-selective electrodes, a silver billet electrode (Ag, 99.9999%) was applied.

Electrodes were connected directly to a Radiometer pHM 26 pH meter. With most of the electrodes, this caused no problems because of their relatively low impedances. Only the chloride and bromide ion-selective electrodes have very high impedances, and when this pair of electrodes was connected to the pH meter, electrical noise became a problem. This was diminished by placing the titration vessel in a tightly fitting, earthed Faraday cage. The signals from the pH meter were applied to a two-channel recorder (Servogor 2s

RE571) where they were registered both in the integral and first-derivative form. The end-points were determined graphically from the peaks on the derivative titration curves.

The titrants were added continuously from an automatic piston burette (Radiometer ABU 12) at a rate of 0.360 ml min^{-1}.

Procedure

Vessels of 50 or 100-ml were used and the necessary volumes of the test solutions were added from semiautomatic burettes. Then distilled water, potassium nitrate solution, and alcohol were added in amounts suitable to achieve the required contents at the second end-point. The total volume of the solution was 30—40 ml. The solution was mixed with a magnetic stirrer, and the electrodes were immersed. After the initial potential had stabilized, the titration was started with simultaneous connection of the automatic burette and the recorder.

The rate of addition of the titrant was especially important. The inflection points for all titrations were shifted to values higher than those stoichiometrically expected; this was most pronounced in the fluoride titration. The basic reason for this shift is, of course, that stabilization of the potential is very slow near the equivalence point in continuous precipitation titrations. Therefore, the rate of addition of the titrant must be the same in both the titrant standardization and the determination of mixtures. Moreover, standardizations must be carried out in the same way and under the same conditions as for determinations of mixtures. Where necessary the corresponding indicating ion-selective electrode can be coupled with an SCE through a salt bridge. The end-points of these titrations were determined graphically, from the maximum of the derivative titration curve. In this way, the maximal corrections for chemical and electrochemical factors influencing the determination of these ions in mixtures can be achieved.

RESULTS AND DISCUSSION

Titration of halides with silver nitrate solution

The first attempt at application of potentiometric titrations with two different indicator electrodes involved the determination of binary chloride, bromide, and iodide mixtures with silver nitrate solution. All suitable combinations of electrodes, Cl^-, Br^-, I^-, and S^{2-} ion-selective, and silver metal were investigated. The silver metal and sulphide-selective electrodes showed almost equal responses in all titrations. A certain advantage of the metal electrode was its faster potential equilibration, i.e. the sharper break on the curve; this was particularly pronounced when the more soluble salts, AgBr and AgCl, were formed. This was the reason for further investigation of the metal electrode.

Each pair of electrodes was investigated in various solvents: water, ethanol, methanol, and isopropanol (50% and 70% at the second end-point).

Addition of organic solvents suppressed the potential change and led to poor reproducibility of the titration curves. Therefore these titrations were done in aqueous solutions.

In order to improve precipitation characteristics and minimize adsorption, various electrolytes were added in amounts sufficient to keep the ionic strength constant (about 0.1). Although Motonaka et al. [10] recommended the use of aluminium(III) nitrate or lanthanum(III) nitrate as the best coagulating agents, these salts would interfere with the fluoride determination and therefore they were not considered. The best coagulant properties were shown by potassium nitrate, especially in determinations of mixtures containing iodide or bromide.

It was established that any initial pH in the range 3—7, which was regulated by adding nitric acid, did not significantly influence the shapes of the titration curves; acidifying the solutions did not lead to better results. Hence the titrations were done in the originally approximately neutral solutions.

Titration of iodide—bromide mixtures. For titrations of these mixtures, the following electrode pairs were examined: S^{2-}/Ag, I^-/Br^-, S^{2-}/I^-, and S^{2-}/Br^-. With the S^{2-}/Ag pair the potential jump for iodide disappeared in all media, while the titration curves recorded with the S^{2-}/I^- and S^{2-}/Br^- electrode pairs showed poor reproducibility. The most suitable indicator system proved to be the I^-/Br^- pair and this was used for end-point determination in the titrations of this mixture in aqueous solutions (Fig. 1). The integral titration curve 1 (Fig. 1) has a signal change at the second equivalence point like a first derivative. With increasing rate of addition of the titrant, this peak increased, but the end-point was shifted to lower values (probably because of increased adsorption on the precipitate). The increase in the peak with the rate of addition of titrant is due to the influence of kinetic factors on the establishment of the equilibrium potential.

The results of determinations given in Table 1 show that iodide can be determined more accurately than bromide. The largest error was obtained in determinations of the 5:1 iodide—bromide mixture (Br^-, —6%), which

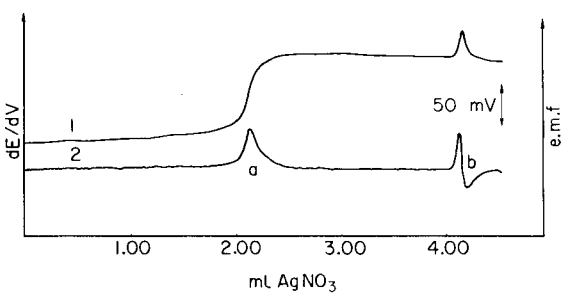

Fig. 1. Differential potentiometric titration curves of the mixture I^- (a) + Br^- (b) (mole ratio 1:1) obtained by titration with 0.0250 M $AgNO_3$: (1) integral (e.m.f. axis); (2) derivative (dE/dV axis). Indicator electrodes: I^-/Br^- pair. V is the volume of titrant added.

TABLE 1

Results of differential potentiometric titrations of binary halide mixtures with 0.0250 M $AgNO_3$
(Six titrations were done in each case)

Mixture	Electrode pair	Ion	1:1 mole ratio			5:1 mole ratio			1:5 mole ratio		
			a[a]	b	c	a	b	c	a	b	c
I^-—Br^-	S^{2-}/SCE	I^-	6.72	—	0.3	32.26	—	0.07	6.68	—	0.4
		Br^-	4.19	—	0.2	4.18	—	0.4	20.52	—	0.07
	I^-/Br^-	I^-	6.71	99.8	0.3	32.51	100.79	0.24	6.52	97.6	0.5
		Br^-	4.07	97.1	0.6	3.94	94.2	1.2	20.70	100.88	0.37
Br^-—Cl^-	Br^-/SCE	Br^-	4.22	—	0.2	20.41	—	0.20	4.22	—	0.2
	Cl^-/SCE	Cl^-	1.88	—	0.2	1.88	—	0.2	9.13	—	0.1
	Br^-/Cl^-	Br^-	4.19	99.3	0.2	20.34	99.66	0.30	4.30	101.9	0.4
		Cl^-	1.82	96.8	0.5	1.87	99.5	1.6	8.94	97.9	0.3

[a] a, mg of the ion found; b % recovery from mixture; c, standard deviation (%).

can be mostly attributed to adsorption of bromide on the silver iodide precipitate.

Titration of bromide—chloride mixtures. Under the same conditions as for the previous mixture, the use of Br^-/Cl^- ion-selective electrodes proved to be most suitable. The addition of potassium nitrate in this case was not just convenient but essential for the appearance of the second break (for chloride) in the titration curve.

From Table 1, it can be seen that the largest error in determination of components of the mixture was obtained for chloride at the mole ratio 1:1 (about −3%). This can be considered as a good result compared to the accuracy of the usual argentimetric determinations of chloride in this mixture.

Titration of iodide—chloride mixtures. In contrast to expectation, the continuous titration of this mixture did not give good results. With each ion-selective electrode pair, and with the I^-/SCE or Cl^-/SCE pairs also, the titration curves contained a ridge at the iodide equivalence point. Instead of an abrupt change, a double potential jump was observed, resulting in two more or less separated peaks in the derivative titration curves. The appearance of the two-step potential change in this case seems to be related to the asymmetry of the titration curve near the iodide equivalence point and to unstabilized potentials in these continuous titrations. The slope of the e. m. f. change in the first jump was much greater than that in the second one. In discontinuous titrations, the ridge on the curve disappeared and the slope was sharp, which indicates that kinetic factors have a significant effect in the continuous titrations. However, since the end-point of the continuous titration of iodide was not sufficiently defined, the iodide—chloride mixture was not included in the serial determinations.

Titration of fluoride-containing mixtures

Silver fluoride is readily soluble, and fluoride is best titrated with lanthanum(III) or thorium(IV) solutions, which do not form insoluble products with the other halides at low concentrations. Accordingly, halide mixtures containing fluoride can be titrated by using suitable solutions of Ag(I)—La(III) or Ag(I)—Th(IV). For the end-point determinations in such titrations, a fluoride-selective electrode was coupled with each of the above-mentioned ion-selective electrodes. Consecutive determinations were then done with the best combination. All titration curves had to be recorded with increased recorder sensitivity near the equivalence point of the fluoride titration, because of the much smaller potential change at this point.

Since the potentiometric titration of fluoride is not satisfactory for low concentrations in aqueous solutions [11] because of the small potential change at the end-point, it is now conventional to add some organic solvent. The best titration characteristics were found with ethanol (50% or 70% at the second end-point). Again conventionally, the titrations were done in the absence of free acid or buffer, to avoid the increased solubility caused by

acidity and to avoid the formation of mixed complex ions in the presence of acidic buffers.

Titration of iodide—fluoride mixtures. With all the electrode pairs investigated, the potential break for iodide had about the same steepness whereas the end-point determination for fluoride tended to be troublesome. The best properties were shown by the S^{2-}/F^- pair, which gave a more pronounced potential change in the fluoride titration. Thus, all further determinations were carried out with these electrodes. The addition of alcohol was more effective at 50% than at 70%. In the latter case, the peak in the derivative titration curve was deformed, probably because of slow establishment of stable potentials near the equivalence point.

A typical titration curve for the mixture is shown in Fig. 2. As expected, the potential jump for the iodide titration (1a) is much greater and sharper than that for fluoride (1b). The two changes are of opposite signs. After the first potential jump, there is a gradual potential increase of the sulphide-selective electrode, which is compensated by the opposite potential change of the fluoride-selective electrode. At the second end-point, the potential jump is about a quarter that at the first end-point, hence different recorder sensitivities are desirable.

The results given in Table 2 show that the 1:2 and 5:2 I^-—F^- mixtures can be determined very accurately. The results for the 1:10 mixture are omitted because the end-point of the fluoride titration could not be located with satisfactory precision. Possibly with a titrant containing more lanthanum(III) the potential jump would be better.

Titration of bromide—fluoride mixtures. These titrations involve much the same problems as in the previous example. Although the e. m. f. change near the end-point of the bromide titration is about half that obtained for iodide, it can be used successfully in all mixtures. The best titration curves were

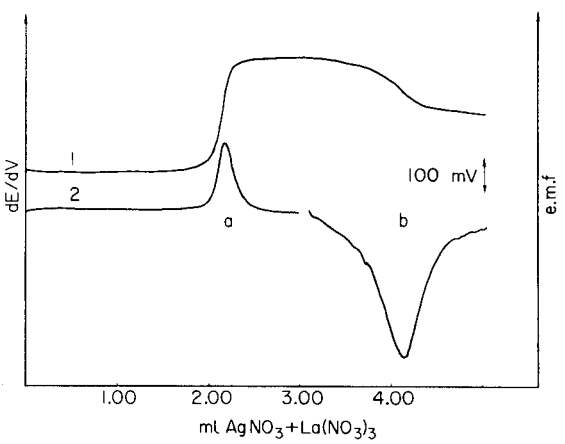

Fig. 2. Differential potentiometric titration curves of the mixture I^- (a) + F^- (b) (mole ratio 1:2) obtained by titration with 0.0250 M $AgNO_3$—0.00833 M $La(NO_3)_3$: (1) integral; (2) derivative. S^{2-}/F^--selective electrode pair.

TABLE 2

Results of differential potentiometric titrations of binary halide mixtures with 0.0250 M $AgNO_3$—0.00833 M $La(NO_3)_3$ (Six titrations were done in each case)

Mixture	Electrode pair	Ion	1:2 mole ratio			5:2 mole ratio			1:10 mole ratio		
			a[a]	b	c	a	b	c	a	b	c
I^-—F^-	I^-/SCE	I^-	6.70	—	0.4	32.13	—	0.21	—	—	—
	F^-/SCE	F^-	1.97	—	0.6	1.97	—	0.6	—	—	—
	S^{2-}/F^-	I^-	6.80	101.5	0.7	32.38	100.78	0.24	—	—	—
		F^-	1.96	99.5	0.4	2.00	101.5	0.3	—	—	—
Br^-—F^-	Br^-/SCE	Br^-	4.15	—	0.2	20.16	—	0.11	4.15	—	0.2
	F^-/SCE	F^-	2.13	—	0.6	2.13	—	0.6	9.91	—	0.2
	Ag/F^-	Br^-	4.14	99.8	0.6	20.15	99.95	0.07	4.30	103.6	0.3
		F^-	2.12	99.5	0.8	2.21	103.8	0.5	9.91	100.0	0.4
Cl^-—F^-	Cl^-/SCE	Cl^-	1.92	—	1.0	8.97	—	0.2	—	—	—
	F^-/SCE	F^-	2.13	—	0.5	2.13	—	0.5	—	—	—
	S^{2-}/F^-	Cl^-	1.88	97.9	0.8	8.97	100.0	0.1	—	—	—
		F^-	2.14	100.5	1.2	2.32	108.9	1.6	—	—	—

[a]See footnote to Table 1.

obtained in 70% ethanol with the Ag/F^- electrode pair. Results of determination of the components of the mixture at three mole ratios (Table 2) show very good agreement with the results obtained for these ions separately.

Titration of chloride—fluoride mixtures. Here the S^{2-}/F^- electrode pair in 70% ethanol proved most satisfactory. The results (Table 2) are acceptable for the 1:2 mole ratio, but with 5:2 mole ratio the fluoride results are very high. In the 1:10 mixture, the end-point for fluoride could not be determined precisely.

OTHER POSSIBILITIES

A hydrolytic end-point detection in the titration of fluoride with thorium(IV) or lanthanum(III) has already been described [7—9]. In the present work, when the fluoride-selective electrode was replaced by a glass electrode, it was found that the shapes of the titration curves were improved. Thanks to the sudden pH change near the equivalence point of the fluoride determination (about 1.5 units) and the faster response of a pH electrode compared to the fluoride electrode, the peaks obtained allow precise determination of the end-point. This was true for all the electrode pairs tested. The results obtained for fluoride in mixtures with iodide, bromide or chloride using the glass indicator electrode were 5—10% lower than those obtained in analogous continuous titrations of the same amounts of fluoride with the fluoride-selective electrode. However, when the fluoride solutions were standardized by discontinuous titration with the fluoride-selective electrode, the results obtained with the glass electrode were in good agreement.

An example of a titration of a four-component mixture of halides is given in Fig. 3. When the fluoride-selective electrode is replaced by a glass electrode, better titration curves can be obtained in 50% acetone than in 50% ethanol. Obviously, acetone must not be used if the electrode membranes or the adhesives dissolve in it.

Instead of lanthanum(III), thorium(IV) can be used in combination with silver(I) as the titrant. For the same amounts of iodide and fluoride as those shown in Table 2, a 0.0250 M $AgNO_3$—0.00625 M $Th(NO_3)_4$ solution was satisfactory with the glass electrode but with the fluoride-selective electrode, the potential jump at the fluoride end-point was small and diffuse. Results obtained with a glass/iodide-selective electrode pair were in good agreement with the results of visual determination of fluoride with methyl thymol blue indicator [12]. The fluoride-selective electrode gives satisfactory results in titrations of fluoride mixtures when a stronger (>0.02 M) thorium(IV) titrant is appropriate.

In further tests, mixtures of thiocyanate with fluoride (Fig. 4) and hexacyanoferrate(III) and fluoride were titrated with 0.0250 M $AgNO_3$ + 0.00833 M $La(NO_3)_3$. In 75% methanol with the Ag/F^- and Ag/glass electrode pairs, the shapes of the titration curves and the results were analogous to those for the previously described mixtures.

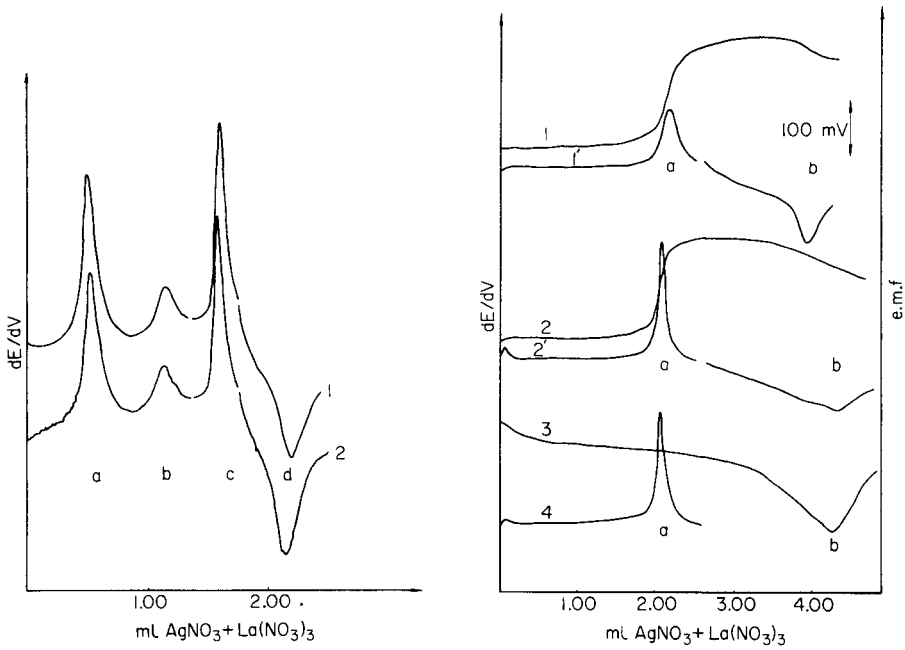

Fig. 3. Differential potentiometric titration curves of the mixture I^- (a) + Br^- (b) + Cl^- (c) + F^- (d) (mole ratio 1:1:1:4) obtained by titration with 0.0500 M $AgNO_3$ + 0.0156 M $La(NO_3)_3$: (1) derivative in 50% acetone; (2) derivative in 50% ethanol. Indicator electrodes: (1) Ag/glass; (2) Ag/F^-.

Fig. 4. Differential potentiometric titration curves of the mixture SCN^- (a;4) + F^- (b;3) (mole ratio 1:2) obtained by titration with 0.0250 M $AgNO_3$ + 0.00833 M $La(NO_3)_3$ using the electrode pairs: Ag/glass (1,1'), Ag/F^- (2,2'), F^-/SCE (3); Ag/SCE (4). Titration curves: (1,2) integral; (1',2',3,4) derivative.

The general conclusion can be drawn that differential potentiometry with ion-selective electrodes can be applied successfully for determinations of anion mixtures, within certain concentration limits, which may cause difficulties by other techniques.

REFERENCES

1 K. M. Stelting and S. E. Manahan, Anal. Chem., 46 (1974) 592.
2 K. M. Stelting and S. E. Manahan, Anal. Chem., 46 (1974) 2118.
3 M. J. D. Brand and G. A. Rechnitz, Anal. Chem., 42 (1970) 616.
4 I. C. Popescu, C. Liteanu and A. Mocanu, Rev. Roum. Chim., 20 (1975) 397.
5 D. H. Chou and L. C. Sams, Jr., Microchem. J., 14 (1969) 507.
6 W. Selig, Microchem. J., 20 (1975) 388.
7 F. F. Gaál, Lj. S. Jovanović and V. D. Canić, Fresenius Z. Anal. Chem., 272 (1974) 117.
8 F. F. Gaál, Lj. S. Jovanović and V. D. Canić, Bull. Soc. Chim. Beograd, 41 (1976) 383.
9 F. F. Gaál, Lj. S. Jovanović and V. D. Canić, Fresenius Z. Anal. Chem., 282 (1976) 439.
10 J. Motonaka, S. Ikeda and N. Tanaka, Anal. Chim. Acta, 105 (1979) 417.
11 J. J. Lingane, Anal. Chem., 39 (1967) 881.
12 W. Selig, Analyst, 93 (1968) 118.

Analytica Chimica Acta, 120 (1980) 93—99

DETERMINATION OF CALCIUM IN SILICATE ROCKS BY POTENTIOMETRIC TITRATION WITH ETHYLENEGLYCOL-BIS-(2-AMINOETHYLETHER)TETRAACETIC ACID AND A CALCIUM-SELECTIVE ELECTRODE

JAROSLAV KOTEK and JAN DOLEŽAL*

Department of Analytical Chemistry, Charles University, Albertov 2030, 128 40 Prague 2 (Czechoslovakia)

(Received 15th April 1980)

SUMMARY

The method reported for the determination of calcium in silicate rocks involves titration with ethyleneglycol-bis(2-aminoethylether)tetraacetic acid (EGTA) to a potentiometric end-point. A Crytur calcium-selective electrode is used; the selectivity constants ($K_{Ca,X}$) are less than 10^{-3} for Mg, Ba, Sr, K and Na. The method can be used for calcium contents of 2% or higher (and exceptionally for lower contents), in the presence of up to 60% Mg, 33% Al, 17% Fe, 5% Ba, 5% Ti, and 2.5% Mn. Al, Fe and Ti are masked with sulphosalicylic acid, barium is precipitated as its sulphate, and manganese is bound as its cyanide complex. If the magnesium content is less than that of calcium, EDTA can be used as titrant, magnesium being masked with acetylacetone.

Complexiметric determination of calcium in the presence of high concentrations of magnesium is difficult. Most methods require precipitation of magnesium as $Mg(OH)_2$ and calcium is titrated with EDTA in a strongly alkaline medium (pH 12.5) using a suitable indicator such as murexide, calcein—fluorexone, calcon, eriochrome blue black R or its derivatives [1, 2]. However, the magnesium hydroxide formed complicates the indicator colour change and calcium ions are adsorbed on its active surface. Many authors have attempted to suppress these interferences by a suitable choice of pH, or by adding sucrose, gelatine, polyvinyl alcohol or carboxy-methylcellulose to suppress the calcium ion adsorption; various methods of precipitating $Mg(OH)_2$ and many indicators have also been tested. However, the interference from $Mg(OH)_2$ has never been completely eliminated.

The use of EGTA is more satisfactory, because the stability constants of the Ca—EGTA and Mg—EGTA complexes are sufficiently different (log $K_{Ca-EGTA}$ = 11.0 and log $K_{Mg-EGTA}$ = 5.2). A difficulty encountered here is the lack of a suitable indicator; some authors have tried to circumvent this problem by using complicated procedures that are difficult to apply in practice [3—7].

The situation was improved by introducing calcium-selective electrodes in potentiometric titrations of calcium in the presence of magnesium [8].

Because the selectivity of the electrodes originally used was not very high (e.g. $K_{Ca,Mg} = 3 \times 10^{-2}$ for the Orion 92-20 electrode and 10^{-2} for the Radiometer calcium Selectrode), satisfactory results were not obtained in the presence of large amounts of magnesium [9—13]. Only the development of electrodes with higher selectivity ($K_{Ca,Mg}$ less than 10^{-3}) will permit the determination of calcium in the presence of high magnesium contents. The use of the suitable selective Crytur 20-15 electrode is described in the present paper.

EXPERIMENTAL

Instrumentation and chemicals

The equipment included an E536 Potentiograph with a 10-ml E535 Dosimat burette (Metrohm, Switzerland), a Crytur 20-15 calcium-selective electrode (Monokrystaly, Turnov, Czechoslovakia), and a calomel reference electrode (Laboratorní přístroje, Prague, Czechoslovakia).

All the chemicals used were of p.a. purity (Lachema, Czechoslovakia) except for EGTA (Merck; Titraplex VI). As titrants, 0.05 M solutions of EGTA and EDTA were prepared; 19.01 g of EGTA was dissolved in 100 ml of 1 M NaOH and diluted with water to 1 l, and 18.61 g of EDTA (disodium salt) was dissolved in water and diluted to 1 l.

Recommended procedure for the determination of calcium in silicate rocks

A 1 g sample is fused in a platinum crucible with 2—3 g of cesium carbonate [11] or with 10 g of Na_2CO_3 and 1 g of K_2CO_3 [14]. The solution obtained is diluted, after removing silica, to 250 ml; the hydrochloric acid concentration should be 0.7—0.8 M. To a 10-ml aliquot (or a standard solution of 0.01 M Ca^{2+}) are added 2 ml of 1 M sulphosalicylic acid. The solution turns red in the presence of iron(III). If iron is not present, 1—2 drops of 1% (w/v) iron(III) chloride solution are added. The solution is stirred and slowly neutralized with ammonia liquor, until the colour changes to yellow and remains the same after addition of another drop of ammonia; 3 more drops of ammonia are then added. If barium (0.1—5%) is present, 2 ml of 2% (w/v) ammonium sulphate solution are added before the neutralization. In the presence of manganese (0.03—2.5%), 1 ml of 10% (w/v) potassium cyanide and 0.1—0.2 ml of 30% hydrogen peroxide are added after the neutralization and the solution is vigorously stirred for 5 min. For higher contents of manganese, more cyanide must be added, the amount of peroxide remaining the same. Before the titration the solution is diluted with water to about 50 ml.

For samples containing less magnesium than calcium, EDTA can be used as the titrant. The procedure is the same as above, except that 2 ml of 1 M acetylacetone are added before the neutralization to mask magnesium.

RESULTS

Potentiometric titration of calcium with EDTA

The Crytur electrode exhibits, according to the manufacturer, an $E = f(\log[Ca^{2+}])$ dependence with a slope of about 22 mV, over the concentration range 10^{-1}—10^{-5} M Ca^{2+}. Measurements with three electrodes yielded values of 21, 19 and 22 mV in the present work.

Titrations of calcium in 100 ml of 0.1 M ammonia buffer of pH 9.5—10 with a 0.05 M EDTA standard solution exhibited a relative standard deviation of less than 2.5% in the concentration range 2×10^{-4}—2×10^{-3} M Ca^{2+}.

Titration of calcium in the presence of magnesium with EDTA was studied first in strongly alkaline medium, the Mg^{2+} being precipitated as $Mg(OH)_2$. In titrations of 2 mg of calcium in the presence of 12 mg of magnesium in 100 ml of 0.1 M NaOH with 0.05 M EDTA, the results were 0.15 mg lower than required by theory, although the well-developed potentiometric curves obtained showed a potential jump of about 300 mV at the end-point. The negative error is evidently caused by adsorption; an attempt to suppress this by adding glycerol (2 ml or a 50% solution) or polyethyleneglycol (m.w. 1540) in the same amount before making the test solution alkaline resulted in an error of —5%. However, the measured potentials were poorly reproducible, because of the presence of the solid phase in the solution.

Masking with acetylacetone was tested for suppression of the magnesium(II) interference [8]. Titrations of 5 mg of calcium in 100 ml of a 0.1 M ammonia buffer of pH 9.5—10 containing 2×10^{-2} M acetylacetone were satisfactory provided that not more than 5 mg of magnesium was present.

In analyses of silicate rocks, high contents of aluminium and iron must be masked. The use of triethanolamine was unsuccessful, because competitive formation of the aluminium and iron acetylacetone complexes occurred. Sulphosalicylic acid was found to be much better; 2 ml of a 1 M solution sufficed for masking 13 mg of aluminium and 7 mg of iron. The titration curve of 5 mg of calcium with 0.05 M EDTA in the presence of 5 mg of magnesium, 7 mg of iron and 13 mg of aluminium after addition of 2 ml of 1 M acetylacetone and 2 ml of sulphosalicylic acid in an ammoniacal buffer of pH 9.5 (total volume 100 ml) exhibited a $\Delta E/\Delta$ ml value of 12 mV/0.1 ml at the end-point. It can be seen from Table 1 that the content of magnesium must not exceed that of calcium if accurate results are to be obtained.

Potentiometric titration of calcium with EGTA

Because of the great difference in the stabilities of the EGTA complexes of calcium and magnesium, the determination of 5 mg of calcium was not affected even by 24 mg of magnesium. However, magnesium hydroxide precipitated in the presence of higher magnesium contents, causing sorption of calcium. This effect was removed by decreasing the pH to 8.2—8.5; this

did not change the shape of the potentiometric curve. Table 2 summarizes the results of the determination of calcium with EGTA in the presence of elements that are commonly present in silicate rocks. Iron, aluminium and titanium were masked with sulphosalicylic acid (2 ml of a 1 M solution), barium was reliably removed as $BaSO_4$ and manganese(II) was converted to the $[Mn(CN)_6]^{3-}$ complex after neutralization. Cyanide also masks Cu^{2+}, Ni^{2+}, Zn^{2+}, Co^{2+} and Cd^{2+}, but these elements rarely occur in silicate rocks at interfering concentrations. Lead ions are commonly masked by thioglycolic acid in complexometry.

If manganese(II) is not masked, the consumption of the titrant corresponds to the sum Ca + Mn, which can be used for determination of manganese; however, the content of Cu, Ni, Zn, Co and Cd must be negligible.

TABLE 1

Titration of 5 mg of calcium with 0.05 M EDTA in the presence of Mg, Fe and Al, in an ammonia buffer of pH 9.5
(0.02 M sulphosalicylic acid and 0.02 M acetylacetone added; total volume 100 ml)

Element	Taken (mg)	Ca found (mg)	Note
Ca	5	5.00	—
Ca + Mg	5 + 5	4.98	Mg masked with acetylacetone
Ca + Mg + Fe	5 + 5 + 7	5.00	Fe masked with sulphosalicylic acid
Ca + Mg + Al	5 + 5 + 13	5.00	Al masked with sulphosalicylic acid
Ca + Mg + Fe	5 + 13 + 7	5.04	Titration curve is drawn out

TABLE 2

Titration of 2 mg of calcium with 0.05 M EGTA in the presence of various metal ions in an ammonia buffer of pH 8.3
(0.04 M sulphosalicylic acid added; total volume 50 ml)

Element	Taken (mg)	Ca found (mg)	Element	Taken (mg)	Ca found (mg)
Ca	2	2.00[a]	Ca + Ti	2 + 2	1.98[d]
Ca + Cs	2 + 80	2.00[b]	Ca + Ba	2 + 2	2.00[f]
Ca + Na	2 + 230	1.99[c]	Ca + Mn	2 + 1	2.00[g]
Ca + Mg	2 + 24	2.02	Ca + Cs + Mg + Al + Fe + Ba + Ti + Mn	2 + 80 + 24 + 13 + 7 + 2 + 2 + 1	2.02[b,d,f,g,h]
Ca + Al	2 + 13	2.02[d]			
Ca + Fe	2 + 7	2.02[d]	Ca + Na + Mg + Al + Fe + Ba + Ti + Mn	2 + 230 + 24 + 13 + 7 + 2 + 2 + 1	1.99[c,d,f,g,i]
Ca + Ba	2 + 2	2.08[e]			

[a]See curve A in Fig. 1. [b]Cs content in 10 ml of decomposed sample. [c]Na content in 10 ml of decomposed sample. [d]Al, Fe and Ti masked with sulphosalicylic acid. [e]Ba precipitated, drawn out curve. [f]Ba precipitated as $BaSO_4$. [g]Mn masked by KCN as $[Mn(CN)_6]^{3-}$. [h]See curve B in Fig. 1. [i]See curve C in Fig. 1.

The effect of high concentrations of cesium and sodium ions was tested because Cs_2CO_3 and Na_2CO_3 are used for sample decomposition. The acidic solution (0.15 M HCl) was neutralized with ammonia to pH 8.3. In Fig. 1 are shown the potentiometric curves for calcium alone (curve A) and in the presence of Cs^+, Mg^{2+}, Al^{3+}, Fe^{3+}, Ba^{2+}, Ti^{4+} and Mn^{2+} (curve B) or in the presence of Na^+, Mg^{2+}, Al^{3+}, Fe^{3+}, Ba^{2+}, Ti^{4+} and Mn^{2+} (curve C). The contents of the elements are given in Table 2. The $\Delta E/\Delta$ ml values at the equivalence point were 40 mV/0.1 ml for curve A, 22 mV/0.1 ml for curve B and 17.0 mV/0.1 ml for curve C. It can be seen from Table 2 that all the elements at the given concentrations have negligible effects on the determination of calcium. Small changes in the consumption are caused by small differences in the slopes of the potentiometric curves.

A comparison of curves B and C in Fig. 1 shows that decomposition with cesium carbonate is advantageous, because the molar concentration of cesium (0.012 M) is substantially lower than that of sodium (0.2 M) in the final solution. As far as the effect of the ammonia buffer is concerned, changes in pH between 8—10 are without effect on the shape of the curves. However, ammonium ions affect the response of the calcium-selective electrode similarly to sodium ions. Their concentration is determined by the amount of hydrochloric acid in the sample solution after decomposition, and the slope of the titration curve decreases with increasing concentration of ammonium ion. This decrease is also affected by other components in the solution and thus a limiting concentration of hydrochloric acid cannot be determined exactly. However, 0.15 M chloride does not markedly affect the shapes of the curves.

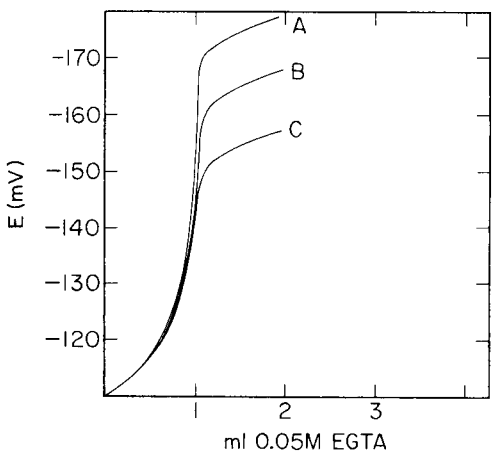

Fig. 1. Potentiometric curves for the titration of calcium with 0.05 M EGTA in 50 ml of ammonia buffer of pH 8.3, in the presence of 0.04 M sulphosalicylic acid, 0.08% $(NH_4)_2SO_4$, 0.2% KCN, 0.06% H_2O_2, with the calcium-selective indicator electrode. Curve A: 2 mg Ca. Curve B: 2 mg Ca in the presence of 80 mg Cs, 24 mg Mg, 13 mg Al, 7 mg Fe, 2 mg Ba, 2 mg Ti and 1 mg Mn. Curve C: As for B, but with 230 mg Na instead of 80 mg Cs.

TABLE 3

Determination of calcium in standard samples
(5 determinations were done on each sample)

Sample	Average found	Standard deviation s	Certified value	Titrant
Serpentinite (% CaO)[a]	1.59	0.05	1.61 ± 0.12	EGTA
Magnesite MK-Košice (% CaO)[b]	0.569	0.052	0.581 ± 0.039	EGTA
Soil 5 (% Ca)[c]	2.38	0.03	2.2[d]	EGTA
	2.41	0.05		EDTA

[a]Obtained from the Mining University, Ostrava, Czechoslovakia. [b]Obtained from Labora, Czechoslovakia. [c]Analytical Quality Control Services, I.E.A.E., Seibersdorf, Austria. [d]Tentative value only.

Determination of calcium in standard samples

The method was tested on three standards: serpentinite from Vězná near Rozná [14], magnesite MK-Košice, and I.A.E.A. Soil 5. Table 3 summarizes the results. Statistical evaluation was based on the Student *t* test at the 95% probability level.

Serpentinite and magnesite were selected for their extreme magnesium contents (37.49 and 45.22% MgO). Because the contents of iron and aluminium were relatively low, the sample volume could be increased to 25 ml (serpentinite) or 50 ml (magnesite), thus improving the limit of determination. The values found agree well with the certified values. Standard soil was selected because of the possibility of using either EGTA or EDTA as titrants. Sample solution volumes were 20 ml. The results of the two sets of determinations agree well, but the determination with EDTA is subject to a larger error. Only a tentative recommended calcium content was available for this standard and the results of determination agreed reasonably well with it. It should be emphasized that under these conditions the methods tested operate close to their limit of determination; however, they can be used to check the results obtained by other methods such as spectrophotometry or atomic absorption spectrometry.

The authors are obliged to Dr. M. Semler of Monokrystaly in Turnov for kindly providing calcium-selective electrodes.

REFERENCES

1 See e.g. G. Schwarzenbach and H. Flaschka, Complexometric Titrations, Methuen, London, 1969. Komplexon-Methoden, B. Siegfried, Zofingen, 1948.
2 J. Neumann, J. Ditz and V. Suk, Fresenius Z. Anal. Chem., 239 (1968) 167; Chem. Listy, 62 (1968) 1330; Fresenius Z. Anal. Chem., 251 (1970) 298; Collect. Czech. Chem. Commun., 36 (1971) 3023.
3 A. Ringbom, G. Pensar and E. Wänninen, Anal. Chim. Acta, 19 (1958) 525.

4 F. S. Sadek, R. W. Smidt and C. N. Reilley, Talanta, 2 (1959) 38.
5 R. Přibil and V. Veselý, Talanta, 13 (1966) 233.
6 R. Přibil and J. Adam, Talanta, 24 (1977) 177.
7 J. Adam and R. Přibil, 22 (1977) 645.
8 See e.g., J. Koryta, Anal. Chim. Acta, 61 (1972) 329; 91 (1977) 1.
9 T. F. Christiansen, J. E. Busch and S. C. Krogh, Anal. Chem., 48 (1976) 1051.
10 J. M. van der Meer, G. den Boef and W. E. van der Linden, Anal. Chim. Acta, 82 (1976) 309.
11 M. Mascini, Anal. Chim. Acta, 56 (1971) 316.
12 Z. Šulcek and M. Huka, Sklář Keram., 28 (1978) 204.
13 Z. Šulcek, P. Povondra and J. Doležal, Crit. Rev. Anal. Chem., 6 (1977) 255.
14 Z. Klika, V. Zamarsky and J. Weiss, Scientific Papers of the University of Mining, Ostrava 12, No. 1 (Mining—Geological Series), paper No. 412, 1976, p. 13.

Analytica Chimica Acta, 120 (1980) 101—109

TWO-PHASE BUFFER SYSTEMS IN WHICH ACID DIMERIZATION OCCURS IN THE ORGANIC PHASE†

T. J. JANJIĆ* and E. B. MILOSAVLJEVIĆ

Chemical Institute, Faculty of Sciences, University of Belgrade, P.O. Box 550, 11001 Belgrade (Yugoslavia)

(Received 30th April 1980)

SUMMARY

Two-phase buffer systems in which acid dimerization occurs in the organic phase are described. The equations for the dependence of buffer capacity on pH and for evaluation of dilution effects in two-phase buffers of this type are derived and experimentally verified. The rule of additivity of buffer capacities is not valid for the two-component, two-phase buffers investigated because mixed dimers are formed in the organic phase.

Two-phase buffer systems have been described [1—3], and it has been shown [1] that they have important advantages over classical single-phase buffers. The dilution effects in such buffers have been studied [1, 2]. Multi-component two-phase buffer systems which have a considerable buffer capacity over a wide pH range have been investigated [3].

For the preparation of two-phase buffer systems with a buffered aqueous phase, the organic solvent should be practically insoluble in water. In the great majority of such solvents, acid dimerization occurs; the influence of this effect on the buffer capacities of the corresponding two-phase buffers is reported in the present paper.

MATHEMATICAL CONSIDERATIONS

The effect of dimerization equilibrium on the dependence of buffer capacity (β_{HA}) on pH

The equilibria in single-component two-phase buffer systems such as are investigated here are summarized in Fig. 1. Species without a subscript are in the aqueous phase and those with the subscript "org" are in the organic phase.

In the systems investigated the following mass balance equation is valid (the charges of individual ions are omitted)

$$C_{tot}^{app} = C_A + C_{HA} + \alpha(C_{HA})_{org} + 2\alpha(C_{H_2A_2})_{org} \quad (1)$$

†This work was presented in part at the 22nd Annual Meeting of the Serbian Chemical Society, Belgrade, Yugoslavia, January, 1980.

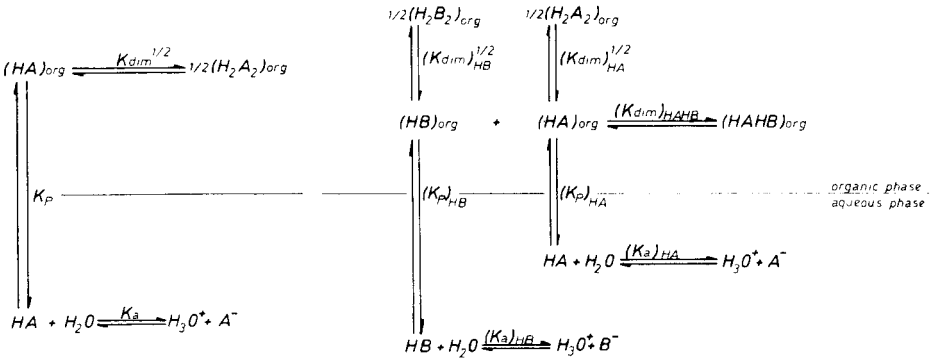

Fig. 1. Equilibria in a single-component two-phase buffer system.

Fig. 2. Equilibria in a two-component two-phase buffer system (acid—base pairs HA/A^- and HB/B^-).

where C_{tot}^{app} is the apparent total concentration of the acid—base pair, i.e., the analytical concentration if the total amount of the acid—base pair were dissolved in the aqueous phase only, and α is the ratio of the organic and aqueous phase volumes ($\alpha = V_{org}/V_w$).

From eqn. (1) and equilibrium constant expressions, defined as $K_a^M = a_H C_A/C_{HA}$, $K_p = (C_{HA})_{org}/C_{HA}$, $K_{dim} = (C_{H_2A_2})_{org}/(C_{HA})^2_{org}$, we obtain

$$C_b \approx C_A = -\frac{(K_a^M)^2 + K_a^M a_H + \alpha K_a^M K_p a_H}{4\alpha K_p^2 K_{dim} a_H^2} + \left[\left(\frac{(K_a^M)^2 + K_a^M a_H + \alpha K_a^M K_p a_H}{4\alpha K_p^2 K_{dim} a_H^2}\right)^2 + \left(\frac{(K_a^M)^2 C_{tot}^{app}}{2\alpha K_p^2 K_{dim} a_H^2}\right)\right]^{1/2} \quad (2)$$

where $a_H = 10^{-pH}$ and C_b is the concentration of strong base which, if strongly basic and very dilute solutions are excluded, is nearly equal to the concentration of the anionic base C_A.

Differentiation, dC_b/da_H, of eqn. (2) and replacement of da_H by $-2.3\, a_H dpH$, gives the following relationship for the buffer capacity (β_{HA})

$$\beta_{HA} = 2.3\left[\left(\frac{3K_1 a_H + K_2 a_H^2 + 2(K_a^M)^2}{2K_3 a_H^2}\right) \times \left((K_a^M)^2 + 2K_1 a_H + K_2 a_H^2\right)^{-1/2} - \frac{2K_a^M + K_4 a_H}{2K_3 a_H^2}\right] \quad (3)$$

For the sake of simplicity, complex constants K_1 to K_4 are introduced into eqn. (3); they are defined as: $K_1 = K_a^M(\alpha K_p + 1)$; $K_2 = (\alpha K_p + 1)^2 + 8\alpha C_{tot}^{app} K_{dim} K_p^2$; $K_3 = (2\alpha K_{dim} K_p^2)/K_a^M$; and $K_4 = \alpha K_p + 1$.

Dilution effect

Dilution effect in two-phase buffers of this type can be calculated from the equation

$$\Delta pH = \log \frac{\{(\alpha_{bd}K_p + 1) - [(\alpha_{bd}K_p + 1)^2 + 8\alpha_{bd}K_p^2 K_{dim}(C_{tot}^{app} - C_A)_{bd}]^{1/2}\}(C_A)_{ad}\alpha_{ad}}{\{(\alpha_{ad}K_p + 1) - [(\alpha_{ad}K_p + 1)^2 + 8\alpha_{ad}K_p^2 K_{dim}(C_{tot}^{app} - C_A)_{ad}]^{1/2}\}(C_A)_{bd}\alpha_{bd}}$$

$$+ \log \frac{y_{ad}}{y_{bd}} \qquad (4)$$

where y is the activity coefficient; subscripts bd and ad denote the conditions before and after dilution of the two-phase buffer. The derivation of eqn. (4) is essentially analogous to that of the corresponding equation (valid for two-phase buffer systems in which acid dimerization does not occur) derived previously by [2].

Two-component two-phase buffer systems

In Fig. 2 are summarized the expected equilibria in two-phase buffer systems that contain components of two acid-base pairs HA/A^- and HB/B^- in the aqueous phase. It can be seen that the existence of the mixed dimer HAHB in the organic phase is assumed in addition to the dimers H_2A_2 and H_2B_2.

If C_{tot}^{app} for both acid–base pairs is equal, the mass-balance equation valid for these systems can be presented in the form

$$C_A\left(1 + \frac{a_H}{(K_a^M)_{HA}} + \frac{\alpha a_H (K_p)_{HA}}{(K_a^M)_{HA}}\right) + C_A^2\left(\frac{2\alpha(K_p)_{HA}^2(K_{dim})_{HA}a_H^2}{(K_a^M)_{HA}^2}\right)$$

$$= C_B\left(1 + \frac{a_H}{(K_a^M)_{HB}} + \frac{\alpha a_H (K_p)_{HB}}{(K_a^M)_{HB}}\right) + C_B^2\left(\frac{2\alpha(K_p)_{HB}^2(K_{dim})_{HB}a_H^2}{(K_a^M)_{HB}^2}\right) \qquad (5)$$

If very basic and very dilute systems are excluded, the charge-balance equation valid for two-component two-phase buffers is $C_b = C_A + C_B$. The concentrations C_A and C_B can be evaluated at a given pH from this equation and eqn. (5) and the concentrations of all other species can be calculated from the corresponding expressions or the equilibrium constants K_a^M, K_p and K_{dim}. This enables the mixed dimerization constant to be evaluated since $(K_{dim})_{HAHB} = (C_{HAHB})_{org}/(C_{HA})_{org}(C_{HB})_{org}$.

EXPERIMENTAL

All experiments were performed at constant ionic strength (I = 0.1), sodium chloride being added when necessary. To maintain constant ionic strength during titrations, sodium salts of the organic acids were titrated with standard hydrochloric acid solution. In all cases benzene or toluene was the organic solvent, and the organic and aqueous phases were equal in volume.

All titrations were done in a nitrogen atmosphere to exclude the effect of carbon dioxide. For calculations, suitable programs were used with a Texas Instruments TI-59 programmable calculator. Other experimental arrangements were the same as described earlier [1, 2].

Suitable rearrangement of eqn. (2) give

$$\left(\frac{C_{tot}^{app}K_a^M}{\alpha a_H C_A} - \frac{K_a^M - a_H}{\alpha a_H}\right) = K_p + \left(\frac{2C_A a_H}{K_a^M}\right) K_p^2 K_{dim} \quad (6)$$

or $Q = K_p + PK_p^2 K_{dim}$ (6a)

This linear relationship permits experimental evaluation of the equilibrium constants K_p and K_{dim} from the intercept and slope of the straight line obtained when Q is plotted as a function of P. Data necessary for this evaluation can be obtained by potentiometric (pH) titration of organic acid in the corresponding two-phase system.

For decanoic acid in the solvent system benzene/water, the following values were found for the equilibrium constants: log K_p = 2.94, log K_{dim} = 2.43. The set of data points was taken from the τ-interval 0.1—0.7, where τ is the fraction titrated.

RESULTS AND DISCUSSION

The effect of dimerization equilibrium on the dependence of buffer capacity (β_{HA}) on pH

Theoretical buffer curves ($\beta_{HA} = f(pH)$), calculated by eqn. (3) using several different values for K_p and K_{dim}, are presented in Fig. 3. It can be seen that for $K_{dim} = 10^2$, increase in K_p causes a shift of the buffer curves towards higher pH values. For a tenfold increase in K_p, this shift is about one pH unit. At that, maximum buffer capacity values change only slightly, and for $C_{tot}^{app} = 0.1$ M, the values are about 7×10^{-2}. Accordingly, it can be concluded that the two-phase buffer systems investigated in this paper have larger maximum buffer capacities than systems in which acid dimerization does not occur [1]. From Fig. 3, it can also be seen that when K_{dim} decreases (K_p remaining constant) the buffer curves are shifted towards lower pH values with a simultaneous decrease in the maximum buffer capacity. Buffer curves when K_{dim} is very small are almost identical with the corresponding curves for systems in which dimerization does not occur. All the buffer curves presented in Fig. 3 are asymmetrical, and deviations from symmetry are more pronounced for larger K_{dim} values.

From eqn. (3), it may be seen that for the two-phase buffer systems considered, buffer capacity is not proportional to the apparent total concentration of the acid—base pair (C_{tot}^{app}), in contrast to the two-phase buffers described earlier [1].

To prove the validity of the theoretical considerations, two-phase buffer systems that contained acid—base pairs of propanoic, hexanoic or decanoic acid were investigated with benzene or toluene as the organic solvent.

For calculations of the buffer capacity at a given pH (eqn. 3), it is necessary to know the mixed acidity constant for a given ionic strength (K_a^M), the constants K_p and K_{dim}, the ratio of the phase volumes (α), and the apparent

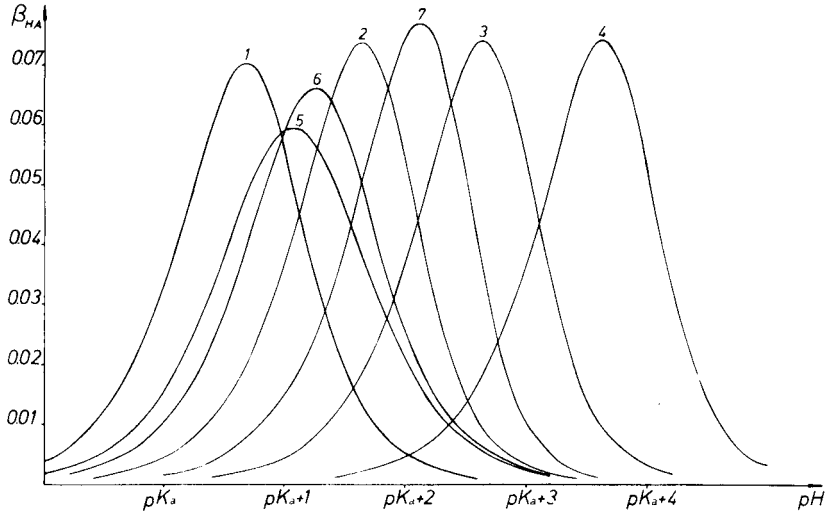

Fig. 3. Influence of K_p and K_{dim} on the buffer curves, $\beta_{HA} = f(pH)$. For curves 1—4, $K_{dim} = 10^2$ and $K_p = 1$ (curve 1), $K_p = 10$ (curve 2), $K_p = 10^2$ (curve 3), $K_p = 10^3$ (curve 4). For curves 5—7, $K_p = 10$ and $K_{dim} = 1$ (curve 5), $K_{dim} = 10$ (curve 6), $K_{dim} = 10^3$ (curve 7). For all curves $C_{tot}^{app} = 0.10$ M, $\alpha = 1$ and I = 0.

total concentration of the acid—base pair (C_{tot}^{app}). The numerical values of the equilibrium constants used for calculating the theoretical buffer curves of the systems investigated experimentally are given in Table 1. The experimental data for the selected two-phase buffers are presented in Figs. 4 and 5, along with the theoretical buffer curves calculated by eqn. 3. It can be seen that the experimental values of the function $\beta_{HA} = f(pH)$ are in good agreement with those calculated theoretically. It can be concluded that the experimental evidence completely confirms the validity of the theoretical considerations.

Dilution effect

The dilution effects for the three two-phase buffers investigated are presented in Table 2, from which it can be seen that the change in pH on

TABLE 1

Values of equilibrium constants (references are given in brackets)

Acid	pK_a	Solvent pair	log K_p	log K_{dim}
Propanoic	4.87 [4]	Benzene/H_2O	−1.22 [6]	1.96 [6]
		Toluene/H_2O	−1.34 [6]	2.12 [6]
Hexanoic	4.88 [5]	Benzene/H_2O	0.63 [6]	1.88 [6]
		Toluene/H_2O	0.54 [6]	2.03 [6]
Decanoic	4.90[a]	Benzene/H_2O	2.94[b]	2.43[b]

[a]Estimated by extrapolation of the functional dependence of pK_a on number of carbon atoms for a homologous series of *n*-carboxylic acids (C = 4—9); pK_a values from ref. [7].
[b]Determined experimentally in this study.

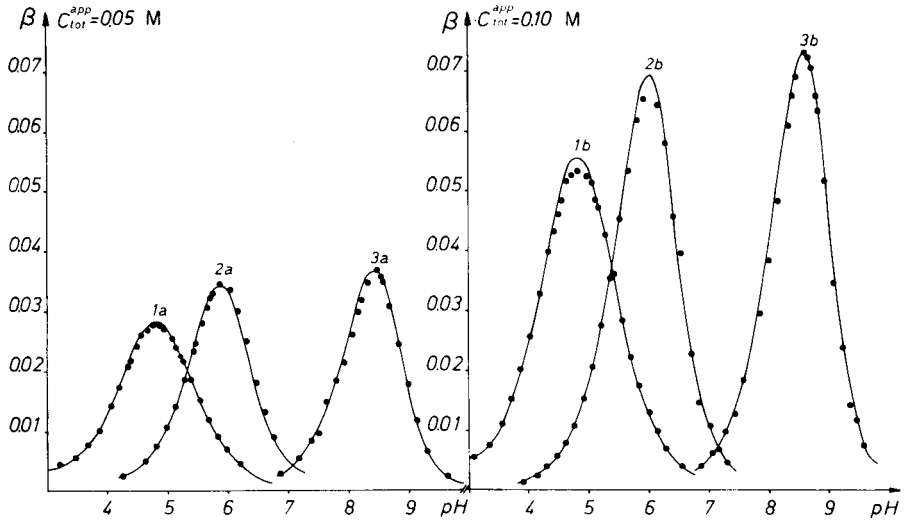

Fig. 4. Experimental data points (•) and calculated theoretical curves (—) (see text) for the buffer capacities of two-phase buffers containing propanoic acid (curves 1a and 1b), hexanoic acid (curves 2a and 2b), and decanoic acid (curves 3a and 3b). Solvent pair, benzene/water (1 + 1), I = 0.1, t = 25°C.

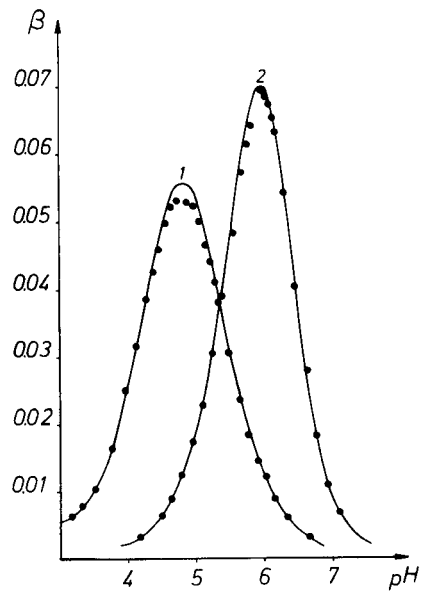

Fig. 5. Experimental data points (•) and calculated theoretical curves (—) (see text) for the buffer capacities of two-phase buffers containing propanoic acid (curve 1) and hexanoic acid (curve 2). Solvent pair, toluene/water (1 + 1), C_{tot}^{app} = 0.10 M, I = 0.1, t = 25°C.

TABLE 2

Dilution effects in two-phase buffers I[a], II[b] and III[c]

Buffers diluted with	pH Values					
	Measured			Calculated[d]		
	I	II	III	I	II	III
5.24 ml of H_2O	5.79	5.75	8.39	5.79	5.75	8.40
10.48 ml of H_2O	5.70	5.65	8.29	5.71	5.67	8.31
15.72 ml of H_2O	5.62	5.58	8.22	5.64	5.60	8.23
15.72 ml of H_2O + 15.72 ml of benzene (toluene)[e]	5.80	5.76	8.40	5.79	5.75	8.38

[a]Prepared by mixing 15.00 ml of 0.0985 M $CH_3(CH_2)_4COONa$, 0.716 ml of 1.032 M HCl and 15.72 ml of benzene (pH = 5.90).
[b]Prepared by mixing 15.00 ml of 0.0985 M $CH_3(CH_2)_4COONa$, 0.716 ml of 1.032 M HCl and 15.72 ml of toluene (pH = 5.86).
[c]Prepared by mixing 15.00 ml of 0.1000 M $CH_3(CH_2)_8COONa$, 0.727 ml of 1.032 M HCl and 15.72 ml of benzene (pH = 8.51).
[d]Calculated from eqn. (4). The activity coefficients were calculated by the Davies equation: $-\log y = 0.509\, z^2[I^{1/2}/(1 + I^{1/2}) - 0.2\, I]$.
[e]The ionic strength of the aqueous phase was maintained constant by addition of NaCl.

twofold dilution of the aqueous phase is about −0.28 pH units. The agreement between the experimentally measured pH values and those calculated according to eqn. (4) is good.

It was shown earlier [2] that no change in pH occurs when both phases of a two-phase buffer are diluted in such a way that their ratio remains unchanged and if the ionic strength of the aqueous phase is kept constant. However, the results in Table 2 show that this is not the case when acid dimerization occurs in the organic phase of a two-phase buffer. The pH values of the buffers investigated, after twofold dilution of both phases (at constant ionic strength), are lower than the corresponding values before dilution. This depression in pH may be used as a qualitative potentiometric criterion for establishing whether dimerization of the organic acid occurs in the organic solvent tested (only formic and to a lesser extent acetic acid form higher oligomers [8]).

Mathematically, it can be proved that the largest depression (−0.15 pH units) would be expected when species A^- and $(H_2A_2)_{org}$ are so predominant that the concentrations of all other species in the system can be neglected. The depressions in pH on twofold dilution of both phases of the two-phase buffer systems tested lie in the theoretically expected limits, and amount to −0.10, −0.10 and −0.11 pH units for buffers I, II and III, respectively (see Table 2).

Two-component two-phase buffer systems

Two two-component buffers in the benzene/water solvent system were examined. The first buffer contained the acid–base pairs of propanoic and

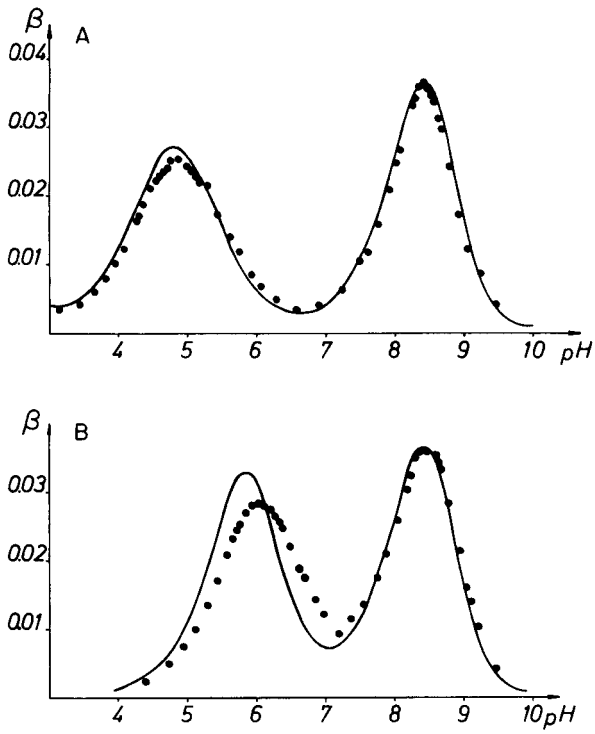

Fig. 6. Buffer capacity as a function of pH for a two-component two-phase buffer containing (A) propanoic and decanoic acids, and (B) hexanoic and decanoic acids. (•) Experimental values; (—) calculated sum of buffer capacities of the corresponding single-component two-phase buffers. Solvent pair, benzene/water (1 + 1), C_{tot}^{app} = 0.05 M for each acid—base pair, I = 0.1, t = 25°C.

decanoic acids, and the second was made up of hexanoic and decanoic acids. The results of experimental determinations of the dependence of β on pH are presented in Fig. 6 along with the calculated sum of the buffer capacities of the corresponding single component two-phase buffers. It can be seen that the rule of additivity of buffer capacities is valid in the pH range in which neutralization of the apparently weaker acid occurs (higher pH values). This is understandable, for the apparently stronger acid is almost completely neutralized in this pH range, so that formation of mixed dimers occurs only to an insignificant extent. However, the additivity rule is not valid in the pH range in which neutralization of the apparently stronger acid occurs because mixed dimers can then be formed in appreciable concentrations.

For the hexanoic—decanoic system, in which deviations from the additivity rule are more pronounced, mixed dimerization constant $(K_{dim})_{HAHB}$ was evaluated (see Mathematical Considerations). The results obtained are summarized in Table 3. The relatively good agreement of the values of $(K_{dim})_{HAHB}$ obtained at different pH values may be taken as indirect

TABLE 3

Values of mixed dimerization constant for hexanoic and decanoic acids

pH	6.55	6.40	6.30	6.20	6.10	6.00	5.80	5.70
$\log (K_{dim})_{HAHB}$	2.35	2.39	2.41	2.42	2.43	2.44	2.46	2.47

proof that deviations from the rule of additivity of buffer capacities are caused by formation of the mixed dimers in the organic phase of the two-phase buffer.

The authors are grateful to the Serbian Republic Research Fund for financial support.

REFERENCES

1 T. J. Janjić and E. B. Milosavljević, Anal. Chem., 50 (1978) 597.
2 T. J. Janjić and E. B. Milosavljević, Bull. Soc. Chim. Beograd, 43 (1978) 553.
3 T. J. Janjić, E. B. Milosavljević and M. K. Srdanović, Anal. Chim. Acta, 107 (1979) 359.
4 H. S. Harned and R. W. Ehlers, J. Am. Chem. Soc., 55 (1933) 2379.
5 J. F. Dippy, J. Chem. Soc., (1938) 1222.
6 B. P. Nikol'ski (Glavnyi Ed.), Spravochnik Khimika, Vol. 3, Khimiya, Moscow, 1964, pp. 475, 480.
7 G. Kortüm, W. Vogel and K. Andrussow, Dissociation Constants of Organic Acids in Aqueous Solution, Butterworth, London, 1961, pp. 244, 249.
8 N. A. Izmailov, Elektrokhimiya Rastvorov, Khimiya, Moscow, 1976, p. 249.

Analytica Chimica Acta, 120 (1980) 111—120

THE ELECTROCHEMICAL REACTIONS OF COPPER(II) AND COPPER(I) CHLORIDE IN N,N-DIMETHYLFORMAMIDE

ROBERT D. BRAUN

Department of Chemistry, Box 44370, University of Southwestern Louisiana, Lafayette, LA 70504 (U.S.A.)

(Received 12th June 1980)

SUMMARY

Polarographic, voltammetric and controlled-potential coulometric studies of copper(II) and copper(I) chloride in dimethylformamide are reported. The two chloride complexes of copper(II) are reduced in a total of three electrochemical steps to two copper(I)-chloride complexes and to copper(0). The two copper(I)-chloride species are reduced to copper(0) and oxidized to copper(II)-chloride complexes. The dissociation constant of the tetrachlorocuprate(II) complex has been polarographically estimated to be 10^{-25}.

Copper(II) chloride has been extensively used [1—4] as an oxidizing agent in oxidation—reduction titrations in N,N-dimethylformamide (DMF). During those titrations the copper(II) was apparently reduced to copper(I). Since copper(II) nitrate and copper(II) perchlorate are directly reduced to copper(0) [5] during electrochemical reactions, and since copper(II) is known to form complexes with chloride [6], it appears likely that copper(I) is stabilized in DMF, as it is in water [7], by complexation with chloride. The present study was undertaken to examine the electrochemical reactions of copper(II) and copper(I) chloride in DMF.

EXPERIMENTAL

Chemicals

N,N-Dimethylformamide (Baker Analyzed Reagent) was stored under a dry nitrogen atmosphere and was used without further purification. Reagent-grade copper(II) chloride dihydrate and copper(I) chloride were used in this study. A 0.1 M tetrabutylammonium perchlorate (TBAP) solution was used as the electrolyte solution except where otherwise indicated. Reagent-grade silver nitrate was used in the reference-electrode, filling solution. All chemicals were stored in desiccators. High purity, dry nitrogen was used to deaerate samples prior to electrochemical study, and to protect the solvent and the cell solutions from the atmosphere.

Apparatus

A model 174a Polarographic Analyzer (Princeton Applied Research) was coupled to an Omnigraphic 2000 x—y recorder (Houston Instrument) for polarography and voltammetry, and to an Omniscribe strip-chart recorder (Houston Instrument) for controlled-potential coulometry. A silver—0.010 M silver nitrate reference electrode and a platinum auxiliary electrode were used. The silver nitrate reference solution was prepared daily. All potentials reported in this paper are relative to the silver—silver nitrate reference electrode. The indicator electrode was either a platinum disc (0.1 mm diameter), a dropping mercury electrode (d.m.e.), or a hanging mercury drop electrode (h.m.d.e.; area = 2.2 mm^2) depending upon the study. The working electrode used for controlled-potential coulometry was either a mercury pool or a platinum foil.

The platinum disc electrode was pretreated before each trial by dipping in concentrated nitric acid, rinsing with deionized water and acetone, and then polishing dry with a laboratory tissue while the electrode was rotated at 1200 rpm. Voltammetric studies with the rotated platinum disc electrode (r.p.d.e.) were done at 1200 rpm. The water-jacketed, three-compartment cell was maintained at 25.0°C except in the temperature studies. The two outer compartments in the cell were separated from the center compartment by medium-porosity glass frits.

RESULTS AND DISCUSSION

Copper(II) chloride

Copper(II) chloride was polarographically examined over the concentration range from 0.1 mM to 10.5 mM. Polarograms of copper(II) chloride solutions contained one anodic and three cathodic waves (Fig. 1, curve A). The anodic wave occurred at —0.25 V. Polarograms of lithium chloride solutions in DMF (Fig. 1, curve B) contained two anodic waves at half-wave potentials of about - 0.25 V and —0.6 V. Apparently the anodic wave observed in copper(II) chloride solutions corresponds to one of the chloride waves. The more negative anodic wave was not observed in copper(II) chloride solutions until after controlled-potential coulometry at —1.4 V (see later discussion).

The half-wave potential ($E_{1/2}$, V) of the first cathodic wave (wave I_c) varied with concentration (20 solutions between 0.35 and 5.5 mM) according to the equation: $E_{1/2} = 0.012C - 0.326$. At concentrations greater than about 3 mM, a maximum associated with the wave made $E_{1/2}$ measurements unreliable. It is interesting to note that this wave is at a slightly more positive potential than the wave owing to reduction of copper(II) perchlorate to copper(0) [5] which occurs at —0.383 V. The variation in $E_{1/2}$ with concentration of the second and third cathodic waves (II_c and III_c) appeared to be completely random and can be attributed to slight daily variations in the reference electrode potential and other experimental parameters. The half-wave potentials of wave II_c and wave III_c were —0.600 ± 0.009 V (16 trials)

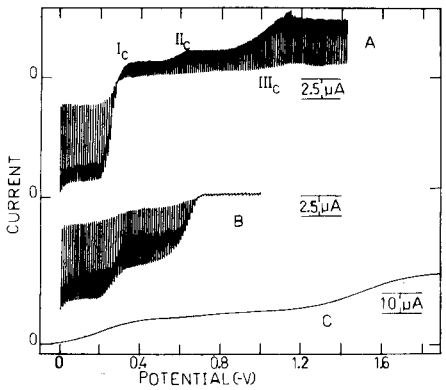

Fig. 1. (A) A polarogram of 1.6 mM $CuCl_2$; (B) a polarogram of 4.8 mM LiCl; (C) a voltammogram obtained at a r.p.d.e. of 1.3 mM $CuCl_2$.

and −0.97 ± 0.02 V (19 trials) respectively. (All uncertainties listed in this paper are expressed as standard deviations.) The $E_{1/2}$ of wave III_c was often difficult to measure accurately as a consequence of the maximum associated with the wave.

A polarographic study was performed on a 1.3 mM copper(II) chloride solution at seven temperatures between 10 and 40°C. The temperature coefficients of the half-wave potentials for the cathodic waves were 0.5 mV/degree for I_c, −1.2 mV/degree for II_c and −2.0 mV/degree for III_c. These values are within the expected range for reversible electrode reactions [8a]. The corresponding relative temperature coefficients for the diffusion currents (i_d) were 1.5%/degree for I_c, 1.1%/degree for II_c and 0.9%/degree for III_c. These values are sufficiently close to the theoretical value of about 1.3%/degree [8b] to indicate the absence of slow chemical steps in the electrochemical reductions associated with each of the three cathodic waves.

Plots of potential as a function of $\log[i/(i_d - i)]$ were obtained on the rising portions of the three cathodic waves for five samples of varying concentrations. In each case these log plots were linear. The average slopes of the log plots were −0.027 ± 0.006 V/decade (I_c), −0.059 ± 0.003 V/decade (II_c) and −0.087 ± 0.013 V/decade (III_c). The average slope of the log plots for I_c is near the theoretical slope (−0.030 V/decade) for a reversible 2-e transfer, and the average slope of the log plots for II_c is identical to the theoretical slope for a reversible 1-e transfer. The slopes of the log plots for wave I_c could have been affected by the proximity of the anodic wave and should be viewed with suspicion. The slopes of the log plots for wave III_c were not near the theoretical value for any reversible reaction and can be taken as evidence of the irreversibility of that particular electrochemical reaction.

The diffusion current of each of the three cathodic waves increased linearly with the square root of the corrected mercury column height (h_{corr}) for

eight column heights between 40.5 cm and 100.5 cm, and $i_d/h_{corr}^{1/2}$ slightly decreased with h_{corr}. These results are expected for electroactive species which obey the Ilkovic and Koutecky equations [8c], and indicate diffusion control of the polarographic wave heights.

Controlled-potential coulometry at a mercury-pool working electrode was done at −0.5 V on the plateau of wave I_c. The calculated value of n was 0.9 ± 0.2 mol of electrons transferred for each mole of copper(II) chloride (5 trials). Polarograms obtained after each electrolysis revealed the disappearance of I_c and an increase in the height of the anodic wave. During three of the five electrolyses, the heights of waves II_c and III_c decreased; however, these waves never completely disappeared.

Controlled-potential coulometry on a mercury pool at a potential (− 0.8 V) on the plateau of II_c yielded a calculated n of 0.89 ± 0.09 (5 trials). After each of these electrolyses, I_c and II_c had disappeared and III_c had significantly decreased in height. After each electrolysis the anodic wave increased in height, and in three of the five cases a second anodic wave at about − 0.6 V appeared.

The decrease in i_d of II_c and III_c after controlled-potential coulometry on the plateau of I_c, and the decrease in i_d of III_c upon electrolysis on the plateau of II_c appears to indicate that a slow chemical equilibrium exists between the chemical species associated with each wave. If the chemical equilibrium had been rapid, exhaustive electrolysis on any of the three waves would have resulted in a complete disappearance of all three waves. If there were no chemical equilibria between the species, electrolysis of a wave at a potential which was positive would have had no effect upon the i_d for the wave.

Controlled-potential coulometry at −1.4 V on the plateau of III_c yielded a calculated n of 2.00 ± 0.06 (7 trials). After electrolysis at −1.4 V, all three cathodic waves disappeared, and only the two anodic waves characteristic of chloride (Fig. 1, curve B) were observed.

Since reduction of copper(II) to copper(0) can be easily recognized as a copper plate if the electrolysis is done at a platinum working electrode, several studies were performed using platinum indicator and working electrodes. Prior to each electrolysis, copper(II) chloride solutions were examined at a r.p.d.e. (Fig. 1, curve C). The potential of the r.p.d.e. was scanned from +1 to −3 V. Prior to electrolysis no anodic peaks were observed; however, two cathodic peaks at about −0.2 and −1.4 V were seen. The wave at −0.2 V was broad and, at concentrations below 1 mM, consisted of two waves which apparently overlap at higher concentrations. This wave probably corresponds to I_c and II_c observed at the d.m.e. The wave at −1.4 V apparently corresponded to III_c at the d.m.e.

Controlled-potential coulometry at −0.5 V at a platinum-foil working electrode on the plateau of the first cathodic wave yielded a calculated n of 1.0 ± 0.1 (4 trials). The color of the solution changed from yellow to colorless during these electrolyses indicating removal of the $CuCl_4^{2-}$ [6]

complex from the solution. After these electrolyses, the −0.2 V cathodic wave was replaced with an anodic wave at +0.3 V. During each electrolysis the −1.4 V cathodic wave either completely disappeared or significantly decreased in height. A copper plate did not form on the working electrode during these studies.

Solutions of lithium chloride in DMF have a single anodic wave at +0.5 V. Consequently the +0.3 V anodic wave observed after electrolysis of copper(II) chloride solutions cannot be attributed to chloride. Since the chloride wave was not present prior to or after the electrolysis, apparently no free chloride exists in copper(II) chloride solutions, i.e., essentially all of the chloride is complexed with copper. The polarographic anodic wave at −0.25 V which was observed in copper(II) chloride solutions is probably due to oxidation of mercury to a mercury—chloride complex. The 0.3 V anodic wave is apparently due to a copper(I)—chloride species (see later discussion).

Controlled-potential coulometry at −1.6 V at a platinum-foil working electrode on the plateau of the more negative cathodic wave (observed at the r.p.d.e.) yielded an n of 2.1 ± 0.3 (3 trials). The solution turned from yellow to colorless during these electrolyses, and a copper plate formed on the electrode. After each of these electrolyses, only the anodic chloride wave was observed. Clearly the product of this electrolysis was copper(0).

The diffusion currents associated with each of the cathodic polarographic waves increased with concentration, but the increases were not linear (Fig. 2). The sum of the diffusion currents of I_c and II_c and of I_c, II_c and III_c did increase linearly with concentration. Either of these plots could be used for the determination of copper(II) chloride solutions in DMF.

The lack of linearity of plots of diffusion current as a function of copper(II) chloride concentration for the individual cathodic waves, and the linearity of the plots of total wave height can be interpreted to indicate a shift with total concentration in the relative concentrations of the chemical

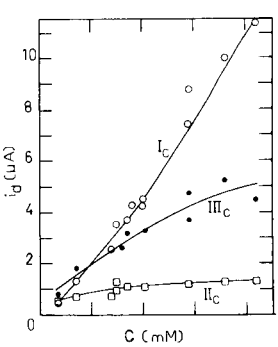

Fig. 2. The variation in polarographic diffusion current with concentration for the three $CuCl_2$ waves.

species associated with each wave. This could only occur if the chemical species associated with each of the three cathodic waves were in chemical equilibrium with each other. This conclusion is in agreement with that obtained from the coulometric studies.

An attempt was made to determine polarographically the degree of chloride complexation of the copper(II) species associated with each of the three cathodic polarographic waves. A series of five 1.5 mM copper(II) solutions were prepared which contained lithium chloride at concentrations varying from 0.05 to 0.09 M. The ionic strength of each solution was maintained at 0.1 M by the addition of TBAP. Although I_c was completely obscured by the large anodic wave associated with chloride, II_c and III_c were visible. A plot of $E_{1/2}$ as a function of $\log[Cl^-]$ for II_c and III_c yielded straight lines with slopes of −0.06 V/decade and −0.13 V/decade respectively. Since the reduction product of wave III_c has been shown to be copper(0), the overall electrochemical reaction associated with III_c must be $CuCl_p^{2-p} + 2e + Hg = Cu(Hg) + pCl^-$, for which the slope of the $E_{1/2}$ vs. $\log[Cl^-]$ plot should be −0.059 p/2 at 25°C [8d]. By setting the theoretical slope equal to the observed slope, it is clear that p = 4 for III_c, i.e., the chemical species which is reduced at III_c is $CuCl_4^{2-}$.

The reduction taking place at II_c has been shown from log-plot slopes and coulometry to be a 1-e reaction. The general equation for this reduction is $CuCl_p^{2-p} + e = CuCl_q^{1-q} + (p - q)Cl^-$ for which the theoretical $E_{1/2}$ vs. $\log[Cl^-]$ slope at 25°C is $-0.059(p - q)$[8d]. By comparing the theoretical slope with the observed slope, p − q is found to be 2. Since only two copper(II)—chloride complexes ($CuCl_4^{2-}$ and $CuCl^+$) in DMF are known, it is apparent that II_c corresponds to $CuCl_4^{2-} + e = CuCl_2^- + 2Cl^-$.

An estimate of the dissociation constant of the copper(II) tetrachloride complex can be obtained from the shift in $E_{1/2}$ between that observed for uncomplexed copper(II) perchlorate solutions ($E_{1/2}$ = −0.383 V) [5] and that observed for copper(II) solutions containing 0.09 M LiCl by use of eqn. 1 [8d].

$$(E_{1/2})_c - (E_{1/2})_s = 0.0296\left(\log K_D - \log\frac{f_s}{f_c} - \log D_c^{1/2}/D_s^{1/2} - 2\log 0.09 f_{Cl^-}\right) \quad (1)$$

Here, the c subscript refers to the complex and the s subscript refers to the copper(II) perchlorate solution, f is the activity coefficient, D is the diffusion coefficient, and K_D is the dissociation constant. If the activity coefficients are estimated using Debye—Hückel theory, and the diffusion coefficients of the complexed and uncomplexed copper(II) are assumed to be approximately equal, K_D is calculated to be 10^{-25}.

Triangular-sweep voltammetry at a h.m.d.e. was performed on several copper(II) chloride solutions at scan rates of 0.02, 0.05, 0.1, 0.2 and 0.5 V s^{-1}. In each case cathodic peaks were observed at about −0.3 and −1.1 V while anodic peaks occurred at about −0.2 and −0.9 V (Fig. 3, curve A). Application of the diagnostic criteria of Nicholson and Shain [9] to the cathodic peaks yielded ambiguous results.

Copper(I) chloride

Copper(I) chloride was polarographically studied over the concentration range from 0.1 to 8 mM. Polarograms of copper(I) chloride solutions contained one anodic and two cathodic waves (Fig. 4, curve A). The anodic wave occurred at about the same potential as the anodic copper(II) chloride wave. The $E_{1/2}$ of the anodic wave was slightly concentration-dependent as shown by the equation: $E_{1/2} = 0.0025C - 0.257$ (29 solutions studied). The first cathodic wave had an $E_{1/2}$ value of −0.36 ± 0.01 V (15 trials). The $E_{1/2}$ of the first cathodic wave did not appear to vary with changing concentration. The second cathodic wave had an $E_{1/2}$ value of −0.91 ± 0.02 V (27 trials) which did not vary with concentration. A maximum was usually associated with the −0.91 V wave.

The half-wave potentials and the diffusion currents of the three polarographic waves of 1.1 mM copper(I) chloride were measured at intervals of 5°C between 10 and 40°C. The temperature coefficients of the half-wave potentials for the anodic, first cathodic and second cathodic waves were, respectively, −0.7, 1.3 and 0.8 mV/degree. The corresponding relative temperature coefficients of the diffusion currents were 0.8, 1.4 and 1.2%/degree. These values are within the range of expected values for reversible electrode reactions with no slow chemical steps [8a, b].

Log plots (see earlier discussion) obtained on the rising portions of the three polarographic waves were linear. The slopes of the log plots were 0.042 ± 0.005 V/decade (anodic wave; 5 trials), −0.059 ± 0.005 V/decade (−0.36 V cathodic wave; 5 trials), and −0.115 ± 0.008 V/decade (−0.91 V cathodic wave; 5 trials). These data suggest that the anodic wave and the −0.91 V cathodic wave correspond to irreversible electrochemical reactions while the −0.36 V cathodic wave corresponds to a reversible 1-e electrochemical reaction.

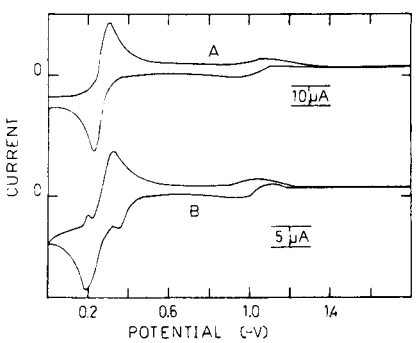

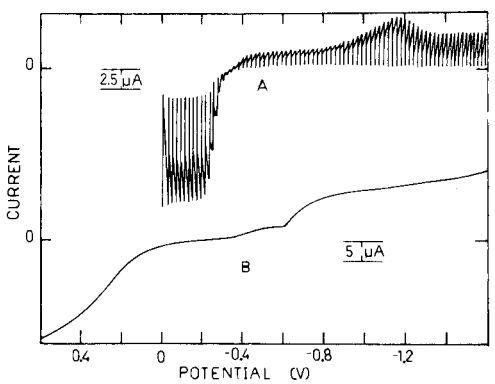

Fig. 3. Triangular-sweep voltammograms obtained at a h.m.d.e. (A) 2.8 mM $CuCl_2$ at a scan rate of 0.05 V/s; (B) 1.4 mM CuCl at a scan rate of 0.1 V/s.

Fig. 4. Voltammograms of 2 mM CuCl obtained at (A) a d.m.e. and (B) a r.p.d.e.

The variations in i_d with $h_{corr}^{1/2}$ and in $i_d/h_{corr}^{1/2}$ with h_{corr} were measured with 1.0 mM copper(I) chloride at eight mercury column heights. The results were those expected for electroactive species which obey the Ilkovic and Koutecky equations. This indicates diffusion control of the wave height for the three polarographic waves.

Controlled-potential coulometry was performed at a mercury-pool working electrode on the plateau of each of the two cathodic waves. At an applied potential of −0.7 V, on the plateau of the first cathodic wave, the calculated n was 0.5 ± 0.1 mol of electrons transferred for each mole of copper(I) chloride (5 trials). Polarograms obtained after each electrolysis revealed that the first cathodic wave had disappeared. In four of the five trials the second cathodic wave decreased in height indicating a slow chemical equilibrium between the chemical species responsible for the two waves.

After controlled-potential coulometry at a potential of −1.2 V on the plateau of the second cathodic wave, the calculated n was 1.0 ± 0.1 (5 trials). Polarograms obtained after the electrolyses revealed the disappearance of both cathodic waves, the disappearance (or decrease in height) of the original anodic wave, and the appearance of the two anodic chloride waves. This indicates that the anodic wave observed in copper(I) chloride solutions is, at least partially, due to oxidation of a copper(I) species. The anodic wave is most likely due to the combination of a wave from chloride, which was observed in copper(II) chloride solutions, and a wave from oxidation of copper(I), i.e, both waves occur at nearly the same potential and overlap.

Controlled-potential coulometry was also done with a platinum-foil working electrode at potentials on the plateaus of the voltammetric waves obtained at a r.p.d.e. Voltammograms obtained while using a r.p.d.e. had one anodic wave at +0.30 ± 0.01 V (8 trials) and two cathodic waves (Fig. 4, curve B). The $E_{1/2}$ values of the cathodic waves varied with concentration (C, range 0.9—3 mM) according to the equations: $E_{1/2} = 0.025C - 0.485$ and $E_{1/2} = 0.025C - 0.715$.

Controlled-potential coulometry performed at +0.6 V on the plateau of the anodic wave yielded a calculated n of 1.0 ± 0.1 (5 trials). After each exhaustive electrolysis, voltammograms and polarograms of the sample solutions contained waves at approximately those potentials observed in copper(II) chloride solutions. It is interesting to note that although the anodic wave observed at the r.p.d.e. completely disappeared during the electrolysis, the polarographic anodic wave significantly decreased in height but did not disappear. This is further evidence that the anodic wave observed at the d.m.e. is a combination of two waves caused by oxidation of copper(I) to copper(II) and mercury to a mercury—chloride complex.

Because of the proximity of the two cathodic waves, controlled-potential coulometry at a platinum-foil working electrode was not performed on the plateau of the first wave and before the second wave. At an applied potential of −2 V, on the plateau of the second cathodic wave, the calculated n was 0.98 ± 0.01 (5 trials). During each electrolysis copper plated on the platinum

working electrode. After each electrolysis the voltammograms and polarograms obtained with the sample solutions showed those anodic waves typical of chloride.

The diffusion currents associated with the anodic polarographic wave and the first cathodic polarographic wave of copper(I) chloride solutions increased linearly with concentration. The diffusion current for the second cathodic wave also appeared to increase with concentration, but the data were too scattered (27 solutions) to conclude that the increase was linear.

Studies to determine the degree of chloride complexation of the copper(I) species in solution were unsuccessful. The anodic chloride wave associated with the large concentrations of chloride used in this study completely obscured the anodic and first cathodic waves. Although the second cathodic wave was still visible, the maximum associated with this wave made it impossible to obtain the accurate measurements of $E_{1/2}$ required for this study.

Triangular-sweep voltammetry of three copper(I)—chloride solutions was performed at the h.m.d.e. (Fig. 3, curve B) and at the platinum disc electrode. Scan rates of 0.02, 0.05, 0.1, 0.2, 0.5 and 1 V s^{-1} were utilized during these studies. Application of the diagnostic criteria of Nicholson and Shain [9] to the cathodic peaks observed during the forward scans did not permit limitation of the electrochemical reaction mechanism associated with each peak to a single possibility.

Electrochemical reactions

The electrochemical reactions which are undergone by the several copper(II)—chloride species can be summarized by

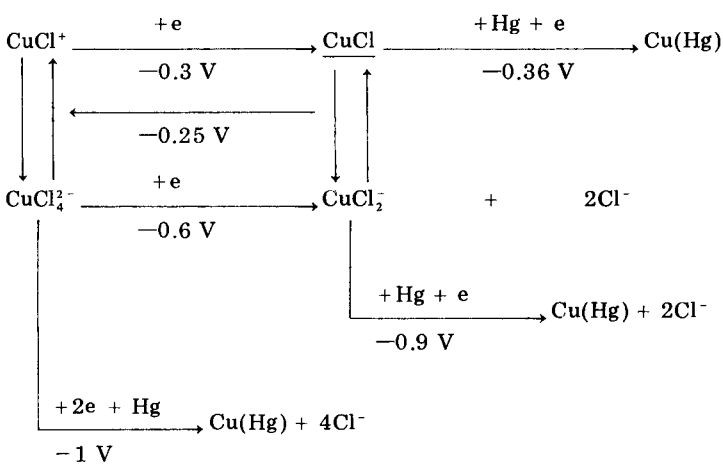

The potentials listed are those observed at the d.m.e. The third cathodic wave of copper(II) chloride has been shown coulometrically to correspond to reduction to copper(0). The polarographic complexation study has shown that the chloride complex responsible for this wave is $CuCl_4^{2-}$. The second

cathodic wave of copper(II) chloride has similarly been shown to be due to the reduction of $CuCl_4^{2-}$ to $CuCl_2^-$. Since the anodic wave at − 0.25 V increased in height after electroanalysis on the plateau of both I_c and II_c, it can be concluded that the —0.25 V wave is due to the oxidation of $CuCl_2^-$, the reduction product of I_c, or both. Since there apparently are two copper(I)—chloride complexes which are in chemical equilibrium with each other, any of these three possibilities is reasonable. It is important to remember that the −0.25-V anodic polarographic wave is probably due to both a copper(I) species and to oxidation of mercury to a mercury—chloride complex.

The first cathodic wave of copper(II) chloride was coulometrically shown to be due to reduction to a copper(I) species. Complexation data were not available, however, since only two soluble copper(II)—chloride complexes are known in DMF and since reductions of $CuCl_4^{2-}$ have already been assigned to II_c and III_c, it is likely that I_c is due to reduction of $CuCl^+$ to a copper(I) species. Although the identity of this copper(I) species is unknown, it can safely be assumed to be a copper(I)—chloride complex since uncomplexed copper(I) is not stable in DMF [5]. The copper(II)—chloride complexes have been shown by polarograms obtained on solutions after coulometry on the first two cathodic waves to be in a slow chemical equilibrium with each other.

The two cathodic waves in copper(I) chloride solutions have been coulometrically shown to be due to reduction to copper(0). Apparently the species responsible for the two cathodic waves are in chemical equilibrium as shown by polarograms obtained after controlled-potential coulometry on the plateau of the first wave. The anodic wave was coulometrically shown to be oxidized on platinum to the copper(II)—chloride complexes.

Although the copper(II) chloride solutions undergo several electrochemical reactions, it is apparent that at applied potentials that are greater (i.e. more positive) than − 0.36 V, the copper(II) species are all reduced to copper(I). Apparently these reactions are those which have been observed in oxidation—reduction titrations. All of the electrochemical reactions are summarized in the above scheme, where the identity of the underlined copper(I)- chloride complex is not known with certainty and where $CuCl_2^-$ and/or the unknown copper(I)—chloride complex could be oxidized to either $CuCl^+$ or $CuCl_4^{2-}$ which then reacts to yield some of the other.

REFERENCES

1 J. F. Hinton and H. M. Tomlinson, Anal. Chem., 33 (1961) 1502.
2 R. D. Braun and J. T. Stock, Anal. Chim. Acta, 60 (1972) 167.
3 R. D. Braun and J. T. Stock, Anal. Chim. Acta, 60 (1972) 250.
4 J. T. Stock and L. M. Doane, Anal. Chim. Acta, 86 (1976) 317.
5 R. D. Braun, Anal. Chim. Acta, 99 (1978) 325.
6 R. D. Braun, Fresenius Z. Anal. Chem., 285 (1977) 47.
7 F. A. Cotton and G. Wilkinson, Advanced Inorganic Chemistry, Interscience, New York, 1962, p. 750.
8 L. Meites, Polarographic Techniques, 2nd edn., J. Wiley, New York, 1965, (a) p. 288; (b) p. 139; (c) pp. 132—133; (d) Ch. 5.
9 R. S. Nicholson and I. Shain, Anal. Chem., 36 (1964) 706.

Analytica Chimica Acta, 120 (1980) 121—127

THE DETERMINATION OF ARSENIC BY ELECTROTHERMAL ATOMIC ABSORPTION SPECTROMETRY WITH A GRAPHITE FURNACE
Part 2. Determination of Arsenic(III) and Arsenic(V) After Extraction

D. CHAKRABORTI, W. De JONGHE and F. ADAMS*

Department of Chemistry, University of Antwerp (U.I.A.), B-2610 Wilrijk (Belgium)

(Received 30th May 1980)

SUMMARY

A procedure is described for the sequential determination of arsenite and arsenate in samples of natural waters. It is based on the extraction of arsenic(III) with ammonium sec-butyl dithiophosphate and measurement, after re-extraction into water, by graphite-furnace atomic absorption spectrometry. Reduction of arsenic(V) allows its subsequent determination. The method is applied to fresh and sea water samples. The detection limit is 6 ng l^{-1}.

Usually for determinations of arsenic in environmental samples, the total content of the element is considered adequate. Recent research has shown that the predominant arsenic-containing species present in the environment are inorganic arsenite and arsenate and some organic compounds, especially dimethylarsenic and monomethylarsonic acid. A dynamic relationship exists whereby oxidation—reduction and biomethylation processes provide ways for interconversions of the arsenic compounds. Arsenic is widely distributed in nature and is used in agriculture in large quantities. The differences in toxicity among inorganic arsenic(III) and arsenic(V) and the organoarsenicals has generated an impetus for the development of species-specific determinations in environmental samples, and many speciation methods are now available.

The first analytical procedure for selective determinations was put forward by Braman and Foreback [1] who used a procedure based on selective reduction with sodium tetrahydroborate and separation of the volatile arsines by selective volatilization from a cold trap. The final detection was made by the d.c. discharge emission technique. Various other procedures use the same hydride generation with other detectors for the final detection, e.g. microwave plasma emission [2], flame atomic absorption spectrometry [3], graphite furnace atomic absorption spectrometry (g.f.a.a.s.) [4, 5] and electron capture and flame ionization after gas chromatographic separation [4].

Johnson and Pilson [6] developed a spectrophotometric method for inorganic arsenite and arsenate, whereas Peoples et al. [7] used spectrophoto-

metry for distinguishing between inorganic and organic arsenic within certain concentration ranges. Another colorimetric method [8] for arsenic(III) and (V) determinations suffers from interferences by many common cations and anions. Some procedures have also been described based on a polarographic distinction between arsenite, arsenate and the organic species [9, 10].

Several studies have been based on chelate extraction followed by direct g.f.a.a.s. [11, 12]. One procedure uses the extraction of arsenic as the iodide into chloroform followed by re-extraction into water [13]; it cannot differentiate between arsenic(III) and arsenic(V). The present study deals with the use of ammonium sec-butyldithiophosphate in hexane for preconcentrating arsenic(III) in the presence of arsenic(V) and a number of contaminants. The reagent was already known to be selective for the chelation and extraction of arsenic(III) [14]. Re-extraction into water provides a useful increase in sensitivity for the determination by g.f.a.a.s. and circumvents many of the problems described earlier [15—17] which severely limit the determination of arsenic in the graphite furnace. Reduction of arsenic(V) to arsenic(III) allows its subsequent determination in environmental and other samples.

EXPERIMENTAL

Instrumentation and reagents

The atomic absorption apparatus was the same as that described earlier [15]. All measurements were done at the 193.7-nm arsenic resonance line and absorbances were read as peak heights from the built-in peak-reading device of the spectrometer. The slit width was 1 mm. The furnace was flushed with argon at an internal flow rate of 300 ml min^{-1} and an external rate of 900 ml min^{-1}. The optimum time/temperature program for a 20-μl injected solution was as follows: dry at 90°C for 20 s, ash at 1100°C for 20 s, atomize at 2600°C for 10 s, and glow out at 2700°C for 10 s. Nickel sulphate (100 μg Ni ml^{-1}) was used as a stabilizing agent for atomization.

All chemicals used were of analytical-reagent grade. Distilled deionized water was used for all the experiments.

Arsenic(III) standard (1 mg As ml^{-1}). Arsenic(III) oxide (0.1320 g) was dissolved in 2 ml of 1 M sodium hydroxide. To the solution was added 0.5 ml of 4.5 M hydrochloric acid and distilled water to give a final volume of 100 ml. A secondary standard solution was prepared daily by 100-fold dilution.

Arsenic(V) standard. A Merck Titrisol standard solution of arsenic(V) oxide in water was used.

Preparation of reducing reagent. A 20-ml portion of 4.5 M hydrochloric acid was slowly added to 40 ml of 1.48 M sodium hydrogensulphite solution in a 100-ml flask; 40 ml of 0.056 M sodium thiosulphate solution was added to give a yellow solution. The reducing reagent was prepared freshly when required. The stock solutions of sodium hydrogensulphite and sodium thiosulphate could be re-used when stored in the refrigerator.

Preparation of the extraction reagent. The method was similar to that used for the preparation of aliphatic esters of thiophosphoric acids [18—20]. Phosphorus(V) sulphide (111 g) was transferred to a three-necked flask fitted with a dropping funnel, a stirrer and a condenser. Benzene was added in an amount just sufficient to cover the phosphorus sulphide. The flask was warmed on a water bath at about 75°C. Sec-butanol (150 g) was added dropwise while stirring. The temperature was kept between 70°C and 80°C during this addition, after which it was raised to about 85°C and kept there for 2 h with constant stirring. The entire reaction should be carried out in a fume hood as hydrogen sulphide is evolved. About 20 g granular activated charcoal was added and the mixture filtered; the filtrate may be coloured. Dry ammonia was passed through the filtrate so that a precipitate appeared. After saturation of the suspension with ammonia, the solid was filtered off and air-dried. The amount recovered was about 200 g. It was purified by crystallization from benzene. Shiny white flakes of ammonium butyldithiophosphate (ABDP, yield 150 g) were obtained. It may be further recrystallised to obtain higher purity. Required for $C_8H_{22}NO_2PS_2$, 5.4% N, 24.75% S, 37.1% C, 8.5% H; found, 5.5% N, 24.75% S, 37.2% C, 8.3% H.

Preparation of a 0.05 M ABDP solution in hexane. A 0.6475-g portion of the reagent was dissolved in 42 ml of water. About 8.3 ml of concentrated hydrochloric acid was added, and the white precipitate that appeared was extracted into hexane (toluene or carbon tetrachloride might also be used). The final volume was made up to 50 ml. A 0.01 M solution in hexane was used for all extractions. The stock solution was stable for at least a month.

Determination of arsenic(III) and arsenic(V)

The sample 500 or 1000 ml was transferred to a separatory funnel. About 10 ml of concentrated hydrochloric acid was added followed by 10 ml of the 0.01 M ABDP solution in hexane. The funnel was shaken vigorously for 2—3 min and allowed to settle until any haziness disappeared, which took 10—15 min. The organic layer was transferred to a 50-ml separatory funnel and the aqueous layer was extracted with a further 5 ml of the ABDP solution. The combined extracts (A) contained the arsenic(III) and the aqueous layer the arsenic(V).

To the aqueous portion containing arsenic(V) was added about 35 ml of the reducing reagent. The solution was shaken for 3—5 min, 10 ml of 0.01 M ABDP solution was added and the above extraction procedure was repeated. The extract (B) contained the arsenic(V) from the original solution.

In a 50-ml separatory funnel extract A was washed twice with 10 ml of water and the aqueous layer was rejected. The organic layer was extracted twice with 2-ml portions of bromine-water. The aqueous portion which now contained the arsenic was collected in a 5-ml flask and mixed with 100 μl of (1 + 1) nitric acid, 50 μl of hydrogen peroxide and 500 μl of the nickel sulphate solution. The solution remained slightly yellow at the beginning but became colourless a few minutes after the addition of the hydrogen peroxide.

The analysis of the solution by g.f.a.a.s. using the above procedure gave the amount of arsenic(III) in the original solution. The use of a similar procedure with the extract B gave the amount of original arsenic(V).

Blank values were measured under identical conditions. For the analysis of natural water samples, the determination of arsenic(III) was done on 1 l of water and arsenic(V) on 500 ml.

RESULTS AND DISCUSSION

To confirm that ABDP is suitable for the extraction of arsenic(III) but not arsenic(V), various amounts of arsenic(III) and (V) in 500 ml of water were extracted using the procedure described. Table 1 shows the results of determinations of arsenic(III), arsenic(V) and mixtures. The blank values were 54 ± 2 ng l^{-1} for arsenic(III) and 194 ± 2 ng l^{-1} for arsenic(V). These values include standard deviations calculated from five results. The detection limit for both forms of arsenic, using the criterion of three times the standard deviation of the blank, was 6 ng l^{-1}. Linear calibration curves for arsenic(III) and (V) are shown in Fig. 1. They are not quite identical since they were measured using different graphite tubes.

Another reducing agent commonly used for reducing arsenic(V) to arsenic(III), tin(II) chloride (40% in 11 M hydrochloric acid) with potassium iodide (15%) was also also investigated. However, at low concentrations of arsenic it

TABLE 1

Determinations of arsenic(III) and arsenic(V)

Oxidation state	As added (μg)[a]	As(III) found (μg)[b]	Recovery (%)	As(V) found (μg)[b]	Recovery (%)
As(III)	0.10	0.09	90	<0.006	—
	0.50	0.48	96	<0.006	—
	0.25	0.23	92	<0.006	—
	0.75	0.71	94	<0.006	—
As(V)	0.50	<0.006	<1	—	—
	0.25	<0.006	<1	—	—
	0.75	<0.006	<1		
As(V) (after reduction)	0.10	<0.006	<1	0.09	90
	0.50	<0.006	<1	0.47	94
	0.25	<0.006	<1	0.23	92
	0.75	<0.006	<1	0.71	94
As(III) and As(V)	0.25 As(III) 0.25 As(V)	0.24	96	0.23	92
	0.25 As(III) 0.75 As(V)	0.23	92	0.71	94
	0.75 As(III) 0.25 As(V)	0.72	96	0.23	92

[a]To 500 ml of water. [b]Each result is the mean of 3 determinations.

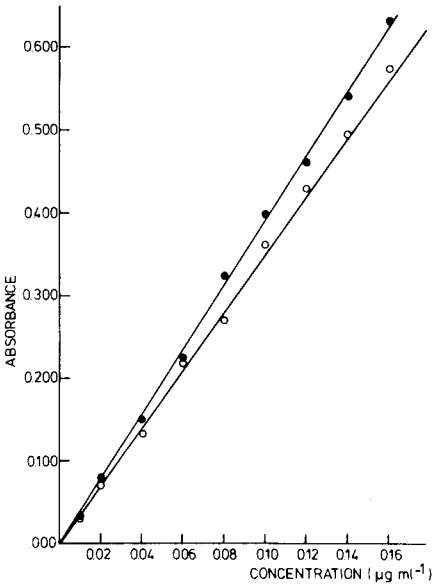

Fig. 1. Calibration curves for arsenic(III) (•) and arsenic(V) (○) using gas-stop during the atomization stage. Concentrations are those in final aqueous solution.

was not effective. Toluene and carbon tetrachloride were examined for the extraction of arsenic(III). They gave comparable results, but hexane was chosen because of the faster separation of the aqueous and organic layers and its lower toxicity.

Hydrogen peroxide is important for the final determination by g.f.a.a.s. Without its addition, low and irreproducible results were obtained. For the final measurements from 5 ml of aqueous solution, the amount of 30% hydrogen peroxide added should be 50—100 μl. At lower peroxide concentrations, absorbance readings were much reduced and became irreproducible; at higher concentrations the peak heights again decreased.

Variation in the hydrochloric acid concentration from 0.1 to 1 M had no influence on the extraction of arsenic(III).

In the earlier work [15], it was found that various elements interfered in the direct determination of arsenic, especially when sodium or potassium were present together with sulphate. All these interferences are adequately removed by the solvent extraction process. To observe the effect of a number of interferences, a synthetic river water [21] (composition in mg l^{-1}: $CaCl_2 \cdot 2H_2O$, 294; NaCl, 216; $MgSO_4 \cdot 7H_2O$, 86; KCl, 9.5; $(NH_4)_2HPO_4$, 7.3) and synthetic sea water [22] (composition in g l^{-1}: NaCl, 23.9; $MgCl_2$, 5.07; Na_2SO_4, 3.99; $CaCl_2$, 1.12; KCl, 0.667; $NaHCO_3$, 0.196; KBr, 0.098; H_3BO_3, 0.027; $SrCl_2$, 0.024; NaF, 0.003) were prepared. To 500 ml of this water known amounts of arsenic(III) and (V) were added and determined by the procedure described. The data in Table 2 show that the recovery of both species was more than 90%.

TABLE 2

Recovery of arsenic(III) and arsenic(V) from 500 ml of synthetic river and sea waters

Synthetic water	Arsenic added (μg)		As(III) found (μg)[a]	Recovery (%)	As(V) found (μg)[a]	Recovery (%)
	(III)	(V)				
River	0.25	0.75	0.23	92	0.71	94
	0.50	0.50	0.47	94	0.47	94
	0.75	0.25	0.71	94	0.23	92
Sea water	0.25	0.75	0.23	92	0.72	96
	0.50	0.50	0.47	94	0.46	92
	0.75	0.25	0.72	96	0.23	92

[a]Mean of 3 determinations.

Table 3 shows the results obtained for some natural water samples. The results for sea water agree with previously published data [4], i.e. 0.016—0.034 ppb of arsenic(III) and 1.49—1.75 ppb for arsenic(V). In the same study, the arsenic(V) concentration in river water was shown to be appreciably larger than that of arsenic(III).

Conclusions

The determination of arsenic in environmental samples by graphite-furnace atomic absorption spectrometry is inaccurate as a result of severe interferences by a number of common cations and anions, particularly sodium, potassium, aluminium and sulphate. An extraction procedure based on the use of ammonium sec-butyldithiophosphate in hexane, and re-extraction into water suitably concentrates arsenic and effectively removes all interferences. Since the reagent is selective for arsenic(III), the method allows speciation between arsenite and arsenate. Down to 6 ng l^{-1} of both

TABLE 3

Determination of arsenic(III) and arsenic(V) in natural samples[a]

Sample	As(III) found (μg l^{-1})	As(V) found (μg l^{-1})	Total (μg l^{-1})
Tap water[b]	0.006	3.88	3.88
Sea water[c]	0.025	1.38	1.41
Rain and water-soluble dust[d]	0.214	4.85	5.06
Lake water[e]	0.255	2.50	2.75
River water[f]	0.026	15.5	15.5

[a]Each result is the average of 3 determinations. [b]Chlorinated laboratory tap water. [c]10 km from North Sea coast, collected 5 m below the surface. [d]One month in a collection flask on the roof of a 3-storey university building. [e]University lake water. [f]Near a metal factory, Scheldt river.

species can be detected; this limit is the result of arsenic present in the reagents used, otherwise the procedure could be adapted to even lower concentration levels.

This research was carried out within the framework of the National Research and Development Program on the Environment of the Interministerial Commission for Science Policy, Belgium.

REFERENCES

1 R. S. Braman and C. C. Foreback, Science, 182 (1973) 1247.
2 Y. Talmi and D. T. Bostik, Anal. Chem., 47 (1975) 2145.
3 J. S. Edmonds and K. A. Francesconi, Anal. Chem., 48 (1976) 2019.
4 M. O. Andreae, Anal. Chem., 49 (1977) 820.
5 A. U. Shaikh and D. E. Tallman, Anal. Chim. Acta, 98 (1978) 251.
6 D. L. Johnson and M. E. Q. Pilson, Anal. Chim. Acta, 58 (1972) 289.
7 S. A. Peoples, J. Lakso and T. Lais, Proc. West. Pharmacol. Soc., 14 (1971) 178.
8 S. S. Sandhu, Analyst, 101 (1976) 856.
9 F. T. Henry, T. O. Kirch and T. M. Thorpe, Anal. Chem., 51 (1979) 215.
10 F. T. Henry and T. M. Thorpe, Anal. Chem., 52 (1980) 80.
11 K. C. Tam, Environ. Sci. Technol., 8 (1974) 734.
12 T. Kamada, Talanta, 23 (1976) 835.
13 A. W. Fitchett, E. H. Daughtrey Jr. and P. Mushak, Anal. Chim. Acta, 79 (1975) 93.
14 D. Chakraborti, Ph.D. Thesis, Jadavpur University, Calcutta, 1972.
15 D. Chakraborti, W. De Jonghe and F. Adams, Anal. Chim. Acta, 119 (1980) 331.
16 T. Kamada, T. Kumamaru and Y. Yamamoto, Bunseki Kagaku, 24 (1975) 89.
17 T. Inui, N. Fudagawa and A. Kawase, Fresenius Z. Anal. Chem., 299 (1979) 190.
18 T. W. Mastin, G. R. Norman and E. A. Weilmvenster, J. Org. Chem., 67 (1945) 1662.
19 V. P. Wystrach, E. O. Hook and G. L. M. Christopher, J. Am. Chem. Soc., 21 (1956) 705.
20 W. E. Bacon and J. F. Bork, J. Am. Chem. Soc., 27 (1962) 1484.
21 E. Bruninx, Philips Research Reports, Eindhoven, The Netherlands, 30 (1975) 177.
22 J. P. Riley and G. Skirrow, Chem. Oceanogr. Vol. 2, 2nd edn., p. 601, Academic Press, London, 1975.

Analytica Chimica Acta, 120 (1980) 129—139

CHEMICAL SPECIATION OF MERCURY IN NATURAL WATERS

P. D. GOULDEN* and D. H. J. ANTHONY
National Water Research Institute, Burlington, Ontario L7R 4A6 (Canada)
(Received 15th January 1980)

SUMMARY

Improved sensitivity of the cold-vapour atomic absorption method for mercury can be obtained by equilibrating the reduced sample with a small volume of air at 90°C. An automated system has been developed that has a detection limit of 1 ng Hg l^{-1}. By changing the reducing conditions three species of mercury can be differentiated and determined, inorganic mercury, arylmercury compounds such as phenylmercury(II) chloride, and alkylmercury compounds such as methylmercury(II) chloride. Speciation of mercury in natural waters is possible.

The speciation of mercury forms in environmental samples is of interest in order to determine the routes by which mercury passes through the ecosystem and because of the differing toxicities of the various forms. In biological samples such as fish where the mercury levels range up to 100 μg kg^{-1}, it is possible to determine methylmercury either by selective extraction, separation by chromatography followed by quantification, or by chemical speciation by a method such as that described by Magos [1]. The latter method utilizes atomic absorption detection of mercury vapour taking advantage of the fact that methylmercury and inorganic mercury are reduced to elemental mercury under different conditions. For samples such as natural waters, rain and snow, the direct measurement methods have not been sufficiently sensitive to allow chemical speciation such as this.

In the present work, effort has been directed towards lowering the detection limit (currently 0.01 μg Hg l^{-1}) of the mechanized method used here for total mercury. The factors affecting the partitioning of mercury between a liquid and gas phase have been studied. With these results it is possible to define the parameters that must be used in an analytical system for mercury in order to obtain a certain sensitivity. It is shown that in a mechanized system, with partitioning at 90°C and absorbance measurement at room temperature, it is possible to obtain a detection limit of 1 ng Hg l^{-1}. It has been found possible to distinguish three classes of mercury compounds by changing the chemical reduction system. These three classes are inorganic mercury, arylmercury compounds such as phenylmercury(II) salts, and alkylmercury compounds. With a detection limit of 1 ng Hg l^{-1}, this scheme of chemical speciation can be used for the examination of 'clean' natural waters, rain, and melted snow.

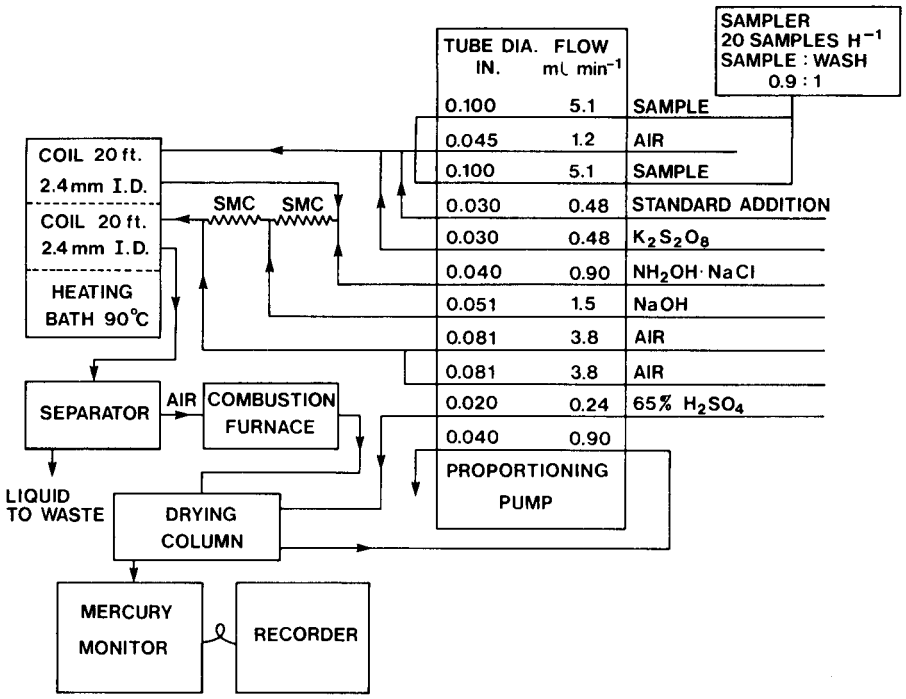

Fig. 1. Manifold for total mercury determination.

EXPERIMENTAL

Apparatus

The manifolds used are shown in Figs. 1 and 2. The sampler is a Sampler IV (Technicon Corp.) fitted with 16 mm × 10 mm sample tubes. The pump is a 20-channel proportioning pump (Carlo Erba); the heating bath (Technicon Corp.) is fitted with a proportional temperature controller (Model 72, Yellow Springs Instrument Co. Inc.). Details of the drying column are shown in Fig. 3. The combustion furnace is made from silica tubing, 0.7 cm o.d., 15 cm long, wrapped with 28-gauge Chromel heating wire connected to a variable transformer. The temperature of the furnace was measured with a thermocouple and controlled manually at 900 ± 50°C. The combustion tube is packed with cobalt oxide catalyst (Beckman Instruments). The mercury monitor (Laboratory Data Control) originally fitted with 0.7 cm × 30 cm cells has the sample cell sleeved with 0.7-cm o.d. borosilicate tubing to give an effective inside diameter of 0.4 cm so that the cell volume is reduced.

The absorption columns used to determine partition coefficients with sulfuric acid and to absorb mercury vapour in potassium dichromate—sulfuric acid solution as a confirmation test were similar to the drying column in Fig. 3 except that the internal diameter was 0.7 cm. Columns ranging in length from 10 cm to 30 cm were used to confirm that equilibrium was reached.

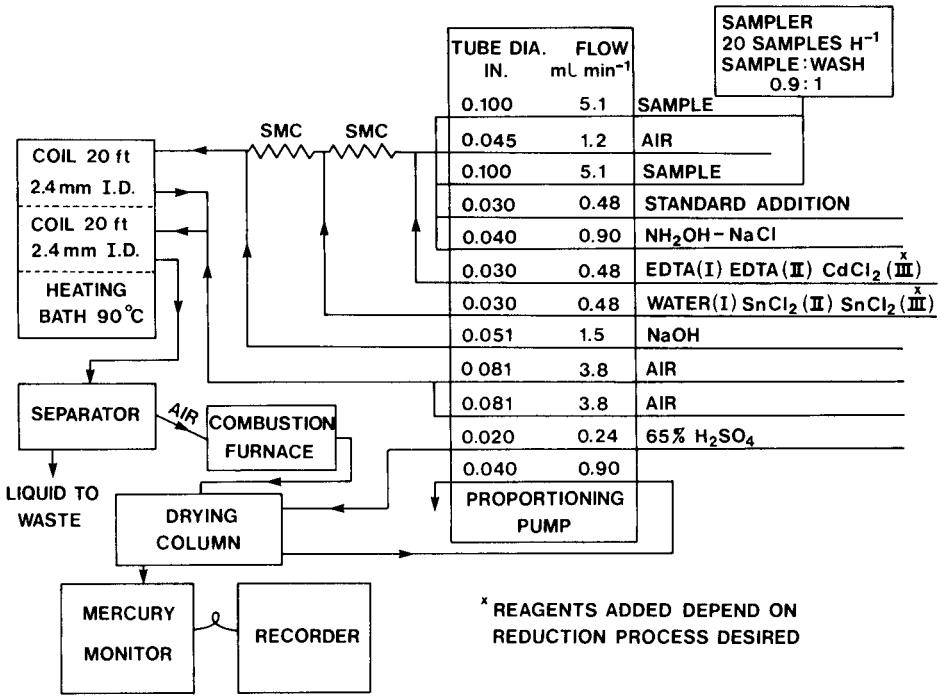

Fig. 2. Manifold for mercury speciation. The asterisks indicate that the reagents added depend on the reduction process required.

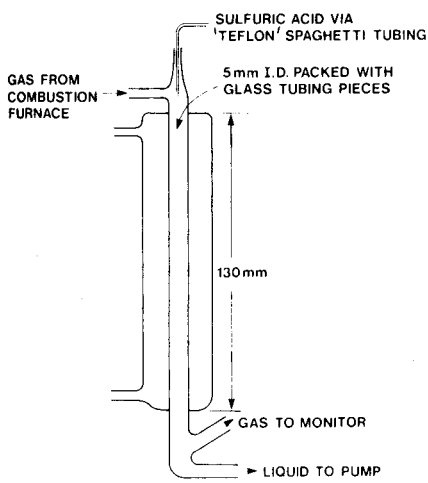

Fig. 3. Drying column.

The gas chromatograph used to confirm the presence of methylmercury was a Hewlett Packard Model 5700A fitted with a ^{63}Ni electron capture detector. The effluent gas from this detector was mixed with oxygen and passed through a combustion furnace similar to the one above, to the mercury monitor.

Reagents

The reagents used are 0.5 M potassium peroxydisulfate, 0.61 M hydroxylammonium sulfate in 5.1 M sodium chloride, 0.27 M disodium ethylenediaminetetraacetate dihydrate, 12.5 M sodium hydroxide, 0.01 M cadmium chloride, and 0.44 M tin(II) chloride dihydrate in 2 M hydrochloric acid.

Procedure

For a determination of total mercury, samples are run using the manifold shown in Fig. 1. The sample is segmented with air and then mixed with potassium peroxydisulfate and water through the "standard addition" line. The mixture is then digested in the first coil of the heating bath to convert all forms of mercury to inorganic mercury. The digested sample is mixed with the hydroxylamine—sodium chloride reagent and sodium hydroxide, more air is added, and the mixture is passed to the second coil in the heating bath. The elemental mercury produced equilibrates between the liquid and air phases in this coil. The liquid and air are separated in the phase separator. The gas stream, containing the mercury vapour, passes through the combustion furnace where organic materials are destroyed. The gas stream is then dried with sulfuric acid in the cooled, packed column and passed to the mercury monitor for absorbance measurement. A calibration curve is obtained by sampling standard solutions of mercury(II) chloride and this is used to determine the levels of mercury in the samples. When the manifold is first set up, calibration curves using mercury(II) chloride and methylmercury(II) chloride are compared to confirm that complete conversion of methylmercury(II) compounds to mercury is obtained. Periodically, the effect of sample matrix is determined by pumping a sample continuously and adding various mercury(II) chloride and methylmercury(II) chloride standards through the "standard addition" line. Comparison of these results with the normal calibration curve enables any effect of sample matrix to be seen.

It should be noted that in this process, no acid is added in the oxidation step except that which is used as a sample preservative. This is because it has been shown [2] that as the acid concentration increases there is a decrease in the efficiency of oxidation by peroxydisulfate.

For speciation, the manifold shown in Fig. 2 is used. The sample is segmented with air and the hydroxylamine—sodium chloride reagent is added. One of the reagent mixtures shown as I, II or III and sodium hydroxide are added, and the sample flow is passed to the first coil in the heating bath where reduction to mercury takes place. This solution is equilibrated with added air in the second coil in the heating bath and from then on the system is the same as the total mercury system above.

The reagent mixtures (I, II and III) and their uses in speciation are as follows. Reagent mixture I is EDTA and water. This reagent with hydroxylamine in an alkaline solution reduces inorganic mercury to mercury. Reagent mixture II is EDTA and tin(II) chloride. With this reagent, inorganic mercury and aryl compounds such as phenylmercury(II) compounds are reduced to mercury. Reagent mixture III is cadmium chloride and tin(II) chloride. With this reagent, all forms of mercury, including methylmercury, are reduced to elemental mercury.

Up to 10 samples are run in turn, using each of these three reagent mixtures. Immediately afterwards, standards of mercury(II) chloride, phenylmercury(II) chloride, and methylmercury(II) chloride in preservative solution are processed under the same three conditions to obtain calibration curves. Comparison of the results of the three determinations allows differentiations among the three mercury species. Often the concern is only for the detection of methylmercury which is given by the difference between determination with reagents III and II. Comparison of the results with reagent III and the total mercury determination with peroxydisulfate oxidation gives confirmation of the total mercury level in the sample.

The effect of sample matrix was determined with the "standard addition" line as described above, with standards of mercury(II), phenylmercury(II) and methylmercury(II) chloride.

Procedures for preliminary and confirmatory studies

The partition coefficients at the various temperatures were determined by a method similar to that used by Koirtyohann and Khalil [3]. A standard mercury solution was pumped continuously, using the reagents for total mercury, and the plateau height was recorded. The solution was re-sampled and re-equilibrated with a fresh air stream in a jacketed packed column controlled at the particular temperature of the heating bath and the absorbance of this air stream was measured. The partition coefficients were then calculated from these two absorbance readings and the liquid and gas flow rates. From Fig. 4 it is seen that at some gas-to-liquid ratios the concentration of mercury in the air stream, and hence the absorbance, is not sensitive to changes in the partition coefficient. Hence, in these determinations the volume ratios were manipulated so that the measurements were made under conditions for which change of one unit in the partition coefficient corresponded to a change in concentration factor of at least 0.1.

The procedure used to provide additional assurance that the absorbance in the mercury monitor was due to mercury vapour was as follows. The sample was sampled continuously and the absorbance observed. The gas was then diverted through an absorption column on its way to the mercury monitor. A solution of 0.03 M potassium dichromate in 3.6 M sulfuric acid was passed down the absorption column. This solution was shown to absorb mercury vapours quantitatively. The solution leaving the column was collected and later the mercury content was determined by adding tin(II) chloride, equi-

librating it with air, and measuring the absorbance with the mercury monitor. The disappearance of the absorbance signal when the gas passes through the absorption column, and the quantitative regeneration of the mercury vapours provided further confirmation that the absorbance measured by the mercury monitor was due to mercury. The confirmation tests for methylmercury were as follows. Sodium chloride (10% by weight) was added to each sample and the solution was extracted with benzene. The benzene extracts were evaporated to small volume and injected into a gas chromatograph. The column used (2 m long, 2 mm i.d.) was packed with 20% Carbowax 20 M on GasChrom Q. The column temperature was 190°C and the injection temperature was 200°C. The carrier gas was nitrogen at 50 ml min^{-1}. After the gas had passed through the electron capture detector, oxygen (6 ml min^{-1}) was added and the gas was passed to the mercury monitor via the combustion furnace. This confirmed that the peak seen by the electron capture detector and attributed to methylmercury by its retention time, did contain mercury. The solvent peak, whose time was shown by the electron capture detector, was manually vented and was not passed to the mercury monitor.

METHOD OPTIMIZATION

The maximum sensitivity of the cold vapour method is achieved when all the mercury from as large a sample as possible is transferred to the minimum amount of air that is needed to make the absorption measurement. In the present work, efforts were made to achieve optimum transfer of the mercury to a small volume of air by controlling the partitioning conditions and to design the hydraulic system, so that the only significant noise was from the electronics of the measuring instrumentation.

Under equilibrium conditions, the factors that affect the concentrations of mercury in the liquid and air streams are the ratio of liquid-to-air volume and the gas/liquid partition coefficient (K). The ratio of concentration in the gas to that originally in the liquid, here called the concentration factor (c), is given by the expression $c = [K^{-1} + V_g\ V_l^{-1}]^{-1}$, where V_g and V_l are the volumes of gas and liquid, respectively. The values of the concentration factor for various partition coefficients and various volume ratios are shown in Fig. 4. The partition coefficients under various conditions of acid concentration and temperature were determined by Koirtyohann and Khalil [3], who found a value of about 0.4 at 25°C. Similar values were found here. The commonly-used systems operate at room temperature so that the maximum concentrations of mercury in the air stream at different volume ratios are given by line A-A in Fig. 4. Thus, in order to achieve a significant increase in sensitivity, the partition coefficient must be controlled. This can be done by changing the operating conditions so that the absolute value is changed, by changing the effective partition coefficient with the use of a counter-current air—liquid flow system, or by an absorption—desorption system.

Clifton [4] has noted the increase in absorbance signal when the temperature of the mercury reduction system is raised from 10 to 40°C. Koirtyohann and Khalil [3] found that the partition coefficient increased from 0.4 to 0.7 over the range 10—90°C. In the present work, the apparent partition coefficient, K_a, was determined as a function of solution matrix and temperature.

In these determinations, the air was equilibrated with the liquid at a certain temperature, the air was separated, cooled to 25°C and dried, and the absorbance was measured. The ratio of the concentration of mercury in this cooled, dried air to the concentration of mercury in the liquid is the apparent partition coefficient. (When this system is used for separation and measurement, K_a may be used in place of K in Fig. 4.) The results (Table 1) show that K_a is affected by the concentration of alkali or acid in the liquid and that a value of K_a of about 5 can be obtained by raising the temperature to 90°C. With a partition coefficient of this magnitude, it is believed that the concurrent flow system, with its inherent advantage of maintaining sample integrity and achievement of equilibrium conditions, can provide sufficient sensitivity, and alternative ways of obtaining high effective partition coefficients were not pursued. It is possible to obtain still higher partition coefficients by raising the temperature even higher and, in fact, to strip the mercury from solution with steam. However, the water that vaporizes with the mercury must be removed and the choice of 90°C was made as an optimum situation where K_a is of adequate magnitude and the amount of water vaporized is 'reasonable'. (The 8.8 ml min^{-1} of air contains 0.017 ml min^{-1} of water.)

The system was required for the routine analysis of samples at a minimum rate of 20 samples per hour. This places some constraints on the volume ratios of air-to-liquid that can be used because of the volume of the sample cell in the mercury monitor and the amount of sample that can be conveniently handled in a 'Technicon Sampler IV'. This resulted in the air-to-liquid volume ratio of 0.6 that is used in the manifold shown. If a different type of sampler was used, or if the samples were handled manually, the sensitivity could be changed as shown by line B-B in Fig. 4.

TABLE 1

Effects of temperature and matrix on partition coefficients

Temperature (°C)	Partition coefficient			
	0.6% H_2SO_4	20% H_2SO_4	2% NaOH	4% NaOH
10	0.4	0.5	0.5	0.6
25	0.5	0.6	0.7	0.7
50	0.8	1.4	1.5	1.7
70	2.0	2.5	2.7	3.0
90	3.8	4.1	4.6	5.0

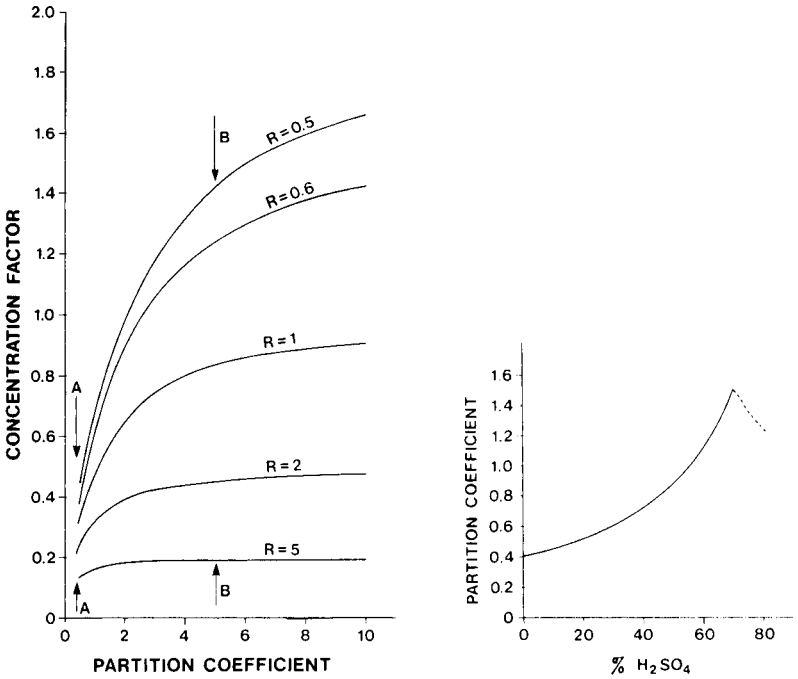

Fig. 4. Concentration factor for various volume ratios and partition coefficients. $R = V_g V_l^{-1}$. A-A shows the range of concentration factors available at room temperature. B-B shows the range available at 90°C.

Fig. 5. Partition coefficient for sulfuric acid solutions.

To avoid problems of water mist in the detector, and to improve the noise characteristics, it was found desirable to dry the air stream chemically. This was most conveniently done with sulfuric acid in the column shown in Fig. 3. To establish the best sulfuric acid concentration, the partition coefficients of mercury between air and various concentrations of sulfuric acid were determined. These results (Fig. 5) indicate that the partition coefficient increases with concentration, until a concentration of about 75% by weight is reached. Above this concentration, the mercury is absorbed by the sulfuric acid and cannot be re-volatilized by sparging with air.

In the system used for total mercury with peroxydisulfate oxidation, the amplitude of the variations in the baseline trace is equivalent to about 0.3 ng Hg l^{-1}. For a factor of three times this noise, the detection limit is about 1 ng Hg l^{-1}. The relative standard deviations obtained in replicate determinations were 1.2%, 1.9%, 2.3%, and 5% at mercury levels of 200, 50, 20 and 10 ng Hg l^{-1}, respectively. The detection limits and precision of the determinations of other mercury species are similar to these.

To carry out the chemical speciation, an automatic method is not needed here from the viewpoint of handling many samples. However, it is con-

venient to use the system with the mechanized sampler, and the sensitivity and precision are sufficiently good for the method to be used with natural water samples, rain and melted snow.

RESULTS AND DISCUSSION

Speciation

Synthetic samples. Several compounds at the 0.2 μg Hg l^{-1} level were analyzed by using the various reducing conditions described above. The results (Table 2) show that three types of mercury compounds can be distinguished: inorganic mercury, compounds such as phenylmercury(II) chloride, and compounds such as methylmercury chloride. Ethoxyethylmercury(II) chloride and methoxyethylmercury(II) chloride gave some response under the conditions for determining inorganic mercury.

Natural samples. Typical results on natural water samples are shown in Table 3. It is seen that some of these samples contain methylmercury and that in some samples this may amount to 20% of the total mercury. None of the samples contained any organomercury other than methylmercury. These results came from the analysis of a batch of eighteen lake water samples and ten rain samples, all of which had detectable levels of total mercury. Twelve of the water samples and all of the rain samples contained only inorganic mercury.

The samples that contained methylmercury were analyzed by the extraction—chromatographic procedure described above. The only organomercury that was found was methylmercury and there was agreement to within ±20% with the results obtained by the chemical speciation.

Sample preservation

The water samples collected here for a total mercury determination are preserved by the addition of 1% (by volume) sulfuric acid and 0.05% potassium dichromate. There has been discussion on the need for this type of preservative [5]. The effect of this on the various organomercury compounds shown in Table 1 was determined by a series of storage tests. The materials at levels of 0.2 μg Hg l^{-1} were stored at room temperature and periodically monitored. It was found that they were all converted to inorganic mercury, the most resistant being methylmercury and diphenylmercury which were about 50% converted in 30 days. The conversion is a function of the dichromate addition. When they were stored in 1% sulfuric acid for 30 days, the phenyl, diphenyl, methyl, and ethyl compounds showed negligible conversion to inorganic mercury. Thus it would appear that for speciation work, two samples should be taken, one preserved with the dichromate—sulfuric acid mixture and one preserved with sulfuric acid alone. Prompt analysis is also an assurance of more valid results.

TABLE 2

Effect of digestion conditions on mercury determined for selected compounds

Compound (200 ng Hg l^{-1})	Mercury determined (ng l^{-1})			
	I[a]	II[a]	III[a]	IV[b]
$HgCl_2$	204	210	202	200
$C_2H_5O \cdot C_2H_5HgCl$	41	196	204	198
$CH_3O \cdot C_2H_5HgCl$	56	192	194	202
C_6H_5HgCl	6	214	206	208
$(C_6H_5)_2$ Hg	4	186	192	182
C_2H_5HgCl	5	12	214	216
CH_3HgCl	4	10	208	200

[a]Speciation reagents in Fig. 2. [b]Total mercury after peroxydisulfate oxidation.

TABLE 3

Mercury determined in selected water samples

Sample No.[a]	Mercury determined (ng l^{-1})				Difference (III—II)	
	I[b]	II[b]	III[b]	IV[c]	(ng Hg l^{-1})	% of Total
1	31	30	33	33	3	10
2	82	84	96	94	12	12
3	61	60	73	70	13	18
4	103	102	112	114	10	9
5	110	111	139	140	28	20
6	164	167	178	189	11	6
7	108	106	110	108	—	—
8	61	60	58	61	—	—
9	22	26	26	23	—	—
10	18	20	20	22	—	—

[a]Samples 1—8 are lake waters; samples 9 and 10 are rain water. [b]Speciation reagents in Fig. 2. [c]Total mercury using peroxydisulfate oxidation.

Interferences

The most serious potential interference in the method arises from volatile organic materials which absorb the 253.7-nm radiation in the mercury monitor. However, these are destroyed in the oxidizing furnace. For example, benzene at a level of 10 mg l^{-1} in a sample gives an apparent mercury reading, without the furnace, of 0.4 μg Hg l^{-1}. Comparison of the results from treatments III and IV (see Table 3), also offers some indication of spurious mercury results because of the presence of organic materials.

Other interferences, reported to occur in an acidic reduction system, do not present any difficulties in the alkaline reduction system used here. For example, high chloride levels which are reported to interfere because of production of chlorine in the peroxydisulfate oxidation [6] do not interfere

here in that way since any chlorine produced is completely absorbed in the alkaline solution. However, it was found that when high chloride levels are present, organic materials may not be completely oxidized, e.g., benzene (10 mg l^{-1}) in a sample, completely oxidized in fresh water, was only 60% oxidized in synthetic sea water. However, it has been shown [7, 8] that free chlorine and bromine are extremely efficient reagents for breaking down organomercury compounds even in the presence of unoxidized organic material. This was confirmed in the present work. Standard additions of methylmercury to sewage samples with a chemical oxygen demand of 500 mg l^{-1} gave complete recovery of mercury even in the presence of 4% sodium chloride. The combustion furnace gives protection against unoxidized volatile organic materials.

Alkaline volatile materials such as ammonia and amines do not interfere because any material that is volatilized is absorbed by the sulfuric acid used in the drying column. There was no interference from ammonium chloride (500 mg l^{-1}).

The ionic strength of the solution has some effect on the recovery of mercury in the reduction process using hydroxylamine alone. The sodium chloride is added in this process to swamp out any differences between samples and standards.

The work of Magos [1] and of Umezaki and Iwamoto [9] indicates that, with a reduction system of hydroxylamine with tin(II) chloride, only inorganic mercury should be reduced in the absence of copper or cadmium. In the present work, the situation was found to be not quite so simple. With many natural waters, particularly waters of high salinity such as those from Western Canada, it was found that standard additions of methylmercury gave significant recovery of mercury even when copper or cadmium was not added. With some waters, added methylmercury (200 ng Hg l^{-1}) was 40% reduced to elemental mercury. This is presumably because of other trace metals present acting as reduction catalysts. It was found that the addition of EDTA in the manifold prevented this unusual reduction of methyl and ethyl mercury.

REFERENCES

1 L. Magos, Analyst, 96 (1971) 847.
2 P. D. Goulden and D. H. J. Anthony, Anal. Chem., 50 (1978) 953.
3 S. R. Koirtyohann and M. Khalil, Anal. Chem., 48 (1976) 136.
4 A. P. Clifton, Int. J. Environ. Anal. Chem., 4 (1975) 47.
5 J. Carron and H. Agemian, Anal. Chim. Acta, 92 (1977) 61 (and references therein).
6 H. Agemian and A. S. Y. Chau, Anal. Chem., 50 (1978) 13.
7 D. E. Becknell, R. H. Marsh and W. Allie, Anal. Chem., 43 (1971) 1230.
8 B. J. Farey, L. A. Nelson and M. G. Rolph, Analyst, 103 (1978) 656.
9 Y. Umezaki and K. Iwamoto, Jpn. Analyst, 20 (1971) 173.

Analytica Chimica Acta, 120 (1980) 141—146

REDUCTION OF CHEMICAL INTERFERENCE AND SPECIATION STUDIES IN THE HYDRIDE GENERATION—ATOMIC ABSORPTION METHOD FOR SELENIUM

P. N. VIJAN* and D. LEUNG

Laboratory Services Branch, Ontario Ministry of the Environment, 125 Resources Road, Rexdale, Ontario M9W 5L1 (Canada)

(Received 18th February 1980)

SUMMARY

A simple procedure is described for reducing the chemical interference of heavy metal ions with the hydride—atomic absorption spectroscopic method for the determination of selenium. This is achieved through the formation of stable chlorocomplexes of these ions in 7.5 M HCl. Up to 30 μg Cu(II) ml^{-1}, 500 μg Ni(II) ml^{-1}, and 500 μg Fe(III) ml^{-1} do not interfere. Recoveries of selenium from standard reference samples, fortified with known interfering concentrations of heavy metals, range between 92 and 101%. The reducing property of hydrochloric acid is used to differentiate between Se(IV) and Se(VI) species.

The hydride generation—atomic absorption spectroscopic (a.a.s.) method for the determination of selenium suffers from interferences by $\mu g\ g^{-1}$ amounts of copper, nickel and precious metal ions in solution [1—4]. These ions interfere chemically by inhibiting the conversion of selenium into its hydride. Whereas precious metals are rarely present in environmental samples, copper, nickel and related heavy metals are quite common. While some information on the elimination of such interferences is available [1, 5, 6], proposed procedures have not proven completely satisfactory. The present paper utilizes the ability of hydrochloric acid to form chlorocomplexes with commonly occurring heavy metals, typically copper and nickel [7], thus virtually eliminating their interference. This reducing property of hydrochloric acid may also serve to differentiate between the tetravalent and hexavalent forms of selenium.

EXPERIMENTAL

Apparatus and reagents

The sample manifold is illustrated in Fig. 1. Various instruments and accessories used were the same as described previously [1].

Distilled water was used for preparation of standard and reagent solutions, and analytical reagent-grade chemicals were used. All test solutions were prepared from 1000 $\mu g\ ml^{-1}$ stock standards of individual elements. A

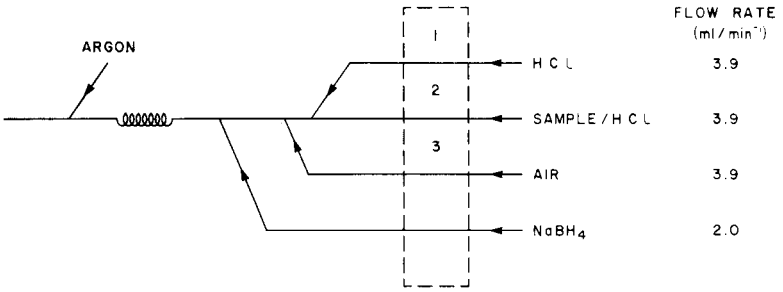

Fig. 1. Schematic diagram of the manifold.

1 μg Se(IV) ml^{-1} solution was prepared by serial dilution with 1% nitric acid of a 1000 μg Se(IV) ml^{-1} solution prepared from high-purity selenium. A 1 μg Se(VI) ml^{-1} solution was prepared by a dropwise addition of 0.004 M potassium permanganate to 10 ml of 10 μg Se(IV) ml^{-1} solution until the appearance of light pink colour. The volume was then made to 100 ml with 1% nitric acid. A 1.0 % (w/v) solution of sodium tetrahydroborate was prepared in 0.1 % sodium hydroxide. A 6:3:1 mixture of nitric, sulfuric, and perchloric acids was used for sample digestion.

Procedure

Standard Reference Material (SRM) samples, containing 1—4 μg of selenium were accurately weighed into 250-ml Erlenmeyer flasks equipped with air condensers. A few glass beads and 15 ml of the digestion mixture were added to each flask and heated slowly and gently until copious white fumes of sulfur trioxide evolved. The digests were then diluted to 100 ml at room temperature.

Various test solutions for interference studies were prepared to contain 20 ng Se ml^{-1} in appropriate concentrations of hydrochloric acid. Speciation test solutions were prepared by adding identical aliquot pairs of 1 μg Se(VI) ml^{-1} and 1 μg Se(IV) ml^{-1} solutions to two sets of six 25-ml volumetric flasks and diluting the contents of one set to 25 ml with 1 M HCl and the other set with 9 M HCl.

RESULTS AND DISCUSSION

Curve b in Fig. 2 shows the relationship between hydrochloric acid concentration and the selenium signal. A significant decrease in signal is noticed when the acid concentration of the mixed stream exceeds 8 M, the decrease is ca. 22% at 9 M and 33% at 10.5 M HCl. This loss in sensitivity may be due to decreased residence time of atoms in the quartz tube on account of accelerated reaction of sodium tetrahydroborate at high acidities. Thus some control is necessary to maintain the acid concentration of the mixed stream between 6 and 8 M in order to achieve optimum sensitivity as well as desirable freedom from interference by heavy metals.

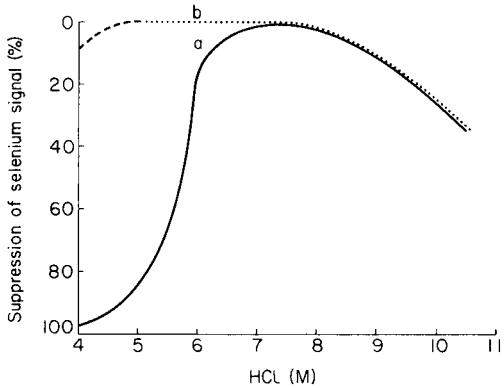

Fig. 2. Effect of hydrochloric acid on absorbance signal of selenium (20 ng ml^{-1}): (a) in presence of 20 μg Cu(II) ml^{-1}; (b) in absence of Cu(II).

Curve a in Fig. 2 illustrates the effect of hydrochloric acid concentration on samples containing copper(II). It is obvious that the interference of 20 μg Cu ml^{-1} with the absorption signal of 20 ng Se ml^{-1} is virtually eliminated when the acid concentration of the sample reaches 6 M. Since 9 M acid is drawn through the reagent line, the effective hydrochloric acid concentration of the mixed stream is 7.5 M. This acid concentration may also be optimum for maximum sensitivity and freedom from interferences for manual hydride generation methods. Nickel, cobalt, iron, and other related heavy metal ions show similar behavior. To evaluate the chlorocomplexation procedure, 20 ppm copper solutions were prepared in 1 M and 9 M HCl. The solution prepared in 1 M acid produced a black precipitate of elemental copper on reaction with tetrahydroborate whereas the one prepared in 9 M acid remained clear. The solution containing 20 μg Cu(II) ml^{-1} had a characteristic yellowish colour, with absorbance at 400 nm increasing linearly with increase in hydrochloric acid concentration from 0 to 12 M. The degree of complexation was maximum in 12 M HCl. Replacement of hydrochloric acid with an equivalent amount of sodium chloride in the presence of 6 M sulfuric or perchloric acid did not produce the desired results. Sulfuric acid, although known to form sulfato complexes of lesser stability [7], failed to yield the desired reduction in interference. The use of perchloric or nitric acid did not reduce interferences under similar experimental conditions.

Table 1 shows the effect of increasing concentrations of interfering ions on the absorbance of 20 ng Se ml^{-1}. The test solutions were prepared in 6 M HCl with 9 M acid feeding through the reagent line. Ions of other heavy metals such as cadmium, zinc, manganese, cobalt, vanadium, and chromium did not interfere. As much as 500 ppm nickel(II) or iron(III) did not interfere significantly. Up to 30 ppm strontium(II) or phosphate did not affect the complete recovery of 20 ng Se ml^{-1}. Most environmental samples are unlikely to contain such high concentrations of these species. In samples such as minerals and metals, containing high concentrations

of these elements, coprecipitation of selenium prior to the measurement step may be the preferred approach. Interference by precious metal ions could not be removed, although they are known to form chlorocomplexes. However, their occurrence in environmental samples is unlikely.

Table 2 contains the results of determinations of selenium in four National Bureau of Standards (NBS) reference material samples and three EPA water standards spiked with Cu(II), Ni(II), and Fe(III). The results are in close agreement with the certified values.

An in-house sewage sludge sample containing 1.50 ppm selenium was analysed 10 times to determine the precision of the method. A mean value of 1.52 ppm was determined with a relative standard deviation of 2.5%. No selenium signal could be obtained on this sample when processed by the previous method [1] because of interference by heavy metals. An alternative digestion with 1:1 H_2SO_4—HNO_3 mixture containing 0.1% vanadium pentoxide was also tried on NBS and sewage samples. The digestions were satisfactory and the high concentration of dissolved vanadium did not interfere. Unlike the previous method [1], the wash solution in the present work was 9 M HCl instead of distilled water. This did not affect the performance of the system and allowed the uninterrupted generation of

TABLE 1

Influence of heavy metal ions on selenium signal from a 20 ng Se(IV) ml^{-1} solution

Interfering ion	Amount ($\mu g\ ml^{-1}$)	% Suppression	Interfering ion	Amount ($\mu g\ ml^{-1}$)	% Suppression
Cu(II)	15	0	Ni(II)	500	2
Cu(II)	30	10	Fe(III)	50	0
Cu(II)	100	30	Fe(III)	100	5
Ni(II)	100	0	Fe(III)	500	10

TABLE 2

Determination of selenium in reference samples spiked[a] with interfering ions

Sample	Se found[b] ($\mu g\ g^{-1}$)	Certified value ($\mu g\ g^{-1}$)	Recovery (%)
Albacore Tuna, SRM 50	3.84 ± 0.10	3.96 ± 0.2	97
Bovine Liver, SRM 1577	1.05 ± 0.05	1.10 ± 0.1	95
Wheat Flour, SRM 1567	1.00 ± 0.10	1.10 ± 0.2	92
Rice Flour, SRM 1568	0.38 ± 0.05	0.40 ± 0.1	95
EPA 1	8.8 ng ml^{-1}	8.7 ng ml^{-1}	101
EPA 2	24.1 ng ml^{-1}	24.0	100.4
EPA 3	16.0 ng ml^{-1}	16	100

[a]Sample solutions spiked with 10, 25, 25 ppm of Cu(II), Ni(II), Fe(III), respectively.
[b]Mean of triplicate determination.

hydrogen during the wash cycle. It also prevented the accumulation of metals in the manifold. Loss of signal by accidental contamination of the manifold with heavy metals can be restored by two to three washings with concentrated nitric acid. Use of a non-metallic sampling probe is recommended.

In addition to complexing heavy metal ions and furnishing hydrogen ions for the chemical reaction, hydrochloric acid plays an important role as a reducing agent. Selenium(VI) does not convert to its hydride unless it is reduced to the tetravalent state. Figure 3 illustrates the effect of increasing concentration of hydrochloric acid on the degrees of conversion of Se(VI) to Se(IV). The reduction is incomplete in 4.5 M HCl but goes to completion when the hydrochloric acid concentration in the mixed stream reaches 7.5 M. Use of nitric acid in place of hydrochloric acid reduced the signals. Further support to the reducing property of hydrochloric acid was lent by the facts that a 250-μg aliquot of 2 μg Se(VI) ml^{-1} solution diluted to 25 ml with 1 M HCl produced no signal while full signal was restored when a 250-μl aliquot of 2 μg Se(VI) ml^{-1} was first mixed with 2 ml of concentrated hydrochloric acid and then diluted to 25 ml with water. Although the final acid concentration in both cases was 1 M, in the latter instance, the hydrochloric acid concentration was approximately 10.7 M before dilution. This momentary high acid concentration caused the complete conversion of Se(VI) to Se(IV). It also suggests that the reduction is fairly rapid. Once the reduction is complete, subsequent dilution does not affect the valency of selenium.

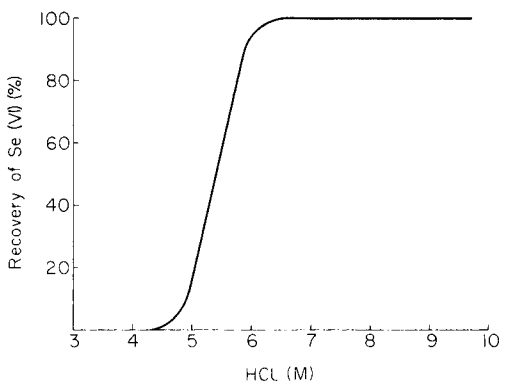

Fig. 3. Effect of hydrochloric acid on reduction of selenium(VI) to selenium(IV) (20 ng ml^{-1}).

This difference in behaviour of the hexa- and tetravalent forms of selenium offered an interesting opportunity to differentiate between the two species. Total selenium was determined in 9 M HCl and selenium(IV) in 1 M HCl media. The difference between the two was equivalent to selenium (VI). This is demonstrated by data in Table 3. A speciation study may be possible only in natural waters free of interfering ions or containing such low ionic concentrations of copper, nickel, iron, and related heavy metals which do not interfere in $\leqslant$ 4 M hydrochloric acid.

TABLE 3

Influence of hydrochloric acid concentration on selenium determinations

Se added (ng ml^{-1})		Se found (ng ml^{-1})		
Se(IV)	Se(VI)	1 M HCl	9 M HCl	Difference
0	20	0.1	20.1	20.0
4	16	3.9	20.4	16.5
8	12	7.8	20.2	12.4
12	8	12.2	19.9	7.7
16	4	16.0	20.2	4.2
20	0	19.8	20.0	0.2

We thank the Director of the Laboratory Services Branch for his support and encouragement in carrying out this work.

REFERENCES

1 P. N. Vijan and G. R. Wood, Talanta, 23 (1976) 89.
2 A. E. Smith, Analyst, 100 (1975) 300.
3 D. D. Siemer, Analyt. Lett, 8 (5) (1975) 323.
4 F. D. Pierce and H. R. Brown, Anal. Chem., 49 (1977) 1417; 48 (1976) 693.
5 M. Bedard and J. D. Kerbyson, Can. J. Spectrosc., 21 (1975) 64.
6 G. F. Kirkbright and M. Taddia, At. Absorpt. Newsl., 18 (1979) 68.
7 T. Moeller, Advanced Text Book of Inorganic Chemistry, 7th edn., J. Wiley, New York, 1958, pp. 237 and 428.

Analytica Chimica Acta, 120 (1980) 147—154

DETERMINATION OF TRACES OF CHLORIDE IN SOLUTION BY MICROWAVE-INDUCED PLASMA EMISSION SPECTROMETRY USING CHLORINE GENERATION

J. F. ALDER*, QINHAN JIN** and R. D. SNOOK

Department of Chemistry, Imperial College, London SW7 2AY (Gt. Britain)

(Received 12th May 1980)

SUMMARY

The method described for the determination of traces of chloride in solution by microwave-induced argon plasma emission spectrometry is based on the evolution of chlorine from a potassium permanganate solution in sulphuric acid and measurement of the chlorine molecular emission at 257 nm. The detection limit is 10 ng of chloride and the log—log calibration plots are linear over ranges of 0.025—100 μg of chloride, depending on the orientation of the plasma. Potential interfering elements are shown not to present any major problems.

The determination of traces of chloride in solution or solid matrices is difficult; neutron activation analysis is frequently used [1—4]. Other techniques that have been examined are cathodic stripping voltammetry [5], microwave-induced plasma emission spectrometry (m.i.p.e.s.) [6–10] and indirect flame emission spectrometry [11].

Since the excitation energy of chlorine is high and its principal resonance line lies in the far-ultraviolet region of the spectrum [12], it is difficult to determine chlorine directly by flame atomic emission or absorption spectrometry [13]. The sensitivity of the spectrographic determination of chlorine in solution by the copper-spark method [14] or by means of a hollow cathode [15] is also poor; values of 10 ppm [14] and 3 ppm [15], respectively, were reported. In recent years, several papers on the determination of trace chlorine in gas chromatographic effluents by m.i.p.e.s. have appeared. Dagnall et al. [7] used an atmospheric argon microwave-induced plasma as an element-selective detector for gas chromatography; a detection limit of 4.5×10^{-9} g s^{-1} was reported for the 257-nm chlorine molecular band. Bache and Lisk [6] and McLean et al. [8] used a reduced-pressure helium microwave-induced plasma; the detection limit for chlorine was 6×10^{-11} g s^{-1} for the Cl(I) 479.5-nm line. Beenakker [9] used a novel cavity to operate a helium or argon microwave-induced plasma at atmospheric pressure and reported an improvement in detection limits for the halogens

**On leave from Department of Chemistry, Jilin University, Changchun, People's Republic of China.

(7×10^{-12} g s^{-1} for chlorine). Hanai et al. [10] used an atmospheric "Surfatron" plasma and obtained a detection limit of 1×10^{-9} g s^{-1}. None of these authors has applied their methods to the determination of chloride in solution or solids.

In this paper, a method for generating chlorine from solution is described; this gives a significant improvement in the capability of m.i.p.e.s. for the determination of chloride.

EXPERIMENTAL

Instrumentation

The basic configuration of the instrumentation is shown in Fig. 1 and the details of the components employed are listed in Table 1. The by-pass tap 1 serves to keep the plasma alight when tap 2 is turned off to permit sample injection and to generate chlorine.

Reagents

Analytical-reagent grade materials were employed throughout. Stock solutions of 1000 ppm chloride were prepared by dissolving sodium chloride in distilled water. Working solutions were prepared daily.

The generating solution was prepared by dissolving 0.3 g of potassium permanganate in 25 ml of concentrated sulphuric acid, and allowing to stand overnight.

Procedure

A 7.5-ml portion of generating solution was transferred to the generating cell (25 ml). After being stirred under an argon flow for 20 min, this solution was ready for use. Tap 2 was turned off and tap 1 on to keep the plasma alight. A 50-μl aliquot of sample solution was injected into the cell through the side-arm. A minute later, the chlorine generated was swept into the plasma by turning on tap 2 and turning off tap 1. The chlorine molecular emission signal at 257 nm was measured, using the optimum operating conditions given in Table 2, and displayed on the recorder.

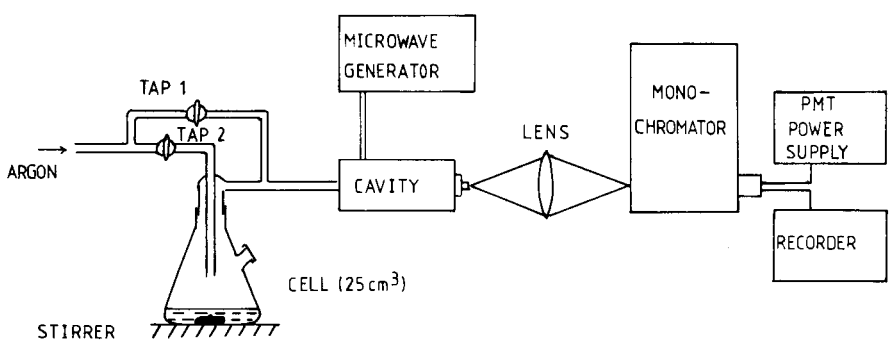

Fig. 1. Schematic diagram of instrumentation and generating cell.

TABLE 1

Specifications of equipment

Microwave generator	Microtron 200 (EMS Ltd., Wantage, Berkshire) and reflected power meter
Cavity	Evenson ¾-wave; silica tube (2.0 mm i.d., 4.0 mm o.d.)
Spectrometer	Rank Hilger D330, 33-cm focal length Czerny–Turner scanning monochromator (1200 lines mm^{-1} grating blazed at 300 nm); reciprocal linear dispersion, 2.7 nm mm^{-1}; measured resolution, 0.08 nm at 15-μm slit width
Optics	Plasma imaged in 1:1 ratio on to entrance slit with one 7.5-cm focal length fused silica lens
Photomultiplier	EMI 6256B
Chart recorder	Oxford 3000 series (250 ms for f.s.d.)
Sample application	50-μl Jencons micropipette with disposable polypropylene tips

TABLE 2

Optimum operating conditions for determination of chloride in solution

Generator net forward power	60 W	Entrance slit width	50 μm
Photomultiplier	1100 V	Entrance slit height	2 mm
Argon flow rate	1.0 l min^{-1}	Exit slit width	50 μm
Sample solution volume applied	50 μl	Wavelength	257.6 nm

RESULTS AND DISCUSSION

Wavelength

The most intense spectral line of chlorine in the u.v.–visible region is Cl(II) at 479.5 nm, although it is observed only weakly in the spectra from both r.f. plasmas [16] and microwave-induced plasmas, as are the atomic lines Cl(I) at 439.0 nm and 452.6 nm. Pearce and Gaydon [17] pointed out that the chlorine molecular emission band at 257 nm is the most sensitive for chlorine compounds, a fact corroborated in this work; the signal at the 257-nm band was about 25 times greater than that for Cl(I) at 439.0 nm for the same plasma conditions and chlorine partial pressure.

In this work, two maxima were found in the molecular emission spectrum from chlorine, at 256.8 nm and 257.6 nm (Fig. 2). At 257 nm there is interference, probably from the Mn(II) 257.6-nm line, arising from carry-over of a manganese(VII) compound, but it can be eliminated by measuring at an adjacent wavelength and controlling the analytical conditions (especially the argon flow rate and slit width).

Method of chlorine generation

Several reagents for generating chlorine from solutions were investigated. They included potassium peroxodisulphate, potassium dichromate and

cerium(IV) sulphate, all in sulphuric acid, but the best was potassium permanganate in concentrated sulphuric acid. Such a solution, however, is somewhat unstable when freshly prepared, forming manganese(VII) oxide (Mn_2O_7) which decomposes to manganese(IV) oxide and oxygen [18]. The oxygen released makes the plasma unstable, but this can be avoided by standing the solution overnight before use to permit stabilization.

Since manganese(VII) oxide decomposes at 55°C, heating the generating solution to accelerate the release rate of chlorine is not feasible; in fact, the reaction between chloride and the generating solution is rapid enough not to require heating. When signals were repeatedly recorded every 50 s for about 10 s for a single sample, the peak heights obtained decreased in a geometric series (Fig. 3). The general expression for the peak heights obtained is $h_n = h_1 g^{n-1}$, where h_n is the peak height of the nth peak, h_1 is the height of the first peak and g is a proportionally constant. This result agrees with the assumption that the rate of chlorine release is merely controlled by the distribution of chlorine between gas and liquid phases in the generating cell. The value of g obtained from 16 experiments was 0.70 and the relative standard deviation was 4.7%.

Optimization of operation parameters

Pure aqueous standard chloride solutions were used to optimize the experimental variables in the instrumental system and to determine the best attainable sensitivity and precision. The forward microwave power, reflected power, cavity position, argon flow rate, chlorine generating cell volume, generating

Fig. 2. Chlorine band emission from the microwave-induced plasma. Lower spectrum is from argon alone; upper spectrum is from argon + 1% chlorine.

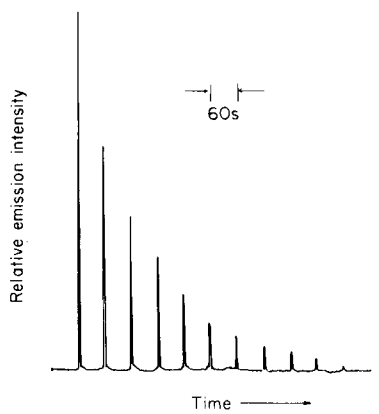

Fig. 3. Chlorine emission peak heights recorded at 1-min generation time intervals for a single chloride sample.

solution volume, concentration of potassium permanganate, sample solution volume, slit width and photomultiplier e.h.t. used were varied independently in order to establish the optimal conditions reported in Table 2.

Two positions of the cavity were studied, the plasma being placed perpendicular or parallel to the monochromator axis. When the cavity was held perpendicularly (i.e. vertically), the log—log calibration graph obtained had a slope of 2.0 at its linear portion (Fig. 4). When the cavity was held horizontally, the detection limit was significantly improved but the slope log—log plot was 0.61 and the signal reproducibility was worse.

Argon flow rate significantly influenced both the background emission and the chlorine molecular emission. The best signal-to-background ratio was obtained at an argon flow rate of 1.0 l min^{-1} for both cavity positions (Fig. 5). The effect of the forward microwave power when the cavity was held horizontally is shown in Fig. 6. When the power was over 80 W the plasma became unstable.

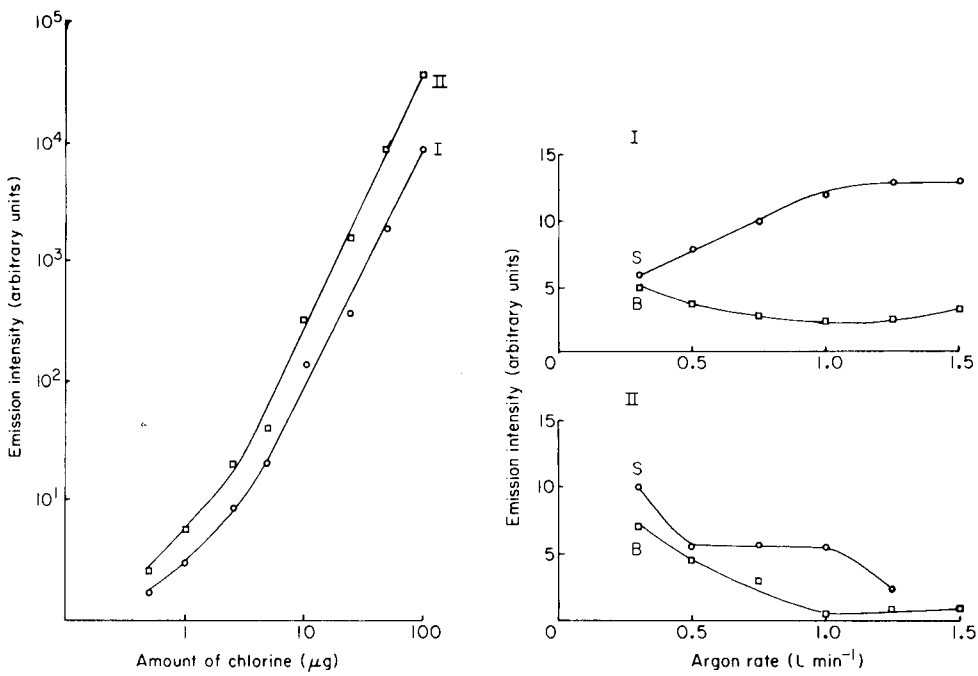

Fig. 4. Chlorine calibration curves derived from (I) first peak height measurement (slope, 2.0); (II) sum of peak height series (slope, 2.1). Plasma held perpendicularly to the monochromator axis.

Fig. 5. Emission intensity of chlorine band (S) and background (B) as a function of argon flow rate: (I) vertical plasma; (II) horizontal plasma.

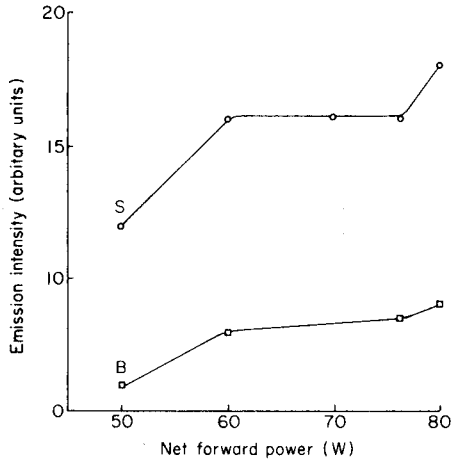

Fig. 6. Emission intensity of chlorine band (S) and background (B) as a function of forward microwave power (cavity held horizontally).

Calibration graph, detection limit and interferences

Under the optimal operating conditions, calibration curves similar to curve I of Fig. 4 were found to be linear over the range 0.025—25 μg (cavity held horizontally) or over the range 5—100 μg (cavity held perpendicularly) of chloride. The detection limits, defined as the mass of chloride required to produce a signal twice the standard deviation of the blank, were 10 ng and 200 ng, respectively. For the determination of chloride at low concentrations (<25 μg) the horizontal configuration is best; for higher concentrations, the vertical configuration is more useful.

When the sum of the peak heights, from repeated degassing of a sample vs. log [Cl], was used, the log—log calibration graph was nearly parallel to the log—log plot based on the first signal alone (Fig. 4). Since the peak-heights decreased in a geometric series, the sum of the peak heights could be calculated from the first peak height. The constant g was measured from a large number of experiments and the sum of all peak heights, H_{sum}, was calculated from $H_{sum} = h_1(1 - g^n)/(1 - g)$. From the viewpoint of signal-to-noise ratio, there is no advantage in doing this calculation, because the resultant relative standard deviation (r.s.d.) will increase as well as the signal magnitude. Thus only the first peak height and precision need be measured in order to gain a true representation of the concentration of chloride in the sample. Any improvement in the efficiency of chloride release from the solution will show itself as a decrease in the value of g.

Potential interferences

The effects of some potentially interfering elements, which are known to have serious effects on microwave plasmas, were studied. The results obtained are shown in Table 3. The r.s.d of the signal for 0.25 μg of chloride was 9%

TABLE 3

Effects of potential interfering elements on the signal obtained for 0.25 μg of chloride

Element	Added as	Ratio element: Cl (w/w)	Change in signal (%)[a]
Mercury	Nitrate	1000	0[b]
Tellurium	Nitrate	500	0
Fluorine	Sodium	40	+6
Bromine	Sodium	20	+8
Iodine	Potassium	40	+9

[a]Mean of three replicates. The r.s.d. for 0.25 μg Cl^- alone was 9%. [b]See text.

so there is no significant interference from I, Br, F, Te or Hg at the levels studied. The effect of mercury is more complex than appears from Table 3. If a sample of chloride contaminated with a 1000-fold amount of mercury is introduced into the cell, the signal from chlorine is unaltered. The presence of the mercury, however, apparently causes rapid destruction of the oxidizing properties of the solution (the deep colour of the solution lightens), and subsequent additions of chloride would result in much diminished signals.

Capacity of the generation solution

The oxidizing power of the solution will be reduced by dilution through repeated sample injections. The main limit, however, is decomposition of the generating solution. Addition of a total volume of 1.5 ml of sample solution into 7.5 ml of generating solution caused significant decomposition of the generating solution, giving spectral interference from manganese emission at 257.6 nm; the mechanism of this decomposition is not certain, but probably involves manganese(VII) oxide.

Conclusion

The method described provides a useful rapid and direct determination of traces of chloride in aqueous solution. An improvement in sensitivity could be obtained by improving the rate of generation of chlorine from the solution. Attempts to reduce the solubility of chlorine by adding various salts (e.g. sodium, potassium or silver sulphate) and ultrasonic agitation of the solution proved fruitless; heating the reaction mixture resulted only in decomposition of the reagents before any significant improvement could be noted.

This general approach of chemical separation and isolation of volatile species prior to their introduction into a microwave-induced plasma avoids the major drawback of this plasma for routine analysis as it largely overcomes the serious matrix effects commonly found with this technique.

We are grateful to the Royal Society, London, for a grant to purchase the monochromator and equipment.

REFERENCES

1 C. Ballaux, R. Dams and J. Hoste, Anal. Chim. Acta, 43 (1968) 1.
2 H. Akaiwa, E. Tajima and S. Aizawa, Radioisotopes, 20 (1971) 165.
3 J.Hoste, J. Radioanal. Chem., 19 (1974) 7.
4 A. V. Nikolaev, E. N. Gilbert, M. M. Goldshtein and I. G. Yudelerich, Igv. Sib. Otd. Akad. Navik. SSSR, Ser. Khim. Nauk., (1977) (6) 50 (see Chem. Abstr., 88 (1977) 145629P).
5 I. E. Davidson and W. Franklin, Anal. Chem., 51 (1979) 2127.
6 C. A. Bache and D. J. Lisk, Anal. Chem., 39 (1967) 786.
7 R. M. Dagnall, T. S. West and P. Whitehead, Anal. Chem., 44 (1972) 2074.
8 W. R. McLean, D. L. Stanton and G. E. Penketh, Analyst, 95 (1973) 432.
9 C. I. M. Beenakker, Spectrochim. Acta, 31B (1976) 483; 32B (1977) 173; 33B (1978) 53.
10 T. Hanai, S. Coulombe, M. Moisan and J. Hubert, Proc. Int. Winter Conf. 1980 on Developments in Atomic Plasma Spectrochem. Analysis, San Juan, Puerto Rico, 1980.
11 B. Gutsche, R. Herrmann, M. Höhne and K. Rüdiger, Spectrochim. Acta, 33B (1978) 609.
12 G. F. Kirkbright and M. J. Adams, 5th Int. Conf. At. Spect., Melbourne, 1975.
13 R. Herrmann, in R. Mavrodineanu (Ed.), Analytical Flame Spectroscopy, Macmillan, London, 1970, p. 502.
14 W. H. Tayler and M. S. W. Webb, AERE Report R3875 (1961), p. 14.
15 N. K. Rudneskii, Zh. Prikl. Spektrosk., 25 (1976) 921.
16 J. F. Alder and J. M. Mermet, Spectrochim. Acta, 28B (1973) 421.
17 R. E. B. Pearse and A. G. Gaydon, The Identification of Molecular Spectra, 3rd edn., Chapman and Hall, London, 1965.
18 G. D. Parkes, Mellor's Modern Inorganic Chemistry, Longman, London, 1967.

Analytica Chimica Acta, 120 (1980) 155—162

DIRECT MEASUREMENT OF IRON IN SERUM BY ELECTROTHERMAL ATOMIC ABSORPTION SPECTROMETRY

KAYOKO NAKAMURA*, HIROKO WATANABE and HIROTAKE ORII

Department of Radiology, Tokyo Metropolitan Institute of Medical Science, Hon-Komagome, Bunkyo-ku, Tokyo 113 (Japan)

(Received 15th April 1980)

SUMMARY

A simple and rapid method is described for the determination of iron in serum by atomic absorption spectrometry with a graphite furnace atomiser. The serum is diluted 40 times with water, and injected into the graphite tube. Optimal conditions are established, and interferences from proteins and salts eliminated. Since the procedure requires no sample pretreatment such as protein precipitation or wet digestion, contamination and losses by co-precipitation are excluded. The method can determine any species of iron in serum.

Iron is the most abundant heavy metal in higher animals. In tissues, blood and body fluids, it is involved in a large number of enzyme reactions as an activator, or in the transport of oxygen. The content of iron in biological materials is one of the important factors in clinical diagnosis. Hemochromatosis, anemia, or late pregnancy can be diagnosed from serum iron levels [1]. Methods for the routine determination of serum iron, involve the precipitation of serum proteins followed by the measurement of iron in the supernatant liquid either spectrophotometrically [2] or by atomic absorption spectrometry [3, 4]. For precipitation, 1.0 ml or more of serum (2.0 ml of whole blood) is required.

Electrothermal atomic absorption spectrometry has often been recommended for biological materials because small amounts of samples can be analysed without pretreatment [5—10]. Olsen et al. [9] reported the determination of serum iron by atomic absorption spectrometry with a graphite furnace. They described the interferences of proteins in the direct determination, and proposed treatment with trichloroacetic acid before the injection of samples into the carbon tube. In this method, however, purification of trichloroacetic acid was necessary to exclude contamination from the commercial reagent. It seems to be desirable to avoid the precipitation step, not only to minimize contamination problems and simplify the procedure, but to exclude errors arising from the co-precipitation of iron and proteins. Therefore, a direct method is preferable, if it is accurate. The greatest source of inaccuracy in electrothermal methods, appears to be the differences of heating program between samples and working standards and interferences

of protein and salts. In the method of Glenn et al. [10], interferences were eliminated by injection of 1-μl aliquots of sample. However, this procedure required special precautions.

This paper demonstrates that the direct injection of much diluted serum samples minimizes interferences from salts and proteins on the determination of iron by electrothermal atomic absorption spectrometry.

EXPERIMENTAL

Apparatus

A model 460 atomic absorption spectrometer (Perkin-Elmer Corp. Norwalk, CT) with a deuterium arc background corrector in conjunction with an HGA-2100 graphite furnace (Perkin-Elmer) was used. The atomizer consisted of a cylindrical graphite tube (6 mm i.d., 28 mm long). A multi-element Intensitron hollow cathode lamp for Al, Ca, Cu, Zn, Mg, Si and Fe was operated at 30 mA for iron determinations, at 248.6 nm with a spectral band width of 0.2 nm. A continuous flow of nitrogen (47.7 l min^{-1}, setting 30 on the HGA controller) was directed through the tube. After the tube was carefully aligned to give a maximum signal, it was cleaned by making a few firings until no peaks were observed in the recorder. Samples or standard solutions were added to the graphite tube directly with an Eppendorf micropipette with disposable tips. Pipet tips were soaked for at least one day in 1 M hydrochloric acid, then thoroughly rinsed with distilled water. A new tip was used for each sample; 50-μl aliquots were used throughout.

Chemicals

All chemicals were of analytical grade. Standard iron(III) chloride (1000 ppm Fe) solution (in 0.1 M HCl; Wako Chemicals) was used to prepare working standards by dilution with 0.1 M HCl. A 10% (w/v) trichloroacetic acid solution, and a 7.5% solution containing 1.5% ascorbic acid were prepared. The latter solution was stable for 2 weeks.

Protein solutions. Solutions containing 20% (w/v) albumin, 20% (w/v) globulin or 0.3% (w/v) transferrin (all from Sigma Chemicals) were prepared.

Hemoglobin standard. Whole blood (2 ml) was washed thrice with 0.9% (w/v) sodium chloride solution. Red cells were lysed by freezing and thawing. The exact hemoglobin content was determined by the cyanmethemoglobin method using a Wako kit (Wako Chemicals) [11]. Working solutions were prepared by appropriate dilution with water.

Synthetic serum solution. This was prepared by dissolving 0.88 g of NaCl, 37 mg of KCl, 2 mg of $MgCl_2$, 10 mg of $CaCl_2$, 0.17 g of $NH_4H_2PO_4$, 0.1 g of glucose and 30 mg of urea in 100 ml of water. (150 mM NaCl, 5 mM KCl, 0.002% $MgCl_2$, 0.01% $CaCl_2$, 15 mM $NH_4H_2PO_4$, 0.1% glucose and 0.03% urea) [12].

Serum was prepared for analysis by the method described by Sasaki et al. [13].

Deionized distilled water, in which no iron could be detected, was used throughout.

Procedures

Determination of proteins in serum. Trace amounts of hemoglobin in serum were determined with *o*-tolidine [14]. The contents of albumin and globulin were measured using Wako kits (Wako Chemicals) [15]. Transferrin was measured as total iron binding capacity by Ramsay's method [16].

Precipitation procedure for investigating protein interference. This was based on the method of Olsen et al. [9], with some modifications. Serum (100 μl) was mixed with an equal volume of 10% trichloroacetic acid solution, heated at 90°C for 15 min, and centrifuged at 2500 rpm for 10 min. The supernatant liquid was diluted with water, an aliquot was introduced to the graphite tube, and iron was determined by the same procedure as in the dilution method (below).

Dilution procedure. Serum (25 μl) was diluted and mixed with 1 ml of water and 50 μl was injected into the graphite tube. After drying at 100°C for 60 s, and charring for 55 s, including a ramp time of 30 s, up to 1000°C, atomization was done at 2400°C for 8 s. The iron atomic absorption signals were measured with background correction, with 8-s integration.

Wet digestion procedure. Serum (1 ml) was digested with 1 ml of concentrated nitric acid and then with 0.5 ml of concentrated sulfuric acid and 0.1 ml of concentrated perchloric acid. The digested sample was diluted to exactly 10 ml with water, and iron was determined in the sample by extraction with thiocyanate and 1, 10-phenanthroline into methyl isobutyl ketone [17].

Precipitation procedure for iron determination by flame a.a.s. (Table 4). This was based on the procedure of Makino and Takahara [18], with some modifications. Serum (2.0 ml) and 4.0 ml of 7.5% trichloroacetic acid solution containing 1.5% ascorbic acid, were mixed, left at room temperature for 5 min, and centrifuged at 3000 rpm for 15 min. Iron in the supernatant liquid was measured by flame a.a.s. as described by Olson and Hammlin [3].

RESULTS AND DISCUSSION

Effect of atomizing and charring temperatures

As shown in Fig. 1, with 50 μl of aqueous iron standard (1.5 ng of iron), the peak area was constant at atomizing temperatures between 2200°C and 2700°C. For a serum sample diluted with water, the peak area increased with increasing atomizing temperature up to 2600°C. When the temperature was higher than 2500°C, two peaks were produced probably because of other elements in the serum. The optimum response was attained at 2400°C. The atomizing time of 8 s provided total atomization for both standards and diluted serum, allowing complete return of the signal to the baseline.

The charring stage is essential to remove components of the sample matrix

that are more volatile than iron. Figure 2 shows that the temperature of the charring cycle also affected the iron atomization signal. Above 1100°C, the peak area decreased. This was consistent with a loss of iron by volatilization preceding atomization. This was almost the same for serum, except that smoking or spattering appeared between the drying and charring stages, probably because of the proteins in the serum. This effect could be eliminated by using the ramp mode to increase the charring temperature from 100°C to 1000°C. Under these conditions, the peak area was constant for 40—60 s charring time. The optimal charring time for a 50-μl serum sample was 55 s, including a ramp time of 30 s. The optimal conditions for operating the HGA-2100 graphite furnace are included in the analytical procedure (see Experimental).

Calibration

The calibration plot obtained under the optimal conditions with standard iron solutions was linear for 0—3.0 ng of iron. The relative standard deviation was 2.1% for 10 replicate measurements of 2.0 ng of iron. A series of sera with different amounts of iron was prepared by adding appropriate amounts of standard iron solution to a serum sample. The responses for these solutions were again linear, with the same slope as for the standard iron solutions. Therefore, the calibration curve made by using standard iron solutions is suitable for the determination of iron in serum.

Effect of other blood components

Normal human serum contains 140 mM Na^+, 4.4 mM K^+, 5.0 mM Ca^{2+} and 0.25 mM Mg^{2+} [19]. Taking into account the dilution of the serum,

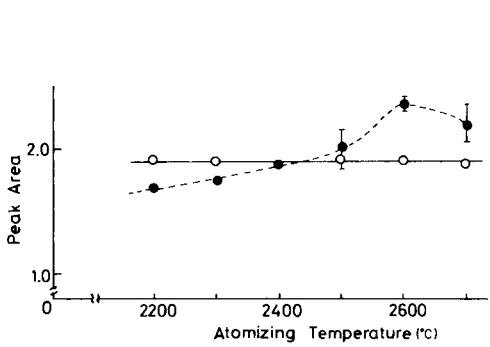

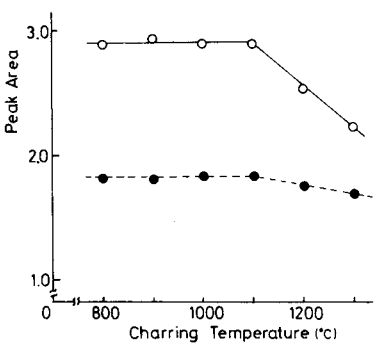

Fig. 1. Effect of atomizing temperature: (○) $FeCl_3$ solution (1.5 ng Fe), (●) serum diluted with water (1.0 ng Fe injected). Drying at 100°C for 60 s; charring at 1000°C for 55 s; atomizing time, 8 s.

Fig. 2. Effect of charring temperature: (○) $FeCl_3$ solution (2.0 ng Fe), (●) serum diluted with water (1.0 ng Fe injected). Drying at 100°C for 60 s; charring time, 55 s; atomizing at 2400°C for 8 s.

the effect of these ions on the determination of iron was investigated. Table 1 indicates that these ions did not interfere under the conditions used (which included background correction). Likewise, iron in the synthetic serum gave good recoveries under these conditions.

The concentrations of albumin, globulin and transferrin in normal human serum are reported to be 43 mg ml^{-1}, 30 mg ml^{-1} and 3 μg Fe ml^{-1} (total iron-binding capacity), respectively [19]. Serum also contains small concentrations of hemoglobin (ca. 50 μg ml^{-1}), when gross hemolysis cannot be observed [20]. Taking into account the dilution of the serum, the effect of these proteins on the determination of iron was investigated. As shown in Table 2, none of the proteins affected the determination. The iron contained in commercial albumin or globulin powder (4.87 or 1.34 μg g^{-1}, respectively) could be recovered satisfactorily. Hemoglobin contains about 3.47 mg g^{-1} of iron [2], thus iron could not be detected in 0.8 μg ml^{-1} hemoglobin solution. Iron in

TABLE 1

Effect of salts on the determination of iron (10 ppb)

Samples	Peak area	Recovery (%)
$FeCl_3$	0.67	
$FeCl_3$ + 1.5 mM NaCl	0.63	95
$FeCl_3$ + 0.05 mM KCl	0.66	99
$FeCl_3$ + 0.05 mM $CaCl_2$	0.65	98
$FeCl_3$ + 0.05 mM $MgCl_2$	0.64	96
$FeCl_3$ in synthetic serum[a]	0.67	100

[a]See text.

TABLE 2

Effect of proteins on the determination of iron (10 ppb)

Samples	Peak area	Recovery (%)
$FeCl_3$	0.67	
1.0 mg ml^{-1} albumin	0.86	
$FeCl_3$ + 1.0 mg ml^{-1} albumin	1.53	100
1.0 mg ml^{-1} globulin	0.65	
$FeCl_3$ + 1.0 mg ml^{-1} globulin	1.27	92
0.8 μg ml^{-1} hemoglobin	0.00	
$FeCl_3$ + 0.8 μg ml^{-1} hemoglobin	0.67	100
30 μg ml^{-1} transferrin	0.00	
$FeCl_3$ + 5 μg ml^{-1} transferrin	0.65	97
$FeCl_3$ + 30 μg ml^{-1} transferrin	0.67	100

30 μg ml^{-1} transferrin solution also could not be detected (commercial transferrin powder was apo-transferrin, 90% iron-free). It has been reported [21] that the determination of iron in serum is dependent on the degree of saturation of transferrin with iron. Table 2 indicates that transferrin, whether iron-saturated or not, did not affect the determination of iron by the present method.

It was found, further, that excessive amounts of albumin, globulin, hemoglobin or transferrin did not have a significant effect on the determination of iron by the proposed dilution method, whereas the recoveries of iron by the precipitation method were much decreased by the proteins (Table 3). Contamination from the trichloroacetic acid could be observed.

Determination of iron in serum

Iron in serum was determined by the dilution method and by the wet digestion, and precipitation methods. The results obtained are shown in Table 4. Few significant differences were observed between the dilution and wet digestion methods, suggesting that any species of iron in serum can be detected by the dilution method. However, the dilution method yielded consistently higher results, than the precipitation method even after the iron derived from hemoglobin had been subtracted. The iron in serum was reported by Holmberg and Laurell [22] to be completely bound to a specific protein, designated transferrin or siderophilin. The difference between the dilution and precipitation methods is probably due either to the incomplete separation of iron from proteins, or to the co-precipitation of iron and proteins. Table 4 also indicates that when more varieties of proteins were present, such as in hemolyzed rat sera 1, 2 and 3, the greater were the differences observed. Therefore, co-precipitation of iron and

TABLE 3

Effect of proteins on the determination of iron in serum

Samples	Fe found (ppm)		Recovery (%)	
	Present method	Other method [9]	Present method	Other metho
Normal serum[a]	1.66	1.42		
Serum containing 100 mg ml^{-1} albumin	1.36	1.24	82	87
Serum containing 50 mg ml^{-1} globulin	1.69	1.12	102	79
Serum containing 1.14 mg ml^{-1} hemoglobin	1.85	0.62	111	44
Serum containing 5.5 mg ml^{-1} transferrin	1.56	1.02	94	72

[a]Albumin, globulin, hemoglobin and transferrin were 47.6 mg ml^{-1}, 23.1 mg ml^{-1}, 124 μg ml^{-1}, and the equivalent of 311 mg Fe ml^{-1}, respectively.

TABLE 4

Comparison of methods for the determination of iron in serum

Samples	Fe found (ppm)		
	Dilution method	Wet digestion method	Precipitation method
Human serum 1	1.72 (1.56)[a]	1.72	1.21
Human serum 2	0.89 (0.81)	0.85	0.91
Human serum 3	1.58 (1.50)	1.52	1.18
Human serum 4	0.85 (0.74)	0.78	0.62
Human serum 5	0.76 (0.62)	0.71	0.36
Rat serum 1	4.50 (3.12)	4.69	1.93
Rat serum 2	4.25 (3.04)	4.28	2.06
Rat serum 3	3.92 (2.91)	3.72	1.66

[a]Values in parentheses are those obtained after subtraction of the iron derived from hemoglobin; hemoglobin was determined by using *o*-tolidine, and the iron derived from hemoglobin was calculated on the basis of 3.42 μg of iron in 1 mg of hemoglobin.

proteins is the more probable cause of the negative error. Study of this problem is in progress.

In conclusion, the dilution procedure proposed is very promising for providing a rapid and accurate means for measuring iron in serum without pretreatment.

We are grateful to Professor Takejiro Ozawa of Saitama University for many suggestions and a critical reading of the manuscript.

REFERENCES

1 S. E. Miller and J. M. Weller, Textbook of Clinical Pathology, Williams and Wilkins Co., Baltimore, MD, 1971, p. 265.
2 S. M. Lewis, Am. J. Clin. Pathol., 56 (1971) 543.
3 A. D. Olson and W. B. Hammlin, Clin. Chem., 15 (1969) 438.
4 A. Zettner, L. C. Sylvia and L. Capacho-Delgado, Am. J. Clin. Pathol., 45 (1966) 533.
5 K. Fujiwara, Y. Umezawa, Y. Numata, K. Fuwa and S. Fujiwara, Anal. Biochem., 94 (1979) 386.
6 D. I. Paynter, Anal. Chem., 51 (1979) 2086.
7 J. P. Matousek and B. J. Stevens, Clin. Chem., 17 (1971) 363.
8 V. Giridhar and F. W. Sunderman, Sr., Clin. Chem., 19 (1973) 671.
9 E. D. Olsen, P. I. Jatlow, F. J. Fernandez and H. L. Kahn, Clin. Chem., 19 (1973) 326.
10 M. T. Glenn, J. Savory, S. S. Fein, R. D. Reeves, C. J. Molnar and J. D. Winefordner, Anal. Chem., 45 (1973) 203.
11 K. Matsubara, Jpn. J. Clin. Pathol., 14 (1966) 29.
12 T. Makino and K. Takahara, Symp. Clin. Chem., 17 (1977) 47.
13 K. Sasaki, N. Ueda, M. Kitamura and T. Nakayama, Sampling of Human Components—Blood, Kohdansha Scientific, Tokyo, 1972, p. 22.
14 A. F. Beau, Am. J. Clin. Pathol., 38 (1962) 111.

15 B. T. Doumas, W. A. Watson and H. G. Biggs, Clin. Chim. Acta, 31 (1971) 87.
16 W. N. H. Ramsay, Clin. Chim. Acta, 2 (1957) 214.
17 K. W. Kirky and R. H. A. Crawley, Anal. Chim. Acta, 19 (1958) 363.
18 T. Makino and K. Takahara, Jpn. J. Clin. Pathol., 25 (1977) 767.
19 T. Ishii, Modern Medical Technology 6, Clinical Chemistry (Part II), Igaku Shoin, Tokyo, 1975, p. 673.
20 K. Takano, M. Okuda, J. Ohtake, M. Inoue and I. Suzuki, Jpn. J. Clin. Pathol., 17 (1969) 164.
21 T. J. Giovvanniello, in D. Seligson (Ed.), Serum Iron and Iron-binding Capacity in Standard Methods of Clinical Chemistry, Vol. IV, Academic Press, New York, 1963.
22 C. G. Holmberg and C. B. Laurell, Acta Chem. Scand., 1 (1947) 944.

Analytica Chimica Acta, 120 (1980) 163—170

THE DETERMINATION OF NITRITE BY ULTRAVIOLET ABSORPTION SPECTROMETRY IN THE GAS PHASE

AUGUSTA SYTY* and RICHARD A. SIMMONS

Department of Chemistry, Indiana University of Pennsylvania, Indiana, PA 15705 (U.S.A.)

(Received 19th March 1980)

SUMMARY

Aliquots of nitrite-containing solutions are injected into small aliquots of 8 M hydrochloric acid and the evolved gases are swept by a stream of carrier gas through an absorption cell where transient absorbance in the gas phase is measured at 195 nm. The detection limit is 0.2 μg NO_2^- ml^{-1} with the calibration curve remaining linear to 65 μg NO_2^- ml^{-1}. Reproducibility is reflected in 2.4% relative standard deviation from the mean at the 5 μg NO_2^- ml^{-1} level. There is no interference from CO_3^{2-}, NO_3^-, SO_4^{2-}, Br^-, CN^-, CNO^-, or NH_4^+, but SCN^-, I^-, S^{2-} and SO_3^{2-} interfere.

Reported methods for the determination of nitrite make use of a variety of instrumental techniques, but colorimetric methods have been the most thoroughly studied and the most frequently used. Colorimetric methods for nitrite are very often based on the Griess reaction, i.e. the reaction of nitrite with a primary aromatic amine to form a diazonium salt which is then coupled with another aromatic compound to form an azo dye whose absorbance is measured. A common combination of reagents used for the Griess reaction has involved the nitrosation of sulfanilic acid followed by coupling with α-naphthylamine to produce a dye with an absorption maximum around 520 nm. The original Griess method offered good sensitivity ($\epsilon = 3.2 \times 10^4$ l mol^{-1} cm^{-1}) and adequate precision with relative standard deviation (r.s.d.) of 2.5% [1]. Other combinations of nitrosatable compounds and coupling reagents have been tried and, since α-naphthylamine was found to be carcinogenic, the use of N-(1-naphthyl)-ethylenediamine as coupling reagent and of sulfanilamide has become common. With this pair of reagents, absorbance is measured around 540 nm, the molar absorptivity of the dye is 2.7×10^4 l mol^{-1} cm^{-1} [1], the calibration curve remains linear up to about 0.7 μg NO_2^- ml^{-1} [2], and the detection limit is of the order of 0.002 μg NO_2^- ml^{-1}. Although the Griess reaction offers the advantage of excellent sensitivity, it also has several limitations. For example, control of pH, temperature and concentration of reagents is critical. Griess reagents deteriorate on storage even when refrigerated. The color-developing reaction has to be timed due to instability of the dye and to numerous side-reactions. Samples being tested should not contain oxidants, reductants or other colored solutes.

Copper ions must be absent because they catalyse the decomposition of the diazonium salt [3]. Several metal ions interfere by precipitation [4].

The purpose of this paper is to report a rapid and precise absorption spectrometric method for the determination of nitrite which does not involve preparation of any colored compounds and which is subject to very few interferences. Nitrite-containing solutions are injected into hydrochloric acid, and the nitrogenous gases evolved in the reaction are swept by a stream of carrier gas to a flow-through absorption cell where transient absorbance is measured at 195 nm. The technique for the determination of SO_3^{2-}, S^{2-}, I^-, Br^-, as well as the NH_4^+ ion, by chemical evolution of volatile products followed by u.v. absorption spectrometry in the gas phase, was described in earlier reports by Syty and co-workers [5—9]. Evolution of gaseous products and measurement of absorbance in the gas phase with different apparatus, has also been used by Cresser and Isaacson [10, 11].

EXPERIMENTAL

Apparatus

Absorbance of the evolved gases was measured with a Perkin-Elmer model 460 atomic absorption spectrometer, with readout presented on a 10-mV stripchart recorder. The spectrometer was modified for non-flame measurement of transient molecular absorbance in the gas phase by simple removal of the head from the nebulizer/burner and its replacement with a 15-cm long 2.5-cm diameter quartz-ended flow-through absorption cell supported by a holder which fits into the neck of the nebulizer/burner. The deuterium arc lamp, whose normal function in the spectrometer is to provide background correction, served as the only source of radiation. Absorbance measurements were taken at 195 nm with a slit setting of 2 nm.

The glass reaction vessel used to combine the reagents and evolve the absorbing gases has been described and illustrated previously [6—9]. Essentially, it consists of a cylindrical glass vessel of about 60-ml capacity (2.8 cm i.d. tapering to 1.5 cm i.d. at the bottom). Aliquots of hydrochloric acid are introduced into the vessel from a 25-ml buret attached to a glass side-arm by means of a short sleeve of Tygon tubing. Sample solutions are injected into the reaction vessel via a septum-covered sidearm by means of a 1.00-ml Hamilton syringe with Chaney adaptor. The carrier gas enters the reaction vessel through a glass tube which follows the vertical axis of the vessel down to within about 1 cm of the bottom, its end being tapered to about 1 mm i.d. The carrier gas bubbles vigorously through the few milliliters of liquid, mixing the reagents and sweeping the evolved gases out of the reaction vessel to the flow-through absorption cell via a sidearm and a length of Tygon tubing. After passage through the absorption cell, the gas stream is vented into the atmosphere. Spent reagents are drained through the stopcock fitted at the bottom of the vessel. The flow of carrier gas is never interrupted; the baseline on the recorder is established with nitrogen bubbling through the

fresh aliquot of acid and continuously flowing through the absorption cell. A Matheson flowmeter is used to regulate the carrier gas flow rate.

No effort was made to remove the water and hydrogen chloride vapors which were present in the carrier gas stream emerging from the reaction vessel. When a desiccant ($CaSO_4$) was interposed between the vessel and the absorption cell, the height of the recorded absorbance signals decreased by about 30%. To avoid introducing the variable of relative desiccant freshness, no desiccant was used in collecting the data for this report. The continuous presence of water and hydrogen chloride vapors in the gas stream is essentially constant and becomes part of the background over which the analytical signal is measured.

Procedure

The deuterium arc lamp is allowed to warm up for a few minutes. A 5.00-ml aliquot of 8.0 M HCl is delivered into the reaction vessel from the side-arm buret. The nitrogen pressure is set at 10 psi, the flow rate is adjusted to 1.45 l min^{-1}, and the recorder is turned on to establish the baseline. With the carrier gas flowing uninterrupted and with the pen recording, a 1.00-ml aliquot of nitrite-containing solution is rapidly injected through the septum-covered port into the acid solution. Because of rapid evolution of nitrosyl chloride, an absorbance signal causes a rapid deflection of the pen on the recorder, reaching a maximum in 11 s and then trailing down more slowly (Fig. 1). The analytical absorbance signal is measured from the baseline to the maximum of the recorded peak. Usually, the recorder is turned off and the reaction vessel is drained as soon as the peak maximum is recorded. A fresh 5-ml aliquot of acid is then immediately delivered into the vessel and the recorder is turned on to re-establish the baseline. The apparatus is thus ready for the next injection of nitrite in less than 1 min. It is of course obvious that draining the reaction vessel before the recorded absorbance signal has returned to the baseline means that much nitrosyl chloride is lost with the discarded acid without evolution into the gas phase and passage through the absorption cell. This, however, introduces no error into the determination because it is the peak height rather than the peak area of the recorded signal which is measured. Recorded peak heights are very reproducible under constant conditions and, as the data presented below will show, remain proportional to concentration of nitrite over a reasonable range. The main advantages of draining the reaction vessel immediately after the absorbance maximum has been recorded are the speed with which the peak maximum is reached (11 s) as compared to the length of time required to record the entire absorbance trace (ca. 170 s), and the convenience of measuring the heights of peaks as compared to measuring the areas under the very skewed absorbance curves. Standard solutions of nitrite are prepared by weighing reagent-grade sodium nitrite and by appropriate dilutions with distilled water.

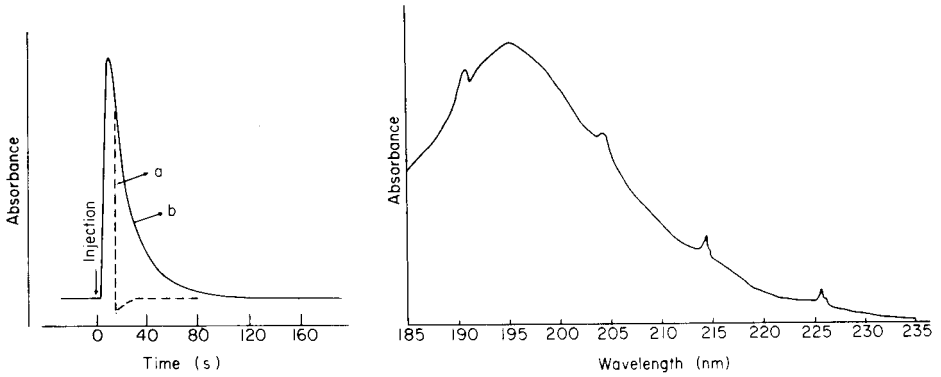

Fig. 1. Recorded absorbance signal. (a) Vessel drained immediately after the peak maximum is passed and refilled with fresh acid. (b) Vessel not drained until after the entire absorbance signal has been recorded.

Fig. 2. Absorbance spectrum of the gases evolved upon injection of nitrite into 8 M HCl.

RESULTS AND DISCUSSION

Absorption spectrum

By making repeated injections of a 100 μg NO_2^- ml^{-1} solution into fresh aliquots of 8.0 M HCl while the wavelength was varied over the range 180—235 nm, the absorption spectrum shown in Fig. 2 was obtained. The spectrum was confirmed by trapping some of the evolved gases and making a scan on a Cary 14. The absorbance maximum occurs between 192 and 199 nm. The data for this report were collected at 195 nm.

It is probable that the evolved gases consist either of nitrosyl chloride formed by the reaction $NaNO_2 + 2\ HCl \rightarrow NOCl + NaCl + H_2O$ [12], or of a mixture of nitrosyl chloride and of oxides of nitrogen. Injection of nitrite into aliquots of acids other than hydrochloric acid gave greatly reduced absorption signals. Thus, the absorbance signal of 0.845 decreased to 0.158 when 8.0 M HCl was replaced by 8.0 M H_2SO_4, and further decreased to 0.044 when 8.0 M HNO_3 was used as the acid medium. These results support the expectation that the injection of nitrite into hydrochloric acid leads to the evolution of predominantly or entirely nitrosyl chloride whereas reactions with other acids evolve oxides of nitrogen. Most of the data in this report were collected for 8.0 M HCl.

Effect of carrier gas flow rate

Repeated injections of 1.00 ml of a 50.00 μg NO_2^- ml^{-1} solution into fresh 5.00-ml aliquots of 8.0 M HCl were made at nitrogen flow rates varying from 0.300—2.00 l min^{-1}. The data presented in Fig. 3 indicate that given the dimensions of the particular reaction vessel being used, flow rates between 1.45 and 1.77 l min^{-1} gave rise to the most intense absorbance signal. Most

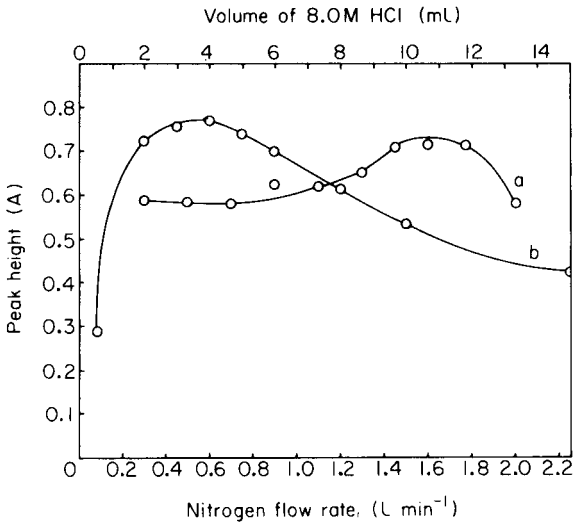

Fig. 3. Effects of nitrogen flow rate and acid volume on absorbance (a) Nitrogen flow rate. (b) Acid volume.

of the data were collected at 1.45 l min^{-1}. Flow rates above 1.77 l min^{-1} caused such vigorous bubbling in the reaction vessel that the precision of determination was affected adversely, possibly because of the increased probability of water mist reaching the absorption cell and the sharpness of the recorded peaks, which enhanced the significance of the small inadvertent variations in the rate of manual injection of samples by syringe. As the data in Fig. 3 indicate, variation of the carrier gas velocity has a remarkably small effect on signal intensity. Earlier studies employing similar apparatus have encountered similar effects during the evolution of other gases [6—9].

Effect of acid volume and concentration

When the volume of 8 M HCl delivered into the reaction vessel prior to injecting 1-ml aliquots of a 50 μg NO_2^- ml^{-1} solution was varied from 0.50 ml to 15.00 ml, the data included in Fig. 3 were collected. Volumes in the 2—5 ml range yielded the best signal level.

The absorbance was significantly affected by the concentration of the hydrochloric acid solution used. Thus, injected nitrite aliquots which caused an absorbance of 0.845 with 8.0 M HCl, gave an absorbance of only 0.576 with 6.0 M HCl, 0.336 with 5.0 M HCl, 0.045 with 3.0 M HCl and 0.006 with 1.0 M HCl. It is expected that the use of concentrations above 8.0 M would cause further increases in signal intensity, but such concentrations were not tested.

Fresh acid aliquots versus repeated injections into the same aliquots

Since the quantity of 8.0 M HCl consumed by reaction with the injected 1-ml aliquots of aqueous 1—1000 μg NO_2^- ml^{-1} solutions is minute, the need

for changing the acid between injections was investigated. Ten successive injections of 1.00 ml of a 100.0 μg NO_2^- ml^{-1} solution were made, without draining the vessel after each injection. For comparison, ten similar injections were also made into fresh 8.0 M HCl aliquots, draining the reaction vessel and refilling following each injection.

Injections made into the same aliquot of acid yielded peak heights which decreased gradually from an absorbance of 0.889 for the first injection to an absorbance of 0.196 for the tenth injection. The areas under the entire recorded absorbance peaks showed only some random variation (r.s.d. = 3.3%) and, whereas the time required to reach peak maximum exhibited only a slight increase (from 11 to 19 s), the time required to achieve a complete flushing of the reaction train and the return of the pen to the baseline increased from 170 to 375 s.

By contrast, the ten repeated injections into fresh aliquots of acid exhibited only slight random variations in both the measured peak heights (r.s.d. = 0.4%) and peak areas (r.s.d. = 1.8%). The time required to reach the peak maximum remained constant at 11 s and that required to flush out the reaction train and re-establish the baseline on the recorder remained constant at close to 170 s.

Consequently, in the interests of precision and speed of determination, injections should always be made into fresh aliquots of acid. Furthermore, even though fresh acid aliquots permit adequate reproducibility in peak areas, it is preferable to drain the reaction vessel and refill it with the next acid aliquot as soon as the peak maximum is recorded because recording and measuring just peak heights is slightly more precise and very much faster than recording the entire absorbance signals and measuring the areas under the peaks.

Stability of nitrite solutions

The stability of nitrite solutions ranging from 5—100 μg NO_2^- ml^{-1} was tested both in water and in 0.1 M NaOH. Fresh solutions were prepared, stored in plastic bottles, and kept for six months. At the end of that time, the solutions were evaluated against freshly prepared standards. The slight differences in the signals were within the normal variation caused by the injection technique. The nitrite solutions were concluded to be stable in both water and 0.1 M NaOH. Working standards prepared in water were used in the rest of this study. Although solutions which stood unopened showed no decay, dilute working standards, which were frequently unstoppered to pour out aliquots for use, did undergo a slight decrease in nitrite concentration over several months. Consequently, fresh nitrite solutions were prepared periodically as a precaution.

Precision, detection limit and dynamic range

A series of seven repeated injections at several levels of nitrite concentration yielded the following values for percentage standard deviation from the

mean: 2.4% at 5.00 μg NO_2^- ml^{-1}, 1.4% at 40.00 μg NO_2^- ml^{-1}, and 0.4% at 100.0 μg NO_2^- ml^{-1}. Low as it is, the variation is attributed predominantly to inability to make very rapid manual syringe injections at exactly the same rate. Inasmuch as 5.00 μg NO_2^- ml^{-1} gives an average absorbance signal of 0.0547, the detection limit (defined as the concentration which yields a signal twice the standard deviation) is 0.23 μg NO_2^- ml^{-1}.

The linear portion of the calibration curve, prepared by plotting the height of the recorded peak as a function of nitrite concentration of the 1.00-ml aliquots injected into 8.0 M HCl, extends to about 65 μg NO_2^- ml^{-1}. The performance of the method was evaluated by calculating the terms in the regression equation $y = (a \pm s_a)\,x + (b \pm s_b)$ with s_{yx} where a and b are slope and intercept of the calibration curve and s_a and s_b are standard deviations of slope and intercept and s_{yx} is standard error of y on x. The data yielded the following values for all terms: $a = 0.01203$, $b = 0.00132$, $s_a = 0.00003$, $s_b = 0.00016$ and $s_{yx} = 0.002$.

Interferences

The effect of concomitant anions was studied by testing a series of solutions containing 60.0 μg NO_2^- ml^{-1} (as the sodium salt) and 3000 μg ml^{-1} potential interfering ion (as Na or K salts). Solutions containing the potential interfering ion (3000 μg ml^{-1}) alone were also tested. The following anions had no effect on the nitrite signal: CO_3^{2-}, NO_3^-, SO_4^{2-}, Br^-, CN^-, CNO^-; none caused any absorbance when injected alone.

The anions which did affect the nitrite absorbance signal are listed in Table 1. Thiocyanate and iodide reacted with nitrite in solution but did not cause any absorbance signals when injected alone. Sulfide and sulfite interfered because of interaction with nitrite in solution and evolution of H_2S and SO_2, both of which gases absorb at 195 nm. In testing the sulfide interference, ammonium sulfide was used as the source of the anion. The ammonium ion itself (injected as chloride) had no effect on the signal.

Conclusion

The proposed method for the determination of nitrite in aqueous solution offers several advantages compared to the colorimetric methods for nitrite based on the Griess reaction. No reagents other than 8 M HCl are required, eliminating all concerns of reagent preservation and of timed color development. A complete run can be made in less than 2 min. The method is simple and direct. The reaction vessel can be easily constructed by anyone familiar with rudimentary glass-blowing techniques. Any atomic absorption instrument with a built-in u.v. continuum background corrector light source can be employed.

The limitation of the proposed method is its moderate sensitivity. The detection limit is 0.2 μg NO_2^- ml^{-1} and the linear portion of the calibration curve extends to 65 μg NO_2^- ml^{-1}, compared with a detection limit of 0.002 μg NO_2^- ml^{-1} and linearity up to 0.7 μg NO_2^- ml^{-1} for the Griess colorimetric method.

TABLE 1

Interfering anions

Anion added	Concentration (μg ml^{-1})	Observed signal intensity (%) relative to that of nitrite (60 μg ml^{-1})	
		In presence of interfering ion	Interfering ion alone
None		100	—
Thiosulphate	3000	42	0
Iodide	3000	4	0
Sulfide	912	164	175
Sulfite	3000	137	145

Interferences in the proposed method are few. Aside from concomitants which can oxidize or reduce nitrite in solution, and whose effect is therefore irreducible in most methods for nitrite, the only concomitants which interfere in the proposed method are those which cause rapid evolution of volatile products which absorb at 195 nm upon mixing with hydrochloric acid.

The proposed determination of nitrite by ultraviolet absorption spectrometry in the gas phase offers a good alternative to colorimetric methods for nitrite.

The authors thank Gregory L. Malcolm for carrying out some preliminary investigations on this project.

REFERENCES

1 J. B. Fox, Jr., Anal. Chem., 51 (1979) 1493.
2 R. N. Fiddler, J. Assoc. Off. Anal. Chem., 60 (1977) 594.
3 S. Marczenko, Spectrophotometric Determination of Elements, J. Wiley, New York, 1976, pp. 395—6.
4 J. R. Clear and M. Roth, in I. M. Kolthoff, P. J. Elving and E. B. Sandell (Eds.), Treatise on Analytical Chemistry, Part II, Vol. 5, Ch. Nitrogen, Interscience, New York, 1961.
5 A. Syty, Anal. Chem., 45 (1973) 1744.
6 H. E. Winkler and A. Syty, Environ. Sci. Technol., 10 (1976) 913.
7 G. Nicholson and A. Syty, Anal. Chem., 48 (1976) 1481.
8 A. Syty, Anal. Chem., 51 (1979) 911.
9 C. C. Muroski and A. Syty, Anal. Chem., 52 (1980) 143.
10 M. S. Cresser and P. J. Isaacson, Talanta, 23 (1976) 885.
11 M. S. Cresser, Analyst, 102 (1977) 99.
12 J. Jander and U. Engelhardt, in C. B. Colburn (Ed.), Developments in Inorganic Nitrogen Chemistry, Vol. 2, Ch. 3, Elsevier, New York, 1973, p. 142.

Analytica Chimica Acta, 120 (1980) 171—176

DETERMINATION OF METHYLCYCLOPENTADIENYLMANGANESE-TRICARBONYL BY GAS CHROMATOGRAPHY—ATOMIC ABSORPTION SPECTROMETRY AT ng m^{-3} LEVELS IN AIR SAMPLES

M. COE, R. CRUZ and J. C. VAN LOON

Department of Geology, Chemistry and the Institute for Environmental Studies, University of Toronto, Toronto, Ontario M5S 1A1 (Canada)

(Received 2nd June 1980)

SUMMARY

A procedure is given for the determination of methylcyclopentadienylmanganese tricarbonyl (MMT) at ng m^{-3} concentrations in air. The method involves trapping of MMT in a small segment of gas chromatographic column and then determination by gas chromatography with an electrothermal atomic absorption detector. The detection limit of the procedure is 0.05 ng m^{-3}. Air samples from an underground car-park (when MMT was detected) were found to contain between 0.1 and 0.3 ng m^{-3} MMT. MMT was not detected in any of the street air samples taken.

Methylcyclopentadienylmanganesetricarbonyl (MMT) is added to many of the so-called "unleaded" gasolines sold in North America, as an antiknock compound. Levels of MMT in these gasolines average about 0.16 g gal^{-1}. MMT was discovered and patented by Ethyl Corporation and there is little information in the scientific literature concerning this compound. The current widespread distribution of MMT as a gasoline additive makes it essential that a method be developed for its determination in environmental samples. Most procedures for the determination of MMT are indirect relating it to the total manganese found in a sample. Turkel'traub et al. [1] described a gas chromatographic procedure for the related compound cyclopentadienylmanganesetricarbonyl (CMT). Only one procedure, that of Uden et al. [2], has been reported for the direct determination of MMT. This latter procedure is for the relatively high levels of MMT found in gasoline. In the following paragraphs, a procedure is outlined for the gas chromatographic/atomic absorption determination of MMT directly at ng m^{-3} levels in air.

The techniques of analytical atomic spectrometry can be used to advantage in the study of metal compounds, as metal specific detectors for chromatography. Uden et al. [2] used d.c. argon plasma emission spectrometry as the detector in their work. The detection limit obtainable by d.c. argon plasma emission for manganese is poorer than for electrothermal atomic absorption. Thus this latter detector was chosen in the current work because of the very low levels of MMT expected in environmental samples.

EXPERIMENTAL

Apparatus and reagents

A Perkin-Elmer 603 atomic absorption spectrometer was used with a Perkin-Elmer HGA 2100 furnace. A deuterium arc background corrector was employed. A Pye gas chromatograph (Series 104) was interfaced to the graphite furnace using a tantalum connector as previously described [3]. A glass chromatographic column (2.3 m long, 6 mm o.d.) was packed with 3% OV-1 on high-performance Chromosorb W (80/100 mesh). The gas from the chromatograph was transferred to the furnace through teflon-lined aluminium tubing.

The gas chromatographic set up is illustrated in Fig. 1. (A) connects to a nitrogen cylinder. (B) is the sample oven containing the sample trap and 4-way valve. (C) is the gas chromatograph connected through a standard injection valve to the column. (D) is the graphite furnace. The operating conditions for the gas chromatograph and the graphite furnace were as shown in Table 1.

Samples of air were collected in teflon-lined aluminium U-tubes (30 cm long, 3 mm o.d.) packed with 3% OV-1 on Chromosorb W (80/100 mesh). These tubes were placed in a water—ice cooling bath. Air entered through an air filter previously described [3] and was pumped through the U-tube trap at about 70 ml min^{-1} using a vacuum pump. The length of sampling time and the average flow rate, checked frequently during sampling, were used to compute sample volume.

MMT (Alfa Division, Ventron Corporation, Danvers, Massachusetts) was diluted in isooctane to produce the working standards. These standards were prepared fresh daily.

Procedures

Air samples were collected for various periods of up to 100 h and were retained in a freezer until run.

The gas chromatographic system is assembled as shown in Fig. 1. All transfer lines between the sample oven (B) and the gas chromatograph (C) and thence to the graphite furnace (D), must be wrapped in 36-W heating tape and held at 150°C throughout the procedure.

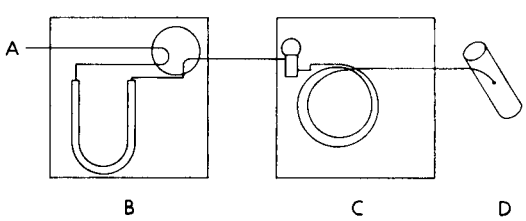

Fig. 1. Gas chromatograph system.

TABLE 1

Instrumental operating conditions

Gas chromatography		Atomic absorption spectrometry	
Carrier gas flow rate	80 ml min^{-1}	Ash 300°C	120 s (dry cycle)
Oven temperature program	115°C isothermal	Atomize 1800°C	240 s (char cycle)
Injection port temperature	150°C	Internal gas flow	0
Outlet and transfer tube temperature	150°C	External gas flow (N_2)	60 ml min^{-1}
		Wavelength	279.5 nm
		Slit 4	(0.7 nm)
		Background correction mode, Scale expansion (× 5)	

With the 4-way valve in the sample oven in the bypass position, the sample trap is placed in the cool sample oven and connected with Swagelok fittings. The nitrogen carrier gas flow rate is adjusted to 100 ml min^{-1} (which reduces to 80 ml min^{-1} when the sample trap is switched on). The sample oven is heated at 150°C for 10 min (no flow through the sample tube). The 4-way valve is then turned to start the flow through the sample tube, and the atomic absorption furnace program is initiated immediately. The gas chromatograph is run isothermally at 115°C. Gas flow is continued until the MMT peak has been recorded.

Calibration is done by injecting an appropriate μl standard of MMT directly into the cooled, spent, sample tube in the sample oven. The above procedure is then followed exactly as for the sample.

RESULTS AND DISCUSSION

Optimization of the procedure

Collection of MMT. Because of the very low levels of MMT expected in air and other environmental samples, it was necessary to employ a method of preconcentration. Two possibilities exist: (1) the MMT can be trapped in a solvent contained in a bubbler; or (2) the MMT can be trapped on an adsorber held at very low temperature. Both of these strategies were tried.

A micro bubbler containing hexane was cooled in an ice bath. After collection of the sample the hexane volume was reduced to 0.4 ml. A 10-μl aliquot was injected into the gas chromatograph. The detection limit using this approach was about 0.02 μg m^{-3} of air for an 8-h sampling period. This was shown to be too poor for the present purposes.

The second trapping strategy is that outlined in the proposed procedure above. MMT is collected on a teflon-lined U-tube containing packing material similar to that used in the gas chromatographic columns. It was necessary to build a sample oven which contained a 4-way valve (which allows by-passing of the sample U-tube) so that any lines or other components carrying MMT

could be heated. This is because MMT has a relatively high boiling point and tends to condense out on cool transfer lines.

Decomposition of MMT in transfer lines. In a similar study of tetraalkyllead compounds, the problem of decomposition of these compounds in the metal transfer lines was noted. Teflon-lined tubing prevented this problem and was used as a precaution in this study as well.

Calibration. Ideally it would be desirable to inject standard solutions through the injection valve for calibration and avoid collection on the sample trap. However, the chromatographic peaks obtained by direct injection and those obtained using the sample trap had slightly different retention times and were differently shaped. Thus, it was necessary to inject the calibration standard onto the spent sample U-tube and follow the procedure exactly as for the samples. Peak area rather than peak height was used in the calculations.

Comparison of atomizers. Interfacing of gas chromatography and atomic absorption occurs through the atomizer. When best atomic absorption sensitivity is required, a commercial electrothermal atomizer (furnace or rod) is usually chosen. These devices are relatively expensive and are not available in all atomic absorption laboratories to be tied up for this purpose. Thus it was of interest to determine the relative detection limits obtainable for inexpensive homemade quartz-tube atomizers which were developed for a study of tetraalkyllead compounds [3].

These atomizers consist of a quartz tube wrapped with heating wire or a slotted quartz tube held in an air—acetylene flame. The relative detection limits of the wire-wrapped quartz tube and the Perkin-Elmer HGA 2100 were the same, whereas that of the slotted quartz tube was 20 times greater in comparative tests with MMT. Thus, if desired, a quartz tube wrapped in heating wire can be used in place of the commercial furnace with no penalty to be paid in detection limit.

It is interesting to note that MMT atomizes readily giving free manganese atoms at the relatively low temperature of 1000°C attainable with the heating wire wrapped quartz tube atomizer. This temperature is in marked contrast to 2700°C often recommended as the atomization temperature in the commercial graphite furnace atomizers. In this regard, it was found necessary, for maximum sensitivity, to align the manganese hollow-cathode lamp so that the optical beam just grazed the inner surface of the quartz tube nearest the gas inlet. Sensitivities obtained in the center of the tube are greatly reduced.

Analysis of air samples

Air samples of up to 15 m^3 were taken at a variety of locations on the streets of Toronto. No MMT was detected in any sample (detection limit 0.05 ng m^{-3}). This compares with 14 ng m^{-3} for total tetraalkyllead compounds found in street air in similar locations. Samples were then collected in an underground car-park beneath the Chemistry and Physics buildings at the University of Toronto. In a few of these samples MMT was detected.

Figure 2 shows the chromatograms obtained when a calibration standard

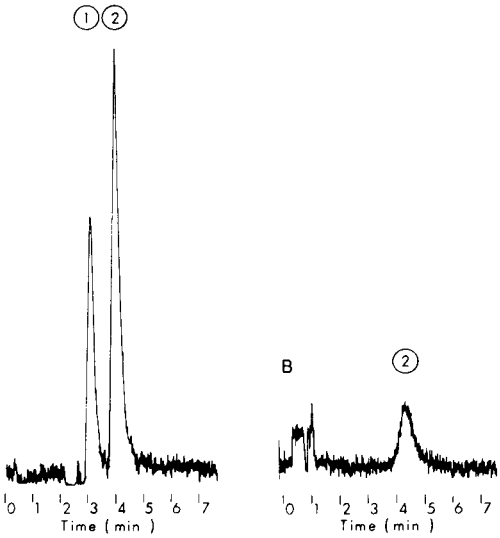

Fig. 2. (A) Chromatograph for standard sample containing MMT and CMT. (B) Chromatogram of an air sample taken in an underground car-park.

containing CMT which can be used as an internal reference if desired [2]) and MMT were run according to the proposed procedure. The level of MMT in the air sample was 0.3 ng m^{-3}. Other samples yielded values between 0.1 and 0.3 ng m^{-3}. It should be noted that the retention times of the MMT peak shown in the chromatogram for the air sample and the calibration standard are slightly different (ca. 0.2 min). It was not uncommon to have this variation which reflects the reproducibility problems found when sample traps are used.

It is interesting to speculate as to why the MMT levels in air are so much lower than those of tetraalkyllead when it is likely that a large fraction of the vehicles are using "unleaded" gasoline containing MMT. To this end, a cursory study of MMT in air was attempted.

MMT, liquid and vapor, was injected into clear 2-l glass bottles kept in the light and in the dark. Samples were then taken of the contained air and isooctane rinsings of the bottle walls at various intervals. Results of these studies suggest that MMT is quickly decomposed in air, more quickly in the light than in the dark. This conclusion must be treated as highly qualitative since a number of problems were encountered during this work.

Regarding this experiment, it was particularly difficult to keep the MMT suspended in the air. There is a great tendency for this compound to condense out on the sides of the bottles. Apart from making sampling difficult, this calls into question whether such a system is valid for determining the stability of MMT in air. Obviously, a full-scale separate study (well beyond the scope of this work) would be very important and should be undertaken.

The relative low volatility of MMT (i.e. its tendency to condense out on

surfaces) may also be a reason for the very low levels detected in air samples even in an underground car-park. With this in mind, the filter papers used for filtering particulate samples from the air in the MMT gas sampling train were rinsed and in some cases refluxed with isooctane. The rinsings were then injected into the gas chromatograph as a test for the presence of MMT, but in no case was MMT detected.

It is important to point out that tests done on exhaust samples taken from cars which were burning "unleaded" gasoline showed no MMT (detection limit 0.1 ng m^{-3}). This is consistent with a similar study of tetraalkyllead compounds [3]. Thus most of the MMT detected in the air samples is due to evaporation and spillage, etc.

This work was supported by a grant from the Ontario Ministry of the Environment, Research Grants Program and by Perkin-Elmer Corporation, Norwalk, Connecticut who supplied all the atomic absorption equipment. Thanks are also due to the Canada Center for Inland Waters, Burlington, Ontario, who lent the gas chromatograph.

REFERENCES

1 G. N. Turkel'traub, B. M. Luskina and S. V. Syavtsillo, Khim. Tekhnol. Topl. Masel, 12 (1967) 58.
2 P. C. Uden, R. M. Barnes and F. P. DiSanzo, Anal. Chem., 50 (1978) 852.
3 B. Radziuk, Y. Thomassen, Y. K. Chau and J. C. van Loon, Anal. Chim. Acta, 105 (1979) 255.

Analytica Chimica Acta, 120 (1980) 177—186

GAS CHROMATOGRAPHIC METHOD FOR THE DETERMINATION OF SELENITE AND TOTAL SELENIUM IN SEA WATER

C. I. MEASURES* and J. D. BURTON

Department of Oceanography, The University of Southampton, Southampton SO9 5NH, Hampshire (Gt. Britain)

(Received 15th February 1980)

SUMMARY

A method is described for the determination of dissolved selenite and total selenium in natural waters. The detection limit is approximately 10 pmol l^{-1} and the reproducibility ±2.4% (1σ) at 394 pmol l^{-1}. A 100-ml sample containing selenite is reacted with 4-nitro-*o*-phenylenediamine to form 5-nitropiazselenol which is extracted into toluene and then determined by gas chromatography with an electron-capture detector. Other forms of selenium can be determined after photo-oxidizing samples under controlled pH conditions. This leads to a reproducible proportionation of species between selenite and selenate. The method has been used successfully to analyze samples both at sea and in the laboratory.

The geochemical cycle of selenium is not well understood, particularly in the marine environment where low concentrations of selenium are encountered. Early methods of sea water analysis [1, 2] using co-precipitation for preconcentration required large samples because of the insensitivity of the final spectrophotometric determination. Neutron activation analysis [3], provides good sensitivity, but is not readily available and also involves delays in obtaining results. Sugimura and Suzuki [4] used a fluorimetric determination, but a slow preconcentration step was still required with a sample volume of 5 l.

The use of gas chromatography with an electron-capture detector after extraction of 5-nitropiazselenol has been reported by Shimoishi [5] for coastal waters. The method had the advantage of requiring only a small sample but lacked the sensitivity for precise analysis at the levels found. In later work, Shimoishi and Tôei [6] used 1,2-diamino-3,5-dibromobenzene as the reagent and obtained a ten-fold improvement in sensitivity.

A further problem encountered in determinations of selenium in sea water is the oxidation state of the element. Sillen [7] predicted from equilibrium modelling that selenate would be the thermodynamically favoured form in sea water of pE 12.5. It has been calculated [8] that this predomin-

*Present address: Department of Earth and Planetary Sciences — 54-1318, Massachusetts Institute of Technology, Cambridge, MA 02139, U.S.A.

ance should be true for sea water of pH 8.1 for any $pE > 6.8$. Sillen's prediction, while contrary to their own, prompted Chau and Riley [2] and Shimoishi [5], whose methods were specific for selenium(IV), to adapt their techniques in order to detect and determine selenium(VI). However, they were unable to detect selenium(VI) in their samples (limits of detection, 126 and 253 pmol l^{-1}, respectively).

Recent work [6, 9—12] has shown that in fact both selenium(IV) and selenium(VI) are present in oceanic water. Shimoishi and Tôei [6] and Cutter [12] have reported methods which are capable of measuring and differentiating both oxidation states in sea water; both methods require precise control of conditions to obtain quantitative conversions of selenium(VI) to selenium(IV).

This paper reports a method which has been used successfully for routine determination of both selenium(IV) and total selenium at sea [10, 11]. The method, which is an improvement of the method of Shimoishi [5], has a detection limit of approximately 10 pmol l^{-1} (0.8 ng l^{-1}) and incorporates a simple photo-oxidation procedure which results in the reproducible proportionation of all selenium species between selenium(IV) and selenium(VI), allowing rapid and precise determination of both selenite, total selenium (and selenate by difference) in sea water. The method presented is an improvement of the procedure used for the analysis of samples collected in the N. E. Atlantic [10]. The modifications have improved the precision and sensitivity of the method.

EXPERIMENTAL

Solutions and reagents

4-Nitro-o-phenylenediamine solution (1%). Dissolve 1 g of 4-nitro-*o*-phenylenediamine (Aldrich Chemical Co.) in a mixture of 9 ml of concentrated hydrochloric acid and 91 ml of deionized water. Extract by shaking with 30 ml of redistilled toluene for 5 min. Discard the organic phase and repeat the extraction a further four times. Store the prepared reagent in the dark under refrigeration (4°C) with a fresh 30-ml layer of toluene. Before use, shake the reagent for 5 min and allow to separate. Under these conditions, the reagent is stable for more than four weeks.

Borax solution (0.1 M). Dissolve 3.81 g of disodium tetraborate (A. R.) in 100 ml of deionized water.

Redistilled toluene. Redistil sulphur-free toluene, checking the distillate for purity by injection into the gas chromatograph.

Selenium(IV) standards. Dissolve an appropriate amount of selenium dioxide in distilled water. Prepare serial dilutions to provide working standards of 50 pmol Se ml^{-1}. Standards deteriorate fairly rapidly and are therefore prepared as needed from the solid, not from dilution of stock solution.

Selenium(VI) standards. Prepared from sodium selenate.

Apparatus

The Hewlett-Packard 5736A gas chromatograph used was equipped with a 10-mCi ^{63}Ni electron-capture detector. Injections (3 μl) were made using a S.G.E. 10-μl syringe fitted with a repeating adaptor. The operating conditions were: injection heater 200° C, column oven 195° C; detector oven 350°C; gas (95% argon, 5% methane) flow 70 ml min^{-1}. The column used was a 6 ft. × 1/8 in. (i.d.) glass column packed with 3% 10C (Applied Science) on silylated Chromosorb W (Chromosorb W-HP or similar).

Recommended procedures

Selenium(IV). To 100 ml of a freshly collected sample, add 2 ml of 1% 4-nitro-*o*-phenylenediamine solution and ensure that the pH of the sample is less than 1.8. Stand the sample in a stoppered vessel at room temperature, out of direct sunlight, for 2 h. Add 1 ml of redistilled toluene and shake for 5 min on a wrist-action shaker or for 2 min by hand. Transfer to a separating funnel, and after 5 min, run the aqueous phase to waste and store the toluene extract in a screw cap vial with a teflon-lined cap. The extract is stable indefinitely if kept in a freezer at —4°C.

Total selenium. Place 100 ml of the sample in a quartz silica tube of 2.5-cm diameter. Add 2 ml of 0.1 M borax solution and approximately 50 μl of 30% hydrogen peroxide. Irradiate the sample for 5 h, using a 1250-W medium-pressure mercury lamp. At the end of irradiation, allow the tube to cool before proceeding with the method for selenium(IV). These samples require the addition of more acid to adjust to a pH of less than 1.8.

Measurement of extracts. Inject 3-μl aliquots of samples into the gas chromatograph. Measure the height of the 5-nitropiazselenol peak and compare with the calibration curve constructed from standards adjusted to the same volume and carried through the complete derivative procedure. Standards or previously measured samples should be run at regular intervals to allow for variations in detector sensitivity. If peak heights are used for measurements, injection volumes of standards and samples must be the same. The calibration curve was found to be linear over the range 10—3000 pmol l^{-1}.

RESULTS AND DISCUSSION

Formation of derivative

The reaction between 4-nitro-*o*-phenylenediamine and selenium(IV) as selenite yields 5-nitropiazselenol and is specific for selenite. The mechanism of the reaction for the unsubstituted *o*-phenylenediamine has been discussed by Barcza [13].

Experiments using both ^{75}Se tracer and gas chromatography to optimize reaction conditions indicated that when 2 ml of a 1% (w/v) solution of 4-nitro-*o*-phenylenediamine was used per 100 ml of sample, maximum recovery could be achieved after 45 min at room temperature (25° C). The use of a lower reagent concentration (2 ml, 0.2% w/v) reduced the magnitude of

spurious peaks associated with the reagent but led to an inordinately long reaction time (14 h at 25°C). The reaction was faster at 80°C but this promoted reagent decomposition. The observation of similar reagent decomposition induced by exposure to sunlight led to reactions being carried out in subdued light. A study of the effect of sample pH on the reaction (Fig. 1) showed a marked reduction in recovery above pH 1.8, in agreement with earlier results [14].

Initial experiments in which 100-ml samples were extracted with 2 ml of redistilled toluene indicated that the maximum recovery of derivative was 90% relative to 7-ml samples. Calculations yielded a distribution coefficient of 415, in reasonable agreement with an earlier value of 367 [14]. With two sequential 1-ml extractions, recoveries of 96% were achieved. This procedure was used in the N. E. Atlantic work [10]; however, in order to simplify the method and increase its sensitivity, later samples [11] were processed using a single 1-ml extraction [6]. Calculations indicated that this would lead to 80% extraction of piazselenol. Standards for the method were prepared by extracting known amounts of selenium(IV) in distilled water, or sea water free of selenium(IV), under the same conditions as for samples, so that incomplete extraction was unimportant. Heptane and hexane did not extract the derivatives, in contrast to the findings of Gosink and Reynolds [15].

Interferences

Surface samples of oceanic water, naturally free of selenium(IV), were used to examine the effect of the addition of various ions on the recovery of selenium(IV) spikes. The results (Table 1) indicate that in the presence of 2 ml of 0.1 M EDTA per 100 ml of sample, none of the ions studied interfered at concentrations between 10 and 100 times their normal sea-

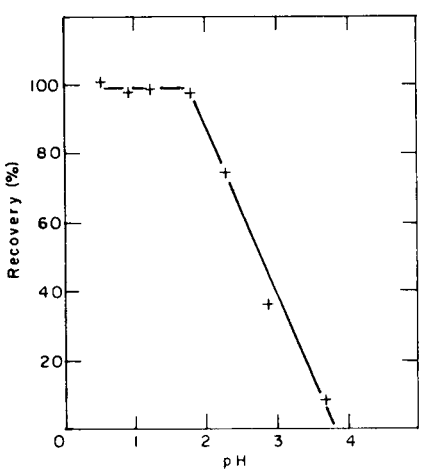

Fig. 1. Effect of sample pH on extraction of selenium.

TABLE 1

Recovery[a] of selenium in the presence of diverse ions and 2×10^{-3} M EDTA

Diverse ion	NO_3^-	NO_2^-	PO_4^{3-}	SiO_2	x[b]	V(V)	Cr(III)	Cr(VI)	Mn(II)	Mn(IV)
Conc. added[c] ($\mu g\ l^{-1}$)	6000	300	600	5000		15	6	6	20	20
Recovery (%)	100	105	97	109[d]	95[e]	98	104	103	98	100

Diverse ion	Fe(II)	Fe(III)	Co(II)	Ni(II)	Cu(II)	Zn(II)	As(V)	Cd(II)	Sn(IV)
Conc. added[c] ($\mu g\ l^{-1}$)	300	30	0.8	20	20	50	400	0.5	0.1
Recovery (%)	106	103	101	107[e]	102	100	104	100	96

[a]Samples used for spiking were filtered surface sea water (100 ml), naturally free of selenite, spiked with 3.45 ng of Se as selenous acid.
[b]NO_3^-, NO_2^-, PO_4^{3-} and SiO_2 added simultaneously in the concentrations mentioned.
[c]Diverse ion spike concentrations were those added to the natural levels in the samples.
[d]4 ng Se l^{-1} in blank. [e]2 ng Se l^{-1} in blank.

water maxima. In the case of addition of silicon and nickel, the high recovery was attributed to selenium in the reagents used for spiking. This conclusion is based on evidence of traces of selenium in even ultra-pure reagents [16—18] and the lack of any relation between reaction time and blank sizes; the latter rules out the possibility of a slow reaction between the diverse ion and the reagent producing a derivative with a retention time similar to the piazselenol used. Although these interference studies were done with EDTA added, later work showed that there was no detectable difference between oceanic samples processed with and without EDTA, which was therefore omitted from the final procedure.

Gas chromatography

Various columns were tested for the separation of the 5-nitropiazselenol. Stationary phases of intermediate and polar type produced the best separations of the piazselenol from the peaks of naturally occurring materials which are co-extracted from sea-water samples. Two types of column used in most work were: (1) 6.7% OV17 plus 8.2% QF-I on 80—100-mesh acid-washed Chromosorb W pretreated with dimethylchlorosilane and (2) 3% 10C (Applied Science) on 60—80 mesh acid-washed Chromosorb W. The 3% 10C column was used most recently (Fig. 2).

The identity of the 5-nitropiazselenol peak from extracted samples was confirmed by using standards prepared from the pure compound dissolved in toluene. Retention times for extracts and pure standards were identical on all columns used. Peak heights obtained from the dissolved standards were the same (within 3%) as those of extracted standards when corrected for expected losses in the extraction procedure (Table 2).

TABLE 2

Comparison of standards

	Aqueous standard[a]	5-Nitropiazselenol[b]
Selenium (3 μl nominal)	10.38 pg	10.6 pg
Adjusted for recovery (98%)	9.94 pg	
Adjusted for backwash (89%)	8.84 pg	
Peak height (3 μl)	128 mm	149 mm
Peak height (pg)	14.4 mm	14.0 mm

[a]Selenite spike in deionized water carried through the derivatization procedure.
[b]Standard prepared by dissolving recrystallized 5-nitropiazselenol in toluene and measuring directly.

Photo-oxidation

Early experiments in which samples of estuarine water were photo-oxidized in order to release organically bound material showed very large (6—7 fold) increases in available selenium(IV). Experiments in which spikes of selenium(VI) and selenium(IV) were added to samples of distilled water which were then irradiated, indicated that under similar irradiation conditions identical recoveries were obtained in the form of selenium(IV). Further experiments in which the pH of the samples before irradiation was varied indicated that recovery as selenium(IV) could be increased with increasing pH (Fig. 3). Although increased recovery as selenium(IV) could be obtained with pH greater than 9, the formation of precipitates at these pH values when sea-water samples are used introduces unacceptable uncertainties.

TABLE 3

Reproducibility of recovery of selenium as selenite after photo-oxidation

Sample	Salinity (‰)	No. of replicates	Coefficient of variation (%)	Recovery (%)
Estuarine water[a]	32	6	4.5	75
Estuarine water[a]	32	6	5.6	77
Estuarine water[a]	32	6	4.6	69
Estuarine water[a]	20	6	2.5	73
River water[a]	—	6	1.9	77
Deionized water[a]	—	6	4.5	75
				Average 74 ± 3
Sea water[b]	35	5	5.5	86
Sea water[b]	35	5	5.7	89
Sea water[b]	35	2		86

[a]With a 1000-W u.v. lamp. [b]With a 1250-W u.v. lamp.

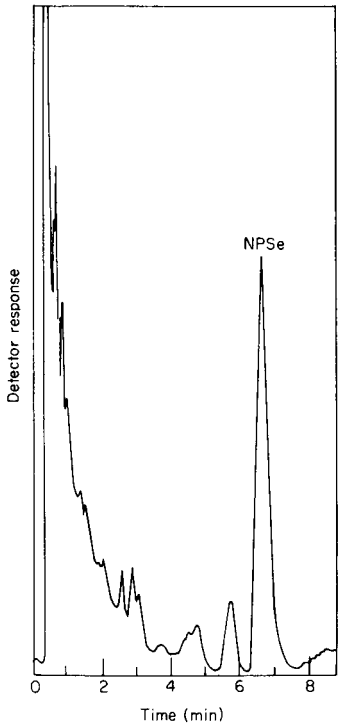

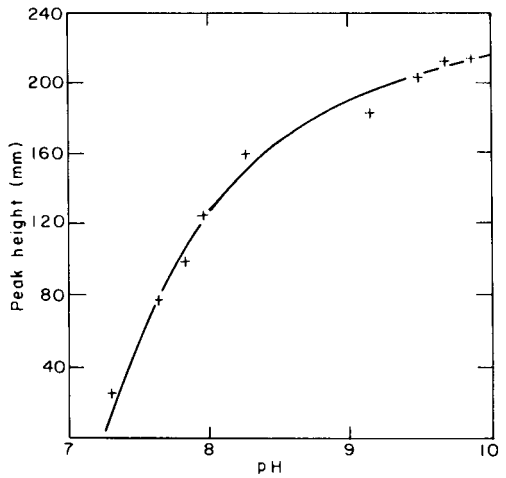

Fig. 2. Chromatogram of an oceanic sample. Column, 3% 10-C silanized Chromosorb W column. Conditions as in Experimental; attenuation ×16. The sample was sea water (11°02'N, 140°05' W depth 742 m) containing 537 pmol Se(IV) l^{-1}.

Fig. 3. Effect of sample pH during photo-oxidation on recovery as selenite.

Irradiation of samples of water with differing salinities indicated (Table 3) that, under the recommended buffering conditions, recovery of selenium as selenium(IV) averaged 74 ± 3% with no significant differences between samples of different salinities. Later experiments with a different u.v. irradiation apparatus and a 1250-W lamp yielded recoveries as selenium(IV) of 86 ± 6%.

Mechanisms

The photo-induced redox reactions occurring in samples of natural waters are poorly understood. The proportionation of selenium between the tetravalent and hexavalent oxidation states is at first surprising but is paralleled by findings on nitrate. Armstrong et al. [19] observed partial reduction of nitrate to nitrite during irradiation of sea water. Shuali et al. [20] reported the same phenomenon for nitrate in distilled water and noted a pH dependence, with maximum reduction to nitrite occurring in samples irradiated at pH 10. The mechanism they proposed for the observed behaviour involves photo-induced decomposition of the nitrate ion. The similar pH effect on the

nitrate and selenate systems indicates that the mechanism of the observed behaviour of selenium may well be similar to that for nitrate. The photo-induced decomposition mechanism is also consistent with the higher yield of selenium(IV) observed with the 1250-W lamp.

Limit of detection, precision and recovery

The limit of detection of the proposed method was generally 4 fmol absolute, which is equivalent to 25 pmol Se l^{-1} using a 100-ml sample; this was later improved to approximately 10 pmol l^{-1}. The coefficient of variation as determined by replicate determinations is shown in Table 4. The values were obtained on a variety of samples under different conditions. The first value for oceanic water indicates a coefficient of variation of less than 5% at 342 pmol l^{-1}. This was improved using a single 1-ml toluene extraction

TABLE 4

Reproducibility of selenite determination

Sample	No. of replicates	Av. Se (pmol l^{-1})	Coefficient of variation (%)
Spiked distilled water	6	1962	3.3
^{75}Se spike in sea water	6	—	1.9
Ocean water[a]	8	342	4.5
Distilled water	6	63	28
Ocean water[b]	6	394	2.4
Ocean water duplicates[b]	2	1928, 1928	
	2	677, 663	
	2	1239, 1240	
	2	249, 227	

[a]Performed during routine analysis at sea.
[b]Performed by modified technique (single 1-ml extraction).

TABLE 5

Recovery of selenite spikes[a]

Sample	Selenium (pmol)			
	Initial	Added	Recovered	Recovery (%)
Photo-oxidized estuarine water	112	44	155	98
Estuarine water	19	44	61	97
Ocean water[b]	38	44	84	105
	29	44	75	105
Ocean water[b] (surface)	0	44	44	100

[a]Samples extracted by the original double extraction method. [b]Performed during routine analysis at sea.

TABLE 6

Comparison of extracts of stored samples with those extracted at sea

Depth (m)	Species determined	Selenium (pmol l^{-1})		Difference (%)
		At sea	Stored	
400	Se(IV)	315	335	+6
988	Se(IV)	610	635	+4
75	Se(IV)	54	42	−23
4821	Total	2026	2048	+1
1878	Total	1529	1544	+1

to less than 3% at 394 pmol l^{-1}. Recovery using a variety of samples when compared to standards taken through the same procedure (Table 5) was quantitative within the precision of the technique.

Storage

Comparison of samples extracted at sea with those extracted in the laboratory (Table 6) indicated that for samples acidified to pH 2 with hydrochloric acid and stored in either glass or linear polyethylene containers there was no significant change in concentration in either oxidation state over a period of 4.5 months in agreement with earlier results [4, 21]. Profiles of selenium at two oceanic stations produced by a combination of shipboard extractions and laboratory extractions of stored samples showed no significant differences between the two techniques.

One of us (C. I. M.) thanks the University of Southampton for the Research Studentship which made this work possible.

REFERENCES

1 M. Ishibashi, T. Shigematsu and Y. Nagasawa, Rec. Oceanogr. Wks. Jpn., New Ser., 1 (1953) 44.
2 Y. K. Chau and J. P. Riley, Anal. Chim. Acta, 33 (1965) 36.
3 D. F. Schutz and K. K. Turekian, Geochim. Cosmochim. Acta, 29 (1965) 259.
4 Y. Sugimura and Y. Suzuki, J. Oceanogr. Soc. Jpn., 33 (1977) 23.
5 Y. Shimoishi, Anal. Chim. Acta, 64 (1973) 465.
6 Y. Shimoishi and K. Tôei, Anal. Chim. Acta, 100 (1978) 65.
7 L. G. Sillen, in M. Sears (Ed.), Oceanography, American Association for the Advancement of Science, Washington, DC, 1961, p. 549.
8 C. I. Measures, Ph.D. Thesis, University of Southampton, 1978.
9 Y. Sugimura, Y. Suzuki and Y. Miyake, J. Oceanogr. Soc. Jpn., 32 (1976) 235.
10 C. I. Measures and J. D. Burton, Earth Planet. Sci. Lett., 46 (1980) 385.
11 C. I. Measures, R. E. McDuff and J.M. Edmond, Earth Planet. Sci. Lett., (1980) in press.
12 G. A. Cutter, Anal. Chim. Acta, 98 (1978) 59.
13 L. Barcza, Mikrochim. Ichnoanal. Acta, (1964) 136.
14 M. Tanaka and T. Kawashima, Talanta, 12 (1965) 211.
15 T. A. Gosink and D. J. Reynolds, Mar. Sci. Commun., 1 (1975) 101.
16 Y. Shimoishi and K. Tôei, Talanta, 17 (1970) 165.

17 Y. Shimoishi, Bull. Chem. Soc. Jpn., 44 (1971) 3370.
18 A. Meyer, E. Grallath, G. Kaiser and G. Tölg, Fresenius Z. Anal. Chem., 281 (1976) 201.
19 F. A. J. Armstrong, P. M. Williams and J. D. H. Strickland, Nature, 211 (1966) 481.
20 U. Shuali, M. Ottolenghi, J. Rabani and Z. Yelin, J. Phys. Chem., 73 (1969) 3445.
21 V. Cheam and H. Agemian, Anal. Chim. Acta, 113 (1980) 237.

Analytica Chimica Acta, 120 (1980) 187—192

SENSITIVE DERIVATIZATION REAGENTS FOR THE RESOLUTION OF CARBOXYLIC ACID ENANTIOMERS BY HIGH-PERFORMANCE LIQUID CHROMATOGRAPHY

JUNICHI GOTO, NOBUHARU GOTO, ATSUKO HIKICHI, TOMOKO NISHIMAKI and TOSHIO NAMBARA*

Pharmaceutical Institute, Tohoku University, Aobayama, Sendai 980 (Japan)

(Received 28th April 1980)

SUMMARY

Two highly sensitive, chiral derivatization reagents, D- and L-1-aminoethyl-4-dimethylaminonaphthalene, were synthesized from 1-dimethylaminonaphthalene. Condensation of carboxylic acids with the chiral reagent was readily effected in the presence of a water-soluble carbodiimide. The diastereoisomeric amides formed from N-acetylamino acid and α-arylpropionic acid enantiomers were efficiently resolved by normal phase chromatography (μPorasil column) with hexane/ethyl acetate or hexane/tetrahydrofuran as a mobile phase. With a fluorescence detector (excitation 320 nm, emission 395 nm), the detection limit was 0.1 ng.

Liquid chromatography has been widely used for the separation of enantiomers in two ways: introduction of an asymmetric environment intramolecularly by conversion to diastereoisomers [1] and intermolecularly by the use of chiral stationary or mobile phases [2]. In connection with pharmacokinetic studies of enantiomeric drugs, a new derivatization reagent providing diastereoisomers which would be more readily distinguishable and would give higher sensitivity, was required. In previous papers [3—5], the preparation of chiral derivatization reagents for the resolution of enantiomeric amines by high-performance liquid chromatography (h.p.l.c.) was described. The present paper deals with the synthesis of chiral derivatization reagents having a fluorophore which gives high sensitivity with a fluorescence detector, and the applicability of these reagents to the resolution of carboxylic acid enantiomers by h.p.l.c.

EXPERIMENTAL

Equipment

A model ALC/GPC 202 R401 high-performance liquid chromatograph (Waters Assoc., Milford, MA, U.S.A.) equipped with a Hitachi Model 650-10LC spectrofluorimeter (excitation 320 nm; emission 395 nm) was used. Samples were applied by a Waters Model U6K sample loop injector (effective

volume, 2 ml). A μPorasil column (1 ft. × 0.25 in. i.d.; Waters Assoc.) was used under ambient conditions.

All melting points were taken on a micro hot-stage apparatus and are uncorrected. Optical rotations were measured on a JASCO Model DIP-4 automatic polarimeter. Nuclear magnetic resonance (n.m.r.) spectra were recorded on a JEOL Model PS-100 spectrometer at 100 MHz using tetramethylsilane as an internal standard; abbreviations used are *s* for singlet, *d* for doublet, and *m* for multiplet.

Synthesis of derivatization reagents

The reactions may be outlined as follows:

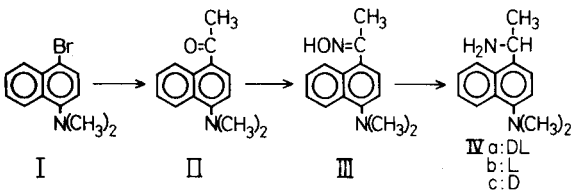

1-Aceto-4-dimethylaminonaphthalene (II). To a stirred suspension of magnesium (1.2 g) and methyl iodide (2 drops) in anhydrous ether (60 ml) was added dropwise a solution of 1-bromo-4-dimethylaminonaphthalene (I; 10 g) in anhydrous ether (20 ml). The mixture was stirred at room temperature for 3 h. The resulting Grignard reagent was added dropwise to a stirred solution of acetonitrile (3.3 g) in anhydrous ether (20 ml) at room temperature, and the mixture was stirred further for 30 min. The reaction mixture was decomposed with 10% hydrochloric acid (50 ml) under ice-cooling over a period of 30 min and neutralized with 10% (w/v) sodium hydroxide solution. The resulting solution was extracted with ether. The organic layer was washed with water, dried (Na_2SO_4), and evaporated. The oily residue was subjected to column chromatography on silica gel (50 g). Elution with hexane/ethyl acetate (5:1) gave II (2 g) as a pale red oil.

1-Aceto-4-dimethylaminonaphthalene oxime (III). A solution of II (2 g), hydroxylammonium chloride (3 g) and sodium acetate (5 g) was boiled under reflux for 2 h. After removal of the precipitate by filtration, the filtrate was evaporated. The oily residue was subjected to column chromatography on silica gel (40 g). Elution with hexane/ethyl acetate (5:1) and recrystallization of the eluate from methanol gave compound III (700 mg) as pale brown needles (m.p. 152—153°C). Calculated for $C_{14}H_{16}N_2O$: 73.7% C, 7.1% H, 12.3% N; found: 73.8% C, 6.9% H, 12.2% N. N.m.r. (CCl_4)δ: 2.24 (3H, *s*, $-CH_3$), 2.84 (6H, *s*, $-N(CH_3)_2$), 6.86—8.26 (6H, *m*, Ar—H), 9.40 (1H, *m*, =N—OH).

DL-1-Aminoethyl-4-dimethylaminoaphthalene (IVa). To a stirred solution of III (1 g) in a mixture of ethanol (20 ml) and 15% NaOH (20 ml), was added portionwise Raney nickel (700 mg) under ice-cooling, and the suspension was stirred for 4 h. After removal of the catalyst by filtration, the filtrate was concentrated and extracted with ether. The organic layer was washed

with water, dried (Na_2SO_4), and evaporated. The oily residue was subjected to column chromatography on silica gel (8 g). Elution with 1 M methylamine in ethyl acetate/ethanol (3:1) gave IVa (800 mg) as a colorless oil. N.m.r. ($CDCl_3$)δ: 1.46 (3H, *d*, J = 8 Hz, $-CH_3$), 1.64 (2H, *s*, $-NH_2$), 2.84 (6H, *s*, $-N(CH_3)_2$), 4.83 (1H, *d*, J = 8 Hz, $-CH<$), 7.01—8.28 (6H, *m*, Ar—H). Hydrogen chloride was passed into a solution of IVa in ether to give a crystalline product. Recrystallization from methanol/ether gave the hydrochloride of IVa as colorless needles (m.p. 239—240°C, decomp.). Calculated for $C_{14}H_{19}ClN_2$: 67.0% C, 7.6% H, 11.2% N; found: 66.7% C, 7.8% H, 11.0% N.

Optical resolution of IVa. To a solution of IVa (384 mg) in ethanol (2 ml) was added a solution of D-α-methoxy-α-methyl-1-naphthaleneacetic acid [4] (428 mg) in ethanol (5 ml). The resulting precipitate was collected by filtration and fractionally crystallized from ethanol several times. The salt was decomposed with 10% NaOH solution and the free base was extracted with ether. The organic layer was washed with water, dried (Na_2SO_4), and evaporated to provide the L-base (IVb; 100 mg) as a colorless oil. Treatment with hydrogen chloride gave the hydrochloride of IVb as colorless needles (m.p. 240—241°C, decomp.; $[\alpha]_D^{15}$ — 17.7°; *c* = 0.37, methanol). Calculated for $C_{14}H_{19}ClN_2$: 67.0% C, 7.6% H, 11.2% N; found: 66.8% C, 7.7% H, 11.0% N. The mother liquor was treated with L-α-methoxy-α-methyl-1-naphthaleneacetic acid [4] in the manner described above to give the hydrochloride of the D-base (IVc; 80 mg) as colorless needles (m.p. 243—244°C, decomp.; $[\alpha]_D^{15}$ + 17.3°; *c* = 1.4, methanol). Calculated for $C_{14}H_{19}ClN_2$: 67.0% C, 7.6% H, 11.2% N; found: 67.2% C, 7.7% H, 11.3% N.

Materials

Amino acids were kindly donated by Ajinomoto Co. (Kawasaki, Japan). Optically active ibuprofen and indoprofen were obtained by fractional crystallization of L-α-methylbenzylamine salts of commercially available racemates. Other reagents were purchased from Tokyo Kasei Co. (Tokyo, Japan). Solvents were purified by distillation prior to use. All the reagents were of analytical-reagent grade.

Derivatization procedure

To a solution of carboxylic acid (ca. 500 μg) in pyridine (0.2 ml) or dichloromethane (0.2 ml) containing tri-n-butylamine (20 μl) were added reagent IVc (ca. 500 μg) and 1-ethyl-3-(3-dimethylaminopropyl)-carbodiimide hydrochloride (ca. 1 mg); the solution was then allowed to stand at room temperature for 3 h. The reaction mixture was extracted with ethyl acetate. An aliquot (5 μl) was injected into the chromatograph.

RESULTS AND DISCUSSION

Preparation of the reagents

The design of a promising derivatization reagent for the liquid chromatographic resolution of carboxylic acid enantiomers via diastereoisomers requires

the incorporation of suitable structural features, i.e. chirality leading to efficient resolution, a function reactive toward the carboxylic acid group, and a suitably strong fluorophore. These requirements led to the preparation of an optically active dimethylaminonaphthalene derivative having a primary amino function because the dimethylaminonaphthalene moiety should enhance the sensitivity for fluorimetric monitoring. Our effort was initially directed to the synthesis of D- and L-1-aminoethyl-4-dimethylaminonaphthalenes.

The reaction of the freshly prepared Grignard reagent with acetonitrile proceeded readily to provide compound II in reasonable yield. Condensation with hydroxylamine gave the oxime III which on reduction gave the required compound IVa. The optical resolution of IVa was accomplished by repeated fractional crystallization, providing the desired enantiomers IVb and IVc. The optical purity of both chiral reagents was more than 99.5% as judged by the usual criteria.

Application to h.p.l.c.

The applicability of these reagents to the separation of carboxylic acid enantiomers by h.p.l.c. was then investigated. Condensation of N-acetylamino acids with the chiral reagent was effected in the presence of water-soluble carbodiimide under alkaline conditions:

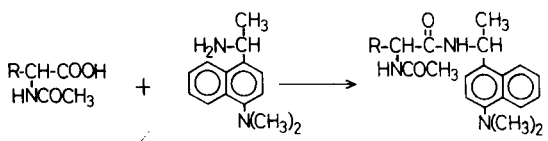

The derivatized enantiomers showed a single peak of the theoretical shape and provided excellent sensitivity (excitation wavelength 320 nm, emission wavelength 395 nm) with a detection limit of 0.1 ng. No racemization of the product or derivatization reagent occurred, even after prolonged reaction.

It is sufficiently substantiated that amide diastereoisomer can be separated more efficiently by normal-phase rather than reversed-phase chromatography [3, 4]. In actuality, no satisfactory separation of the diastereoisomers formed from N-acetyl DL-amino acids was obtained on a μBondapak C_{18} column. In contrast, each of the diastereoisomer pairs was separated on a μPorasil column when hexane/ethyl acetate was used as the mobile phase. The retention and resolution values of nine pairs of diastereoisomers produced with reagent IVc are listed in Table 1. The k' and α values refer to the capacity ratio and separation factor for a pair of diastereoisomers, respectively. The resolution value, R, was calculated from the equation $R = 2(t_{R_2} - t_{R_1})/(W_1 + W_2)$, where t_{R_1} and t_{R_2} are retention times, and W_1 and W_2 are the bases of triangles derived from the peaks. It is evident from the data that the complete separation was obtained for all the pairs of N-acetylamino acids. The R value increased with increasing carbon number of the alkyl residue at the α-position

TABLE 1

Separation of diastereoisomeric amide derivatives of N-acetyl-DL-amino acids (Column, μPorasil. Mobile phase, hexane/ethyl acetate (1:3). Flow rate, (A) 1.0 ml min^{-1}, t_0 = 2.5 min, (B) 3.0 ml min^{-1}, t_0 = 0.8 min)

Amino acid	k'		α	R	Flow rate
	L	D			
Alanine	11.20	13.40	1.20	1.17	B
α-Aminobutyric acid	6.93	11.33	1.63	3.47	A
Valine	3.20	7.07	2.21	6.44	A
Norvaline	4.00	8.60	2.15	6.27	A
Leucine	2.73	7.00	2.56	8.10	A
Norleucine	4.00	7.73	1.93	5.83	A
Proline	22.80	34.00	1.49	1.89	B
Phenylglycine	2.00	4.63	2.32	6.53	A
Phenylalanine	3.10	6.33	2.04	6.30	A

TABLE 2

Separation of diastereoisomeric amide derivatives of DL-α- arylpropionic acids (Column, μPorasil. Mobile phase, (A) hexane/ethyl acetate (10:3), (B) hexane/tetrahydrofuran (5:1). Flow rate, 1.0 ml min^{-1}, t_0 = 2.5 min)

Drug	k'		α	R	Mobile phase
	D	L			
Ibuprofen	1.36	2.05	1.51	4.30	A
	1.32	1.98	1.50	3.80	B
Indoprofen	19.10	24.70	1.30	3.65	A
	15.40	18.30	1.18	3.00	B
Naproxen	3.04	4.37	1.44	3.60	A
	2.79	3.80	1.36	3.14	B

among the former six substrates. No exceptions were observed in the elution order of each pair of enantiomers; N-acetyl L-amino acids were eluted before the corresponding D-enantiomers.

This derivatization method was further applied to the separation of DL-α-arylpropionic acids which are currently used as anti-inflammatory drugs.

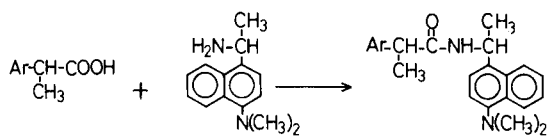

As listed in Table 2, DL-ibuprofen, indoprofen, and naproxen were completely resolved on a μPorasil column when hexane/ethyl acetate (10:3) or hexane/tetrahydrofuran (5:1) was used as the mobile phase. The use of the former solvent system appears to be somewhat more efficient for resolution.

In conclusion, this derivatization procedure for h.p.l.c. of carboxylic acids proved to be excellent not only for the resolution of enantiomers but also in providing sensitive fluorimetric monitoring. The highly sensitive method may serve for the determination of α-arylpropionic acid drugs in biological fluids for pharmacokinetic studies. In addition, the application of the present method to the separation and determination of biologically active substances having a carboxylic acid group should be a fertile field for study.

The authors are indebted to the staffs of the central analytical laboratory of this Institute for elemental analyses and spectral measurements. This work was supported in part by a Grant-in-Aid for Scientific Research from the Ministry of Education, Science and Culture of Japan.

REFERENCES

1 T. Tamegai, M. Ohmae, K. Kawabe and M. Tomoeda, J. Liq. Chromatogr., 2 (1979) 1229.
2 P. E. Hare and E. Gil-Av, Science, 204 (1979) 1226.
3 T. Nambara, S. Ikegawa, M. Hasegawa and J. Goto, Anal. Chim. Acta, 101 (1978) 111.
4 J. Goto, M. Hasegawa, S. Nakamura, K. Shimada and T. Nambara, J. Chromatogr., 152 (1978) 413.
5 J. Goto, N. Goto, A. Hikichi and T. Nambara, J. Liq. Chromatogr., 2 (1979) 1179.

Analytica Chimica Acta, 120 (1980) 193—207

THE SIMULTANEOUS DETERMINATION OF THE PROSTAGLANDINS BY CHEMOSPECIFIC DEUTERATION WITH SEPARATION AND QUANTIFICATION BY COMBINED GAS CHROMATOGRAPHY — CHEMICAL IONIZATION MASS SPECTROMETRY

ROBERT G. MEGARGLE*, LAURENCE E. SLIVON, JOSEPH E. GRAAS and A. HARRY ANDRIST*

Department of Chemistry, The Cleveland State University, Cleveland, OH 44115 (U.S.A.)

(Received 28th January 1980)

SUMMARY

A new gas chromatography/mass spectrometry (g.c./m.s.) procedure is described which simultaneously quantifies eight prostaglandins using one internal standard. The method could easily be extended to include more prostaglandins. The basis of the new method derives from two developments; 1) the discovery of quantitative chemospecific deuteration conditions for the C_5—C_6 double bonds of the prostaglandins (PG_2), and 2) the development of special computer software to solve the analytical problem. Eight prostaglandins, present in the 1—100 ppm range, were determined with errors only occasionally over 10%. Substantially better performance may be expected with a more stable mass spectrometer. Samples with only 2 prostaglandins showed errors only occasionally over 1%.

The prostaglandins [1], along with the prostaglandin endoperoxides [2], the thromboxanes [3] and prostacyclin [4] are a ubiquitous family of oxygenated fatty acids which are known to possess a number of profound biological activities. They are biosynthesized in ppm quantities in both male and female mammalian cells and, at this concentration level, act as potent intermediary regulators of a vast array of organ functions, including reproductive physiology, central nervous system activity, lipid metabolism, blood flow and pressure, smooth muscle activity, endocrine gland secretions, respiratory action, and digestive secretions [1]. The past decade has witnessed dramatic progress in the complete elucidation of the mechanism of prostaglandin biogenesis as well as the individual physiological activities. Further advances in this important and rapidly developing area of biochemistry would be significantly enhanced by the development of a reliable, simultaneous quantitation method for a variety of prostaglandins. The extremely low concentrations of prostaglandins, in the range 10^{-6}—10^{-12} g ml^{-1}, in most biological samples constitutes the major problem in any realistic analytical scheme. The analytical problem is complicated by the unusual sensitivity of prostaglandins toward acids, bases, and oxygen, resulting in autoxidation, elimination and rearrangements. These problems have pre-

cluded application of the more conventional analytical techniques for fatty acids. Several procedures for the prostaglandins have been developed, including several involving direct measurement without separation: 1) bioassay [5], 2) spectrophotometric determination [6], 3) enzymatic determination [7], 4) receptor assay [8], 5) isotope derivative assay [9], 6) radioimmunoassay [10]; and several including a separation step: 7) extraction and chromatography [11], 8) high-performance liquid chromatography (h.p.l.c.) [12], 9) gas chromatography [13], and 10) combined gas chromatography/mass spectrometry [14]. The representative sensitivities of these methods, as well as examples of prostaglandins determined by each, are given in Table 1.

These currently available analytical techniques are selective for only certain prostaglandins and/or only one or two prostaglandins per analysis. In this study, a new analytical procedure is described for the simultaneous quantification of eight prostaglandins utilizing one internal standard. The new method was made possible by a combination of four distinct factors. First, reaction conditions were discovered which permit the quantitative as well as chemospecific deuteration of the C_5—C_6 double bonds of the PG_2 series to produce species that are distinct mass spectrometrically. Second, chemical ionization mass spectrometry (c.i.m.s.) produced relatively simple spectra for these reduced PG's with a few significant ions at high mass. Third, the selective capability of the mass spectrometer as a gas chromatography detector was exploited. Fourth, computer software was developed specifically to solve this analytical problem utilizing selected ion monitoring (s.i.m.) and a variation of the simultaneous equations method.

The prostaglandins chosen to perfect the new technique were PGA_1, PGA_2, PGB_1, PGB_2, PGE_1, PGE_2, $PGF_{1\alpha}$, and $PGF_{2\alpha}$. The experimental design for the new method involved the selective reduction of the C_5—C_6 *cis* double bonds with molecular deuterium to produce unique masses, and derivatization to enhance chromatographic characteristics, followed by separation and quantification by combined gas chromatography/mass

TABLE 1

Prostaglandin analytical methods

Method	Detection limit (g ml^{-1})	PG examples	Method	Detection limit (g ml^{-1})	PG examples
Spectrophotometry	10^{-6}	E,A,B	G.c./m.s.	10^{-10}	E,A,F,B
Fluorescence	10^{-6}	E	Radioimmunoassay	10^{-11}	E,F,A
Zimmerman reaction	10^{-6}	E,A,B	Receptor assay	10^{-11}	E
Flame ionization g.c.	10^{-7}	E,A,F,B	Isotope derivative assay	10^{-12}	E
Enzymatic	10^{-9}	E,A,F	Electron capture g.c.	10^{-12}	B
Bioassay	10^{-9}	E,A,F	G.c./m.s./com.	10^{-12}	E,A,F,B

spectrometry/computer (g.c.—m.s.—com.). This technique provides the following advantages not yet attained by other available methods. First, reduction of the C_5—C_6 double bonds decreases autoxidation, which increases storage lifetime. Second, tetra-substituted double bonds do not undergo catalytic reduction [15]. Therefore, deuterium incorporation eliminates the coincidence in molecular weight that exists between the PGA's and the PGB's, which differ only in the position of the endocyclic double bond. Third, deuterium incorporation also reduces all members of the PG_2 series to the PG_1 series, which enhances detectability, yet allows for mass spectrometric discrimination between PG_2 and PG_1 species thanks to the stable isotopic label. Fourth, the technique allows the total amount of each prostaglandin to be determined simultaneously in one sample.

GENERAL CONSIDERATIONS

Deuteration and derivatization

Early experiments on the catalytic reduction of PGE_2 to PGE_1 in 50% yield revealed the utility of tris(triphenylphosphine)chlororhodium(I) as a remarkably selective reagent [16]. These findings were extended considerably in 1973 by Lincoln et al. [17] to encompass the selective reduction of PGE_2-15-acetate methyl ester to PGE_1-15-acetate methyl ester in 80% yield. Recently, total chemical selectivity, i.e. chemospecificity, has been achieved in the homogeneous hydrogenation as well as deuteration of C_5—C_6 and endocyclic C_{10}—C_{11} prostaglandin double bonds without rearrangement or partial reduction of C_{13}—C_{14} or C_8—C_{12} double bonds [18].

The new method utilizes protection of the C_{13}—C_{14} double bond as the C_{15}-trimethylsilyl ether and protection of the carboxyl group as the methyl ester before reduction under molecular hydrogen or deuterium with tris (triphenylphosphine)chlororhodium(I) in 60:40 acetone—benzene at 25°C. Six specifically deuterated prostaglandin derivatives shown in Fig. 1 have been prepared in quantitative yield with this reaction. The individual transformations [18] are (ME and TMS indicate methyl ester and trimethylsilyl ether; the numbers in parentheses refer both to the reaction and to the derivatives listed in Fig. 1)

$PGF_{2\alpha}$-ME-$(TMS)_3$ → 5,6-dideuterio-$PGF_{1\alpha}$-ME-$(TMS)_3$ (1)

PGE_2-ME-$(TMS)_2$ → 5,6-dideuterio-PGE_1-ME-$(TMS)_2$ (2)

PGB_2-ME-TMS → 5,6-dideuterio-PGB_1-ME-TMS (3)

3,3,4,4-tetradeuterio-$PGE_{2\alpha}$-ME-$(TMS)_3$ → 3,3,4,4,5,6-hexadeuterio-$PGF_{1\alpha}$-ME-$(TMS)_3$ (4)

PGA_2-ME-TMS → 5,6,10,11-tetradeuterio-11-deoxy-PGE_1-ME-TMS (5)

PGA_1-ME-TMS → 10,11-dideuterio-11-deoxy-PGE_1-ME-TMS (6)

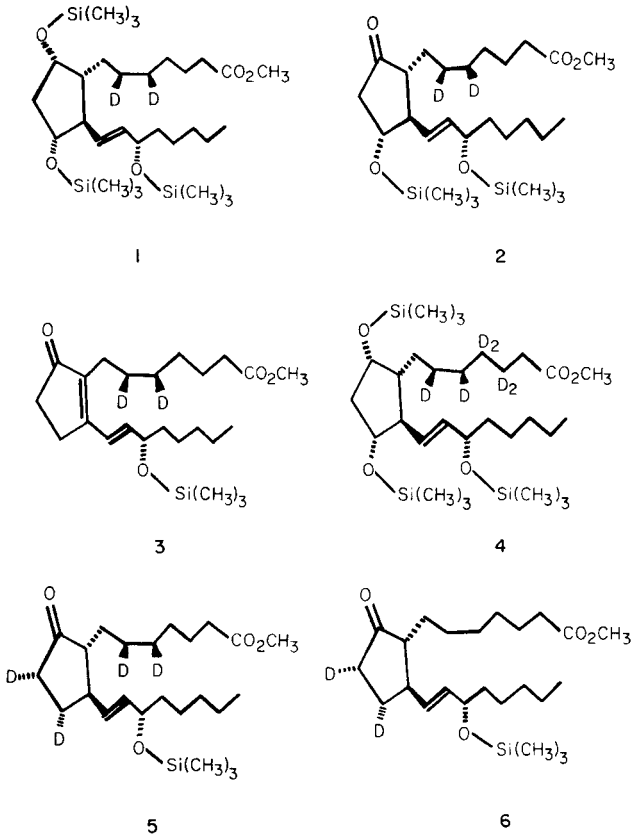

Fig. 1. Prostaglandin derivatives.

The 9-keto prostaglandin derivatives produced in reactions 2, 3, 5, and 6, above, were converted to methoxime derivatives prior to g.c.—m.s.—com. analysis as indicated in Fig. 2.

The demonstration of complete chemical selectivity [19] (olefins do not undergo *E—Z* isomerization during rhodium-catalyzed hydrogenation [20]) in the homogeneous deuteration of derivatized prostaglandins is not only the chemical basis of the analytical procedure, but also a new and far more convenient labeling technique [21] for producing isotopically substituted prostaglandins. Such labeled substrates should prove to be excellent internal standards for related g.c.—m.s.—com. prostaglandin determinations as well as interesting starting materials for detailed metabolic tracer studies.

Mass spectrometry of prostaglandins

In combination with gas chromatography, mass spectrometry [22] continues to be the premier analytical technique in this area of research. The added advantages of chemical ionization mass spectrometry (c.i.m.s.)

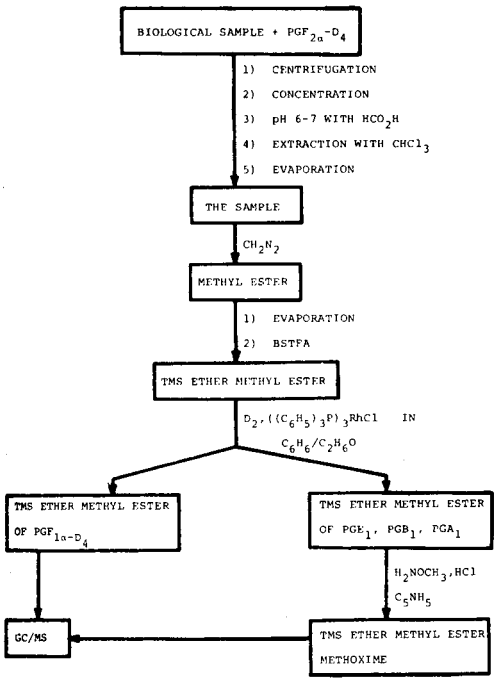

Fig. 2. Sample treatment scheme.

[23] over electron-impact mass spectrometry (e.i.m.s.) were recognized [24] early in the development of analytical methods for the prostaglandins [25].

The methane c.i.m. spectra of the prostaglandin derivatives synthesized for this study reveal the expected functional group elimination processes. A prominent $(M-15)^+$ is observed for all trimethylsilyl ethers as well as a strong $(M-89)^+$, $(M+H-(CH_3)_3SiOH)^+$. A fragment at $(M-81)^+$, $(M+H-CH_3-OH)^+$, is present in spectra of PGA, PGB, and PGE derivatives. This observation suggests fragmentation from the methoxime functionality common to the derivatives of A, B, and E series PG's and not from the methyl ester functionality common to all the PG derivatives. This conclusion is supported by the methane c.i.m. spectrum of the cyclopentanone methoxime where the base peak is $(M-31)^+$. Moreover, the methane c.i.m. spectrum of methyl stearate shows only a small $(M-31)^+$ peak. The absence of a major $(M-15)^+$ in these two spectra suggests that its presence in the spectra of the prostaglandin derivatives is a direct consequence of trimethylsilyl ether fragmentation of a methyl group.

Addition ions at $(M+29)^+$ and $(M+41)^+$ arise from ethyl and allyl cation additions. Significant fragmentation corresponding to $(M-71)^+$ and $(M-173)^+$ in the PGE derivatives comes from cleavage at C_{15}—C_{16}, the allylic bond. The PGF derivatives show multiple loss of $(CH_3)_3SiOH$. In fact, $(M-179)^+$ resulting from the loss of two such groups is the base peak for the PGF

derivatives. No significant $(M+1)^+$ peak, $(M+H)^+$, is observed in the c.i.m. spectra of the PGF derivatives. Only a small $(M+1)^+$ with a correspondingly small $(M-1)^+$ is observed for PGE derivatives, while it is the base peak for PGB derivatives.

Although not all of the fragments in the methane c.i.m. spectra of the PG derivatives have been fully characterized (as have the e.i. spectra [26]), one significant observation comes from our deuterium-labeled compounds. When the C_5—C_6 double bonds of the 10, 11-dideuterio—PGA_2, PGB_2, PGE_2, and $PGF_{2\alpha}$ derivatives have been reduced with molecular deuterium, a 2-amu shift of all the ions in the *m/z* 300—600 range is observed; therefore, none of the ions observed in this region corresponds to loss of the C_1—C_7 side chain.

Quantitative method

There was no unique mass associated with each prostaglandin that showed an intense ion fragment that did not also have some interference from g.c. column bleed, system contamination, or ion fragments from co-eluting compounds. The elution patterns of the four classes of prostaglandin derivatives are shown in Fig. 3. Two chromatographic peaks are observed for the A and E prostaglandin derivatives; these are due to the *syn* and *anti* orientations of the methoxime functionality. Rather than try to find better g.c. conditions, it was decided to treat the entire set of overlapping peaks as a single entity and use the data system to resolve the overlap. A variation of the method of linear simultaneous equations [27—31] was used.

One *m/z* was chosen to be principally representative of each of the eight prostaglandins plus the internal standard. The ion chosen for the A and E prostaglandin arises from the molecular ion plus a proton, but loss of the TMSOH group. The B prostaglandin peak used was the (M+1) ion, where the E prostaglandin peak chosen was the molecular ion minus a methyl group. Those chosen are listed in the heading of Table 2, and represent a trade-off between a desire for a minimum in interference from other prostaglandins against a need for strong relative intensity for that specific prostaglandin.

In this variation of the linear equation method, the usual matrix A was formed where each coefficient a_{ij} was the ratio of the ion current at the ith *m/z* to the total ion current at all nine *m/z*'s when pure prostaglandin j was measured by itself. Ion source and other experimental conditions were carefully maintained from these cracking pattern determinations through

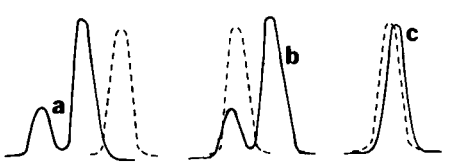

Fig. 3. G.c. elution profiles of the derivatized (a) PGA's, (b) PGE's and (c) PGB's relative to the PGF derivatives (dotted lines), which had the same retention time in each case.

TABLE 2

The coefficient matrix for the simultaneous quantification of 8 prostaglandins

Component and representative *m/z*									
	D_2PGA_1	D_4PGA_1	$PGF_{1\alpha}$	$D_2PGF_{1\alpha}$	$D_6PGF_{1\alpha}$	PGB_1	D_2PGB_1	PGE_1	D_2PGE_1
m/z	(366)	(368)	(407)	(409)	(413)	(452)	(454)	(526)	(528)
366	82.10	7.71	0.29	0.49	0.08	10.98	6.07	27.63	4.40
368	6.53	81.92	0.29	1.68	0.55	0.99	8.45	17.95	32.86
407	0.78	0.56	83.01	7.32	0.48	0.86	2.09	1.54	1.29
409	2.78	4.23	15.56	88.71	1.91	0.57	9.62	1.24	4.31
413	0.45	2.37	0.21	1.05	96.48	0.13	6,45	0.50	0.68
452	0.91	0.84	0.05	0.12	0.14	75.20	7.54	19.75	5.69
454	6.39	2.31	0.19	0.11	0.08	11.07	59.29	4.53	28.14
526	0.00	0.03	0.24	0.08	0.14	0.11	0.27	22.79	0.49
528	0.00	0.00	0.12	0.39	0.07	0.02	0.18	4.02	22.09

the rest of the work. The coefficients that were obtained from three determinations are shown in Table 2. The standard deviation was less than 2% of each matrix element value. Note that in most cases there is mass spectral overlap, caused by normal isotopic composition, between the PG_1 and PG_2 forms of deuterium after the reduction of the C_5—C_6 bond. Also note that there are additional fragmentation interferences appearing in the table, particularly with the E prostaglandins, where diagonal dominance of the matrix fails. This anomaly is due to the extensive fragmentation of the E prostaglandin derivatives as well as the presence of a small impurity in the E samples. Since it was also present in the standards, it does not affect the accuracy of these determinations, but its absence may slightly alter the matrix elements for the E columns.

The SIM computer program operates the mass spectrometer and measures the areas under each of the nine chosen *m/z*'s corresponding to the g.c. peak of the chromatographed sample. Since the entire prostaglandin sample is treated as one g.c. peak, the result is only nine numbers. Multiplication of the inverse matrix A^{-1} by the nine-element vector of areas from SIM yields a new nine-element vector with entries that are independently related to the amount of each prostaglandin j. The first eight values are divided by the ninth, the internal standard, and then multiplied by the concentration of that standard. This gives eight values, d_j, related to concentration but independent of injection volume and instrument parameters that cause equal effects on all prostaglandins. Finally, a known mixture is used to determine eight sensitivity factors, S_j, such that the product d_jS_j yields the concentrations of the eight prostaglandins in the same units used to specify the known mixture.

This last factor represents our variation on the standard technique and accounts for ionization efficiency and other factors that determine the proportionality between detector signal at the *m/z* chosen and the amount of sample.

EXPERIMENTAL

Materials

Prostaglandin starting materials. PGA_1, PGE_1, $PGF_{2\alpha}$, D_4-$PGF_{2\alpha}$, PGE_2, PGB_2, and PGA_2 were supplied through the courtesy of Drs. U. Axen and J. E. Pike (Upjohn Company, Kalamazoo, Michigan). PGB_1 was prepared by the known procedure [14].

Solvents. Reagent-grade cyclohexane, benzene, and acetone were distilled under nitrogen, thoroughly degassed, and stored over 4A Molecular Sieves under nitrogen.

Tris(triphenylphosphine)chlororhodium(I). The homogeneous hydrogenation catalyst was prepared as described by Osborn et al. [19] using triphenylphosphine freshly recrystallized from ethanol.

Diazomethane. A standard diazomethane generator was constructed from a 2 × 15-cm tube. Diazomethane was transferred from the generator to the sample in a stream of dry nitrogen. A 2-ml portion of diethyl ether was added to the generator, followed by 2-ml of diethylene glycol monobutyl ether, 250 mg of N-methyl-N-nitroso-*p*-toluenesulfonamide (Diazald), and an additional 3-ml portion of anhydrous diethyl ether. Dry nitrogen was bubbled through the generator and into the sample tube as a 1-ml portion of 60% aqueous potassium hydroxide was added to the Diazald solution.

5,6-Dideuteration of Prostaglandins

An outline of the procedure starting from biological samples is given in Fig. 2. Tetradeuterio-$PGF_{2\alpha}$ was added as an internal standard to such samples. The following method describes the dideuterio synthesis of a mixture of known prostaglandins substituted for the box in Fig. 2 called the sample. A 1-ml sample containing a known amount of prostaglandin was placed in a 1.0 × 7.5-cm culture tube followed by 1-2 ml of dry diethyl ether. Diazomethane was generated as described above and bubbled through the sample solution until a yellow coloration persisted. The sample was concentrated to a 1-ml volume in a stream of dry nitrogen, transferred to a clean 24-ml one-neck round-bottomed flask, and evaporated to dryness in a stream of dry nitrogen at 50°C; 200 ml of bis-trimethylsilyltrifluoroacetamide (BSTFA) was then added to the dry residue. The flask was stoppered and the silylation was conducted for 2 h at 25°C. The flask was fitted with a teflon gas-entry stopcock and transferred to a glove box containing an atmosphere of dry nitrogen. About 25—50 mg of tris(triphenylphosphine) chlororhodium(I) [19] was added to the flask, followed by 5 ml of a 2:3 (by volume) benzene—acetone mixture. A rubber septum was placed over the end of the gas-entry stopcock before the flask was evacuated to 180 torr using house vacuum and a syringe needle connection. Immediately following evacuation, 99.5 atom percent deuterium gas was added to the 25-ml flask from a 25-ml syringe. The reaction flask was removed from the glove box and placed on a wrist-action shaker for 20 h. The sample was evaporated

at 90°C under vacuum. The residue was taken up in dry cyclohexane and filtered through 2 mm of Florisil to remove the catalyst. The sample was evaporated to dryness in a stream of dry nitrogen and redissolved in enough cyclohexane to give 1 ml of solution for the g.c./m.s. steps.

In this exact manner, reactions 1—6 were carried out, both individually and in a mixture. With all these reactions, no starting material or side products were detected by g.c./m.s. in the resulting solutions.

Program

The program for control of the mass spectrometer and acquisition of areas under selected *m/z* peak profiles is described elsewhere [32]. Automatic shift correction and autoranging features were utilized. In the selected ion-monitoring mode for this application, the data acquisition program produces ten double precision numbers for each g.c. peak. One is the total ion current formed by adding the intensities of the nine masses monitored and is the signal that was used to define g.c. profiles for the peak-start and peak-end detection algorithm. The other nine numbers are areas under individual *m/z* profiles for the g.c. peak. An integration time of 17 ms was selected and background subtraction was employed, using the mass scan just before g.c. peak-start definition.

The nine area-under-peak results from the acquisition portion of the program were analyzed by the modified linear equation method described in this paper, using an assembly language program. This was done after acquisition of all the g.c data, which in most cases, consisted of several injections of standards and samples. The inverse matrix, A^{-1}, was computed separately and the results assembled as a part of the program. Sensitivity factors were determined at the start of a work session, assembled as a short data segment on another minicomputer, and loaded into a space reserved for them in memory. The use of specific experimental data as a part of the operating software reduces versatility, but was necessary to save the memory space normally allocated to data input and computational routines.

Instrument

A Finnigan 1015D g.c./m.s. was used with a data system constructed and programmed in-house. The data system consisted of a Texas Instruments 960A minicomputer and silent 700 terminal with cassette tape, a Tektronix 613 storage oscilloscope, a MFE x-y plotter, and a custom-designed interface allowing data acquisition and control of the mass spectrometer. All mass spectral measurements were performed under methane chemical ionization conditions. Studies with $D_2PGF_{1\alpha}$ and PGE_1 support previous findings [33] of minimal effects on spectra of variations in source pressure and electron energy. Values of 725 ± 25 μm and 140 ± 10 eV were maintained. Source temperature variations caused dramatic changes in sensitivity and the fragmentation pattern of $D_2PGF_{1\alpha}$ and is one instrument condition that must be carefully controlled. An operating value of 75°C was selected as the

lowest possible value that could be reliably maintained. This was accomplished by using the source heater to hold the temperatures with only intermittent use of the filament to avoid overheating. Higher temperature caused lower sensitivity at the higher masses.

Repeller potential, ion energy, and lens voltage settings were also found to affect the mass spectral patterns. The repeller was held at 0 V to increase ion–molecule collisions and the lens was set between −20 and −40 V to give the best high mass sensitivity possible without loss of resolution. The ion energy and the r.f. generator were tuned frequently during each work session, using FC-43 as a benchmark, so that the intensity of the *m/z* 414 peak was exactly 67% of the intensity of the *m/z* 219 peak while maintaining unit resolution between these fragments and their ^{13}C isotopes. This frequent tuning was necessary to correct for ion source and rod contamination, as well as r.f. generator or other instrument instabilities.

Gas chromatographic separation was carried out with a 1.5 m × 2 mm i.d. glass U-shaped column packed with 3% OV-101 on Chromosorb W-HP, and using methane as carrier gas. The glass column was deactivated with 5% dimethyldichlorosilane in toluene prior to packing. The column was temperature-programmed following injection from 240 to 275°C at a rate of 20°C min^{-1}. The output of the g.c. was passed to the mass spectrometer through a glass capillary and vacuum diverter supplied by the g.c./m.s. manufacturer.

RESULTS AND DISCUSSION

The matrix coefficients were determined at the beginning of the project and found to be relatively reproducible through careful control of the source conditions. The sensitivity factors, however, seem to depend on the state of cleanliness of the source and rods, plus possibly other instrument factors, and need to be determined at each work session. Thus, fragmentation patterns can be reproduced over a period of several months, but the instrument sensitivity varies daily.

An indication of the sources of error in this analysis can be seen in Table 3. Columns 1 and 2 give the composition of the standard mixture used to determine the sensitivity factors for the first work session. Column 3 gives the average area and standard deviation under each of the nine *m/z* peak profiles, listed in the same order as in Table 2. The relative standard deviations are less than 5% in all cases. This uncertainty in peak area determination is the normal mass spectrometer irreproducibility, and is due principally to variations in source conditions, minor r.f. generator drift, and detector noise. Column 4 shows the results of the multiplication of the column 3 vector by the inverse matrix A^{-1} and, therefore, consists of numbers related to concentration of the prostaglandin in column 1, but without the cross-contributions contained in the numbers in column 3. Note that the standard deviations increase only slightly after matrix multiplication. The individual experimental results that were used to produce columns 3 and 4 were normalized relative

TABLE 3

Concentration of each prostaglandin in the nine component reference mixture and the resulting sensitivity factors for first work session

(1) Prostaglandin	(2) Conc. (ng μl^{-1})	(3) Relative area m/z ± s.d	(4) Relative signal of PG ± s.d.	(5) Sensitivity factor ± r.s.d.
PGA_1	94.75	17.02 ± 0.30	11.33 ± 0.37	0.4780 ± 3.95
PGA_2	119.2	15.90 ± 0.03	13.12 ± 0.20	0.5193 ± 1.85
$PGF_{1\alpha}$	114.7	7.04 ± 0.08	6.89 ± 0.09	0.9513 ± 3.42
$PGF_{2\alpha}$	87.50	8.97 ± 0.06	6.18 ± 0.06	0.8091 ± 2.21
$D_4PGF_{2\alpha}$	112.5	7.37 ± 0.17	6.42 ± 0.18	1.000 —
PGB_1	146.2	28.04 ± 0.21	33.58 ± 0.33	0.2488 ± 2.73
PGB_2	123.0	12.22 ± 0.03	9.49 ± 0.16	0.7400 ± 1.77
PGE_1	95.25	1.87 ± 0.09	7.78 ± 0.38	0.7007 ± 7.59
PGE_2	94.50	1.52 ± 0.07	5.22 ± 0.26	1.03 ± 7.60

to the total signal of the nine readings before averaging to eliminate effects such as differing injection volume. The last column of Table 3 shows the sensitivity factors computed directly from the unnormalized data (also used to produce column 3) and the percentage standard deviations of each of these numbers. The larger uncertainty for the E prostaglandin sensitivity factors arises in part from the small g.c. peak area produced at m/z 526 and 528 for these molecules. The choice of these m/z's is the result of a less-than-satisfactory compromise, necessitated because more intense peaks in the mass spectrum of E prostaglandin occurred at m/z's where there were serious interferences from other prostaglandins. Also, the m/z's chosen to measure the PGE's are at high mass where instrument stability is poorest.

Six text solutions containing all nine prostaglandins were prepared for the first work session by dilution of a single stock solution of the eight analyte prostaglandins plus addition of a constant concentration of internal standard. They were subjected to analysis with only the concentration of internal standard supplied to the program. There are obvious systematic errors which caused mostly low results from the analyses (Table 4).

A second work session was conducted with a new set of five test solutions and a new determination of the sensitivity factors, shown in Table 5. The differences in sensitivity factors from the first work session might be due to instrument source or rod contamination or errors in actual sample concentration due to degradation or preparation errors. This time, each test solution was prepared by combination of aliquots from individual standards of each prostaglandin, a method that should aggravate the measurement errors if solution preparation is an important source of uncertainty. Errors in the stock solutions could still be a source of systematic discrepancy, however.

The high relative standard deviation of the E prostaglandin coefficients is still present in the second work session. The possibility of magnification of

TABLE 4

Results for the first work session for simultaneous determination of eight prostaglandins

Sample	1	2	3	4	5	6	Sample	1	2	3	4	5	6
PGA_1							PGB_1						
known	0.00	7.58	18.95	37.90	56.85	75.00	known	0.00	11.70	29.25	58.50	87.75	11
found	0.04	7.31	19.10	38.38	55.08	80.93	found	0.00	9.89	24.32	49.92	71.57	10
error	—	−3.6	+0.8	+1.3	−3.1	+7.9	error	—	−15.5	−16.9	−14.7	−18.4	−1
PGA_2							PGB_2						
known	0.00	9.54	23.85	47.70	71.55	95.40	known	0.00	9.84	24.60	49.20	73.80	9
found	0.02	6.70	20.44	38.01	55.08	92.85	found	0.05	8.84	21.22	43.07	62.03	8
error	—	−29.8	−14.3	−20.3	−23.0	−2.7	error	—	−10.2	−13.7	−12.5	−15.9	−1
$PGF_{1\alpha}$							PGE_1						
known	0.00	9.18	22.95	45.90	68.85	91.80	known	0.00	7.62	19.05	38.10	57.15	7
found	0.24	6.56	16.99	35.61	48.85	75.54	found	0.13	5.32	13.76	29.66	44.81	6
error	—	−28.5	−26.0	−22.4	−29.1	−17.7	error	—	−30.2	−27.8	−22.2	−21.6	−1
$PGF_{2\alpha}$							PGE_2						
known	0.00	7.00	17.50	35.00	52.50	70.00	known	0.00	7.56	18.90	37.80	56.70	7
found	0.19	8.90	19.61	40.30	50.98	72.18	found	0.32	5.32	14.86	31.02	47.53	6
error	—	+27.1	+12.1	+15.1	−2.9	+3.1	error	—	−29.6	−21.4	−17.9	−16.2	−1

TABLE 5

Sensitivity factors and results of benchmark analysis for the second work session

Prostaglandin	Known conc.	Sensitivity factor av. ± s.d.	Found conc.	R.s.d.	Error
PGA_1	37.90	0.3002 ± 0.0051	35.72	6.58	−5.8
PGA_2	63.60	0.4485 ± 0.0396	69.90	12.80	9.9
$PGF_{1\alpha}$	64.26	0.4198 ± 0.0189	67.69	2.47	5.3
$PGF_{2\alpha}$	46.67	0.4016 ± 0.0069	45.41	3.11	−2.7
PGB_1	39.00	0.1409 ± 0.0040	39.06	1.31	+0.2
PGB_2	32.80	0.2244 ± 0.0043	31.94	5.57	−2.6
PGE_1	50.80	0.6394 ± 0.1727	50.80	7.81	0
PGE_2	48.42	0.8512 ± 0.1717	51.88	10.58	+7.2

the PGE errors in the matrix calculation, due to the higher off-diagonal terms in the E columns, was considered. Calculations with synthetic data show that small errors in the matrix do get magnified, especially in the E and A prostaglandin results, but not to an extent that would account for all the variations in the E prostaglandin results.

The biggest difference during the second work session involved the care taken to achieve instrument stability and reproducibility. This time, the solution used to determine the sensitivity factors was run every 3rd or 4th injection as a benchmark to help insure that instrument drift was not interfering with the results. The mass spectrometer was retuned after each benchmark run if changes were observed. Retuning was required several times during the second work session.

The results of the second work session are shown in Table 6. Each solution was measured twice. Note that the errors this time are smaller, only occasionally over 10%, and are both positive and negative in direction. The problems in the first work session, therefore, might be due to improperly determined sensitivity factors, but are more likely the result of mass spectrometer drift. The errors are not larger for the A and E prostaglandins, as would be expected if matrix errors were an important cause of difficulty. Also, since the internal standard is an F prostaglandin, and the F results are not significantly better than the others, problems with changing sensitivity factors are not especially indicated. The internal standard could be expected to correct for such changes in the F values more than the others.

As a further check on the sources of error, the benchmark results, run nine times during the second work session, were subjected to the analytical program. The results are shown in the second part of Table 5. Note that the actual errors are within the relative standard deviations and are of the same order of magnitude as the test solutions. Since this solution, run throughout the work session, is the same one used at the beginning to determine the sensitivity factors, the errors in Table 5 are indicative of the limitations of the instrument for simultaneous determination of eight unknowns with one internal standard.

As a less stringent test, the entire approach was repeated with a sample consisting of only two F prostaglandins and the tetradeuterio-$PGF_{2\alpha}$ internal standard. The coefficient matrix and sensitivity factor determination are shown in Table 7. The results of seven test solutions are given in Table 8. Except for two determinations, the errors are less than 1%. In sample 5, the

TABLE 6

Results for the second work session for simultaneous determination of eight prostaglandins

Sample	1	2	3	4	5	Sample	1	2	3	4	5
PGA_1						PGB_1					
known	0.00	15.16	22.74	30.32	37.90	known	0.00	15.60	23.40	31.20	39.00
found	0.00	12.38	20.82	30.80	32.58	found	0.00	15.36	23.88	31.69	39.48
error	—	−18.3	−8.4	+1.6	−14.0	error	—	−1.5	+2.0	+1.6	+1.2
PGA_2						PGB_2					
known	0.00	25.44	38.16	50.88	63.60	known	0.00	13.12	19.68	26.24	32.80
found	0.08	27.68	41.42	58.44	66.53	found	0.04	12.92	17.46	23.28	32.84
error	—	+8.8	+8.5	+14.9	+4.6	error	—	−1.5	−11.3	−11.3	+0.1
$PGF_{1\alpha}$						PGE_1					
known	0.00	18.36	27.54	36.72	45.90	known	0.00	20.32	30.48	40.64	50.80
found	0.05	20.14	28.42	40.84	47.86	found	1.18	17.76	28.10	38.54	50.78
error	—	+9.7	−3.2	+11.2	+4.3	error	—	−12.6	−7.8	−5.2	−0.1
$PGF_{2\alpha}$						PGE_2					
known	0.00	18.66	28.00	37.33	46.67	known	0.00	19.37	29.05	38.73	48.42
found	0.00	17.78	28.44	40.73	44.19	found	0.40	19.66	27.81	44.52	51.04
error	—	−4.7	+1.6	+9.1	−5.3	error	—	+1.5	−4.3	+19.9	+5.4

TABLE 7

Coefficient matrix and sensitivity factors for determination of F prostaglandins

m/z	$PGF_{1\alpha}$	$PGF_{2\alpha}$ ($D_2PGF_{1\alpha}$)	$D_4PGF_{2\alpha}$ (D_6PGF_2)
407	85.17 ± 0.76	7.28 ± 0.07	0.75 ± 0.08
409	14.12 ± 0.42	91.60 ± 0.21	2.32 ± 0.03
413	0.69 ± 0.34	1.10 ± 0.14	96.92 ± 0.09
Conc. for S_j (ng μl^{-1})	76.50	58.50	76.50
S_j av. ± s.d.	1.316 ± 0.001	0.9632 ± 0.0115	1.000 (defined)

TABLE 8

Results of determination of only F prostaglandins

Sample	1	2	3	4	5	6	7
$PGF_{1\alpha}$							
Known	0.00	15.30	30.60	76.50	30.60	15.30	76.50
Found	0.00	15.24	30.16	75.78	30.56	15.27	72.65
Error (%)	—	+0.40	−1.44	−0.94	−0.13	−0.20	−5.03
$PGF_{2\alpha}$							
Known	0.00	11.70	23.40	58.50	0.00	58.50	11.70
Found	0.00	11.80	23.47	58.20	0.00	57.94	11.82
Error (%)	—	+0.85	+0.30	−0.51	—	−0.96	−0.43

program correctly interpreted the absence of $PGF_{2\alpha}$ even though there was measured ion current at the principle *m/z* monitored for that derivative.

Real urine samples were spiked with the nine prostaglandins and subjected to the new analytical scheme, but preliminary results indicated that further development will be required before the method can be applied to biological samples. A blank urine indicated the presence of a substance that co-eluted with the prostaglandins and had ions with the same *m/z* values as those chosen for PGA_2, and $PGF_{1\alpha}$. The mass spectra of these compounds showed they were not prostaglandins. The next phase of the study is to develop a sample treatment step that both concentrates the prostaglandins and removes the interfering impurities.

The application of linear simultaneous equations to complex s.i.m. data has been shown to produce reliable quantitative data on a mixture of prostaglandins that have been reduced to a single chemical species with varying degrees of isotopic substitution. It is believed that similar reliability would have been observed for the multi-component case had instrument stability been more favorable. The derivatization scheme employing complete selective deuteration of the C_5—C_6 (and C_{10}—C_{11} when present) double bonds of the

prostaglandins reduces the number of chemically distinct species for determination. The selective deuteration procedure has the ability to differentiate the isomeric PGA's and PGB's which has not been accomplished previous to the application of homogeneous deuteration. The reactions are quantitative for C_5—C_6 and C_{10}—C_{11} double bonds but totally unreactive toward the tetrasubstituted C_8—C_{12} double bond.

REFERENCES

1 K. C. Nicolaou, G. P. Gasic and W. E. Barnette, Angew. Chem. Int. Ed. Engl., 17 (1978) 293 (and references cited therein).
2 M. Hamberg and B. Samuelsson, Proc. Natl. Acad. Sci. USA, 70 (1973) 899.
3 J. Svensson, M. Hamberg and B. Samuelsson, Acta Physiol. Scand., 94 (1975) 222.
4 S. Moncada, R. Gryglewski, S. Bunting and J. R. Vane, Nature, 263 (1976) 663.
5. See, e.g., P. J. Piper and J. R. Vane, in P. Mantegazza and E. W. Horton (Eds.), Prostaglandins, Peptides, and Amines, Academic Press, London, 1969.
6 See, e.g., N. H. Andersen, J. Lipid Res., 10 (1969) 320.
7 See, e.g., F. M. Matschinsky, D. Shanahan and J. Ellerman, Anal. Biochem., 60 (1974) 188.
8 See, e.g., M. Smigel and J. Frolich, Prostaglandins, 6 (1974) 537.
9 E. Bojesen and K. Buchave, Biochem. Biophys. Acta, 280 (1972) 614.
10 See, e.g., E. Granstom, H. Kindahl and B. Samuelsson, Prostaglandins, 12 (1976) 929.
11 See, e.g., R. L. Spraggins, J. Org. Chem., 38 (1973) 3661.
12 See, e.g., K. Carr, B. J. Sweetman and J. C. Frohlich, Prostaglandins, 11 (1976) 3.
13 See, e.g., B. S. Middleditch and D. M. Desiderio, Prostaglandins, 2 (1972) 115.
14 See, e.g., B. J. Sweetman, J. C. Frohlich and J. T. Watson, Prostaglandins, 3 (1973) 75.
15 R. L. Augustine, Catalytic Hydrogenation, M. Dekker, New York, 1965.
16 G. K. Koch and J. W. Dalenberg, J. Labelled Compd., VI (1970) 395.
17 F. H. Lincoln, W. P. Schneider and J. E. Pike, J. Org. Chem., 38 (1973) 951.
18 A. H. Andrist and J. E. Graas, Prostaglandins, 18 (1979) 631.
19 J. A. Osborn, F. H. Jardine, J. F. Yound and G. Wilkinson, J. Chem. Soc. A, (1966) 1711.
20 K. E. Koenig and W. S. Knowles, 175th National Meeting of the American Chemical Society, Anaheim, California, March, 1978, Abstract No. ORGN 154.
21 A. Rosegay and D. Taub, Prostaglandins, 12 (1976) 785.
22 P. F. Crain, D. M. Desiderio, Jr. and J. A. McCloskey, in J. M. Lowenstein (Ed), Mass Spectrometry of Prostaglandins, Methods of Enzymology, Lipids, Vol. XIV, Part B, Academic, New York, 1973.
23 W. J. Richter and H. Schwartz, Angew. Chem. Int. Ed. Engl., 17 (1978) 424.
24 D. M. Desiderio and K. Hagele, J. Chem. Soc. Chem. Commun., (1971) 1074.
25 W. D. Lehmann and H. R. Schulten, Angew. Chem. Int. Ed. Engl., 17 (1978) 221.
26 B. S. Middleditch and D. M. Desiderio, J. Org. Chem., 38 (1973) 2204.
27 R. W. Kiser, Introduction to Mass Spectrometry and its Applications, Prentice-Hall, New Jersey, 1965, pp. 216—223.
28 J. H. Beynon, R. A. Saunders and A. E. Williams, The Mass Spectra of Organic Molecules, Elsevier, New York, 1968, pp. 33—36.
29 J. H. Beynon, Mass Spectrometry and its Application to Organic Chemistry, Elsevier, New York, 1960, pp. 424—432.
30 T. L. Isenhour and P. C. Jurs, Introduction to Computer Programming for Chemists, Allyn-Bacon, 1972, pp. 265—269.
31 B. J. Millard, Quantitative Mass Spectrometry, Heyden, London, 1978.
32 R. Megargle and L. Slivon, manuscript in preparation.
33 M. S. B. Munson, Anal. Chem., 43 (1971) 28A.

Analytica Chimica Acta, 120 (1980) 209—215

DETERMINATION OF SMALL AMOUNTS OF SOME SULFONAMIDE DRUGS BY RESONANCE RAMAN SPECTROMETRY

S. SATO, S. HIGUCHI and S. TANAKA*

Department of Industrial Chemistry, Faculty of Engineering, The University of Tokyo, Hongo, Bunkyo-ku, Tokyo (Japan)

(Received 21st April 1980)

SUMMARY

Resonance Raman spectrometric determinations of eight sulfonamide drugs are discussed. All the samples were colorless and exhibited no resonance Raman effect with argon ion laser excitation. After conversion to colored derivatives by diazotization and coupling reactions of the aromatic primary amine moiety, the sulfonamides could be determined from their resonance Raman spectra; the detection limits were about 2×10^{-8} M. However, the method cannot be used for identification of the individual drugs because the spectra obtained exhibited exactly the same spectral features. In order to obtain characteristic spectra, color development for the R—NH_2 molecule produced by hydrolysis of the sulfonamide with hydrochloric acid was examined. Three of the samples tested (sulfathiazole, sulfisoxazole and sulfisomezole) gave colored derivatives by a common chemical reaction system; the resonance Raman spectra then obtained exhibited characteristic spectral patterns.

Resonance Raman spectrometry has recently received considerable attention as a new analytical technique which offers both high sensitivity and the excellent selectivity inherent in vibrational spectrometry. This technique is often effective in the identification and the determination of trace amounts of compounds having closely related structures. Resonance Raman spectrometric determinations of trace amounts of some phenylamide pesticides have been reported [1]. The samples were converted to colored products by means of hydrolysis, diazotization and coupling. In this paper, an analogous approach is described for the application of resonance Raman spectrometry to sulfonamides.

The sulfonamide drugs are widely used as chemotherapeutic agents. They are all structurally similar having molecular structures of the type, $H_2N—C_6H_4—SO_2—NH—R$, where R is H, $C(NH)NH_2$ or a heterocyclic group such as pyridine, pyrimidine, isoxazole and thiazole ring. Since most of the drugs and their preparations are complex mixtures consisting of various components, specific analysis for an individual drug usually encounters difficulties. Furthermore, applications to clinical tests and estimations of purity require determinations of small amounts of the drugs in complex mixtures. Thus, analytical methods with high sensitivity as well as excellent

selectivity are desirable. At present, small amounts of sulfonamides are mainly determined by colorimetry, although h.p.l.c. assay and mass spectrometry have been recommended [2, 3]. The colorimetric methods have adequate sensitivity but lack selectivity, because the absorption bands of the colored derivatives lie in the same wavelength region [4].

In the investigation reported here, which is another attempt to widen the applicability of resonance Raman spectrometry by introducing color reactions, the principal effort was directed to development of a method which could identify as well as determine sulfonamide drugs. This aim was only partly accomplished, but it is demonstrated that resonance Raman spectrometry can be applied to the identification and determination of small amounts of some sulfonamide drugs.

EXPERIMENTAL

Instrumentation

The Raman spectra were measured with a JASCO Model J-800 Laser Raman spectrometer. A Spectra-Physics Model 164 argon ion laser was used as an excitation source. The laser was operated at 488.0 nm with 200mW of power at the samples. The detector was an HTV-R-464 photomultiplier. Depending on the noise levels of the spectra, the scans were repeated 4—16 times to improve the S/N ratios. The sample cell was rotated at 2500 rpm to avoid the influence of local heating of sample solutions and the possible decomposition of samples.

Test substances

The samples used are shown in Table 1. The identities of the samples were confirmed by referring their i.r. spectra to standard charts. The Raman spectra were all measured for aqueous solutions.

Procedures

Procedure A (for the formation of azo dyes). An aliquot (2 ml) of the aqueous 10^{-4} M solution of the sulfonamide was transferred to a 10-ml volumetric flask, and 2 ml of 2 M hydrochloric acid (to give pH 1—2) and 0.5 ml of 0.1% (w/v) sodium nitrite solution were added. After 3 min, 0.5 ml of a 0.5% (w/v) solution of ammonium sulfamate was added, followed after 2 min by 0.5 ml of a 0.1% (w/v) solution of N-(1-naphthyl)ethylenediamine solution. After 2 min, the mixture was diluted to 10 ml for measurement.

Procedure B (for hydrolysis). The sample was hydrolyzed with 6 M hydrochloric acid by refluxing for 3.5 h. After cooling, the solution was made alkaline with 30% sodium hydroxide solution, and extracted with four 25-ml portions of chloroform. The residue (*p*-aminobenzenesulfonic acid, etc.) was discarded, and the extract was evaporated to give the $R—NH_2$ compound. For the method of color development, see Results and Discussion.

TABLE 1

The sulfonamides used in the present investigation: 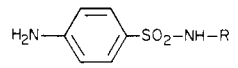

R	Name	Yield of R–NH_2 on hydrolysis (%)	R	Name	Yield of R–NH_2 on hydrolysis (%)
H	Sulfanilamide	–		Sulfathiazole	64.6[a]
	Sulfaguanidine	–	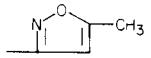	Sulfisomezole	76.2[a]
	Sulfapyridine	92.4[a]	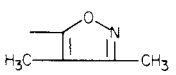	Sulfisoxazole	48.1[b]
	Sulfadiadine	–	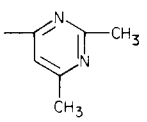	Sulfisomidine	–

[a]As described in Procedure B. [b]8 M HCl for 10 min.

RESULTS AND DISCUSSION

Raman spectra of sulfonamide drugs

The usual Raman spectra of the sulfonamide drugs were first measured. Some of the results are shown in Fig. 1; strong bands appear in the 1200—1000 cm^{-1}, 850—800 cm^{-1} and 700—550 cm^{-1} regions. These Raman spectra confirm that the characteristic spectral patterns obtained for each of the drugs are adequate for identification purposes, i.e., the difference of the R structure in $H_2N—C_6H_4—SO_2—NH—R$ is reflected well in the usual Raman spectra. This must be contrasted with the case of the resonance Raman spectra described below. Be that as it may, applications of the usual Raman spectrometry are limited to cases where the concentrations are higher than about 10^{-2} M.

Resonance Raman spectra of the products obtained by color reaction of the aromatic primary amine moiety

A basic investigation of the resonance Raman spectrometry of the sulfonamides was carried out. As all the samples under test were colorless, colored derivatives were required in order to obtain resonance Raman spectra. Accordingly, as a first step, the simplest available reaction was utilized: azo dyes were prepared by diazotization and coupling reactions of the primary amine moiety of the sulfonamides. The detailed operations of the reactions were based on the method of Bratton and Marshall [4]; the procedure is

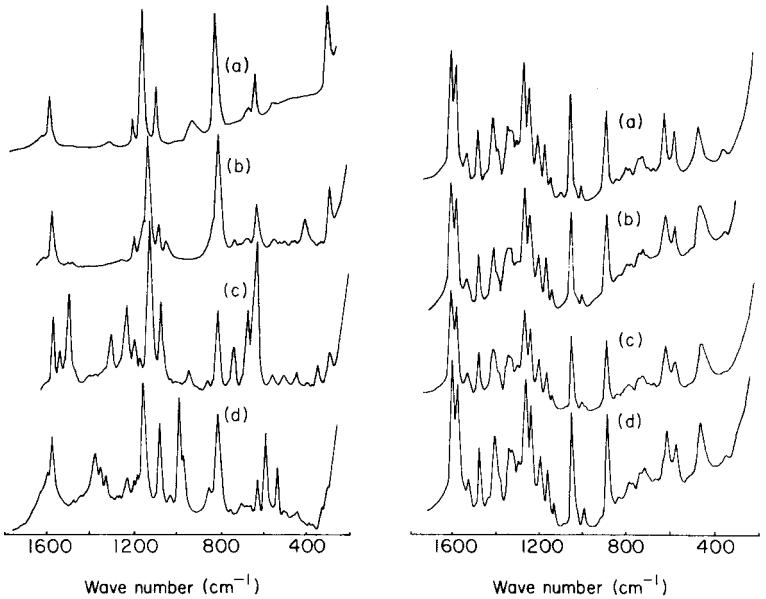

Fig. 1. The Raman spectra for about 0.1 M aqueous solutions of some sulfonamides: (a) sulfanilamide; (b) sulfaguanidine; (c) sulfathiazole; (d) sulfisomezole.

Fig. 2. The resonance Raman spectra of the azo compounds obtained by Procedure A from (a) sulfanilamide; (b) sulfathiazole; (c) sulfapyridine; (d) sulfaguanidine. Sulfonamide concentration, 2×10^{-5} M.

given in the Experimental section. The resonance Raman spectra obtained for the colored products thus prepared are shown in Fig. 2. In principle, resonance Raman spectrometry has the excellent selectivity inherent in vibrational spectrometry although this characteristic is often not attainable in the case of conventional spectrophotometry. However, in this particular case, the spectra of the colored derivatives exhibit exactly the same Raman spectral patterns (Fig. 2) so that the method is not suitable for the selective determination of individual sulfonamides although it is useful for the identification and determination of trace components in a given sample as a group of sulfonamides. Comparison of Figs. 1 and 2 emphasizes that the characteristic bands corresponding to each of the drugs did not appear in the resonance Raman spectra of the colored derivatives obtained by the reaction in alkaline solution with N-(1-naphthyl)ethylenediamine as coupling reagent.

The following interpretation of these results is speculative. If the colored products obtained are described by R″—N=N—C_6H_4—SO_2NH—R (where R″ represents the N-(1-naphthyl)ethylenediamine substituent), it can be assumed that the electron transfer sequence between the R—NH— group and the part of the molecule containing the azo group, which is responsible for the absorption band in the visible region considered here, is disrupted by the intervening SO_2 group. Therefore, the R—NH— group plays little part in the

color development, and so the vibrations in the R—NH— group are not under the influence of the resonance Raman effect. Since the R″—N=N—C_6H_4— structure is exactly the same for all the samples, it follows that identical spectral features are observed in the resonance Raman spectra for the different samples. This experimental fact seems worthwhile reporting as an example of the peculiar phenomena that may be encountered in resonance Raman spectrometry.

As for the sensitivity attainable by using such resonance Raman spectra, it was established that the detection limit for the sulfonamides tested is about 2×10^{-8} M; the sensitivity of this method is therefore about an order of magnitude higher than that of standard colorimetry. This result agrees with the conclusion for other samples reported previously [1].

Resonance Raman spectra for the colored derivatives of R—NH_2 produced by hydrolysis

In an attempt to obtain characteristic spectra for each of the drugs tested, color development of the R—NH_2 molecules produced by hydrolysis of sulfonamides was examined, the resonance Raman spectra being measured for the colored derivatives obtained. The hydrolysis of sulfonamides is generally regarded as more difficult than that of alkyl or allyl amides. In the procedure adopted (see Procedure B in the Experimental section), the samples were hydrolyzed by refluxing for 3.5 h with 6 M hydrochloric acid. After extraction with chloroform and evaporation of the extract, the identities of the R—NH_2 compounds produced were confirmed by comparing their i.r. spectra with standard charts. The R—NH_2 compounds corresponding to each of the drugs were obtained without contamination from by-products such as *p*-aminosulfonic acids or unhydrolyzed sulfonamides. The yields of the R—NH_2 compounds are listed in Table 1. However, some of the sulfonamides with a heterocyclic group of the pyrimidine type were still difficult to hydrolyze.

After the hydrolyzates for each sample had been obtained, the best method for color development was examined. Several color-forming reagents were tested: 2-thiobarbituric acid [5], nitrosylsulfuric acid [6], β-naphthoquinone sulfonic acid [7]; the methods of El-Dib and Aly [8] and Bratton and Marshall [4] were also used. However, for the samples concerned, these methods were found to be effective, at best, for only one of the derived amines treated, except for the method of Bratton and Marshall [4]. Application of the Bratton—Marshall method to three samples (i.e., 2-aminothiazole from sulfathiazole, 3,4-dimethyl-5-aminoisoxazole from sulfisoxazole and 5-methyl-3-aminoisoxazole from sulfisomezole) gave conversion to useful stable colored products. At present, however, there seems to be no procedure of color development that is applicable to all the derived R—NH_2 compounds, and further studies are necessary.

Figure 3 shows the resonance Raman spectra of the colored products corresponding to the above-mentioned three sulfonamide drugs.

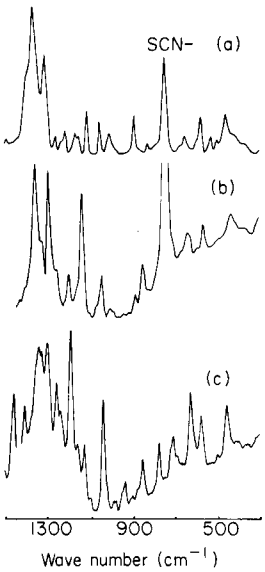

Fig. 3. The resonance Raman spectra of azo compounds obtained by Procedures B and A from (a) sulfisomezole (2×10^{-5} M); (b) sulfathiazole (2×10^{-4} M); (c) sulfisoxazole (1×10^{-4} M).

As is well known, the appearance of fluorescence background interferes badly with measurements of Raman spectra. In the present case, the solutions of the colored products exhibited a strong background of this type when exposed to the laser beam irradiation, and reduction of this background was essential for obtaining clear spectra. After various tests, it was found that the addition of sodium thiocyanate as a quencher was effective. Thus, the spectra shown in Fig. 3 were obtained for solutions containing 2—3% (w/v) of sodium thiocyanate. As can be seen from Fig. 3, the resonance Raman spectra obtained are sufficiently characteristic for each of the samples, and exhibit specific bands which reflect the difference in the structures of the R group in the sulfonamide drugs. Accordingly, these spectra can be applied to the selective determination of small amounts of the drugs, though the applicability of the present method is limited to a small number of samples.

CONCLUSION

This approach to the application of resonance Raman spectrometry to the determination of colorless samples, such as sulfonamide drugs, by using color reactions made some important aspects of the method clear. First, it was proved that in resonance Raman spectrometry there is a peculiar case in which the selectivity is completely lost; this is rarely encountered in vibrational spectrometry. Second, there is a limit of the applicability for methods in which samples are transformed to colored products by chemical deriva-

tization reactions, though there is room for further studies concerning the present samples. It should be noted that this problem of applicability is related primarily to colorimetric procedures. Finally, it can be concluded that, despite these problems, resonance Raman spectrometry has the latent possibility of becoming a powerful technique for the microanalysis of sulfonamide drugs, which has both high sensitivity and excellent selectivity.

REFERENCES

1 S. Higuchi, O. Aiko and S. Tanaka, Anal. Chim. Acta, 116 (1980) 1.
2 S. C. Su, A. V. Hartkopf and B. L. Karger, J. Chromatogr., 119 (1976) 523.
3 R. Davis, D. T. Hurst and A. R. Taylor, J. Appl. Chem. Biotechnol., 27 (1977) 543.
4 A. C. Bratton and E. K. Marshall, Jr., J. Biol. Chem., 128 (1939) 537.
5 R. G. Shepherd, Anal. Chem., 20 (1948) 1150.
6 J. G. Fisher, in H. F. Mark (Ed.), Kirk—Othmer Encyclopedia of Chemical Technology, Vol. 20, Interscience, U.S.A., 1969, p. 193.
7 F. Feigl, Spot Tests in Organic Analysis, Elsevier, Amsterdam, 1965, p. 314.
8 M. A. El-Dib and O. A. Aly, J. Ass. Off. Anal. Chem., 55 (1972) 1276.

Analytica Chimica Acta, 120 (1980) 217—226

INFLUENCE OF MATRIX ON RELATIVE SENSITIVITY FACTORS IN SPARK-SOURCE MASS SPECTROMETRIC ANALYSIS

MINAO ITO*, SHOKI SATO and KAZUO YANAGIHARA

Central Research Laboratory, Daido Steel Co. Ltd., 2-30 Daido-Cho, Minami-Ku, Nagoya (Japan)

(Received 17th June 1980)

SUMMARY

In spark-source mass spectrometric analysis, relative sensitivity factors are commonly used for sensitivity correction. The influence of matrix elements (aluminum, iron, copper and molybdenum) on such factors was studied under similar experimental conditions. The factor relative to iron, which is contained in the above four metals, varied with the matrix, but an equation based on the independent correlation of matrix and measured element with a physical property of these elements, was satisfactory. Melting point gave a better multiple correlation than boiling point or heat of sublimation. From this equation under given experimental conditions, it should be possible to calculate relative sensitivity factors in the absence of reference materials.

The sensitivity of spark-source mass spectrometric analysis for various trace elements differs remarkably. In order to correct such different sensitivities, it is common to use a relative sensitivity factor (r.s.f.) which is a sensitivity ratio for a measured element and a matrix or other element. These factors have been obtained experimentally by measuring standard samples. However, investigations have been carried out to estimate them from physical properties, because it is very difficult to obtain a comprehensive list of these factors experimentally. Relations between experimental factors and physical properties such as melting point [1], boiling point [2, 3], heat of sublimation [4—8], ionization potential [4—6], covalent radius [5, 8], ionization cross-section [6, 7], and temperature for constant vapor pressure [9] have been studied and effective estimation equations have been obtained. However, many of those reports deal with studies of such factors in a single matrix and there are few reports which deal with the influence of matrices on those factors. These studies show that the factors can be expressed as ratios of the physical properties of a measured element and those of an internal standard element.

In contrast, there are many reports which deal with the influence of experimental conditions on an r.s.f. The factors have been shown to be influenced by the shape of the sample electrodes [10], spark-gap width [11], spark voltage, repetition frequency and accelerating voltage [12], tempera-

ture of the sample electrode [13], etc. Magee and Harrison [11] demonstrated that spark-gap width influences the sensitivity for major component elements. Van Hoye et al. [13] reported that the sensitivity for elements having a low melting or boiling point varies greatly with sparking conditions. In a previous report [1], it was shown that the content of metals such as chromium, manganese and cobalt has less influence on the r.s.f. than the content of nickel or silicon.

The above considerations lead to the conclusions that it is inadequate to express the r.s.f. only as a ratio of a physical property of a measured element to that of an internal standard element, and that the equation for calculating the r.s.f. should contain a factor determined by the measurement conditions [13]. Moreover, the influence of the physical properties of matrix elements on the r.s.f. will differ from that of the measured element.

In the work described here, various elements in steel, copper, aluminum and molybdenum samples were studied under constant conditions of measurement by means of peak-switching electrical detection and sensitivity ratios with respect to matrix elements were determined in order to clarify the influence of matrices. As similar measuring conditions as possible were chosen for the four metals. Other conditions which cannot be the same were also examined so that their influence on the r.s.f. could be minimized. Finally, the relation between an r.s.f. and the physical properties of measured and matrix elements was studied.

EXPERIMENTAL

Apparatus

A JEOL JMS-OIBM mass spectrometer with electrical detection equipment was used. The electrical detection system was operated by magnetic peak-switching with a Hall probe magnetic monitor; this operation allowed coverage of the entire mass range at a constant accelerating voltage. The spark-gap width was kept constant with an automatic spark-gap controller which operates via the spark breakdown voltage.

Sample preparation

AA1-5, AB1-4 and AC4 (Johnson Matthey Chemicals) were used as standard aluminum samples and CC1, 3 and 4, CB0, 2 and 4—8 and CA5 (Johnson Matthey Chemicals) were used as standard copper samples. NBS 461–468, NBS 442—444 and Daido Steel standards were used as standard steel samples. Daido Steel standards were used as standard molybdenum samples. The composition ranges of these standards are shown in Table 1.

The samples were machined into two cylindrical electrodes, 15–20 mm long with a diameter of 3 mm. These electrodes were etched with dilute hydrochloric acid, rinsed in distilled water and cleaned in high-purity ethanol with the aid of an ultrasonic cleaner. After drying, the electrodes were

TABLE 1

Composition of the standard samples (wt. %)

Element	Steel	Aluminum	Copper	Molybdenum
Be			0.003—0.03	
C	0.04—0.5			
Mg		1.9		
Al				0.0002—0.0003
Si	0.03—0.5	0.06—0.7	0.0002—0.05	0.003—0.009
Ca	0.001—0.002		0.0002—0.0004	
Ti	0.004—0.3	0.002—0.1		
V	0.002—0.3			
Cr	0.002—20	0.4		
Mn	0.03—5	0.002—2	0.0001—0.05	
Fe		0.06—0.8	0.0002—0.06	0.0005—0.006
Co	0.008—1		0.0001—0.05	
Ni	0.003—10	0.003—0.08	0.0001—0.05	0.0001—0.007
Cu	0.02—0.5			
Ge	0.001—0.004			
As	0.008—0.1		0.002—0.02	
Se	0.03—0.2		0.002—0.02	
Zr	0.004—0.2		0.003—0.02	0.002—0.01
Nb	0.001—0.3			0.002—0.1
Mo	0.005—0.3			
Ag	0.002—0.004		0.0003—0.003	
Sb	0.04—0.2		0.003	
Te	0.02—0.06		0.003—0.02	
Ta	0.002—0.4			0.004—0.06
W	0.01—0.2			0.01—0.4
Pb	0.0006—0.04			
Bi	0.01—0.03			

mounted on the electrode holders in the source chamber, and pre-sparked for an appropriate time.

Procedure

Experimental parameters of the four kinds of metal are shown in Table 2. For the purpose of clarifying relations between a matrix and an r.s.f., it is necessary that experimental parameters are similar for different matrices. However, when different parameters had to be used, the influence of those parameters on the r.s.f. was examined, and then those parameters were changed so little that their influence on the r.s.f. could be neglected.

Matrix elements were chosen as the internal standard elements because, in routine analysis, it is inconvenient to choose a common element as the internal standard element. And, as described by Kai and Miki [4], the standard deviations of measurement are less when a matrix element is chosen as the internal standard.

TABLE 2

Experimental parameters used for the metal samples

Experimental parameter	Fe	Al	Cu	Mo
Spark breakdown voltage (kV)	56	40	48	56
Repetition frequency (Hz)	1000	300	1000	1000
Pulse length (μs)	40	40	40	40
Spark gap (μm)	35	40	35	20

RESULTS AND DISCUSSION

Effects of experimental parameters on r.s.f. values

The spark gap is one of the factors which influences the r.s.f., and so the gap should be kept constant. However, the relation between spark gap and spark breakdown voltage is different for different matrices, as shown in Fig. 1, and good precision requires stable sparks, which are attainable at different ranges for each matrix. For this reason, the relation between spark gap and r.s.f. was examined for each matrix, using spark gaps in the stable spark range. Figures 2—5 show these relations for each matrix. The spark gaps in Table 2 were chosen to be as similar as possible within the spark-gap ranges which do not influence the r.s.f. greatly.

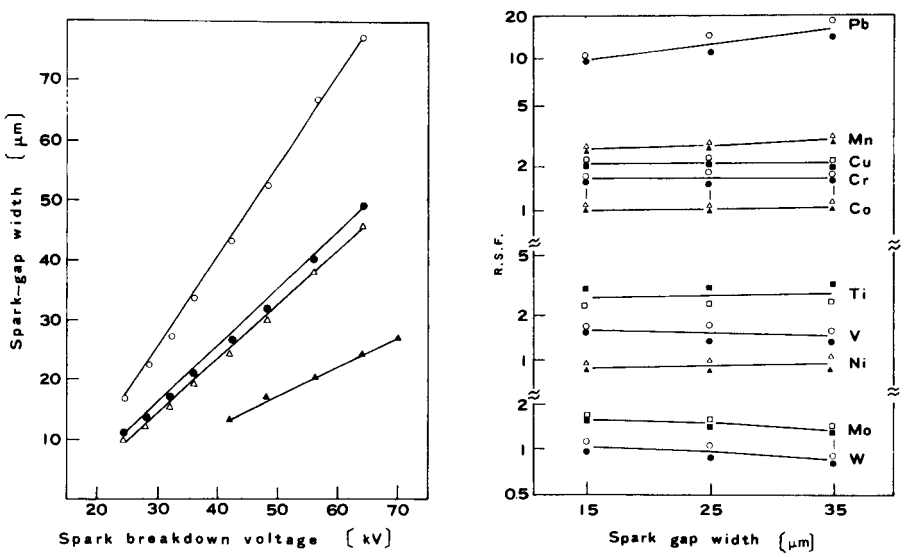

Fig. 1. Correlation between spark breakdown voltage and spark-gap width in different matrices: (○) Al; (●) Cu; (△) Fe; (▲) Mo.

Fig. 2. Effect of spark-gap width on r.s.f. for steel: open symbols, NBS 462; closed symbols, NBS 443.

The repetition frequency influences the temperature of the sample electrodes and thus influences the r.s.f. values. For steel, copper and molybdenum, 1000 Hz was employed (Table 2), but this frequency rapidly consumes an aluminum sample. Figure 6 shows the influence of repetition frequency on intensities in an aluminum matrix sample; 300 Hz was chosen as a suitable frequency.

Raising the ion multi-voltage increases the amplification. However, there is a possibility of counting loss at high incidence rates. The influence of ion multi-voltage on the counting loss for each matrix was therefore examined. For example, there are four isotopes ^{54}Fe, ^{56}Fe, ^{57}Fe and ^{58}Fe in iron, of abundance 5.8, 92, 2.2 and 0.33%, respectively. Spectra were measured at different ion multi-voltages. Figure 7 shows the relation between ion multi-voltage and the intensities of each iron isotope corrected for isotopic abundance; it is clear that the counting loss becomes larger above 0.8 kV for ^{56}Fe than for ^{58}Fe which is least abundant, but for ^{57}Fe, which is usually used as an internal standard, the counting loss does not increase at voltages below 1.0 kV. As a result of other similar investigations, it was clarified that counting losses are negligible for measurement at ion multi-voltages of 0.9, 0.8 and 1.0 kV for ^{65}Cu, ^{27}Al and ^{97}Mo, respectively.

Relative sensitivity factors obtained

Forty-six samples of the four kinds of metals were each measured twice; r.s.f. values were calculated with reference to matrix elements as internal standards and were averaged for each element measured in each metal.

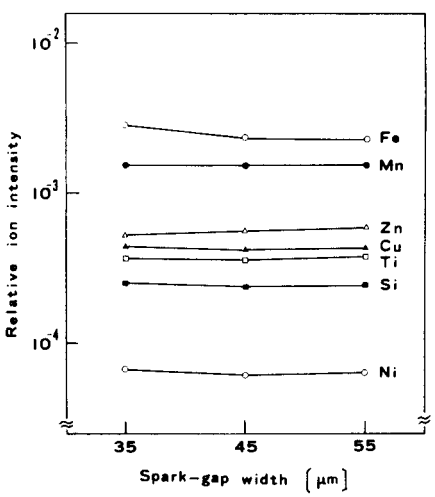

Fig. 3. Effect of spark-gap width on relative ion intensity for an aluminum sample (Johnson Matthey AA5).

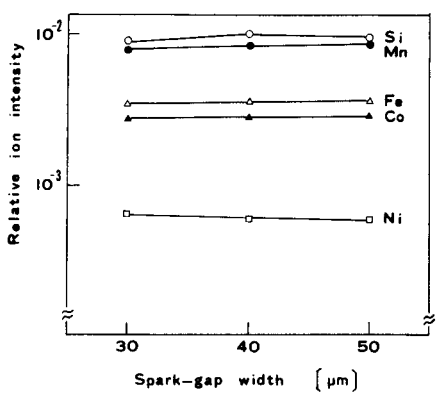

Fig. 4. Effect of spark-gap width on relative ion intensity for a copper sample (Johnson Matthey CB0).

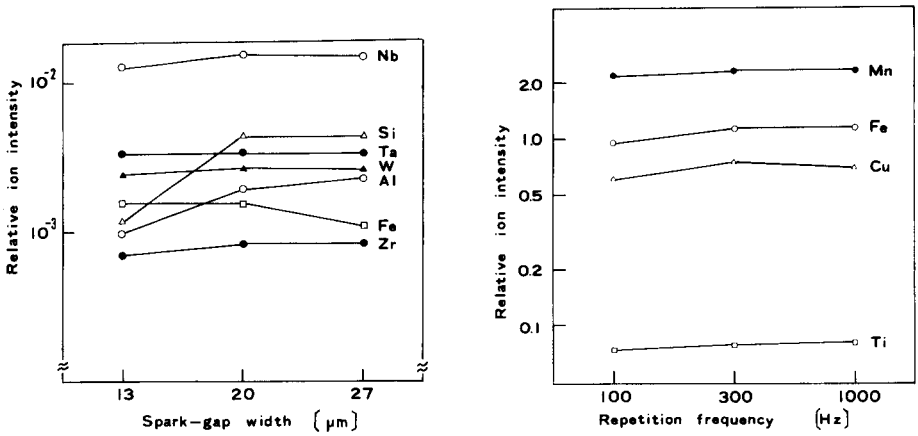

Fig. 5. Effect of spark-gap width on relative ion intensity for a molybdenum sample (Daido Steel standard).

Fig. 6. Effect of repetition frequency on relative ion intensity for an aluminum sample (Johnson Matthey AA2).

These values are shown in Table 3. In this table, it is to be expected that the r.s.f. values for different matrices differ because the matrix element is taken as the internal standard. To put these values on the same basis, iron, which is found in all the matrices, was taken as an internal standard, and the r.s.f. values for elements which were measured in at least two matrices were

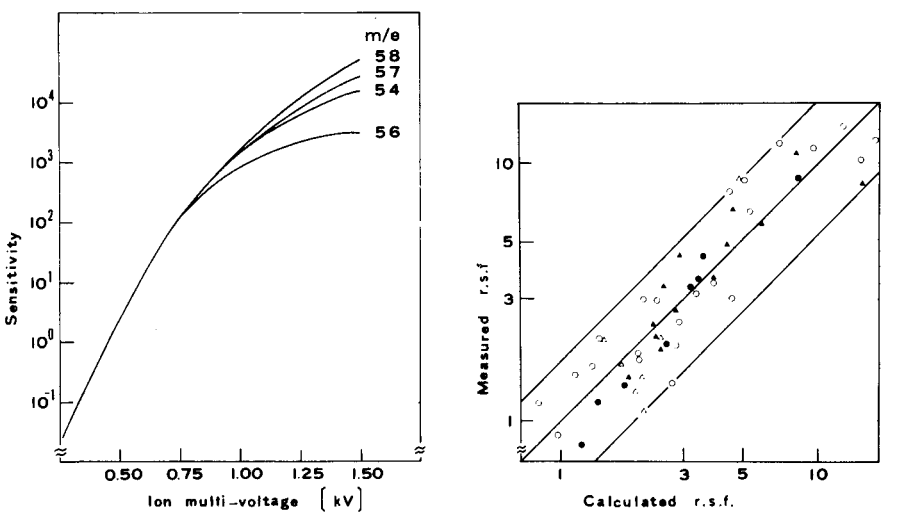

Fig. 7. Correlation between ion multi-voltage and sensitivity (intensity corrected for isotopic abundance) for iron.

Fig. 8. Correlation between measured and calculated r.s.f. values using the multiple regression formula $\log(\text{r.s.f.}) = 3.481 - 1.411 \log Mp_1 + 0.471 \log Mp_2$.

TABLE 3

Experimental r.s.f. values for steels, aluminum, copper and molybdenum (matrix element = 1.0)

Element	Steel	Al	Cu	Mo	Element	Steel	Al	Cu	Mo
Be			2.7		Ge	3.0			
C	1.2				As	6.4		6.6	
Mg		8.7			Se	12.3		8.3	
Al		1.0		8.8	Zr	3.0		1.5	2.0
Si	2.4	1.5	3.4	4.4	Nb	2.2			1.4
Ca	8.6		4.9		Mo	1.7			1.0
Ti	3.0	1.7			Ag	7.8		3.6	
V	1.9				Sb	12.0		5.8	
Cr	1.8	2.1			Te	11.4		11.0	
Mn	3.2	2.1	4.5		Ta	1.6			1.2
Fe	1.0	1.3	2.4	3.3	W	0.9			0.8
Co	1.4		2.1		Pb	13.9			
Ni	2.0	1.1	1.9	3.6	Bi	10.2			
Cu	3.5		1.0						

recalculated. Table 4 shows the values obtained. It can be seen that these r.s.f. values are larger in a steel matrix than in the other matrices. Moreover, the values for a particular element in the other matrices agree fairly well, except for aluminum. It should also be noted that the r.s.f. of a matrix element in its own matrix is smaller than that in the other matrices, i.e. an r.s.f. is larger if the internal standard is a matrix element. Thus the influence of the matrix elements on an r.s.f. is different from that of other elements. Therefore, the relationships between r.s.f. values based on matrix elements and the physical properties of the measured elements were studied for each matrix. It was recognized earlier for steel samples [1] that melting point and heat of sublimation correlated well with r.s.f. values, and that heating and vaporizing processes greatly influenced these values. In the present

TABLE 4

Experimental r.s.f. values for steels, aluminum, copper and molybdenum (iron = 1.0)

Element	Steel	Al	Cu	Mo	Element	Steel	Al	Cu	Mo
Al		0.77		2.7	Se	12.3		3.5	
Si	2.4	1.2	1.4	1.3	Zr	3.0		0.63	0.61
Ca	8.6		2.0		Nb	2.2			0.42
Ti	3.0	1.3			Mo	1.7			0.30
Cr	1.8	1.6			Ag	7.8		1.5	
Mn	3.2	1.6	1.9		Sb	12.0		2.4	
Co	1.4		0.88		Te	11.4		4.6	
Ni	2.0	0.85	0.79	1.1	Ta	1.6			0.36
Cu	3.5		0.42		W	0.9			0.25
As	6.4		2.7						

investigation, therefore, relations with melting and boiling points and heat of sublimation were studied. The suggested correlation between the r.s.f. and a particular physical property of the measured element (X_i) was r.s.f. = $a'X_i^b$, i.e. log (r.s.f.) = a + $b$log X_i, where a, a' and b are constants. In each matrix, correlation coefficients and regression formulae were obtained by using the logarithmic equation. These are shown in Table 5, which indicates that melting point has a better correlation that the other properties, except for aluminum. The r.s.f. values estimated from the regression formulae using melting points for aluminum, copper, iron and molybdenum are 6.44, 3.49, 2.81 and 1.36, respectively. These relatively large values coincide with the low sensitivity of matrix elements in these matrices. This also agrees with the findings of Van Hoye et al. [14] for an iron matrix.

The slopes of the melting point regression equations for the four matrices in Table 5 are somewhat similar. This suggests that the influence of different matrices could be included in constant a in the above equation, rather than in b. Thus, by separating the effect of the matrix property (X_m) the general equation becomes

$$\log(\text{r.s.f.}) = a'' + b \log X_i + c \log X_m \quad (1)$$

where a'', b and c are constants. Multiple regression formulae and correlation coefficients between all the values in Table 3 and melting and boiling points and heat of sublimation were calculated according to this equation, as before. These are shown in Table 6. The correlation between r.s.f. and melting point was again best, with the correlation coefficient almost equal to those for individual matrices. The r.s.f. values estimated by the multiple

TABLE 5

Regression formulae and correlation coefficients for each matrix

Matrix	Regression formula[a]	Correlation coeff.
Fe	log(r.s.f.) = 4.713 − 1.309log *Mp*	0.921
Al	log(r.s.f.) = 6.925 − 2.060log *Mp*	0.830
Cu	log(r.s.f.) = 4.554 − 1.280log *Mp*	0.894
Mo	log(r.s.f.) = 6.234 − 1.763log *Mp*	0.986
Fe	log(r.s.f.) = 5.226 − 1.370log *Bp*	0.815
Al	log(r.s.f.) = 6.838 − 1.901log *Bp*	0.925
Cu	log(r.s.f.) = 4.082 − 1.044log *Bp*	0.854
Mo	log(r.s.f.) = 9.784 − 2.609log *Bp*	0.953
Fe	log(r.s.f.) = 3.629 − 1.569log ΔHs	0.892
Al	log(r.s.f.) = 3.242 − 1.529log ΔHs	0.934
Cu	log(r.s.f.) = 3.276 − 1.433log ΔHs	0.855
Mo	log(r.s.f.) = 5.068 − 2.214log ΔHs	0.980

[a] *Mp*: Melting point (K); *Bp*: boiling point (K); ΔHs: heat of sublimation (kcal mol^{-1}).

TABLE 6

Multiple regression formulae and correlation coefficients for the four matrices

Multiple regression formula[a]	Multiple correlation coeff.
$\log(\text{r.s.f.}) = 3.481 - 1.411\log Mp_1 + 0.471\log Mp_2$	0.914
$\log(\text{r.s.f.}) = 2.458 - 1.404\log Bp_1 + 0.819\log Bp_2$	0.817
$\log(\text{r.s.f.}) = 1.848 - 1.633\log \Delta Hs_1 + 0.928\log \Delta Hs_2$	0.880

[a]Subscript 1 indicates the measured element and 2 the matrix element.

regression melting point formula corresponded fairly well to the measured values, as shown in Fig. 8, the coefficient of variation being 33%.

Although the contributions of matrix elements and measured elements to the r.s.f. have been differentiated, it is unnecessary to consider counting losses because the ion multi-voltage was adjusted to a value where counting losses were negligible. Also, the influence of concentration on the r.s.f. has often been described. In the present investigation, however, such an effect was observed only when the concentration range was wide, as for nickel in steels. If the concentration influences the r.s.f., the contribution of matrix elements will differ from that of measured elements, whose concentration is usually very small. In this study, melting point generally correlated better with the r.s.f. than other physical properties, which suggests that fractional melting is one of the factors governing the r.s.f. and causes the difference between b and c of eqn. (1). However, this discussion is based on the results from only one measurement condition and therefore, the contribution of matrix elements and measured element should be investigated further, under different conditions. It is expected, however, that r.s.f. values of unknown matrices under given measurement conditions may be estimated if each constant in eqn. (1) is obtained for such measurement conditions.

CONCLUSIONS

Relative sensitivity factors in spark-source mass spectrometric analysis of various metals are influenced by the kind of matrix. Factors for aluminum, steel, copper and molybdenum matrices were measured under similar experimental conditions. The relation between r.s.f. values and physical properties of matrix and measured elements, shows that r.s.f. values related to matrix elements have irregular values if a definite element is chosen as an internal standard for various matrices. For the estimation of an r.s.f., therefore, an equation is obtained in which the physical properties of the measured element and matrix element are independent parameters, and thus the factor is not influenced by the nature of the matrix.

REFERENCES

1 M. Ito and K. Yanagihara, Bunseki Kagaku, 22 (1973) 10.
2 N. W. H. Addink, Fresenius Z. Anal. Chem., 206 (1964) 81.
3 N. W. H. Addink, in R. I. Reed (Ed.), Mass Spectrometry, Academic Press, New York, 1965, p. 223.
4 J. Kai and M. Miki, Mass Spectrom. (Tokyo), 12 (1964) 81.
5 B. B. Goshgarian and A. V. Jensen, 12th Annual Conf. on Mass Spectrometry and Allied Topics, Montreal, 1964.
6 G. Vidal, P. Galmard and P. Lanusse, Methodes Phys. Anal. GAMS, 4 (1968) 404.
7 R. E. Honig, Advances in Mass Spectrometry, Vol. 3, Institute of Petroleum, London, 1966, p. 101.
8 M. Ménétrier, Methodes Phys. Anal. GAMS, 4 (1968) 153.
9 J. M. McCrea, 15th Annual Conf. on Mass Spectrometry and Allied Topics, Pittsburgh, PA, 1968.
10 J. Franzen and K. D. Schuy, Advances in Mass Spectrometry, Vol. 4, Institute of Petroleum, London, 1968, p. 449.
11 C. W. Magee and W. W. Harrison, Anal. Chem., 45 (1973) 852.
12 N. Yamaguchi, R. Suzuki and O. Kammori, Bunseki Kagaku, 18 (1969) 3.
13 E. Van Hoye, F. Adams and R. Gijbels, Int. J. Mass Spectrom. Ion Phys., 30 (1979) 75.
14 E. Van Hoye, F. Adams and R. Gijbels, Talanta, 26 (1979) 285.

Analytica Chimica Acta, 120 (1980) 227—236

EFFETS DE SURFACE DANS LE DOSAGE PAR ACTIVATION NEUTRONIQUE DU SOUFRE

R. DELMAS* et M. FEDOROFF

Centre d'Etudes de Chimie Métallurgique du C.N.R.S. 15, Rue Georges Urbain, 94400 Vitry-sur-Seine (France)

G. REVEL

Laboratoire Pierre Süe, C.E.N. Saclay, B.P. n° 2, 91190 Gif-sur-Yvette (France)

(Reçu le 17 avril 1980)

SUMMARY

Surface effects in the determination of sulfur by neutron activation analysis

Thermal neutron activation analysis leads to overestimated sulfur contents in some metals. This phenomenon was studied for samples of iron. It is attributed to ineffective chemical etching arising from dissolution of the metal through a surface layer which retains impurities, especially sulfur-35. Significant amounts of this isotope are produced at the surface through the $^{35}Cl(n, \gamma)^{35}S$ reaction. Experimental modifications which lead to the correct sulfur concentration are proposed.

RESUME

L'utilisation de l'activation neutronique pour doser le soufre selon la réaction $^{34}S(n, \gamma)^{35}S$ conduit à en surestimer la teneur dans certains métaux. Nous avons étudié ce phénomène sur des échantillons de fer. Après avoir exclu plusieurs hypothèses nous avons établi que le décapage du fer par certains milieux s'effectue par passage du métal à travers une couche superficielle qui retient des impuretés de surface dont le soufre-35. Cet isotope est produit en quantité très importante à partir du chlore présent à la surface selon la réaction $^{35}Cl(n, \gamma)^{35}S$. Nous proposons des modes opératoires qui permettent de s'affranchir de ce phénomène et d'obtenir la teneur exacte du soufre dans le fer.

Un avantage essentiel de l'analyse par activation, est que la teneur au voisinage de la surface et la teneur en volume de l'élément dosé peuvent être aisément discriminées par un décapage après irradiation. Ceci permet de s'affranchir d'une cause d'erreur difficile à éliminer dans les autres méthodes analytiques. Cependant dans quelques rares cas il a été signalé que cette cause d'erreur subsiste. Des travaux antérieurs [1—3] ont montré que la teneur en soufre de certains métaux (Fe, Ni, Cu, Mo), déterminée par activation dans les neutrons thermiques en utilisant la réaction $^{34}S(n, \gamma)^{35}S$, était surestimée d'un ordre de grandeur après un décapage chimique de plusieurs centaines de micromètres. Le phénomène n'a pas été constaté avec des échantillons d'aluminium et de magnésium.

Les auteurs avançaient l'hypothèse d'une diffusion de ^{35}S créé en surface par la réaction $^{35}Cl(n, p)^{35}S$. La pollution naturelle des surfaces en chlore (environ 1 $\mu g\ cm^{-2}$ sur le fer) et le fait que, dans nos conditions d'irradiation, à masses égales, le chlore produit 30 à 40 fois plus de ^{35}S que le soufre, font que la quantité de ^{35}S créée à la surface des échantillons est particulièrement importante.

D'autres travaux [4] ont mis en évidence une pénétration profonde de l'oxygène dans le fer et le niobium (non observée dans Ni, Pt, Mo), immergés dans l'eau et soumis à une irradiation neutronique. Qualitativement le phénomène est analogue à celui observé avec le soufre, mais il est établi par une méthode différente: dosage par réaction nucléaire directe et abrasion ionique des couches successives.

Nous avons choisi d'étudier le système ^{35}S—Fe car les phénomènes y ont une grande ampleur. Notre travail vise à en donner une explication et à proposer une méthode qui conduise à un dosage exact de la teneur intrinsèque des échantillons. Dans un précédent article [5], nous avons décrit nos premiers travaux à ce sujet. Après avoir mis au point une méthode sélective et rapide de séparation de ^{35}S radiochimiquement pur, nous avons pu déterminer sa répartition dans des tranches décapées successivement dans le métal irradié.

Deux résultats importants avaient été obtenus: (1) le soufre radioactif provient bien du chlore de surface; (2) les histogrammes observés sont incompatibles avec une diffusion thermique accélérée par les joints de grains et les défauts créés par l'irradiation neutronique [6].

Dans le présent travail, nous étudions dans quelle mesure la distribution apparente du soufre en profondeur est liée au mode de décapage, quelle est sa répartition en surface et si le phénomène est spécifique du soufre.

METHODES ET RESULTATS

Influence du mode de décapage

Si le phénomène observé est réellement une diffusion en profondeur, il ne doit pas dépendre du mode de décapage. Jusqu'à présent, deux méthodes de décapage chimique avaient donné des pénétrations apparentes de ^{35}S analogues. L'une utilisait comme bain de décapage HNO_3 11 M [2], l'autre une solution H_2O_2 30%—HF 2% [5]. Nous utilisons ici une méthode d'abrasion. Des tranches d'une épaisseur de 10 μm environ sont obtenues au moyen d'un papier abrasif 600. Le métal pulvérulent déposé sur l'abrasif est dissous par une solution H_2O_2 30%—HF 2%. Le soufre est ensuite séparé chimiquement par la méthode établie précédemment [5] et la radioactivité de ^{35}S est mesurée.

L'abrasion conduit à une décroissance de la teneur en soufre plus rapide que pour un décapage chimique (Fig. 1A et B). On atteint un palier qui correspond à une teneur apparente en soufre proche de la limite de détection (d'autant plus élevée, que la masse de fer décapée est faible), mais légèrement

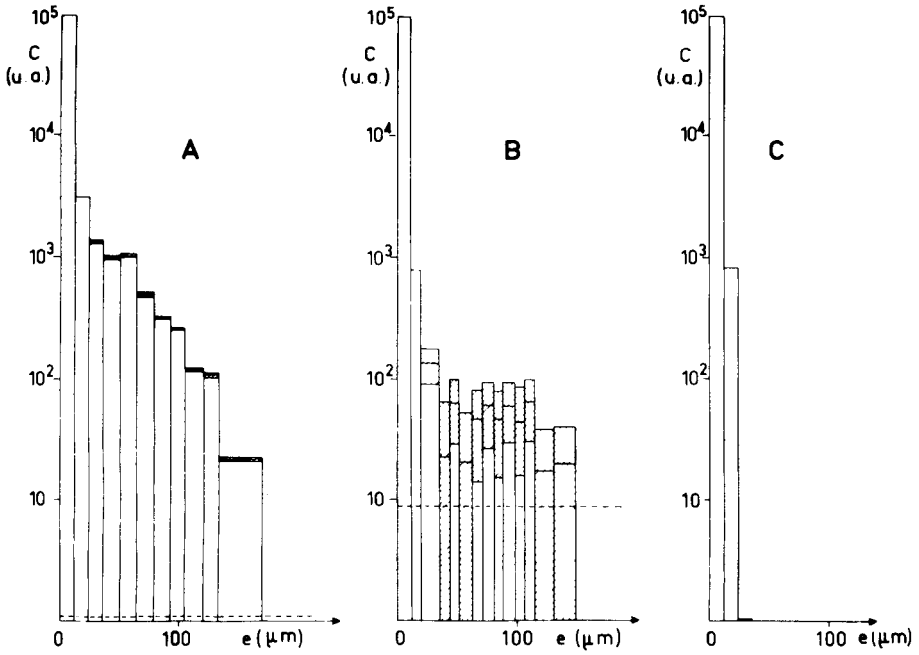

Fig. 1. Concentration apparente C du soufre (en unités arbitraires, la concentration de la première tranche étant prise égale à 10^5) en fonction de l'épaisseur décapée e en μm. Les rectangles hachurés donnent l'intervalle d'erreur avec une confiance de 95%. Les pointillés correspondent à la teneur réelle (0,8 $\mu g\ g^{-1}$). (A) Décapages chimiques par le milieu H_2O_2—HF; (B) abrasion mécanique; (C) répartition calculée dans les conditions de la Fig. 1A en supposant que la redéposition est seule en cause.

supérieure à la teneur réelle dans les échantillons. Ceci est attribué à une imperfection intrinsèque de l'abrasion qui l'avait faite écarter au tout début des expériences: une partie du métal abrasé s'incruste ce qui conduit à une contamination de la tranche $(n + 1)$ par la tranche n. Au cours d'une autre expérience nous avons évité ce risque en alternant abrasions et décapages. Dans ce cas on atteint la teneur réelle en soufre qui est de 0,8 $\mu g\ g^{-1}$ sur un échantillon de fer étalon de teneur certifiée fourni par le Bureau National de Métrologie. L'ensemble de ces expériences montre que la contamination en soufre est localisée dans une zone très proche de la surface des échantillons.

Pour confirmer ce résultat nous avons utilisé un réactif qui n'attaque le fer qu'avec une vitesse très lente, alors que les oxydes sont dissous rapidement. Il s'agit de l'acide chlorhydrique 6 M désaéré par barbotage d'azote [7]. Trois décapages successifs de 30 min enlèvent 99,8% de la radioactivité initiale en ^{35}S. L'épaisseur de métal enlevée est inférieure à 1,5 μm. Il faut enlever plus de 100 μm de métal par décapage avec le bain H_2O_2—HF, pour atteindre le même pourcentage.

Régularité des décapages par le milieu H_2O_2—HF

L'hypothèse d'une diffusion en volume étant écartée, la qualité du décapage

déjà étudiée [5], a fait l'objet d'un nouvel examen. Il est évident qu'une mauvaise procédure de décapage peut conduire à une apparente pénétration en volume si la vitesse de l'attaque n'est pas uniforme sur toute la surface.

Pour étudier l'évolution du profil de la surface au cours des décapages nous avons utilisé un échantillon enrobé dans une résine acrylique, poli à l'alumine, et sur lequel du ^{35}S avait été déposé. Chaque point de la surface était repéré par ses trois coordonnées au moyen d'un microscope optique. Le système utilisé permettait de positionner l'échantillon sur la platine du microscope de façon reproductible après chaque décapage. La coordonnée de profondeur était obtenue par mise au point micrométrique. Un fil de platine également enrobé dans la résine servait de référence. Les irrégularités de la surface ont en outre été mesurées à l'aide d'un palpeur mécanique et par interférométrie à polarisation d'après Nomarski. L'activité en ^{35}S a été mesurée dans chaque tranche décapée.

La Figure 2 montre l'evolution du profil au cours de 5 décapages successifs, observée par microscopie optique. La radioactivité qui se manifeste après plusieurs décapages n'est pas due à la persistance de zones non attaquées. Les mesures indiquent que la vitesse d'attaque n'est pas la même d'un point à l'autre au cours d'un même décapage. D'autre part, en un même point la vitesse n'est pas constante d'un décapage à l'autre; ces deux variations ont le même écart-type 2,7 $\mu m\ min^{-1}$. L'épaisseur moyenne enlevée par rapport à la surface initiale, généralement déterminée par pesée, est définie avec un écart-type de 3 μm quels que soient l'épaisseur décapée et le nombre de décapages, ce qui montre le caractère aléatoire des variations. Les accidents de surface observés par interférométrie et au moyen d'un palpeur ont une amplitude qui n'est jamais supérieure à 3 μm. Par ailleurs, la répartition de ^{35}S dans les tranches est analogue à celle de la Fig. 1A.

Rôle du redépôt à partir de la solution

Lorsque la surface de l'échantillon est en contact avec une solution radioactive, on peut définir un coefficient de redéposition exprimé en centimètre égal au rapport de la radioactivité déposée par unité de surface à la radioactivité par unité de volume de la solution après établissement de l'équilibre. Nous avons fait de nombreuses mesures de ce coefficient en utilisant des échantillons non irradiés et en faisant varier les conditions expérimentales: fer très peu ou très fortement oxydé, solutions décapantes (H_2O_2 30%—HF 2%) ou non (H_2O). Les solutions contenaient du soufre radioactif sous forme sulfate et de 0 à 1 mg cm^{-3} de sulfate d'ammonium utilisé comme entraineur. Ces expériences ont montré que la variation du coefficient de redéposition avec la concentration d'entraineur est négligeable devant celle due à l'état d'oxydation de la surface. Le coefficient de redépôt varie de 10^{-5} cm (fer préalablement décapé et en contact avec la solution décapante, donc peu oxydé) à 10^{-1} cm (fer fortement oxydé en contact avec une solution non décapante).

Dans l'hypothèse la plus défavorable (coefficient égal à 10^{-1} cm), nous avons calculé la répartition apparente du soufre en la supposant due unique-

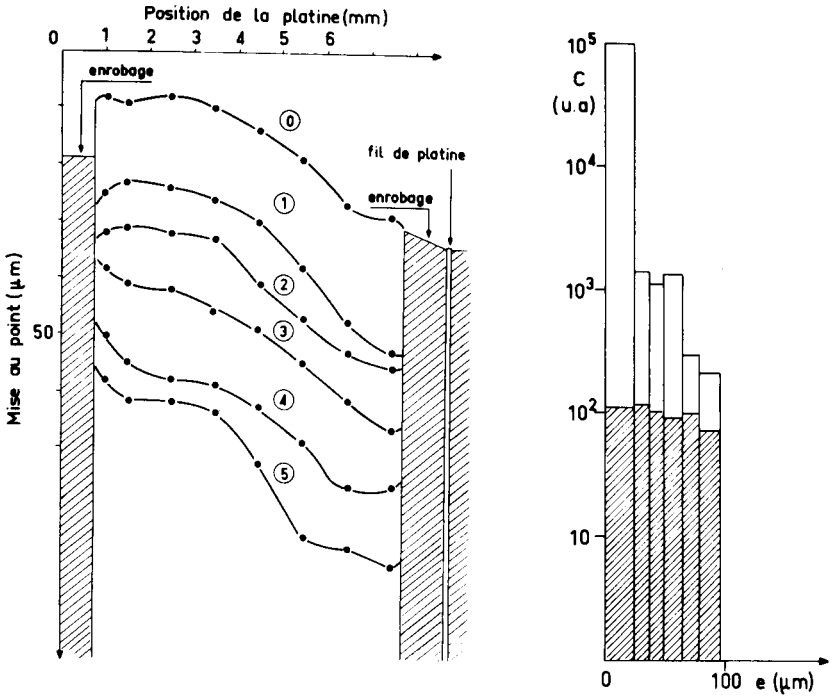

Fig. 2. Evolution du profil d'une coupe diamétrale d'un échantillon au cours de cinq décapages successifs observée par microscopie optique. On indique la position de la platine du microscope (mm) en abscisse et le réglage de mise au point micrométrique en ordonnée.

Fig. 3. Répartition du ^{35}S après décapage par H_2O_2—HF d'un échantillon de fer poli, non irradié, sur lequel on a déposé du ^{35}S. En ordonnée la concentration C en soufre est prise arbitrairement égale à 10^5 u.a. pour la première tranche. Les rectangles hachurés représentent les limites de détection.

ment à la redéposition. La courbe calculée (Fig. 1C) montre qu'au delà de 30 µm la redéposition contribue pour moins de 0,2% à l'activité obtenue après décapage chimique (Fig. 1A). Les conditions choisies étant extrêmes (échantillon fortement oxydé, pas de lavage de la surface entre deux décapages), nous sommes donc fondés à exclure l'explication du phénomène par la redéposition.

Répartition du phénomène en surface

Les résultats précédents indiquent que l'entraînement du soufre au cours des décapages est dû à un phénomène de surface. Ceci est confirmé par le fait que l'irradiation n'est pas nécessaire pour que le phénomène se produise. Le décapage par tranche d'un échantillon non irradié sur lequel a été déposé du ^{35}S conduit à l'obtention d'un histogramme analogue à celui de la Fig. 1A. Nous avons voulu vérifier par autoradiographie si le soufre était réparti uniformément à la surface, ou si sa concentration était affectée par la structure

superficielle de l'échantillon. L'utilisation d'échantillons non irradiés permet de détecter ^{35}S sans interférence.

Un échantillon est mis en contact avec une solution fortement radioactive en ^{35}S. On procède au décapage par tranches avec le milieu H_2O_2—HF. La mesure de la radioactivité des tranches permet d'établir la répartition de ^{35}S. Chaque décapage est précédé d'un examen macrographique (× 5) et d'une autoradiographie sur film Kodak 4489.

Nous avons tout d'abord utilisé un échantillon fraîchement poli, brillant à l'examen microscopique et donc peu oxydé. La répartition de ^{35}S (Fig. 3) est analogue à celle d'un échantillon oxydé en cours d'irradiation. Au delà de 100 μm on tombe au-dessous de la limite de détection en raison de la faible activité retenue. Des autoradiographies n'ont pu être effectuées que sur la première tranche par manque de sensibilité. On observe une répartition non uniforme du soufre sans qu'elle puisse être reliée à des accidents de surface.

Nous avons alors procédé aux mêmes expériences sur un échantillon fortement oxydé de façon à obtenir un dépôt important de ^{35}S. Cette oxydation a été réalisée par contact prolongé avec une solution HNO_3 10^{-2} M contenant des ions Cu^{2+} de façon à faciliter l'attaque électrochimique du fer. La radioactivité en ^{35}S est encore décelable après 200 μm de décapage. La Figure 4 donne un exemple de ce qui est observé par macrographie et autoradiographie. Le ^{35}S n'est pas réparti uniformément à la surface; il y a corrélation entre les zones de forte radioactivité et celles où l'oxydation est visible. Cette concordance persiste tout au long des décapages alors que globalement la radioactivité décroît. La forte oxydation de la surface amène à considérer cette expérience comme partiellement représentative du phénomène étudié, car elle conduit à un décapage plus irrégulier que dans les conditions expérimentales habituellement utilisées.

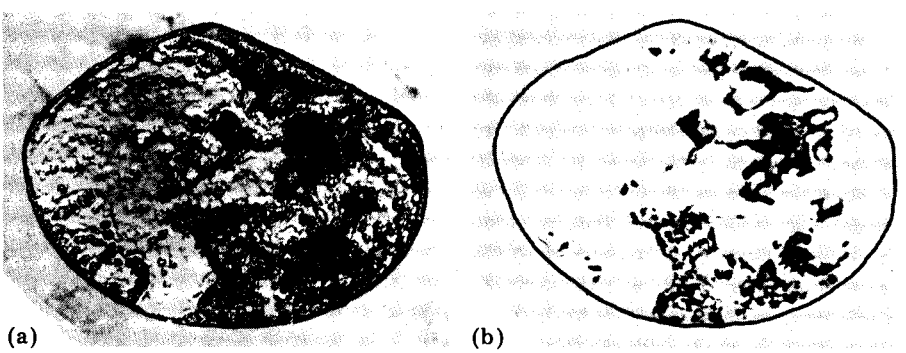

Fig. 4. Macrographie (a) et autoradiographie (b) d'un échantillon de fer oxydé avec dépôt de ^{35}S après décapages par le bain H_2O_2—HF (× 2,5). Le soufre apparaît en noir sur l'autoradiographie.

Spécificité du phénomène

Il était intéressant de savoir si le gradient en ^{35}S dans les tranches de décapage est un phénomène spécifique au soufre, ou s'il a été simplement décelé à cause de la forte radioactivité produite à partir du chlore de surface par la réaction $^{35}Cl(n, \gamma)^{35}S$. Dans ce cas un autre élément que le soufre devrait produire un phénomène analogue, si sa radioactivité par unité de surface est suffisamment élevée. Nous avons choisi le cobalt qui peut devenir fortement radioactif grâce à la réaction $^{59}Co(n, \gamma)^{60}Co$ et qui a des propriétés chimiques très différentes de celles du soufre.

Pour pouvoir comparer valablement le comportement du soufre et du cobalt, nous avons irradié un échantillon contaminé en chlorure de cobalt. Après irradiation nous avons décapé des tranches par la méthode habituelle (H_2O_2—HF). Nous mesurons d'abord la radioactivité-γ du ^{60}Co après élimination du ^{59}Fe par extraction à l'hexone [5]. Le rendement de séparation en ^{60}Co est mesuré en incorporant un traceur ^{57}Co au bain de décapage. Ensuite nous effectuons la séparation chimique du soufre par la méthode déjà décrite [5], applicable en présence de cobalt. Nous mesurons alors la radioactivité-β de ^{35}S.

Les résultats sont reproduits sur la Fig. 5 en normalisant les radioactivités par rapport à la deuxième tranche. La première tranche contient relativement plus de cobalt que de soufre. Par contre, à partir de la deuxième tranche, la teneur des deux éléments décroît de façon identique.

DISCUSSION

Les résultats obtenus après abrasion mécanique et après attaque chimique ont montré que le phénomène observé n'est dû ni à une diffusion profonde dans le métal, ni à une pénétration dans des piqûres ou cavités. Deux hypothèses pouvaient être avancées pour expliquer le phénomène: soit un décapage irrégulier dû à des vitesses d'attaque différentes sur certaines zones de la surface, soit le maintien du soufre à la surface au cours des décapages. L'examen de l'efficacité du décapage par plusieurs méthodes montre qu'il ne subsiste pas de zones peu attaquées pouvant retenir ^{35}S: les accidents de surface ont une amplitude nettement inférieure à l'épaisseur décapée.

Nos expériences ayant montré que le redépôt à partir de la solution intervenait pour une part négligeable dans le phénomène, nos résultats ne peuvent s'expliquer que par un passage en solution beaucoup plus lent pour le soufre que pour le fer. Au cours de la dissolution anodique d'un alliage Ni—S à faible teneur en soufre (de l'ordre de 50 ppm), il a été mis en évidence un enrichissement de la surface en soufre qui augmentait jusqu'à atteindre un état stationnaire correspondant à une dizaine de couches monoatomiques de soufre [8]. Les mêmes auteurs ont également étudié un échantillon de nickel recouvert d'une couche monoatomique de soufre et établi que celle-ci se maintenait intacte au cours de la dissolution jusqu'au delà du potentiel de passivation du métal pur.

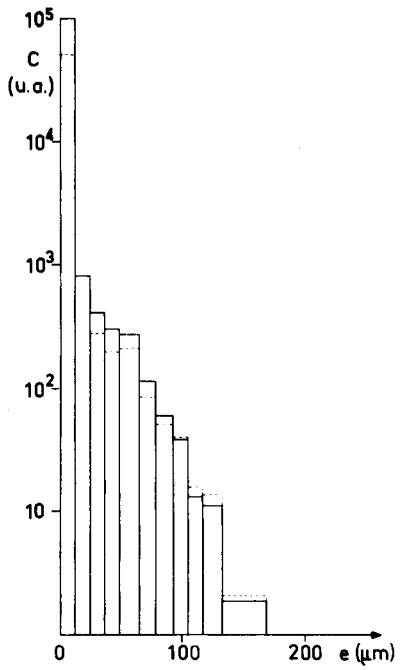

Fig. 5. Répartition de ^{60}Co (traits continus) et ^{35}S (traits pointillés) d'un échantillon de fer irradié avec dépôt de $CoCl_2$. La concentration de la première tranche en cobalt est prise arbitrairement égale à 10^5 u.a. Les concentrations en soufre et en cobalt de la deuxième tranche sont prises arbitrairement égales.

L'analogie est évidente, mais outre qu'il s'agit du fer, notre cas présente plusieurs différences. Des travaux effectués par ailleurs [9] ont montré qu'une monocouche de sulfure adsorbée à la surface d'un monocristal de fer correspondait à un atome de soufre pour deux atomes de substrat. Dans nos expériences, le ^{35}S produit à partir du chlore n'est pas en quantité suffisante pour former une monocouche. Il en représente au plus un millième dans l'exemple de la Fig. 1A, soit 1 atome pour 2000 du substrat. Les ions sulfate utilisés comme entraîneur s'adsorbent à la surface au cours du décapage; la capacité de rétention de la surface en début de décapage atteint 100 anions de sulfate pour un atome de substrat en supposant que l'aire de l'échantillon est la même que son aire géométrique. Remarquons que dans le cas du cobalt le radioisotope est produit en présence de son entraîneur, et la quantité de cobalt adsorbé est également de l'ordre de 100 atomes pour un atome de substrat (exemple de la Fig. 1A). Dans les conditions de dissolution utilisées (H_2O_2—HF, HNO_3 ou bien HCl), le soufre suit l'entraîneur sulfate, il se trouve donc probablement sous cette forme et non sous forme sulfure. D'autre par, les échantillons utilisés par les auteurs [8] sont monocristallins et exempts d'oxygène.

Plusieurs de nos expériences semblent montrer d'ailleurs que l'oxyde joue un rôle dans le phénomène: il y a corrélation entre la radioactivité en ^{35}S et la

quantité d'oxyde, l'acide chlorhydrique 6 M désaéré qui dissout sélectivement l'oxyde, met plus facilement le soufre en solution que le milieu H_2O_2—HF.

Par ailleurs [10], les propriétés de rétention de l'oxyde ferrique hydraté ont été systématiquement étudiées en milieu HNO_3 0,1 M. Dans ces conditions, les ions sulfate sont irréversiblement fixés avec formation d'un composé peu soluble. Par contre, les ions Co^{2+} ne présentent aucune affinité. Ces expériences ont été faites en milieu HNO_3 0,1 M alors que l'existence de notre phénomène a été établie dans les milieux HNO_3 11 M et H_2O_2 30%—HF 2%.

Dès à présent à défaut d'une explication totale et définitive du phénomène observé, nous avons mis au point les conditions permettant le dosage exact du soufre dans le fer au moyen de la réaction $^{34}S(n, \gamma)^{35}S$. Deux solutions peuvent être retenues: soit effectuer un recuit sous hydrogène à 850°C et irradier sous ampoule scellée; soit, si l'échantillon est préparé et irradié sans précautions particulières, effectuer après irradiation le traitement suivant: l'échantillon doit être lavé deux à trois fois par HCl 6 M désaéré, ensuite décapé fortement (500 μm) par alternance d'abrasions et de décapages par le milieu H_2O_2 30%—HF 2%. Les attaques chimiques par ce dernier milieu ont seulement pour but de nettoyer la surface entre deux abrasions; un décapage trop prononcé pourrait enrichir la surface en soufre. Un dernier lavage par HCl 6 M désaéré permet de parer à cette éventualité.

Les dosages réalisés par l'un ou l'autre de ces procédés donnent une teneur de 0,8 $\mu g\ g^{-1}$ de soufre dans nos échantillons. Cette valeur est dix fois supérieure à nos limites de détection. Elle correspond à la teneur certifiée par le Bureau National de Métrologie.

Conclusion

Nos expériences ont apporté un progrès à la compréhension des causes d'erreur dans la détermination de la teneur en soufre des échantillons de fer par la réaction $^{34}S(n, \gamma)^{35}S$. Les hypothèses de diffusion profonde au cours de l'irradiation, de redépôt à partir de la solution et de décapage irrégulier ont été écartées. Les teneurs apparentes élevées en soufre sont dues à une fixation de celui-ci à la surface et à son maintien partiel au cours de l'attaque chimique. De nouvelles expériences seront nécessaires pour préciser la nature des liaisons de l'impureté fixée et le rôle de l'oxyde, mais dès maintenant nous proposons des méthodes conduisant à un dosage exact.

BIBLIOGRAPHIE

1 M. Cuypers, J. Le Héricy, J. Cuypers et Ph. Albert, C.R. Acad. Sci. Paris, 261 (1965) 5494.
2 Ph. Albert, J. Blouri, Ch. Cleyrergue, N. Deschamps et J. Le Héricy, J. Radioanal. Chem., 1 (1968) 297, 389, 431.
3 M. Fédoroff, C.R. Acad. Sci. Paris, 271 C (1970) 399.
4 M. Boissier-Chermette, Thèse Lyon, 1974.
5 R. Delmas, M. Fédoroff et G. Revel, Radiochem. Radioanal. Lett., 30 (1977) 3, 209-218.
6 Y. Adda, M. Beyeler et G. Brebec, Thin Solid Films, 25 (1975) 107.

7 S. Menasce, Rev. Mét., 59 (1962) 249.
8 J. Oudar et P. Marcus, Applications of Surface Science, 3 (1979) 1, 48.
9 J. Oudar et E. Margot, Colloque International C.N.R.S. n° 187, Structure et Propriétés des Surfaces des Solides, Paris, 1969, pp. 123—130.
10 M. Guillaume, Analusis, 1 (1972) 7, 467.

Analytica Chimica Acta, 120 (1980) 237—248

ION FLOTATION STUDIES OF THE CHLOROCOMPLEXES OF SOME PLATINUM GROUP METALS

EUGENE W. BERG* and DANIEL M. DOWNEY

Department of Chemistry, Louisiana State University, Baton Rouge, LA 70803 (U.S.A.)

(Received 8th April 1980)

SUMMARY

The anionic chlorocomplexes of Au(III), Pt(IV), Pd(II), Ir(IV), Ir(III) and Rh(III) can be floated from aqueous solutions with cationic surfactants of the type RNR'_3Br. The flotation behavior of each metal is reported with respect to variations of hydrochloric acid and sodium chloride concentrations, the R and R′ chain lengths, initial surfactant concentrations and initial metal ion concentrations. The flotation behavior of the metals is compared to the anion-exchange selectivity coefficients and a flotation selectivity sequence of Au(III) > Pt(IV), Ir(IV), Pd(II) > Ir(III) > Rh(III) is generally observed. Nearly 100% of Au(III), Pt(IV), Ir(IV) and Pd(II) can be recovered from dilute solutions using the ion flotation procedures.

The flotation of particulate matter has been used in the ore industry since 1912 for the recovery of valuable minerals from crushed ores. It was not until 1959, however, that Sebba [1] first proposed that ions may be selectively removed from aqueous solution by flotation. The ion flotation process involves the addition of an ionogenic surfactant (collector) to a solution containing ions of opposite charge (colligend) and foaming by passing air or nitrogen through the solution. The collector may form either a precipitate or a soluble product with the colligend; in either case, colligend—collector ion pairs are floated and form a scum or sublate on the surface of the solution as the foam collapses. The solid sublate may be easily removed for further processing. Thus ion flotation is both a separation and concentration process. Ions are often successfully floated from 10^{-7} to 10^{-4} M solutions and may be concentrated by factors of 10^4 or 10^5.

Numerous cationic and anionic complexes have been floated since Sebba's initial work [2—4]. However, the platinum group metals have not yet undergone an extensive, systematic flotation study even though it was suggested as early as 1962 by Sebba [5]. Several flotation studies of the individual platinum group metals have been published: gold [6—8], platinum [9, 10], palladium [9, 11] and ruthenium [12]. No flotation studies for osmium, rhodium or iridium have been noted in the literature.

The present paper reports on the ion flotation properties of the chlorocomplexes of Au(III), Pt(IV), Pd(II), Ir(IV), Ir(III) and Rh(III). These metals

exist in hydrochloric acid solutions as $AuCl_4^-$, $PtCl_6^{2-}$, $PdCl_4^{2-}$, $IrCl_6^{2-}$, $IrCl_6^{3-}$ and $RhCl_6^{3-}$, respectively. Cationic surfactants of the type RNR'_3^+ were chosen for study, where R and R′ are primary and secondary alkyl chains. Osmium and ruthenium were not studied because of their complex aqueous chemistry.

Many variables have been shown to influence ion flotation processes and these have been discussed by Pinfold [13]. In this paper, the influence of several variables on the flotation of each platinum metal chlorocomplex is presented. These variables are sodium chloride concentration, hydrochloric acid concentration, initial collector concentration, initial metal chlorocomplex concentration and the surfactant primary and secondary alkyl chain lengths. Significant differences in the degree and rate of flotation are noted for several of these metals, and possible separation methods are suggested.

Finally, the optimum ion flotation conditions for quantitatively recovering the various metals from dilute aqueous solutions are presented.

EXPERIMENTAL

Sample and reagents

Hexachloroplatinate(IV), tetrachloropalladate(II) and tetrachloroaurate-(III) stock solutions were prepared by dissolving the high-purity metals (A. D. Mackay, Inc.) in aqua regia, fuming to dryness with hydrochloric acid and storing in 2 M HCl. An iridium(IV) stock solution was prepared by dissolving high-purity sodium hexachloroiridate(IV) (Alfa-Ventron Chemical Co.) in 6 M HCl and passing chlorine gas through the solution for several hours to ensure complete oxidation to iridium(IV). After boiling to dryness, the final iridium solution was made up in 2 M HCl. Iridium(III) solutions were prepared as needed by boiling aliquots of the Ir(IV) stock solution with 0.25 ml of 10% hydroxylammonium chloride for 10 min [14]. High-purity sodium hexachlororhodate(III) (Alfa-Ventron) was refluxed for several hours in concentrated hydrochloric acid. The final rhodium(III) solution was made up in 2 M HCl.

Aliquots of the stock solutions of Ir, Pd, Pt and Au were irradiated with thermal neutrons from ^{252}Cf in the LSU Nuclear Science Center to produce the radiotracers summarized in Table 1. As there is no suitable tracer for rhodium, the tin(II) chloride method of Sandell [15] was used for the determination of rhodium.

Quaternary ammonium surfactants were prepared by the standard procedure of reacting tertiary amines with long-chain alkyl bromides. The long chain of the resulting surfactant may be considered to be the primary chain. Alkyl bromides of primary chain length C-8 to C-18 (Eastman Chemical Co.) were reacted with trimethylamine (Aldrich Chemical Co.) to give surfactants of varying primary chain length and constant secondary chain length. The C—16 alkyl bromide was also reacted with triethylamine, tripropylamine and tributylamine (Aldrich Chemical Co.) to give surfactants of constant

TABLE 1

Major isotopes produced by neutron activation of the platinum group metals

Isotope	Half-life	Major energies (MeV)	Isotope	Half-life	Major energies (MeV)
Rhodium-104 m	4.35 min	0.057, 0.078	Platinum-195 m	4.0 d	0.031
Palladium-109	13.43 h	0.088	Platinum-197	18.3 h	0.077, 0.191
Iridium-192	74.2 d	0.316, 0.468	Gold-198	2.7 d	0.412
Iridium-194	19.2 d	0.328			

TABLE 2

Elemental content of surfactants used for floating the platinum group metals

Surfactant	Abbreviation	Theoretical			Found		
		%C	%H	%N	%C	%H	%N
Hexadecylamine hydrochloride	HAC	69.41	12.78	5.06	69.72	12.58	4.92
Hexadecyltrimethylammonium bromide	HTMAB	62.62	11.62	3.84	62.77	11.13	3.76
Hexadecyltriethylammonium bromide	HTEAB	65.00	11.90	3.44	64.96	11.85	3.22
Hexadecyltripropylammonium bromide	HTPAB	66.93	12.13	3.12	67.06	11.65	3.05
Hexadecyltributylammonium bromide	HTBAB	68.54	10.27	2.85	68.19	10.01	2.55
Octyltrimethylammonium bromide	OTMAB	52.38	10.38	5.55	52.51	10.02	5.13
Decyltrimethylammonium bromide	DTMAB	55.71	10.79	5.00	55.86	10.61	4.89
Dodecyltrimethylammonium bromide	DDTMAB	58.43	11.11	4.54	58.32	10.86	4.48
Tetradecyltrimethylammonium bromide	TTMAB	60.70	11.39	4.16	61.01	11.40	4.06
Pentadecyltrimethylammonium bromide	PTMAB	61.70	11.50	4.00	62.24	11.42	3.90
Octadecyltrimethylammonium bromide	ODTMAB	64.26	11.81	3.57	64.13	11.38	3.46

primary chain length and varying secondary chain length. Finally, hexadecylammonium hydrochloride was prepared by bubbling anhydrous hydrogen chloride through a solution of hexadecylamine (Eastman Chemical Co.) in ether and recrystallizing the salt from diethyl ether—ethanol. All surfactant stock solutions were prepared as 0.1 and 0.02 M solutions in absolute ethanol. The surfactants employed and the results obtained in purity checks are presented in Table 2.

Ion flotation procedure

Ion flotation experiments were carried out in a glass column made by lengthening to 30 cm an ordinary 60-ml Buchner funnel with a fine glass fritted disc (Fisher Scientific Co.). A port was drilled 1 cm above the frit and fitted with a rubber septum for sample removal. Nitrogen was saturated with water and bubbled through the sintered glass frit (4—5-μm nominal porosity) at a flow rate of 10 cm^3 min^{-1}.

The total volume of each sample solution prepared for flotation was 100 ml. The concentration of all solutes present in each sample prepared for flotation was dependent on which variable was under investigation; all others were held constant. In the general case, all sample solutions [except those containing Ir(IV)] were prepared in 100-ml volumetric flasks by adding

enough metal chlorocomplex solution to give a final concentration of 5×10^{-5} M. An additional aliquot of 2 M HCl was added to give a final concentration of 0.01 M HCl. Exactly 1 ml of an ethanolic 0.02 M surfactant stock solution was then added by pipet and the solution brought to volume and mixed for 10 min before flotation. The total ethanol added in all cases was 1 ml per 100 ml of solution.

For the investigation of iridium(IV) flotation, an additional step was involved in the preparation of samples. Quaternary ammonium functional groups have been shown to reduce Ir(IV) partly to Ir(III) [16]. In order to counteract the reducing effect of the surfactants, 0.25 ml aliquots of a 1% cerium(IV) sulfate solution in 10% sulfuric acid were added to both the surfactant and the iridium(IV) before mixing. In addition, the Ir(IV):Ce(IV) mixture was heated for several minutes in a 140°C oil bath before mixing with the surfactant.

Procedures for preliminary tests

The length of the primary and secondary chains of the quaternary ammonium surfactants was the first parameter investigated for influence on the flotation of the platinum metal chlorocomplexes. The sample solutions were prepared as described in the general case.

For studies involving the influence of HCl or NaCl concentration, the sample solutions were prepared for each metal as in the general case with selected surfactants. In addition, aliquots of stock solutions of HCl or NaCl were added to give final solutions ranging from 0.01 to 3.0 M HCl or NaCl in 100 ml.

For studies involving the variation of surfactant concentration, sample solutions were prepared as in the general case except that aliquots of selected surfactant solution for each metal were added to give concentrations ranging from 0 to 0.001 M.

The concentration of metal chlorocomplex remaining in the bulk solution at any time after beginning flotation, C_t, was determined in the following manner in order to estimate the extent of flotation. Samples were removed from the flotation column with a syringe and determined by counting the activity of each radiotracer in 1—5-ml aliquots with a 2 × 2-in. NaI(Tl) well crystal detector coupled with a TMC 401D multichannel analyzer or spectrophotometrically for rhodium. By dividing C_t by the original concentration, C_0, and plotting the ratio vs. flotation time, curves were obtained for the rate of removal. The percentage of metal ion floated was calculated as % floated $= (1 - C_t/C_0)(100)$.

Recovery studies were conducted by preparing 200-ml sample solutions containing initial metal concentrations of 2.5×10^{-4} M. For the flotation of Ir(IV), Pt(IV) and Pd(II), enough HTPAB was added to give a final concentration of 6.0×10^{-4} M. The Ir(IV) solutions were also treated with cerium(IV) as described above. The surfactant concentrations allow an excess of 1×10^{-4} M over the stoichiometric ratio to provide foam for supporting the sublates.

TABLE 3

Percentage of the platinum metals floated with surfactants of various chain lengths, R, as a function of time
(Initial conditions: [Metal] = 5×10^{-5} M, [$RN(CH_3)_3Br$] = 2×10^{-4} M, pH = 2, N_2 flow rate = 10 cm^3 min^{-1})

R	Time (min)	Amount floated (%)					
		Au(III)	Pd(II)	Pt(IV)	Ir(IV)	Ir(III)	Rh(III)
C-8	30	50	0	0	0	0	0
	120	53	0	0	0	0	0
	240	53	0	0	0	0	0
C-10	30	60	10	8	9	9	0
	120	62	10	10	9	9	0
	240	65	10	10	11	10	0
C-12	30	75	38	92	95	28	8
	120	85	40	93	98	30	9
	240	95	40	93	98	30	10
C-14	30	70	70	92	92	49	18
	120	82	72	94	95	50	20
	240	95	72	94	97	50	20
C-15	30	65	85	92	85	48	19
	120	92	90	95	90	50	22
	240	100	90	96	90	50	22
C-16	30	54	95	80	75	53	21
	120	81	98	82	82	55	25
	240	95	100	85	84	55	25
C-18	30	50	80	40	60	45	25
	120	76	90	45	73	49	30
	240	88	92	50	75	50	30

Exactly 100 ml of each sample solution was transferred to the column for flotation. After passing nitrogen through each solution for 2 h, each sublate was collected for analysis, after the bulk liquid had been drained off, by washing the column with acetone and collecting the wash liquid in a flask. After the acetone had been removed by rotary evaporation, the sublate was wet-ashed with nitric acid and fumed with hydrochloric acid. Finally, the recovered metals were prepared in 2 M HCl solution and the amounts recovered were determined (Table 3).

RESULTS AND DISCUSSION

Influence of primary chain length on flotation

The length of the long (primary) hydrocarbon chain of surfactants has been shown to influence greatly the degree of flotation of particulates [17] and ions [18]. Therefore, seven surfactants of the type $RN(CH_3)_3Br$, where

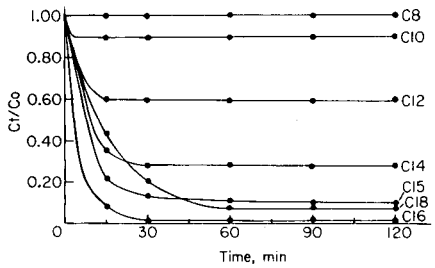

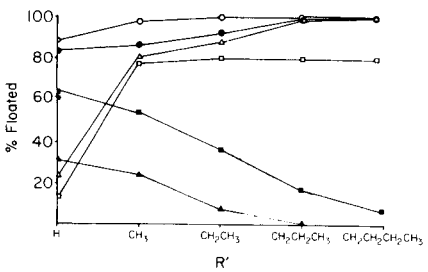

Fig. 1. Effect of varying surfactant primary chain length on flotation of Pd(II) with surfactants of the type $RN(CH_3)_3Br$. Initial conditions: $[PdCl_4^{2-}] = 5 \times 10^{-5}$ M, $[RN(CH_3)_3Br] = 2 \times 10^{-4}$ M, pH 2, N_2 flow rate 10 cm^3 min^{-1}.

Fig. 2. Effect of varying secondary chain length on percentage floated for each metal after 2 h with surfactants of the type $C_{16}H_{33}NR'_3Br$. Initial conditions: [Metal] = 5×10^{-5} M, $[C_{16}H_{33}NR'_3Br] = 2 \times 10^{-4}$ M, pH 2.0, N_2 flow rate 10 cm^3 min^{-1}. (△) Pt(IV); (□) Au(III); (○) Pd(II); (●) Ir(IV); (■) Ir(III); (▲) Rh(III).

R was an unbranched hydrocarbon chain of chain length C-8 to C-18, were prepared for floating the chlorocomplex anions of the platinum group metals.

Figure 1 presents the curves for the rate of removal by flotation of $PdCl_4^{2-}$ with each of the surfactants. Similar curves were obtained for $IrCl_6^{2-}$, $IrCl_6^{3-}$, $RhCl_4^{3-}$, $AuCl_4^-$ and $PtCl_6^{2-}$. The percentage of each metal floated as a function of time is given in Table 3. Precipitates were formed in the bulk solution when surfactants of chain length C-12 and greater were mixed with Pd(II), Pt(IV), Ir(IV) and Au(III). Rh(III) and Ir(III) formed precipitates in the bulk solution only with the C-16 and C-18 surfactants. None of the metals could be quantitatively recovered from the bulk solutions by filtering the precipitates.

It was found that as the surfactant chain length was increased, the time required to reach steady state for the flotation of all the metal ions also increased. In addition, the percentage of metal chlorocomplex floated generally increased with increasing chain length, reached a maximum and then began to decrease. In order to explain these trends, several properties of surfactants will be discussed.

The concentration of a surfactant in the gas–liquid interface is dependent, in part, on the length of its hydrocarbon chain. As the hydrocarbon chain length increases from one surfactant to another of the same type, the concentration of the surfactant in the surface layer increases relative to its concentration in the bulk solution. Since ion flotation utilizes only the surfactant in the interfacial layer for flotation of the colligend, it follows that the amount of colligend floated also increases as the surfactant chain length increases. However, the stability of the foam head formed by bubbling gas through the solution is proportional to chain length. Foam heads are desirable because they support the sublate and prevent redispersion into the bulk solution; however, very stable heads result in lower fractions of metal

floated because much of the surfactant is entrained in the foam and is unavailable for collecting the colligend by reflux action.

The low flotation observed for the C-8 and C-10 surfactants may be attributed to their low surface activity and to the formation of unstable foam heads. The optimum chain lengths for maximum flotation appear to be C-14 or C-15. For C-16 and C-18 surfactants, the degree of flotation generally decreases because of the formation of stable foams. As the foam stabilities increase, longer equilibration times are observed because the rate of surfactant reflux is slower.

Finally, the selectivity sequence for each surfactant may be evaluated by noting the maximum fraction of each metal chlorocomplex floated. The data in Table 3 show that the flotation of all the metals studied except gold(III) reaches a maximum within 2 h. In 4 h, the C-15 surfactant floated 100% of the gold(III) whereas the C-12, C-14 and C-16 surfactants floated only 95% of the gold(III). Generally, the selectivity sequence at steady state is $AuCl_4^-$ > $PdCl_4^{2-}$, $PtCl_6^{2-}$, $IrCl_6^{2-}$ > $IrCl_6^{3-}$ > $RhCl_6^{3-}$. If the charges of the platinum group metal chlorocomplexes are considered, then the sequence observed for flotation of the anions is monovalent > divalent > trivalent anions.

These data are in disagreement with Pinfold [13] who predicted that as the ionic charge increases, the fraction floated would increase. However, the distribution coefficients of the platinum metals for quaternary ammonium ion-exchange resins [19, 20] indicate selectivities in the order of $AuCl_4^-$ > $PdCl_4^{2-}$, $PtCl_6^{2-}$, $IrCl_6^{2-}$ > $IrCl_6^{3-}$ > $RhCl_6^{3-}$. It is reasonable to assume that the forces which cause the strong binding of Au(III), Pd(II), Pt(IV) and Ir(IV) to anion-exchange resins would also cause strong binding to the quaternary ammonium surfactants; which, in turn, results in greater degrees of flotation for these metals.

Influence of secondary chain length on flotation

Surfactants of constant primary chain length and varying secondary chain length were also prepared for the flotation studies of the platinum group metals. These surfactants were of the type, $C_{16}H_{33}NR'_3^+$, where R′ was either H, methyl, ethyl, n-propyl or n-butyl. The percentage of each metal chlorocomplex floated after 2 h was calculated and is plotted vs. secondary chain length in Fig. 2.

For all metals studied except gold(III), the flotation data presented indicates the maximum amount of metal floated. After 4 h of flotation, the gold(III) is floated to 95%, 98%, 100% and 100% by trimethyl-, triethyl-, tripropyl- and tributyl-ammonium surfactants, respectively. Thus for all the surfactants studied, except RNH_3^+, the flotation sequence at steady state is Au(III) > Pd(II), Pt(IV), Ir(IV) > Ir(III) > Rh(III).

For Pd(II), Pt(IV), Ir(IV) and Au(III), the percentage of metal floated increases with increasing secondary chain length. However, the percentage of Ir(III) and Rh(III) floated decreases with increasing secondary chain

length. An increase in percentage floated with increasing chain length was expected for reasons explained before, because the surface activity of the surfactant also increases with secondary chain length.

The decrease in percentage floated is thought to be the result of the charge and size of the Rh(III) and Ir(III) chlorocomplexes. The $RhCl_6^{3-}$ and $IrCl_6^{3-}$ ions are comparable in size to the tetramethylammonium ion. Thus as the length of the secondary chains are increased, the size of the quaternary ammonium ion becomes very large relative to the platinum metal chlorocomplexes. Pd(II), Pt(IV) and Ir(IV) require only a 2:1 mole ratio of surfactant to metal for flotation. However, the Rh(III) and Ir(III) require a 3:1 mole ratio. Apparently, the crowding of three large ammonium groups around the small anions is sterically unfavorable and leads to a reduction in flotation.

Influence of sodium chloride and hydrochloric acid on flotation

Other studies [9, 16, 21] have utilized the differences in formation constants of chloride complexes of metals (e.g., Fe^{3+}, Hg^{2+}) at various chloride concentrations to effect flotation separation. Because of the difficulty involved in preparing the various chloro–aquo species of the platinum group metals, all of these experiments involved the addition of the metals in their fully chloro-substituted forms in hydrochloric acid solution. However, it is still of importance to know the effects of excess of chloride on the flotation processes of these metals because of the numerous industrial procedures involving brine or hydrochloric acid media.

Figure 3 indicates the variation of percentage floated for the various metals in 0.01—3.0 M chloride as NaCl and HCl, respectively, with the surfactant hexadecyltripropylammonium bromide (HTPAB) after flotation for 2 h. The rhodium(III) data are those obtained with the surfactant hexadecyltrimethylammonium bromide (HTMAB) as rhodium(III) is not floated by HTPAB.

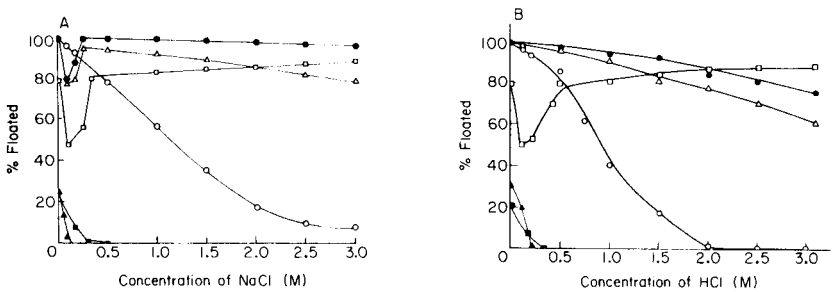

Fig. 3. Effect of (A) varying NaCl concentration at pH 2.0, and (B) varying HCl concentration, on percentage floated for each metal after 2 h. Initial conditions: [Metal] = 5×10^{-5} M, [HTMAB] = 2×10^{-4} M (for Rh(III) flotation), [HTPAB] = 2×10^{-4} M (for Ir(IV), Pt(IV), Ir(III), Pd(II) and Au(III) flotation), N_2 flow rate 10 cm^3 min^{-1}. (△) Pt(IV); (□) Au(III); (○) Pd(II); (●) Ir(IV); (■) Ir(III); (▲) Rh(III).

For solutions containing up to 3.0 M sodium chloride, colloidal precipitates are observed in the bulk solution when the Pt(IV), Ir(IV) or Au(III) is mixed with the surfactant, HTPAB. In dilute hydrochloric acid, precipitation is also observed, but for hydrochloric acid concentrations greater than 1.0 M, there is no precipitation observed with Pt(IV) or Ir(IV). Pd(II), Ir(III) and Rh(III) do not form precipitates with HTPAB and Rh(III) and Ir(III) form precipitates with other surfactants only in very dilute chloride solutions.

The flotation of gold(III) initially decreases as the HCl or NaCl concentration increases, then increases as the chloride concentration increases. The same phenomenon was observed for Pt(IV) and Ir(IV) in NaCl solutions, but not in HCl solutions. Observations similar to these were explained in a previous study by Walkowiak and Bartecki [11].

As the chloride concentration increases, the percentage floated for all metals except gold(III) decreases. The flotation of Pd(II) decreases to zero in $\geqslant$ 2.0 M HCl, and the degree of flotation for Rh(III) and Ir(III) is reduced to zero in solutions containing $\geqslant$ 0.3 M chloride. These data are in agreement with the anion-exchange distribution coefficients obtained for the platinum metals eluted with various concentrations of hydrochloric acid [19, 20]. For all the metals except gold(III), the distribution coefficients decrease with increasing hydrochloric acid concentration.

Influence of surfactant and metal chlorocomplex concentration on flotation

It is important to know if variations in the initial concentrations of either the surfactant or colligend result in significant differences in the percentage of metal floated. For the first series of experiments, the metal chlorocomplex concentration was fixed and the surfactant concentration was varied. The percentage of metal chlorocomplex floated vs. the concentration of surfactant is plotted in Fig. 4. For the second series of experiments, the surfactant concentration was held constant and the metal chlorocomplex concentration was varied. The percentage of metal chlorocomplex floated vs. the initial metal chlorocomplex is plotted in Fig. 5. For both series of experiments, gold(III) was floated with PTMAB; the other metals with HTPAB.

The sublate salt contains a stoichiometric amount of colligend and collector. Therefore, to float 100% of univalent and divalent ions, the surfactant must be present in at least 1:1 and 2:1 molar amounts, respectively. Figures 4 and 5 indicate that 100% of the metal chlorocomplex ions are floated only when there is an excess of collector. An excess of collector is necessary to provide a foam support which prevents redispersion of the sublate into solution.

Figures 4 and 5 indicate that the careful control of initial concentrations of both the surfactant and metal ions is not critical for achieving 100% flotation as long as there is an excess of collector added. It is interesting to note that in other studies [13, 16, 22] flotation was found to pass through a maximum with increasing surfactant/metal ion ratios. The decrease in the

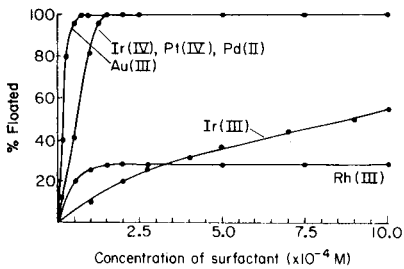

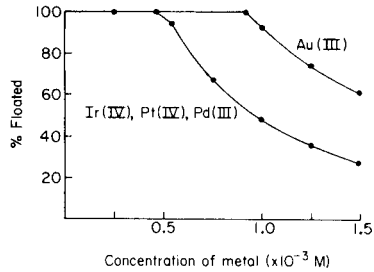

Fig. 4. Effect of varying surfactant concentration on percentage of metal floated after 2 h. Initial conditions: [Metal] = 5×10^{-5} M, pH 2, N_2 flow rate 10 cm^3 min^{-1}. PTMAB was used to float Au(III). HTPAB was used to float Ir(IV), Pt(IV), Pd(II) and Ir(III). HTMAB was used to float Rh(III).

Fig. 5. Effect of varying initial metal concentration on percentage of metal floated after 2 h. Initial conditions: [HTPAB] = 1×10^{-3} M (for Pt(IV), Pd(II) and Ir(IV) flotation), [PTMAB] = 1×10^{-3} M (for Au(III) flotation), pH 2.0, N_2 flow rate 10 cm^3 min^{-1}.

TABLE 4

Recovery data for Au(III), Ir(IV), Pd(III) and Pt(IV)

Metal	Surfactant	Amount (mg)		%	Method of determination [Ref.]
		added	recovered		
Au(III)	PTMAB	4.924	4.913	99.8	Hydroquine [24]
Au(III)		4.924	4.920	99.9	
Au(III)		4.924	4.890	99.3	
Ir(IV)	HTPAB	4.805	4.796	99.8	Mixed acids [25]
Ir(IV)		4.805	4.810	>100	
Ir(IV)		4.805	4.798	99.8	
Pd(II)	HTPAB	2.660	2.645	99.4	Diethyldithiocarbamate [26]
Pd(II)		2.660	2.615	98.3	
Pd(II)		2.660	2.639	99.2	
Pt(IV)	HTPAB	4.877	4.791	98.2	Diethyldithiocarbamate [27]
Pt(IV)		4.877	4.803	98.5	
Pt(IV)		4.877	4.862	99.7	

percentage of colligend floated was attributed to the formation of micelles, or to the "coating" of the colloidal sublate with surfactant molecules which render it hydrophilic. Even though a flotation maximum was not observed in these studies, it is important to realize that a large excess of surfactant produces a large volume of foam which reduces the usefulness of ion flotation as a concentrating procedure.

Recovery by ion flotation

The practical advantage of ion flotation is that the technique may be used to recover ions from dilute solution. Data are presented in Table 4 for Au(III),

Pt(IV), Ir(IV) and Pd(II) which indicate that these metals may be quantitatively recovered from dilute solutions when floated under optimum conditions. As the condensed foam volume in all cases was found to be less than 0.5 ml, enrichments of 200-fold were obtained.

The platinum metals may be collected from dilute solutions by passing the solutions through anion-exchange resins, but their recovery from these resins is often a tedious task involving soxhlet extractions for long periods under extreme conditions [23]. Thus, the simple, one-step wet ashing of the sublate with nitric acid for recovering the metal chlorocomplexes yields considerable improvement over their recovery from ion exchange resins.

Separation by ion flotation

A separation by ion flotation of a binary mixture of two ions can be obtained if the conditions are adjusted so that one ion floats while the other remains in the bulk solution. The data presented above indicate that separations of Au(III), Pd(II), Pt(IV) and Ir(IV) from Ir(III) and Rh(III) are possible because the percentage of Ir(III) and Rh(III) floated decreases to zero as the chloride concentration increases and as the surfactant secondary chain length increases. Furthermore, the separation of Au(III), Pt(IV) and Ir(IV) from Pd(II) is possible by adjusting the hydrochloric acid concentration.

Single-stage, batch flotation procedures for mixtures of the platinum metals based on these observations will be presented in forthcoming papers.

REFERENCES

1 F. Sebba, Nature, 184 (1959) 1062.
2 R. B. Grieves, Chem. Eng. J. (Lausanne), 9 (1975) 93.
3 A. N. Clark and D. J. Wilson, Sep. Purif. Methods, 7 (1978) 55.
4 P. Somosundaran, Sep. Sci., 10 (1975) 93.
5 F. Sebba, Ion Flotation, Elsevier, New York, 1962, p. 93.
6 W. Charewicz and J. Niemiec, Nukleonika, 14 (1969) 113.
7 W. Walkowiak and R. B. Grieves, J. Inorg. Nucl. Chem., 38 (1976) 1351.
8 W. Walkowiak, D. Bhattacharyya and R. B. Grieves, Anal. Chem., 48 (1976) 975.
9 W. Charewicz and W. Walkowiak, Sep. Sci., 7 (1972) 631.
10 W. Walkowiak and A. Bartecki, Nukleonika, 18 (1973) 209.
11 W. Walkowiak and A. Bartecki, Nukleonika, 18 (1973) 133.
12 F. Kepak and J. Kriva, Sep. Sci., 5 (1970) 385.
13 T. A. Pinfold, in R. Lemlich (Ed.), Adsorptive Bubble Separation Techniques, Academic Press, New York, 1972, p. 53, p. 70.
14 S. I. Ginzburg, Analytical Chemistry of the Platinum Group Metals, Halsted Press, New York, 1975, p. 298.
15 E. B. Sandell, Colorimetric Determination of Traces of Metals, 3rd edn., Interscience, New York, 1959, p. 769.
16 R. B. Grieves and W. Charewicz, Anal. Lett., 7 (1974) 233; J. Inorg. Nucl. Chem., 36 (1974) 2371.
17 D. W. Fuerstenau, in R. Lemlich (Ed.), Adsorptive Bubble Separation Techniques, Academic Press, New York, 1972, p. 113.
18 R. B. Grieves, D. Bhattacharyya and J. K. Ghosal, Colloid Polym. Sci., 254 (1976) 507.
19 S. S. Berman and W. A. E. McBryde, Can. J. Chem., 36 (1958) 835.

20 K. A. Kraus and F. Nelson, J. Am. Chem. Soc., 76 (1968) 339.
21 B. L. Karger and M. W. Miller, Anal. Chim. Acta, 48 (1969) 273.
22 R. B. Grieves and D. Bhattacharyya, Sep. Sci., 3 (1968) 185.
23 S. S. Berman and W. A. E. McBryde, Can. J. Chem., 36 (1958) 845.
24 W. B. Pollard, Analyst (London), 62 (1937) 597.
25 G. H. Ayres and Q. Quick, Anal. Chem., 22 (1950) 1403.
26 W. B. Pollard, Analyst (London), 67 (1942) 184.
27 W. B. Pollard, Trans. Inst. Min. Met., 47 (1937) 331.

Analytica Chimica Acta, 120 (1980) 249—254

QUANTITATIVE SEPARATION OF LANTHANIDES AND SCANDIUM FROM BARIUM, STRONTIUM AND OTHER ELEMENTS BY CATION-EXCHANGE CHROMATOGRAPHY IN NITRIC ACID

F. W. E. STRELOW

National Chemical Research Laboratory, P.O. Box 395, Pretoria 0001 (Republic of South Africa)

(Received 27th May 1980)

SUMMARY

The lanthanides plus yttrium and scandium are separated from Ba, Sr, Ca, Mg, Pb(II), Bi(III), Zn, Mn(II) and U(VI) by eluting these elements with 2.0 M nitric acid from a column of AG50W-X8 cation exchange resin (200—400 mesh). The lanthanides are retained and can then be eluted with 4 M nitric or hydrochloric acid. Separations are quantitative and applicable to microgram and millimolar amounts of the lanthanides and the other elements. Elements such as Cu(II), Co(II), Ni(II), Cd, Hg(II), Tl(I), Ag, Be, Ti(IV) and the alkali metals should accompany barium quantitatively according to their known distribution coefficients. Relevant elution curves and results of analysis of synthetic mixtures are presented.

Most elements can be separated from the lanthanides by elution with 1.75 M hydrochloric acid [1] from a cation-exchange resin column. The only elements which accompany the lanthanides are Y, Sc, Zr, Hf, Ba and Sr (partially). An even better separation from aluminium, iron(III) and most other elements can be obtained by eluting these with 3.0 M hydrochloric acid containing 50% ethanol [2], but all the strontium and part of the calcium are retained together with the lanthanides in addition to the elements named above. Furthermore, during the anion-exchange separation of the lanthanides in nitric acid mixture with methanol or other organic solvents [3—6], barium again is found with the medium and strontium with the heavier lanthanides; Pb(II), Bi(III) and U(VI) are also retained. In some cases considerable amounts of barium and strontium occur together with lanthanides in ores such as the bastnäsite standards IGS40 and IGS41 of the British Institute of Geological Sciences. A method for the complete separation of barium and strontium from lanthanides at a wide range of concentration ratios therefore should be of some interest. Separation by the classical hydroxide precipitation is rather unsatisfactory when the amounts of lanthanides and barium plus strontium are widely different. Separation is possible by cation exchange in α-hydroxyisobutyrate, but has been applied only to radiotracer amounts [7, 8] and the presence of large amounts of the organic reagent does not seem to be very attractive. Even larger separation factors can be obtained by

using EDTA or other aminopolycarboxylic acids of a suitable pH as eluting agents. Differences in complex stability constants between the lanthanides and barium or strontium range from about 6 to more than 12 orders of magnitude. Again the presence of the complexing agent makes this approach less attractive for further work and, in addition, ion-exchange kinetics in the presence of EDTA often are not very favourable. A volatile inorganic acid would be much more attractive as eluting agent.

It has been shown that strontium and especially barium have considerably lower distribution coefficients in nitric than in the corresponding concentrations of hydrochloric acid [9]. An investigation of available distribution coefficient data [10] shows that the use of 2.0 M nitric acid as eluting agent and an 8% cross-linked resin should offer good prospects for a separation. Gadolinium and europium have the lowest distribution coefficient of the lanthanides with a value of about 29, while that for barium is about 12. The separation factor for the most critical elements is therefore rather small and relatively large columns are required for the separation of larger amounts. Many other elements such as lead, calcium and all the other di- and monovalent elements should accompany barium and strontium. The quantitative aspects of this separation were investigated in detail and the results are presented below. Scandium, which has a coefficient even smaller than gadolinium, was included in the investigation.

EXPERIMENTAL

Reagents and apparatus

Lanthanides and yttrium and scandium oxides of $\geqslant 99.9\%$ purity (Fluka AG, Buchs, Switzerland) were dissolved in dilute nitric acid. All other reagents were of analytical-reagent grade. Water was distilled and then passed through an Elgastat deionizer. The resin was the AG50W-X8 sulphonated polystyrene cation exchanger (200—400 mesh; Bio-Rad Laboratories, Richmond, California). Borosilicate glass tubes of 24-mm bore, with fused-in glass sinters of No. 2 porosity and a buret tap at the bottom and a B19 ground-glass joint at the top were used as columns.

A Varian-Techtron AA5 instrument was used for atomic absorption measurements.

Elution curves

A resin containing 90 ml (30 g; 20 cm long) of AG50W-X8 resin (200—400 mesh) was prepared and equilibrated with 0.1 M nitric acid. A solution containing 2.2 mmol of barium and 1 mmol of gadolinium in about 50 ml of 0.5 M nitric acid was passed onto the column and the ions were washed onto the resin with 0.1 M nitric acid. Barium followed by gadolinium were then eluted with 2.0 M nitric acid using a flow rate of 2.5 ± 0.3 ml min^{-1} throughout. Fractions of 25-ml volume were taken with an automatic fractionator from the beginning of the elution step. The excess of acid in the fractions was removed by evaporation on a water bath and the amounts of the elements

in the fractions were determined. Barium was determined by atomic absorption spectrometry (a.a.s.) in 0.5 M hydrochloric acid using a nitrous oxide—acetylene flame, a wavelength of 553.5 nm, and 1000 ppm of potassium as flame ionization suppressor. Suitable dilution was applied when required. Large amounts of gadolinium were determined gravimetrically as the oxide after precipitation with ammonia, and small amounts by complexometric titration with 0.001 M EDTA at pH 5.5 using xylenol orange as indicator. The experimental elution curve is shown in Fig. 1A.

Figure 1B shows an experimental curve for a mixture of 2 mmol of barium and 1 mmol of scandium using exactly the same conditions. Ytterbium (1 mmol) appeared in the eluate at about 950 ml and 2 mmol of the same element did so after about 750 ml of 2 M nitric acid had been passed through the column. No lanthanum could be detected in the first 1000 ml of eluate when 1 mmol of this element were present; when 2 mmol were present, it appeared at about 950 ml in the eluate. Figure 2 shows an experimental curve for a mixture of 2.2 mmol of strontium and 2.3 mmol of lanthanum. The elution with 2.0 M nitric acid was terminated after 500 ml had been passed and the elution of lanthanum was continued with 4.0 M nitric acid. The other lanthanides are less strongly adsorbed than lanthanum. Calcium and magnesium are eluted even ahead of strontium, and most other divalent elements behave in the same way.

Quantitative separations

Appropriate volumes of a lanthanide or yttrium or scandium and of one other element were measured out accurately and mixed. The solution containing between 0.1 and 0.5 M nitric acid was passed onto a column containing 90 ml of AG50W-X8 cation-exchange resin as described above under "Elution curves", and the ions were washed onto the resin with small portions of 0.1 M nitric acid. The "other element" was then eluted with 500 ml of 2.00 M nitric acid at a flow rate of 2.5 ± 0.3 ml min^{-1} and finally the lanthanide, yttrium or scandium was eluted with 400 ml of 4.00 M nitric acid at the same flow rate. The eluates were evaporated to small volumes, transferred to small beakers and the elements determined by suitable methods. Two blank runs were carried through the separation procedure and the results corrected accordingly. The quantitative results obtained are presented in Table 1 and the analytical methods used are summarized in Table 2.

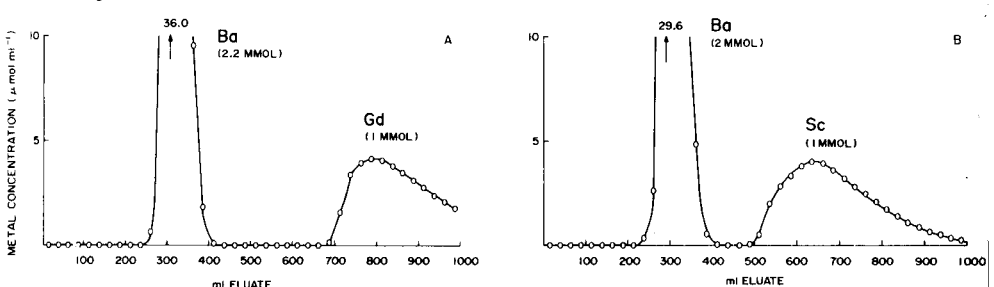

Fig. 1. Elution curve for (A) Ba—Gd and (B) Ba—Sc with 2.0 M HNO_3. Conditions as in text.

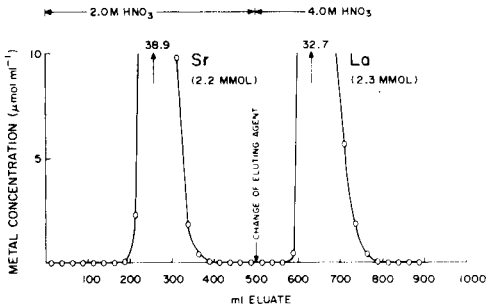

Fig. 2. Elution curve Sr—La with nitric acid. Conditions as in text.

DISCUSSION

The method described provides a useful means for the quantitative separation of the lanthanides plus yttrium and scandium from Ba, Sr, Ca, Mg, Pb(II), Bi(III), Zn, Mn(II) and U(VI). With columns of the described size, separations are quantitative and quite satisfactory for amounts ranging from less than 1 μmol of barium or the other elements to more than 2 mmol and from less than 1 μmol of the lanthanide group to at least 2 mmol of La, Ce, Pr, Yb and Lu but only slightly more than 1 mmol of Gd and Eu, the elements of this group which are least strongly adsorbed in nitric acid. The other

TABLE 1

Quantitative separations of synthetic mixtures

Taken		Found[a]	
Lanthanide (mg)	Other element (mg)	Lanthanide (mg)	Other element (mg)
Yb 162.6	Ba 271.8	162.7 ± 0.1	271.9 ± 0.2
Yb 0.994	Ba 271.8	0.992 ± 0.003	271.8 ± 0.2
Yb 325.2	Ba 0.272	325.2 ± 0.2	0.271 ± 0.003
Yb 325.2	Sr 174.2	325.1 ± 0.2	174.7 ± 0.2
Yb 162.6	Ca 80.42	162.6 ± 0.1	80.41 ± 0.04
Yb 162.6	Mg 48.04	162.6 ± 0.1	48.05 ± 0.03
Yb 162.6	Pb(II) 208.6	162.7 ± 0.1	208.6 ± 0.1
Yb 162.6	Bi(III) 207.1	162.6 ± 0.1	207.0 ± 0.2
Yb 162.6	Zn 130.5	162.5 ± 0.1	130.5 ± 0.1
Yb 162.6	Mn(II) 110.6	162.6 ± 0.1	110.5 ± 0.1
Yb 162.6	U(VI) 238.8	162.7 ± 0.1	238.8 ± 0.1
Gd 155.7	Ba 271.8	155.6 ± 0.1	271.9 ± 0.2
La 279.8	Ba 271.8	279.7 ± 0.2	271.8 ± 0.3
Y 89.44	Ba 271.8	89.46 ± 0.05	271.7 ± 0.2
Sc 23.13	Ba 271.8	23.13 ± 0.02	271.8 ± 0.2
Sc 46.26	Ba 271.8	46.18 ± 0.03	271.9 ± 0.2

[a]Mean of triplicate determinations.

TABLE 2

Analytical methods used

Element	Method
Yb, Gd, La, Y	Gravimetrically as the oxide after precipitation as the oxalate from 0.1 M hydrochloric acid. Small amounts (and elution curves) of Yb by a.a.s. with a nitrous oxide—acetylene flame, the 398.8-nm line, and 2000 ppm potassium as flame ionization buffer.
Sc	Titration with EDTA at pH 3.5; xylenol orange indicator.
Ba	Gravimetrically as $BaSO_4$; small amounts by a.a.s. with a nitrous oxide—acetylene flame, the 553.5-nm line; and 2000 ppm potassium as flame ionization buffer.
Sr	Gravimetrically as $SrSO_4$; ethanol added after precipitation.
Ca, Mn(II)	Titration with EDTA in excess of ammonia; methylthymol blue indicator; hydroxylammonium chloride present for Mn(II).
Mg	Titration with EDTA at pH 10; eriochrome blue-black B indicator.
Pb(II), Zn	Titration with DCTA at pH 5.5; xylenol orange indicator.
Bi(III)	Titration with EDTA at pH 1; xylenol orange indicator.
U(VI)	Gravimetrically as U_3O_8 after precipitation with CO_2-free ammonia solution.

lanthanides are somewhere in between. Scandium is adsorbed even less strongly than gadolinium and has a distribution coefficient of about 24. Only up to about 0.5 mmol can be separated with some safety margin. When about 1 mmol is present, the separation becomes marginal (Fig. 2) and about 2 μmol can appear in the "other element" fraction when the cut is made at 500 ml. Barium shows a slight low-level tailing and 26 ± 4 μg were found in the ytterbium fraction when 271.8 mg were present originally. The cross-contamination therefore was about 0.01% at this level. The amount of ytterbium (162.6 mg present) found in the barium fraction was below 0.5 μg, the detection limit of the method used.

Many other elements, though not investigated in detail, should accompany barium quantitatively because of their known distribution coefficients [10]. These elements include Cu(II), Co(II), Ni(II), Cd, Hg(II), Tl(I), Ag, Be, Ti(IV) and all the alkali metals. Indium, Ga, Al and Fe(III) are very similar to scandium in their behaviour. Small amounts of up to about 0.5 mmol accompany the lanthanides quantitatively. For larger amounts the separation becomes unsatisfactory. These trivalent elements can be separated from the lanthanides by cation exchange in 1.75 M hydrochloric acid [1] or in 3.00 M hydrochloric acid containing 50% or 60% ethanol [2]. The only other elements which accompany the lanthanides are zirconium, hafnium, and thorium. Thorium is retained by the column when the lanthanides are eluted with 425 ml of 4.0 M hydrochloric acid instead of 400 ml of nitric acid. Furthermore, all three elements can be separated from the lanthanides by anion exchange in dilute sulphuric acid [11]. The method is applicable to the accurate analysis of minerals and rocks containing both the lanthanides and the heavy alkaline earths as major components, but it also should have many other applications.

REFERENCES

1 F. W. E. Strelow, Anal. Chim. Acta, 34 (1966) 387.
2 F. W. E. Strelow and C. Baxter, Talanta, 16 (1969) 1145.
3 R. A. Edge, Anal. Chim. Acta, 29 (1963) 321.
4 J. P. Faris and J. W. Warton, Anal. Chem., 34 (1962) 1077.
5 I. Roelandts, G. Duykaerts and A. O. Brunfelt, Anal. Chim. Acta, 73 (1974) 141.
6 J. Alstad and A. O. Brunfelt, Anal. Chim. Acta, 38 (1967) 185.
7 A. P. Baerg and R. M. Bartholomew, Can. J. Chem., 35 (1957) 980.
8 L. Wish, Anal. Chem., 33 (1961) 53.
9 F. W. E. Strelow, Anal. Chem., 32 (1960) 1185.
10 F. W. E. Strelow, R. Rethemeyer and C. J. C. Bothma, Anal. Chem., 37 (1965) 106.
11 F. W. E. Strelow and C. J. C. Bothma, Anal. Chem., 39 (1967) 595.

Analytica Chimica Acta, 120 (1980) 255—266

STUDIES ON THE SEPARATION OF ANIONS WITH 8-HYDROXYQUINOLINIUM ION AS COUNTERION

MAO-SUNG KUO[a] and HORACIO A MOTTOLA*

Department of Chemistry, Oklahoma State University, Stillwater, OK 74078 (U.S.A.)

(Received 10th March 1980)

SUMMARY

Distribution constants, K_D, for 8-hydroxyquinolinium—anion pairs and for a series of inorganic and organic anions are reported between aqueous acidic phases and 1-butanol and 3-methyl-1-butanol. As expected, K_D values are larger for anions with relatively large crystal radius (e.g., $Cl^- < I^- < R—SO_3^-$), smaller for anions containing either hydroxyl or carboxyl groups favoring solvation by water (e.g., HSO_4^-, $HSeO_3^-$, $H_2PO_4^-$, $C_6H_5COO^-$, CH_3COO^-) and larger in solvents with larger solubility parameters (e.g., 4-methyl-2-pentanone < 3-methyl-1-butanol < 1-butanol). Distribution constants between aqueous solutions and 8-hydroxyquinoline immobilized (chemically) on controlled-pore glass are estimated for a series of aromatic and aliphatic sulfonates. Aromatic sulfonates show substantially larger K_D values than aliphatic sulfonates. Batch equilibration data were used to design chromatographic (liquid—solid) separation of a few sulfonates.

Solvent extraction of ion-pairs and liquid—liquid and liquid—solid chromatographic separations involving ion-pair formations is a well recognized technique in analytical chemistry. For certain chemical species (e.g., pharmaceutical drugs and some other organic compounds) the efficiency of extraction and selectivity are better with ion-pairs than in other extraction systems involving the partition of molecular (uncharged) species [1]. Inorganic anions [2, 3] and hydrophilic organic compounds [4] have been successfully extracted and separated after ion-pair formation. Ion-pair formation and distribution between two immiscible phases has particular advantages for aprotic ions (e.g., quaternary ammonium ions, sulfonates, organic sulfates) and for compounds that are difficult to extract in uncharged form (e.g., amino acids and aminophenols) [5].

As early as 1952, Dyrssen [6] investigated the distribution of 8-hydroxyquinoline between acidic aqueous solutions and 4-methyl-2-pentanone (methyl isobutyl ketone) and reported the extraction of 8-hydroxyquinolinium ion, H_2Q^+, as an ion-pair with perchlorate ion. Dyrssen proposed a simplified model to account for the ion-pair extraction and estimated the value of the distribution constant, $K_D(H_2Q^+, ClO_4^-)$, for the ion-pair species as

---

[a]Permanent address: Department of Chemistry, Tunghai University, Taichung, Taiwan, Republic of China.

0.11. Dyrssen's model and approach was later applied by Mottola and Freiser [7] to the extraction of the same species into 3-methyl-1-butanol (isopentyl alcohol). They reported a value of 0.8 for the corresponding distribution constant, which showed the expected increase with increasing solubility parameter of the organic solvent [7]. Hydrogensulfate anion was only poorly extracted under the same conditions [7]. These earlier observations, suggesting the use of 8-hydroxyquinolinium ion for the chromatographic separation of anions, motivated the studies presented in this paper. These can be organized into three distinct groups itemized in this paper as: (1) batch distribution studies of a variety of organic and inorganic anions with 8-quinolinium ion and between aqueous acidic solutions and 3-methyl-1-butanol or 1-butanol; (2) batch distribution studies for some hydrocarbon sulfonates between aqueous solution and 8-hydroxyquinoline immobilized (by chemical attachment) on controlled-pore glass; and (3) chromatographic separation of some arenesulfonates using immobilized 8-hydroxyquinoline.

LIQUID—LIQUID DISTRIBUTION OF 8-HYDROXYQUINOLINIUM—ANION PAIRS

Experimental

Reagents. Organic solvents and all chemicals used were of analytical-reagent grade. Deionized—distilled water was used for preparation of aqueous solutions. The alcohols were purified by shaking with 0.01 M NaOH (2:1 volume ratio) and then rinsing with deionized—distilled water to remove potential oxidants [8].

Apparatus. A Corning 7 pH meter equipped with a Sargent S-300070-10, miniature combination electrode was used for pH measurements. Temperature control of water baths was provided by a Brinkman IC-2 regulator—circulator. Spectrophotometric measurements were done with a Bausch and Lomb Spectronic 505 and matched 1-cm quartz cells. A custom-made shaker was used throughout the batch equilibrations reported; it is based on an air-driven mechanism provided by a vacuum motor for a windshield wiper of the type commonly used in automobiles.

Procedure. A volume (10 or 15 ml) of solution of 8-hydroxyquinoline of known concentration in 1-butanol or 3-methyl-1-butanol was shaken with an equal volume of an aqueous phase in 30-ml vials stoppered with plastic caps. The ionic strength of the aqueous phase was adjusted to 0.10 by addition of a sodium salt (e.g., $NaHSO_4$, NaCl, $NaClO_4$, or Na_2SO_4) and the pH adjusted to the desired value by addition of sulfuric acid. The two phases were contacted for 15 min in the shaker (31 excursions/min). Beyond 15 min of shaking, no significant difference in the distribution ratio values was observed. While separation of the phases occurred rapidly after extraction, the solutions were allowed to stand for 1 h at 25 ± 0.2°C in a water bath to insure complete phase separation at constant temperature. The volume of each phase was found to be unchanged after this equilibration.

After phase separation, an aliquot of the aqueous phase was removed by

dipping a pipet into the aqueous layer while exerting a positive pressure through the empty pipet to prevent the entrance of organic solvent. The pH of this aliquot was measured as the equilibrium pH value. Another aliquot portion of convenient size (generally 5 ml) of the aqueous phase was transferred to a 20-ml beaker and its pH adjusted as closely as possible to 1.0 by dropwise addition of 1.0 M HCl or other acid. The solution was then quantitatively transferred to a 25-ml volumetric flask by rinsing and diluting to the mark with 0.10 M HCl or other acid previously used. The same procedure was followed with blanks run with solvent containing no 8-hydroxyquinoline. The absorbance of the aqueous phase so treated was measured at 360 nm against the blank and the concentration of 8-quinolinium ion found by reference to a calibration curve prepared in a similar way. Molar absorptivities varied slightly with the acid used (see Table 1).

Results and discussion

Dyrssen's simplified model for the solvent extraction of 8-hydroxyquinolinium—anion ion-pairs leads to the following equation [6]:

$$D = K_{D(H_2Q^+, A^-)} + K_{a_1} \cdot K_{D(HQ)} \cdot [H^+]^{-1} \quad (1)$$

which suggests the determination of $K_D(H_2Q^+, A^-)$ values by plots of the distribution ratio, D as a function of $1/[H^+]$ and extrapolation to $(1/[H^+]) = 0$. The slope of these plots should be equal to the product $K_{a_1} \cdot K_D(HQ)$, the first ionization constant for 8-hydroxyquinolinium ion and the distribution constant of 8-hydroxyquinoline in the corresponding organic solvent—water pair, respectively. Table 2 lists values of K_D obtained by applying this approach to the experimental data. Not included are data for periodate, which as a rather strong oxidizing agent is unstable in acidic medium. The change of D values (and by extension the partition constant value obtained by extrapolation) for the periodate ion-pair over a period of time is shown in Fig. 1. It can be seen that K_D values, as expected, decrease with time. A value close to 1 can, however, be estimated for $K_D(H_2Q^+, IO_4^-)$. The tab-

TABLE 1

Molar absorptivities (ϵ) at 360 nm for 8-hydroxyquinolinium ion in different media

Medium	ϵ ($\times 10^3$ l mol^{-1} cm^{-1})	Medium	ϵ ($\times 10^3$ l mol^{-1} cm^{-1})
0.10 M HCl	1.70	0.59 M H_3PO_4	1.88
0.10 M $HClO_4$[a]	1.72	0.10 M HCl[b]	1.58
0.10 M CH_3COOH	1.83	0.10 M HCl[c]	1.57

[a] A value of 1.65 ± 0.03 × 10^3 cm^{-1} has been reported for the molar absorptivity in 0.10 M perchlorate [7].
[b] 8-Hydroxyquinoline added as the benzoate (Ashland Chemical Co.).
[c] 8-Hydroxyquinoline added as the citrate (Ashland Chemical Co.).

TABLE 2

Distribution constants of 8-hydroxyquinolinium ion in the presence of a variety of anions as obtained by Dyrssen's equation (eqn. 1)
(Temp. = 25 ± 0.2°C; ionic strength = 0.10)

Anion	$K_D(H_2Q^+, A^-)$	$K_D(HQ)^a$	Anion	$K_D(H_2Q^+, A^-)$	$K_D(HQ)^a$
Distribution between 3-methyl-1-butanol and aqueous phases			*Distribution between 1-butanol and aqueous phases*		
HSO_4^-	0.073	203	HSO_4^-	0.39	72.3
$HSeO_3^-$	0.097	70.5	Cl^-	0.55	332
$H_2PO_4^-$	0.15	412	I^-	0.92	563
AsO_2^-	0.15	71.1	ClO_4^-	1.8	1260
Cl^-	0.20	71.1	Penicillinate	0.38	30.7
I^-	0.40	132	*p*-Toluenesulfonate	3.0	1677
ClO_4^-	0.76	304			
$C_6H_5COO^-$	0.13	40.6			
CH_3COO^-	0.21	90.1			

[a]Calculated by dividing the slope of Dyrssen's plot by 1.41×10^{-5}, taken as the K_{a_1} value for 8-hydroxyquinoline [7].

ulated values of $K_D(H_2Q^+, A^-)$ follow the trend to be expected for the nature of the solvent systems involved, the nature of the anion, and the side reactions (protolysis) taking place in the aqueous phase. The increasing order for chloride, iodide and perchlorate, for instance, reflects the fact that chloride, with the smallest crystal radius (larger hydrated-ion radius), would be expected to form the weakest ion-pair and consequently be the most poorly extracted. Large and poorly hydrated ions (e.g., perchlorate or the sulfonates) should form ion-pairs more soluble in the organic phase than the aqueous phase (Fig. 2). If a comparison is made among the oxygen-containing anions, the low values for HSO_4^-, $HSeO_3^-$, $H_2PO_4^-$, $C_6H_5COO^-$, and CH_3COO^- (compared with perchlorate) can be understood: all these anions contain either hydroxyl or carboxyl groups that favor solvation by water and thus produce poor ion-pairing characteristics. As to the extracting organic solvent, $K_D(H_2Q^+, A^-)$ values in 1-butanol are about twice as large as those in isopentyl alcohol. This is to be expected on the basis of the larger solubility parameter of 1-butanol which is due to larger dipole–dipole interactions and greater hydrogen bonding capabilities. At least on a qualitative basis, the Dyrssen model produces K_D values which do not contradict the expected trend. A disturbing aspect, however, is revealed when the slopes of the plots used for K_D estimation are considered. These slopes should all have the same value in a given solvent pair, but this was not the case. Undoubtedly, some of the assumptions made to derive eqn. (1) are not valid. Particularly suspect is the assumption that the factor $K_f[A^-]_{aq}$ (with K_f as the formation constant for the ion-pair in the aqueous and subscript aq indicating the aqueous phase) must have a value close to 1 if the following reactions are considered:

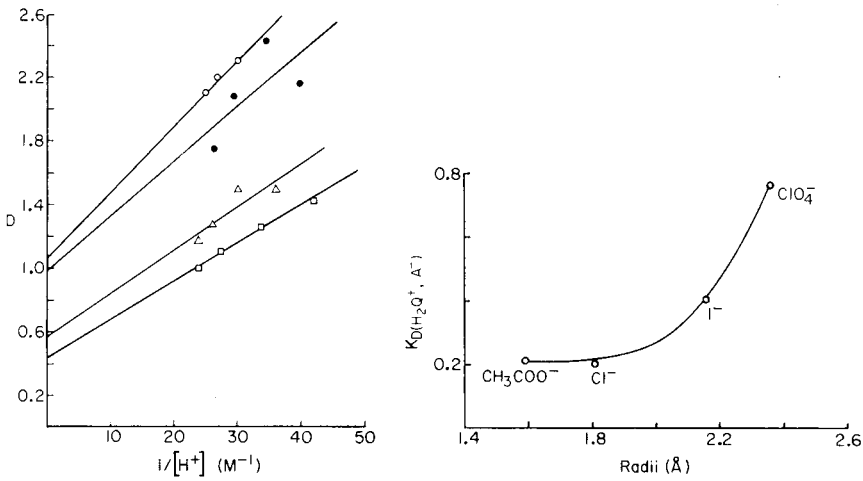

Fig. 1. Dyrssen's plots for extraction of 8-hydroxyquinolinium—periodate ion-pairs into isopentyl alcohol from acidic aqueous solutions; ionic strength = 0.10 M; 25.0 ± 0.2°C. Time after equilibration: (○) 2.5 h; (●) 3.0 h; (△) 3.5 h; (□) 45.0 h.

Fig. 2. Plot of ion-pair distribution constant (obtained from Dyrssen's plots) for some selected anions as a function of anion crystal radius. Data for isopentyl alcohol from Table 2. Crystal radii taken from Y. Marcus, Introduction to Liquid State Chemistry, J. Wiley, New York, 1977, pp. 250, 251.

$$(H_2Q^+)_{aq} + (A^-)_{aq} \rightleftharpoons (H_2Q^+, A^-)_{org} \quad (2)$$

$$(H_2Q^+)_{aq} \rightleftharpoons (H^+)_{aq} + (HQ)_{aq} \quad (3)$$

$$(HQ)_{aq} \rightleftharpoons (HQ)_{org} \quad (4)$$

$$(H^+)_{aq} + (A^-)_{aq} \rightleftharpoons (HA)_{aq} \quad (5)$$

for which the following equilibrium constants apply. K_{ex}^{-} (H_2Q^+, A^-) is the equilibrium (extraction) constant for reaction (2); K_{a1} is the H_2Q^+ ionization constant for reaction (3); $K_D(HQ)$ is the partition constant for neutral 8-quinolinol, i.e. reaction (4); and $1/K_a(HA)$ is the reciprocal of the ionization constant for the protonated species of the pairing anion in reaction (5). Derivation of D from the reactions shown above leads to:

$$D = K_{ex\,(H_2Q^+, A^-)}\,[H^+]\,[A^-]_{aq} + K_{D(HQ)} \cdot K_{a1}/([H^+] + K_{a1}) \quad (6)$$

Equation (6) reduces to eqn. (1) if $K_{a1} \ll [H^+]$, say by a factor of 10^{-3}, and if $K_f[A^-]_{aq}$ is close to 1. $K_f = [H_2Q^+, A^-]/[H_2Q^+]\,[A^-]$ in the aqueous phase.

The first condition is valid for 8-quinolinol at pH about 1—2 (K_{a1} for 8-quinolininium ion close to 10^{-5}) but the second condition becomes the doubtful one. A knowledge of K_f and $[A^-]_{aq}$ from independent experiments is needed, however, to confirm or end this suspicion.

The qualitative correlation of $K_D(H_2Q^+, A^-)$ values obtained from Dyrssen's

treatment with the trend expected from solvent and anion properties, however, permits some confidence in them as guidance for the design of chromatographic separations.

DISTRIBUTION STUDIES INVOLVING 8-HYDROXYQUINOLINIUM ION IMMOBILIZED ON CONTROLLED-PORE GLASS

Experimental

Reagents and materials. Two types of supports were used in these studies. One was a commercially available (until recently) type (Corning Glass Works, distributed by Pierce Chemical Co., Rockford, Illinois) 8-hydroxyquinoline/CPG-550; this product had a particle diameter in the range of 177—840 μm, an average pore size of 55.0 nm, a typical surface area of 70 $m^2\ g^{-1}$, and a reported capacity of 0.03 mmol of bonded 8-hydroxyquinoline per g of resin. Plain, controlled-pore glass beads (CPG; Corning Glass Works distributed by Pierce Chemical Company) had the same pore size and surface area as the 8-hydroxyquinoline/CPG-550 but smaller particle diameter (37—74 μm).

The second type of support used was synthesized here. The starting material was aminopropyl CPG (Electro-Nucleonics, Fairfield, NJ) with 125—177-μm particle diameter, 54.4-nm mean pore size, 1.24-$cm^3\ g^{-1}$ pore volume, and 57-$m^2\ g^{-1}$ surface area. The procedure of Weetal [9] was modified in part by use of later information [10].

A 2-g portion of CPG—AMP was weighed out in a 50-ml beaker. After introduction of a solution of *p*-nitrobenzoyl chloride (2.84 g) in chloroform (25 ml) containing 5% triethylamine (1.94 g), the mixture was covered with aluminium foil and allowed to react overnight. The glass beads were then separated from the solution by filtering the mixture through filter paper. The treated glass beads were transferred to a 400-ml beaker by using 100 ml of 0.30 M sodium dithionite solution. The solution was heated at about 70°C with constant stirring for about 1.5 h. Some gases (HCl and SO_2) were expelled.

After cooling the mixture to room temperature, it was filtered as described above. The glass beads were transferred to another 400-ml beaker by use of 48 ml of 2 M HCl and the mixture chilled in an ice bath (ice + NaCl) at 0°C to −10°C. Sodium nitrite (1.2 g) was then added slowly with stirring for about 30 min. Foam was formed and the solution turned brownish yellow. The obtained mixture was placed in a vacuum desiccator and gases were evacuated for another 30 min using a water pump.

The liquid was then decanted and the beads washed with 100 ml of cold deionized—distilled water, 100 ml of cold 1% sulfamic acid solution, and twice more with 100-ml portions of cold deionized—distilled water. The diazotized glass was coupled to 8-hydroxyquinoline by adding 50 ml of saturated 8-hydroxyquinoline solution in 0.05 M Na_2CO_3 and stirring for about 40 min. A deep dark red color appeared. After filtering, the CPG—8HQ resin was washed with deionized—distilled water until the filtrate was

colorless. The product was finally air-dried.

All other chemicals used were of analytical-reagent grade.

Apparatus. For the atomic absorption determination of copper to ascertain the capacity of the prepared resin, a Perkin-Elmer Model 290B spectrometer was used with an Intensitron No. 2252 hollow-cathode lamp (Perkin-Elmer). Acetylene and air (1:1 ratio) were used as fuel and oxidant, respectively.

All pH measurements were made with a Beckman Zeromatic pH meter and a Sargent S-300070-10 miniature combination electrode. A Heath Model EU-20B strip chart recorder was connected to the pH meter to check pH readings at equilibrium.

In distribution studies involving the chloride ion as counterion, chloride concentration at equilibrium was determined potentiometrically with an Orion Model 801A digital pH/mV meter, an Ag^+/S^{2-} ion-selective electrode (Orion Model 94-16A) and a sleeve-type double-junction reference electrode (with Orion 90-00-02 inner filling solution and Orion 90-00-03, 10% KNO_3 outer filling solution). The chloride concentration was indirectly estimated by determining the free silver ion remaining after reaction with a known excess of silver nitrate added to the solution under study.

Aromatic sulfonates were determined by use of their absorption of radiant energy in the u.v. region of the spectrum and with the aid of a Bausch and Lomb Spectronic 505 and matched 1-cm quartz cells.

Aliphatic sulfonic acids were determined by potentiometric acid—base titration.

Procedure used in distribution studies. The experimental approach was similar to that described in the liquid—liquid distribution studies section. In place of the organic solvent containing 8-hydroxyquinoline, a known weighed amount of immobilized reagent (in the neighbourhood of 0.6 g) was equilibrated with the aqueous phase (3.00 ml) by shaking for 30 min. Beyond 20 min of shaking, no significant difference in the values of distribution ratios was observed.

Samples of immobilized reagent were re-used after repeated washing with deionized—distilled water and drying at about 120°C for 1 h. Pre-conditioning of the immobilized reagent was done by washing four more times with deionized—distilled water and removal of the excess of water.

Results and discussion

Table 3 summarizes comparative data on the capacity and pK_a characteristics of the Corning and the laboratory-prepared materials. Figure 3 depicts the distribution constant values obtained for a few sulfonate anions and chloride ions. The K_D^* values are defined as: K_D^* = (mmol of anion on the resin/g resin)/(mmol of anion in solution/ml). For comparison, results using plain CPG chips are included; similar results were obtained with the commercial and the laboratory-prepared resins. The K_D^* values follow the trend expected from the increase in hydrophobicity with increasing numbers of methyl or aryl carbons in the counterion. The pH trend is the expected

TABLE 3

Capacity and acid—base behavior of commercial and laboratory-synthesized 8-hydroxyquinoline—CPG resins

	Corning resin	Laboratory-made resin
Amount of copper taken up (mmol g^{-1} of resin)	0.18_4	0.38_9
pK_a ($CPG—H_2Q^+ \rightleftharpoons CPG—HQ + H^+$)	3.38 ± 0.10	3.28 ± 0.10

[a]Results are average of 6 determinations. For comparison, the pK_a value for 8-hydroxyquinoline under identical conditions was found to be 4.76 ± 0.05, a value in reasonable agreement with reported values, which range from 4.5 [11] to 5.23 [12]. The values reported here for pK_a of the immobilized 8-hydroxyquinolinium ion on CPG are comparable with the value of 3.3 reported by Jezorek and Freiser [13] for Porasil—8-hydroxyquinoline resin.

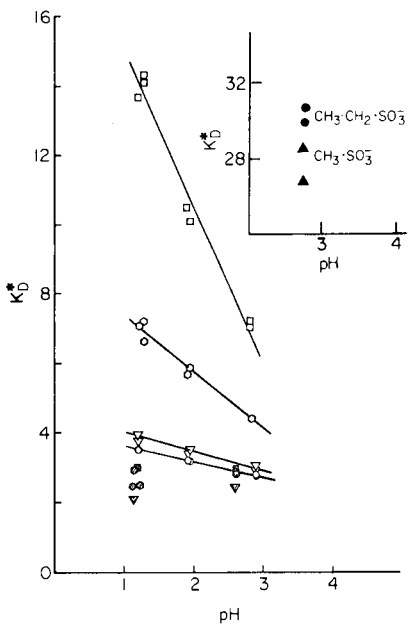

Fig. 3. K_D^* values (definition in text) for a series of aromatic and aliphatic sulfonates between CPG—8-hydroxyquinoline and acidic aqueous phases. Chloride is included for comparison. Ionic strength of aqueous phase: 0.10 M; 25.0 ± 0.2°C. Open symbols, CPG—8HQ; solid symbols, plain CPG. (○) 1-naphthalene; (▽) 2-mesitylene; (◇) *p*-toluene; (□) benzene.

one for ion-pairing and above a pH of 3 (in agreement with the pK_a value reported in Table 3) K_D^* values become small, rather constant with pH, and close to the values obtained with plain glass.

The results collected in Figure 3 suggest that immobilized 8-hydroxy-

quinolinium ion on CPG is potentially useful for (a) a group separation of aliphatic from aromatic sulfonates, and (b) column chromatographic separation of aromatic and aliphatic sulfonates utilizing the CPG—$8H_2Q^+$, A^- system as packing material. It should be noted that the mechanical strength of the inorganic silicate backbone of this packing is an advantage for high-pressure operation. This prompted the exploratory work reported below.

CHROMATOGRAPHIC SEPARATION OF SOME AROMATIC SULFONATES WITH CPG—8-HYDROXYQUINOLINE AS PACKING MATERIAL

Experimental

Reagents and materials. Most of the chemicals and solutions used were as described in previous sections of this paper. The materials used as packing materials, prepared in this laboratory, were of two particle sizes: 125—177 μm and 37—74 μm, respectively.

Apparatus. The liquid chromatograph used was of a low-pressure type. Detection was provided by a Bausch and Lomb Spectronic 505 spectrophotometer with a 185-μl volume, 10-mm path length flow cell (Type 178-Q-10, Markson Science, Inc., Del Mar, California). A low-pulsation pump was used for solution transport (Gilson Minipuls 2). The column was a capillary glass tube (99 × 0.20 cm) slurry packed with the CPG—HQ. A coarse-frit, sintered glass disc was glued with epoxy to the bottom of the column. Two three-way teflon valves (Hamilton Co., Reno, Nevada) were connected to the top and bottom of the column as convenient devices to get rid of trapped bubbles. The rotary injection valve, located at the top of the column, was constructed as described by Hansen and Růžička [14] for injection in unsegmented continuous-flow determinations. The sample loop was constructed from microbore Tygon tubing (Cole Parmer Co., Chicago, Illinois) of 0.51 mm i.d. giving a volume of 8 μl.

Since even the lowest available chart speed (about 3.3 cm min^{-1}) in the built-in recorder of the Spectronic 505 provided traces inappropriate for direct reproduction, chromatograms were analyzed and retraced with the help of a Hewlett-Packard 9825A desk-top computer and a Hewlett-Packard 9862A plotter. Analysis and simulated retraced figures were based on a Poisson distribution [15, 16] to account for the residual adsorption observed, probably as a result of a residual interaction of the benzene rings with the —Si—OH structure.

Results and discussion

Because of sample availability, the results reported are limited to benzenesulfonate, *p*-toluenesulfonate, 2-mesitylenesulfonate, and 1-naphthalenesulfonate. Preliminary work with an open column (49 × 0.60 cm) indicated that good separation could be obtained by using the resin in its chloride form and perchlorate as the eluting counterion. Column dimensions and

other experimental parameters were selected so as to obtain reasonable separation of benzenesulfonate and *p*-toluenesulfonate and the effect of flow rate on resolution is analyzed in the different graphs presented in Fig. 4.

Resolution was calculated from

$$R_s = [(t_R)_{i+1} - (t_R)_i] / [\tfrac{1}{2}(w_{i+1} + w_i)]$$

in which i is the elution order, t_R the retention time and w the width at base in min. This formula was used for convenience and in recognition of its relative value in the light of approximate symmetry in the retraced chromatograms. Critical evaluation of the factors experimentally variable within the constraints of the setup used indicated that good separation could be obtained for benzenesulfonate and *p*-toluenesulfonate by using 0.10 M $HClO_4$ at a flow of 0.20 ml min^{-1}. After elution of *p*-toluenesulfonate, and in order to decrease the time for determination, a combination of flow and concentration gradient had to be applied. The ionic strength of the eluant was increased from 0.10 to 0.44 M in about 50 min and the flow rate was simultaneously increased from 0.22 ml min^{-1} to 0.35 ml min^{-1}. Figure 5 shows a typical chromatogram. The resolution for the first two compounds is 0.99; baseline resolution seems possible (R_s = 1.5) with a 225-cm column of the same characteristics as that used to obtain the chromatogram of Fig. 5 on

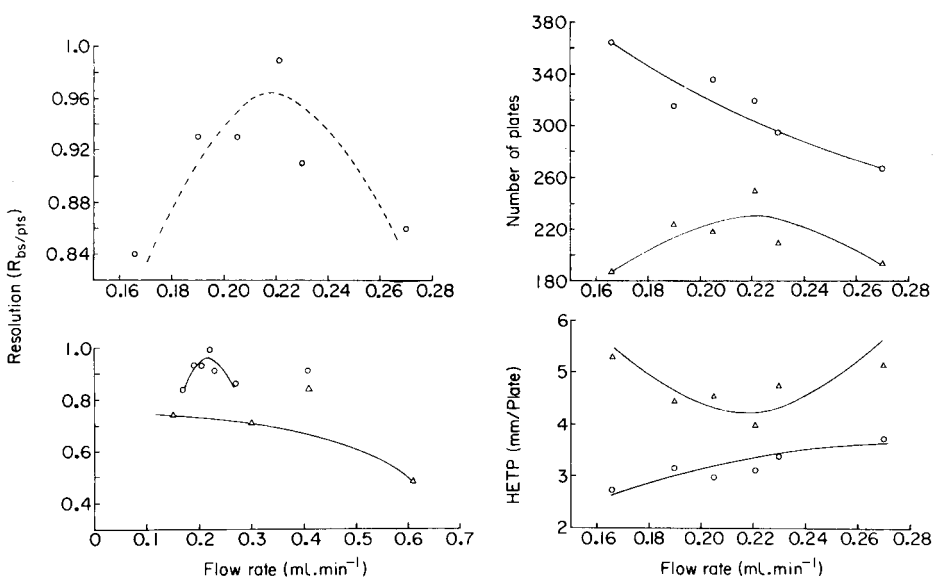

Fig. 4. Effect of flow rate, number of theoretical plates, and plate height for chromatographic separation of benzene sulfonate and *p*-toluenesulfonate. Resolution vs. flow rate: (○) particle size (37—74 μm); (△) particle size 125—177 μm. Number of plates and HETP vs. flow rate: (○) benzenesulfonate; (△) *p*-toluenesulfonate.

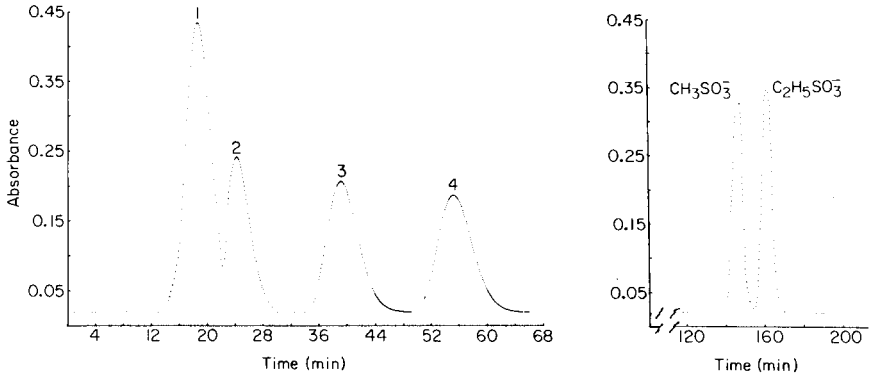

Fig. 5. Computer-retraced chromatogram: (1) benzenesulfonate; (2) *p*-toluenesulfonate; (3) 2-mesitylenesulfonate; (4) 1-naphthalenesulfonate.

Fig. 6. Computer-predicted chromatogram for methanesulfonate and ethanesulfonate. Elution at pH 2.8 and flow rate (assumed constant) of 0.35 ml min^{-1}; column length, 99 cm; column i.d., 0.20 cm.

the assumption that the resolution is proportional to the square root of column length. Figure 6 is a computer-simulated chromatogram for the separation of methanesulfonate and ethanesulfonate in the column used to obtain the separation of the aromatic sulfonates illustrated in Fig. 5. A constant flow rate and constant eluant concentration were assumed and distribution data presented in earlier sections were used to predict retention parameters. The information presented in Figs. 5 and 6 is illustrative of the group separation (aromatic vs. aliphatic) and the species separation of aromatic sulfonates described in this paper. The importance of sulfonate species separation and determination has been reviewed recently [17].

The authors acknowledge the help of Mr. Heinz Hall with construction of all custom-made parts used in this work.

REFERENCES

1 G. Schill, in J. A. Marinsky and Y. Marcus (Eds.), Ion Exchange and Solvent Extraction: A Series of Advances, Vol. 6, M. Dekker, New York, 1974, Ch. 1.
2 Y. Marcus and A. S. Kertes, Ion-Exchange and Solvent Extraction of Metal Complexes, Wiley—Interscience, London, 1969.
3 U. Mayer, Coord. Chem. Rev., 21 (1976) 159.
4 G. Schill, K. O. Borg, R. Modin and B. A. Persson, in E. Wanninen (Ed.), Essays on Analytical Chemistry (in memory of Professor Anders Ringbom), Pergamon, New York, 1977, pp. 379—395.
5 E. Eksborg and G. Schill, Anal. Chem., 45 (1973) 2092.
6 D. Dyrssen, Svensk Kem. Tidskr., 64 (1952) 213.
7 H. A. Mottola and H. Freiser, Talanta, 13 (1966) 55.
8 G. H. Morrison and H. Freiser, Solvent Extraction in Analytical Chemistry, J. Wiley, New York, 1957, p. 249.

9 H. H. Weetal, Biochim. Biophys. Acta, 212 (1970) 1.
10 General Catalog, Pierce Chemical Company, P.O. Box 177, Rockford, IL, 61105, 1976—1977, pp. 274—296.
11 I. M. Kolthoff, Chem. Weekbl., 24 (1927) 606.
12 S. Lacroix, Anal. Chim. Acta, 1 (1947) 260.
13 J. R. Jezorek and H. Freiser, Anal. Chem., 51 (1979) 366.
14 E. H. Hansen and J. Růžička, J. Chem. Ed., 56 (1979) 677.
15 S. L. Meyer, Data Analysis for Scientists and Engineers, J. Wiley, New York, 1974, Ch. 24.
16 P. R. Bevington, Data Reduction and Error Analysis for the Physical Sciences, McGraw-Hill, New York, 1969, Ch. 3.
17 Mao-Sung Kuo and H. A. Mottola, CRC Crit. Rev. Anal. Chem., 10 (1) (1980).

Analytica Chimica Acta, 120 (1980) 267—277

EXTRACTION BEHAVIOR OF ION-PAIRS OF AZO-DYE CATIONS AND THEIR ANALYTICAL APPLICATIONS

SHOJI MOTOMIZU* and KYOJI TÔEI

Department of Chemistry, Faculty of Science, Okayama University, Tsushima-naka, Okayama-shi (Japan)

(Received 16th April 1980)

SUMMARY

The extraction of ion-pairs of monovalent organic acid anions and inorganic anions with 4-(4-diethylaminophenylazo)-N-alkylpyridinium cation (azo-dye cation) is described. The alkyl groups studied were methyl, ethyl, propyl, butyl and benzyl groups. The ion association, distribution and extraction constants for the ion-pairs were determined from partition equilibrium studies. These azo-dye cations can extract chelate anions containing sulfonic acid groups into chloroform. The cobalt complex of 2-nitroso-1-naphthol-4-sulfonic acid is extracted quantitatively into chloroform with the propyl derivative as a 1:3 Co: dye complex; measurement of the absorbance of the extracted ion-pair provides a very sensitive determination of cobalt, the apparent molar absorptivity in chloroform being 1.66×10^5 l mol^{-1} cm^{-1} at 566 nm. The methyl derivative is suitable for cation extraction of monovalent anions such as the complex nickel anion of 4-chloro-2-nitroso-1-naphthol, and anionic surfactants. The possibilities for application of these azo-dye cations in extraction-spectrophotometric determinations are very large.

Ion-pairs have become widely used in analytical chemistry, especially for the separation of ions by extraction, precipitation, flotation and partition chromatography. Solvent extraction is one of the most important and useful separation procedures, because the extract can be used subsequently for spectrophotometric, fluorimetric and atomic-absorption determinations. Extraction-spectrophotometric determinations of ion associates have advantages in enhancement of sensitivity and selectivity, as different cationic or anionic dyes with large molar absorptivities and varying extraction properties can be selected. Cationic dyes such as methylene blue, rhodamine B and crystal violet, have been preferred for anionic surfactants, many complex halogen anions and chelate anions [1]; in such procedures, the molar absorptivities often reach 1×10^5 l mol^{-1} cm^{-1}. Chelate anions possessing sulfonic acid groups have often been extracted into chloroform, 1,2-dichloroethane or butanol as ion pairs with quaternary ammonium ions, the metal ions being determined via the absorption of the chelates themselves. However, such chelate anions have rarely been extracted with commonly available cationic dyes. This aspect is examined in the present paper.

Dyes such as derivatives of azine, thiazine, oxazine and triphenylmethane proved not to be useful either because the anion was not extracted or

because an excessive amount of the dye was co-extracted. 4-(4-Diethylaminophenylazo)-N-alkylpyridinium cations (I) were capable of extracting

(I) 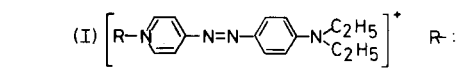 R- : CH_3-, C_2H_5-, C_3H_7-, C_4H_9-, 

chelate anions possessing sulfonic acid groups into chloroform. Measurement of the absorbance of the azo dye in the extracted ion-pair provided very sensitive spectrophotometric determinations of metal ions. Such extraction–spectrophotometric methods with the azo-dye cation can be applied to the previously reported extraction systems with quaternary ammonium ions, as well as to determinations of anionic surfactants and monovalent chelate anions. Accordingly, these azo-dye cations should become very useful ion-pair reagents, and so the relevant distribution equilibria for some simple anions were also studied.

EXPERIMENTAL

Apparatus and reagents

Absorbances were measured on a Schimazu UV300 recording spectrophotometer and a Schimazu QV50 spectrophotometer in glass cells of 10-mm path length. An Iwaki (Model V-S Type KM) shaker was used for horizontal shaking of the 25-ml stoppered test tubes used for extraction.

4-(4-Diethylaminophenylazo)-N-alkylpyridinium salts (cationic azo-dyes). 4-(4-Diethylaminophenylazo)pyridine was synthesized as described by Faessiger and Brown [2]. The recrystallized product was dissolved in a benzene solution of alkyl halide (methyl iodide, ethyl iodide, propyl iodide, butyl bromide or benzyl bromide), and the solution was refluxed for 3—5 h for alkylation of pyridine derivative. The products precipitated (crystalline) were filtered on paper and washed with fresh benzene until the filtrate was scarcely colored. The N-alkylpyridinium halides obtained were dissolved in water and the solutions were passed through an anion-exchange resin (Dowex SBR-P, Cl^- form) in a glass column (20 cm long and 2 cm diameter). The eluate was transferred to a suitable volumetric flask and diluted to the mark with water.

Anion solutions. Sodium salts of monovalent anions were dissolved in distilled water. Solutions of organic acids (phenol, benzoic acid, benzenesulfonic acid, naphthoic acid and naphthalenesulfonic acid and their derivatives) were prepared by dissolving their sodium salts in water or by dissolving the acids in sodium hydroxide solution. For weak acids, the solutions were adjusted to pH values two or three units above their pK_a values. The pH values of the solutions must be in the range 5—10; at pH <5, some parts of the azo-dye cation are protonated to become CH^{2+}, and at pH > 10, some parts become COH, which is yellow and is easily extracted into chloroform.

Extracting solvents. Commercially available chloroform, 1,2-dichloroethane, chlorobenzene, isobutyl methyl ketone(MIBK), nitrobenzene, benzene

and toluene were used without further purification. These solvents were saturated with water by shaking with water before use.

2-Nitroso-1-naphthol-4-sulfonic acid (Nitroso-NW acid). The reagent was obtained by nitrosation of 1-naphthol-4-sulfonic acid in an acidic aqueous solution with sodium nitrite [3]. The crude nitroso compound was recrystallized twice from acidic water. Aqueous solutions were used. The commercially available reagent may be used if it is recrystallized.

All reagents used, except the reagents synthesized, were of analytical reagent grade.

Determination of the equilibrium constants

An extraction system in which a monovalent cation (C^+) reacts with a monovalent anion (A^-) to form only one kind of ion-pair ($C^+ A^-$) in the aqueous phase, and in which the extracted ion-pair does not dissociate or aggregate, involves the following equilibria.

The ion association constant for a monovalent cation and an anion in an aqueous solution, K_A, refers to the reaction

$$C^+ + A^- \rightleftharpoons C^+ A^-; K_A = [C^+ A^-]/[C^+][A^-] \quad (1)$$

The distribution coefficient of the ion pair ($C^+ A^-$) between the aqueous and organic phases, K_D, refers to the equilibrium

$$C^+ A^- \rightleftharpoons (C^+ A^-)_{org}; K_D = [C^+ A^-]_{org}/[C^+ A^-] \quad (2)$$

where the subscript org refers to the organic phase and the aqueous concentrations are unmarked.

The distribution ratio of C^+ between the aqueous and organic phases, D, and the extraction constant, K_{ex}, refer to

$$D = [C^+ A^-]_{org}/([C^+] + [C^+A^-]) \quad (3)$$

$$K_{ex} = [C^+ A^-]_{org}/[C^+][A^-] = K_A K_D \quad (4)$$

From eqns. (1—4), the following equation can be derived

$$D^{-1} = K_D^{-1} + (K_{ex}[A^-])^{-1}$$

When activities are used instead of concentrations, then

$$D^{-1} = (f^0_{(org)}/K_D^T f^0) + (f^0_{(org)}/K_{ex}^T f^+ f^- [A^-]) \quad (5')$$

where K_D^T and K_{ex}^T are the relevant constants, and f^+, f^-, f^0 and f^0_{org} are the activity coefficients for C^+, A^-, $(C^+ A^-)$ and $(C^+ A^-)_{org}$, respectively. When the concentrations of the ions are relatively small and the Debye—Hückel limiting law is applicable, then eqn. (5′) becomes

$$D^{-1} = (K_D^T)^{-1} + (K_{ex}^T f^2 [A^-])^{-1} \quad (5'')$$

The plots of D^{-1} against $(f^2 [A^-])^{-1}$ or $[A^-]^{-1}$ must be linear; from the intercept of the y-axis and the slope, K_D^T or K_D and K_{ex}^T or K_{ex} can be calculated.

Procedure. An appropriate amount of the aqueous solution of the azo dye (chloride, C^+Cl^-) was transferred to a separatory funnel and the sodium salt solution of the anion (A^-) was added in a 10—100-fold molar excess over the azo dye. This solution was shaken with suitable amounts of organic solvent. The separated organic phase was then shaken with a fresh anion (A^-) solution containing a 10—100-fold molar excess of the azo dye. Then 5-ml portions of the organic phase and of an aqueous solution containing various amounts of the anion (A^-) were shaken in a 25-ml stoppered test tube for about 30 min to complete the extraction equilibrium. After phase separation, the absorbance of the organic or aqueous phase was measured at the maximum wavelength of the azo dye, and the distribution ratio (D) was calculated from the original absorbance of the organic phase and the absorbance of the organic or aqueous phase after shaking with the anion solution. The concentration of the anion (A^-) in the aqueous phase was obtained by adding the concentration of the azo-dye cation (C^+) in the aqueous phase to the original concentration of anion in the aqueous phase. In almost all cases, the concentration of anion was much higher than that of the azo dye in the aqueous phase, and the concentration of the ion pair ($C^+ A^-$) in the aqueous phase could be neglected compared with the concentration of anion (A^-). The values of D^{-1} were plotted against $(f^2[A^{-1}])^{-1}$ or $[A^-]^{-1}$ and the intercept and slope were calculated by the least-squares method. The ion-association constant, K_A, was calculated by dividing the value of K_{ex} by the value of K_D.

When the distribution coefficient of the ion pair, K_D, was very large, its value became uncertain. In such cases, only the value of K_{ex} was obtained.

RESULTS AND DISCUSSION

Determination of the equilibrium constants for monovalent anions

All five azo-dye cations mentioned above were examined, and equilibrium constants, the K_{ex}, K_D and K_A values were calculated. The plots of D^{-1} against $[Cl^-]^{-1}$, $[I^-]^{-1}$ and $[ClO_4^-]^{-1}$ for the ethyl azo-dye derivative are shown in Fig. 1 as examples. As expected, the plots were all linear. The plots of D^{-1} against $(f^2[I^-])^{-1}$ and $(f^2[ClO_4^-])^{-1}$ are also shown in Fig. 1; the activity coefficient, f, was calculated from $-\log f = 0.5\, I^{1/2}$ (where I is the ionic strength). These plots were also straight lines and the values of K_D^T and K_{ex}^T obtained were almost the same as K_D and K_{ex}. The plots of eqn. (5) were therefore used for convenience. In Table 1, the results obtained for the azo-dye cations studied and for tetradecyldimethylbenzylammonium (zephiramine) and methylene blue are listed. The wavelengths of maximum absorption (λ_{max}) of the ion pair in chloroform are also shown in Table 1.

In general, the larger the value of log K_{ex}, the better will be the extraction of the ion-pair. It is generally considered that the bulkier and more organophilic the ion, the better will be the extraction of the ion-pair. Accordingly, the extraction of the ion-pair increases as the radius of the inorganic ion increases or as the azo-dye cation becomes increasingly organophilic. These

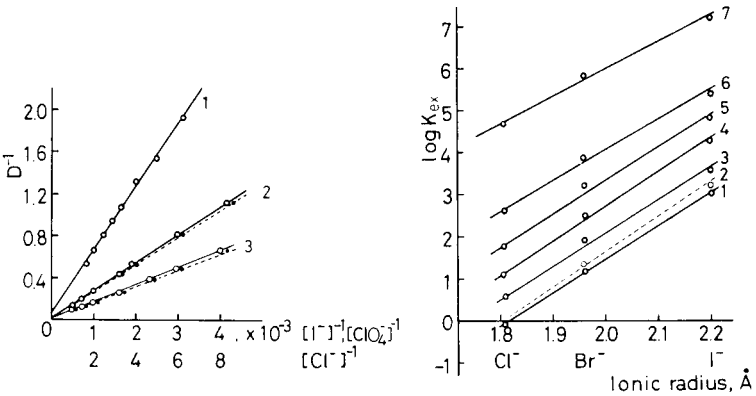

Fig. 1. The plots of D^{-1} against $[A^-]^{-1}$ and $(f^2[A^-])^{-1}$ for the ethyl derivative of the azo dye. (1) Chloride; (2) iodide; (3) perchlorate; (——) $[A^-]^{-1}$; (---) $(f^2[A^-])^{-1}$.

Fig. 2. The plots of log K_{ex} against the ionic radius of the halide ion. (1) CH_3-derivative of the azo dye; (2) methylene blue; (3) C_2H_5-derivative; (4) C_3H_7-derivative; (5) C_4H_9-derivative; (6) $C_6H_5CH_2$-derivative; (7) zephiramine.

trends are clarified in Fig. 2 for halide ions. With the organic anions, it was found that the ion-pair containing the sulfonate ion was more readily extracted than the ion-pair containing the carboxylate ion. The introduction of a nitro group, or of a hydroxyl group in the *o*-position of the carboxylate, or the change from a phenyl group to a naphthyl group, increased the percentage extraction, whereas the introduction of a hydroxyl group in the *m*- or *p*-position decreased the percentage extraction. A reliable measure of bulk is difficult to find for organic anions, and so the values of log K_{ex} were plotted against the value of log K_{ex} of the ion-pair formed between the corresponding anion and the ethyl azo-dye derivative (see Fig. 3). The plots for the methyl, propyl, butyl and benzyl derivatives, and for methylene blue and zephiramine, showed good linearity with very similar slopes.

As mentioned above, K_{ex} can be evaluated from the slope of the D^{-1} vs. $[A^-]^{-1}$ plot; the accuracy is relatively good when log K_{ex} lies in the range 1—5. In contrast, K_D must be evaluated from the intercept of the y-axis, so that its value is easily affected by variations in the slope and the accuracy is less than that of K_{ex}. However, it is possible to say that, in general, the bulkier the anion, the larger log K_D. The values of log K_A, obtained as described under Experimental, are again, less accurate than those of log K_{ex}; the trends are similar to those for log K_D.

It is worth noting that the log K_{ex} values increase as the wavelength of maximum absorption of the ion-pair in the organic phase becomes longer.

Extracting solvent

Benzene, toluene, MIBK, chlorobenzene, chloroform, 1,2-dichloroethane and nitrobenzene were examined. In general, the ion-pairs of monovalent

TABLE 1

Equilibrium constants obtained between aqueous and chloroform phases for the five azo-dye derivatives, methylene blue and zephiramine

Anion	log K_{ex}	log K_D	log K_A	λ_{max} (nm)	Anion	log K_{ex}	log K_D	log K_A
CH_3-derivative					*C_3H_7-derivative*			
Cl^-	−0.08	0.02	−0.10	563	Cl^-	1.11	1.44	−0.33
Br^-	1.19	0.68	0.51	565	Br^-	2.49	1.41	1.08
I^-	3.01	1.49	1.52	567	I^-	4.26	1.43	2.83
ClO_4^-	3.16	1.30	1.86	567	ClO_4^-	4.48	1.48	3.00
ReO_4^-	3.56	1.62	1.94	571	Benzoate	1.73	1.17	0.56
Benzoate	0.60	−0.14	0.74	555	Naphthoate	2.96	1.44	1.52
4-NO_2-benzoate	1.80	0.19	1.61	562	Benzenesulfonate	3.16	1.07	2.09
3-NO_2-benzoate	1.75	0.28	1.47	561	Naphthalenesulfonate	4.65	1.45	3.20
2-OH-benzoate	2.31	0.70	1.61	562				
Naphthoate	1.85	0.29	1.56	558	*C_4H_9-derivative*			
Benzenesulfonate	1.88	0.45	1.43	560	Cl^-	1.79	1.11	0.68
4-OH-benzenesulfonate	0.99	−0.19	1.18	563	Br^-	3.20	1.20	2.00
4-NO_2-benzene-sulfonate	3.07	0.64	2.43	566	I^-	4.80	1.38	3.42
					Benzoate	2.30	1.12	1.18
3-NO_2-benzene-sulfonate	3.13	1.00	2.13	565	Naphthoate	3.51	1.08	2.43
					Benzenesulfonate	3.78	0.93	2.85
Naphthalenesulfonate	3.26	0.72	2.54	561	Naphthalenesulfonate	5.16	1.51	3.65
4-Nitrophenolate	2.55	1.59	0.96	580				
					$C_6H_5CH_2$-derivative			
C_2H_5-derivative					Cl^-	2.62	0.87	1.75
Cl^-	0.57	0.74	−0.17	559	Br^-	3.84	1.17	2.67
Br^-	1.90	1.00	0.90	563	I^-	5.37	—	—
NO_3^-	1.84	0.85	0.99	563	Benzoate	3.14	0.83	2.31
I^-	3.54	1.70	1.84	567	Naphthoate	4.16	—	—
ClO_4^-	3.79	1.96	1.83	568	Benzenesulfonate	4.35	2.35	2.00
ReO_4^-	4.11	1.80	2.31	570	Naphthalenesulfonate	5.61	—	—
Benzoate	1.19	0.16	1.03	560				
4-NO_2-benzoate	2.43	0.65	1.78	565	*Methylene blue*			
3-NO_2-benzoate	2.38	0.61	1.77	565	Cl^-	−0.10	0.82	−0.92
2-OH-benzoate	2.84	1.00	1.84	560	Br^-	1.35	0.40	0.95
Naphthoate	2.35	0.63	1.72	559	I^-	3.20	1.27	1.93
Benzenesulfonate	2.54	1.12	1.42	562	ClO_4^-	3.32	1.22	2.10
4-OH-benzenesulfonate	1.48	0.46	1.02	564	Benzenesulfonate	1.51	0.47	1.04
4-NO_2-benzene-sulfonate	3.74	1.62	2.12	565	Naphthalenesulfonate	3.34	0.66	2.68
3-NO_2-benzene-sulfonate	3.68	1.42	2.26	566	*Zephiramine*			
					Cl^-	4.67	2.52	2.15
Naphthalenesulfonate	3.75	2.00	1.75	561	Br^-	5.88	2.62	3.26
4-Nitrophenolate	3.39	1.73	1.66	581	I^-	7.44	3.29	4.19
3-Nitrophenolate	3.0	—	—	577				

anions with the azo-dye cations were too easily extracted into nitrobenzene for equilibrium constants to be calculated, whereas they were not sufficiently extracted into benzene, toluene and MIBK. Some results obtained with chlorobenzene and 1,2-dichloroethane are listed in Table 2. Of the solvents examined, the order of extractability was usually nitrobenzene > 1,2-dichloroethane > chloroform > chlorobenzene > MIBK, benzene, toluene.

TABLE 2

The equilibrium constants obtained between aqueous and organic phases (chlorobenzene or 1,2-dichloroethane)

Anion	log K_{ex}	log K_D	log K_A	λ_{max}[a] (nm)
C_2H_5-derivative with 1,2-dichloroethane				
Cl^-	0.42	—	—	583
Br^-	1.82	1.13	0.69	583
I^-	3.96	1.36	2.60	583
NO_3^-	2.42	1.73	0.69	583
Benzenesulfonate	3.01	1.10	1.91	583
Naphthalenesulfonate	4.58	1.33	3.25	582
$C_6H_5CH_2$-derivative with 1,2-dichloroethane				
Cl^-	2.47	0.44	2.03	590
Br^-	3.97	1.07	2.90	590
NO_3^-	4.37	1.06	3.31	590
$C_6H_5CH_2$-derivative with chlorobenzene				
Cl^-	−0.78	—	—	558
Br^-	0.96	0.15	0.81	564
I^-	3.07	0.81	2.26	568

[a]The maximum absorption wavelength of the ion-pair.

Extraction of cobalt complex of 2-nitroso-1-naphthol-4-sulfonic acid and determination of the extraction constant for the cobalt complex anion and reagent

Cobalt ion reacts with 2-nitroso-1-naphthol-4-sulfonic acid (nitroso-NW acid, H_2R) to form a 1:3 complex anion, CoR_3^{3-}. Previously, this complex anion was extracted with zephiramine into chloroform [4]. In the present work, triphenylmethane dyes (malachite green, brilliant green and crystal violet), xanthene dyes (rhodamine B and rhodamine 6 G), a thiazine dye (methylene blue) and the azo-dye derivatives discussed in this paper were examined instead of zephiramine. In general, the dye cations, except the azo-dye cations, were extracted into nitrobenzene, 1,2-dichloroethane or chloroform as the ion-pair with chloride so that reagent blanks were large. In contrast, these dye cations were only slightly extracted into chlorobenzene, toluene and benzene so that reagent blanks were small; unfortunately, the ion-pairs formed with the complex cobalt anion were also poorly extracted.

All the five azo-dye derivatives discussed here formed chloroform-extractable ion-pairs with the complex cobalt anion; the composition of the ion-pair extracted was found to be 1:3 cobalt complex: azo-dye cation by the mole ratio method, when the propyl and butyl derivatives were examined. The ion-pairs formed with chloride were not readily extracted. The excess of reagent (in the form R^{2-}) was also scarcely extracted into chloroform whereas excess in the form of HR^- was extracted. The cobalt-containing ion-pair

could be extracted into 1,2-dichloroethane but the reagent blank was larger than with chloroform while the extraction of the cobalt complex was less efficient.

The equilibrium constants, K_{ex}, K_D and K_A could be obtained for monovalent anions and cations from eqn. (5), but this was not possible for multivalent anions and cations. Accordingly, log K_{ex} was evaluated for R^{2-} and the complex cobalt anion (CoR_3^{3-}) by assuming that the concentration of the ion-pair in the aqueous phase was negligibly small compared with the total concentrations of the reactants in the aqueous phase and that the ion-pair extracted into chloroform did not dissociate. The results obtained for the ethyl and propyl derivatives are listed in Table 3. These values were plotted in Fig. 3, in which the value of log K_{ex} divided by the valency of the anion was used. These plots lie on the line for monovalent anions. The extraction constants for the complex cobalt anion, R^{2-} and HR^-, for the methyl, butyl and benzyl derivatives were not determined but their values could be estimated from the linear relationship in Fig. 3.

The curves of percentage extraction against log [C^+], calculated from log K_{ex}, are shown in Fig. 4. It can be seen that the nitroso-NW acid in the R^{2-} form is less easily extracted than HR^- or the complex anion; almost all the cobalt complex is extracted and almost all the reagent (in the R^{2-} form) remains in the aqueous phase at concentrations of about 10^{-4} M for the ethyl derivative or 2.5×10^{-5} M for the propyl derivative. Accordingly, the excess of reagent must be present in the R^{2-} form in the aqueous phase to keep the reagent blank small. As the acidity constant, pK_{a2}, for the hydroxyl proton is 6.16 [4], the pH of the aqueous phase must be adjusted above 8.2 to remove the large excess of reagent from the organic phase.

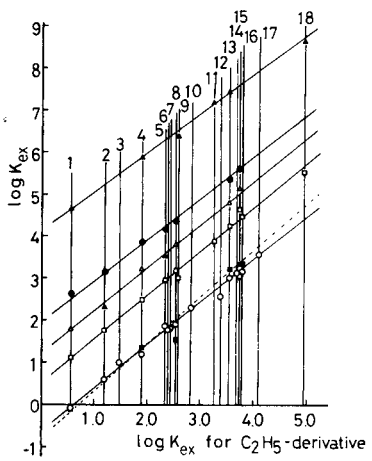

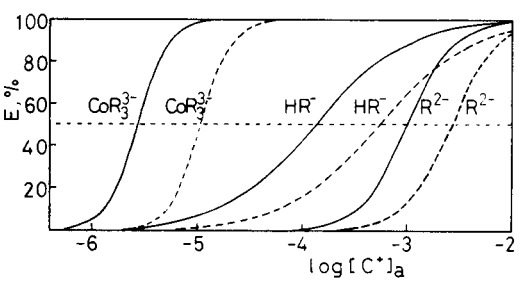

Fig. 3. Plots of log K_{ex} against log K_{ex} for the C_2H_5-derivative of the azo dye. Cations: (○) CH_3-derivative; (▪) methylene blue; (□) C_3H_7-derivative; (△) C_4H_9-derivative; (•) $C_6H_5CH_2$-derivative; (▲) zephiramine.

Fig. 4. Percentage extraction of HR^-, R^{2-} and CoR_3^{3-} against the concentration of azo-dye cation. H_2R: 2-nitroso-1-naphthol-4-sulfonic acid. C^+: (----) C_2H_5-derivative of the azo dye; (——) C_3H_7-derivative.

TABLE 3

Extraction constants for 2-nitroso-1-naphthol-4-sulfonic acid (H_2R) and its cobalt complex into chloroform

Cation	log K_{ex}		
	CoR_3^{3-}	R^{2-}	HR^-
C_2H_5-derivative	14.89 ± 0.20	5.14 ± 0.25	3.26 ± 0.11
C_3H_7-derivative	16.63 ± 0.27	5.99 ± 0.27	3.86 ± 0.08
Zephiramine	25.91	12.73	7.17

Extraction—spectrophotometric determination of cobalt with nitroso-NW acid and azo-dye cations

General procedure. The aqueous cobalt solution (5 ml) was pipetted into a stoppered test tube, and 0.5 ml of aqueous 10^{-3} M nitroso-NW acid solution and 0.5 ml of aqueous buffer solution (pH 8.6, 1 M Na_2HPO_4) were added. After addition of a suitable amount (see Table 4) of aqueous azo-dye solution, the mixture was shaken with 5 ml of chloroform for 10 min. After phase separation, the absorbance of the chloroform phase was measured at the maximum absorption wavelength (see Table 4).

The optimal amounts of azo-dye solution, above which the absorbance of the extracted ion-pair remained maximum and constant, and at which the reagent blank was relatively small and constant are given in Table 4. With the benzyl derivative, as estimated from Fig. 3, extraction of the reagent (even as R^{2-}) and so the reagent blank were very large; hence this cation was not examined in detail. From the calibration curves obtained by using the above procedure, the propyl derivative was judged to be the best reagent of the five because of the relatively large molar absorptivity and the low reagent blank. In Fig. 5, the absorption spectra for the propyl derivative are shown. The linear range for the calibration plots was 5×10^{-7}—5×10^{-6} M cobalt(II); for 2×10^{-6} M solution, the coefficient of variance was 0.72% ($n = 9$).

TABLE 4

The molar absorptivities (ϵ) of the cobalt complexes in chloroform[a]

Cation	λ_{max} (nm)	ϵ ($\times 10^4$ l mol^{-1} cm^{-1})	Absorbance of reagent blank	Cation added
CH_3-derivative	564	9.9	0.083	2 ml of 2×10^{-3} M
C_2H_5-derivative	564	16.8	0.090	0.5 ml of 2×10^{-3} M
C_3H_7-derivative	566	16.6	0.062	0.5 ml of 10^{-3} M
C_4H_9-derivative	566	13.5	0.128	1 ml of 10^{-4} M

[a]With 10^{-4} M 2-nitroso-1-naphthol-4-sulfonic acid at pH 8.6.

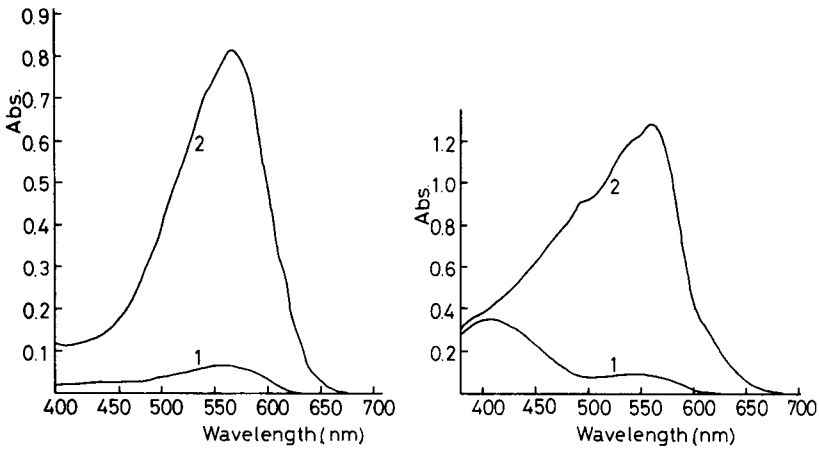

Fig. 5. Absorption spectra of the ion-pair of cobalt—nitroso-NW acid complex anion with the C_3H_7-derivative of the azo dye in chloroform. Nitroso-NW acid, 1×10^{-4} M; azo-dye cation, 10^{-4} M. (1) Reagent blank; (2) [cobalt(II)] = 5×10^{-6} M. Chloroform reference; pH 8.6.

Fig. 6. Absorption spectra of the ion-pair of nickel—4-chloro-2-nitroso-1-naphthol complex anion with the CH_3-derivative of the azo dye in chloroform. 4-Chloro-2-nitroso-1-naphthol, 2×10^{-4} M; azo-dye cation, 4×10^{-4} M. (1) Reagent blank; (2) [Ni^{2+}] = 2×10^{-5} M. Chloroform reference; pH 6.

CONCLUSIONS

The results obtained for the extraction of the ion-pairs formed between the azo-dye cations and monovalent anions indicate that iodide, perchlorate and perrhenate ions can be extracted quantitatively into chloroform and determined spectrophotometrically by using the chloride of the azo-dye derivatives. In this paper, the effect of the alkyl group in the organic anion on the extraction constant has not been discussed in detail. However, the extraction constant (log K_{ex}) became larger (about $0.6 \times n$) than that of the parent organic anion when the alkyl group, C_nH_{2n+1}—, was introduced into the parent organic anion for series such as benzenesulfonate, alkylsulfonate, benzoate and carboxylate [5], as well as when alkyl groups (methyl, ethyl, propyl and butyl) were contained in the azo-dye cation. Thus anionic surfactants such as alkylbenzenesulfonate, alkylsulfate and alkylsulfonate can be extracted quantitatively into chloroform even with the methyl azo-dye derivative, and a procedure for the extraction—spectrophotometric determination of anionic surfactants in river water has been reported [6]; one shaking extracted the surfactants quantitatively and the molar absorptivity of the ion-pair in chloroform was 6.2×10^4 l mol^{-1} cm^{-1} at 564 nm.

These azo-dye cations can also be applied to the extraction of monovalent chelate anions formed as follows: $M^{n+} + (n + 1)\,HR \rightleftharpoons MR^-_{n+1} + (n + 1)H^+$. For example, nickel(II) reacts with nitrosonaphthol derivatives to form NiR_3^-, where R^- is 1-nitroso-2-naphthol, 2-nitroso-1-naphthol or their halogen

derivatives [7]. Of these nickel-containing anions, the complex formed with 4-chloro-2-nitroso-1-naphthol can be extracted quantitatively into chloroform with the methyl azo-dye derivative reported here. The absorption spectra are shown in Fig. 6. The molar absorptivity was 6.2×10^4 l mol^{-1} cm^{-1} at 557 nm (pH 7.2).

The azo-dye cations examined in this work should prove to be very useful and widely applicable reagents for extraction-spectrophotometric determinations. Their application to anions possessing sulfonic acid groups seems to be particularly useful and general from the point of view of developing highly sensitive methods.

REFERENCES

1 Z. Marczenko, Mikrochim. Acta (Wien), (1977) 651.
2 R. W. Faessiger and E. V. Brown, Trans. K. Acad. Sci., 24 (1963) 106; (Chem. Abstr., 60, 14465g).
3 K. Tôei and S. Motomizu, Nippon Kagaku Zasshi, 92 (1971) 92.
4 S. Motomizu and K. Tôei, Anal. Chim. Acta, 89 (1977) 167.
5 K. Tôei, S. Motomizu and S. Hamada, Abstr., 40th Ann. Meeting of the Chem. Soc. Jpn., III (1979) 998.
6 K. Higuchi, S. Monya, Y. Shimoishi, H. Miyata and K. Tôei, Bunseki Kagaku, 29 (1980) 180.
7 K. Tôei, S. Motomizu and H. Yokosu, Anal. Chim. Acta, 110 (1979) 329.

Analytica Chimica Acta, 120 (1980) 279—287

SALTING-OUT OF POLAR SOLVENTS FROM AQUEOUS SOLUTION AND ITS APPLICATION TO ION-PAIR EXTRACTIONS

YUKIO NAGAOSA

Faculty of Engineering, Fukui University, 3-chome, Bunkyo, Fukui 910 (Japan)

(Received 14th January 1980)

SUMMARY

Water-miscible polar solvents such as acetonitrile, 1-methyl-2-pyrrolidone and hexamethylphosphoramide can be separated from their aqueous solutions by salting-out. The McDevit—Long equation is useful in explaining the salting-out of polar solvents (whether water-miscible or not). The cobalt(II) complex with 2,2′-bipyridine can be extracted quantitatively as the ion-pair into these solvents from saturated ammonium sulphate solution containing a 10-fold molar excess of perchlorate ion. In the acetonitrile system, high distribution ratios can be obtained at high concentrations of multivalent inorganic salts and at low temperatures.

The solubility of a substance in water often decreases on the addition of an inorganic salt. This salting-out phenomenon can be valuable in increasing the extractability of metal complexes in liquid—liquid distribution [1—3]. When a water-miscible solvent is salted-out from aqueous solution, phase separation results from the decreased solubility of the solvent. Fujinaga and Nagaosa [4] have shown that acetonitrile is a very suitable solvent for use in polarographic methods after salting-out extraction. This salting-out technique would seem promising in general extraction chemistry, as certain ion-pairs could be extracted into polar water-miscible solvents, analogously to extractions into, say, nitrobenzene [5] or propylene carbonate [6]. Further, it is of interest to compare behaviour in salting-out extractions with that in conventional extractions.

The present paper describes the salting-out and phase separation of various polar solvents from their aqueous solutions in terms of the McDevit—Long theory [7]. Several polar solvents are shown to be effective in extracting the cobalt(II) complex formed with 2,2′-bipyridine as its ion-pair. Acetonitrile is used to examine the effects of experimental factors on the extractability.

EXPERIMENTAL

Reagents and apparatus

Tris(2,2′-bipyridine)cobalt(II) perchlorate was prepared as described by Burstall and Nyholm [8] and its purity was checked by elemental analysis. Acetonitrile was distilled from phosphorus pentoxide. The other organic

solvents were purified by standard methods [9]. Inorganic salts and 2,2′-bipyridine (reagent grade; Nakarai Chemicals Co. Ltd) were used without further purification. Redistilled water was used throughout.

Differential pulse polarography of cobalt(II) in acetonitrile was done as described previously [10]. A Hitachi Model 139 spectrophotometer was used for absorbance measurements. Conductivity was measured in a glass cell equipped with platinized platinum electrodes by a Yokogawa Model CM-1DB conductometer in a thermostat at 25°C. A Toa-Denpa HM-5A pH meter was used for pH checks.

Solubility tests

The organic solvent was added to 10.0 ml of an aqueous salt solution from a 2.0-ml buret until the solution began to cloud; the solubility of the solvent in the salt solution was determined from the volume added. The solubility of the cobalt(II) complex in aqueous acetonitrile was determined polarographically [10] after dissolution of an aliquot of the saturated solution in 10.0 ml of an acetonitrile solution which was 0.1 M in tetrabutylammonium perchlorate (TBAP) and 0.2 M in 2,2′-bipyridine (final concentrations).

Extraction procedures

In a stoppered 50-ml cylindrical glass tube (calibrated before use), an aqueous salt solution containing cobalt(II) and perchlorate (or chloride) was shaken with an organic solution containing 2,2′-bipyridine until equilibrium was achieved (within about 5 min). The two phases were allowed to separate. The recovered aqueous phase was shaken with 10.0 ml of an acetonitrile solution which was 0.2 M in 2,2′-bipyridine, 0.02 M in sodium perchlorate, and 0.1 M in TBAP, after saturation with ammonium sulphate; in this stage, the cobalt(II) remaining in the initial aqueous phase was extracted quantitatively into the acetonitrile phase. A 5-ml portion of this acetonitrile phase was transferred to a polarographic cell, in order to determine the amount of cobalt(II) in the aqueous phase, w_{aq}; if necessary, the solution was diluted with the same acetonitrile solution as that used in the extraction, i.e. the solution used for polarography was 0.2 M in 2,2′-bipyridine and 0.1 M in TBAP. The amount of cobalt(II) was determined after standard additions of 0.1 M tris(2,2′-bipyridine)cobalt(II) perchlorate solution in acetonitrile.

The distribution ratio (D) is given by $D = (w_t - w_{aq})V_{aq}/w_{aq}V_{org}$, where w_t, V_{aq}, and V_{org} represent the total amount of cobalt(II) taken, and the volumes of the aqueous and the organic phases after the extraction, respectively. The distribution ratios given are the averages of three determinations. The extraction efficiency (%E) was calculated from the equation: $E = 100D/[D + (V_{aq}/V_{org})]$.

In the acetonitrile extraction, the amount of cobalt(II) in the acetonitrile phase, w_{org}, was determined after appropriate dilutions. The amount of cobalt(II) in the aqueous phase was calculated by difference from the total amount taken. Accordingly, $D = w_{org}V_{aq}/(w_t - w_{org})V_{org}$.

The pH of the aqueous phase after extraction was 6.5—7.5. The water content of the organic phase was determined by Karl Fischer titrations.

RESULTS AND DISCUSSION

Salting-out and phase separation of polar solvents from aqueous solutions

Preliminary experiments showed that several water-miscible polar solvents could be salted-out from aqueous solutions on addition of inorganic electrolytes, phase separation being obtained. In order to clarify the reactions involved, the solubilities of polar solvents in aqueous saturated salt solutions were determined and equations proposed in the literature were applied.

The salting-out of nonelectrolyte from aqueous solutions is often correlated by the Setschenow equation [11]: $\log f = \log S_0/S = k_s C_s$, where f, S_0, S, k_s and C_s are the activity coefficients of the nonelectrolyte (or polar solvent), the solubilities of the solvent in water and in aqueous salt solution, the salting-out coefficient and the concentration of the aqueous salt solution, respectively. In Fig. 1 are shown the linear plots obtained for the logarithm of the solubilities of acetonitrile and propylene carbonate against ammonium sulphate concentration. Straight lines were also obtained for the other polar solvents tested over the salt concentration range 0.5—3.0 M. All salting-out coefficients determined from these plots were positive (see Fig. 2), i.e., the salt lowered the solubility of the polar solvent in water.

The k_s values obtained depended on the solvent and the salt used. This result can be explained by using the McDevit—Long equation [7, 12], which was derived on the basis of the increase in the internal pressure of water;

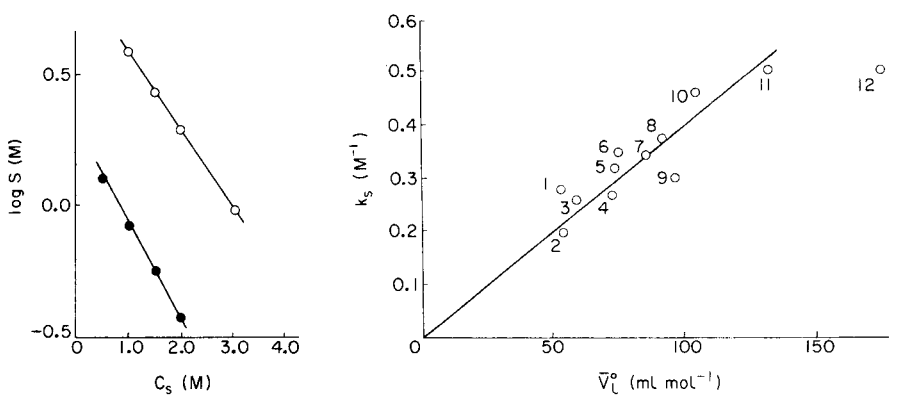

Fig. 1. Plots of log S vs. C_s for salting-out of acetonitrile and propylene carbonate from ammonium sulphate solutions of different concentrations. (○) Acetonitrile; (●) propylene carbonate.

Fig. 2. A plot of k_s vs. $\bar{V}_1^\circ$ for salting-out of various polar solvents from ammonium sulphate solution: (1) acetonitrile; (2) nitromethane; (3) ethanol; (4) nitroethane; (5) acetone; (6) 1-propanol; (7) propylene carbonate; (8) butanol; (9) 1-methyl-2-pyrrolidone; (10) benzyl alcohol; (11) 2-butoxyethanol; (12) hexamethylphosphoramide.

$k_s = \overline{V}_1^\circ(V_s - \overline{V}_s^\circ)/2.3RT\beta_0$, where $\overline{V}_1^\circ$ and $\overline{V}_s^\circ$ are the partial molar volumes of the nonelectrolyte (1) and the salt at infinite dilution, V_s is the molar volume of the liquid salt, and β_0 is the compressibility of water. A nearly linear relationship between the salting-out coefficient for the polar solvent and its molar volume was obtained with ammonium sulphate as salting-out agent (Fig. 2). Only hexamethylphosphoramide had an appreciably lower k_s value than that predicted by the plot. The k_s values of acetonitrile and propylene carbonate were plotted against the value of $(V_s - \overline{V}_s^\circ)$ for the four chloride salts (Fig. 3). The straight lines indicate that large salting-out coefficients were obtained with barium chloride and with the strongly hydrated electrolytes. According to the McDevit—Long theory, the internal pressure of water increases when electrolytes are solvated preferentially with water, because of its high dielectric constant; as a result, the hydrated ion layer excludes a polar solvent molecule. Because of this salting-out effect [13], the solubility of the polar solvent in the aqueous solution decreases, leading to phase separation. Of the watermiscible polar solvents of small molar volume, relatively inert solvents such as acetonitrile, acetone and dioxane were easily separated from aqueous solutions by salting-out, whereas N,N-dimethylformamide, pyridine and methanol could not be separated by addition of any salt. Solvent properties such as basicity, hydrophobicity and molecular structure must affect the solubility in water. Hexamethylphosphoramide(HMPA), 1-methyl-2-pyrrolidone(MPDN) and 2-butoxyethanol, which are water-miscible polar solvents of large molar volume, were salted-out easily with ammonium sulphate to form an organic phase. It seems that the molar volume of the water-miscible solvent is a major factor in this type of phase separation.

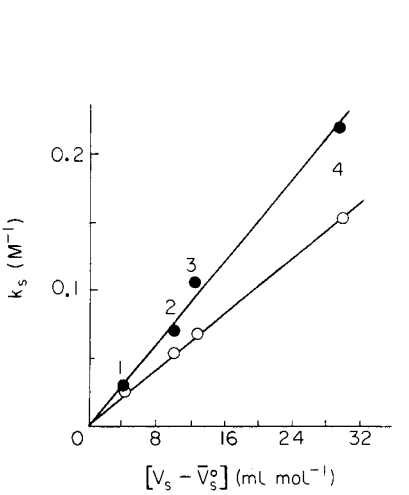

Fig. 3. Plots of k_s vs. $(V_s - \overline{V}_s^\circ)$ for the salting-out of acetonitrile (○) and propylene carbonate (●) from various salt solutions: (1) NH_4Cl; (2) KCl; (3) NaCl; (4) $BaCl_2$.

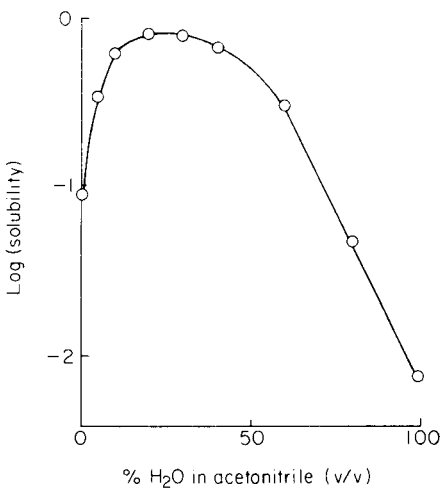

Fig. 4. The solubility (mol l^{-1}) of tris(2,2'-bipyridine)cobalt(II) perchlorate in various acetonitrile—water solutions (v/v%).

Salting-out extraction of the cobalt(II) complex with 2,2'-bipyridine into various polar solvents

Various polar solvents were examined for extraction of the chloride or perchlorate ion-pairs of the cobalt(II) complex with 2.0 M ammonium sulphate (Table 1). In the chloride system, better extraction was obtained with hexamethylphosphoramide or 1-methyl-2-pyrrolidone than with the other solvents tested; this difference in extractability may be due to solvent basicity (e.g., donor number [14]) or molar volume [15]. Nitromethane and nitroethane were better solvents in the perchlorate system. The other solvents listed in Table 1 provided almost complete extraction (>98%) when saturated ammonium sulphate solution was used instead of a 2.0 M solution. Under the same conditions, negligibly small extractability was observed with less polar organic solvents such as 1-propanol, 1-butanol, benzyl alcohol, and 2-butoxyethanol. These results indicate that polar water-miscible solvents should be highly advantageous for the ion-pair extraction if organic solvents containing halogens or nitro groups are unfavourable for the analytical technique used for the final determination [10, 16]. In this study, a large counter-anion was also found to be effective for the ion-pair extraction of the metal chelate cation [1, 3]. Not very surprisingly, an appreciable amount of water was contained in the organic phase of these water-miscible polar solvents after phase separation. The water content of the organic phase varied with the solvent used.

TABLE 1

Extraction of the cobalt(II) complexes into various polar solvents
(The aqueous solution was made 2×10^{-3} M in cobalt(II) chloride (or perchlorate) and 2 M in ammonium sulphate. The organic solution was made 0.2 M in 2,2'-bipyridine. The initial volumes of the two solutions were each 20.0 ml, except for 10.0 ml of MPDN or HMPA.)

Solvent	Chloride system		Perchlorate system		
	D[a]	$\%E$[b]	D	$\%E$	Water content (v/v%)
Acetonitrile	0.603	40.3	1.43	61.6	16.1
Acetone	2.98	86.1	3.34	86.9	32.3
Propylene carbonate	0.832	44.9	6.99	87.5	6.07
Ethanol	3.31	90.1	4.61	92.7	51.5
1-Methyl-2-pyrrolidone	29.4	98.3	26.8	98.1	56.1
Hexamethylphosphoramide	7.41	92.6	6.95	92.1	52.3
Nitromethane	0.216	17.7	41.0	97.6	2.77
Nitroethane	0.197	16.4	29.3	96.7	1.23

[a]Distribution ratio. [b]Extraction efficiency.

TABLE 2

Extraction of the cobalt(II) complex from aqueous 1 M solution of various salts into acetonitrile
(The aqueous solution (1 M salt) was made 2×10^{-3} M in cobalt(II) and 2×10^{-2} M in $NaClO_4$. The acetonitrile solution was made 0.2 M in 2,2'-bipyridine. The initial volume of each solution was 20.0 ml.)

Salt	*D*	*%E*	Water content(%)	Salt	*D*	*%E*	Water content(%)
1 NH_4Cl	1.23	20.9	38.7	6 $BaCl_2$	15.2	91.5	15.2
2 KCl	1.50	39.0	23.4	7 $SrCl_2$	17.6	92.1	14.5
3 NaCl	2.06	48.3	23.6	8 $AlCl_3$	22.1	94.4	10.0
4 $MgCl_2$	10.0	86.6	13.9	9 $(NH_4)_2SO_4$	4.46	83.1	17.1
5 $CaCl_2$	12.3	88.9	14.3				

Salting-out extraction of the cobalt(II) complex with 2,2'-bipyridine into acetonitrile from aqueous 1.0 M salt solutions

Various salting-out agents were examined for the extraction of the cobalt-(II) complex into acetonitrile. The results (Table 2) indicate that better extractability was obtained with salts of multivalent ions: the order of extractability was Al>Sr>Ba>Ca>Mg>Na>K>NH_4 with respect to the chloride salts. It is of interest to note that this order is quite similar to the Hofmeister series or the lyotropic series [17] concerning the salting-out effect. The position of ammonium sulphate lay between the alkaline earth and alkali metal salts. Further, the water content of the acetonitrile phase after the extraction increased in the order Al<Mg<Ca<Sr<Ba<K<Na<NH_4, which is contrary to the series obtained by Dobry-Duclaux [18]. In conclusion, the cobalt(II) complex and water are transferred together to the acetonitrile phase, but the trends in their extractability are opposite.

The distribution ratios presented in Table 2 may also be discussed in relation to the solubility (S) of tris(2,2'-bipyridine)cobalt(II) perchlorate in the aqueous salt solution. The logarithm of the partition coefficient (P) of a species is proportional to log S^{-1} in an ideal liquid—liquid distribution system [19]. In the acetonitrile extraction, the mutual solubility between the two phases was too high for direct application of this relationship. However, in an attempt to establish some relationship between the extractability and solubility of the species, the solubilities of the cobalt(II) complex were measured for aqueous acetonitrile solutions of various compositions. The results obtained (Fig. 4) showed that the solubility of the cobalt(II) complex was at a maximum with water contents of about 25% in acetonitrile, and decreased at high and low water contents. The water content of the acetonitrile phase after the extraction ranged from 15 to 40% for all the salts except aluminium chloride (see Table 2); over this range, the cobalt(II) complex had an approximately constant solubility (Fig. 4). The solubility of the cobalt(II) complex in water was also observed to increase linearly with the content of acetonitrile in the aqueous solution. In Fig. 5, log D was therefore plotted

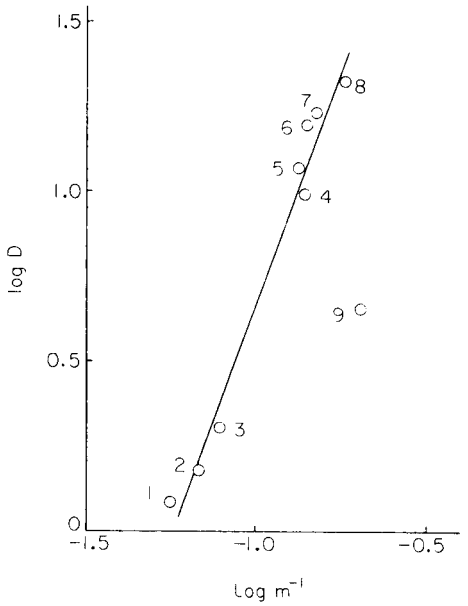

Fig. 5. Relationship between D and the solubility (m) of acetonitrile in various salt solutions. See Table 2 for key to the numbers.

against the negative logarithm of the acetonitrile solubility (m in mol l^{-1}) in aqueous 1.0 M salt solutions, instead of log S^{-1}; the relationship is linear except in the case of ammonium sulphate. It therefore seems reasonable to suggest that the solubility of acetonitrile in the aqueous phase governs the distribution ratio; i.e., decreasing solubility of acetonitrile in aqueous phase increases the extraction of the cobalt(II) complex.

Effect of experimental conditions on the extraction

It is generally recognized that the salting-out effect increases with aqueous salt concentration. The effect of sodium chloride concentration on the extraction of the cobalt(II) complex was examined at 25°C. The results

TABLE 3

Effect of sodium chloride concentration on extraction[a]

NaCl concentration (M)	D	%E	Water content (v/v%)
1.0	2.06	48.3	23.6
2.0	3.79	71.2	11.4
3.0	6.51	82.5	8.4
4.0	12.1	90.2	7.2

[a]The experimental conditions were the same as those described in Table 2.

(Table 3) show that the percentage extraction increased at higher concentrations of sodium chloride, as would be expected from the decreased solubility of acetonitrile in more concentrated salt solutions. The contents of water and sodium chloride in the acetonitrile phase decreased as the salt concentration increased, but the separate roles of the two substances could not be established clearly.

The initial volume of 4.0 M sodium chloride solution was then varied from 10.0 to 60 ml, while the initial volume of acetonitrile was kept to 20 ml. The distribution ratios obtained were constant over the whole volume range tested (Table 4); this can be predicted by the constant solubility of acetonitrile in 4.0 M sodium chloride, despite the change of initial volume of the salt solution. The extraction efficiency, however, decreased with an increase in the initial volume of the salt solution, because the recovered volume of the acetonitrile phase decreased (see the equation for determining $\%E$).

The effect of temperature on the extraction was investigated over the range 15—30°C (Table 5). The D and $\%E$ values decreased with increasing temperature, whereas the solubility of acetonitrile in 1.0 M sodium chloride increased. The negative dependency of the extractability on temperature is probably due to endothermic dissolution of acetonitrile in the salt solution. The reciprocal relationship between water content and extractability is also shown in Table 3.

Nature of the extracted species

Conductivity was measured for 0.16—1.6 × 10^{-2} M tris-(2,2′-bipyridine)-cobalt(II) perchlorate in acetonitrile and in an acetonitrile solution containing 15% water. The plots of the equivalent conductance against the square root of the complex concentration were linear. This suggests that the cobalt(II)

TABLE 4

Effect of initial volume of the aqueous phase (4.0 M sodium chloride) on extraction[a]

Volume (ml)	10.0	20.0	30.0	40.0	50.0	60.0
D	12.6	12.1	12.2	12.3	12.4	12.2
$\%E$	95.6	90.2	83.7	76.2	67.4	56.7

[a]The other experimental conditions were the same as those described in Table 2.

TABLE 5

Effect of temperature on extraction with 1.0 M sodium chloride as the aqueous phase[a]

Temperature(°C)	D	$\%E$	Water content (v/v%)
15.0	2.64	56.6	18.6
20.0	2.31	51.9	21.0
25.0	2.06	46.5	23.6
30.0	1.86	41.8	26.3

[a]The other experimental conditions were the same as those described in Table 2.

complex is a strong electrolyte in the two solutions [20]. In the view of the molar absorptivity, it is likely that the cobalt(II) complex is extracted as the dissociated species $[Co(bip)_3:(ClO_4)_2]$ into the acetonitrile phase.

The author is grateful to Prof. T. Fujinaga, Kyoto University, for many helpful discussions and to Dr. M. Satake, Fukui University, for his continuing encouragement

REFERENCES

1 Y. Marcus and A. S. Kertes, Ion Exchange and Solvent Extraction of Metal Complexes, Wiley—Interscience, London, 1969, p. 597.
2 G. H. Morrison and H. Freiser, Solvent Extraction in Analytical Chemistry, Wiley—Interscience, New York, 1966, p. 43.
3 D. Dyrssen, J. O. Liljenzin and J. Rydberg, Solvent Extraction Chemistry, North-Holland, Amsterdam, 1967.
4 T. Fujinaga and Y. Nagaosa, Bull. Chem. Soc. Jpn., 53 (1980) 416.
5 P. F. Collins, H. Diehl and G. F. Smith, Anal. Chem., 31 (1959) 1862.
6 B. G. Stephens and H. A. Suddeth, Anal. Chem., 39 (1967) 1478.
7 W. F. McDevit and F. A. Long, J. Am. Chem. Soc., 74 (1952) 1773.
8 F. H. Burstall and R. S. Nyholm, J. Chem. Soc., (1952) 3570.
9 I. A. Riddick and W. B. Bunger, Technique of Chemistry, Vol. VII, Organic Solvents, Wiley—Interscience, New York, 3rd edn., 1970.
10 Y. Nagaosa, Anal. Chim. Acta, 115 (1980) 81.
11 J. Setschenow, Z. Phys. Chem., 4 (1889) 117.
12 F. A. Long and W. F. McDevit, Chem. Rev., 51 (1952) 119.
13 J. H. Stern and A. Hermann, J. Phys. Chem., 71 (1967) 306.
14 V. Gutmann, Electrochim. Acta, 21 (1976) 661.
15 Y. Yoshimura and N. Suzuki, Anal. Chim. Acta, 85 (1976) 383.
16 C. E. Matkovich and G. D. Christian, Anal. Chem., 45 (1973) 1915.
17 S. Glasstone and D. Lewis, Elements of Physical Chemistry, Van Nostrand, New York, 1960, p. 585.
18 A. Dobry-Duclaux, Chem. Ztg., 76 (1952) 805.
19 C. Hansch, J. E. Quinlan and G. L. Lawrence, J. Org. Chem., 33 (1968) 347.
20 S. Motomizu, K. Toei and T. Iwachido, Bull. Chem. Soc. Jpn., 42 (1969) 1006.

Analytica Chimica Acta, 120 (1980) 289—296

SEPARATION OF URANIUM FROM NATURAL WATERS ON CHELEX-100 RESIN

P. PAKALNS

Australian Atomic Energy Commission Research Establishment, Lucas Heights, NSW, 2232 (Australia)

(Received 10th March 1980)

SUMMARY

Uranium can be separated from fresh waters on Chelex-100 resin by careful control of the resin pH at 4.6 when sample solutions are adjusted to 3.9—4.7 after addition of 1,2-diaminocyclohexanetetraacetic acid. The interference of up to 500 μg of phosphate is avoided by addition of thorium(IV) at pH 3.9—4.0. After elution with 2 M nitric acid, uranium is determined spectrophotometrically with 4-(2-pyridylazo)resorcinol. Uranium can be concentrated from sea water at its natural pH without masking when the column is conditioned at pH 7.0 and a fluorimetric determination is used. The maximum recovery is 93% by spectrophotometry and 90% by fluorimetry. Interference by surfactants, sodium tripolyphosphate, NTA and EDTA at concentrations of 20 mg l^{-1} reduces recoveries to 84—91%. Vanadium(V) interferes slightly in the spectrophotometric method.

Sulcek and Povondra [1] have shown that, after the addition of 1,2-diaminocyclohexanetetraacetic acid (DCyTA) to solutions in the pH range 3.5—7, uranium can be separated quantitatively from many cations on Dowex-1 resin in the ammonium form. Earlier, Florence and Farrar [2] had adjusted the aqueous solutions to pH 3 before separation and reported that, after separation on the resin in the sodium form, the only interference in the spectrophotometric determination of uranium with 4-(2-pyridylazo)resorcinol (PAR) was caused by vanadium(V), which forms a weak complex with DCyTA and is partially absorbed by the resin. When the Chelex-100 resin column and the solution were adjusted to the same pH, a robust concentration scheme for many metals could be readily achieved in natural waters with metal recoveries better than 92% [3].

This paper describes the use of Chelex-100 resin for the preconcentration of uranium from polluted and unpolluted fresh and saline waters. After careful resin pH adjustment, uranium was determined by either the spectrophotometric PAR method [2], or the fluorimetric method based on extraction from saturated calcium nitrate—EDTA [4] or acid-deficient aluminium nitrate salting-out solutions [5]. High uranium concentrations were determined spectrophotometrically with PAR [2], whereas for μg l^{-1} levels the fluorimetric method was preferred.

EXPERIMENTAL

Columns and reagents

The Chelex-100 exchange columns were prepared with 3 ml of resin as described previously [3] and were conditioned with 20 ml of a solution (pH 4.6) containing 136 g of sodium acetate trihydrate and 58 ml of glacial acetic acid per litre.

DCyTA solution (50 g l^{-1}). Dissolve 50 g of 1,2-diaminocyclohexanetetra-acetic acid in 800 ml of water by adjusting the pH of the suspension to 6.0 with 10% sodium hydroxide. Dilute to 1 l.

Washing solution (pH 5.5). Dissolve 8 g of ammonium acetate in 800 ml of water. Adjust to pH 5.5 with acetic acid. Dilute to 1 l.

Recommended procedures

Sample preparation. After sampling, filter the water through a 0.45-μm membrane filter, and analyse the sample immediately. If necessary, the sample may be stored in acid-washed polythene bottles after the addition of 2.5 ml of 15 M nitric acid per litre of filtrate; in this case, the results may differ from the unacidified sample. Before analysis, adjust the pH to 4.0 after the addition of the DCyTA solution.

Analytical method (a) (for total phosphate between 25 and 500 μg). Transfer a sample to a beaker and add 2.0 ml of the DCyTA solution to each 25-ml aliquot. Add 1.0 ml of aqueous thorium nitrate solution (1 g Th l^{-1}) and, if required, adjust the pH of the solution to between 3.9 and 4.0. Pass the solution through the resin column at a rate of 2 ml min^{-1}. Rinse the beaker with 5 ml of water, add the washings to the column, then wash the resin with 20 ml of the washing solution using the same flow rate. Elute uranium with 20 ml of 2 M nitric acid into a 100-ml tall beaker. Add 1 ml of 72% perchloric acid and evaporate the solution to dryness on a hotplate at medium temperature. Dissolve the salts in 10 ml of water and determine uranium spectrophotometrically with PAR.

For the fluorimetric determination, dissolve the salts in 5 ml of 1 M nitric acid, add 25 ml of salting-out solution [4], and transfer it to a 50-ml separating funnel. Extract into 2.00 ml of methyl isobutyl ketone and then determine uranium.

Analytical method (b) (for total phosphate less than 25 μg). Determine uranium in the above manner, but do not add 1 ml of thorium solution; if necessary, adjust the pH between 3.9 and 4.7.

The recovery of uranium should be determined by carrying a solution containing approximately 120 μg of uranium through the procedure. The maximum recovery at 23°C is 93%. The absorbance of the blanks varies between 0.000 and 0.001.

RESULTS AND DISCUSSION

A preliminary investigation was carried out to determine the optimum pH of the resin column giving the maximum recovery of uranium from 25-ml

aliquots of solutions prepared from distilled water or sea water, each containing 2.0 ml of DCyTA solution. The resin was conditioned by adding 20 ml of various 1 M solutions at different pH (Table 1). The results show that the highest recovery of uranium (93%), measured against an aqueous uranium standard, was obtained when the resin column was conditioned with 1 M sodium acetate—acetic acid buffer of pH 4.6. After the addition of DCyTA, the pH values for the distilled and sea-water samples were 6.4 and 3.9, respectively. The sea water had a greater buffering capacity than distilled water in the resin column conditioned at pH $\geqslant$5.5, so that the lower pH was maintained and so the uranium recoveries from sea water were higher. It should be possible to determine uranium in sea water after conditioning the resin at pH 5.5, although at that pH, phosphate interference would not be overcome by the addition of thorium (see below). Uranium recoveries were also determined from distilled and sea-water samples without DCyTA for resin columns preconditioned as above. To maintain a constant pH, the distilled water samples were prepared in corresponding 0.1 M conditioning solutions; after the separation, the resin was washed with 20 ml of the same 0.1 M conditioning solution. After conditioning the resin column with a 1 M solution of pH 7.0, a sea-water sample was passed through the column at its natural pH of 8.2, the column being washed with 20 ml of 0.1 M conditioning solution of pH 7.0. The results given in Table 1 show that, in the presence of DCyTA, maximum adsorption of uranium from fresh and saline waters was obtained when the pH of the sample was about pH 4.6 but, without the addition of DCyTA, the maximum recovery from fresh waters was obtained at pH 5.5. This optimum pH for the separation of uranium on

TABLE 1

The effect of various conditioning solutions on the recovery of uranium (120 μg U) in the presence and absence of DCyTA after separation on Chelex-100 resin (3 ml; 50—100 mesh) 25 ml sample

Conditioning solution (1 M) 20 ml added	pH	Recovery (%)[a]			
		With DCyTA		Without DCyTA	
		Distilled water	Sea water	Distilled water	Sea water
Nil	10.3	69	83	—	—
Na acetate	8.6	86	90	86	—
NH_4 acetate	7.0	86	90	86	93
NH_4 acetate[b]	5.5	89	93	93	—
Na acetate[b]	4.6	93	93	88	—
Na acetate[b]	4.6	83[c]	—	—	—
Na acetate[b]	4.6	93[d]	—	—	—

[a]Compared with standard uranium solution (120 μg U). [b]pH adjusted with acetic acid. [c]200-ml sample, 16 ml of 5% DCyTA added, pH 6.30. [d]200-ml sample, 16 ml of 5% DCyTA added, pH 4.70.

Chelex-100 resin from ground waters has also been reported by Hathaway and James [6]. Although Riley and Taylor [7] reported that uranium could not be adsorbed on the resin column from sea water, results have shown that uranium can be separated directly, with a maximum recovery of 93%, from such samples if the Chelex-100 resin is previously conditioned at pH 7.0 with 1 M ammonium acetate solution.

Effect of different waters on column pH

The above results showed that Chelex-100 resin conditioned at pH 4.6 could be used to separate uranium from 25-ml samples of fresh and saline waters. With such small samples, the pH of the effluent stays close to the pH of the column (4.75). To separate uranium from larger volumes, however, the change in the pH of the effluent has to be known, because the recovery of uranium from 200 ml of distilled water is only 83% (Table 1). To examine this pH change, 200-ml volumes of distilled and natural waters at various pH values were passed through the resin column conditioned at pH 4.75; the pH of the effluent was measured at 10-ml intervals. The results in Fig. 1 show that it should be possible to separate uranium from 25-ml volumes of distilled and river waters at their original pH after addition of DCyTA, because the effluent pH of 5.10 has increased just slightly above the pH of the column of 4.75 (curves 1 and 6). One the pH of the effluent exceeded 5.1, the adsorption (and recoveries) of uranium decreased (Table 1). If, after the addition of DCyTA, the pH of fresh waters is adjusted to pH 4.7, the pH of the effluent remains nearly constant below pH 5.0 (curves 2 and 7). If the pH is adjusted to 4.0, that of the effluent will remain above 4.0 (curve 3) which is the lowest pH giving the maximum recovery of 93% (Table 2).

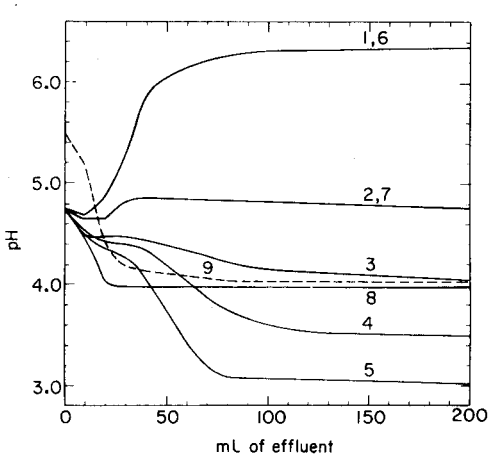

Fig. 1. Effect of distilled, river and sea waters on the pH of the effluent. pH of resin column 4.75, except for curve 9. DCyTA added before pH adjustment. Distilled water, pH: (1) 6.30; (2) 4.70; (3) 4.00; (4) 3.50; (5) 3.00. River water, pH: (6) 6.30; (7) 4.70. Sea water, pH: (8) 3.90; (9) (pH of column 5.50) 3.90.

TABLE 2

The effect of probable interferences on the recovery of uranium in the presence of DCyTA on Chelex-100 resin column conditioned at pH 4.6, for 25-ml samples containing 120 μg U

Interference	Conc. (mg l^{-1})	Th added (mg)	pH of soln.	Recovery (%)[a]	Interference	Conc. (mg l^{-1})	Th added (mg)	pH of soln.	Recovery (%)[a]
Distilled water					*Distilled water*				
—	—		4.7	93	Sodium	20	—	4.7	89
—	—	—	3.5	86	tripolyphosphate	20	1	4.0	89
—	—	—	3.0	86	Washing powder	20	—	4.7	87
Phosphate	1	—	4.7	92		20	1	4.0	87
	5	—	4.7	82	NTA	20	—	4.7	84
	20	—	4.7	35		20	1	4.0	90
	20	1	6.2	30	EDTA	20	—	4.7	84
	20	1	4.7	90		20	1	4.0	91
	20	1	4.0	93	V(V)	0.1[d]	—	4.7	5
	40	1	4.0	84	Th	—	1	4.0	52[e]
	40	2	4.0	84	*Polluted creek water*				
	100	5	4.0	54	Phosphate	23	1	4.0	89
	2.5	1	4.0	93[b]		13	1	4.0	88[f]
	10	4	4.0	87[b]	*Tidal water*				
	—	—	4.7	90[c]	Phosphate	<0.05	—	4.7	90[b]
	20	1	4.0	91[c]	*Sea water*				
Anionic	20	—	4.7	90	Phosphate	1	—	3.9	93[g]
detergent	20	1	4.0	87		5	—	3.9	91
Nonionic	20	—	4.7	91	—	20	—	3.9	70
detergent	20	1	4.0	87	—	—	—	8.0	3.5[b,h,i]
						—	—	3.9	3.4[b,i]

[a]Compared with standard uranium solution. [b]200-ml sample. [c]Samples containing 0.12 and 1.2 μg of uranium, determined fluorimetrically with calcium nitrate—EDTA salting-out solution. [d]Total amount added in mg; no U added; this produced a colour equivalent to 5 μg U. [e]Thorium adsorbed on resin column in μg; no U added. [f]40-ml sample. [g]The same recovery was obtained on a 200-ml sample without the addition of 1 mg Th, and containing 500 μg of phosphate with 1 mg Th added. [h]Column conditioned with 20 ml of 1 M ammonium acetate and after separation washed with washing solution of pH 5.5. No DCyTA added. [i]Results in μg U l^{-1}. No U added.

The pH of sea water after the addition of DCyTA decreased to 3.9 and the final pH of the effluent was about 4.0 (curve 8). Uranium in sea water can be separated using a resin column conditioned at pH 5.5 (Table 1); curve 9 indicates a fast drop in the pH of the effluent and therefore good recoveries (93%). The pH at the top of the resin column is lower than indicated by the effluent.

For solutions adjusted to pH 3.5 and 3.0, curves 4 and 5 indicate that adsorption of uranium should be good from a 25-ml volume, but the recoveries were only 86% (Table 2). Any large volume of solution adjusted to a pH below 3.9 will produce an effluent having a pH below 3.9 (curves 4 and 5) and recoveries will then be low.

Washing solution

After the adsorption of uranium, the resin column must be washed to remove residual DCyTA from the column because the nitric and perchloric acid mixture does not destroy the DCyTA completely on fuming. A dark

organic residue appears in the beaker, which will explode if the residue is fumed to dryness. To overcome this danger, a washing solution was needed with a pH low enough not to elute uranium in the presence of DCyTA yet high enough not to elute any uranium after the removal of DCyTA (Table 1). A solution of 0.1 M ammonium acetate at pH 5.5 removed DCyTA without any loss of uranium. Sodium acetate—acetic acid (pH 4.6) or distilled water washing solutions gave 88 and 86% recoveries, respectively.

Study of interferences

The effect of interfering ions and results of uranium determination in sea water are shown in Table 2.

Phosphate interferes badly because its complex with uranium prevents complete adsorption, being unretained by the resin. With phosphate at 1 mg l^{-1} in a 25-ml solution, 92% recovery was obtained, but this decreased rapidly with increasing phosphate concentration. Thorium(IV) was added to complex phosphate ion; 1 mg of thorium(IV) permitted the determination of uranium in the presence of phosphate up to 20 mg l^{-1} in a 25-ml sample. The total amount of phosphate tolerable in a sample (at any volume) was 500 μg. An increase in the thorium concentration, or dilution of the sample, did not improve uranium recoveries, and the pH of the solution had to be lowered from 4.7 to 4.0 to obtain the maximum recovery of 93%.

Unpolluted sea water would not require an addition of thorium since the phosphate concentration is very low, but when polluted water is analysed for uranium, the phosphate levels must be known to enable selection of sample size and, if necessary, to add 1 mg of thorium. The tidal water sample had a salinity of 24‰, the phosphate was below 0.05 mg l^{-1} and the methylene blue reactive substances (MBRS) were 0.095 mg l^{-1}. Thorium was not added and the recovery of added uranium from a 200-ml sample was 90%.

The two water samples were collected from creeks receiving effluent from activated sludge treatment plants and contained phosphate formed by the hydrolysis of tripolyphosphate. The sample volumes used for the recovery tests contained total phosphate concentrations of 575 (25 mg PO_4 l^{-1}) and 520 (13 mg PO_4 l^{-1}), respectively. After acid hydrolysis of tripolyphosphate, the corresponding total phosphate was 26 and 15 mg PO_4 l^{-1} and the MBRS were 0.36 and 0.90 mg l^{-1}, respectively. Uranium recoveries were 88—89% because of the combined effect of various substances in a treated sewage effluent. Recoveries of uranium added to 200-ml samples from creeks supplying drinking water to Sydney were 93%.

The effects of detergents and complexing agents were determined at concentrations of 20 mg l^{-1} in 25-ml volumes, with and without the addition of 1 mg of thorium. Anionic detergent (LAS, linear alkyl sulphonate, 100% active material), nonionic detergent (nonyl ethoxylate, 100% active material), washing powder (15% LAS and 25% sodium tripolyphosphate) and sodium tripolyphosphate gave recoveries of 87—91%, probably because of incomplete removal of metal from the resin column with nitric acid eluant [3]. The two

complexing agents, nitrilotriacetic acid (NTA) and EDTA, form strong complexes with uranium [2]. Therefore some reduction in the uranium recoveries was expected (84%) but the addition of thorium improved the recoveries to 90—91%.

Vanadium(V) in the presence of DCyTA was adsorbed on the resin to the extent of 10%; 10 μg of vanadium produced a colour with PAR equivalent to 5 μg of uranium. The fluorimetric method is free from vanadium interference.

Thorium was adsorbed on the column to the extent of 5.2% in the range of 1—5 mg of thorium tested. This small amount of thorium did not interfere with the spectrophotometric determination or with the calcium nitrate—EDTA fluorimetric procedure. During the extraction from acid-deficient aluminium nitrate salting-out solution, approximately 20% of thorium was extracted into methyl isobutyl ketone; hence about 1 μg of thorium was present in a pellet used for the fluorimetric determination. Sabol and Rider [8] have shown that 1 μg of thorium will produce an interference less than 1% by quenching.

The reported 93% recoveries of a uranium standard solution were obtained at a laboratory temperature of 23°C. In summer when the temperature rose to 33°C, the recovery decreased to 86%.

Determination of uranium in sea water

The uranium concentration in an unacidified sea-water sample, collected from a beach in Sydney, New South Wales, was determined by using the direct separation method and the DCyTA complexing procedure. In the direct method, the resin column was conditioned with a 1 M ammonium acetate solution of pH 7.0, a 200-ml sample of sea-water was passed through the column, the column was washed with 20 ml of 0.1 M ammonium acetate solution of pH 5.5 and uranium eluted with 20 ml of 2 M nitric acid. After adding 1 ml of perchloric acid, the eluate was fumed to dryness and uranium determined fluorimetrically. In the DCyTA complex procedure, 16 ml of DCyTA complexing solution was added to the 200-ml sea-water sample and the separation of uranium was carried out as recommended in the Analytical Method (b). The uranium concentrations, calculated on the basis of 90% recovery, were 3.5 and 3.4 $\mu g\ l^{-1}$, respectively; this is in good agreement with published results of $3.3 \pm 0.2\ \mu g\ U\ l^{-1}$ in sea water [9]. The 90% recovery for the fluorimetric determination of microgram amounts of uranium (Table 2) is 3% less than the maximum obtained for the spectrophotometric method; this is to be expected because of the interference in the fluorimetric method by sodium perchlorate (25 mg) in the fumed residue [4, 5].

REFERENCES

1 Z. Sulcek and P. Povondra, Collect. Czech. Chem. Commun., 32 (1967) 3140.
2 T. M. Florence and Y. Farrar, Anal. Chem., 35 (1963) 1613.
3 P. Pakalns, G. E. Batley and A. J. Cameron, Anal. Chim. Acta, 99 (1978) 333.

4 P. Pakalns and L. E. Ismay, Mikrochim. Acta, 1976 I, 297.
5 P. Pakalns and L. E. Ismay, Mikrochim. Acta, 1976 II, 217.
6 L. R. Hathaway and G. W. James, Anal. Chem., 47 (1975) 2035.
7 J. P. Riley and D. Taylor, Anal. Chim. Acta, 40 (1968) 479.
8 W. W. Sabol and B. F. Rider, USAEC Report KAPL-1477, 1956.
9 T. L. Ke, K. G. Knauss and G. C. Mathieu, Deep-Sea Res., 24 (1977) 1005.

Analytica Chimica Acta, 120 (1980) 297—304

IMPROVED ASSAYS FOR HYDRALAZINE AND HYDRALAZINE PYRUVIC ACID HYDRAZONE IN HUMAN PLASMA

T. M. LUDDEN*

College of Pharmacy, The University of Texas-Austin, Austin, TX 78712 (U.S.A.)

L. K. LUDDEN, J. L. McNAY, H. B. SKRDLANT, P. J. SWAGGERTY and A. M. M. SHEPHERD

Department of Pharmacology, The University of Texas Health Science Center, San Antonio, TX 78284 (U.S.A.)

(Received 10th March 1980)

SUMMARY

Previous determinations of hydralazine and hydralazine pyruvic acid hydrazone based on derivatization and high-performance liquid chromatography have been modified to improve the detection limits of the hydralazine assay and the selectivity of the hydralazine pyruvic acid hydrazone technique. The lower limits of determinations of hydralazine and hydralazine pyruvic acid hydrazone are 2 and 25 ng ml^{-1}, respectively. The application of this technique to the determination of these substances in human plasma is demonstrated.

Hydralazine (1-hydrazinophthalazine, HDZ) has clinical application as a direct acting vasodilator. Although HDZ has been in clinical use for over 20 years, the lack of selective and sensitive techniques for its determination in biological fluids has hampered studies concerning its disposition and pharmacokinetics. Many earlier assay procedures [1—5] are now known to be nonselective owing to the conversion of circulating HDZ hydrazones, particularly the pyruvate hydrazone (HPH), back to HDZ [6, 7]. Proveaux et al. [8] have reported a procedure for the conversion of HDZ to s-triazolo-(3,4a)phthalazine followed by fluorescent detection of the derivative after separation by high-performance liquid chromatography (h.p.l.c.). The selectivity of this procedure has not been evaluated. Degen [9] has described a gas–liquid chromatographic procedure using a nitrogen-specific detector to quantify 1-(3,5-dimethyl-1-pyrazolyl)phthalazine formed by reacting unchanged HDZ with 2,4-pentanedione at room temperature for 1 h. Although the yield is only 40%, this is compensated by the inclusion of a derivatizable internal standard. At a concentration of 680 ng ml^{-1}, HPH did not significantly affect the hydralazine standard curve. The detection limit was about 10 ng ml^{-1}.

Recently, a method was reported for the determination of hydralazine

p-anisaldehyde hydrazone (HPAH) following derivatization of unchanged HDZ in human plasma with *p*-anisaldehyde at room temperature for 7 min [10]. Under the assay conditions HPH, (20 μg ml^{-1}) yielded less than 0.1 mol % HDZ. The detection limit for hydralazine was 5 ng ml^{-1} but good precision was achieved only at concentrations of 10 ng ml^{-1} or above. The results of a preliminary study of the pharmacokinetic behavior of HDZ in healthy human subjects [11] has indicated that levels of unchanged hydralazine are low after oral or intravenous dosing and that additional assay sensitivity is required for certain pharmacokinetic studies.

This report describes modifications of recently published h.p.l.c. procedures [10, 12] that permit selective determination of plasma HDZ concentrations down to 2 ng ml^{-1} and HPH concentrations down to 25 ng ml^{-1}. In addition, evidence is presented which suggests that the formation of HPAH is catalyzed by a substance present in plasma.

EXPERIMENTAL

Reagents and chemicals

Ethyl acetate, acetonitrile and methanol were purchased as glass-distilled solvents; no further processing was necessary. Hydralazine hydrochloride (Sigma Chemical Co.), hydralazine hydrochloride (USP reference standard; U.S. Pharmacological Convention, Inc., Rockville, MD) and *p*-anisaldehyde (Eastman Kodak Co.) were also used. Hydralazine pyruvic acid hydrazone and hydralazine *p*-anisaldehyde hydrazone were prepared and their identity and purity were verified by combined gas chromatography—mass spectrometry as previously described [10].

Derivatization

To determine the appropriate derivatization time, 200 ng of hydralazine was added to each of twelve 3-ml blank plasma samples containing 10 μl of *p*-anisaldehyde. After 3, 5, 7, 10, 15, and 20 min at about 23°C, duplicate samples were extracted as described below and subjected to h.p.l.c. separation. The relative heights of h.p.l.c. peaks were determined.

The efficiency of derivatization of HDZ was determined by comparing the recoveries of HPAH from four 3-ml samples containing 100 ng ml^{-1} standard HDZ and from four 3-ml blank plasma samples to which an equimolar concentration (173 ng ml^{-1}) of HPAH had been added prior to extraction.

Since attempts to assay hydralazine in aqueous media other than plasma using this procedure had been unsuccessful, an effort was made to demonstrate the apparent necessity of a plasma constituent. First, an ultrafiltrate (CF25 Filter Amicon Corp., Lexington, MA) of fresh human plasma was prepared and used in place of plasma. The relative heights of the HPAH peaks obtained using the ultrafiltrate were compared to those obtained when the original plasma sample was used.

It was also possible to demonstrate the necessity of a plasma constituent

by sequentially diluting plasma with 0.1 M phosphate buffer, pH 7.4, and using these solutions instead of plasma.

Extraction

After derivatization, samples were prepared for injection onto the h.p.l.c. column as described previously [10] except that 10 ml of ethyl acetate was used to extract the derivatized HDZ. No buffer was added prior to extraction. Extraction efficiency for HPAH was evaluated by comparing the peak heights of HPAH for four 3-ml plasma samples to which HPAH (173 ng ml^{-1}) had been added before extraction and for four extracts of blank plasma samples to which the same amount of HPAH was added just before injection onto the h.p.l.c. column.

The aqueous phase was prepared for HPH determination using a modification of the procedure described by Haegele et al. [12]. A portion (3 ml) of 0.1 M potassium phosphate buffer, pH 7.4, with 10 mM ethylenediamine tetraacetic acid (EDTA) and 18 ml of methanol were added and the samples placed in the dark at 4°C for about 1 h to allow precipitation of proteins. Following centrifugation for 20 min, 8 ml of supernatant liquid was withdrawn, and evaporated on a rotary evaporator. The residue was then submitted to h.p.l.c. separation and HPH determination as described by Haegele et al. [12].

Chromatography

The residue of each ethyl acetate extract was dissolved and chromatographed as previously described [10] except that the pH of the aqueous portion of the mobile phase was 3.0 instead of 3.4. The residue of each deproteinated aqueous phase was dissolved and chromatographed as previously described [12].

To prepare standard curves, 3 ml of human plasma and 10 μl of *p*-anisaldehyde were placed in an 18-ml culture tube fitted with a polytef-lined screw cap. Fresh solutions of HDZ (6 ng μl^{-1}) in normal saline and HPH (150 ng μl^{-1}) in 0.1 M potassium phosphate buffer, pH 7.4, with 10 mM EDTA were prepared just before use. Appropriate volumes of each solution were added to yield HDZ concentrations of 2—160 ng ml^{-1} and HPH concentrations of 50—1000 ng ml^{-1}. Each sample was mixed immediately and allowed to react for 10 min. Extraction and chromatography were done as described above.

Studies were also done in which the standard curves obtained with frozen plasma from a local blood bank were compared with those obtained with fresh plasma.

Selectivity. Blank plasma samples were spiked with HDZ at concentrations of 2—160 ng ml^{-1}. These were processed in duplicate and compared to identical duplicate standards to which HPH (1 ng ml^{-1}) had been added. Varying concentrations of HPH (50—600 ng ml^{-1}) were added to blank plasma and taken through the assay. The resulting standard curve was compared to an identical standard curve to which HDZ (300 ng ml^{-1}) had also been added.

Potential interference from 3-methyl-s-triazolo(3,4a)phthalazine, 1-hydrazinophthalazinone and 4-(2-acetylhydrazino)phthalazinone, metabolites of hydralazine, was also evaluated.

Precision. Intra-assay precision was evaluated by preparing and assaying quadruplicate standard samples containing HDZ concentrations of 2, 4, 12, 40, 80, and 160 ng ml^{-1} and HPH concentrations of 50, 100, 300, 500, 700, and 1000 ng ml^{-1}.

Human volunteers

Unchanged hydralazine in plasma was determined in two healthy male subjects (1 and 2) and one hypertensive male patient (3), all previously found to be slow acetylators by sulfamethazine phenotyping [13]. Subjects 1 and 2 received an oral dose of hydralazine hydrochloride (0.5 mg kg^{-1}) as a solution in distilled water. Subject 3 received 1 mg kg^{-1} as oral tablets (Apresoline; Ciba-Geigy, Ardsley, NY). In addition, the study was repeated in Subject 3 after seven consecutive 1 mg kg^{-1} oral doses.

Blood samples were drawn into chilled, evacuated tubes containing EDTA as anticoagulant and the red cells were immediately separated by centrifugation at 4°C for 5 min at 2000 g; 3 ml of plasma was added to a culture tube containing 10 μl of *p*-anisaldehyde and vortexed. Unknown samples were then treated exactly like standard curve samples described above.

RESULTS

The retention times of HPAH and HPH were 6.3 and 5.0 min for their respective chromatographic conditions. Detection limits were 2 ng ml^{-1} and 25 ng ml^{-1} for HDZ and HPH, respectively. The use of mobile phase at pH 3.0 instead of 3.4 [10] significantly improved the separation of HPAH from endogenous material. Derivatization efficiency of HDZ was found to be 92.3% while extraction recovery of HPAH was 84.9%. As shown in Fig. 1, there is little additional derivatization of HDZ after 10 min at room temperature. Therefore, a derivatization time of 10 min was chosen for all subsequent studies using a 3-ml plasma sample.

Comparison of HDZ standard curves with and without HPH and of HPH standard curves with and without HDZ yielded no significant differences. At concentrations of 20 μg ml^{-1}, 3-methyl-s-triazolo(3,4)phthalazine, 1-hydrazinophthalazinone, and 4-(2-acetylhydrazino)phthalazinone did not interfere with either assay.

Attempts to assay HDZ in the absence of plasma were unsuccessful by this derivatization procedure. Peak heights for HPAH obtained from such samples were only 0—40% of those obtained from plasma and were quite variable. Similar results were obtained for a plasma ultrafiltrate. Results from the plasma dilution study (Fig. 2) indicate that about a 25% concentration of plasma is required to yield a good recovery of HPAH. Standard curves prepared from frozen blood bank plasma were not different from those prepared from fresh plasma.

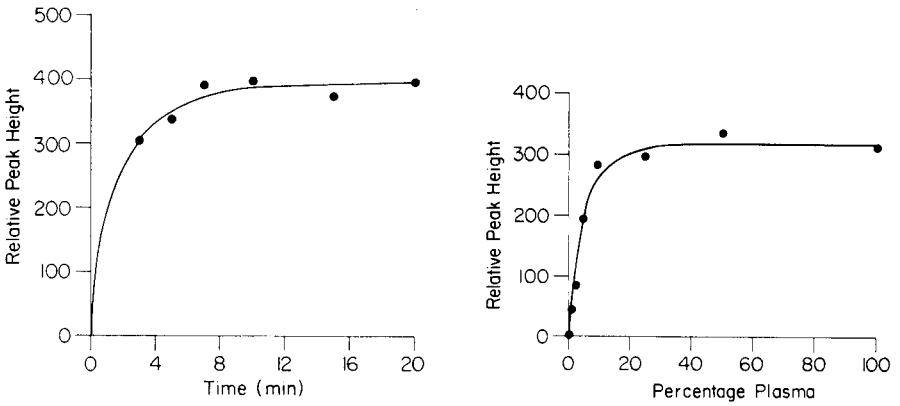

Fig. 1. Estimation of minimum derivatization time. Each point is the mean of two determinations.

Fig. 2. Effect of dilution on the plasma hydralazine assay.

The results of the intra-assay precision study are shown in Table 1. The mean coefficients of variation were 6.9 and 14.0% for HDZ and HPH, respectively. Plasma concentration versus time data for the three volunteers are shown in Table 2. Concentrations of HPH were not determined in Subject 1. Subjects 1 and 2, who both received only 0.5 mg kg^{-1} doses as a solution, exhibited low HDZ concentrations that peaked 20—30 min after drug administration. Concentrations of HDZ dropped below the assay limits after 75—90 min. Plasma HDZ concentrations in the hypertensive patient (Subject 3) who received 100 mg as tablets, both as a single dose and again after seven consecutive 100-mg doses every 12 h, exhibited considerably higher plasma HDZ levels. Peak concentration occurred 40—60 min after the dose and were still detectable at 3 h. Concentrations of HDZ after multiple doses were higher than after the single dose in this subject, but subsequent studies in seven additional hypertensive patients [14] have failed to substantiate this finding.

TABLE 1

Intra-assay precision of hydralazine and hydralazine pyruvic acid hydrazone assays

Hydralazine added (ng ml^{-1})	Relative peak height[a]	Hydralazine found (ng ml^{-1})	Hydralazine pyruvic acid hydrazone added (ng ml^{-1})	Relative peak height[a]	Hydralazine pyruvic acid hydrazone fou (ng ml^{-1})
2	16.5 ± 1.6	2.18	50	24.5 ± 4.6	50.7
4	29.5 ± 2.4	4.07	100	44.4 ± 6.5	101
12	84.5 ± 5.0	12.1	300	123 ± 9.6	297
40	250 ± 15.4	36.0	500	212 ± 13.5	520
80	537 ± 17.3	77.7	700	258 ± 45.8	637
160	1152 ± 95.2	167	1000	424 ± 58.9	1053

[a]Mean ± SD (n = 4).

TABLE 2

Concentrations of hydralazine and hydralazine pyruvic acid hydrazone after oral administration to three human volunteers

Time	Plasma concentration (ng ml^{-1})						
	Subject 1 Single dose[a]	Subject 2 Single dose[a]		Subject 3			
				Single dose[b]		Multiple dose[b]	
	HDZ	HDZ	HPH	HDZ	HPH	HDZ	HPH
0	0.0[c]	0.0	0.0	0.0	0.0	0.0	335
5	<2.0[d]	—	—	—	—	—	—
10	15.8	0.0	<25	0.0	0.0	0.0	386
15	—[e]	25.0	—	—	—	—	—
20	24.8	41.9	36.5	0.0	0.0	0.0	388
25	—	34.6	—	0.0	0.0	0.0	—
30	27.1	9.3	80.4	0.0	0.0	0.0	416
35	—	16.8	—	<2.0	0.0	<2.0	—
40	6.4	19.5	102	52.3	227	52.8	496
45	—	12.1	—	156	—	222	—
50	7.5	6.9	—	130	—	203	—
60	3.8	2.1	117	92.6	895	226	963
75	2.2	<2.0	—	19.8	—	54.4	—
90	<2.0	0.0	98.8	11.4	927	40.0	1129
105	<2.0	—	—	5.8	—	16.0	—
120	0.0	—	60.3	5.7	764	12.8	980
150	—	—	80.4	<2.0	791	8.0	1000
180	—	—	65.8	2.1	822	4.8	816
240	—	—	<25	—	723	—	804
360	—	—	29.2	—	590	—	645
480	—	—	29.2	—	300	—	229

[a]0.5 mg kg^{-1} as a solution. [b]1 mg kg^{-1} as four 25-mg tablets. [c]Indicates no evidence of HDZ or HPH. [d]Indicates evidence of HDZ or HPH but concentration is not quantifiable. [e]Sample either not obtained or not assayed.

Concentrations of HPH in Subjects 2 and 3 peaked at about 90 min and then declined rather slowly. Quantifiable amounts were still present 8 h after doses were given. Accumulation of HPH during multiple dosing in Subject 3 is clearly illustrated by a predose HPH concentration of 335 ng ml^{-1}. Comparisons of relative HDZ and HPH concentrations in Subjects 2 and 3 indicated that HPH concentrations almost always exceed HDZ concentrations by 5—10 fold or more.

DISCUSSION

Most previously published procedures [1—5] for the determination of HDZ in biological fluids are nonselective because labile plasma metabolites of hydralazine are also measured [6, 7]. Recently published procedures

[9, 10] appear to be more selective but have a limit of about 10 ng ml^{-1} for precise quantification. A method with a detection limit of 3 ng ml^{-1} has been reported [8] but the selectivity of this technique has not been adequately evaluated. The currently described h.p.l.c. method has good selectivity in that the major identified plasma metabolite of HDZ, namely HPH, does not interfere, and it provides for precise quantification of HDZ down to 2 ng ml^{-1}. There is loss of precision in determining HPH when this procedure is used instead of the original method [12] but there is improved selectivity in that unchanged HDZ is not converted to HPH during the process.

In vivo and in vitro animal studies [15, 16] of HPH indicate that it does not possess sufficient vasodilatory activity to account for the prolonged antihypertensive effect observed following HDZ administration. However, the determination of this metabolite in combination with a nonselective gas–liquid chromatographic procedure [3] permits estimation by difference of the acid-labile plasma metabolites of HDZ other than HPH [14]. These yet-unidentified metabolites may play a role in the pharmacological effect of HDZ.

The use of an extraction step and separate chromatographic procedures for HDZ and HPH permits the selection of optimum conditions for the determination of both compounds. While deletion of the ethyl acetate extraction and use of solvent programming for chromatographic separation would simplify the overall procedure, there is a significant loss in sensitivity for both HPAH and HPH.

The application of the analytical technique was illustrated for two healthy subjects and one hypertensive patient, all known to be slow acetylators. Fast acetylators have lower HDZ concentrations after oral dosing but a considerable portion of the plasma level time profile following a 1 mg kg^{-1} oral dose can still be described by using this procedure [14]. The sensitivity is also adequate for describing the pharmacokinetics of HDZ after a 0.3 mg kg^{-1} intravenous dose [17]. While the complexity of the assay does not lend itself to use in routine monitoring of HDZ therapy, it will serve as a research tool for acquiring pharmacokinetic information concerning the factors that influence HDZ disposition in man.

This work was supported by grants from the Texas Affiliate, Inc., the American Heart Association and NIH grant GM24092. We thank Ms. Barbara Boyle and Ms. Beverly Keeton for their help in preparing this paper, and Drs. W. Reiss and K. Schmid (Ciba-Geigy, Ltd., Basel, Switzerland) for their generous gift of authentic 4-(2-acetylhydrazino)-phthalazinone.

REFERENCES

1 R. Zacest and J. Koch-Weser, Clin. Pharmacol. Ther., 13 (1972) 420.
2 S. B. Zak, M. F. Bartlett, W. E. Wagner, T. G. Gilleran and G. Lukas, J. Pharm. Sci., 63 (1974) 225.
3 D. B. Jack, S. Brechbüler, C. H. Degen, C. Zbinden and W. Riess, J. Chromatogr., 115 (1975) 87.
4 S. B. Zak, G. Lukas and T. G. Gilleran, Drug Metab. Dispos., 5 (1977) 116.
5 D. W. Schneck, J. S. Sprouse, K. Miller, J. E. Vary, F. O. DeWitt and A. H. Hayes, Jr., Clin. Pharmacol. Ther., 24 (1978) 714.
6 P. A. Reece, P. E. Stanley and R. Zacest, J. Pharm. Sci., 67 (1978) 1150.
7 P. A. Reece and R. Zacest, Clin. Exp. Pharmacol. Physiol., (1979) 207.
8 W. J. Proveaux, J. C. O'Donnell and J. K. H. Ma, J. Chromatogr., 176 (1979) 480.
9 P. H. Degen, J. Chromatogr., 176 (1979) 375.
10 T. M. Ludden, L. K. Goggin, J. L. McNay, K. D. Haegele and A. M. M. Shepherd, J. Pharm. Sci., 68 (1979) 1423.
11 A. M. M. Shepherd, T. M. Ludden, K. D. Haegele, T. Talseth and J. L. McNay, Res. Commun. Chem. Path. Pharmacol., 26 (1979) 129.
12 K. D. Haegele, H. B. Skrdlant, T. Talseth, J. L. McNay, A. M. M. Shepherd and W. A. Clementi, J. Chromatogr., 187 (1980) 171.
13 W. Olson, J. Miceli and W. Weber, Clin. Pharmacol. Ther., 23 (1978) 204.
14 A. M. M. Shepherd, T. M. Ludden, M.-S. Lin and J. L. McNay, Clin. Pharmacol. Ther., 27 (1980) 286.
15 T. Talseth, K. D. Haegele, J. L. McNay, H. B. Skrdlant, W. A. Clementi and A. M. M. Shepherd, J. Pharmacol. Exp. Ther., 211 (1979) 509.
16 A. M. M. Shepherd, W. A. Clementi, K. D. Haegele, J. L. McNay, T. M. Ludden, H. B. Skrdlant and T. Talseth, Clin. Res., 27 (1979) 317A.
17 T. M. Ludden, A. M. M. Shepherd, M.-S. Lin and J. L. McNay, Clin. Pharmacol. Ther., 27 (1980) 268.

Analytica Chimica Acta, 120 (1980) 305—311

AUTOMATIC DETERMINATION OF INORGANIC CARBON IN SURFACE WATERS

JOAN CROWTHER* and W. B. MOODY

Water Quality Section, Ontario Ministry of the Environment, Rexdale, Ontario M9W 5L1 (Canada)

(Received 5th June 1980)

SUMMARY

An automated colorimetric procedure was developed for the determination of inorganic carbon in the range 0.3—40.0 mg l^{-1}, and then modified to handle concentrations in the range 0.01—2.00 mg l^{-1}. The procedure entailed conversion of carbon dioxide equilibria products to carbon dioxide. By gas dialysis, a portion of this gas was dissolved in a weakly buffered alkaline phenolphthalein solution, and inorganic carbon was determined by measuring the loss in color of the indicator. Calibrations were linear within 1% full scale. When surface water samples were processed by the subject and by alternative methods, the colorimetric carbon results were lower by approximately 1% full scale.

The concern with acid precipitation has led to studies of lakes with low natural alkalinities where the effects of acid rain are exacerbated. These investigations require knowledge of hydrogen carbonate buffering capacity and frequently entail primary productivity measurements. In both cases, a sensitive analytical procedure for inorganic forms of carbon is required. To be suitable, methods should be automated to handle the work load.

For determining both dissolved organic and dissolved inorganic carbon, Goulden [1] introduced an automated dual-channel procedure which utilized infrared detectors. To determine dissolved organic carbon, DiLiddo [2] modified this procedure primarily by changing to colorimetric detection. The latter was based on the diffusion of carbon dioxide through a gas dialyzer into a weakly buffered alkaline phenolphthalein solution and measurement of the resultant loss in color at 550 nm. It seemed feasible that an automated analytical method for inorganic carbon could be developed by combining a simple extraction step with DiLiddo's colorimetric detection system. It was assumed that determination of dissolved inorganic carbon equilibria products would suffice, as the concentration of particulate inorganic carbon in the test waters of interest was expected to be insignificant.

EXPERIMENTAL

Apparatus

For the low analytical range, culture tubes (25 × 150 mm) with polyseal cone caps were used as sample containers. Determinations required an Auto-

Analyser system including a large industrial model sampler, modified to accept the tall culture tubes by lowering the base plate, a peristaltic pump, an AAII colorimeter, and a single-pen chart recorder. Other modules needed were a variable-temperature heating bath (157-B273-39) plus temperature controller (170-B173-02) and two gas dialyzers (177-B077-01 and 177-B008-01) equipped with carbon dioxide-permeable membranes (157-B129); the path length for each gas dialyzer was 15 cm. Figure 1 is a schematic diagram of the flow system. Contamination from the atmosphere was minimized by drawing air requirements for reagent and manifold lines through a gas-scrubbing train consisting of two wash bottles, one filled with 20% (v/v) sulphuric acid to remove any ammonia and the other containing 6.2 M sodium hydroxide to strip carbon dioxide. For the high range, only one gas dialyzer was required, and the heating bath was omitted (Fig. 2).

A Beckman Model 915A Total Carbon Analyzer and a Varian 920 gas chromatographic unit with standard thermal conductivity detectors were employed to provide control data.

Reagents

All reagents and standards were prepared with deionized, distilled water that had been flushed with nitrogen for 1 h. For the low range, calibration standards were prepared daily by diluting a sodium hydrogencarbonate

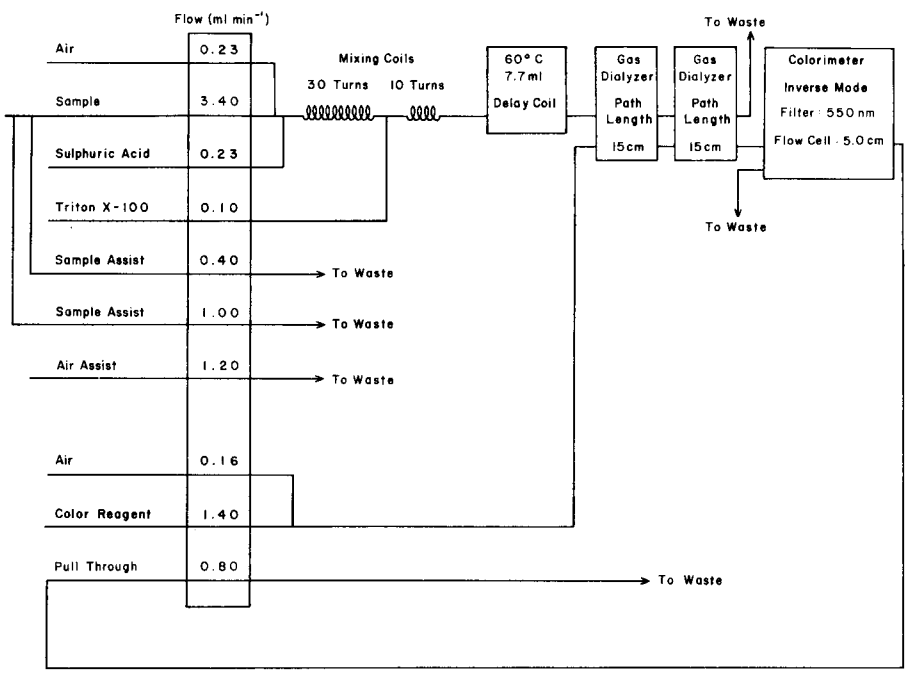

Fig. 1. Low analytical range manifold for determination of inorganic carbon in surface waters.

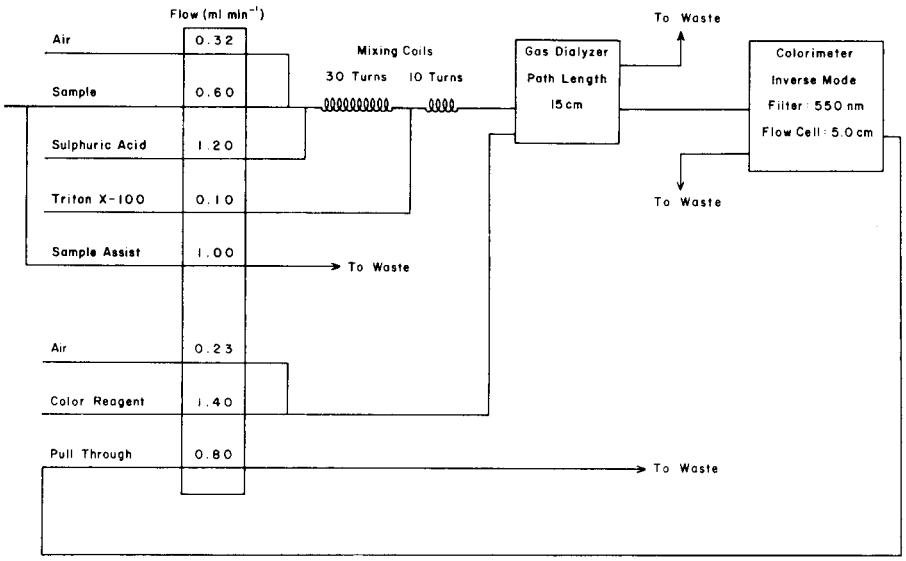

Fig. 2. High analytical range manifold for determination of inorganic carbon in surface waters.

(200 mg C l^{-1}) solution stored in sealed glass ampules. For the high range, standards were prepared from a refrigerated stock solution of sodium hydrogencarbonate (1000 mg C l^{-1}), and these standards could be used for 3—5 days before the blank problem became significant. Analyses required a 0.25 M sulphuric acid solution. To prepare the color reagent, three stock solutions needed were: (a) wetting agent containing equal volumes of isopropanol and Triton X-100 (Rohm and Haas Co.); (b) phenolphthalein (1 g dissolved in 100 ml of methanol); and (c) buffer. The buffer was prepared by dissolving 5.0 g of sodium hydrogencarbonate and 2.5 g of sodium tetraborate decahydrate in approximately 950 ml of water and then adjusting the pH of the solution with 0.5 M sodium hydroxide to the range 9.45—9.50. After dilution to 1 l, the flask was promptly stoppered. The working color reagent was prepared by diluting 2.0 ml of phenolphthalein stock to 1900 ml and adding 50.0 ml of buffer stock and 1.0 ml of wetting agent stock. After further dilution to 2 l and mixing, the reagent was quickly transferred to a low-actinic glass bottle (2-l capacity) and capped or connected to the gas-scrubbing train. The air space above the reagent was minimized and the solution was prepared 2—16 h before use so that the reaction resulting from the inevitable brief exposure of the reagent to air had been completed. The baseline on the chart recorder drifted upwards during determinations if the air space above the color reagent still contained carbon dioxide. A Triton X-100 working reagent was prepared by diluting 10 ml of the wetting agent stock solution to 1 l. The air supply to the wash water reservoir of the sampler was also drawn through the gas scrubbing train.

Procedure

For the low range, samples were collected by field staff in 25 × 150 mm culture tubes with polyseal cone caps. The tubes were completely filled and capped leaving no air bubble. Samples were processed within 24 h by presenting these culture tubes directly to the AutoAnalyzer system. This collection procedure eliminated errors arising from sample transfers.

One 12-l batch of nitrogen-flushed deionized, distilled water was prepared daily, and utilized for preparing standards, wash water, and blanks. A small portion of this water was acidified to pH 2 with sulphuric acid and reflushed with nitrogen to provide two acidified blanks. With the heating bath set at 60°C, a stable baseline for the AutoAnalyzer system was obtained. Then one acidified blank was processed using the setting from the previous day for the standard calibration knob; typically this blank was equivalent to -0.02 mg C l^{-1}, a value which indicated that carbon dioxide had been stripped efficiently from the water supply. When the baseline had re-stabilized after about 10 min, the system was calibrated, and the calibration data were plotted to determine the blank. Sampling time and wash cycle were both 2 min. The colorimeter was operated in the inverse mode on Damp 1 setting. Although the drum of the sampler was loaded with standards and samples, the caps were removed from only ten culture tubes at a time. Thus the operator was obliged to attend the system every 40 min. At the conclusion of the run, another "acid" blank was processed to ensure that the system had not become contaminated with carbon dioxide during the operation.

As the resolution for the high analytical range was only 0.2 mg C l^{-1}, some of the restrictions required for the low range were omitted: (a) continuity of sample containers from field through measurement was not mandatory; (b) both standards and samples were exposed to the atmosphere throughout the run; (c) the colorimeter signal was not damped; and (d) the rate of determinations was increased to 24 h^{-1}. The daily calibration was checked to ensure that the blank was <0.2 mg C l^{-1}.

RESULTS AND DISCUSSION

High analytical range

A procedure was developed for determining inorganic carbon at the levels expected in most surface waters, i.e., full scale was 40.0 mg C l^{-1}. For this system (Fig. 2), the sample was acidified to convert hydrogencarbonate equilibria products to carbon dioxide. Then the stream was mixed with the air that had been stripped of carbon dioxide, and passed over a gas dialyzer fitted with a carbon dioxide-permeable membrane. A reproducible portion of carbon dioxide was extracted into a weakly buffered alkaline phenolphthalein solution, and carbon was determined by measuring the loss in absorbance of this reagent at 550 nm. The color reagent described by DiLiddo [2] was tested, but it was found that resultant calibrations were not linear. To overcome this problem, DiLiddo's color reagent was modified by

lowering the pH to 9.3, and slightly increasing the buffering capacity by replacing sodium carbonate with sodium tetraborate. Standards were prepared from sodium hydrogencarbonate because they were more stable when exposed to the atmosphere than standards prepared from sodium carbonate or carbonate/hydrogencarbonate combinations. Hydrogencarbonate standards changed less than 0.2 mg C l^{-1} when exposed to the atmosphere for 8 h. When this system was calibrated, full scale absorbance change was approximately 0.4 units, and calibrations were linear within 0.2 mg C l^{-1}. The standard deviation for replicate determinations ranged from 0.17 to 0.30 mg C l^{-1} depending on the carbon content of the samples (Table 1). The system was also evaluated by comparison with the inorganic carbon channel of a Beckman 915A Total Carbon Analyzer [3] which had been calibrated for the range 2—100 mg C l^{-1}. Supernatant liquids from 62 surface waters were processed by both procedures, and the data were subjected to linear regression analysis: Y on X where X referred to the colorimetric data (Table 2). For the linear regression, the slope was 0.992 with a standard deviation of 0.005; the intercept was 0.246 mg C l^{-1} with a standard deviation of 0.095 mg C l^{-1} and the standard error of estimate was 0.308. Colorimetric results were lower by an average of 0.18 mg C l^{-1}. Over the past three years, this procedure has proven both precise and rugged.

Low analytical range

When special studies required a more sensitive inorganic carbon procedure, the above system was modified so that full scale was 2.00 mg C l^{-1}. Sample and color reagent flow rates were altered, and the manifold was expanded to include an extra gas dialyzer and a heating bath set at 60°C (Fig. 1). Full scale absorbance change for this system was about 0.15 units.

Although there was slight evidence of curvature, deviations from linearity did not exceed 0.02 mg C l^{-1}. Six standards were processed and results were plotted daily to determine the blank which ranged from —0.02 to 0.06 mg C l^{-1}, and averaged 0.025 mg C l^{-1} with a standard deviation of 0.029 mg C l^{-1} for 20 observations. Carbon standards could be exposed to the atmosphere for 1 h if the carbon concentration was 0.40 mg l^{-1} or greater; at lower concentrations, the average change was 0.021 mg C l^{-1}. Provided standards

TABLE 1

Precision of replicate analyses of surface waters

High range (full scale = 40.0 mg C l^{-1})			Low range (full scale = 2.00 mg C l^{-1})		
Sample concn. range (mg l^{-1} C)	No. of samples	S. d. (mg C l^{-1})	Sample concn. range (mg C l^{-1})	No. of samples	S. d. (mg C l^{-1})
<8.0	118	0.17	<0.40	21	0.003
8.0—20.0	57	0.30	0.40—1.00	9	0.013
20.0—40.0	84	0.28	1.00—2.00	28	0.020

TABLE 2

Intercomparison of inorganic procedures based on analyses of surface waters

Statistical parameter[a]		High range (f.s.d.=40.0 mg C l^{-1})	Low range (f.s.d.=2.00 mg C l^{-1})
No. of samples		62	57
Linear regression (Y on X)			
Slope and s. d.		0.992(0.005)	0.913(0.026)
Intercept and s. d. (mg C l^{-1})		0.246(0.097)	0.125(0.032)
Standard error of estimate		0.308	0.00656
Differences ($Y - X$) for range:			
<20%	No. of samples	31	2
	Av. difference and s. d. (mg C l^{-1})	0.13(0.46)	0.065
20—50%	No. of samples	16	35
	Av. difference and s. d. (mg C l^{-1})	0.28(0.59)	0.045(0.077)
50—100%	No. of samples	15	20
	Av. difference and s. d. (mg C l^{-1})	0.08(0.61)	−0.016(0.097)
<100%	No. of samples	62	57
	Av. difference and s. d. (mg C l^{-1})	0.18(0.53)	0.024(0.088)

[a] X refers to colorimetric data.

were capped between determinations, changes in concentration over a 24-h period were less than 0.02 mg C l^{-1} for the entire calibrated range.

Precision was estimated by processing routine samples in duplicate. The standard deviation increased from 0.003 to 0.020 mg C l^{-1} depending on the carbon content of the samples (Table 1).

To estimate perishability, samples were processed on successive days; the average decrease in inorganic carbon was 0.030 mg l^{-1} compared with a standard deviation of 0.039 mg C l^{-1} for 23 samples. As these samples were at least one day old with reference to the time of sampling, another series of tests was performed. Eight samples were collected simultaneously at one site, and processed at 15-min intervals with the first vial analyzed 5 min after collection. The results were 2.24, 2.24, 2.24, 2.32, 2.24, 2.24, 2.24, 2.28 mg C l^{-1}. Finally, the first vial, which had been exposed to the atmosphere for 2 h, was reanalyzed; the inorganic carbon had decreased from 2.24 to 2.10 mg l^{-1}. These results suggest that the procedure is valid for low-level inorganic carbon determinations provided that sample exposure to the atmosphere is restricted.

An interference study was conducted by mixing the test solution with a blank or carbon standard within the manifold; solution strengths, however, were adjusted such that flow rates and concentrations at the gas dialyzers were unchanged. This technique avoided interactions with the atmosphere. The results of the study showed that 8 common cations (Al(III), NH_4^+, Ca(II), Fe(III), Mg(II), Mn(II), K^+, and Na^+) and 7 common anions (F^-, Cl^-, NO_3^-, NO_2^-, PO_4^{3-}, SiO_3^{2-} and SO_4^{2-}) were not detected as carbon and that carbon spikes were recovered within 2%. At the 50 mg l^{-1} level, humic and tannic acids did not interfere. Sulphide, however, was detected as inorganic carbon; 1 mg S^{2-} l^{-1} was equivalent to 0.6 mg C l^{-1}.

The method intercomparison utilized a gas chromatographic procedure. The latter was similar to that described by Murray et al. [4], but the column packing was 30% HMPA (hexamethylphosphoramide) [5] on acid-washed 60—80 mesh Chromosorb W instead of Porapak Q. When full scale was 2.00 mg C l^{-1}, this chromatographic system had a variable blank (0.06—0.31 mg C l^{-1}), and showed abrupt changes (5—10%) in sensitivity. Imprecision, as measured by standard deviation, was about three times that of the colorimetric method. Actually these known deficiencies led to the development of the colorimetric method. The intercomparison was conducted by analyzing 58 surface water samples by both procedures, and evaluating the data by linear regression analysis: Y on X where X referred to the colorimetric data (Table 2). The slope was 0.913 with a standard deviation of 0.026; the intercept was 0.125 mg C l^{-1} with a standard deviation of 0.032 mg C l^{-1}, and the standard error of estimate was 0.0066. Given the problems with the gas chromatographic system, this level of agreement was considered adequate.

Although the colorimetric system for determining low levels of inorganic carbon required considerable care in preparation of standards and reagents, the resultant data were both precise and relatively free from interference effects. At these levels, however, inorganic carbon is a perishable parameter requiring prompt analysis and limited exposure to the atmosphere.

REFERENCES

1 P. D. Goulden, Water Res., 10 (1976) 487.
2 J. DiLiddo, Paper presented at the 7th Technicon International Congress, New York, 1976.
3 C. E. von Hall and V. A. Stenger, Anal. Chem., 39 (1976) 503.
4 D. A. J. Murray, D. Povoledo and R. V. Schmidt, Field Analysis of Dissolved Gases in Lake Waters by Gas Chromatography, Water Quality Parameters, ASTM STP 573, American Society for Testing and Materials, 1975, p. 391.
5 J. W. Swinnerton, V. J. Lennebom and C. H. Cheeck, Anal. Chem., 34 (1962) 1509.

Analytica Chimica Acta, 120 (1980) 313—320

GROUND- AND EXCITED-STATE PROTOTROPIC EQUILIBRIA OF SOME HYDROXYLATED BENZO(a)PYRENES

A. C. CAPOMACCHIA* and F. L. WHITE

Department of Pharmaceutics, School of Pharmacy, The University of Georgia, Athens, GA 30602 (U.S.A.)

(Received 24th March 1980)

SUMMARY

Fluorescence excitation and emission spectroscopy are used to determine the ground and excited-state acid dissociation constants for 3-OH- and 9-OH-benzo(a)pyrene as well as the 4,5-, 7,8-, and 9,10-dihydrodiol derivatives. These constants and spectral shifts arising from substituent placement are used to show that in the vicinity of the hydroxyl substituents there is a greater charge localization for 9-OH-benzo(a)pyrene than for 3-OH-benzo(a)pyrene in both ground and lowest excited singlet states, and that for 9,10-dihydrodiol there is greater charge localization than for 4,5- and 7,8-dihydrodiol in the ground state. These results are briefly correlated with the carcinogenic potential of benzo(a)pyrenes.

For the past twenty years workers in the area of benzo(a)pyrene (BP) metabolite identification have been using fluorimetric assay procedures [1—5]. Initially the procedure relied solely on the native fluorescence of the BP metabolite(s) [1]. Later workers found that alkaline solutions enhanced the sensitivity of the method; therefore alkali extractable metabolites were monitored [2]. For the most part, these metabolites are monohydroxy derivatives of BP formed spontaneously from arene oxides which are intermediates in the metabolism of BP [6]. The dihydroxy derivatives are dihydrodiols and are formed from the parent hydrocarbon through the intermediate formation of simple epoxides which are hydrated to the dihydrodiol by epoxide hydrase [7].

To the best of our knowledge the protolytic behavior of these agents has never been reported. Therefore, the present study was undertaken. The compounds examined were five hydroxy derivatives of BP which have also been shown to be its major metabolites [6, 7]: 3-OH-BP, 9-OH-BP, trans-4,5-dihydro-4,5-diol, trans-7,8-dihydro-7,8-diol and trans-9,10-dihydro-9,10-diol.

EXPERIMENTAL

Materials

The benzo(a)pyrenes, 3-OH-BP, 9-OH-BP, trans-4,5-dihydro-4,5-diol-BP, trans-7,8-diol-BP and trans-9,10-dihydro-9,10-diol-BP (J. N. Keith, ITT Research Institute, Chicago, IL) were available in lots of 5 mg or less. All compounds were used without further purification but were determined to be pure by comparing the respective absorption and corrected fluorescence excitation spectra of their dilute ethanolic solutions, by their fluorescence emission, and by h.p.l.c. Stock ethanolic solutions (ca. 1.0×10^{-6} M) of these agents were prepared fresh weekly and stored in the dark at 10°C. Daily purity checks were conducted to ensure that no decomposition had occurred. Solid samples were kept in a freezer at −10°C. Basic solutions were prepared by dilution of carbonate-free sodium hydroxide with distilled, deionized water. The latter was also used to make acidic solutions from Baker reagent-grade sulfuric acid. Sulfuric acid solutions were calibrated by means of the corrected Hammett acidity scale of Jorgenson and Hartter [8]. Solutions for the pH region were prepared by dilution of sulfuric acid or sodium hydroxide solution. Buffer solutions were not used because of their possible interference in fluorimetric titrimetry [9].

Methods

Solutions for fluorimetric study of acid-base character were prepared by adding 100 μl of stock ethanolic hydrocarbon solution to 2 ml of acid or base solution which had been added to a 2-ml cuvette with a volumetric pipet. Addition of ethanolic hydrocarbon solution to acidic or basic solutions resulted in (95 : 5) water-alcohol solution which had no apparent effect on the spectra. After delivery of the hydrocarbon, each solution was mixed rapidly with a teflon paddle. The spectrum of each solution was recorded within 1 min. All acid—base studies were conducted in triplicate. Values of pK_a and pK_a* were obtained graphically from respective plots of fluorescence excitation and emission intensity versus pH or Hammett acidity.

Apparatus

Corrected fluorescence excitation and emission spectra were generated on a Perkin-Elmer MPF-44A spectrofluorimeter in 1-cm quartz cells. Spectra were corrected for the wavelength response of the light source, photomultiplier tube, and optical system by means of a microprocessor. Electronic absorption spectra were taken in 1-cm silica cells on a Cary 118 spectrophotometer. All spectral measurements were conducted at room temperature, 24 ± 2.0°C. A modular Altex h.p.l.c. system with a single-piston pump, a 254-nm single wavelength detector, a μ-Bondapak C-18 column and a CO: PELL ODS pre-column eluted with (7 : 3) methanol—water were used to check PAH purity. Microliter aliquots of ethanolic PAH solutions were delivered with a 100-μl syringe (Precision Sampling Corp.). The pH values were measured with a Corning Model 12 pH meter using a Sensorex 5300 C silver—silver chloride glass combination electrode.

RESULTS

The corrected fluorescence excitation spectra of the neutral and anionic species for both 3-OH-BP and 9-OH-BP are shown in Fig. 1. In the mid-pH region from pH 5 to 7.5 the excitation intensity of 3-OH-BP remains constant. For 9-OH-BP this region of constant intensity is from pH 5 to 8.5. As the pH is increased to 12, the spectral intensity of each compound diminishes rapidly with a mid-point at pH 8.6 and 9.5 for 3-OH-BP and 9-OH-BP, respectively (Table 1). Each compound in the ground-state solvent configuration exhibits a shift to longer wavelengths of its excitation spectrum with increasing pH. The appearance of these new bands corresponds exactly with the disappearance of the ones which lie at shorter wavelengths. The new bands exhibit some loss in vibrational character relative to the latter.

The corrected emission spectra of the neutral and anionic species for both 3-OH-BP and 9-OH-BP are shown in Fig. 2. In the low pH region from pH 1—3 and from pH 2—6 the fluorescence intensities of 3-OH-BP and 9-OH-BP, respectively, are constant. As basicity is increased to pH 10, the emission intensity of each compound decreases with a mid-point at pH 4.3 and 7.8 for 3-OH-BP and 9-OH-BP, respectively (Table 1). Corresponding exactly with the disappearance of the structured emission bands at short wavelength are the appearance of new diffuse emission bands at longer wavelengths.

The excitation and emission spectra for both prototropic species derived from 3-OH-BP lie at longer wavelengths than the corresponding species for 9-OH-BP except for the anions in the lowest excited singlet state which have the same maxima.

Table 2 shows a comparison of the red shift induced by ring hydroxylation

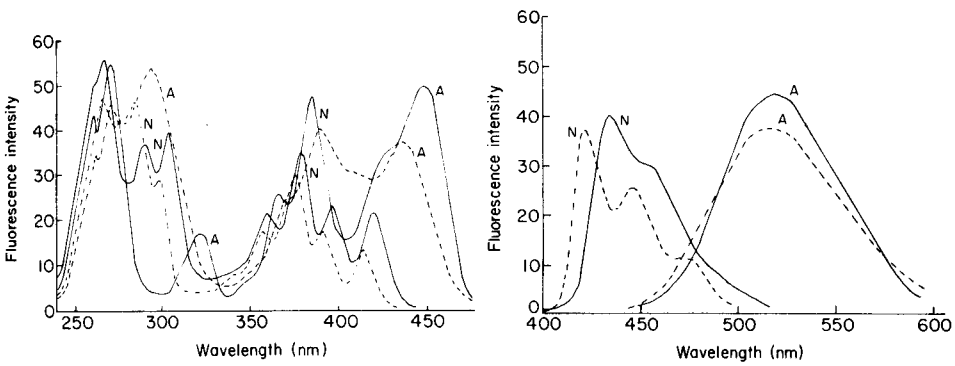

Fig. 1. Corrected excitation spectra for the anion (A) at pH 12 and neutral molecule (N) at pH 6 for 3-OH-BP (——) and 9-OH-BP (---) in aqueous solution. All concentrations are ca. 1×10^{-7} M.

Fig. 2. Corrected emission spectra for the anion (A) at pH 10 and neutral molecule (N) at pH 2 for 3-OH-BP (——) and 9-OH-BP (---) in aqueous solution. All concentrations are ca. 1×10^{-7} M.

TABLE 1

Acid dissociation constants for the ground (pK_a) and lowest excited singlet states (pK_a^*) for some mono- and dihydroxy derivatives of benzo(a)pyrene (BP)

BP	pK_a	Wavelength (nm)	pK_a^*	Wavelength (nm)
3-OH	8.6	450	4.3	420, 520
9-OH	9.5	440	7.8	435, 520
Trans-4,5-dihydro-4,5-diol	12.7	325	~1	385
Trans-7,8-dihydro-7,8-diol	11.8	368	1.0	403
Trans-9,10-dihydro-9,10-diol	13.2	345	0.0	408

TABLE 2

Shifts ($\Delta\nu_a$ and $\Delta\nu_f$, $cm^{-1} \times 10^{-4}$) and Stokes shift (SS, $cm^{-1} \times 10^{-4}$) in the electronic spectra of naphthalene compared to those in benzo(a)pyrene (BP) caused by ring hydroxylation

	$\bar{\nu}_a$[a]	$\Delta\bar{\nu}_a$	SS[3]	$\bar{\nu}_f$[b]	$\Delta\bar{\nu}_f$
Naphthalene	3.20		0.02	3.18	
		0.08			0.53
α-naphthol[c]	3.12		0.52	2.65	
		0.13			0.33
β-naphthol[c]	3.07		0.78	2.85	
Benzo(a)pyrene	2.48		0.02	2.45	
		0.12			0.18
3-OH-BP	2.36		0.08	2.28	
		0.09			0.09
9-OH-BP	2.38		0.03	2.37	

[a]Long-wavelength band absorption or corrected excitation maxima. [b]Fluorescence maxima. [c]From Ref. [10].

in naphthalene and benzo(a)pyrene; it is greater for naphthalene in the lowest excited singlet state whereas the ground states are shifted equivalently. In both the ground and lowest excited singlet states, the naphthols show a greater Stokes shift than the BP phenols.

The corrected fluorescence excitation and emission spectral characteristics of the three dihydrodiol derivatives are shown in Table 3. These compounds are referred to below as 4,5-DBP, 7,8-DBP and 9,10-DBP. The excitation spectral intensities for all three diols are constant in the neutral pH region but diminish as basicity is increased. The mid-points at which this occurs are listed in Table 1. No new bands appear as pH is increased. The emission intensities for all three diols are also constant at neutral pH and diminish rapidly as acidity is increased. The mid-points at which this occurs are in Table 1. Again, no new bands appear as acidity is increased. The excitation

TABLE 3

Corrected excitation and emission spectral features of 4,5-DBP, 7,8-DBP and 9,10-DPB compared to the major absorption, excitation, and emission features of BP and chrysene

	Absorption, excitation (nm)				Emission (nm)		
Chrysene	258	266	320	362[a]	364	382	402[b]
4,5-DBP[c]	266	275	323	364	366	385	407
7,8-DBP[c]	257	292	366	396	402	424	446
9,10-DBP[c]	273	301	345	382	407	429	452
BP[c]	263	296	386	402	406	430	457

[a]Ref. [11]. [b]Ref. [12]. [c]Results from this laboratory.

spectrum of 4,5-DBP shows vibrational fine structure which is retained during the course and at the completion of all acid—base reactions, with appropriate scale expansion. The emission spectrum of 4,5-DBP is quenched with increasing acidity until H_0—4.7 when the spectral band suddenly loses all vibrational features and presents itself as a diffuse band overlaying the original band. This can be attributed to decomposition. The midpoint of quenching was estimated (Table 1).

The low-intensity, long-wavelength excitation spectral bands in the region 350—400 nm and the higher intensity bands in the region 320—370 nm for each dihydrodiol are more affected by substituent placement than are the shorter-wavelength bands in the region 250—310 nm. The long-wavelength bands are positioned in the order 7,8-DBP > 9,10-DBP > 4,5-DBP. The short-wavelength band of 9,10-DBP appears to lie at longer wavelengths than that of 7,8-DBP and shows less vibrational structure than the latter. In the same wavelength region, the spectrum of 4,5-DBP is even less clearly defined than that of the 9,10-derivative and cannot be compared with regard to its position. The excitation and emission spectral position and especially the band form of 4,5-DBP more resemble those of chrysene than the parent compound BP (Table 3). However, the excitation and emission spectra of 7,8- and 9,10-DBP are similar in bandform and position to BP (Table 3).

DISCUSSION

The shift to longer wavelengths of both the excitation and emission spectra for 3-OH-BP and 9-OH-BP, which is due to formation of the phenolate anion, and their increased acidity in the lowest excited singlet state are typical of molecules containing electron-donating substituents. Both indicate a significant charge redistribution in the electron clouds of these molecules. This is especially true in the vicinity of the oxygen atom such that the electronic environment of the hydroxyl-hydrogen atom is altered. This occurs to a greater extent for both the neutral and anionic species of these compounds in the lowest excited singlet state as seen by the relatively greater red shift of their emission spectra.

The comparative alteration in electronic environment of the hydroxyl proton as a function of substituent placement can be seen in Table 1. The pK_a value reported for 9-OH-BP is more basic by nearly one order of magnitude than that for 3-OH-BP. A comparison of these values with those for α-naphthol and β-naphthol (9.23 and 9.46), respectively [1], shows that in the ground state the 3-OH derivative is more acidic than the naphthols whereas 9-OH-BP is slightly more basic. In contrast, the difference in pK_a^* values for the two BP isomers is 3.5 and they are much more basic in the lowest excited singlet state than the above naphthols ($pK_a^* = 2.5$ and 2.81), respectively [13]. The comparative different excited state protolytic behavior of the BP derivatives is presumably due to a decrease in the interaction of the electronic vector of the hydroxyl groups with the molecular dipole moment in the lowest excited singlet state, relative to that of the naphthols. This explanation seems to be borne out by the greater spectral shifts seen from naphthalene after α- or β-hydroxylation compared to those for BP after hydroxylation in either the 3- or 9- position (Table 2), and by the much greater Stokes shifts observed for the isomeric naphthols (Table 2 [10]). The smaller $\Delta\bar{\nu}_f$ values for the hydroxylated benzo(a)pyrenes show that they possess less charge-transfer character than the naphthols and explain, in part, their greater excited-state basicity. Similarly, the greater $\Delta\bar{\nu}_f$ and $\Delta\bar{\nu}_a$ values for 3-OH-BP account for its greater acidity than the 9-isomer, in both ground and lowest excited singlet states, in terms of comparatively greater charge transfer from the 3-oxygen atom. The much smaller Stokes shifts observed for the two BP derivatives indicate much less change in their excited-state dipole moments when compared with the naphthols. Therefore, solvent reorganization processes around their dipoles during relaxation to the lowest excited singlet state and to the thermally relaxed ground state are less extensive in these agents. Furthermore, these processes are less important in 9-OH-BP than in 3-OH-BP. This, of course, shows that charge redistribution is much less in the BP phenols than in the naphthols and less in 9-OH-BP than 3-OH-BP. As a result, there is a greater charge localization in the region of the hydroxyl oxygen atom which is greater for 9-OH-BP, especially in the lowest excited single state.

The pK_a values for 4,5-DBP, 7,8-DBP and 9,10-DBP are much more basic than those reported for the monohydroxy isomers (Table 1). Moreover, the relative basicities of 7,8- and 9,10-DBP seem to be related to the size of their aromatic π-systems. The 9,10-isomer is more basic by 1.4 pH units and its excitation spectrum lies at shorter wavelengths than 7,8-DBP. Both points indicate that the hydroxyl groups on 9,10-DBP are not interacting with the aromatic π-system to the same extent as those on 7,8-DBP. As a result, there is a relatively greater charge localization in the vicinity of the oxygen atoms in 9,10-DBP compared to 7,8-DBP. The comparison excludes 4,5-DBP since it is more closely related, spectroscopically (Table 3) and structurally, to chrysene than BP.

In contrast, the positioning of the 9,10-DBP emission spectrum at slightly

longer wavelengths than that of 7,8-DBP indicates that the relative charge localization observed for the formed compound in the ground state is lost when it is in the lowest excited singlet state. This is reflected by its more acidic pK_a* relative to that of 7,8-DBP.

The higher pK_a reported here for 9,10-DBP compared to 7,8-DBP supports recent studies on the absolute conformation of the dihydroxy groups in these positions [15—17]. These workers showed that the hydroxyl groups on 9,10-DBP are diaxial whereas those on 7,8-DPB are diequatorial. The latter conformation should confer greater planarity to the molecule and increase the charge-transfer character of the hydroxy groups concomitant with a decrease in the basicity of the latter. This is what was observed and is reported here (Tables 1 and 3).

It is currently thought that polycyclic aromatic hydrocarbons such as BP must be metabolically activated before they can exert any biological activity such as causing cancer [18]. Metabolism to the ultimate carcinogen is believed to occur at the "bay region" of these compounds. For BP this is the region between the C-9 and C-11 atoms [6, 7]. Early work has indicated a correlation between epoxide metabolites and the π-bond densities of some aromatic hydrocarbons. This suggested that metabolism to the arene oxide occurred via electrophilic attack by a singlet oxygen on a π-bond [19, 20]. More recently, studies have emerged which support this idea and indicate that metabolic activation occurs through transfer of an electrophilic oxygen atom from an activated P-450 enzyme to an electron-rich area presumably at or near the "bay region" [6, 7]. The importance of this is that there appears to be some correlation between π-electron density and carcinogenic potential [6, 7, 20].

To date, the only way to determine the π-bond densities or electron-rich regions in BP and some of its derivatives has been through molecular orbital calculations. The present paper shows that simple acid—base studies can experimentally indicate and verify predicted regions of π-electron localization for those derivatives or metabolites that undergo prototropic reactions. For example, it is shown that 9-OH-BP and 9,10-DBP in the ground state have a greater charge localization near the "bay region", than do 3-OH-BP, 4,5-DBP and 7,8-DBP. These results based on pK_a values and spectral shifts correlate well with both theoretical calculations and experiments on the metabolic products of BP reported in the literature [6, 7, 17—21].

REFERENCES

1 A. H. Conney, E. C. Miller and J. H. Miller, J. Biol. Chem., 228 (1957) 753.
2 L. W. Wattenberg, J. L. Leong, and P. J. Strand, Can. Res., 22 (1962) 1120.
3 D. W. Nerbert and H. V. Gelboin, J. Biol. Chem., 243 (1968) 6242.
4 W. Dehnen, R. Tomingas and J. Roos, Anal. Biochem., 53 (1973) 373.
5 G. Holder, H. Yagi, W. Levin, A. Y. H. Lu and D. M. Jerina, Biochem. Biophys. Res. Comm., 63 (1975) 1363.
6 P. W. Jones and R. J. Freudenthal (Eds.), Carcinogenesis—A Comprehensive Survey, Vol. 3, Raven Press, NY, 1978.

7 P. L. Grover (Ed.), Chemical Carcinogens and DNA, Vols. I and II, CRC Press, Boca Raton, FL, 1979.
8 M. J. Jorgenson and D. R. Hartter, J. Am. Chem. Soc., 85 (1963) 878.
9 S. G. Schulman and A. C. Capomacchia, J. Phys. Chem., 79 (1975) 1337.
10 S. G. Schulman, Spec. Lett. 6 (1973) 197.
11 H. H. Jaffee and M. Orchin, Theory and Applications of Ultraviolet Spectroscopy, J. Wiley, New York, 1966.
12 C. A. Parker, Photoluminescence of Solutions, Elsevier, Amsterdam, 1968.
13 A. Weller, Z. Physik. Chem. (Frankfurt), 17 (1958) 224.
14 E. Sawicki, Photometric Organic Analysis, Part I, Wiley—Interscience, N.W., 1970, Ch. 10.
15 H. Yagi, J. Akagi, D. R. Thakker, H. D. Mah, M. Koreeda and D. M. Jerina, J. Am. Chem. Soc., 99 (1977) 2358.
16 J. M. Janusz, A. R. Becker and T. C. Bruice, J. Am. Chem. Soc., 100 (1978) 8269.
17 H. Yagi, D. R. Thakker, R. E. Lehr and D. M. Jering, J. Org. Chem., 44 (1979) 3439.
18 E. C. Miller and J. A. Miller, in H. Busch (Ed.), Molecular Biology of Cancer, Academic Press, NY, 1979.
19 E. Boyland, in B. Pullman (Ed.), Electronic Aspects of Biochemistry, Academic Press, NY, 1964.
20 E. Boyland, in E. D. Bergman and B. Pullman (Eds.), Jerusalem Symposia on Quantum Chemistry and Biochemistry I, Israel Academy of Sciences and Humanities, Jerusalem, 1969.
21 A. Dipple, in C. E. Searle (Ed.), Chemical Carcinogens, ACS Monograph 173, Am. Chem. Soc., Washington, DC, 1976, Ch. 5.

Analytica Chimica Acta, 120 (1980) 321—333

EXTRACTION—SPECTROPHOTOMETRIC DETERMINATION OF BORIC ACID WITH 1,8-DIHYDROXYNAPHTHALENE-4-SULFONIC ACID AND ZEPHIRAMINE

TAKASHI KORENAGA, SHOJI MOTOMIZU and KYOJI TÔEI*

Department of Chemistry, Faculty of Science, Okayama University, Tsushima-naka, Okayama-shi, 700 (Japan)

(Received 21st April 1980)

SUMMARY

1,8-Dihydroxynaphthalene-4-sulfonic acid (DHNS) is described as a new reagent for the extraction—spectrophotometric determination of boric acid. The reagent and its boron complex are extracted into 1,2-dichloroethane as ion-associates with tetradecyldimethylbenzylammonium chloride (zephiramine). The extracted complex of boron—DHNS—zephiramine has the composition 1:2:3 and is stable to back-washing with 1 M sodium chloride solution (pH 9.2), whereas the excess of reagent co-extracted is removed to the aqueous phase. The apparent molar absorptivity of the complex in the organic phase is 2.45×10^4 l mol^{-1} cm^{-1} at 341 nm, which is 1.7 times larger than that with chromotropic acid. Addition of EDTA prevents most interferences. The improved method with DHNS is successfully applied to the determination of boron as boric acid in waters. The exchange equilibrium constants, $K_{A^{n-}}^{nX^-}$, for the reagent and complex were also determined for four monovalent anions (X^- = Cl^-, Br^-, NO_3^- and I^-). Some of these constants are compared with those pertaining to chromotropic acid and 1,8-dihydroxynaphthalene.

Several organic reagents forming six-membered rings (e.g., curcumin [1, 2], β-diketones [3], anthraquinones [1, 4, 5] and aliphatic diols [6, 7]) have been developed for the spectrophotometric determination of boron present as boric acid. These reagents hardly react with boric acid in aqueous neutral media at room temperature, whereas 1,8-dihydroxynaphthalene-3,6-disulfonic acid (chromotropic acid) forms a complex with boric acid in aqueous solution over a wide pH range at room temperature [8]. The spectrophotometric determination of boron in natural waters by extraction of the ternary complex formed with chromotropic acid and tetradecyldimethylbenzylammonium chloride (zephiramine) by 1,2-dichloroethane has been reported [9]. A large quantity of reagent (250-fold relative to boron) was necessary for complete complex formation and the large excess of co-extracted reagent was removed from the organic phase according to the principles proposed by Motomizu and Tôei [10]. The extracted complex showed maximal absorption at 351 nm and the apparent molar absorptivity was 1.4×10^4 l mol^{-1} cm^{-1}, which was 3.5 times greater than that in aqueous solution [8]. However, the composition of the ternary complex could not be determined because of the small difference in the extractabilities of the reagent and

boron complex; also the extraction of boron complex with chromotropic acid was fairly incomplete because of the two sulfonic acid groups present in the reagent.

In the work described here, 1,8-dihydroxynaphthalene-4-sulfonic acid (DHNS) was synthesized and tested for the solvent extraction of boric acid, and a greatly improved method was developed for the extraction—spectrophotometric determination of boron with the reagent and zephiramine. The method was then applied to the determination of small amounts of boron in waters. The extraction equilibria of the ion-pairs of the reagent and the boron complex formed with zephiramine were also examined; some of the exchange equilibrium constants obtained were compared with those of chromotropic acid and 1,8-dihydroxynaphthalene. DHNS is shown to be superior to chromotropic acid as a boron reagent, because of the greater extractability of the boron complex.

EXPERIMENTAL

Reagents

1,8-Dihydroxynaphthalene-4-sulfonic acid (DHNS). This was synthesized from sodium 1-amino-8-naphthol-4-sulfonate by fusion at about 200°C [11, 12]. The DHNS sodium salt produced as white flaky crystals was dried under reduced pressure; 1.311 g was dissolved in 500 ml of deionized water to give a 1.00×10^{-2} M solution. The solution was stored in an amber polyethylene bottle at 4°C.

1,8-Dihydroxynaphthalene-3,6-disulfonic acid (chromotropic acid). Chromotropic acid (disodium salt dihydrate; Dojindo Co.) was used as received; 2.001 g was dissolved in 500 ml of deionized water to give a 1.00×10^{-2} M solution, which was stored in the same way as DHNS.

1,8-Dihydroxynaphthalene. This was synthesized from sodium 1-naphthol-8-sulfonate by fusion at 200—230°C [13, 14]; the reagent was dried under reduced pressure and 20 mg was dissolved in 500 ml of deionized water to give a 2.5×10^{-4} M solution. The solution was stored in the same way as DHNS.

Standard boron solution. Boric acid (154.6 mg) was dissolved in deionized water to give 250 ml of 1.000×10^{-2} M solution, which was stored in a polyethylene bottle. Working solutions were prepared by accurate dilution.

Tetradecyldimethylbenzylammonium chloride (zephiramine, ZCl). Zephiramine (Dojindo Co.) was dried under reduced pressure (2—3 mm Hg) at about 50°C and dissolved in deionized water to give an aqueous 1.00×10^{-2} M solution [15]. A 2.00×10^{-3} M solution of zephiramine in 1,2-dichloroethane was also prepared by direct dissolution of the dried reagent.

Buffer solutions. Sulfuric acid—sodium acetate, potassium dihydrogenphosphate—disodium hydrogenphosphate, ammonia—ammonium sulfate, sodium hydrogencarbonate—sodium carbonate and sodium hydroxide solutions were used to adjust the pH of solutions.

Monovalent anion solutions. Solutions of sodium chloride, bromide, nitrate and potassium iodide were prepared in deionized water.

Analytical-reagent grade solvents and other chemicals were used as received.

Apparatus

Equipment included a Hitachi Model 139 spectrophotometer and a Hitachi Model EPS-3T recording spectrophotometer (both with 10-mm silica cells), a Hitachi—Horiba Model F-5ss pH meter equipped with a combined electrode (6026-05T), an Iwaki Model KM shaker (250 strokes min^{-1}), and a Taiyo Kagaku Kogyo Model Monoshin shaker (50 strokes min^{-1}).

Recommended procedure for analysis of waters

Pipette up to 2 ml of the water sample, which has previously been acidified with 0.5 ml of concentrated sulfuric acid per liter and filtered through a 0.45-μm pore membrane filter, into a stoppered 25-ml test tube. Add 1 ml of buffer (1 M sodium acetate—sulfuric acid, pH 4), 1 ml of 0.01 M EDTA and 1 ml of 0.01 M DHNS solutions, in this order. Dilute the solution to 5 ml with deionized water and mix thoroughly. Add 5 ml of 2×10^{-3} M zephiramine in 1,2-dichloroethane and shake with a KM shaker for 10 min. Discard the aqueous phase and add 5 ml of the back-washing solution (which is 1.0 M in sodium chloride and 0.2 M in ammonia—ammonium sulfate at pH 9.2) to the test tube. Shake with a KM shaker for 10 min and then discard the aqueous phase. Repeat the back-washing of the organic phase with another 5-ml portion of the back-washing solution. Measure the absorbance of the organic phase at 341 nm in 10-mm silica cells against a reagent blank obtained with deionized water as reference. Prepare the working curve with standard boron solution in the same way, and use it for the determination (apparent molar absorptivity, 2.45×10^4 l mol^{-1} cm^{-1} at 341 nm, reagent blank 0.119 ± 0.005).

Procedure for distribution studies

An aliquot of the boron solution was transferred to a stoppered 25-ml test tube and the reagent, buffer, zephiramine and monovalent anion solutions were added in that order. After dilution to 5 ml with deionized water, and thorough mixing, 5 ml of the organic solvent was added. The resulting mixture was equilibrated by shaking for 30 min with a KM shaker (30 min sufficed for all the systems studied). After phase separation (if necessary, the test tube was shaken slowly for 10 min with a Monoshin shaker in order to complete and accelerate phase separation [9]), the aqueous phase was taken out and its pH was measured. The organic layer was transferred to a 10-mm silica cell. Absorbances were measured at the optimum wavelength of each organic solution against the respective solvent as reference.

The distribution of the zephiramine was determined by direct measurement of its absorbance (e.g., the molar absorptivity was 482 l mol^{-1} cm^{-1} at 263 nm in 1,2-dichloroethane and 380 l mol^{-1} cm^{-1} at 262 nm in water). All the extraction studies were made at 25 ± 1°C.

RESULTS AND DISCUSSION

Distribution of zephiramine between 1,2-dichloroethane and water

The distribution of ZCl between 1,2-dichloroethane and water was examined in order to consider the extraction mechanism of the boron complex in detail, although it has been worked through for different solvents [10, 16, 17]. In the present work, the distribution ratio (D_{ZCl}) and the extraction constant (K_{ex}^{ZCl}) of zephiramine chloride can be described as

$$D_{ZCl} = [ZCl]_o/([Z^+]_a + [ZCl_a]) \quad (1)$$

$$K_{ex}^{ZCl} = [ZCl]_o/([Z^+]_a[Cl^-]_a) = D_{ZCl}/([Cl^-]_{total} - [ZCl]_o) \quad (2)$$

where the subscripts a and o refer to the aqueous and organic phases, respectively.

The results obtained showed that the extraction constant for 1,2-dichloroethane was $10^{3.61 \pm 0.05}$ (21 determinations) at 25 ± 1°C. For reference, the extraction constants for dichloromethane, chloroform, carbon tetrachloride and 1,1,2,2-tetrachloroethane were found to be $10^{4.23 \pm 0.05}$, $10^{4.73 \pm 0.08}$, $10^{1.39 \pm 0.03}$ and $10^{2.52 \pm 0.10}$, respectively, under the same conditions. The K_{ex}^{ZCl} values depended on the extraction conditions. For example, when acetate buffer solution (0.020 M) and sodium sulfate solution (0.033 M) were added in the extraction systems described above, the K_{ex}^{ZCl} values became $10^{2.67}$ and $10^{4.98}$ for 1,2-dichloroethane and chloroform, respectively.

To examine the effect of monovalent anions (X^-), the distribution of ZX ($X^- = Br^-$, NO_3^- and I^-) between 1,2-dichloroethane and water was also determined. The extraction constants (K_{ex}^{ZX}) for 1,2-dichloroethane were found to be $10^{4.79 \pm 0.04}$ ($X^- = Br^-$), $10^{5.24 \pm 0.06}$ ($X^- = NO_3^-$) and $10^{6.08 \pm 0.07}$ ($X^- = I^-$), respectively.

The plot of log K_{ex}^{ZX} against $1/r_{X^-}$ (r_{X^-} is the crystallographic ionic radius for each monovalent anion [18]) was found to be linear except for the nitrate ion (Fig. 1).

Properties of DHNS

An aqueous solution of the sodium salt of DHNS was colorless and fluorescent. These solutions were stable in an amber polyethylene bottle for at least a month in a refrigerator. In a colorless bottle at room temperature, the solution was not stable. In the solid state, DHNS in an amber glass jar was stable for a year in a refrigerator.

DHNS (H_3R) dissociates in aqueous solution. The hydroxyl group in the *peri*-position is known to be strongly combined with a hydrogen bond [19], so that the third acidity constant, pK_{a3}, could not be obtained. As the sulfonic acid group was dissociated above pH 1, pK_{a1} could also not be determined. The second acidity constant, pK_{a2}, was calculated from

$$pK_a = pH + \log \{(d_2 - d)/(d - d_1)\} \quad (3)$$

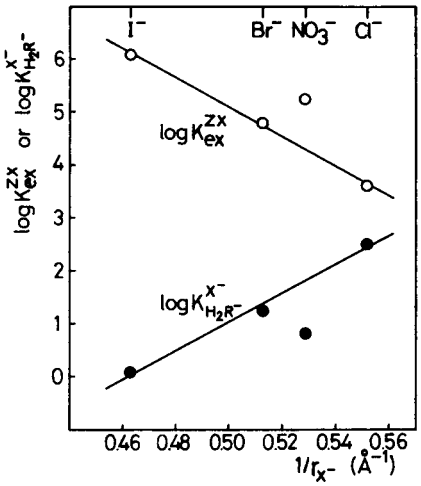

Fig. 1. Relation between log K_{ex}^{ZX} (or log $K_{H_2R^-}^{X^-}$) and the reciprocal of the ionic radii.

where d_1, d_2 and d are the absorbances of the acid form, the base form and the mixed solutions, respectively. The absorption spectra of DHNS (μ = 0.1 (KCl), 25 ± 1°C) are shown in Fig. 2. The isosbestic points occur at 267 and 319.5 nm. In Fig. 3 is shown the plot of log $\{(d_2 - d)/(d - d_1)\}$ against pH, which is a straight line of slope about −1. The pK_{a_2} value (= − log $\{([H^+][HR^{2-}])/[H_2R^-]\}$) was calculated to be 5.25 ± 0.03 (Table 1). For reference, the third dissociation constant of chromotropic acid and the first dissociation constant of 1,8-dihydroxynaphthalene were also determined spectrophoto-

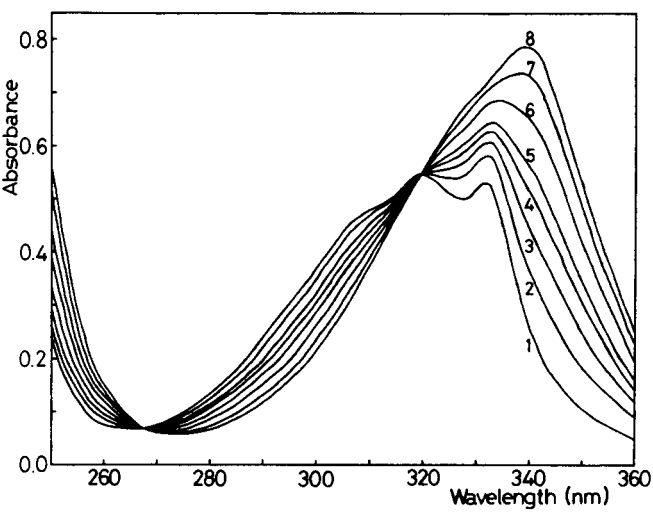

Fig. 2. Absorption spectra of DHNS in aqueous solution. [R] = 7.5 × 10^{-5} M. pH: (1) 3.28, (2) 4.52, (3) 4.95, (4) 5.21, (5) 5.34, (6) 5.69, (7) 6.11, (8) 6.81. Reference: water.

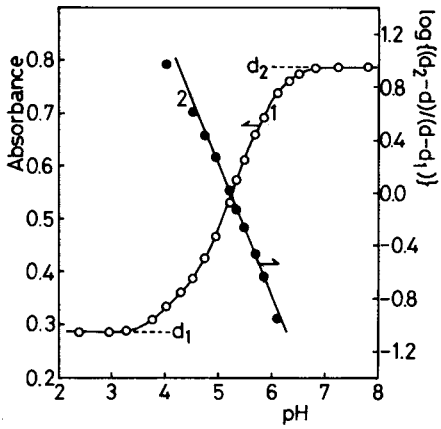

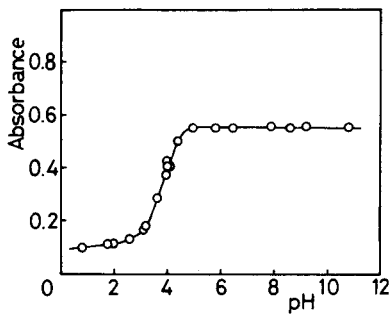

Fig. 3. Plots of the absorbance vs. pH (curve 1) and $\log\{(d_2 - d)/(d - d_1)\}$ vs. pH at 339 nm (curve 2). μ = 0.1 (KCl).

Fig. 4. Effect of pH on the decomposition of the boron complex in the presence of 1M sodium chloride. A 1,2-dichloroethane solution of the boron—DHNS complex formed from 2 × 10^{-5} M boron, 2 × 10^{-3} M DHNS and 2 × 10^{-3} M zephiramine was used after removal of the excess of reagent by back-washing twice with sodium chloride solution. Absorbance was measured at 341 nm against 1,2-dichloroethane.

TABLE 1

Acid dissociation constants calculated (25 ± 1°C, μ = 0.1 (KCl))

Reagent	pK_a	
	This work	Ref.[a]
DHNS	5.25 ± 0.03	5.33 (p) [19]
Chromotropic acid	5.37 ± 0.03	5.53 (p) [19]
		5.36 (p) [20]
		5.44 ± 0.03 (s) [22]
1,8-Dihydroxynaphthalene	6.47 ± 0.04	6.71 (s) [21]

[a]p and s in parentheses denote use of a potentiometric method and a spectrophotometric method in the determination, respectively.

metrically. These are also shown in Table 1. The values found agreed with those reported earlier [19—22].

In aqueous solution, changes in the ultraviolet absorption spectra of DHNS are caused by addition of boric acid at pH 3—10. In general, the reaction rate of boric acid with the reagent in aqueous solution is slow.

Composition of the boron—DHNS complex in 1,2-dichloroethane

To confirm the composition of the boron—DHNS complex the following experiments were carried out in the extraction system using 1,2-dichloroethane

and zephiramine. The effect of pH on the stability of the boron complex was examined as outlined in the procedure for distribution studies, the concentration of the boron complex in 1,2-dichloroethane being determined by measurement at 341 nm (Fig. 4). The complex was found to decompose below pH 5 in the absence of excess of reagent, whereas it was stable when excess of reagent was present. This probably happened because the reagent produced by decomposition of the boron—DHNS complex in solutions without excess of reagent was readily transferred to the aqueous phase in the presence of 1 M sodium chloride. In the absence of sodium chloride, however, the boron complex was scarcely decomposed below pH 5.

In a further experiment, the 1,2-dichloroethane solution of the boron—DHNS complex free from excess of DHNS reagent was allowed to decompose at pH below 5 in the presence of various concentrations of sodium chloride; then the concentration of DHNS in the aqueous solution was measured at 319.5 nm and the concentration of free boron in the aqueous solution was determined by the methylene blue method [23]. The results obtained can be summarized as follows: when the chloride concentrations were varied from 0.5 to 2.0 M at pH about 4, the [DHNS]/[boron] ratio of the boron—DHNS complex obtained by the decomposition procedure varied from 1.76 to 2.02 (12 determinations). When the pH values were varied at about 2 and 3 for chloride concentrations of 0.5, 1.0, 1.5 and 2.0 M, the [DHNS]/[boron] ratio varied from 1.81 to 2.04 (7 determinations). From these results, the composition ratio of the complex (boron: DHNS) was concluded to be 1:2.

Study of extraction equilibria

In the extraction of the ion-associate, the exchange equilibrium constant, $K^{nX^-}_{A^{n-}}$, refers to the following reaction [10]:

$$A^{n-}_{(a)} + nZX_{(o)} \rightleftharpoons nX^-_{(a)} + Z_nA_{(o)} \quad (4)$$

$$K^{nX^-}_{A^{n-}} = ([X^-]^n_a[Z_nA]_o)/([A^{n-}]_a[ZX]^n_o) \quad (5)$$

where A^{n-}, Z^+ and X^- are the n-valent anion, the zephiramine cation and the monovalent anion (chloride, bromide, nitrate and iodide), respectively. The exchange equilibrium constants for A^{n-} and X^- were determined by extracting A^{n-} with ZX into an organic solvent from aqueous solutions containing various amounts of X^- and measuring the concentration of Z_nA in the organic phase.

Exchange equilibrium constant for reagent. At about pH 3, the predominant DHNS species in the aqueous solution is the H_2R^- ion, which reacts with ZX to form a 1:1 ion-pair and is extracted into 1,2-dichloroethane. The exchange equilibrium constants for H_2R^- (the monovalent anion of DHNS) were determined for four monovalent anions ($X^- = Cl^-$, Br^-, NO_3^- and I^-). The plots of log $([Z \cdot H_2R]_o/[H_2R^-]_a)$ against log$([X^-]_a/[ZX]_o)$ were all linear with slopes of about −1. The constants calculated are listed in Table 2.

TABLE 2

Exchange equilibrium constants of the reagents and boron complexes (25 ± 1°C)

		X^-			
		Cl^-	Br^-	NO_3^-	I^-
Reagents					
DHNS	$\log K_{H_2R^-}^{X^-}$	2.51 ± 0.05	1.25 ± 0.07	0.81 ± 0.05	0.09 ± 0.09
	$\log K_{HR^{2-}}^{2X^-}$	4.39 ± 0.07	2.02 ± 0.04	1.10 ± 0.04	−0.40 ± 0.06
Chromotropic acid	$\log K_{H_2R'^{2-}}^{2X^-}$	3.38 ± 0.04	1.06 ± 0.04	0.05 ± 0.04	−1.31 ± 0.08
	$\log K_{HR'^{3-}}^{3X^-}$	5.44 ± 0.03	2.00 ± 0.05	0.62 ± 0.06	−1.61 ± 0.10
1,8-Dihydroxynaphthalene	$\log K_{HR''^-}^{X^-}$	4.49 ± 0.02	3.37 ± 0.08	2.93 ± 0.06	2.02 ± 0.05
Complexes					
Boron—DHNS	$\log K_{BR_2^{3-}}^{3X^-}$	9.77 ± 0.04	6.20 ± 0.07	5.14 ± 0.07	2.13 ± 0.08
Boron—chromotropic acid	$\log K_{BR_2'^{5-}}^{5X^-}$	11.99 ± 0.09	6.19 ± 0.06	3.91 ± 0.07	−0.85 ± 0.09

The plot of log $K_{H_2R}^{X^-}$ against $1/r_{X^-}$ (Fig. 1) was also found to be linear except for the nitrate ion.

At about pH 9, the predominant DHNS species in aqueous solution is the HR^{2-} ion, which reacts with ZX to form a 1:2 ion-associate and is extracted into 1,2-dichloroethane. The exchange equilibrium constants for HR^{2-} (the divalent anion of DHNS) were also determined for four monovalent anions. The plots of $\log([Z_2HR]_o/[HR^{2-}]_a)$ against $\log([X^-]_a/[ZX]_o)$ are linear and their slopes are almost −2. The constants calculated are also listed in Table 2.

For reference, the equilibrium constants for chromotropic acid and 1,8-dihydroxynaphthalene anions between 1,2-dichloroethane and water were also determined (Table 2).

Exchange equilibrium constant for boron complex. The exchange equilibrium constants for the boron—DHNS complex were determined at pH 9 by using a 1,2-dichloroethane solution of the boron—DHNS complex from which the excess of DHNS had been entirely removed (see below). The plots of log D_{boron} (= $\log([Z_3BR_2]_o/[BR_2^{3-}]_a)$ against $\log([X^-]_a/[ZX]_o)$ for the four monovalent anions are shown in Fig. 5. These plots are all straight lines with slopes of about −3. Accordingly, the boron—DHNS compex (A^{n-}) is assumed to be BR_2^{3-}, because of its boron:DHNS ratio of 1:2, and the composition of the ternary boron—DHNS—zephiramine complex in 1,2-dichloroethane is considered to be 1:2:3. Thus the equilibrium constants for the boron—DHNS complex could be obtained with the results indicated in Table 2.

For reference, the complex equilibrium constants for the boron—chromotropic acid complex were also determined (Table 2). The plots of log D_{boron} against $\log([X^-]_a/[ZX]_o)$ for the boron—chromotropic acid complex were all linear and their slopes were almost −5. The composition of the complex may therefore be assumed to be 1:2:5 (boron : chromotropic acid : zephiramine).

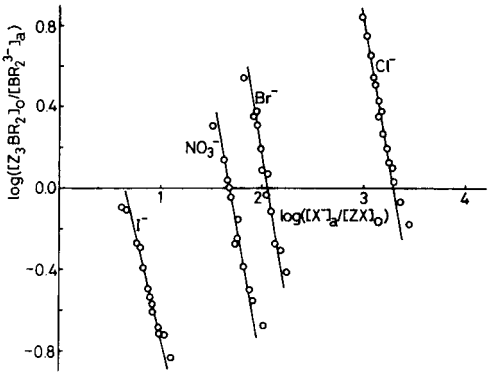

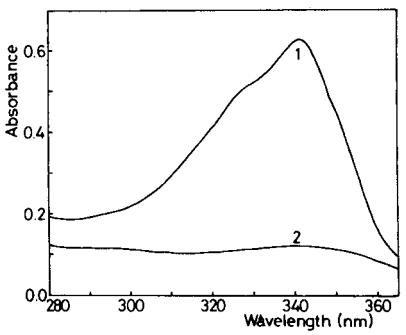

Fig. 5. Plots of $\log([Z_3BR_2]_o/[BR_2^{3-}]_a)$ against $\log([X^-]_a/[ZX]_o)$. $[BR_2^{3-}]_{total} = 1.81 \times 10^{-5}$ M, $[\text{zephiramine}]_{total} = 9.1 \times 10^{-4}$ M, pH 9.0.

Fig. 6. Absorption spectra of the complex and its reagent blank in 1,2-dichloroethane. (1) Complex of boron—DHNS: [boron] = 2×10^{-5} M, [R] = 2×10^{-3} M, [zephiramine] = 2×10^{-3} M (excess of reagent removed by back-washing twice with sodium chloride solution). Reference: 1,2-dichloroethane. (2) Reagent blank of (1) without boron.

Removal of the extracted excess of reagent

On extraction with zephiramine, the large excess of DHNS is co-extracted along with the boron complex into the organic phase, and its removal is necessary for accurate determinations of the absorbance of the boron complex. In previous work [9], chromotropic acid was used as the reagent for the solvent extraction of boron present as boric acid with 4×10^{-3} M zephiramine. After extraction of the boron—chromotropic acid complex, the excess of co-extracted reagent was removed from 1,2-dichloroethane to the aqueous phase by washing with a solution which was 0.6 M in sodium chloride and contained ammonia—ammonium sulfate buffer of pH 9.2.

In the case of DHNS, the excess of reagent could also be removed with alkaline sodium chloride solution. From the equilibrium constants shown in Table 2, the possible concentration of sodium chloride in the back-washing solution can be calculated from the equation

$$\log D_{HR^{2-}} = \log([Z_2HR]_o/[HR^{2-}]_a) = \log K_{HR^{2-}}^{2Cl^-} + 2 \log [ZCl]_o - 2 \log [Cl^-]_a \quad (6)$$

When $[ZCl]_o = 2 \times 10^{-3}$ M and $\log D_{HR^{2-}} = -1$, the concentration of chloride ion can be calculated to be about 1 M. In this work, therefore, a back-washing solution which was 1.0 M in sodium chloride with ammonia—ammonium sulfate buffer of pH 9.2 was used to remove the excess of DHNS reagent.

Application to the determination of boron present as boric acid

Absorption spectra. The absorption spectra of the boron complex and its reagent blank in 1,2-dichloroethane obtained by the recommended procedure using the above back-washing solution are shown in Fig. 6. When the excess of co-extracted reagent in the organic phase is back-washed twice, the best sensitivity for the ternary boron—DHNS—zephiramine complex is obtained at 341 nm. The absorbance of the organic phase was too high to be measured when the excess of co-extracted reagent was not removed. The calibration graph at 341 nm obtained with standard boron solutions according to the recommended procedure was straight and obeyed Beer's law over the range 0—4 × 10^{-5} M boric acid. The apparent molar absorptivity calculated from the slope of the calibration graph was 2.45 × 10^4 l mol^{-1} cm^{-1} at 341 nm, which is 1.7 times greater than that obtained with chromotropic acid [9]. The reagent blank at 341 nm was 0.119 ± 0.005 (7 determinations). These values were reproducible and the calibration graph and the reagent blank are distinctly preferable to those obtained with chromotropic acid for the determination of boron.

Effect of co-existing ions. 1,8-Dihydroxynaphthalene derivatives such as chromotropic acid react with metal ions such as Al^{3+}, Cu^{2+}, Fe^{2+}, Fe^{3+}, Mn^{2+} and UO_2^{2+} [9]. In the recommended procedure, however, these metal ions did not react with DHNS because 1 ml of 0.01 M EDTA was added to the extraction system at pH 4. Therefore, the interferences of these metals could be eliminated by adding EDTA and the other ions generally present in waters such as sea and hot-spring waters [9] did not cause any errors in this improved method. Thus, the recommended procedure allowed boron to be determined in such natural waters without any interferences.

Determination of boron in natural waters. Water samples were treated with 0.5 ml of concentrated sulfuric acid per liter as soon as they were sampled, then filtered through a 0.45-μm membrane filter, and stored in polyethylene bottles at room temperature.

The recommended procedure proved suitable for determining boron down to 0.03 mg l^{-1} in natural water samples such as sea and hot-spring waters (Table 3). Of course, samples with lower concentrations of boron can be handled if a larger volume of sample is used for the determination. The detection limit and the relative standard deviation achieved with the method were 0.01 mg B l^{-1} and less than 4%, respectively.

Boron present in sample solutions as boric acid and as tetraborate can be determined by this method, but not boron present as fluoroborate. In general, natural waters contain boron in the form of boric acid and seldom contain boron in the forms of tetraborate and fluoroborate. Accordingly, the total boron can be determined by use of the recommended procedure using DHNS.

The recovery of boron was examined by adding known amounts of boric acid (0.54 μg as boron) to the sample solutions. The results obtained are also shown in Table 3. These results show that boron in such natural waters

TABLE 3

Determination of boron in waters with DHNS

Sample	Sampling date	Sample volume (ml)	Absorbance[b]	Boron content (mg l^{-1})	Recovery[c] (%)
Seashore at Shibukawa (Okayama Prefecture)	May 4th, 1978	2[a]	0.394 ± 0.017	4.4 ± 0.2	98
Offshore at Teshima (Kagawa Prefecture)	April 23rd, 1978	2[a]	0.403 ± 0.009	4.5 ± 0.1	101
Seashore at Tanohama (Ehime Prefecture)	August 23rd, 1977	2[a]	0.385 ± 0.011	4.3 ± 0.1	100
Seashore at Aoya (Tottori Prefecture)	August 27th, 1977	2[a]	0.349 ± 0.007	3.9 ± 0.1	97
Hot-spring at Misasa (Tottori Prefecture)	August 19th, 1977	2[a]	0.206 ± 0.008	2.3 ± 0.1	103
Hot-spring at Yubara (Okayama Prefecture)	May 3rd, 1978	2	0.030	0.03_4	

[a] Samples were diluted (1 + 9) with deionized water.
[b] Average values of three determinations. The absorbances were measured against a reagent blank.
[c] 0.54 μg of boron as boric acid was added to the samples.

is quantitatively extracted into 1,2-dichloroethane as the ion-associate with DHNS and zephiramine, although the boron complex in the extract is back-washed twice in order to reduce the reagent blank.

CONCLUSION

An improved method was developed for the determination of boric acid with DHNS as the analytical reagent. The method proposed is suitable for the determination of small amounts of boron (as boric acid) in natural waters such as sea and hot-spring waters.

The DHNS reagent is easily extracted into organic solvents such as 1,2-dichloroethane as its ion-pair with zephiramine but can be stripped with a solution containing 1 M sodium chloride at pH 9.2. In contrast, the boron complex with DHNS is extracted into the organic phase with zephiramine but is not stripped with the back-washing solution. Figure 7 shows the percentage extractions of reagents and boron complexes for DHNS and chromotropic acid; these were calculated by using the exchange equilibrium constants for chloride listed in Table 2. Figure 7 indicates that with chromotropic acid, the excess of reagent extracted into 1,2-dichloroethane when 2×10^{-3} M zephiramine is used, is easily back-washed with 0.3 M sodium chloride solution at pH 9.2; in the previous work [9], 4×10^{-3} M zephiramine was used, and 0.6 M sodium chloride solution was necessary for back-washing at pH 9.2. With chromotropic acid, the boron complex was removed partially along with the excess of reagent because of their close equilibrium constants. With DHNS, however, although the excess of reagent was back-washed with 1 M sodium chloride at pH 9.2, the boron complex was hardly removed, as shown in Fig. 7.

In comparison with the previous method based on chromotropic acid [9], the proposed method based on DHNS for the extraction—spectrophotometric

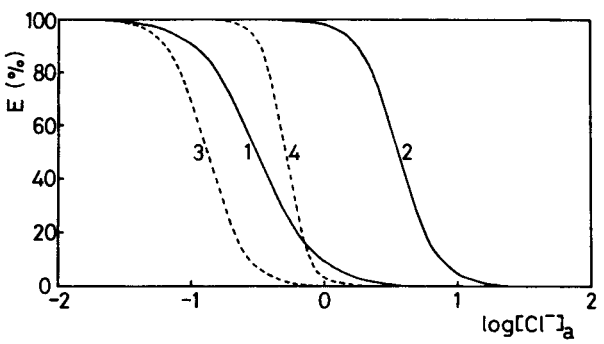

Fig. 7. Percentage extraction of reagents and boron complexes against chloride concentration for 2×10^{-3} M zephiramine. (1) DHNS reagent in the form of HR^{2-}; (2) boron—DHNS complex in the form of BR_2^{3-}; (3) chromotropic acid reagent in the form of HR'^{3-}; (4) boron—chromotropic acid complex in the form of BR'^{5-}_2.

determination of boron possesses the following advantages: (i) the apparent molar absorptivity of the boron complex with DHNS (2.45×10^4 l mol^{-1} cm^{-1} at 341 nm) is 1.7 times larger than that with chromotropic acid (1.4×10^4 l mol^{-1} cm^{-1} at 351 nm); (ii) the difference in extractability between DHNS and its boron complex is larger than that between chromotropic acid and its boron complex so that the separation of excess of DHNS reagent is more easily achieved without loss of the boron complex; (iii) the possibility of concentration of the boron complex with DHNS is greater than that with chromotropic acid because of their extraction constants. DHNS is therefore superior to chromotropic acid as an analytical reagent for the extraction—spectrophotometric determination of boron present as boric acid.

REFERENCES

1 L. Silverman and K. Trego, Anal. Chem., 25 (1953) 1264.
2 L. R. Uppström, Anal. Chim. Acta, 43 (1968) 475.
3 J. L. Lambert, J. V. Paukstelis and R. A. Bruckdorfer, Anal. Chem., 50 (1978) 822.
4 K. Emi, K. Tôei and K. Harada, Nippon Kagaku Zasshi, 78 (1957) 1299.
5 E. C. Cogbill and J. H. Yoe, Anal. Chem., 29 (1957) 1251.
6 D. Dyrssen, L. Uppström and M. Zangen, Anal. Chim. Acta, 46 (1969) 55.
7 B. Egneus and L. Uppström, Anal. Chim. Acta, 66 (1973) 211.
8 D. F. Kuemmel and M. G. Mellon, Anal. Chem., 29 (1957) 378.
9 T. Korenaga, S. Motomizu and K. Tôei, Analyst, 103 (1978) 745.
10 S. Motomizu and K. Tôei, Anal. Chim. Acta, 89 (1977) 167.
11 Bayer and Co., D.R.P. 80315.
12 R. Shibata and M. Okuyama, Nippon Kagaku Kaishi, 57 (1936) 36.
13 H. Erdmann, Justus Liebigs Ann. Chem., 247 (1888) 356.
14 A. P. Lurie, G. H. Brown, J. R. Thirtle and A. Weissberger, J. Am. Chem. Soc., 83 (1961) 5015.
15 K. Tôei and K. Kawada, Jpn. Anal., 21 (1972) 1510.
16 M. Zenki, Jpn. Anal., 25 (1976) 552.
17 H. Hoshino, T. Yotsuyanagi and K. Aomura, Anal. Chim. Acta, 83 (1976) 317.
18 W. M. Latimer, K. S. Pitzer and C. M. Slansky, J. Chem. Phys., 108 (1939) 7.
19 H. Zollinger and W. Büchler, Helv. Chim. Acta, 34 (1951) 591.
20 J. Heller and G. Schwarzenbach, Helv. Chim. Acta, 34 (1951) 1876.
21 H. Musso and H. G. Matthies, Chem. Ber., 94 (1961) 356.
22 M. Sakaguchi, A. Mizote, H. Miyata and K. Tôei, Bull. Chem. Soc. Jpn., 36 (1963) 885.
23 Japan Industrial Standard (JIS), K 0102, 1974.

Analytica Chimica Acta, 120 (1980) 335—345

SPECTROSCOPIC STUDY OF CHLORANIL CHARGE-TRANSFER COMPLEXES OF AMINO ACIDS AND RELATED COMPOUNDS†

BETH Y. LIN and K. L. CHENG*

Department of Chemistry, University of Missouri-Kansas City, Kansas City, MO 64110 (U.S.A.)

(Received 16th November 1979)

SUMMARY

The absorption maxima, molar absorptivities, infrared spectra, compositions, formation constants, and pH dependence of amino acid—chloranil complexes have been determined with purified chloranil. The n-π charge-transfer interaction depends on the presence of an unprotonated amino group; pH 9 is optimal for complex formation, but once formed, the complex is stable in a highly acidic medium and may be quantitatively extracted by hexanol. The molar absorptivities of the chloranil complexes of glycine, iminodiacetic acid, NTA, EDTA, DTPA and TTHA were measured. There is a linear relationship between the logarithm of the molar absorptivities of their chloranil complexes and the number of carboxylic groups in the molecule. There is an inverse linear relationship between the molar absorptivities of chloranil—metal—EDTA complexes and the logarithm of the stability constants of the EDTA chelates. This leads to a new method of determining the stability constants of complexes involving a nitrogen-donating group.

Several spectrophotometric methods are available for determining amino acids, e.g., the ninhydrin method [1], the peri-naphthindan-2,3,4-trione hydrate method [2] and the 3,5-dibromosalicylaldehyde method [3]. Al-Sulimany and Townshend tested 24 amino acids with chloranil at pH 9 [4]. All but 3,4-dihydroxyphenylalanine formed colored complexes with absorption maxima at about 350 nm and high apparent molar absorptivity, ranging from 5000 l mol^{-1} cm^{-1} for cysteine to 28,100 for lysine. The nature of the reaction between chloranil and amino acids is still not known with certainty; it has been proposed that it is based on the formation of charge-transfer complexes [5]. The reaction deserves further study.

Chloranil (2,3,5,6-tetrachloroquinone) is a yellow crystalline substance only slightly soluble in water, but soluble in many common organic solvents. It has a fairly high electron affinity (1.4 eV) [6] and it is known to be a strong electron acceptor forming complexes with various Lewis bases [7].

---

†Part of a M.S. thesis of Beth Y. Lin, University of Missouri-Kansas City, 1974. Presented at the First Federation of Analytical Chemistry and Spectroscopy Meeting, November, 1974, Atlantic City, NJ, U.S.A.

These reactions have been interpreted in terms of charge-transfer theory as proposed by Mulliken [8]. Although complexes of chloranil with polycyclic aromatic hydrocarbons have been studied in detail [9, 10], little attention has been given to the n-π charge-transfer complexes of chloranil [11—13].

This paper presents the absorption maxima and the molar absorptivities of a range of amino acid—chloranil complexes. The electron donors include natural amino acids, synthesized amino polycarboxylic acids, metal—EDTA chelates and peptides. The effects of pH, solvent, temperature and time on the absorbance are discussed. The results obtained suggest that the structure of the amino acid plays an important role in the mechanism of the charge-transfer process, thereby influencing the molar absorptivity. The infrared spectra for some amino acid—chloranil complexes are reported. The solvent extraction of the complexes described offers certain advantages of selectivity and sensitivity. Stability constants for some of the amino acid—chloranil complexes have been calculated.

EXPERIMENTAL

Apparatus and reagents

Spectra in the range 345—450 nm were measured by a Beckman DK-2A double-beam spectrophotometer. A Beckman model DU single-beam spectrophotometer was used for manual absorbance measurements. Infrared spectra were taken with a Perkin-Elmer model 337 grating infrared spectrophotometer.

Chloranil solution. An ethanolic 2.2×10^{-3} M chloranil solution was prepared from chloranil which had been recrystallized from chloroform (m.p. 250°C).

Buffer solutions. The buffers used were 0.05 M phosphate for pH 6 and 7, 0.0125 M (adjusted with HCl) for pH 8, 0.05 M sodium borate for pH 9, 0.025 M sodium hydrogencarbonate (adjusted with sodium hydroxide) for pH 10 and 11, and 0.1 M potassium chloride (adjusted with 0.2 M NaOH before dilution for pH 12 and 13. The reagents used were of analytical grade.

Amino acids. The sources were as follows: tryptophan, DL-serine, L-leucine, glycine, glutamic acid, and tyrosine (Fisher Scientific Co., reagent grade); isoleucine, 2-aminobutyric acid, lysine, proline, methionine, aspartic acid, valine and butylamine (Eastman Kodak Co., reagent grade); sarcosine (Aldrich, 98%); iminodiacetic acid (IDA; Aldrich Chem. Co., 97%); ethylenediaminetetraacetic acid (EDTA; Matheson, Coleman & Bell, 99%); triethylenetetraminehexaacetic acid (TTHA; Dojin Pharmaceutical); diethylenetriaminepentaacetic acid (DTPA; Dojin Pharmaceutical); hydroxyethylethylenediaminetriacetic acid (HEDTA; Eastman Kodak Co.). Mg—EDTA and Zn—EDTA (Baker Chemical Co.) and Cu—EDTA (Eastman Kodak Co.) were also used.

Procedures

Preparation of calibration curve for amino acid with chloranil in aqueous solution. The method used is similar to that reported by Al-Sulimany and Townshend [4]. To 0.0, 0.2, 0.4, 0.6, 0.8 and 1.0 ml of 100 ppm amino acid solution, in a series of 10-ml volumetric flasks, were added 2 ml of 2.2×10^{-3} M chloranil solution (in ethanol) and 2 ml of pH 9 borate buffer. After dilution to volume with water, the mixtures were heated in a water bath at 64—67°C for 10 min in the case of lysine and up to 60 min in the case of histidine and the aminopolycarboxylic acids. The solutions were cooled to room temperature in cold tap water. Absorption spectra (340—450 nm) and absorbance at λ_{max} (355 nm) were measured within 30 min in 1-cm cells against the solution containing no amino acid. The procedures for solvent, temperature, pH and time effect studies were similar.

Preparation of calibration curves for glycine with chloranil in alcohol by solvent extraction. The glycine—chloranil complex was prepared exactly as described above; 5 ml of the solution obtained were placed in a separatory funnel, and 2 ml of 4 M HCl, water, to a total volume of about 10 ml, and exactly 5 ml of hexanol were added. After vigorous shaking for 1 min, the organic layer was separated (addition of sodium chloride helped the separation). The absorbance of the clear hexanol extract was measured at 330 nm in a 1-cm cell against a blank containing all reagents but no amino acid. The calibration curve was prepared by using standard solutions containing 1—5 ppm glycine.

Infrared spectroscopic study of glycine—chloranil complex. Ammonium glycinate was prepared by dissolving glycine in the minimum amount of water, adjusting to pH 9 with ammonia, evaporating the solution to dryness in a Rotavapor and vacuum-drying for 2 h. The 1:1 glycine—chloranil complex was made by mixing 50 ml of 10^{-3} M glycine solution, 50 ml of 10^{-3} M chloranil solution, and sufficient 6 M ammonia solution to give pH 9; the solution was heated in a water bath at 65°C for 20 min, cooled to room temperature under tap water and then evaporated to dryness in a Rotavapor. The solid was vacuum-dried for 2 h. Infrared spectra were measured on KBr discs of the pure amino acid, chloranil, and the amino acid—chloranil complexes.

RESULTS AND DISCUSSION

Effect of conditions on the absorption spectra

Chloranil is capable of forming complexes with amino acids, amines and peptides; the complexes have a new absorption band generally at 350—355 nm at pH 9; proline and methylglycine gave broad peaks at 360 nm and 370 nm, respectively. The formation and the spectra of the complexes were affected by solvent, pH, temperature and time.

Studies [14] of the solvent effect on the intensity of the charge-transfer (CT) absorption band of the iodine—benzene complex showed that the

intensity and the thermodynamic properties change with the type of solvent. The stability of the complex (as measured by the heat of formation) decreases with increasing intensity (oscillator strength) of the CT absorption band, and depends on the solvent. This has been explained on the basis of solvent interaction with iodine and the observed discrepancy of Mulliken's theory [8] of CT interaction in the case of weak CT complexes. For the benzene—iodine complex, the CT interaction is weak, and the solvent plays an important role by interacting with the electron acceptor. It is interesting to see how the solvent affects the spectra of strongly bound complexes.

Spectra of solutions of glycine and nitrilotriacetic acid (NTA) with chloranil in different polar solvents were studied. The u.v. absorption maximum for the glycine—chloranil complex shifted to longer wavelengths as the alcoholic solvent (20%) increased in dielectric constant (ϵ) from isopropanol (347 nm, ϵ = 18.3) to ethanol (352 nm, ϵ = 24.3) and methanol (355 nm, ϵ = 32.6). The same complex was used to study the effect of various organic solvent—water ratios; the absorbance decreased and the absorption maximum shifted as the percentage of organic solvent increased, the direction of the shift depending on the solvent used.

The charge-transfer absorption maxima for solutions of the amino acid—chloranil complexes were found to depend on the pH in the manner described by earlier workers [4, 13, 15]. The absorbance maxima shifted to longer wavelengths when the pH exceeded 5. The absorption peaks of the complexes at various pH values are given in Table 1.

Amino acid—chloranil complexes formed slowly at room temperature, but the reaction rate increased markedly when the solutions were heated in a water bath, the optimum conditions being 64—67°C for 20 min. Absorbance began to decrease when the temperature exceeded 70°C, probably because of evaporation of ethanol [4], or decomposition of chloranil. The required heating time for each complex varied, ranging from only 10 min for lysine to 50 min for glutamic acid and 60 min for histidine at 65 ± 1°C [4].

Molar absorptivities of amino acid—chloranil complexes

When solutions of chloranil (yellow) and amino acids (colorless) were mixed and heated at pH 9, an intensely purple solution was obtained. The absorbance of this solution at 355 nm was proportional to the concentration of amino acids. The molar absorptivity of each complex was calculated (Table 2). The values varied from 5050 l mol^{-1} cm^{-1} for cysteine to 28,100 l mol^{-1} cm^{-1} for lysine, confirming the findings of Al-Sulimany and Townshend [4].

Examination of these values indicates that the structure of the amino acid may have an important influence on the charge-transfer process. Lysine and ornithine, which have two free amino groups, formed complexes with the highest molar absorptivities. Similarly, the molar absorptivity of the diamino butane—chloranil complex is almost double that of the butylamine—chloranil complex (Table 3). Thus the presence of the second amino group seems to

TABLE 1

Maximum absorption wavelengths of some amino acid—chloranil complexes at different pH values

Amino acid	Experimental		Literature [12]	
	pH	λ_{max} (nm)	pH	λ_{max} (nm)
Glycine	7.0	345	5.6	370
	9.0	350	8	360
	11.0	355	10	350
	13.0	385	11	360
Proline	5.0	325	7	375
	8.0	355	9	370
	12.0	365	12	355
Tyrosine	7.0	350	7	360
	12.8	360	13.2	330
NTA	7.0	340		
	9.3	350		
	11.0	352		
EDTA	6.0	333		
	7.0	336		
	9.0	350		
	12.0	367		
HEDTA	8.0	336		
	9.0	350		
	11.0	360		
	5.0	322		
TTHA	5.0	310		
	7.0	331		
	9.0	350		
	11.0	375		

increase the electron density of the donor, thereby increasing the molar absorptivity of the complexes. Also, as shown later, lysine forms a 2:1 chloranil—amino acid complex, which may account for the higher absorbance.

The aspartic acid—chloranil complex had a considerably lower molar absorptivity. This may be explained by the fact that the acid forms a six-membered ring by hydrogen bonding, which withdraws the electrons from the nitrogen atom and thus decreases its electron-donating ability. Glutamic acid, which also contains two carboxylic groups, cannot form a stable five- or six-membered ring, probably because of steric hindrance, has a normal molar absorptivity.

The molar absorptivities of solutions of three aromatic amino acid—chloranil complexes are between 17,380 to 18,300 l mol^{-1} cm^{-1}. However, that of the tyrosine—chloranil complex (which has a hydroxyl group in the benzene ring) is slightly lower than that for phenylalanine; similarly the values for the threonine and hydroxyproline complexes are lower than those for the 2-aminobutyric acid and proline complexes. Since oxygen is more

TABLE 2

Molar absorptivities of chloranil complexes of amino acids in aqueous 20% ethanol

Amino acid	Molar absorptivity ($l\ mol^{-1}\ cm^{-1}$) 355 nm[a]	350 nm[b]	Amino acid	Molar absorptivity ($l\ mol^{-1}\ cm^{-1}$) 355 nm[a]	350 nm[b]
Alanine	16900	17000	Lysine	28076	28100
2-Aminobutyric acid	17500	—	Methionine	19020	15500
Arginine	17391	18700	Ornithine	26060	25600
Aspartic acid	8655	5600	Phenylalanine	18300	18000
Cysteine	5050	5500	Proline	11020	11200
Cystine	21600	18300	Serine	17800	15700
Glutamic acid	14200	11500	Threonine	11900	12100
Glycine	15600	12600	Tryptophan	17380	15500
Histidine	16500	11600	Tyrosine	18000	16000
Hydroxyproline	—	8700	Valine	18400	20500
Isoleucine	20368	20500	Methylglycine	1500	—
Leucine	21200	21000	Sarcosine	4600	—

[a]This work. [b]Values from [4].

electronegative than nitrogen, the hydroxyl group would pull electrons from the system, decreasing the electron density of the amino group, and thus decreasing the molar absorptivity.

Hydrogen bonding can also explain the extremely low molar absorptivity of the cysteine complex. The proton withdraws electrons, making the unshared pair of electrons on nitrogen less available to the chloranil acceptor.

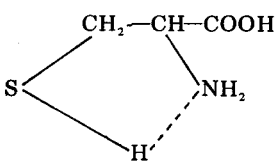

However, in methionine this cannot occur and the lone pair of the amino group is unaffected. The second amino group in cystine increases the basicity of the amino acid, resulting in a high molar absorptivity for its complex.

Six aminopolycarboxylic acids were studied. They reacted with chloranil at pH 9 forming weaker complexes than the amino acids, as evidenced by the decreasing absorbance of solutions of their complexes as the number of carboxylic groups in the molecule increased (Table 3). There is a linear relationship between the logarithm of the molar absorptivity and the number of carboxylic acid groups in a molecule of aminopolycarboxylic acid (Fig. 1). Although N-hydroxyethylethylenediaminetriacetic acid (HEDTA) has three carboxylic acid groups, it also has one electron-withdrawing hydroxyl group, so that the molar absorptivity of its complex is less than those of NTA and EDTA.

TABLE 3

Molar absorptivities (ϵ) of chloranil complexes

Compound	ϵ (355 nm) ($l\ mol^{-1}\ cm^{-1}$)	Compound	No. —COOH	ϵ (350 nm) ($l\ mol^{-1}\ cm^{-1}$)	log K
Amino acids		*Aminopolycarboxylic acids*			
Glycine (Gly)	15600	Glycine	1	15600	
Lysine	28100	IDA	2	7762	
		NTA	3	6500	
Amines		EDTA	4	4500	
Butylamine	16400	HEDTA	3	3000	
Diaminobutane	28200	DTPA	5	2750	
		TTHA	6	2000	
Peptides					
Gly—Gly	8250	*Metal—EDTA chelates*			
Gly—Gly—Gly	9100	Cu—EDTA (CuY^{2-})		950	18.8
Gly—Gly—Gly—Gly	8230	Zn—EDTA (ZnY^{2-})		999	16.5
		Mg—EDTA (MgY^{2-})		1334	8.7
		Na—EDTA (Na_3Y^-)		4500	1.6

[a]Literature values.

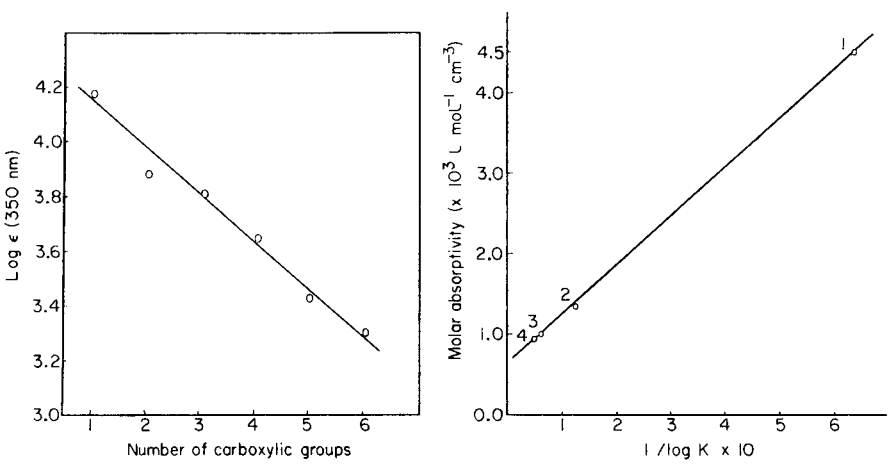

Fig. 1. The relationship between the logarithm of the molar absorptivity of aminopolycarboxylic acid complexes and the number of carboxylic groups in the molecule.

Fig. 2. Molar absorptivity of complexes of metal—EDTA—chloranil complexes as influenced by the stability of the EDTA chelates: (1) $NaHY^{2-}$; (2) MgY^{2-}; (3) ZnY^{2-}; (4) CuY^{2-}.

The reactions of chloranil with metal—EDTA chelates at pH 9 were also studied; their molar absorptivities are included in Table 3. There is an inverse linear relationship between the molar absorptivity and the logarithm of the stability constants of the EDTA chelates. This is shown in Fig. 2. The electron density on the nitrogen atoms of EDTA chelates is decreased as a result of the bond between the nitrogen atoms and the metal ion; consequently, there is

less charge transfer from the EDTA chelates to the chloranil. These results may provide a new and convenient method of determining the stability constants of many complexes.

Table 3 also shows that some simple peptides form chloranil complexes. As all except the terminal amino group are involved in amide linkages, in which the C—N bond has considerable double-bond character, the nitrogen atoms generally have a much diminished tendency to donate their lone pairs of electrons for charge transfer, so that only the terminal amine group is significantly involved in complex formation, and the molar absorptivity is unaffected by the degree of polymerization.

Methylglycine and sarcosine were also studied. The molar absorptivities of their complexes are low, in agreement with the observation that only primary amino groups react with chloranil to give intensely colored complexes.

Composition and stability of amino acid—chloranil complexes

Amino acid—chloranil complexes have always been assumed to form in a 1:1 ratio [13], but there has never been any experimental evidence reported to substantiate this assumption. Therefore, the stoichiometry of the chloranil complexes was studied by Job's method [16] and the mole ratio method.

The Job curves for many of the amino acid—chloranil complexes studied were not ideal because of the appreciable dissociation of the complexes, but by extrapolation of each curve, an apex at about 1:1 is obtained for each of the complexes; stability constants can also be calculated from these plots. The results are given in Table 4. The stability constant for the glycine—chloranil complex in 50% ethanol was reported [12] as only 215 at an apparent pH of 8. This is to be compared with the value reported here namely, 18050. The conditions for complex formation were not clearly given by Birks and Slifkin [12] and may differ significantly from those used here. Moreover, they claimed that the amino acid was in excess when it reacted with chloranil.

TABLE 4

Stability constants (K) of 1:1 amino acid—chloranil complexes

Amino acid	Experimental[a]	Literature [12][b]
	K ($l\ mol^{-1}$)	K ($l\ mol^{-1}$)
Alanine	8440	318
Histidine	7030	—
Glycine	18050	215
Phenylalanine	4080	—
Tyrosine	4910	—
Valine	6860	—

[a] At λ_{max} = 355 nm and pH 9 in aqueous 20% ethanol.
[b] At λ_{max} = 350 nm and pH 8 in aqueous 50% ethanol.

Other reasons may be advanced to explain the large discrepancy in the stability constant values. Previous investigators used impure chloranil, whereas purified chloranil was used in the present study. The low values may result from the formation of the complex at room temperature, at which formation is extremely slow.

The mole ratio method was tested for glycine, lysine, and histidine. The glycine and histidine complexes gave only one break at a ratio of 1:1 (that for histidine is not very abrupt). The first break of the lysine—chloranil complex was at 1:1, but a second break was observed at a 1:2 ratio of lysine to chloranil, indicating that an excess of chloranil reacts with the second amino group of lysine.

Infrared spectra

In an amino acid—chloranil charge-transfer process, the lone pair of electrons on a nitrogen atom interacts with a carbon—oxygen π-orbital in chloranil [13]. An infrared spectrum may give some information about the structure of the complex. The infrared spectrum of the proline—chloranil complex shows two sharp, intense bands at 1600 cm^{-1} and 1400 cm^{-1}. The C=O and C=C bands in the chloranil spectrum occur at 1700 cm^{-1} and 1590 cm^{-1}, which are very close to the carboxylate band (1560—1600 cm^{-1}) in the amino acid. It appears that in the spectrum of the complex there is no 1700 cm^{-1} C=O band. It is difficult to conclude whether the C=O band is missing or has shifted to 1600 cm^{-1}, thus overlapping with another band.

The infrared spectrum of valine has the following bands: N—N stretch, 3350—3130 cm^{-1}; N—H bend 1610 cm^{-1} and 1485 cm^{-1}; carboxyl, 1600—1560 cm^{-1} and 1400 cm^{-1}. These bands overlap with each other to give two broad bands at 2300—3500 cm^{-1} and 1300—1600 cm^{-1}. The complex has a spectrum which is mostly the sum of the spectra of the two components, but with further broadening of these bands. Overall, the infrared spectra of the complexes show only small differences from those of its components, thus emphasizing the weak interaction involved in charge-transfer complexes.

Solvent extraction of amino acid—chloranil complexes

The solvent extraction of amino acid—chloranil complexes has not been reported before. Various solvents were used in an attempt to extract the complexes from aqueous 20% ethanol at pH 9 (Table 5). Little, if any, extraction was achieved. However, it was found that once the complexes had been formed in a basic medium, they were not easily decomposed on acidification. Thus, the amino group must be unprotonated in order to form the complex, and it is likely that the complex formed in a basic medium is negatively charged, and so hydrophilic. On careful acidification, however, the anion is converted to a neutral complex, which may be extracted by an organic solvent [17]. The change in spectrum on acidification of the glycine complex is shown in Fig. 3. Alcohols such as isoamyl alcohol and hexanol are the most suitable solvents for extracting the glycine—chloranil complex (Table 5). The optimum pH of the solution for extraction was 0—1.5 (Fig. 4).

TABLE 5

Extraction of glycine—chloranil complex with different solvents at pH 2.2

Solvent	Absorbance at 330 nm	Solvent	Absorbance at 330 nm
Toluene	0.01	Isobutanol	0.37
Hexyl ether	0.09	Isoamyl alcohol	0.46
Chloroform	0.13	Hexanol	0.47
o-Dichlorobenzene	0.22		

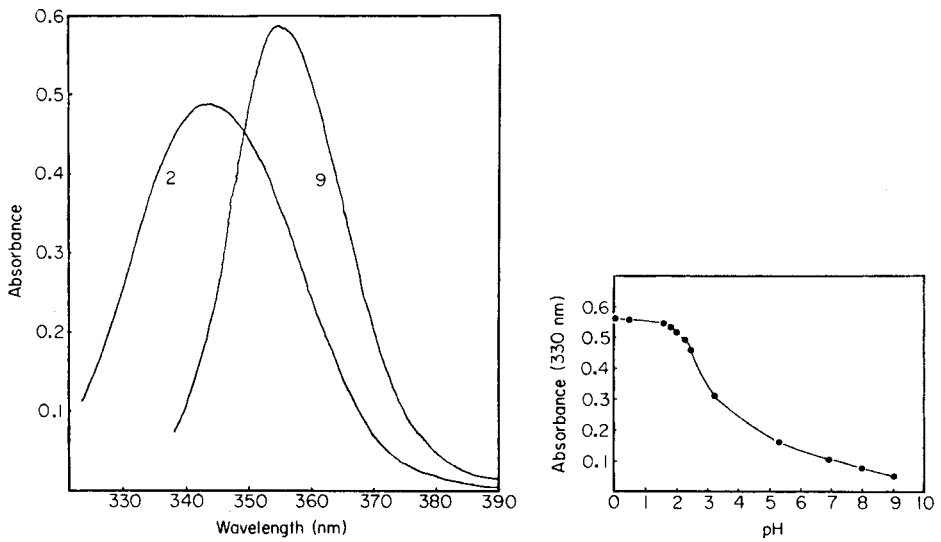

Fig. 3. Shift of the spectrum of the glycine—chloranil complex on acidification. The numbers on the curves indicate pH.

Fig. 4. Absorbance of hexanol solutions of the glycine—chloranil complex extracted from aqueous 20% ethanol solution at various pH values.

A calibration graph obtained for glycine by solvent extraction with hexanol at pH 0.5, measured at 330 nm, was linear with a slope of 0.22 absorbance per ppm of glycine.

It is interesting to note that there are few analytical methods that determine amino acids by a solvent extraction technique. In the present work, which has been reported in detail elsewhere [18], the measurement of glycine is demonstrated, but future work on the extraction of other amino acids and amines, and possible separation processes should be undertaken.

REFERENCES

1 S. Moore and W. Stein, J. Biol. Chem., 211 (1954) 907.
2 R. Riemschneider and J. Wierer, Fresenius Z. Anal. Chem., 193 (1963) 186.
3 K. Yuhi, J. Pharm. Soc. Jpn., 81 (1961) 297.
4 F. Al-Sulimany and A. Townshend, Anal. Chim. Acta, 66 (1973) 195; T. S. Al-Ghabsha, S. A. Rahim and A. Townshend, Anal. Chim. Acta, 85 (1976) 189.
5 M. A. Slifkin, Charge Transfer Interactions of Biomolecules, Academic, London, 1971, p. 53.
6 G. Briegleb, Angew. Chem. (Int. Ed. Engl.), 3 (1964) 617.
7 E. Weitz, Angew. Chem., 66 (1954) 658.
8 R. S. Mulliken, J. Am. Chem. Soc., 74 (1952) 811.
9 W. L. Peticolas, J. Chem. Phys., 26 (1957) 429.
10 J. B. Birks and M. A. Slifkin, Nature, 191 (1961) 761.
11 R. Foster and T. J. Thomson, Trans. Faraday Soc., 58 (1962) 860.
12 J. B. Birks and M. A. Slifkin, Nature, 197 (1963) 42.
13 R. Foster, Organic Charge-Transfer Complexes, Academic, London, 1969, p. 313.
14 B. B. Bhowmik, Spectrochim. Acta, Part A, 27 (1971) 321.
15 J. W. Hancock, C. E. Morrell and D. Rhum, Tetrahedron Lett., 22 (1962) 987.
16 P. Job, Ann. Chim., 9 (1928) 113.
17 K. L. Cheng, Anal. Chem., 28 (1956) 1738; Talanta, 8 (1961) 301.
18 B. Y. Lin, M.S. Thesis, University of Missouri-Kansas City, 1974.

Analytica Chimica Acta, 120 (1980) 347—251

Short Communication

POLAROGRAPHIC DETERMINATION OF THIAMINE AND ITS MONOPHOSPHATE AND PYROPHOSPHATE ESTERS

T. VERGARA, D. MARÍN* and J. VERA

Physical Chemistry Department, University of Murcia, Murcia (Spain)

(Received 21st April 1980)

Summary. A d.c. polarographic method for estimating thiamine and its monophosphate and pyrophosphate esters in the same sample is proposed. The anodic waves of thiamine and its monophosphate and pyrophosphate appear at $E_{1/2}$ values of −0.36 to −0.4 V vs. s.c.e., at pH higher than 9.0, 9.3 and 9.6, respectively. Careful adjustment of pH in separate aliquots to pH 9.0—9.3, 9.3—9.6, and >9.6 allows measurement of waves corresponding to thiamine, thiamine and its monophosphate, and thiamine and its monophosphate and pyrophosphate, respectively. Samples containing thiamine disulfide can also be analysed.

The methods [1—3] hitherto used for the determination of thiamine and its phosphoric acid esters have involved separation of these thiamine compounds and subsequent determination of each compound. There are several methods of determining thiamine by polarography [4—6]. In these methods the catalytic wave in unbuffered solution, or in a cobalt solution, or the reduction wave in alkaline solution, can be used for quantitative assays. The anodic wave that appears at pH 9.0 has proved particularly suitable [7]. In 1966, Robinson [8] wrote that "the only physical method of estimating thiamine that appears to be promising is the polarographic method". Further, the polarographic method has been used to estimate several vitamins in the same sample [9—11]. However, no data are available in literature about the determination of thiamine phosphate esters by polarography. In the present communication, a d.c. polarographic method is reported for the determination of thiamine and its phosphate esters without preceding separation.

Experimental

Polarographic waves were obtained by means of a Radiometer PO4 polarograph using a thermostated cell at 25°C and a saturated calomel electrode (s.c.e.) as reference electrode. The dropping mercury electrode (d.m.e.) used, at a height of 35 cm Hg, had the following characteristics: m = 2.60 mg s^{-1} and t = 2.96 s at −1.50 V (vs. s.c.e.) in a Britton—Robinson buffered solution (pH 9.0, μ = 0.5 M).
All chemicals were of reagent grade.

Results and discussion

Thiamine, thiamine monophosphate (TMP) and thiamine pyrophosphate (TPP) have polarographic activity in Britton—Robinson buffered solutions, showing an anodic wave at basic pH. The anodic waves of thiamine [12], TMP and TPP [13] appear at pH values higher than 9.0., 9.3 and 9.6, respectively. These anodic waves are due to reaction of the thiol forms of these compounds at the dropping mercury electrode [12]: R—SH + Hg → R—SHg + H^+ + e^-. The fact that thiamine, TMP, and TPP react at increasing pH values can be ascribed to the effects of the increasing negative charge of the monophosphate and pyrophosphate groups in basic media. The height of the anodic wave increases with time reaching a limiting value (Fig. 1). The higher the pH, the higher is the limiting value. This happens because conversion to the thiol form is not instantaneous but is favored by increasing pH. At pH > 11.6 the limiting value is pH-independent, the compound being completely in the thiol form.

The half-wave potentials of these compounds are very similar: −400, −370 and −360 mV (vs. s.c.e.) for thiamine, TMP and TPP, respectively. Therefore, the polarograms of a solution containing all three compounds show only one anodic wave (Fig. 2, curve 4). As shown in Fig. 2 (curves 5 and 6), in the range pH 9.0—9.3, the height of the anodic wave of a solution containing thiamine, TMP and TPP is the same as the height for a similar solution containing only thiamine, i.e., at these pH values, only thiamine itself reacts. In Fig. 3, it can be seen that, in the range pH 9.3—9.6, the height of the anodic wave for a solution containing thiamine, TMP and TPP is equal, at its limiting value, to the sum of the heights of the waves for thiamine and TMP separately, i.e., in this pH range, the thiazole ring

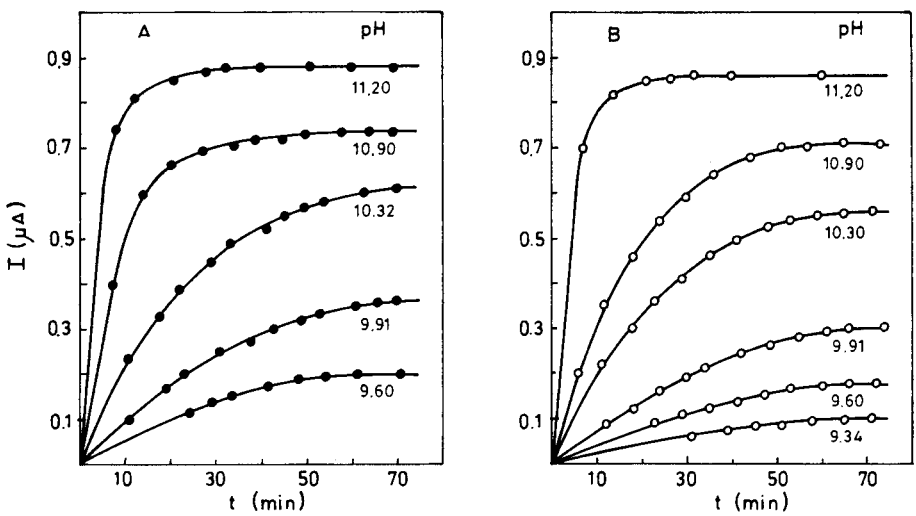

Fig. 1. Variation of the height of the anodic wave with time at various pH values: (A) 0.4 mM TPP, (B) 0.4 mM TPP in Britton—Robinson buffer.

of thiamine and TMP is reactive but that of TPP is not. If the pH of the solution of thiamine, TMP and TPP is increased to more than 9.6, the anodic wave height obtained (Fig. 4) is now equal to the sum of the heights for separate solutions of thiamine, TMP and TPP, all the compounds becoming electrochemically active.

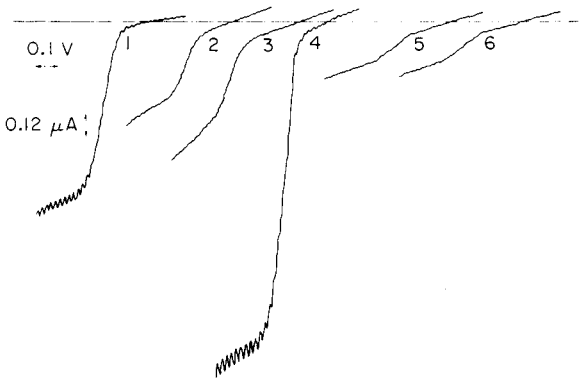

Fig. 2. Polarograms of: (1) 0.4 mM thiamine, (2) 0.4 mM TMP, (3) 0.4 mM TPP, (4) 0.4 mM thiamine + 0.4 mM TMP + 0.4 mM TPP in Britton—Robinson buffer at pH 9.91. Polarograms of: (5) 0.4 mM thiamine, (6) 0.4 mM thiamine + 0.4 mM TMP + 0.4 mM TPP in Britton—Robinson buffer at pH 9.10. In every case, equilibrium has been reached.

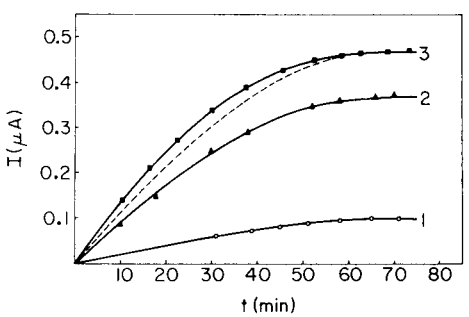

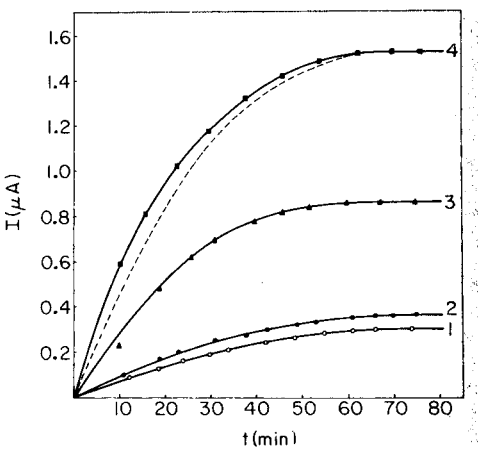

Fig. 3. Variation of the height of the anodic wave with time at pH 9.34: (1) 0.4 mM TMP, (2) 0.4 mM thiamine, (3) (solid line) 0.4 mM thiamine + 0.4 mM TMP + 0.4 mM TPP in Britton—Robinson buffer, (dotted line) sum of curves 1 and 2.

Fig. 4. Variation of the height of the anodic wave with time at pH 9.91: (1) 0.4 mM TMP, (2) 0.4 mM TPP, (3) 0.4 mM thiamine, (4) (solid line) 0.4 mM TMP + 0.4 mM TPP + 0.4 mM thiamine in Britton—Robinson buffer, (dotted line) sum of curves 1, 2 and 3.

These observations can be used in the analysis of samples containing thiamine, TMP and TPP. First, calibration curves are needed for determining the concentrations from the anodic wave heights; the heights used must correspond to the limiting values, i.e., the time-independent wave height when the thiol equilibrium is achieved. Then three equal portions of the sample under study are adjusted to pH > 9.6, pH 9.3—9.6, and pH 9.3—9.0, respectively, and the limiting wave heights for these solutions are measured. These waves correspond, respectively, to the total thiamine, TMP and TPP concentrations, the thiamine and TMP concentrations, and the thiamine concentration alone, and so the concentrations of each component can be calculated by difference. Under these conditions, the lower limit of sensitivity lies in the range 10^{-4}—10^{-5} M. The linear ranges for the calibration graphs were found to be 7.0×10^{-5}—1.0×10^{-3} M for thiamine, 7.0×10^{-5}—9.0×10^{-4} M for TMP and 7.0×10^{-5}—1.0×10^{-3} M for TPP. Of course, any species with $E_{1/2}$ values within ± 100 mV of the thiamine, TMP and TPP waves will cause overlapping, in which case the proposed method is not applicable.

Thiamine in natural products occurs not only as free thiamine and in the form of phosphoric acid esters, but also in the disulfide form [14]. In alkaline medium, 2 mol of disulfide gives 3 mol of thiol according to the stoichiometry already established for this kind of reaction [15]:

$$2\ R{-}S{-}S{-}R + 4\ OH^- \rightarrow 3\ R{-}S^- + R{-}SO_2^- + 2\ H_2O$$

Therefore, if the sample under study contains thiamine disulfide, its solution at any pH exceeding 9.0 would give an anodic wave which would be partly due to thiamine disulfide. However, the disulfide undergoes a 2-e reduction at the d.m.e. giving the corresponding thiol. The following procedure is suitable for determining samples containing thiamine, TMP and TPP in presence of thiamine disulfide: first, the sample is adjusted to about pH8 and electrolyzed at —700 mV, giving a wave; then three portions of this solution are adjusted to the appropriate pH values for analysis by the above procedure. Obviously all the wave heights must be corrected for the wave obtained in the first step and for the dilutions made.

REFERENCES

1 Y. Itokawa and J. R. Cooper, in D. B. McCormick and L. D. Wright (Eds.), Methods in Enzymology, Vol. XVIII, Part A, Academic Press, New York, 1970, pp. 91—92.
2 G. Rindi and L. de Giuseppe, Biochem. J., 78 (1961) 602.
3 K. Oosugi, K. Igarashi and N. Konoha, Vitamins, 48 (1974) 295.
4 J. J. Lingane and O. L. Davis, J. Biol. Chem., 137 (1941) 567.
5 P. Zuman, Organic Polarographic Analysis, Pergamon, London, 1964, p. 189.
6 M. Brezina and P. Zuman, Polarography in Medicine, Biochemistry and Pharmacy, Interscience, New York, 1958, pp. 382—389.
7 R. Strobecker and H. M. Henning, Vitamin Assay, Verlag Chemie, Darmstadt, 1965, p. 80.
8 F. A. Robinson, The Vitamin Co-Factors of Enzyme Systems, Pergamon, London, 1966, p.42.

9 M. E. Schertel and A. J. Shepparo, J. Pharm. Sci., 60 (1971) 1070.
10 J. M. Lopez Fonseca, P. Sanz Pedrero and J. C. Tutor, An. Quim., 69 (1973) 455.
11 B. Tokes and G. Siciu, Rev. Med., 23 (1977) 132.
12 I. Tachi and S. Koide, Vitamins, 4 (1951) 223.
13 D. Marín, T. Vergara, J. Vera and A. Serna, Electrochim Acta, 24 (1979) 405.
14 O. Zima, G. Göttmann, A. Hoffman, L. Hepding and R. Hotovy, Merck's Jber., 67 (1953) 1.
15 J. P. Danehy and K. N. Parameswaran, J. Org. Chem., 32 (1968) 568.

Analytica Chimica Acta, 120 (1980) 353—355

Short Communication

RESACETOPHENONE ISONICOTINIC ACID HYDRAZONE AS A REAGENT FOR THE CATALYTIC POLAROGRAPHIC DETERMINATION OF NANOGRAM QUANTITIES OF VANADIUM(V)

K. MURALI MOHAN and S. BRAHMAJI RAO*

Chemical Laboratories, SVU Autonomous Post-Graduate Centre, Anantapur 515 003 (India)

(Received 14th January 1980)

Summary. The polarographic method proposed for 1—12 ng of vanadium(V) is based on the reduction of bromate, catalysed by the metal ion, with resacetophenone isonicotinic acid hydrazone at pH 5.0. Only iron interferes seriously.

Transition metal ions are known to catalyse the reduction of oxidizing agents [1—5] at the dropping mercury electrode. Rao and Rao [6] observed that vanadium(V) (0.05—0.3 μg ml^{-1}) catalysed the reduction of potassium bromate at pH 5.0. In the present work, it was found that in the presence of resacetophenone isonicotinic acid hydrazone (RPINAH), the reduction of bromate is catalysed by nanogram quantities of vanadium, thus allowing vanadium to be determined at this level.

Experimental

Apparatus. A d.c. recording polarograph (Elicord, Elico Pvt., Ltd., Hyderabad, India), a Lingane-type H-cell and a digital pH meter (LI-120, Elico) were used. The characteristics of the dropping mercury electrode (d.m.e.) were: t = 3.0 s and m = 1.93 mg/drop at 0 V vs. s.c.e. in water.

Reagents. A stock solution (0.1 M) of ammonium metavanadate (Riedel de Hahn, West Germany) was standardized [7] against ammonium iron(II) sulphate. Working solutions (10^{-6} M) were prepared by suitable dilution immediately before use. A methanolic solution (2×10^{-3} M) of RPINAH was prepared; this was further diluted with methanol to 2×10^{-5} M immediately before use. All other chemicals were of analytical-reagent grade. A pH 5.0 buffer solution was prepared from 1 M sodium acetate and 1 M acetic acid.

Synthesis of RPINAH. The synthesis was analogous to that used for *o*-hydroxybenzaldehydeisonicotinoyl hydrazone [8]. Equimolar amounts of isonicotinic acid hydrazide and 2,4-dihydroxyacetophenone in aqueous ethanol were refluxed for 1 h. The compound that separated on cooling was recrystallized from methanol (m.p. 272—273°C (det.); literature value [9] 270—272°C).

Calibration procedure. To different aliquots of vanadium(V) solution (1×10^{-6} M) in a 25-ml volumetric flask were added 2.5 ml of (0.5 M) potassium bromate solution and 5 ml of the methanolic RPINAH solution. The solution was diluted to the mark with twice-distilled water, shaken well and transferred to the polarographic cell. After deoxygenation by bubbling nitrogen for 15 min, the current—voltage curves were recorded. The height of the peak at −0.03 V was measured and plotted against vanadium concentration.

Results and discussion

Typical polarographic curves for the various components of the solution, alone and in admixture, are shown in Fig. 1. It is clear that the presence of RPINAH, bromate and vanadium(V) are essential in order to obtain the large peak at −0.03 V vs. s.c.e. This peak current varied linearly with the concentration of vanadium over the range 1—12 ng ml^{-1}. The RPINAH should be present in not less than 10-fold excess and not more than 200-fold excess over vanadium(V). A large amount of bromate is needed. A surface-active intermediate involving vanadium(V), bromate and the hydrazone may be responsible for the behaviour observed. The catalytic nature of the wave was confirmed by the observations that the mercury column height did not affect the wave heights, and that surfactants such as Triton-X100 and methyl red had no effect on the peaks; also the limiting current is very much larger than would be expected for a diffusion-controlled wave. Similar observations

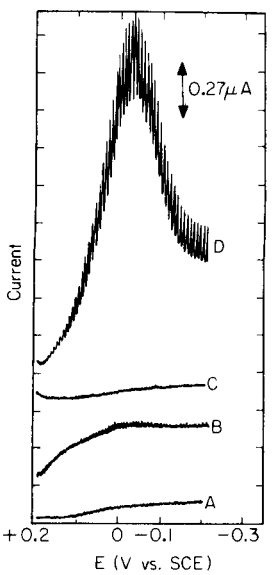

Fig. 1. Polarographic curves for (A) vanadium(V); (B) vanadium(V) + $KBrO_3$; (C) vanadium(V) + RPINAH; (D) vanadium(V) + $KBrO_3$ + RPINAH in pH 5.0 acetate buffer solution. [V(V)] = 16×10^{-8} M; [$KBrO_3$] = 5×10^{-2} M; [RPINAH] = 4×10^{-6} M.

have been made [10] in studies of the molybdenum(VI)--chlorate system in the presence of carboxylic acids.

There were no interferences from Mg(II), Ca(II), Cr(III), Mn(II), Co(II), Ni(II), Zn(II), Al(III), Mo(VI), Cd(II) and Pb(II) even when present in 200-fold amounts (by weight). Iron(III) interfered positively when more than a 5-fold amount was present, whereas copper(II) could be tolerated in 10-fold amounts. Common anions (F^-, Cl^-, Br^-, I^-, SO_4^{2-}) were tolerated in up to 200-fold amounts.

The authors thank the authorities of the SVU Autonomous Post-Graduate Centre, Anantapur for providing the necessary facilities. One of the authors (K.M.M.) is indebted to the University Grants Commission, New Delhi, for a Teacher Research Fellowship and the Besant Theosophical College, Madanapalle for leave.

REFERENCES

1 I. M. Kolthoff and E. P. Parry, J. Am. Chem. Soc., 73 (1951) 2304.
2 W. E. Harris and I. M. Kolthoff, J. Am. Chem. Soc., 67 (1945) 1484.
3 K. Tanaka and K. Nakano, J. Electroanal. Chem., 38 (1972) 482.
4 I. M. Kolthoff and Z. Holdara, J. Electroanal. Chem., 5 (1963) 2.
5 K. Tanaka and K. Nakano, Bull. Chem. Soc., Jpn., 47 (1974) 2222.
6 V. S. N. Rao and S. B. Rao, J. Electroanal. Chem., 108 (1980) 373.
7 I. M. Kolthoff and R. Belcher, Volumetric Analysis, Vol. III, Interscience, New York, 1957, p. 634.
8 P. T. Sah and S. A. Peoples, J. Am. Pharm. Assoc., Sci. Ed., 43 (1954) 513.
9 H.-A. Offe, W. Siefken and G. Domagk (Schenley Industries Inc.) U.S. 192 (Oct. 16, 1956) 2,767. CA 51 (1957) 7431a.
10 E. S. Chikryzova and L. G. Kiriyak, Zh. Anal. Khim., 27 (1972) 1747.

Analytica Chimica Acta, 120 (1980) 357—360

Short Communication

COULOMETRIC TITRATIONS OF ARSENIC(III) AND ANTIMONY(III) WITH ELECTRICALLY GENERATED BROMINE IN ACETIC ACID

T. J. PASTOR*, V. J. VAJGAND and V. V. ANTONIJEVIĆ

Department of Chemistry, Faculty of Sciences, University of Belgrade (Yugoslavia)

(Received 5th May 1980)

Summary. Conditions for the coulometric titrations were investigated. Arsenic(III) could be titrated by continuous or discontinuous generation of bromine, and antimony(III) by discontinuous generation or back-titration. The accuracy and reproducibility depend on the pretreatment of the platinum electrodes.

Bromine is one of the most frequently used reagents for coulometric titrations in aqueous media. It has been successfully used to determine metal ions, inorganic anions, organic compounds and some pharmaceutical products. Arsenic(III) has been titrated in 0.2—1.0 M sulphuric acid [1—8], 1 M hydrochloric acid [9], or dilute acetic acid [10]. The concentration of potassium bromide in the anolyte is usually 0.05—0.5 M. The reagent is generated at a platinum or graphite electrode. Antimony(III) has been determined in the presence of a somewhat higher concentration of hydrochloric acid (2 M) [11, 12].

Conditions for the quantitative electrochemical generation of bromine at a platinum electrode in glacial acetic acid were recently described [13]. Procedures for coulometric titrations of hydroquinone [13] and hydrazines [14] were also developed. This communication describes work which aimed at finding suitable conditions for coulometric determinations of arsenic(III) and antimony(III) in this same solvent.

Experimental

The coulometric titration apparatus with biamperometric end-point detection has already been described [15]. Generation of the reagent was carried out using a current density of 1—5 mA cm^{-2}. The potential between the indicator electrodes was 200—500 mV.

All chemicals were of analytical-reagent grade. Water was removed from them as previously described [13, 15].

Solutions of potassium acetate (0.3—1.3 M) or a 0.2 M solution of sodium perchlorate were used as catholytes. The anolyte was prepared by saturating these solutions with potassium bromide.

Approximately 0.01 M solutions of arsenic(III) chloride and antimony(III) chloride were prepared in acetic acid. Their exact concentrations were

determined by the coulometric method in aqueous media [1, 11].

Procedures. Various procedures were investigated:

I. A definite volume of the solution to be analysed was measured into the anode compartment. The reagent was continuously generated until the end-point was reached.

II. A suitable volume of the solution to be analysed was added to the anode compartment. About 95% of the necessary amount of bromine was continuously generated, and then titration proceeded by discontinuous generation of the reagent in small amounts (for 3—5 s each time at a current of 1—5 mA) until the end-point was reached.

III. The solution to be analysed was added to the anolyte only after 2—90% of the theoretically necessary amount of oxidant had been generated. Titration was completed by continual generation of bromine.

IV. The sample solution was added to the anolyte after 95—97% of the necessary amount of reagent had been generated. Titration was completed by discontinuous generation of bromine.

V. Antimony(III) was also determined by a coulometric back-titration method at room temperature. The desired volume of sample solution was added to the anolyte after an adequate excess of reagent had been generated. After 5—10 min, a known volume of standard arsenic(III) solution was added to the anode compartment. The excess of arsenic(III) was determined by further generation of the reagent. Near the end-point bromine was generated discontinuously.

These general procedures have been described previously in more detail [14—16].

Results and discussion

Preliminary investigations, where generated bromine was titrated with a standard solution of arsenic(III), showed that the reaction was fast and quantitative in a 0.9 M solution of potassium acetate in acetic acid. This indicated the possibility of developing coulometric titration methods for arsenic(III). All the procedures listed above were examined. Thus, for procedures I and II it was found that concentrations of potassium acetate in the supporting electrolyte ranging from 0.3 to 1.3 M did not affect the accuracy of measurements. Because of its low resistance, however, a 0.9 M solution was used throughout. The results of titrations of different amounts of arsenic(III) are presented in Table 1.

The presence of up to 30% water and up to 20% acetic anydride affected neither the accuracy nor reproducibility of the results. Higher concentrations of water and acetic anhydride were not tested.

Procedures III and IV gave results that were 2—3% higher than the theoretical values, regardless of the amount of bromine generated before the solution to be analysed was added to the anolyte. When 2—4 titrations were run in the same anolyte solution by these methods, it was observed in each series of determinations that only the results of the first titration were higher

TABLE 1

Coulometric titration of arsenic(III) in a 0.9 M potassium acetate solution in acetic acid with electrogenerated bromine

Arsenic taken (mg)	No. of titrations	Recovery (%) ± std. dev.		Current (mA)
		Procedure I	Procedure II	
0.716	6	99.0 ± 0.3	99.0 ± 0.7	5.00
0.342	6	100.0 ± 0.5	99.6 ± 0.3	5.00
0.190	6	99.1 ± 0.4	99.4 ± 0.5	2.50
0.105	6	98.8 ± 0.5	99.9 ± 0.5	2.00
0.070	6		99.4 ± 0.4	1.00

than the theoretical values. Thus, the higher results may be attributed to surface changes of the platinum electrodes which occur in the presence of higher concentrations of bromine in the solution before the arsenic(III) is added. In order to prove this assumption, the electrodes were activated before each determination, either by immersing them in a 0.01 M solution of bromine in acetic acid for 2—5 min, or in an aqueous 0.01 M solution of iron(II) sulphate, or by anodic or cathodic polarisation in aqueous 1 M sulphuric acid with a current of 5 mA for 10 min. After activation by bromine, the electrodes were washed by acetic acid; in all other cases they were washed by water, air-dried, and immersed in acetic acid just before use. The chemical activation of electrodes produced slightly more satisfactory results. After pretreatment of the electrodes with bromine or iron(II) sulphate, six consecutive determinations by procedure III gave recoveries of 99.4 ± 0.3% or 99.9 ± 0.3% respectively; after cathodic or anodic polarisation, recoveries were 100.5 ± 0.2% or 100.2 ± 0.3%, respectively.

In a 0.2 M solution of sodium perchlorate the reaction between arsenic(III) and bromine was slow. Various catalysts investigated did not speed up the reaction sufficiently to make it useful. Coulometric methods for determining arsenic(III) by bromine in this supporting electrolyte therefore have not been developed.

The oxidation of antimony(III) with bromine in a 0.9 M solution of potassium acetate in acetic acid was slower than that of arsenic(III). This produced lower results when procedure I was used, even at a low undesirable current density (1 mA cm^{-2}) in the generating circuit. When the generation of bromine near the end-point was discontinuous (procedures II and IV), 0.2—1.1 mg of antimony(III) could be determined with an average error of 1%. The back-titration method produced better results. For six consecutive titrations, a recovery of 99.0 ± 0.3% was obtained; this indicates satisfactory accuracy and good reproducibility.

The authors acknowledge the financial support of the Research Fund of SR of Serbia.

REFERENCES

1 R. J. Myers and E. H. Swift, J. Am. Chem. Soc., 70 (1948) 1047.
2 J. N. Pitts, Jr., D. D. DeFord, T. W. Martin and E. A. Schmall, Anal. Chem., 26 (1954) 628.
3 Q. Fernando, M. A. V. Devanathan, J. C. Rasiah, J. A. Calpin and K. Nakulesparan, J. Electroanal. Chem., 3 (1962) 46.
4 S. Bruckenstein, Anal. Chem., 36 (1964) 2187.
5 G. D. Christian, J. Electroanal. Chem., 11 (1966) 94.
6 W. A. Alexander and D. J. Barclay, J. Electroanal. Chem., 12 (1966) 55.
7 V. J. Jennings, A. Dodson and A. M. Atkinson, Analyst, 97 (1972) 923.
8 V. J. Jennings, A. Dodson and A. Harrison, Analyst, 99 (1974) 145.
9 J. K. Lee and R. N. Adams, Anal. Chem., 30 (1958) 240.
10 G. W. Ewing, Instrumental Methods of Chemical Analysis, McGraw-Hill, New York, 1960, p. 431.
11 R. A. Brown and E. H. Swift, J. Am. Chem. Soc., 71 (1949) 2717.
12 H. L. Richter, Jr., Anal. Chem., 27 (1955) 1526.
13 T. J. Pastor, V. J. Vajgand, V. V. Antonijević and Z. Veličković, Anal. Chim. Acta, 106 (1979) 347.
14 Coulometric Analysis, Conference held at Mátrafüred, Hungary, 17—19 October, 1978, E. Pungor (Ed.), Akadémiai Kiadó, Budapest, 1979, p. 289.
15 T. J. Pastor, V. J. Vajgand and Z. Kićović, Mikrochim. Acta, (1976 II) 525.
16 T. J. Pastor, V. J. Vajgand and V. V. Antonijević, Mikrochim. Acta, (1978 II) 131.

Analytica Chimica Acta, 120 (1980) 361—366

Short Communication

A LIQUID MEMBRANE AMMONIUM-SELECTIVE ELECTRODE BASED ON THE TRIS(2-NITROSO-4-CHLOROPHENOL)IRON(II) ANION

TAKASHI KORENAGA*

Saidaiji Plant, Japan Exlan Co., Ltd., Kanaoka-higashi, Okayama-shi, 704 (Japan)

(Received 14th January 1980)

SUMMARY

Liquid membrane electrodes based on ion-association extraction systems responding to the ammonium ion are described. The tris(2-nitroso-4-chlorophenol)iron(II) anion in a nitrobenzene solution gives an electrode exhibiting Nernstian response in the range $1—10^{-4}$ M ammonium ion (slope, 60 mV) in solutions of pH 4—9. The order of the selectivity coefficients (K_{ij}) is $N(CH_3)_4^+ > NH(CH_3)_3^+ > NH_2(CH_3)_2^+ > NH_3CH_3^+ > K^+ > NH_4^+ > Na^+ > Li^+$.

Cation-selective glass electrodes have been widely used for ammonium determinations in aqueous solutions [1—3]. Ammonium determinations are also possible with the ammonia gas probe [4] and with electrodes containing neutral carrier sequestering agents [5—8]. An ammonium-selective electrode with ammonium tetraphenylborate as the active component has also been investigated [9].

In the present communication, some ammonium-selective electrodes with liquid membranes were prepared by using ion-association extraction systems. Dipicrylaminate, tetraphenylborate, dodecylbenzenesulfonate and tris(2-nitroso-4-chlorophenol)iron(II) were the cation exchangers studied.

Experimental

Reagents. All reagents were of analytical-reagent grade. Tetraphenylborate (TPB) and dodecylbenzenesulfonate (DBS) solutions were prepared from their sodium salts dissolved in distilled water. Dipicrylamine (DPA) was dissolved in an equivalent amount of sodium hydroxide solution.

Tris(2-nitroso-4-chlorophenol)iron(II) (TNI) solution was obtained as follows: 2-nitroso-4-chlorophenol was prepared as the copper complex by nitrosation of *p*-chlorophenol with sodium nitrite in acetic acid containing sodium acetate and copper sulfate. The complex was decomposed with dilute

*Present address: School of Engineering, Okayama University, Tsushima-naka, Okayama-shi, 700, Japan.

hydrochloric acid and the crude product was recrystallized from ethanol [10]. A 1×10^{-2} M solution was prepared by neutralizing with an equivalent amount of sodium hydroxide. Then 100 ml of 1×10^{-3} M iron(II) sulfate solution were transferred to a 500-ml separatory funnel, 100 ml of 1×10^{-2} M 2-nitroso-4-chlorophenol solution and acetate buffer (pH 4.8) were added, and the mixture was left for at least 30 min [11, 12] before extraction with 10 ml of toluene (for 10 min) to remove the unreacted reagent. The 1×10^{-3} M tris(2-nitroso-4-chlorophenol)iron(II) anion remained in the aqueous solution as the sodium salt.

The ammonium stock solution contained ammonium chloride in distilled water. Working solutions were prepared by serial dilutions with distilled water.

Nitrobenzene and 1,2-dichloroethane were used as the extracting solvents without further purification.

Apparatus. A Hitachi-Horiba Model F-5 pH meter equipped with a Yokogawa Model 3046 laboratory recorder was used to measure the membrane potentials. The barrel of an Orion Model 92-07 nitrate ion-selective electrode and an Orion Model 90-02 reference electrode were used.

Preparation and use of the liquid membrane. To a 500-ml separatory funnel were added 100 ml of 1×10^{-3} M ammonium chloride and 100 ml of 1×10^{-3} M TNI. The mixture was shaken with 100 ml of nitrobenzene for 60 min. The aqueous phase was removed and the organic phase was shaken with 100 ml of 1×10^{-3} M ammonium chloride for 60 min. After phase separation, the organic phase was passed through a dry filter paper. This organic solution was diluted to 1×10^{-4} M with nitrobenzene and used as the liquid ion-exchanger. The liquid membrane was supported by a cellulose membrane filter in the manner conventional with Orion electrodes. Except where mentioned, the internal reference solution was aqueous 10^{-2} M ammonium chloride.

Liquid membrane potentials were measured after 5 min; a stable response was achieved after about 1 min when 1×10^{-4} M ammonium chloride solution was measured and the potentials remained constant for at least 1 h. The temperature of the sample solutions was 20 ± 1°C. Solutions were stirred magnetically during the measurements.

Results and discussion

Choice of organic solvent and liquid ion-exchanger. Nitrobenzene and 1,2-dichloroethane were examined as the extracting solvents. Nitrobenzene was preferred because of the wider range of linear response to ammonium ion (Fig. 1). Dodecylbenzenesulfonate (DBS), dipicrylamine (DPA) and tetraphenylborate (TPB) were examined as alternatives to TNI. It is clear from Fig. 2 that the TNI membrane provided the best linear response and that the order of extractability of the ammonium ion with these monovalent organic anions is TNI > DBS > DPA > TPB. It is noteworthy that TNI is a spherical anion and its single charge is distributed over the three chlorine atoms [13].

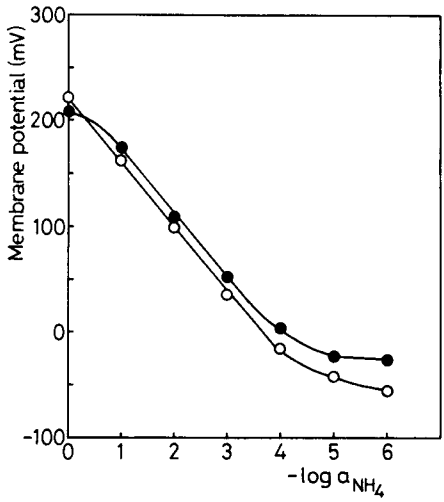

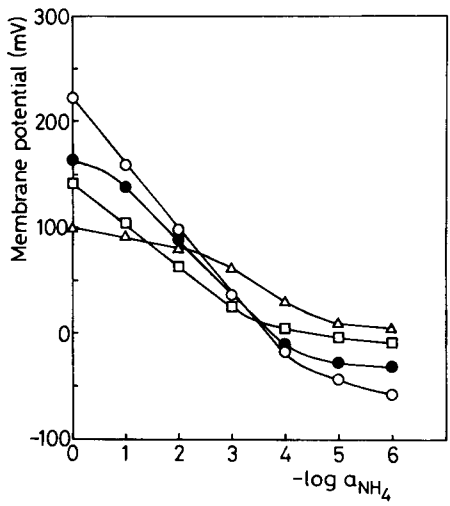

Fig. 1. Electrode response with 1×10^{-4} M ammonium TNI in different organic solvents: (○) nitrobenzene; (●) 1,2-dichloroethane.

Fig. 2. Electrode response with different cation-exchangers (1×10^{-4} M) in nitrobenzene: (○) ammonium TNI; (●) ammonium DBS; (□) ammonium DPA; (△) ammonium TPB.

Figure 2 also shows that the response of the TNI electrode (10^{-4} M) is linear (slope 60 mV/pNH_4) down to 10^{-4} M ammonium chloride. The effect of the concentration of the membrane solute on the membrane potential was studied. An increase in this concentration beyond about $10^{-3.5}$ M caused a drop in the membrane potential. This is probably due to extraction of the membrane solute by the adjacent aqueous solution; hence a dilute organic solution is preferable. The electrical resistance of the membrane, however, increased with decreased concentration of the ion exchanger, so that potential became unstable. Consequently, 1×10^{-4} M was used in the liquid membrane with an aqueous 1×10^{-2} M ammonium chloride reference solution.

Effect of pH. pH adjustments were made by addition of lithium hydroxide and hydrochloric acid. Figure 3 shows that a constant response was obtained from pH 4 to 9 for 10^{-3} M ammonium chloride. The potential increase below pH 3 may be attributed to hydrogen ion interference. That above pH 10 can probably be attributed to lithium ion interference and to ammonia gas permeating the membrane.

Effect of diverse ions. The effects of diverse ions were examined in three series of experiments. The electrode response to alkali metals was in the order $K^+ > NH_4^+ > Na^+ > Li^+$ (Fig. 4). The order of electrode response to alkaline earth metals and aluminium (Fig. 5) was $NH_4^+ > Al^{3+} > Ca^{2+} > Mg^{2+}$; the responses to these divalent and trivalent ions were significant but less than Nernstian. The electrode response to alkylamines (Fig. 6) was $N(CH_3)_4^+ > NH(CH_3)_3^+ > NH_2(CH_3)_2^+ > NH_3CH_3^+ > NH_4^+$. Quaternary ammonium ions

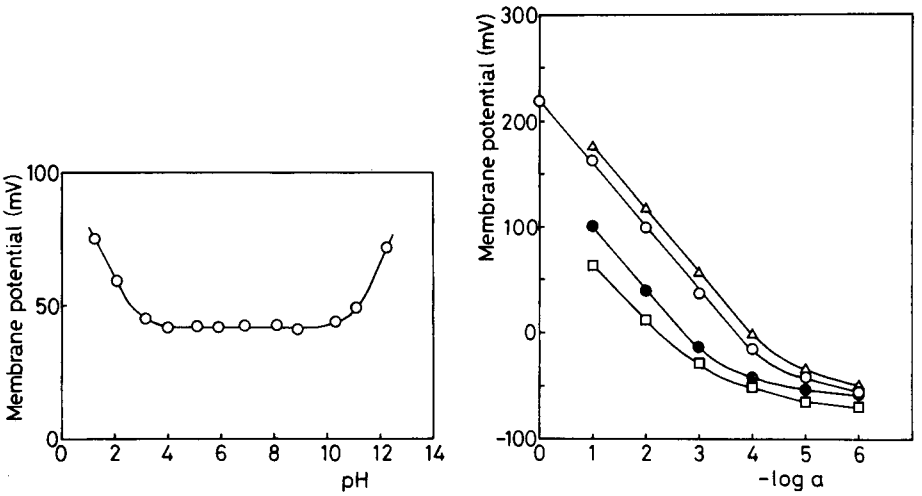

Fig. 3. Electrode response vs. pH for 1×10^{-4} M ammonium TNI in nitrobenzene. Sample solution, 1×10^{-3} M ammonium chloride.

Fig. 4. TNI electrode response to alkali metal ions: (△) K^+, (●) Na^+, (□) Li^+, (○) NH_4^+.

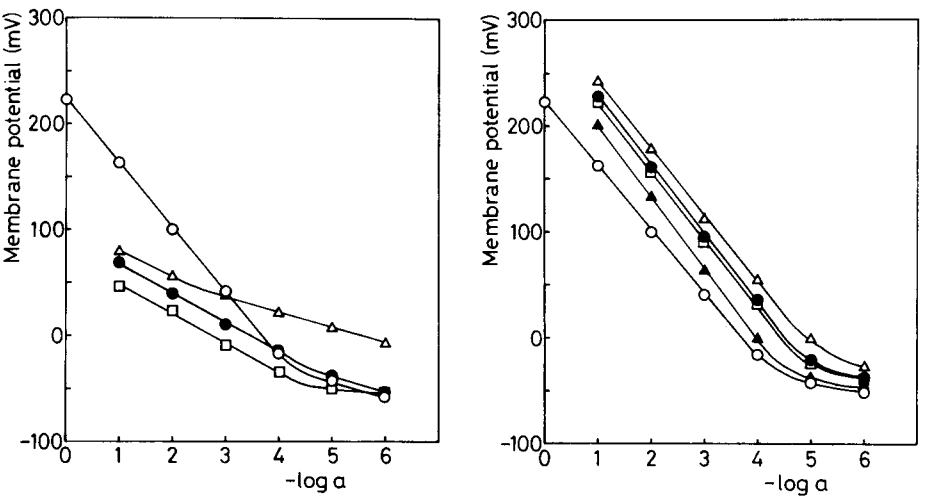

Fig. 5. TNI electrode response to alkaline earth metal and aluminium ions: (●) Ca^{2+}, (□) Mg^{2+}, (△) Al^{3+}, (○) NH_4^+.

Fig. 6. TNI electrode response to alkylammonium ions: (△) $N(CH_3)_4^+$, (●) $NH(CH_3)_3^+$, (□) $NH_2(CH_3)_2^+$, (▲) $NH_3CH_3^+$, (○) NH_4^+.

TABLE 1

Selectivity coefficients (K_{ij}) for various cations with the TNI electrode

Cation	K_{ij}	Cation	K_{ij}
$N(CH_3)_4^+$	15.0	Na^+	0.10
$NH(CH_3)_3^+$	8.4	Li^+	0.03
$NH_2(CH_3)_2^+$	6.7	Ca^{2+}	0.009
$NH_3CH_3^+$	2.4	Mg^{2+}	0.004
K^+	2.0	Al^{3+}	0.008
NH_4^+	1.0		

such as tetrabutylammonium, dodecyltrimethylammonium, and tetradecyldimethylbenzylammonium, and polycations such as poly-N,N-diallyldimethylammonium also gave a response with this electrode.

The selectivity coefficients (K_{ij}) for the TNI membrane (Table 1) were obtained by measuring the membrane potentials in the presence of diverse ions. K_{ij} was estimated as follows: the electrode response in the presence of an interfering ion can be described by [14];

$$E = \text{constant} + 2.303\,(RT/F)\log\{a_{NH_4} + K_{ij}(a_j)^{1/z}\}$$

where z is the charge of the j-ion, K_{ij} is the selectivity coefficient for the j-ion and a_{NH_4} and a_j denote the activities of ammonium ion and j-ion. The a_{NH_4} and a_j activities were approximately given by the molar concentrations because dilute solutions were used.

The order of selectivity coefficients shown in Table 1 for the TNI electrode was also found for the DBS, DPA and TPB membranes. The selectivity coefficients obtained for the TNI membrane in this work agree with those reported for a TPB-plastic membrane [9]. Therefore, it seems likely that the sequence of selectivity is independent of the exchange site species. The selectivity of a liquid membrane electrode is determined by the relative distribution coefficients and mobilities of the primary ion and the competitive ion in the limiting case of complete dissociation [15]. From conductivity measurement of this liquid membrane, it was found that the TNI and its counter cation (i.e. NH_4^+) in nitrobenzene were almost completely dissociated. The sequence of K_{ij} values in Table 1 is therefore consistent with the extractability of the cations into the organic solvents by large monovalent organic anions [16, 17].

The author is greatly indebted to Professor Kyoji Tôei and Dr. Shoji Motomizu of Okayama University for their encouragement, and also to Japan Exlan Co., Ltd. for permission to publish this paper.

REFERENCES

1 G. A. Rechnitz, S. B. Zamochnick and M. Katz, Anal. Chem., 35 (1963) 1322.
2 G. I. Goodfellow and H. M. Webber, Analyst, 97 (1972) 95.
3 G. J. Montalvo and G. G. Guilbault, Anal. Chem., 41 (1969) 1897.
4 Instruction Manual, Ammonia Electrode Model 95-10, Orion Research Inc., Cambridge, MA, U.S.A., 1974.
5 R. P. Scholer and W. Simon, Chimia, 24 (1970) 372.
6 G. A. Rechnitz and E. Eyal, Anal. Chem., 44 (1972) 370.
7 R. E. Cosgrove, C. A. Mask and I. H. Krull, Anal. Lett., 3 (1970) 457.
8 J. Mertens, P. van den Winkel and D. L. Massart, Anal. Lett., 6 (1973) 81.
9 E. Hopîrtean and E. Stefănigă, Rev. Roum. Chim., 20 (1975) 863.
10 T. Korenaga, S. Motomizu and K. Tôei, Nippon Kagaku Zasshi, (1972) 2445.
11 T. Korenaga, S. Motomizu and K. Tôei, Anal. Chim. Acta, 65 (1973) 335.
12 K. Tôei, S. Motomizu and T. Korenaga, Analyst, 100 (1975) 629.
13 K. Tôei (Okayama University), private communication.
14 J. W. Ross, Science, 156 (1967) 1378.
15 R. A. Durst (Ed.), Ion-selective Electrodes, N.B.S. Spec. Publ. 384, U.S. Printing Office, Washington, 1970, p. 5.
16 S. Motomizu, K. Tôei and T. Iwachido, Bull. Chem. Soc. Jpn., 42 (1969) 1006.
17 A. Sadakane, T. Iwachido and K. Tôei, Bull. Chem. Soc. Jpn., 48 (1975) 60.

Analytica Chimica Acta, 120 (1980) 367—370

Short Communication

DETERMINATION OF CYANIDE IN THE PRESENCE OF MERCAPTANS WITH A SELECTIVE-ELECTRODE

J. L. BERNAL*, R. PARDO and J. M. RODRIGUEZ

Department of Analytical Chemistry, Faculty of Sciences, Prado de la Magdalena, Valladolid (Spain)

(Received 3rd September 1979)

Summary. The interfering action of mercaptans on determinations of cyanide with a cyanide-selective electrode can be eliminated by oxidation or by distillation. The procedures are supplied to the analysis of waste waters.

Ion-selective electrodes based on silver iodide and sulphide have been widely used for the determination of cyanide activity [1]. The response model has been studied by several authors [2, 3]. The effect of pH [3—5] and the interferences [6] have also been discussed. For cyanide determinations in media containing interfering compounds, e.g. sulphide, mercaptans or cations forming cyanide complexes, prior distillation of hydrogen cyanide is recommended [7, 8]. In the present communication, the interfering action of three mercaptans is described, and two procedures for eliminating the interference are proposed: one is based on the selective oxidation of mercaptans in presence of cyanide, and the other involves oxidation followed by distillation of hydrogen cyanide.

Experimental

Apparatus. A Philips PW9414 ion-activity meter was used in combination with a Philips IS550—CN cyanide-selective electrode and a Philips R44/2-SD/1 double junction saturated calomel reference electrode with its outer chamber filled with a 2 M KNO_3 solution. The distillation apparatus consisted of a 250-ml distillation flask with three necks, which held a separating funnel, an inlet tube for air and the outlet tube to a condenser. The condenser was joined to a vacuum-type absorber with a gas-dispersion frit and a vacuum line with a clamp for adjustment of suction. The reaction flask was heated electrically.

Reagents. For the cyanide stock solution, 4.199 g of sodium cyanide was dissolved in 1 l of 0.01 M sodium hydroxide. The mercaptan solutions were prepared by dissolving 0.01 mol of the corresponding mercaptan in 1 l of 0.01 M sodium hydroxide. For the TISAB solution, 176.78 g of potassium nitrate, 35.82 g of disodium hydrogenphosphate and 10.0 g of sodium hydroxide were dissolved in 1 l of deionized water.

Determination of cyanide. Mix 50 ml of sample with 25 ml of TISAB and

dilute to 100 ml. Place this solution in a 250-ml beaker, insert the electrodes and read the e.m.f. after stirring continuously for 3 min. Prepare a calibration graph under these conditions for the range 10^{-3}—10^{-6} M cyanide.

Mercaptan oxidation. Mix 50 ml of sample, 25 ml of TISAB and 10 ml of 3% (v/v) hydrogen peroxide, and dilute to 100 ml after 4 min. Determine the cyanide concentration as above.

Mercaptan oxidation and distillation. Place 25 ml of TISAB diluted to 100 ml with deionized water, into the absorber of the distillation apparatus. Place 100 ml of sample in the reaction flask, add 10 ml of 3% (v/v) hydrogen peroxide and heat for 4 min at 50°C. Add 5 ml of saturated mercury(II) chloride solution and 10 ml of 51% (w/v) magnesium(II) chloride solution and connect up the suction (one or two air bubbles per second). Add 15 ml of concentrated sulphuric acid from the separating funnel, and distil for at least 50 min. Remove the solution from the absorber and determine the cyanide concentration as above.

Results and discussion

The TISAB solution used optimizes the pH and the ionic strength. The slope of the calibration graph was −60.8 mV/decade, and the linear range was 10^{-3}—5.0×10^{-6} M, with a detection limit of 8.2×10^{-7} M. To assess the interference of mercaptans, the selectivity coefficients, $K^{pot}_{CN,M}$, for three mercaptans were determined by using the mixed-solutions method [9]. Table 1 shows the results obtained; as the selectivity coefficients exceed unity, the interference is obviously severe. It is therefore necessary to eliminate the mercaptans.

Oxidation method. Iodine is the most selective oxidant for mercaptans, but is clearly unsuitable for the present purpose. Hydrogen peroxide was therefore tested; a reaction time of 4 min was sufficient for the total oxidation of the mercaptans. Apparent selectivity coefficients after the oxidation $(K^{pot}_{CN,M})'$ were determined as before (Table 1). The apparent selectivity coefficients were less than 10^{-3}, indicating that the interferences had been largely eliminated. The characteristics of a calibration line constructed after the oxidation were identical to those obtained for pure cyanide solutions.

TABLE 1

Real and apparent selectivity coefficients of mercaptans

	Mercaptan[a]		
	I	II	III
$K^{pot}_{CN,M}$	4.37	4.79	3.79
$(K^{pot}_{CN,M})'$	9×10^{-4}	4×10^{-4}	1.5×10^{-4}
$(K^{pot}_{CN,M})''$	$<10^{-6}$	$<10^{-6}$	$<10^{-6}$

[a]I, thioglycolic acid; II, 3-mercaptopropionic acid; III, ethyl thioglycolate.

Oxidation—distillation method. The oxidant used was again hydrogen peroxide and sulphuric acid was used to form hydrogen cyanide. The addition of mercury(II) chloride and magnesium(II) chloride helps to break down cyanide complexes and to speed the distillation of hydrogen cyanide. The other parameters of time, temperature, reagent amounts were optimized experimentally. Apparent selectivity coefficients after this treatment, $(K^{pot}_{CN,M})''$ (see Table 1), were less than 10^{-5}, thus the interferences were completely eliminated. The calibration parameters after this treatment were identical to those obtained in the simpler procedures.

The oxidation—distillation method allows the "total" cyanide concentration to be determined because any metal—cyanide complexes are destroyed. In contrast, the oxidation method yields only the "free" cyanide concentration.

Practical applications

The methods were applied in the analysis of waste waters from an industrial plant which utilises hydrogen cyanide and various mercaptans in its processes. In order to compare the procedures properly, four different estimations were used for each sample: (1) direct potentiometry, which gives the "apparent" cyanide concentration; (2) potentiometry after the oxidation treatment, which indicates the "free" cyanide concentration; (3) potentiometry after oxidation and distillation, which gives the "total" cyanide concentration; (4) colorimetric determination of mercaptans in the samples [10].

Table 2 shows the results obtained. The mercaptan concentrations are given rather arbitrarily as ppm of thioglycolic acid because the samples came from a proprietary industrial process and no information was available about which mercaptans were present. From these results, it can be concluded that several of the samples contain cations which form complexes with

TABLE 2

Results obtained for the waste waters

Sample	Apparent cyanide (ppm)	Free cyanide (ppm)	Total cyanide (ppm)	Mercaptan (ppm)
1	38.0	0.03	0.13	23.6
2	10.5	0.23	1.08	4.7
3	4.1	0.19	0.29	1.6
4	15.9	0.03	0.03	9.4
5	5.3	0.12	0.13	2.6
6	0.1	0.03	0.03	0.1
7	1.4	0.03	0.03	0.5
8	431.3	0.03	0.05	202.1
9	41.5	36.4	39.0	4.7
10	10.4	0.14	0.44	8.2

cyanide. Moreover, all the samples have a cyanide concentration higher than that permitted by law. The "apparent" cyanide concentration shows the incorrect results obtained when interferences were not eliminated. The disparity between "free" and "total" concentrations confirms the necessity of using the distillation method in the analysis of industrial samples.

REFERENCES

1 E. Pungor and K. Tóth, Analyst, 95 (1970) 1132.
2 B. Fleet and H. von Storp, Anal. Chem., 43 (1971) 1575.
3 J. Koryta, Anal. Chim. Acta, 61 (1972) 329; 91 (1977) 1.
4 M. Mascini and A. Napoli, Anal. Chem., 46 (1974) 447.
5 M. Gratzl, F. Rakiás, G. Horvai, K. Tóth and E. Pungor, Anal. Chim. Acta, 102 (1978) 85.
6 P. L. Bailey, Analysis with Ion-Selective Electrodes, Heyden, London, 1976.
7 J. L. Penland and G. Fische, Metall. Angew. Chem., 10 (1972) 391.
8 P. J. Cusbert, Anal. Chim. Acta, 87 (1976) 429.
9 E. Pungor and K. Tóth, Anal. Chim. Acta, 47 (1969) 29.
10 C. E. Neubeck and C. V. Smythe, Arch. Biochem., 4 (1944) 435.

Analytica Chimica Acta, 120 (1980) 371—375

Short Communication

DETERMINATION OF TRACES OF PHENOL IN WATERS BY MOLECULAR EMISSION CAVITY ANALYSIS

O. OSIBANJO* and S. O. AJAYI

Department of Chemistry, University of Ibadan, Ibadan (Nigeria)

(Received 19th March 1980)

Summary. Tribromophenol is produced from phenol (10^{-5}—10^{-6} M), filtered off and determined by production of InBr emission at 376 nm in an air—hydrogen—nitrogen flame. Recoveries of 97—99% were obtained from spiked lake water.

Phenolic compounds are environmental pollutants whose presence in surface waters is objectionable because of the unpleasant odours produced when the water is chlorinated. Furthermore, phenols and chlorinated phenols are acutely toxic to fish; certain species can hardly survive in river water containing 0.5—5.0 ppm of phenol [1]. Conventional methods for trace phenol determination involve colorimetric techniques such as those based on coloured diazonium derivatives of phenol [2, 3] or on the complex formed with 4-aminoantipyrine [4]. Apart from being tedious and the reactions being non-stoichiometric, these methods are not specific for phenols, and suffer from many interferences.

Chromatographic techniques which entail fairly long manipulative steps such as extraction, clean-up and separation, have also been applied for the direct determination of trace phenols in waters. Gas chromatography with flame ionisation detection can be applied directly to phenols in water at the ppm level [5] if adequate care is taken to circumvent artefact problems. The detection limit and selectivity are further improved by elaborate phenol pre-concentration by sorption from water onto resins such as Amberlite XAD-2 or XAD-4, and subsequent desorption prior to gas chromatography [6, 7]. Chemical derivatisation allows indirect determination with electron capture detection, but the sensitivity depends on the phenol derivative employed [8—10]. High-performance liquid chromatography has not been widely applied for trace phenol determinations, probably because of the relatively low sensitivity of commercially available detectors, although sensitivity similar to gas chromatography has been reported when the sample is pre-concentrated by sorption on resins [11].

Molecular emission cavity analysis (m.e.c.a.) has already been shown to be a selective and sensitive flame emission technique for the determination of nanogram amounts of halides using an indium-coated stainless steel cavity [12], and rather less sensitive using a tin-lined stainless steel or

aluminium oxy-cavity [13, 14]. As aqueous solutions of phenol are readily brominated at room temperature, the possibility of determining phenol, after the removal of excess of bromine, by measuring the emission of the tribromo derivative in an indium-lined cavity placed in an air—hydrogen—nitrogen flame was investigated.

Experimental

Apparatus. A Pye-Unicam SP900 flame atomic absorption/emission spectrophotometer operating in the emission mode was adapted for m.e.c.a. A premixed flame burner with a circular 18-mm diameter, 16-hole head was attached to the instrument. The design of the sample holder assembly was similar to previous examples [12]. The assembly for supporting the cavity was a carbon steel frame, on top of which was a brass block, which carried a long threaded stainless steel rod (ca. 3 mm diam.) to the end of which was attached the cavity. The cavity was drilled in a stainless steel cylinder, so as to have a diameter of 8 mm and a depth of 5 mm [14, 15]. The cavity could be reproducibly positioned in the flame in line with the spectrometer slit by means of an adjustable knob, which controlled the lateral movement of the cavity in the block on the steel frame. A Perkin-Elmer chart recorder with a response time of 0.5 s was connected to the 0—10 mV output of the instrument.

The cavity was coated with indium by pressing a small amount of indium metal into the cavity. The cavity was introduced into the flame and heated to spread the indium over the walls of the cavity. After cooling with an air blower, the cavity was unscrewed and excess of indium scraped off with a knife, leaving a uniform indium coating inside the walls of the cavity. Usually the cavity coated in this manner was reproducible and could be used for several determinations without renewing the coating.

The gas flow rates were controlled by flow meters (Flow Bits Ltd., Basingstoke, Gt. Britain) after calibration by the conventional soap bubble method. The optimal instrument conditions used are given in Table 1. The instrument was operated in a fume cupboard covered with curtains to prevent any interference from extraneous light.

Calibration procedure. Phenol solution (0.25—1.0 ml of 2×10^{-2} M, or 0.15 M) was added to several 1-l samples of distilled water in 2-l beakers, followed by 10 ml of glacial acetic acid. Liquid bromine (2 ml) was added to each beaker and the solutions stirred at intervals for 20 min. The tribromo

TABLE 1

Instrumental conditions for the determination of phenol by m.e.c.a.

Wavelength	376 nm	Hydrogen	1.6 l min^{-1}
Slit-width	0.40 mm	Nitrogen	3.5 l min^{-1}
Cavity—burner distance	24 mm	Air	1.5 l min^{-1}
Cavity—slit distance	91 mm	Distance of cavity into flame	9 mm

derivative formed in each beaker was filtered off on a small glass-fibre paper (20 min) and washed several times with water (10—20 ml total) until free of residual bromine. The precipitate was allowed to dry in air (15 min) and was then dissolved in 100 ml of ethanol; a 1-ml aliquot was diluted to 10 ml with ethanol, and a 5-μl aliquot was injected into the cavity. The InBr emission obtained on igniting the flame was measured at 376 nm.

Results and discussion

A linear calibration graph was obtained for phenol over the range 0.5×10^{-5}—1.5×10^{-4} M. The coefficient of variation for 10 replicate injections of tribromophenol obtained from a 5.0×10^{-5} M phenol solution was 4%. Figure 1 shows the emission profiles from various amounts of phenol.

The effects of some anions commonly occurring in surface waters were investigated. Chloride, iodide, nitrate, sulphate and phosphate ions were added to 1 l of 5×10^{-5} M phenol solution in weight ratios of 1:1, 10:1 and

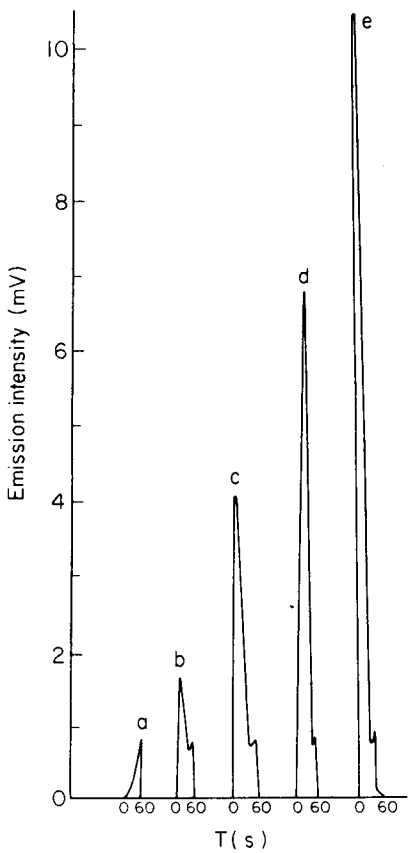

Fig. 1. Emission response profiles for (a) blank; (b) 2.85×10^{-5} M; (c) 5.70×10^{-5} M; (d) 8.55×10^{-5} M and (e) 1.14×10^{-4} M phenol as its tribromo derivative.

TABLE 2

Effect of various anions on the emission intensity of phenol (1 l of 5×10^{-5} M) as tribromophenol

Ion	% Change in intensity caused by ion at molar ratio to phenol of		
	1:1	10:1	100:1
Cl^-	+52	+57	+84
I^-	+50	+94	+100
NO_3^-	−3	−9	−91
SO_4^{2-}	−4	−4	−50
PO_4^{3-}	−67	−77	−81
Combined effect[a]	−1	−70	−100

[a]Of all five ions, each in the ratio stated.

100:1 to phenol, and the phenol was determined by the recommended procedure. Table 2 shows the results obtained. An ion is considered to have interfered if the percentage change in emission intensity is significantly more than twice the coefficient of variation. Thus 1:1 and 10:1 weight ratios of nitrate and sulphate, and the combined effects of all ions at the 1:1 ratio did not interfere with phenol determination.

The serious interference from chloride and iodide probably arises from the formation of chloro- and iodo-phenol derivatives, whose emission peaks (InCl and InI) would overlap with that of tribromophenol (t_m = 12 s) both spectrally and because of inadequate difference in their t_m values. However, the interfering ions are likely to occur at such low levels in natural surface waters as not to interfere with phenol determinations. Samples containing high levels of the interfering ions could be treated previously with silver sulphate to remove chloride, iodide and phosphate while nitrate could be reduced to nitrite and then removed by the addition of sulphamic acid [16].

Determination of phenol in lake water. Water samples were collected in glass bottles at different locations in the Oba Dam Lake. The water samples were mixed together and filtered prior to analysis. Duplicate 1-l portions were taken for analysis. The level of phenol in Oba Dam water was found to

TABLE 3

Recovery studies for phenol determination in 1-l samples of lake water

Sample	Phenol concentration from calibration graph (M)	Phenol recovery (%)
Oba Dam water	0.9×10^{-5}	—
Oba Dam water + 2.85×10^{-5} mol phenol	3.7×10^{-5}	98
Oba Dam water + 8.50×10^{-5} mol phenol	9.2×10^{-5}	98

be 9×10^{-5} M (0.85 ppm) both from the calibration graph and by the method of standard addition. Phenol recovery studies were carried out by spiking the 1-l aliquots. Table 3 shows that a 98% recovery of phenol was obtained.

The authors acknowledge the valuable technical assistance rendered by Messrs. C. O. Okpara and A. O. Bankole.

REFERENCES

1 V. M. Brown, Water Res., 1 (1967) 596.
2 Analytical Methods Committee, Official, Standard and Recommended Methods for Analysis, 2nd edn., Society for Analytical Chemistry, London, 1973.
3 S. Siggia, Quantitative Organic Analysis via Functional Groups, 3rd edn., J. Wiley, New York, 1963.
4 F. Mohler, Jr. and N. Jacob, Anal. Chem., 29 (1957) 1369.
5 K. D. Bartle, J. Elstub, M. Novotny and R. J. Robinson, J. Chromatogr., 135 (1977) 351.
6 Z. Vozňaková and M. Popl, J. Chromatogr. Sci., 17 (1979) 682.
7 D. Chriswell, R. C. Change and J. S. Fritz, Anal. Chem., 47 (1975) 1325.
8 A. T. Shulgin, Anal. Chem., 36 (1964) 20.
9 F. K. Kawahara, Anal. Chem., 40 (1968) 1009.
10 B. Davis, Anal. Chem., 49 (1977) 832.
11 A. W. Wolkoff and R. H. Larose, J. Chromatogr., 99 (1974) 731.
12 D. A. Stiles, Proc. Soc. for Anal. Chem., 11 (1974) 1.
13 R. Belcher, S. A. Ghonaim and A. Townshend, Anal. Chim. Acta, 71 (1974) 255.
14 C. O. Akpofure, R. Belcher, S. L. Bogdanski and A. Townshend, Anal. Lett., 8 (1975) 821.
15 R. Belcher, S. L. Bogdanski, O. Osibanjo and A. Townshend, Anal. Chim. Acta, 84 (1976) 1.
16 R. R. Elton-Bott, Anal. Chim. Acta, 90 (1977) 215.

Analytica Chimica Acta, 120 (1980) 377—382

Short Communication

THERMAL STABILIZATION OF INORGANIC AND ORGANO-SELENIUM COMPOUNDS FOR DIRECT ELECTROTHERMAL ATOMIC ABSORPTION SPECTROMETRY

J. ALEXANDER, K. SAEED and Y. THOMASSEN*

Institute of Occupational Health, Gydas vei 8, Oslo 3 (Norway)

(Received 28th April 1980)

Summary. A ^{75}Se tracer technique is used to show that Sb, Cd, Mn, Mo, Ni, KI, KIO_3, Ag, Th, Tl, Zn and Zr quantitatively stabilize inorganic selenium. Only Mo, Ni and Ag were effective for organoselenium compounds in urine, and only molybdenum was partially successful for blood samples.

The essential role of selenium as a trace metal, its toxic effects at high concentrations in living organisms [1—3] and its influence on the metabolism of the toxicity of other heavy metals [4, 5], necessitates its determination in biological samples by rapid, accurate methods.

Electrothermal atomic absorption spectrometry (e.a.a.s.), when used for the determination of selenium in biological and other complex matrices, is prone to complications because of the high volatility of the analyte. Matrix modification techniques have been proposed to allow increased charring temperatures, and thus decrease the non-specific absorption signals originating from the matrix [6]. Addition of metal ions to the selenium sample is beneficial in that refractory selenides are formed. Earlier studies have shown that copper, iron, molybdenum, nickel, potassium iodide and silver prevented the volatilization of inorganic selenium at low charring temperatures [6—9]. It has recently been demonstrated by tracer techniques that nickel and silver have a strong stabilizing effect on organoselenium compounds present in human blood, while copper and iron had no effect [10]. The use of silver, however, is not favoured for biological samples because of chloride precipitation. The large amount of nickel (0.5%) required to stabilize selenium is unsatisfactory in laboratories where samples are routinely analysed for traces of nickel. In order to avoid contamination of the graphite furnace with nickel, the possibility of using other metals to replace nickel or silver as stabilizing elements was therefore studied. Radioactive selenium was again used to monitor the volatility of the selenium. The effects of the stabilizing agents on the sensitivity was also investigated.

Experimental

Apparatus. A Perkin-Elmer model 5000 atomic absorption spectrometer equipped with selenium electrodeless and deuterium arc lamps, an HGA-500 graphite furnace, an AS-1 automatic sampler, and a Perkin-Elmer model 56 recorder were used. A Perkin-Elmer HGA-76 graphite furnace was used for the isotopic studies. The furnaces were purged with argon. The γ-radiation was measured with a Packard Auto-Gamma scintillation spectrometer.

Reagents and standard solutions. The reagents employed were of analytical reagent-grade quality. A solution of ^{75}Se (as sodium selenite; Radiochemical Centre, Amersham, U. K.) was diluted appropriately with an aqueous 5.0 mM inactive sodium selenite solution.

Commercially-available 1000-ppm standard solutions (BDH) of the following elements were used: antimony, cadmium, cobalt, molybdenum, manganese, mercury, nickel, tin and zinc. The 1000-ppm standard solutions of the other elements were obtained by appropriate solution of cerium(IV) sulphate, cesium chloride, potassium iodate, potassium iodide, palladium chloride, platinum(IV) chloride, silver nitrate, tantalum, thallium(I) nitrate, thorium nitrate, tungsten and zirconium nitrate.

Preparation of in-vivo organoselenium compounds labelled with ^{75}Se. For whole blood, the procedure followed was similar to that described earlier [10]. For urine, Wistar rats were injected intraperitoneally with ^{75}Se-labelled sodium selenite of suitable activity, and kept overnight in metabolism cages for urine collection.

Determination of ^{75}Se activity as a function of ashing temperature. A 20-μl portion of a solution containing ^{75}Se was dispensed into a graphite tube (this corresponded to 3000, 2400 and 1200 cpm in aqueous selenite solution, whole blood and urine, respectively) and dried at 100°C for 40 s. The tube, after cooling, was removed from the furnace and placed in a plastic tube which fitted the counting well in the scintillation spectrometer. The activity was counted for 1 min. The background activity for each graphite tube was determined prior to the injection of the ^{75}Se samples. The net ^{75}Se activity was equivalent to 100% retention of selenium in the graphite tube. Further samples were, after drying as before, ashed at 200–1600°C at 100° intervals.

In another series of tubes, the addition of 20 μl of sample labelled with ^{75}Se was followed by 20 μl of 0.1% (w/v) of test reagent, and the above experiments were repeated. The background counts (20—80 cpm for different tubes) were again subtracted from the measured activities.

Effect of stabilizing reagents on the selenium e.a.a.s. sensitivity. A new graphite tube was used for each reagent solution tested. Aliquots (20 μl) of a 0.2 μg Se ml^{-1} aqueous standard, without and with added 0.1% metal reagent, were dispensed into the tube, dried at 110°C for 25 s (ramp time 15 s), ashed at 500°C for 20 s and atomized at 2200°C using the maximum power mode (internal gas flow 50 ml min^{-1}). The temperature was further increased to 2800°C for 3—4 s to clean the tube. The spectrometer was operated at the

196.0-nm selenium resonance line with a spectral bandwidth of 2.0 nm. The electrodeless discharge lamp was operated at 6 W.

Results and discussion

During the preliminary investigation, it was observed that the volatility of selenium as selenite was increased by the addition of nitric acid. This effect is probably due to the formation of selenates which are known to be more volatile. Therefore, all the metal reagent solutions and the standard solutions used in this work were 3% (w/v) in nitric acid.

Sodium selenite labelled with ^{75}Se. From the results shown in Fig. 1, it is interesting to note the decreased volatility of selenium in the presence of cadmium, antimony, potassium iodate, thallium, manganese, zinc, zirconium and thorium. Potassium iodide is confirmed as being able to decrease the volatility of selenium [11]. The charring temperature can be raised to 1000°C without any loss of selenium. When similar experiments were repeated with potassium chloride solution, selenium began to volatilize at 300°C, indicating the formation of an I—Se compound rather than a K—Se compound. The thermal stability of the selenides which were formed in the graphite furnace showed no correlation with available thermodynamic data; this may be due to formation of more than one selenide. Such selenides vary widely in their physical properties, e.g., melting and boiling point and heat of formation. Selenide formation is a function of temperature and selenides

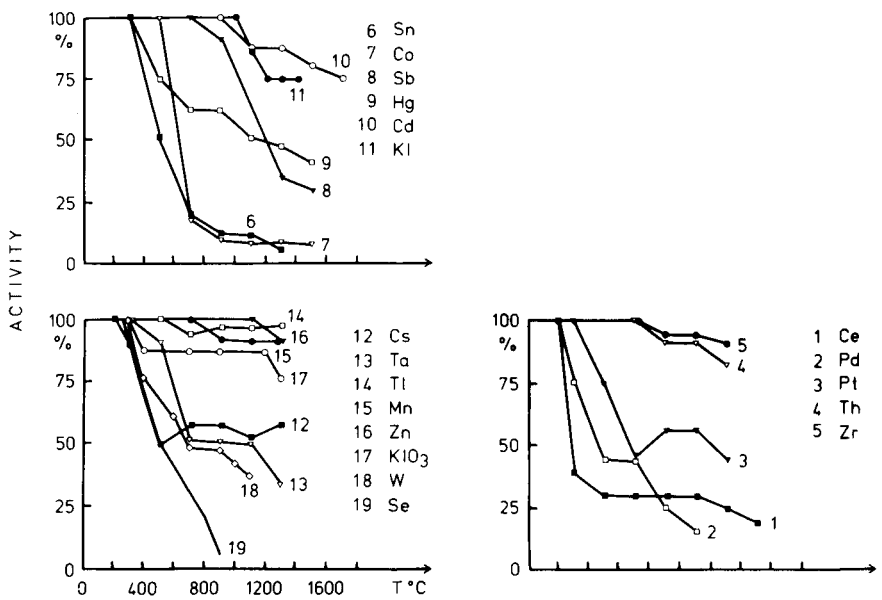

Fig. 1. Retention of activity as a function of the charring temperature for samples of sodium selenite (^{75}Se), with addition of matrix-modifying reagents (1000 μg ml^{-1}). Se = no reagent added.

with different metal to selenium ratios may be expected as the ashing temperature is raised. This might explain the characteristic behaviour of tantalum, cesium, tungsten and platinum with respect to selenium stabilization. As is apparent from Fig. 1, the loss of selenium at 200—300°C in the presence of these elements proceeds little further when the temperature is increased above 500°C and almost 50% of the original activity is retained at 1200°C. If there had been no selenide formation, the activity would have dropped sharply to zero with such an increase in temperature. This may suggest the conversion of more volatile selenium compounds into less volatile selenides with increasing temperature.

Thermal stabilization of inorganic selenium compounds with elements other than copper, iron, molybdenum, nickel, silver and potassium iodide may be of great practical interest. The presence of 1000 ppm of manganese or zinc in the sample matrix makes any matrix modification unnecessary for thermal stabilization of selenium. The properties of thorium and zirconium in forming thermally stable selenides are also of interest; since these two elements are not determined sensitively by e.a.a.s., their contamination of the graphite furnace is of no importance.

In-vivo studies. After the stabilizing effect of different metals on inorganic selenium compounds had been demonstrated, similar studies were repeated by utilizing organoselenium compounds obtained by in-vivo preparation. The only metals tested were those above which had proved to have a significant influence on the selenium volatility. The results obtained from compounds prepared in urine and whole blood are presented in Figs. 2 and 3, respectively.

For urine, Fig. 2 shows that only molybdenum, nickel and silver are effective in preventing the volatility of organically bound selenium (mainly the trimethylselenonium ion). No loss in activity was recorded when the ashing temperatures were raised to 900, 1100 and 1300°C in the presence of molybdenum, nickel and silver, respectively.

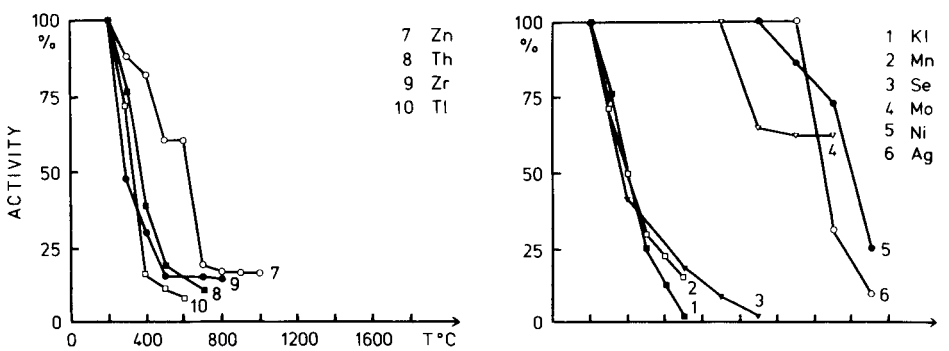

Fig. 2. Retention of activity as a function of the charring temperature for in-vivo prepared rat urine labelled with ^{75}Se, with addition of stabilizing reagents (1000 $\mu g\ ml^{-1}$). Se = no reagent added.

In continuation of earlier work [10], several other metals were studied to determine their influence on the volatility of organoselenium compounds in whole blood. None of the tested metals, however, was able to decrease the selenium volatility (Fig. 3). In the presence of molybdenum, the rapid decrease in activity at 300° C is prevented when the ashing temperature is raised above 400° C. Almost 60% of the original activity then remains up to 1300° C. This behaviour shows that molybdenum does not stabilize quantitatively organoselenium compounds in whole blood. Molybdenum may form stable selenides with some of the organoselenium compounds, while others remain unaffected.

Chemical interferences. Changes in the analyte absorption signal caused by the sample matrix frequently occur in e.a.a.s. Pierce and Brown [12] and Henn [7] have investigated the degree of interference on the selenium sensitivities caused by different ions during electrothermal atomization. However, in these studies the concentration of interfering species was not more than 50 $\mu g\ ml^{-1}$, and it is reasonable to expect a different interference pattern at concentrations of 1000 $\mu g\ ml^{-1}$.

The effects of the elements that stabilize selenium compounds at high temperatures, on the selenium sensitivity are listed in Table 1. The enhancement caused by all the tested reagents, except thallium, is noteworthy. Iron is the stabilizing reagent which stimulates greatest selenium sensitivity, despite the overcompensation problems reported earlier [13]. Large negative signals, probably caused by an overcompensation effect from the deuterium lamp, were recorded for thallium.

During the present study, the strong effect of the graphite tube on the chemical interferences was realized. When one graphite tube was applied to study the enhancement or suppression of the selenium sensitivity, the results were dependent on the sequence of the tested reagents. It is evident that the presence of, e.g., carbide-forming elements such as molybdenum and zirconium will convert the graphite tube slightly to a carbide-coated tube

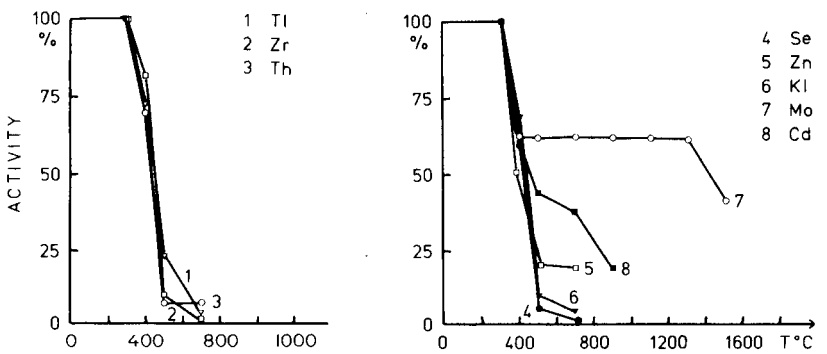

Fig. 3. Retention of activity as a function of the charring temperature for samples of in-vivo prepared whole rat blood labelled with ^{75}Se, with addition of stabilizing reagents (1000 $\mu g\ ml^{-1}$). Se = no reagent added.

TABLE 1

The influence of stabilizing reagents (1000 $\mu g\ ml^{-1}$) on the selenium (0.2 $\mu g\ ml^{-1}$) absorbance

Reagent	Enhancement factor[a]	Reagent	Enhancement factor	Reagent	Enhancement factor
Sb	1.4	Mn	3.2	Th	2.8
Cd	1.3	Ni	2.2	Tl	0.5
Cu	4.1	KIO_3	1.9	Zn	3.4
Fe	4.2	KI	2.0	Zr	2.6
Mo	1.2	Ag	3.0		

[a]Relative to the absorbance of a selenium standard without additive.

with considerably different atomization qualities. It is highly recommended as a general principle that the influence of sample matrices on analyte sensitivity should be studied with graphite tubes which have not previously been used for other elements.

REFERENCES

1 Selenium, Committee on medical and biological effects of environmental pollutants, National Academy of Sciences, Washington DC, 1976.
2 A. T. Diplock, CRC Crit. Rev. Toxicol., 4 (1976) 271.
3 H. E. Ganther, D. G. Hafeman, R. A. Lawrence, R. E. Serfass and W. G. Hockstin (Eds.), Selenium and glutathione peroxidase in health and disease — a review, Vol. II, Academic Press, New York, 1976, pp. 166—234.
4 G. Nordberg (Ed.), Factors influencing metabolism and toxicity of metals, Environ. Health Perspect., 25 (1978) 1.
5 J. Alexander and J. Aaeseth, Biochem. Pharmacol., 29 (1980) 2129.
6 R. D. Ediger, At. Absorpt. Newsl., 14 (1975) 127.
7 E. L. Henn, Anal. Chem., 47 (1975) 428.
8 F. J. Szydlowski, At. Absorpt. Newsl., 16 (1977) 60.
9 M. Ihnat, Anal. Chim. Acta, 82 (1976) 293.
10 K. Saeed, Y. Thomassen and F. J. Langmyhr, Anal. Chim. Acta, 110 (1979) 285.
11 B. Welz, T. Tomoff and E. Wiedeking, Atomic Absorption Application Study No. 656, July 1979, Bodenseewerk Perkin-Elmer, 7770 Überlingen, West Germany.
12 F. D. Pierce and H. R. Brown, Anal. Chem., 49 (1977) 1417.
13 D. C. Manning, At. Absorpt. Newsl., 17 (1978) 107.

Analytica Chimica Acta, 120 (1980) 383–387

Short Communication

MOLECULAR EMISSION CAVITY ANALYSIS
Part 18. Determination of Soluble Sulphate in Waters, Soil, Dusts and other Samples

T. S. AL-GHABSHA[b], S. L. BOGDANSKI[c] and ALAN TOWNSHEND*[a]

Department of Chemistry, University of Birmingham, P.O. Box 363, Birmingham, B15 2TT (Gt. Britain)

(Received 10th July 1980)

Summary. The direct determination of sulphate in waters or vinegar, and in aqueous extracts of soils, dusts and charcoal, is achieved after dilution of the sample with phosphoric acid. The results agree well with those obtained by nephelometry and gravimetry.

The methods available for the determination of traces of sulphate have been reviewed [1]. Most are indirect and time-consuming. They suffer from interferences, so that ion-exchange is very important for the removal of the interfering ions. Thus the procedures become complicated for use in routine analysis. Many of the spectrophotometric and titrimetric methods need expensive reagents. As there is a continuing need for the determination of sulphate in waters and soils, a new method is needed which is simple, sensitive, rapid and free from interferences.

A more promising approach is based on the production of characteristic blue emission bands from sulphur-containing compounds in a hydrogen-based flame, especially using molecular emission cavity analysis (m.e.c.a.). This technique gives sensitive responses from all sulphur compounds [2] including all the sulphur anions [3] and has the added advantage that various sulphur-containing species can simultaneously be determined in admixture based on temporal resolution of the S_2 emission peaks [4, 5]. The technique has already been applied to sulphate in high-purity boiler waters [6].

This communication describes the m.e.c.a. determination of water-soluble sulphate in samples of water, soils and dusts. The developed method is simple, quick and accurate and does not involve precipitation and its associated problems and errors.

Experimental

Apparatus. A modified Evans Electroselenium (EEL) 240 atomic absorption-emission spectrophotometer operating in the emission mode was used

Present addresses:
[a]Department of Chemistry, University of Hull, Hull, HU6 7RK, Gt. Britain.
[b]Department of Chemistry, Mosul University, Iraq.
[c]Doma Instruments Ltd., Unit 19, Forge Trading Estate, Halesowen, Gt. Britain.

[2], with maximal slit 12 (0.91 mm ≡ 3 nm) and gain 7, A Servoscribe 1S chart recorder with a response time of 0.5 s (f.s.d.) was also used. The instrument was used in a dark room as it was sensitive to extraneous light. The cavity used was the hexagonal aperture (maximal diagonal 5 mm) at the end of a 3-cm long stainless steel Allen screw. The cavity had a volume of 45 μl, and was pitched at 7° below the horizontal with the centre of the cavity 20 mm above the top of the burner.

An Evans Electroselenium (EEL) nephelometer was used for the nephelometric measurement of barium sulphate suspensions.

Reagents. Glass-distilled water and analytical-grade reagents were used. Sodium sulphate solution (500 ppm S, 250 ml) was prepared. More dilute solutions were prepared from this stock solution as needed.

Preparation of aqueous solutions from soil, laboratory dust, street dust and charcoal. To a 300-ml beaker, an accurately weighed, 1-g oven-dried soil sample was added, followed by 200 ml of water. The beaker was covered by a watch glass and the contents were digested on a boiling water bath for 15 min. The suspension was filtered through a Whatman No. 40 filter paper and washed with hot water. The filtrate was cooled and made to 250 ml in a volumetric flask with water.

To a 150-ml beaker, a weighed sample of dust (⩽2 g) or charcoal (0.5 g) was added, followed by 70 ml of water. The contents were digested and the suspension was filtered as above. The filtrate was made up to 250 ml with water.

Concentration of impurities in distilled water. To a 1.5-l beaker covered by a watch glass was added 1000 ml of water distilled from an all-glass apparatus. It was boiled until the volume was decreased to 40 ml.

Measurement of sulphate by m.e.c.a. To one of the above solutions or directly to a water sample (⩽22.5 ml) in a 25-ml volumetric flask was added 2.5 ml of 1 M phosphoric acid and the mixture was diluted to volume with water. A 5-μl aliquot of this solution was injected into a cold stainless steel cavity fixed in the optimum position in the hydrogen—nitrogen—air flame (4.1 l H_2 min^{-1}, 5.3 l N_2 min^{-1} and 2.8 l air min^{-1}). The flame was ignited immediately and the emission intensity at 384 nm was recorded as a function of time. When emission was complete the flame was extinguished and the cavity cooled to room temperature with a cold air blower for 2 min before the next sample was injected. The maximum S_2 emission response was measured and used for the determination of sulphate.

Calibration. To a series of 25-ml volumetric flasks were added exactly 0.25, 0.5, 1.0, 1.5 and 2.0 ml of aqueous sodium sulphate solution (50 ppm S), each followed by 2.5 ml of 1 M phosphoric acid, and the solutions were diluted to volume with water. The m.e.c.a. peak height from each was measured using the procedure described above, and plotted against concentration to give the usual sigmoidal calibration graph [3, 7]. The slope of the log—log plot was 1.7, in agreement with previous values [3].

Standard addition procedure for m.e.c.a. To a series of 25-ml volumetric

flasks, each containing exactly the same volume of the sample to be analysed (≤20 ml), were added exactly 0.0, 0.5, 1.0, 1.5, and 2.0 ml of an aqueous sodium sulphate solution (100 ppm S), followed by 2.5 ml of 1 M phosphoric acid, and the mixtures were made up to volume with water. The m.e.c.a. peak height was measured for each solution as described above.

Results and discussion

In all the samples examined, no S_2 emission was observed until the aqueous extract was acidified with phosphoric acid [3]. This also serves to remove metal ion depressive interferences. Under the experimental conditions used, the sulphate peak had a t_m value of 6.5 s.

The technique could be applied directly to most water samples after addition of phosphoric acid, as was previously shown for urine samples [8]. Results obtained are given in Table 1. To confirm the accuracy of the results, measurements were also made by nephelometry as barium sulphate [9] and by a standard addition m.e.c.a. procedure. The results are in good agreement. It should be borne in mind, however, that the sigmoid nature of the m.e.c.a. calibration graph for sulphur compounds makes the interpretation of standard addition procedure for m.e.c.a. somewhat complicated [8]. Nephelometry is less advantageous than m.e.c.a. because it requires additional reagents and has a detection limit at least an order of magnitude poorer. Flanagan and Downie [6] determined sulphate in high-purity waters (20—285 ppb) by multiple evaporation of sample aliquots in the m.e.c.a. cavity. In the present work, the same result was achieved by evaporation of a bulk sample. The m.e.c.a. volatilization system recently reported [10], however, should be superior to both approaches for such dilute samples.

Seven soil samples were analysed for sulphate directly after dilution of the aqueous extract with phosphoric acid and by using the standard addition procedure. The results are compared in Table 2 with those obtained using nephelometric [9] and gravimetric [11] methods. As is evident from the Table, the m.e.c.a. results are in good agreement with the nephelometric

TABLE 1

Determination of sulphate in water samples

Water	Sample vol. (ml)	Emission intensity (mV)[b]	SO_4^{2-} in sample (mg^{-1})		
			M.e.c.a.		Nephelometry
			Direct	Std. add.	
Canal	2	4.8	116	120	117
Rain	10	5.6	26	25	26
Tap	20	3.6	9.8	10	8.5
Distilled	1000[a]	0.6[c]	0.066	—	0.073

[a]Concentrated 25 times. [b]Mean of 3 measurements. [c]Mean of 6 measurements, r.s.d. 2.3%.

TABLE 2

Determination of water-soluble sulphate in Iraqi soils

Sample depth (cm)	Weight (g)	Vol. extract taken[a] (ml)	Emission intensity (mV)[b]	% SO_4^{2-} in soil			
				M.e.c.a.		Nephelometry	Gravimetry[c]
				Direct	Std. add.		
10—40	1.3	8	2.4	0.33	0.34	0.36	0.25
40—100	1.0	8	4.3	0.66	0.70	0.65	0.70
100—140	1.0	2	3.1	2.1	2.1	2.1	2.2
140—160	1.0	2	1.8	1.4	1.4	1.3	1.7
160—190	1.0	2	2.1	1.6	1.7	1.7	1.8
190—250	1.3	2	2.8	1.5	1.5	1.4	1.5
250—300	1.3	0.8	3.1	4.1	4.2	4.3	4.0

[a]From 250-ml samples. [b]Mean of three measurements. [c]Carried out by Mr. Abdulla, Department of Transportation and Environmental Planning, University of Birmingham, using the barium sulphate procedure [11].

TABLE 3

Determination of water-soluble sulphate in dusts[a] and charcoal

Sample wt. (g)	Vol. extract taken (ml)	Emission intensity (mV)[b]	% SO_4^{2-} in sample		Sample wt. (g)	Vol. extract taken (ml)	Emission intensity (mV)[b]	% SO_4^{2-} in sample	
			M.e.c.a.	Nephelometry [9]				M.e.c.a.	Nephelometry [9]
0.45	0.6	2.0	4.8	4.7	0.75	10	6.3	0.35	0.34
0.23	2.5	5.9	4.6	4.5	2.0	22	2.7	0.03	0.04
0.41	0.6	2.2	5.6	5.7	2.0	22	3.0	0.04	0.03
0.50	0.7	2.7	4.5	4.6	2.0	22	3.1	0.04	0.04
0.20	2	4.5	5.4	5.2	2.0	20	3.0	0.04	0.03
0.50	7	3.5	0.52	0.51	0.50[c]	10	2.1	0.28	0.26

[a]Laboratory dusts (>0.5% SO_4^{2-}) and street dusts (≤0.5% SO_4^{2-}), Birmingham. [b]Mean of three measurements. [c]Decolourising charcoal (Hopkin and Williams Ltd.).

and gravimetric results. The direct m.e.c.a. procedure has the advantage of being quicker than the standard addition procedure especially if many samples need to be analysed, and has obvious advantages over the other procedures (Table 3).

Extracts of dusts and charcoal were also readily analysed for sulphate by m.e.c.a. The results obtained again compared favourably with those obtained by nephelometry.

When a vinegar sample (distilled malt vinegar, Sarsons Ltd.) was subjected to m.e.c.a., no S_2 emission was observed unless phosphoric acid was added, indicating that the sulphur was inorganic. The characteristic S_2 emission peak of the vinegar in 0.1 M phosphoric acid was enhanced by the addition of a few drops of sodium sulphate solution indicating that the sulphur was

from sulphate. Furthermore, the t_m value (6.5 s) was the same as that of sodium sulphate under these conditions. The vinegar was found to contain 3.0 mg l^{-1} of sulphate which compared well with that obtained by nephelometry (3.2 mg l^{-1}). The relative standard deviation for six m.e.c.a. measurements was 4%, as compared to 3% for six nephelometric measurements.

Conclusion. Sulphate in aqueous extracts of soils, dusts and charcoal, as well as that present in water samples and vinegar, is readily, accurately and precisely determined by m.e.c.a. The only additional reagent required is dilute phosphoric acid. The procedure is direct, simple and sensitive; ng amounts of sulphate are determined in the μl-samples taken for analysis.

T. S. Al-Ghabsha thanks the University of Mosul, Republic of Iraq, for financial support.

REFERENCES

1 R. Belcher, S. L. Bogdanski, I. H. B. Rix and A. Townshend, Mikrochim. Acta, 11 (1977) 81.
2 R. Belcher, S. L. Bogdanski and A. Townshend, Anal. Chim. Acta, 67 (1973) 1.
3 R. Belcher, S. L. Bogdanski, D. J. Knowles and A. Townshend, Anal. Chim. Acta, 77 (1975) 53.
4 R. Belcher, S. L. Bogdanski, D. J. Knowles and A. Townshend, Anal. Chim. Acta, 79 (1975) 292.
5 M. Q. Al-Abachi, R. Belcher, S. L. Bogdanski and A. Townshend, Anal. Chim. Acta, 86 (1976) 139.
6 J. D. Flanagan and R. A. Downie, Anal. Chem., 48 (1976) 2047.
7 J. H. Glover, Analyst, 100 (1975) 449.
8 R. Belcher, S. L. Bogdanski, I. H. B. Rix and A. Townshend, Mikrochim. Acta, 11 (1977) 91.
9 A. I. Vogel, Quantitative Inorganic Analysis, 3rd edn., Longman, London, 1961.
10 S. L. Bogdanski, I. M. A. Shakir, W. I. Stephen and A. Townshend, Analyst, 104 (1979) 886.
11 British Standard, Method for Testing Soils for Civil Engineering Purposes, British Standards Institution, 1377, 1967.

Analytica Chimica Acta, 120 (1980) 389—393

Short Communication

MESURE PAR PHOTOMETRIE DE FLAMME DU SOUFRE PARTICULAIRE ATMOSPHERIQUE

JEAN GODIN*, JEAN-PIERRE GALLET et CLAUDE BOUDÈNE

INSERMU U 122, Laboratoire de Toxicologie, UER des Sciences Pharmaceutiques, 92290, Chatenay-Malabry (France)

(Reçu le 17 juin 1980)

Summary. Flame photometric measurement of atmospheric particulate sulfur. Particles collected on glass fibre filters washed with nitric acid are introduced into headspace vials containing a reducing mixture of hydroiodic acid, sodium hypophosphite and acetic anhydride. The sulfur concentration in the particles is determined by measurement of generated hydrogen sulfide using a flame photometric detector.

Résumé. Les poussières recueillies sur des filtres de fivre de verre lavés avec de l'acide nitrique sont introduites dans des fioles contenant un mélange réducteur composé d'acide iodhydrique, d'hypophosphite de sodium et d'anhydride acétique. La teneur en soufre des particules est alors déterminée en dosant l'hydrogène sulfuré formé à l'aide d'un détecteur à photométrie de flamme.

Les soufre particulaire représente une part importante des composés soufrés de l'atmosphère et pourrait être à l'origine d'une partie des affections respiratoires humaines. Aussi, depuis quelques années, l'étude des particules contenant du soufre s'est beaucoup développée et de nombreuses techniques de mesure ont été mises au point pour la détermination du soufre particulaire total ou soluble. Ces méthodes ont d'ailleurs fait l'objet de revues récentes [1, 2]. Parmi ces différentes méthodes, seules quelques techniques permettent la détermination du soufre total. Parmi celles-ci, il faut citer la fluorescence-x [3], des techniques d'émission [4, 5] et radiométrique [6].

La photométrie de flamme est largement utilisée pour la mesure des composés soufrés gazeux. Des chercheurs ont tenté de déterminer directement le soufre particulaire sans traitement préalable de l'aérosol. Toutefois l'interférence des composés soufrés gazeux doit être éliminée et il semble que tous les problèmes analytiques ne soient pas résolus; en particulier, il a été montré que la taille des particules et la composition chimique des aérosols avaient une influence sur l'intensité de la réponse du détecteur à photometrie de flamme [7—10].

Afin d'éviter le passage dans le détecteur d'un composé solide hétérogène, nous avons cherché à transformer le soufre particulaire en un composé volatil plus facilement mesurable par cette méthode. Déjà, dans plusieurs techniques

connues de dosage des sulfates ou du soufre particulaire (radiométrie [6] émission de flamme [11], colorimétrie [12, 13]) les composés soufrés ont été transformés en hydrogène sulfuré. Ainsi, les conditions opératoires de l'une des techniques colorimétriques [12] en les adaptant aux conditions particulières d'utilisation du détecteur à photométrie de flamme, nous ont permis de mettre au point notre méthode de dosage.

La technique obtenue a comparativement aux autres méthodes connues les avantages suivants: grande sensibilité, simplicité d'échantillonnage et d'étalonnage, rapidité d'analyse ainsi qu'une utilisation d'un matériel commercialement disponible et relativement peu couteux. Il faut également ajouter qu'il devrait être possible de différencier le soufre soluble du soufre total.

Les prélèvements de poussières sont obtenus par la filtration d'un volume connu d'air à travers un filtre de fibre de verre de petit diamètre. Le filtre est ensuite introduit dans une fiole de réaction contenant le mélange réducteur. Un volume déterminé de la phase gazeuse est alors introduit dans le photomètre de flamme permettant ainsi de déterminer la teneur en soufre des poussières.

Partie expérimentale

Réactifs. Le mélange réducteur est préparé en ajoutant lentement et en refroidissant 20 ml d'anhydride acétique (Merck) à 10 ml d'acide iodhydrique à 57% (Prolabo), puis 5 g d'hypophosphite de sodium anhydre (Prolabo). La solution ainsi obtenue est purifiée en la portant à l'ébullition sous courant d'azote pendant 2 h. L'élimination de l'H_2S peut être suivie en plaçant à la sortie du réfrigérant un tube contenant du Chromosorb W sur lequel a été déposé un mélange d'acétate de plomb (10%) et de glycérine (10%).

Les standards nécessaires aux étalonnages sont obtenus par la dissolution de 444 mg de sulfate de sodium fraîchement desséché, dans un litre d'eau bidistillée (100 μg S ml^{-1}). Cette solution est ensuite diluée 10 et 100 fois (10 et 1 μg S ml^{-1}).

Prélèvements. L'air contenant les particules est aspiré au travers d'un filtre de fibre de verre (Whatman GFC, 25 mm) lavé à l'acide nitrique dilué. Le volume d'air prélevé est déterminé à l'aide d'un rotamètre (pour les volumes inférieurs à 40 l h^{-1}) ou d'un compteur à gaz lorsque le débit est suffisant.

Réduction. Les filtres empoussiérés secs sont mis en contact avec 1 ml de mélange réducteur dans des fioles type pénicilline (OSI) obturées par des disques d'élastomère recouverts de téflon. Avant leur première utilisation, les fioles sont nettoyées avec de l'acide nitrique chaud puis rincées avec de l'eau distillée.

Les fioles contenant le réactif et les filtres sont ensuite portées à 100°C pendant 15 min dans une étuve.

Analyse. Après 30 min de refroidissement à température ambiante, des échantillons de phase gazeuse sont prélevés à l'aide de seringues à gaz de 10, 100 et 250 μl préalablement rincées avec le mélange réducteur. Ils sont ensuite transférés dans un analyseur Tracor HM 270 par l'intermédiaire d'un injecteur à septum placé à l'entrée de la colonne destinée à la mesure du soufre total.

Avant chaque série de dosage, un mélange d'H_2S et d'air est injecté dans l'appareil afin de saturer la colonne et la seringue utilisées pour le dosage. Les injections sont poursuivies jusqu'à hauteur de pic constante.

Les courbes d'étalonnages sont établies en introduisant dans des fioles des quantités connues de sulfate de sodium en solution. Après élimination de l'eau à l'étuve, le contenu des flacons est traité comme les prélèvements.

Résultats et discussion

Les difficultés de dosage de l'hydrogène sulfuré à faibles concentrations sont bien connues [14, 15], ce composé se fixant notamment sur les métaux et le verre. On sait cependant qu'en opérant en milieu acide, on parvient à limiter beaucoup ces inconvénients.

Parmi les facteurs pouvant affecter la formation de l'H_2S à partir des sulfates, nous avons étudié en premier lieu l'influence de la température. On a ainsi constaté qu'à 80°C, la réaction est complète en 45 min environ alors qu'à 100°C elle est terminée en moins de 15 min. On a également constaté que l'H_2S formé, conservé dans les fioles de réaction, est stable pendant plusieurs heures, voire plusieurs jours à température ambiante. Toutefois, on observe, si l'on conserve plusieurs flacons contenant des quantités identiques d'H_2S, que la dispersion des résultats s'élève au cours du temps. Il en est de même si l'on prolonge le temps de réaction au delà de la durée de la réduction des sulfates en H_2S.

En accord avec les études déjà réalisées sur cette réaction, no essais ont montré que l'eau avait une influence très importante sur la quantité d'H_2S libérée dans la phase gazeuse du flacon de réaction. Ainsi, à titre d'exemple, on a observé que si l'on ajoute 20 μl d'eau à 1 ml de réactif contenant 1 μg de S sous forme de sulfate, il n'y a pas de différence de réponse par rapport à un flacon témoin contenant les mêmes réactifs à l'exception de l'eau. Par contre, si l'on ajoute 100 μl d'eau la réponse ne correspond plus qu'à 75% de la quantité initialement présente. Si l'on ajoute 200 μl d'eau la résponse n'est plus que de 20% et si l'on en ajoute 300 μl, elle n'est plus que de 10%.

Comme le montre la Fig. 1 et les écarts type calculés pour chaque teneur de sulfate, la précision des déterminations augmente beaucoup avec la concentration. Notons que cette courbe a été obtenue à partir de mesures réalisées à des jours différents et que la sensibilité de l'appareil varie parfois d'un jour à l'autre. Si les mesures sont réalisées le même jour, leur reproductibilité est meilleure. Ainsi, l'écart type de mesures effectuées sur 28 fioles de 10 ml contenant 1 μg de S (SO_4^{2-}) est de 0.063 μg. Il est de 0.2848 μg pour une quantité de soufre de 5 μg (30 fioles de 50 ml).

Des courbes d'étalonnage similaires à la courbe 1 sont obtenues si l'on modifie le volume des fioles de réaction ou de phase gazeuse injecté. Il a été ainsi constaté que, quelquesoit les conditions opératoires, les courbes sont linéaires dans l'intervalle des log des réponses compris entre 3,6 et 5 approximativement; soit des pics de 200 mm à l'atténuation $\times$ 20 (10^{-7}) et 100 mm à $\times$ 1000 (10^{-7}). Tout en restant à l'intérieur de ces limites et si on

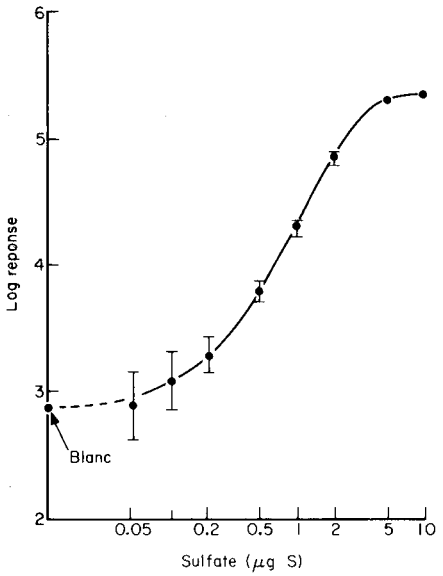

Fig. 1. Courbe d'étalonnage du détecteur à photométrie de flamme. (Les barres en T verticales représentent les écarts-type de 5 déterminations.)

a une idée des teneurs en soufre particulaire de l'atmosphère, des quantités très différentes de soufre peuvent être mesurées en jouant notamment sur le temps de prélèvement, le débit des pompes et le volume des fioles de réaction. Enfin, lors du dosage, il est également possible de modifier le volume de la phase gazeuse injecté dans l'appareil.

De nombreux essais ont été réalisés en utilisant des quantités très différentes de sulfate ainsi qu'en modifiant le volume des fioles de réaction et de la phase gazeuse injecté. En utilisant la partie linéaire des courbes ainsi obtenues, nous avons pu mesurer les teneurs suivantes: fioles de 50 ml, 10 μl injecté, 4,8—28 μg; 20 μl, 2,2—12,5 μg; 50 μl, 0,75—5 μg; fioles de 20 ml, 50 μl injecté, 0,4—2,2 μg; fioles de 10 ml, 50 μl injecté, 0,25—1,5 μg. Ces essais montrent qu'à partir d'une fiole de 50 ml, il est possible de mesurer des quantités de soufre comprises entre 0,75 et 28 μg, mais des volumes de phase gazeuse plus faibles ou surtout plus élevés peuvent être injectés élargissant ainsi les possibilités de la méthode.

Comme le montre la Fig. 1, le réactif contient encore après purification environ 50 ng S ml^{-1}. Par contre, la teneur en sulfate des filtres est peu importante car on ne constate pas de différence entre un échantillon contenant un filtre vierge et le réactif et un échantillon contenant le réactif seulement.

BIBLIOGRAPHIE

1 R. L. Tanner et L. Newman, J. Air Pollut. Control Assoc., 26 (1976) 737.
2 L. Newman, Atmos. Environ., 12 (1978) 113.
3 T. G. Dzubay et R. K. Stevens, Environ. Sci. Technol., 9 (1975) 663.
4 J. D. Husar, R. B. Husar et P. K. Stubits, Anal. Chem., 47 (1975) 2062.
5 S. A. Schubert, J. W. Clayton et Q. Fernando, Anal. Chem., 51 (1979) 1297.
6 J. Forrest et L. Newman, Anal. Chem., 49 (1977) 1579.
7 J. J. Huntzicker, R. S. Hoffman et Chaur Sun Ling, Atmos. Environ., 12 (1978) 83.
8 W. G. Cobourn, R. B. Husar et J. D. Husar, Atmos. Environ., 12 (1978) 89.
9 D. B. Kittelson, R. McKenzie, M. Vermeersch, F. Dorman, D. Pui, B. Liu et K. Whitby, Atmos. Environ., 12 (1978) 105.
10 R. L. Tanner, T. D'Ottavio, R. Garber et L. Newman, Atmos. Environ., 14 (1980) 121.
11 S. L. Bogdanski, I. M. A. Shakir, W. I. Stephen et A. Townshend, Analyst, 104 (1979) 886.
12 L. Gustafsson, Talanta, 4 (1960) 236.
13 J. B. Davis et F. Lindstrom, Anal. Chem., 44 (1972) 524.
14 R. K. Stevens, J. D. Mulik, A. E. O'Keefe et K. J. Krost, Anal. Chem., 43 (1971) 827.
15 D. S. Walker, Analyst, 103 (1978) 397.

Analytica Chimica Acta, 120 (1980) 395—398

Short Communication

SPECTROPHOTOMETRIC DETERMINATION OF COBALT(II) IN THE PRESENCE OF LARGE AMOUNTS OF IRON WITH SALICYLALDEHYDE THIOSEMICARBAZONE

N. SUBBA RAMI REDDY and D. VENKATA REDDY*

Department of Chemistry, SVU Autonomous Post-Graduate Centre, Anantapur 515 003 (India)

(Received 7th May 1980)

Summary. Cobalt(II) reacts instantaneously with the reagent at pH 5.0. The yellow complex has a molar absorptivity of 1.1×10^4 l mol^{-1} cm^{-1}. The method is applied to the determination of cobalt in steels after removal of iron with phosphate.

Salicylaldehyde thiosemicarbazone has been used as an analytical reagent for nickel [1], manganese(II) [2] and for the simultaneous determination of iron and molybdenum [3]. The present communication reports the results obtained in the spectrophotometric determination of cobalt(II) in the presence of large excess of iron. The method is applied to the determination of cobalt in steels.

The spectrophotometric methods most frequently employed for the determination of cobalt utilize nitrosonaphthol reagents. In these methods, copper, nickel, iron and manganese interfere seriously and the excess of reagent shows considerable absorption at the wavelength of maximum absorbance of the complex. The present method offers advantages since manganese does not interfere, copper, nickel and iron can easily be prevented from reacting and the reagent has negligible absorbance at the wavelength of maximum absorbance of the complex. Some of the methods developed for cobalt(II) with hydrazones require a considerable time for maximum colour development whereas in the present case it is almost instantaneous. The reagent is colourless, stable, readily available, selective and sensitive. The colour of its cobalt(II) chelate is stable for more than a week. Extraction is not necessary.

Experimental

Reagents. Salicylaldehyde thiosemicarbazone (SAT) was prepared from ethanolic solutions of salicylaldehyde and thiosemicarbazide by the usual procedure [4]; a 0.2% (w/v) solution was prepared in methanol. Cobalt(II) solutions were prepared from cobalt(II) nitrate hexahydrate and standardized titrimetrically [5]. All other chemicals used were analytical-reagent grade.

Determination of cobalt. To a solution containing 6—120 μg of cobalt

in a 25-ml volumetric flask, add 12 ml of pH 5.0 sodium acetate–acetic acid buffer, 2.5 ml of methanol and 2.5 ml of the 0.2% reagent solution. Shake the contents and dilute to the mark with water. Measure the absorbance in 1-cm cells at 400 nm against a reagent blank.

Determination of cobalt in steel. Dissolve 0.1 g of steel in 10 ml of aqua regia under reflux. Dilute to exactly 100 ml in a volumetric flask with distilled water, and determine cobalt using the procedure described above, adding phosphate (50 mg, as Na_2HPO_4), thiosulphate (60 mg, as $Na_2S_2O_3$) and citrate (19 mg, as the triammonium salt), to prevent iron, copper and nickel, respectively, from reacting. Filter off iron(III) phosphate and measure the absorbance at 400 nm as above.

Results and discussion

Cobalt(II) gives a soluble yellow 1:2 cobalt: SAT complex at pH 3—10, with maximum absorbance at 400 nm at pH 4.5—6.0, as shown in Figs. 1 and 2. Addition of a 5-fold excess of the reagent is necessary for full colour development. The methanol content must not be less than 20% to avoid precipitation of the reagent. Colour formation is instantaneous and the order of addition of the reagents or the buffer has no effect provided that methanol is added before the reagent. Beer's law is obeyed for 0.3—6 ppm of cobalt in the final solution. The molar absorptivity and Sandell sensitivity are $1.1 \pm 0.02 \times 10^4$ l mol^{-1} cm^{-1} and 5.36 ng cm^{-2}, respectively. The relative standard deviation for 10 determinations of 60 μg of cobalt was 1.68%.

plexes with the reagent. However, up to a 100-fold excess of iron may be removed by precipitation with phosphate, and copper and nickel can be masked with thiosulphate and citrate, respectively. The results obtained in the presence of various amounts of iron are given in Table 1. The interference of various other ions on the determination of 60 μg of cobalt(II) was investi-

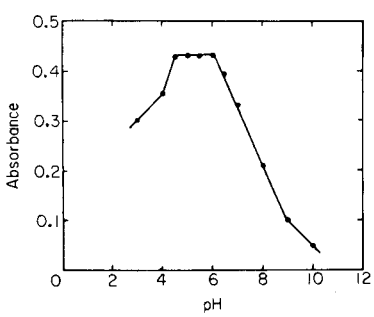

Fig. 1. Absorbance of the cobalt(II) complex as a function of pH.

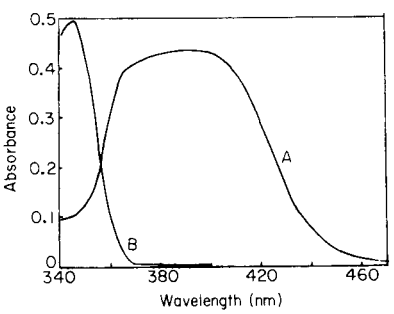

Fig. 2. Absorption spectra: (A) cobalt(II) complex against the reagent blank; (B) reagent blank against aqueous methanol. 4×10^{-5} M Co(II), 2×10^{-6} M SAT.

TABLE 1

Determination of cobalt in the presence of large amounts of iron

Fe:Co[a]	20	40	50	60	80	100
Cobalt found (μg ml^{-1})	0.93	0.90	0.92	0.92	0.91	0.93

[a]0.94 μg Co ml^{-1}.

TABLE 2

Tolerance limits for various ions in the determination of 60 μg of cobalt at pH 5.0

Tolerance[a] limit (μg)	Other ion	Tolerance[a] limit (μg)	other ion
5×10^4	K^+, Na^+, CH_3COO^-, NO_3^-, SO_4^{2-}, ClO_4^-, Br^-, PO_4^{3-}	2×10^3	Th^{4+}, Cd^{2+}
		1×10^3	Zr^{4+}, Te^{4+}
1×10^4	Sr^{2+}, Ca^{2+}, Ba^{2+}, Cl^-, CO_3^{2-}, tartrate	5×10^2	Al^{3+}, Zn^{2+}
5×10^3	Mn^{2+}, Pb^{2+}, SeO_3^{2-}, AsO_4^{3-}, MoO_4^{2-}, $P_2O_7^{4-}$, $B_4O_7^{2-}$	2×10^2	Cr^{3+}, WO_4^{2-}
		1×10^2	Ti^{4+}, Ce^{4+}, Bi^{3+}

[a]Maximum amount giving a deviation $\leqslant \pm$ 2% in absorbance.

TABLE 3

Determination of cobalt in presence of components of steels

Steel	Cobalt conc. (μg ml^{-1})		Steel	Cobalt conc. (μg ml^{-1})	
	Added	Found[a]		Added	Found[a]
Cr—Ni Steel I[b]	0.47	0.47	AISI—316 E[d]	0.47	0.46
	0.71	0.70		0.71	0.72
	0.94	0.93		0.94	0.93
	1.18	1.18		1.18	1.18
AISI—316 T[c]	0.47	0.48			
	0.71	0.71			
	0.94	0.93			
	1.18	1.17			

[a]Mean of 4 determinations. [b]68.15% Fe, 11.84% Ni, 17.77% Cr, 2.15% Mo and 0.09% C. [c]65.1% Fe, 20.7% Cr, 11.4% Ni and 2.8% Mo. [d]64.4% Fe, 19.8% Cr, 13.4% Ni and 2.4% Mo.

gated. The maximum tolerable amounts presented in Table 2 show that the reagent is highly selective.

The effect of the components of steels on the determination of cobalt, using the steel analysis procedure, was investigated by determining cobalt

added in known amounts to solutions of various steel samples. The results, presented in Table 3, are highly satisfactory. Results for an alloy steel are given in Table 4.

Thiosemicarbazones act as chelating agents for metal ions by bonding through the sulphur atom and the hydrazino-nitrogen atom. In the present case, Job [6] curves show that cobalt and SAT combine in a 1:2 molar ratio. A charged complex must be formed, as it is not extractable by solvents such as benzene, chloroform and carbon tetrachloride.

The authors thank Prof. S. Brahmaji Rao, Department of Chemistry, for his interest. N.S.R. is grateful to the University Grants Commission, New Delhi, for the award of a Junior Research Fellowship.

TABLE 4

Determination of cobalt in an alloy steel[a]

Cobalt conc. ($\mu g\ ml^{-1}$)	Taken	0.95	1.42	1.89
	Found	0.94	1.41	1.91

[a]51.15% Fe, 11.22% Ni, 5.09% Cu, 23.72% Co, 6.98% Al, 0.79% Ti, 0.235% Mn, 0.57% Si.

REFERENCES

1 F. Vlacil and K. Vlasta, Sb. Vys. Sk. Chem. Technol., Praze Anal. Chem., 1 (1967) 5.
2 F. Vlacil and D. Valentova, Sb. Vys. Sk. Chem. Technol., Praze Anal. Chem., 3 (1968) 43.
3 D. P. Bendito and F. P. Perez, Microchim. Acta (Wien), 1 (1976) 613.
4 P. P. T. Sah and T. C. Daniab, Rec. Trav. Chim. Pays-Bas, 69 (1950) 1545.
5 A. I. Vogel, A Text Book of Quantitative Inorganic Analysis, Longman, London, 1975, p. 389.
6 P. Job, Ann. Chim., 9 (1928) 113.

Analytica Chimica Acta, 120 (1980) 399—403

Short Communication

AN IMPROVED FLOW INJECTION DETERMINATION OF NITRITE IN WATERS BY USING INTERMITTENT FLOWS

E. A. G. ZAGATTO, A. O. JACINTHO, J. MORTATTI and H. BERGAMIN F°*

Centro de Energia Nuclear na Agricultura, 13.400 Piracicaba, S. Paulo (Brasil)

(Received 19th May 1980)

Summary. An injector—commutator with a 0:1:2 section is employed to achieve intermittent flows without intermittent pumping. The resulting flow injection system is very simple, manually operated, and requires only one peristaltic pump. When applied to the spectrophotometric determination of nitrite in waters, the device leads to an enhancement of the sensitivity and sampling rate without affecting other analytical characteristics. The merging zones approach is employed to decrease consumption of reagents.

In flow injection analysis [1], the recorded peak shape defines the maximum allowable sampling rate for a given degree of carry-over. As the recorded peak shape, and consequently the half-wash time [1], depend on the flow rate, the sampling rate can be increased by employing higher flow rates. However, when long sample residence times are required because of the particular reaction used, there is a limit to the possible increase in pumping rates so that the sampling frequency is also limited. In such cases, a fast flow can be used during the wash time, thus altering the recorded peak shape and increasing the analytical speed [2]. However, a fast flow with intermittent pumping requires the alternate use of two peristaltic pumps [2]. It is shown here that this approach can be simplified by using an injector commutator [3]; only one peristaltic pump without stoppage is required.

The spectrophotometric flow injection method for nitrite in natural waters [3, 4] requires large injected volumes to keep sample dispersion as small as possible, and low flow rates to achieve adequate time for development of the reaction. Under these conditions sensitivity is enhanced, but the sampling frequency is too low with the common flow injection analyzer. An improved system with intermittent flow is described below. The merging zones approach [5—8] is also used to reduce consumption of reagents.

Experimental

Peristaltic pump, tubing, connectors, coils, flow cell, spectrophotometer and recorder were the same as used in previous work [7]. The injector—commutator was similar to those already reported [3, 7, 8]; it consisted of two 2:3:2 commutation sections [8] for injection of samples and reagents,

and one 0:1:2 commutation section to achieve intermittent flow. The device operates in two positions: in the sampling position specified in Fig. 1, the sample (S) is aspirated to fill the sample loop (L_s), the excess being discarded (W); the reagent (R) is pumped to fill the reagent loop (L_R), the excess, slightly diluted by the reagent carrier stream [5], being recovered in vessel V. In this position all streams are employed to wash the analytical path. After switching the injector–commutator (I), the selected sample and reagent volumes are introduced into their carrier streams (C_S and C_R) and flow F is directed back to its origin. The injected sample forms a well defined sample zone which is slowly transported towards the detector, in order to achieve a reasonable mean sample residence time in the analytical path. At point X, the reagent zone meets the sample zone in a synchronized manner and in the following coil (R_C), mixing and chemical reactions occur. After measurement in the flow-through detector (D), the processed sample zone is discarded (W). Switching then brings the injector–commutator back to the position specified in Fig. 1 and another cycle starts. The flows in lines c and d are, therefore, intermittent.

Waste-water samples from Piracicaba, S. Paulo, Brasil, collected and preserved as recommended [9], were analyzed. Before analysis, the samples were filtered. The chemical reactions involved in the determination, and the preparation and storage of reagents, standards and samples have already been reported [3].

The flow injection system indicated in Fig. 1 was employed with the following parameters: sample aspiration rate (S), 3.9 ml min^{-1}; C_S, 2.0 ml H_2O min^{-1}; reagent R [3], 2.0 ml min^{-1}; 20% (v/v) phosphoric acid solution [3] (C_R), 0.4 ml min^{-1}; F, 7.8 ml H_2O min^{-1}; injected sample volume, 500 μl; injected reagent volume, 150 μl; synchronization line a, 25 cm; synchronization line b, 5 cm; connection line XY, 5 cm; reaction coil R_C, 130 cm; wavelength setting, 535 nm.

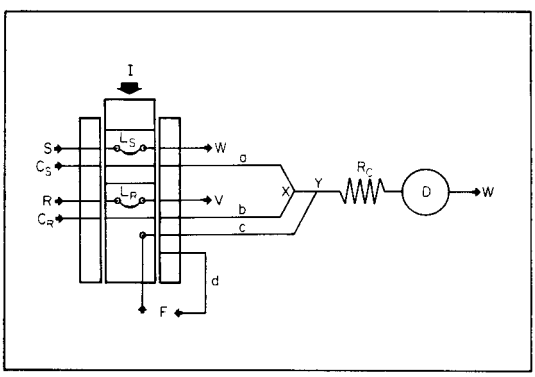

Fig. 1. Flow diagram of the proposed system with the injector–commutator in the sampling position. For details, see text.

The sample dispersion factor was determined as described elsewhere [8], employing a 0.25 ppm $N-NO_2^-$ standard. The same standard was used in a stopped-flow procedure [3] to measure the degree of reaction completion. The precision of the proposed method was estimated by calculating the relative standard deviation of 10 measurements related to a water sample with a nitrite content of 60 ppb $N-NO_2^-$. Recovery was calculated after addition of 3.0 ml of a 1.00 ppm $N-NO_2^-$ standard to 47.0 ml of each assayed sample.

Results and discussion

In the proposed sytem, the time between sample injection and achievement of the top of the peak is about 35 s (Fig. 2), which allows the reaction to proceed to about 88% completion. Without the intermittent flow F, the wash time is about 65 s, assuming a carry-over of 1%. In this situation the analytical frequency (3600/65) is about 55 samples per hour. The intermittent flow reduces the wash time to about 18 s, or 27% of its original value, and the sampling rate becomes dependent on the moment of addition and duration of the intermittent flow. With the proposed method, 70 samples can be run per hour on a routine basis (Fig. 3).

The addition of the intermittent wash solution allows higher sample volumes to be injected without reducing the sampling rate significantly. This leads to an enhancement of the dispersion factor, which causes an increase in sensitivity. With a sample dispersion factor of 0.83, associated with the 88% complete reaction, the proposed method is the most sensitive

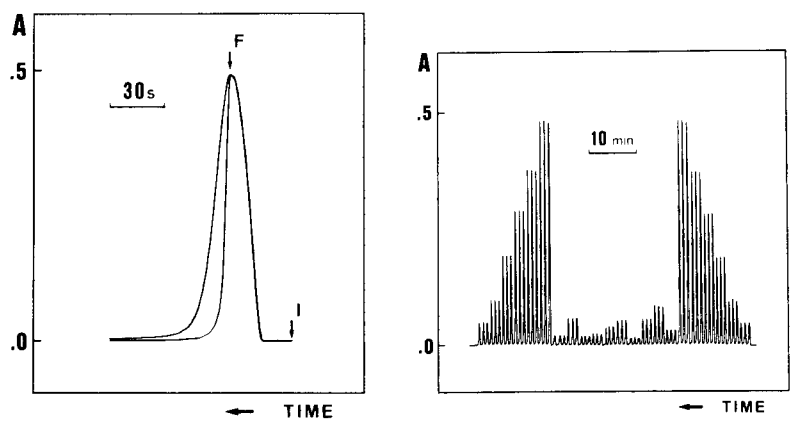

Fig. 2. Effect of intermittent flow on the recorded peak shape. The broader peak was obtained after injection of a 0.25 ppm $N-NO_2^-$ standard and the reagent at moment I without any further switching of flows. The narrower peak was obtained when the injector—commutator was switched to give the intermittent flow at instant F.

Fig. 3. Routine run for nitrite in waste waters. From left to right: six standards (25, 50, 100, 150, 200 and 250 ppb $N-NO_2^-$), ten samples and the standards in the reverse order again. All measurements were made in triplicate.

TABLE 1

Recovery data for the determination of nitrite in waste waters from the Piracicaba region

Sample	Nitrite content (ppb N as NO_2^-)			Recovery (%)
	Before standard addition	After standard addition		
		Expected	Determined	
1	16	75	74	97
2	43	100	98	98
3	29	87	86	99
4	9	68	66	97
5	28	86	84	98
6	20	78	79	101
7	14	73	70	96
8	10	69	71	103
9	30	88	86	98
10	11	70	68	97

of the flow injection procedures so far published for nitrite [2–4]. The proposed method is characterized by a precision of 0.5% relative for a 60 ppb $N—NO_2^-$ water sample. Figure 3 indicates that the linearity of the calibration graph is good and that the system is quite stable. Table 1 shows the recoveries calculated after standard addition.

Conclusions

In flow injection systems, intermittent flow without intermittent pumping is easily achieved with a single 0:1:2 section of an injector–commutator. The resulting system is very simple and is particularly recommended when the chemical processes involved are slow. Since the intermittent wash solution may be added at any moment after the top of the peak has been recorded, the system can be operated manually. When some automatic device is available for injection, a stopped-flow procedure is better than the intermittent flow addition.

Partial support of this project by CNPq (Conselho Nacional de Desenvolvimento Científico e Tecnológico) is greatly appreciated. The authors thank F. J. Krug and B. F. Reis for constructive criticism and Diva Athiê and N. M. Costa Pereira for assistance in preparing the manuscript.

REFERENCES

1 J. Růžička and E. H. Hansen, Anal. Chim. Acta, 78 (1975) 17.
2 J. Růžička and E. H. Hansen, Anal. Chim. Acta, 114 (1980) 19.
3 M. F. Giné, H. Bergamin F°, E. A. G. Zagatto and B. F. Reis, Anal. Chim. Acta, 114 (1980) 191.
4 L. Anderson, Anal. Chim. Acta, 110 (1979) 123.

5 H. Bergamin F°, E. A. G. Zagatto, F. J. Krug and B. F. Reis, Anal. Chim. Acta, 101 (1978) 17.
6 E. A. G. Zagatto, F. J. Krug, H. Bergamin F°, S. S. Jørgensen and B. F. Reis, Anal. Chim. Acta, 104 (1979) 279.
7 B. F. Reis, H. Bergamin F°, E. A. G. Zagatto and F. J. Krug, Anal. Chim. Acta, 107 (1979) 309.
8 B. F. Reis, E. A. G. Zagatto, A. O. Jacintho, F. J. Krug and H. Bergamin F°, Anal. Chim. Acta, 119 (1980) 305.
9 American Public Health Association, American Water Works Association and Water Pollution Control Federation, Standard Methods for the Examination of Water and Wastewater, 14th edn., American Public Health Association, New York, 1975, p. 434.

Analytica Chimica Acta, 120 (1980) 405—409

Short Communication

2-(8-QUINOLYLAZO)-4,5-DIPHENYLIMIDAZOLE — A SENSITIVE EXTRACTION SPECTROPHOTOMETRIC REAGENT FOR MERCURY

SHIGERU MIWA, MASAMICHI FURUKAWA and SHOZO SHIBATA*

Government Industrial Research Institute, Nagoya, Kita-ku, Nagoya (Japan)

(Received 1st April 1980)

Summary. Mercury(II) reacts with 2-(8-quinolylazo)-4,5-diphenylimidazole in aqueous solution; the complex can be extracted with chloroform or 1,2-dichloroethane at pH 4.5—9.5 to give a stable reddish-purple solution. The system conforms to Beer's law; the optimal range in chloroform is 0.05—2 ppm mercury (1-cm cells). Of 25 metal ions investigated, only copper and vanadium interfere seriously. The proposed method is exceptionally sensitive; the molar absorptivity in the chloroform extract is 7.3×10^4 l mol^{-1} cm^{-1} at 580 nm; the Sandell sensitivity is 0.0027 μg Hg cm^{-2}.

A study of some azo compounds containing various heterocycles has been made [1—5] with the object of preparing sensitive organic reagents which have molar absorptivities of the order of 10^5 for different metals; such organic reagents remain quite rare, except perhaps for some ion-association complexes. In this connection, the synthesis of new azo dyes containing 4,5-diphenylimidazole has been reported previously [6].

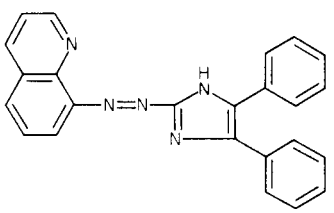

QADI

One of these compounds, 2-(8-quinolylazo)-4,5-diphenylimidazole(QADI) was observed to give with mercury(II) a reddish purple complex which is soluble in various organic solvents. This communication describes the use of QADI as an extraction—photometric reagent for mercury; its sensitivity is compared with other typical reagents for the spectrophotometric determination of mercury in Table 1.

Even in the determination of merely trace amounts of toxic metals such as mercury, beryllium, vanadium, chromium and cadmium, it is desirable that these metals should be recovered in the sample or standard solutions in stable forms. In this regard, spectrophotometric methods are preferable to many other analytical techniques, and this aspect lends greater importance to the development of extremely sensitive new chromogenic reagents.

TABLE 1

Sensitivity and molar absorptivity (ϵ) of some typical reagents for mercury

Reagents	λ_{max} (nm)	Sandell sensitivity (μg Cd cm^{-2})	ϵ ($\times 10^4$ l mol^{-1} cm^{-1})
1 Thiothenoyltrifluoroacetone (benzene)	365	0.0067	3.0
2 Dimethylaminobenzalrhodanine	475	0.0048	4.2
3 *o*, *o'*-Dimethyldithizone (chloroform)	486	0.0039	5.2
4 Dithizone (chloroform)	490	0.0028	7.2
5 QADI (chloroform)	580	0.0027	7.3

Experimental

Reagents. An ethanolic solution of QADI (0.05% w/v) was prepared. The reagent was prepared by coupling 4,5-diphenylimidazole with the diazotate of 2-amino-8-quinoline in alcoholic solution [6]. The buffer solutions were mixtures of 0.1 M sodium acetate and 0.1 M acetic acid, or 0.1 M ammonium chloride and 0.1 M ammonia.

For the standard mercury(II) solution (1.00×10^{-2} M), 2.000 g of mercury was dissolved in 10 ml of concentrated nitric acid and the solution was diluted to 1 l in a volumetric flask with redistilled water.

Organic solvents were purified by standard methods. All solutions were prepared with twice-distilled water from analytical-grade chemicals.

Apparatus. Absorbance curves were measured with a Model 323 Hitachi recording spectrophotometer with 1-cm cells. A Hitachi-Horiba F-7DE type pH meter was used.

Recommended procedure for the determination of mercury. Transfer an aliquot of the slightly acidic sample solution containing 0.5—2.0 μg of mercury to a 50-ml separatory funnel, and dilute to about 20 ml with water. Add 0.5 ml of the ethanolic 0.05% QADI solution and 7 ml of acetate buffer solution (pH 5.0). Mix well, add 10 ml of organic solvent, and shake vigorously for 1—2 min. Transfer the organic phase to a glass-stoppered conical flask, and dehydrate with anhydrous sodium sulfate. Measure the absorbance at 580 nm in 1-cm cells against a reagent blank carried through the same procedure.

If interfering metals are present, transfer an aliquot of the slightly acidic sample solution containing 2—20 μg of mercury to a 50—100-ml beaker, dilute to about 20 ml with water and add 5 ml of 20% (w/v) sodium citrate solution before adjusting to pH 5 with diluted sodium hydroxide or hydrochloric acid. Then continue as described in the above procedure.

Results and discussion

Optimal conditions and sensitivity. The effects of several solvents on the absorbance of the extracted complex were studied. Chloroform was chosen as the solvent for extraction because of the relatively high molar absorptivity obtained. The addition of QADI to a solution containing mercury causes the immediate formation of a reddish-purple complex which is sparingly soluble in water. The absorption spectra of the reagent and of its mercury complex in chloroform are shown in Fig. 1. The absorbance of the reagent is very small at the wavelength of maximum absorbance of its mercury complex.

To establish the optimal pH, standard amounts of mercury and QADI solution were buffered at various pH values. The final pH of each aqueous solution was measured after extraction and the absorbance was measured at 580 nm. A plot of absorbance against pH showed that the absorbance was constant over the range pH 4.5—9.5 but decreased sharply below pH 4 and above pH 10. Subsequent determinations were carried out at pH 5.

The absorbances of a series of solutions containing known amounts of mercury and various amounts of 0.05% dye solution were measured at pH 5. It was found that 0.5 ml of the dye solution sufficed to complex 10 μg of mercury; with higher concentrations of reagent the absorbance was essentially constant.

The time for the absorbance of the complex to reach a stable value was only a few minutes at room temperature, and the absorbance was then stable for at least 3 h. The calibration graph was linear over the range 0.05—2 ppm mercury. The molar absorptivity of the complex and the Sandell sensitivity are shown in Table 1.

Effect of diverse ions. Numerous cations and anions were examined by applying the method to a fixed amount of mercury (20 μg) in the presence of increasing quantities of the ion being studied. Various common anions, except cyanide and EDTA, did not interfere. There were no significant errors from the presence of up to 2 mg of aluminum, lead, chromium, uranium, tungsten, gold, dysprosium, osmium, platinum, thorium, manganese,

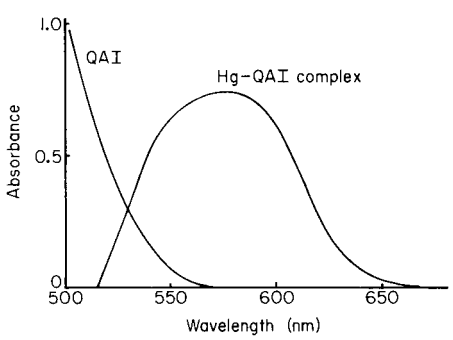

Fig. 1. Absorption spectra of QADI and the Hg—QADI complex (2 ppm Hg) in chloroform.

TABLE 2

Effect of diverse ions (20.0 μg of mercury taken)

Ion	Amount added (mg)	Hg found (μg)	Error (μg)	Ion	Amount added (mg)	Hg found (μg)	Error (μg)
Ag^{+}	0.02	21.0	+1.0	Mo(VI)	0.02	20.7	+0.7
	0.2	22.1	+2.1		0.2	19.1	−0.9
	2.0	23.5	+3.5		2.0	11.4	−8.6
Al^{3+}	0.02	21.5	+1.5	Ni^{2+}	0.2	—[a]	
	0.2	20.1	+0.1	Os^{4+}	0.02	20.5	+0.5
	2.0	20.4	+0.4		0.2	20.7	+0.7
Au^{3+}	0.02	19.7	−0.3		2.0	21.0	+1.0
	0.2	19.5	−0.5	Pb^{2+}	0.02	20.1	+0.1
	2.0	19.0	−1.0		0.2	20.3	+0.3
Bi^{3+}	0.02	21.0	+1.0		2.0	20.2	+0.2
	0.2	20.1	+0.1	Pd^{2+}	0.02	23.9	+3.9
	2.0	15.4	−4.6		0.2	23.1	+3.1
Cd^{2+}	0.02	10.4	−9.6		2.0	24.3	+4.3
Co^{2+}	0.02	—[a]		Pt^{4+}	0.02	20.4	+0.4
Cr^{3+}	0.02	21.0	+1.0		0.2	19.6	−0.4
	0.2	21.1	+1.1		2.0	21.0	+1.0
Cu^{2+}	0.02	—[a]		Th^{4+}	2.0	20.2	+0.2
Dy^{3+}	0.2	21.0	+1.0	Ti^{4+}	0.02	19.9	−0.1
	2.0	20.2	+0.2	U(VI)	0.2	21.1	+1.1
Fe^{3+}	0.02	21.4	+1.4		2.0	21.5	+1.5
	0.2	22.4	+2.4	V^{5+}	0.02	9.6	−10.4
La^{3+}	0.2	20.3	+0.3	W(VI)	2.0	20.4	+0.4
Mg^{2+}	0.2	21.2	+1.2	Zr^{4+}	0.2	20.5	+0.5
	2.0	21.7	+1.7				
Mn^{2+}	0.02	20.9	+0.9				
	0.2	20.7	+0.7				
	2.0	20.3	+0.3				

[a] Off-scale.

TABLE 3

Elimination of interfering ions by citrate (20.0 μg of mercury taken)

Ion	Amount added (mg)	Hg found (μg)	Error (μg)	Ion	Amount added (mg)	Hg found (μg)	Erro (μg)
Ag^{+}	2.0	19.5	−0.5	Mo(VI)	2.0	20.1	+0.1
Bi^{3+}	2.0	20.3	+0.3	Ni^{2+}	0.02	20.2	+0.2
Cd^{2+}	0.02	21.5	+1.5	Pd^{2+}	0.2	20.6	+0.6
Ce^{3+}	2.0	20.6	+0.6	Ti^{4+}	0.2	20.9	+0.9
Co^{2+}	0.02	20.3	+0.3		2.0	18.5	−1.5
Fe^{3+}	2.0	20.6	+0.6	V^{5+}	0.02	5.0	−15.0
La^{3+}	2.0	20.3	+0.3	Zn^{2+}	0.02	20.6	+0.6

magnesium or calcium. The interferences of cadmium, cobalt(II), copper, nickel or zinc could be masked by tartrate or citrate (see Tables 2 and 3). Thus only copper and vanadium(V) interfered seriously.

Nature of complex. The empirical formula of the complex was studied by the continuous variations and mole ratio methods. A typical plot showed unequivocally that a 1:2 HgL_2 complex is formed.

The QADI method is one of the most sensitive and selective spectrophotometric procedures available for the determination of mercury, and should be applicable to many kinds of sample.

REFERENCES

1 S. Shibata, M. Furukawa and Y. Ishiguro, Anal. Chim. Acta, 55 (1971) 231.
2 S. Shibata, M. Furukawa and Y. Ishiguro, Mikrochim. Acta, (1972) 721.
3 S. Shibata, M. Furukawa and K. Toei, Anal. Chim. Acta, 66 (1973) 397.
4 S. Shibata, M. Furukawa and K. Goto, Anal. Chim. Acta, 71 (1974) 85.
5 S. Shibata, M. Furukawa and E. Kamata, Anal. Chim. Acta, 73 (1974) 107.
6 S. Shibata, M. Furukawa and R. Nakashima, Anal. Chim. Acta, 81 (1976) 131.

Analytica Chimica Acta, 120 (1980) 411—414

Short Communication

FLUORESCENT PRODUCTS OF THE REACTION OF MONO-SUBSTITUTED GUANIDINO COMPOUNDS WITH BENZOIN—DIMETHYLFORMAMIDE

MASAAKI KAI, MASATOSHI YAMAGUCHI and YOSUKE OHKURA*

Faculty of Pharmaceutical Sciences, Kyushu University 62, Maidashi, Higashi-ku, Fukuoka 812 (Japan)

(Received 28th May 1980)

Summary. The fluorescent products formed from methylguanidine or phenylguanidine and benzoin in the presence of dimethylformamide are shown to be the corresponding 2-substituted amino-4, 5-diphenylimidazoles. They fluoresce most intensely at pH 9—10 and the fluorescence is stabilized by β-mercaptoethanol.

A sensitive and selective fluorimetric method for the determination of monosubstituted guanidino compounds, based on their reactions with benzoin-dimethylformamide (DMF) reagent in potassium hydroxide solution, has been reported [1]. This communication describes the isolation and characterization of the fluorescent compounds produced from methylguanidine and phenylguanidine.

Experimental

Reagents and apparatus. All chemicals were of reagent grade unless otherwise specified. Double-distilled water was used throughout. Phenylguanidine sulfate was prepared as described by Smith [2]. Uncorrected fluorescence spectra were measured with a Hitachi MPF-4 spectrofluorimeter in 10 × 10 mm quartz cells. Spectral bandwidths of 10 nm were used in both the excitation and emission monochromators. U.v. spectra were measured in ethanolic solution with a Shimadzu UV 200S spectrophotometer, and 10-mm quartz cells. I.r. spectra (KBr pellets) were measured with a Nihonbunko DS 701G spectrometer, mass spectra with a JEOL JMS-01-SG spectrometer, and ^{1}H-n.m.r. spectra with a JEOL JNM-PS-110 spectrometer at 100 MHz, using ca. 15% (w/v) solutions in dimethylsulfoxide-d_6 containing tetramethylsilane as internal standard. The melting points are uncorrected.

Isolation of the product from methylguanidine and its spectral properties. Methylguanidine hydrochloride (4 g) and potassium hydroxide (5 g) were dissolved in 50 ml of methanol. The precipitated potassium chloride was filtered off, and the filtrate mixed with 80 ml of 7.5% (w/v) benzoin solution in methanol, 5 g of DMF and 50 ml of aqueous 8% (w/v) potassium hydroxide solution. The mixture was refluxed for 3 h. After cooling in ice-

water, the white precipitate was removed and the filtrate concentrated to ca. 50 ml in vacuo. The yellow precipitate thus formed was filtered, washed with water, dried in vacuo and dissolved in ca. 10 ml of methanol. The undissolved material was removed and the filtrate evaporated to dryness. The residue was dissolved in a small amount of ethyl acetate, poured on to a glass column packed with ca. 30 g of silica gel (Mallinckrodt, 100 mesh) and eluted with ethyl acetate. The largest fraction which showed a blue fluorescence, was evaporated to dryness. The residue, dissolved in ethyl acetate, was re-chromatographed on a column packed with 35 g of basic alumina (Woelm, activity I) and eluted with the same solvent. The main fraction was evaporated to dryness and crystallized from a mixture of n-hexane and methanol (9:1, v/v) to colorless needles (I; m.p. 170—174°C, decomposition; yield, 54 mg). Calculated for $C_{16}H_{15}N_3$: 77.1% C, 6.1% H, 16.8% N; found 76.8% C, 6.1% H, 16.7% N. U.v. spectrum (in ethanol) λ_{max}nm (log ϵ): 213 (4.28), 227 (4.18), 282 (3.87), 320 (3.97). I.r. spectrum ν_{max}cm^{-1}: 3440 (NH, imidazole), 2760 and 2540 (CH_3), 1548 (aromatic C=C and/or C=N), 770 and 700 (CH, monosubstituted benzene). Mass spectrum m/e: 249 (M^+). ^{1}H-n.m.r. spectrum δ (ppm): 2.82 (3H, doublet, J=5.0 Hz, methyl protons), 5.62 (1H, quartet, J=5.0 Hz, imino proton, exchangeable with deuterium), 7.04—7.48 (1OH, complicated multiplet, aromatic protons), 10.8 (1H, broad singlet, imidazole imino proton, exchangeable with deuterium).

Isolation of the product from phenylguanidine and its spectral properties. Phenylguanidine sulfate (4 g), 3 g of benzoin, and 5 g of DMF were dissolved in 120 ml of methanol. The solution was mixed with 50 ml of aqueous 16% (w/v) potassium hydroxide solution, refluxed for 1 h and cooled in ice-water. The precipitate was removed and the filtrate was concentrated to ca. 50 ml in vacuo. The resulting yellow precipitate was washed with water, dried in vacuo and dissolved in 50 ml of benzene. The undissolved substance was removed and the filtrate was evaporated to dryness in vacuo. The residue, was chromatographed on silica gel and alumina as before, using benzene—ethyl acetate, 9:1 (v/v) as solvent and eluant. The main fraction was evaporated to dryness in vacuo, and crystallized from aqueous 50% (v/v) methanol to colorless needles (II; m.p. 140—142°C, decomposition; yield 110 mg). Calculated for $C_{21}H_{17}N_3 \cdot 1/2H_2O$: 78.7% C, 5.7% H, 13.1% N; found 78.7% C, 5.7% H, 13.0% N. U.v. spectrum (in ethanol) λ_{max} nm (log ϵ): 210 (4.15), 225 (4.03), 278 (4.15). I.r. spectrum ν_{max} cm^{-1}: 3360 (NH, imidazole) 3030 (CH, benzene), 1602 and 1570 (aromatic C=C and/or C=N), 765 and 695 (CH, monosubstituted benzene). Mass spectrum m/e: 311 (M^+, base peak). ^{1}H-n.m.r. spectrum δ(ppm): 7.14—7.60 (15H, complex multiplet, aromatic protons), 8.54 (1H, singlet, imino proton, exchangeable with deuterium), 11.3 (1H, broad singlet, imidazole imino proton, exchangeable with deuterium).

Results and discussion

Fluorescent compounds I and II were shown to be 2-methylamino- and 2-phenylamino-4,5-diphenylimidazole respectively on the basis of the elemental and spectral analyses.

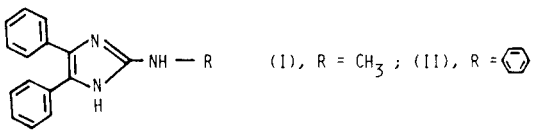

Their excitation and emission spectra were identical with those obtained during the determinations of methylguanidine and phenylguanidine, respectively [1]. In each case, the most intense fluorescence occurred at pH 9—10 (Fig. 1); however this fluorescence was unstable (the rates of loss of fluorescence at pH 9.0 were: I, 22% h^{-1}; II, 52% h^{-1}). The fluorescence could be stabilized by adding β-mercaptoethanol as in the analytical procedure [1].

The reaction of the guanidino compounds with benzoin thus proceeds in a strongly alkaline medium but a change to weakly alkaline conditions must then be made to obtain maximum fluorescence. That change might occur in the analytical procedure [1] because formic acid is formed by decomposition of DMF in the hot, strongly alkaline solution. The condensation products retain the substituted group of the original guanidino compounds and are different from the products formed in the determination of these compounds with 9,10-phenanthroquinone. In the latter reaction, the fluorescent product, 2-amino-1H-phenanthro-[9,10—d]imidazole, has lost the substituted group from the guanidines [3—5].

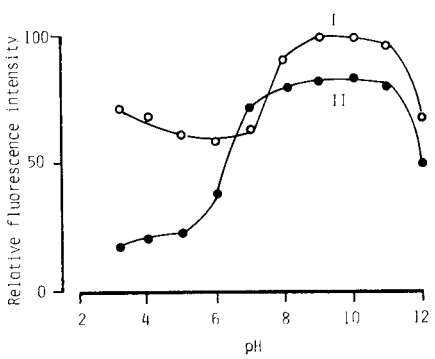

Fig. 1. Effect of pH on the intensity of fluorescence of compounds I and II. Samples (2 nmol) were dissolved in 3 ml of 0.04 M Britton—Robinson buffers of various pHs, and fluorescence was measured at 440 and 430 nm with excitation at 318 and 305 nm, respectively.

The skilful assistance of M. Soejima and Y. Yamashita is acknowledged.

REFERENCES

1 Y. Ohkura and M. Kai, Anal. Chim. Acta, 106 (1979) 89.
2 G. B. L. Smith, J. Am. Chem. Soc., 51 (1929) 476.
3 H. A. Itano and S. Yamada, Anal. Biochem., 48 (1972) 483.
4 H. A. Itano, K. Hirota, I. Kawasaki and S. Yamada, Anal. Biochem., 76 (1976) 134.
5 K. Yasuda and W. S. Chilton, Anal. Biochem., 74 (1976) 609.

Analytica Chimica Acta, 120 (1980) 415—417

Short Communication

DETERMINATION OF 2-AMINO-5-NITROBENZOPHENONE CONTAMINATION IN NITRAZEPAM BY LOW-TEMPERATURE SPECTROPHOSPHORIMETRY

I. HORNYÁK* and L. SZÉKELYHIDI

Research Institute for Technical Physics of the Hungarian Academy of Science, Ujpest I.P.O. Box 76, 1325 Budapest (Hungary)

(Received 14th January 1980)

Summary. 2-Amino-5-nitrobenzophenone (ANB) shows very intense phosphorescence in ethanol glasses at liquid nitrogen temperature. In the same conditions nitrazepam is not phosphorescent. This difference is applied to the determination of ANB contamination in nitrazepam; ANB in the range 5×10^{-9}—2×10^{-4} g ml^{-1} can be determined.

The 1,4-benzodiazepines and compounds with a similar structure are regarded as clinically the most effective and frequently-used minor tranquillizers, exhibiting important muscle relaxant, sedative and anticonvulsant activities. Nitrazepam (1,2-dihydro-7-nitro-5-phenyl-2H-1,4-benzodiazepin-2-one) also possesses these pharmacological activities and also has a moderate hypnotic effect. The compound is synthesized by the method of Sternbach et al. [1], in which the bromoacetamido derivative of 2-amino-5-nitrobenzophenone is treated with ammonia and the resulting compound is cyclized. The product is contaminated by the basic materials of the synthesis, and especially by 2-amino-5-nitrobenzophenone (ANB). Thus the determination of this ANB is very important in quality control. For the determination of ANB, ultraviolet spectrophotometry has normally been applied [2—7]; there are no literature data on its luminescent properties. In this communication, the luminescence characteristics of ANB are outlined and a simple and reliable method for its determination in nitrazepam is described.

Experimental

Apparatus. Phosphorescence was measured with a Hitachi Perkin-Elmer MPF-2A spectrofluorimeter with a phosphoroscope attachment. A 150-W xenon arc lamp was used as the excitation light source. The detector was a Hamamatsu R136 photomultiplier, which has a photocathode spectral response in the range 160—800 nm. Samples were held in the special Hitachi fused quartz micro sample tubes.

Materials. The ANB was obtained from nitrazepam by acid hydrolysis [6]. The compound was recrystallized twice from ethanol and characterized by melting point (162—163°C; literature 161.5°C), u.v. and i.r. spectroscopy, and elementary analysis (calculated for $C_{13}H_{10}O_3N_2$, 64.5% C, 4.1% H,

11.6% N, 19.8% O; found 64.2% C, 4.4% H, 11.6% N, 20.0% O. Different sources of nitrazepam, both commercial and recrystallized products, were examined. All measurements were made in twice-distilled ethanol solution. ANB standard solutions with concentrations in the range 10^{-2}—10^{-8} M were prepared by appropriate dilution.

Procedure. A solution containing ANB was placed in the sample tube, and the tube was then aligned in the quartz Dewar flask containing liquid nitrogen. Phosphorescence, excitation and emission spectra were recorded. From the spectra, the wavelengths of maximum excitation (398 nm) and emission (521 nm) were obtained. The relative intensities of the standard solutions (10^{-8}—10^{-2} M) of ANB were determined at these wavelengths, and corrected for the background phosphorescence. Bandwidths of 5 nm and 10 nm in the emission and excitation monochromators, respectively, were used in quantitative studies.

Results and discussion

ANB shows very intense phosphorescence at 77 K. There are excitation maxima at 271, 332 and 398 nm, and emission maxima at 493, 521 and 550 nm (Fig. 1). For the determination of ANB, intensity values were plotted against concentration. The calibration graph was linear in the concentration range 2×10^{-8}—10^{-3} M. At higher concentrations, the graph deviated from linearity, probably because of concentration quenching. Over the linear part of the graph, the relative standard deviation was 2—3%. In the same conditions, nitrazepam is not phosphorescent so that ANB contamination of nitrazepam can be determined. Quantitative tests were done by adding known amounts of ANB to a pure sample of nitrazepam. For solutions containing 1 mg of nitrazepam per ml and 1.0, 10.0 and 100.0 μg of ANB

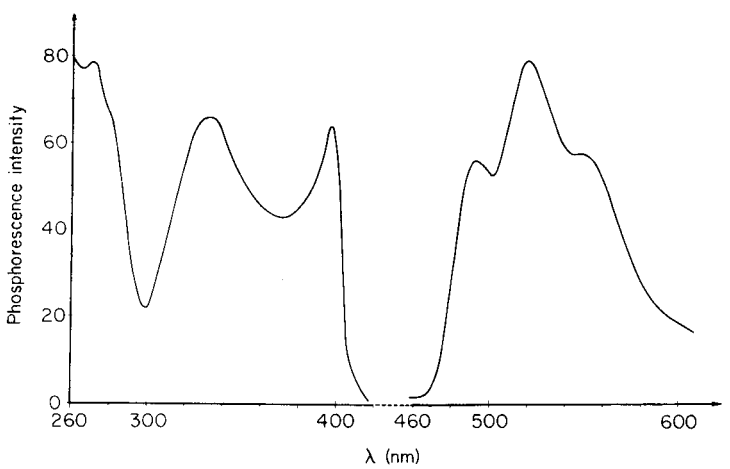

Fig. 1. Phosphorescence excitation and emission spectra of 2-amino-5-nitrobenzophenone (10^{-5} M) in ethanol at 77 K.

per ml, the average results of 6 determinations at each level (with relative standard deviations) were 0.97 (4.2%), 9.85 (3.6%) and 98.00 (4.0%) $\mu g\,ml^{-1}$, respectively.

The sensitivity of the phosphorimetric method and its wide concentration range make it advantageous for the determination of traces of ANB. T.l.c. separation [8] is not required.

REFERENCES

1 L. H. Sternbach, R. I. Fryer, O. Keller, W. Metlesics, G. Sach and N. Steiger, J. Med. Chem., 6 (1963) 261.
2 W. Mayer, S. Erbe and R. Voigt, Pharmazie, 27 (1972) 32.
3 K. H. Beyer and W. Sadée, Dtsch. Apoth. Ztg., 109 (1969) 312; Arzneim. Forsch., 19 (1969) 1929.
4 P. Lafargue, J. Meunier and Y. Lemouthey, J. Chromatogr., 62 (1971) 423.
5 J. Rieder, Arzneim. Forsch., 15 (1965) 1134.
6 O. Pribbilla, Arzneim. Forsch., 15 (1965) 1148.
7 H. Sawada and K. Shinohara, J. Hyg. Chem., 16 (1970) 318.
8 British Pharmacopoeia, 1973.

Analytica Chimica Acta, 120 (1980) 419—422

Short Communication

A SIMPLE AND RAPID METHOD OF COLLECTING RADIONUCLIDES FROM RAIN WATER

TOSHIMASA KIMURA*

Japan Chemical Analysis Center, 295-3, Sanno, Chiba-shi, Chiba Prefecture, 281 (Japan)

TASTUJI HAMADA

Institute of Physical and Chemical Research, 2-1, Hirosawa, Wako-shi, Saitama Prefecture, 351 (Japan)

(Received 12th February 1980)

Summary. A column of mixed powdered ion-exchange resins (Powdex) is proposed for the collection of radionuclides from rain water. The radionuclides are collected efficiently for γ-ray spectrometry. The procedure takes about 1.5 h for 10 l of rain water.

Radionuclides in rain water are determined routinely in various research institutes as well as national and local organizations concerned with environmental monitoring programs. Since most of the radionuclides in rain water are γ-emitters, the main method for their determination is γ-ray spectrometry with a lithium-drifted germanium detector. Several liters of water are taken and the volume is reduced to an appropriate small size to increase the counting efficiency. Evaporation is the commonest technique for the volume reduction [1], but ion-exchange resins are also employed [2].

The use of a powdered ion-exchange resin, called Powdex proved very satisfactory in preliminary tests [3]. In the present communication, the results of further study, especially on the capacity of resin beds and on the measurement of radio-strontium are described. ^{89}Sr and ^{90}Sr, which are important radionuclides in the environment, are β-emitters and consequently, have to be separated from the remaining radionuclides and counted. Radioplutonium should also be monitored, but rain water is not analyzed routinely for these isotopes, which were therefore omitted from the present study.

Experimental

Material and apparatus. All reagents used were of analytical grade. The powdered ion-exchange resin Powdex (PAO and PCH), precoating material Ecocoate, strong basic ion-exchange resin Amberlite 938, and strong acidic ion-exchange resin Amberlite 124 were obtained from Japan Organo Co. Ltd. The filter paper used was 0.45 μm in pore diameter (FM-045; Fuji Photo Film Co.)

Several rain water samples were collected in Saitama Prefecture, Japan.

Radioactivities were determined by γ-ray spectrometry with a 60-cm³ Ge(Li) detector, having 15% relative efficiency and 1.7-keV resolution (FWHM), combined with a 4000-channel pulse-height analyzer. Strontium-89 and -90 were determined by a low background β-ray spectrometer (Picobeta; Fuji Electric Co.).

Method 1. An ion-exchange column (4.5 cm in diameter) was prepared with a mixture of 19 ml of a water slurry of Amberlite 938 (OH^- form; dry weight, 2.7 g) and an equal volume of a water slurry of Amberlite 124 (H^+ form; dry weight, 9.5 g). A rain-water sample containing a trace amount of chloroform, to prevent the growth of microorganisms, was filtered through Whatman 41 and FM-045 papers. The filtrate was introduced into the column at a flow rate of 2 ml min^{-1}. The effluent was evaporated to about 15 ml. Gamma-emitters in the filters, the mixture of ion-exchange resins, and the effluent were determined separately.

Method 2. A mixture of 5 g of powdered anion-exchange resin (PAO; water content 60%; OH^- form) and an equal amount of powdered cation-exchange resin (PCH; water content 60%; H^+ form) was prepared according to the manufacturer's specification. The mixture was transferred to a demountable filter funnel (4.5 cm diameter, 100 cm long) to make a resin bed about 1 cm long. The resin bed was covered with 0.5 g of precoating material. The rain-water sample containing chloroform and 20 mg of strontium ion as a carrier was introduced into the funnel at a flow rate of about 200 ml min^{-1} with suction. The specific resistance of the effluent from the funnel was continuously monitored. The resin and the precoating material were then transferred into a counting vial and mixed thoroughly with a small glass rod. The effluent was evaporated to about 15 ml and transferred to another counting vial. Gamma-emitters in these samples were determined. The resin mixture in the vial was then transferred to a beaker containing 50 ml of 3 M nitric acid, boiled for 2 min, and separated by a filter; this procedure was repeated twice. Strontium ion in the combined filtrate was purified by the fuming nitric acid method [4] and radio-strontium was measured with the β-ray spectrometer. Total strontium was determined by atomic absorption spectrometry.

Results and discussion

Table 1 shows the activities of γ-emitting radionuclides in each fraction obtained by the two methods described above, for separate 3-l rain-water samples collected just after the 23rd nuclear explosion test in the People's Republic of China. The results of method 1 (Table 1) show that ^{95}Zr, ^{141}Ce, and ^{144}Ce were mainly collected on the filter papers, while ^{7}Be and ^{137}Cs were collected in the resin. Most of the radionuclides were recovered in these two fractions, but a little ^{95}Zr, ^{140}Ba, and ^{144}Ce were also detected in the effluent. These results indicate that radionuclides in rain water exist in various physical and chemical forms, (particulate, colloidal, ionic, etc.).

Powdered ion-exchange resin, which is considered to function both as

TABLE 1

Radioactivity (in pCi) found in various fractions of 3-l rain water samples containing short-lived fission products

Nuclide	Method 1			Method 2		
	Filter paper[a]	Resin[b]	Effluent	Resin[c]	Effluent	Recovery[d]
^{7}Be	12.9 ± 4.0	100 ± 5	2.9 ± 1.8	98.3 ± 6.3	0.4 ± 1.0	1.00 ± 0.09
^{95}Zr	16.9 ± 1.4	1.16 ± 0.58	0.85 ± 0.34	12.3 ± 1.5	0.04 ± 0.17	1.00 ± 0.17
^{95}Nb	12.5 ± 0.8	0.35 ± 0.45	0.25 ± 0.19	8.7 ± 0.9	0.09 ± 0.13	0.99 ± 0.14
^{103}Ru	75.9 ± 1.7	20.3 ± 0.8	0.31 ± 0.17	47.7 ± 1.6	0.15 ± 0.12	1.00 ± 0.05
^{106}Ru	24.1 ± 4.0	15.7 ± 2.9	0.57 ± 1.05	12.2 ± 3.4	0 ± 0.69	1.00 ± 0.44
^{125}Sb	10.7 ± 2.1	4.7 ± 1.2	0.48 ± 0.56	6.6 ± 1.7	0 ± 0.46	1.00 ± 0.37
^{131}I	36.8 ± 1.2	33.6 ± 1.1	0 ± 0.61	49.9 ± 2.2	0 ± 0.20	1.00 ± 0.05
^{137}Cs	1.1 ± 0.4	2.17 ± 0.44	0.20 ± 0.18	4.2 ± 0.7	0 ± 0.16	1.00 ± 0.24
^{140}Ba	41.7 ± 2.4	16.6 ± 1.6	1.5 ± 0.7	32.6 ± 3.5	0 ± 0.51	1.00 ± 0.15
^{140}La	54 ± 3	14.5 ± 1.0	0 ± 0.3	24.2 ± 1.7	0 ± 0.3	1.00 ± 0.10
^{141}Ce	51.2 ± 1.2	0.57 ± 0.28	0 ± 0.12	26.1 ± 0.9	0 ± 0.10	1.00 ± 0.05
^{144}Ce	33.1 ± 2.5	4.6 ± 1.3	1.7 ± 0.5	22.2 ± 1.8	0 ± 0.30	1.00 ± 0.11

[a]Whatman 41 and Fuji Photo Film FM-045. [b]19 ml each of Amberlite 938 (OH^-) and Amberlite 124 (H^+) slurries. [c]5 g each of PAO and PCH. [d]The ratio of the radioactivity in the resin bed to that in the resin bed plus effluent.

an ion exchanger and a filter medium, was then applied to the collection of waters. The results of method 2 (Table 1) show that the radionuclides mentioned were essentially absent from the effluent. The ratios of the radioactivity in the resin bed to that found in similar evaporated rain samples are also shown in Table 1.

The maximum volume of rain water that can be treated with the powdered resin bed, was examined by measurement of the specific resistance of the effluent. The results are shown in Fig. 1. When the precoating material was not used, the specific resistance decreased suddenly at 8 l and cracks were then found in the resin bed. The use of precoating material was effective in preventing this cracking, and the bed could then treat 16 l of rain water. The specific resistance of the effluent gradually decreased over 16 l, though bed cracking was not found; this decrease is probably due to the exchange

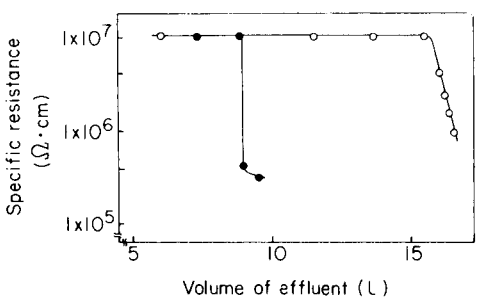

Fig. 1. Change of specific resistance of effluent with volume of effluent: (•) 5 g each of PAO and PCH; (○) 5 g of PAO, 5 g of PCH, and 0.5 g of precoating material.

TABLE 2

Radioactivity (in pCi/10 l of rain water) found in powdered resin bed and effluent

Nuclide	Run 1		Run 2		Run 3		Run 4	
	Resin	Effluent	Resin	Effluent	Resin	Effluent	Resin	Effluent
^{7}Be	218 ± 5	0.10 ± 0.19	139 ± 4	0.44 ± 0.27	142 ± 3	0.10 ± 0.21	256 ± 5	0.15 ± 0.1
^{95}Zr	1.1 ± 0.3	0 ± 0.05	1.2 ± 0.2	0.04 ± 0.06	1.4 ± 0.2	0.06 ± 0.05	2.2 ± 0.3	0.01 ± 0.(
^{95}Nb	2.4 ± 0.3	0 ± 0.05	2.4 ± 0.2	0 ± 0.06	2.0 ± 0.2	0.02 ± 0.06	4.4 ± 0.3	0 ± 0.05
^{106}Ru	4.3 ± 1.2	0 ± 0.18	3.8 ± 1.0	0 ± 0.23	4.5 ± 1.0	0 ± 0.21	8.4 ± 1.3	0.10 ± 0.1
^{125}Sb	2.8 ± 0.7	0 ± 0.24	2.9 ± 0.7	0.09 ± 0.26	4.8 ± 0.7	0 ± 0.24	5.8 ± 0.8	0 ± 0.23
^{137}Cs	5.6 ± 0.4	0.03 ± 0.05	6.4 ± 0.3	0 ± 0.06	6.6 ± 0.3	0 ± 0.05	12.4 ± 0.4	0 ± 0.05
^{144}Ce	31.4 ± 1.1	0.08 ± 0.10	29.4 ± 0.9	0 ± 0.13	23.2 ± 0.9	0 ± 0.11	51.4 ± 1.1	0 ± 0.09
^{89}Sr			0 ± 0.4				0.4 ± 0.5	
^{90}Sr			5.6 ± 0.3				8.9 ± 0.4	
Recovery of Sr (%)	90		78		75		84	

capacities of the anion- and cation-exchange resins. The capacities of the dry resins are 3.5 meq g^{-1} for anions and 4 meq g^{-1} for cations, based on the manufacturer's specification.

Table 2 shows the results of another experiment in which method 2 was applied to four 10-l samples of rain water collected during April to September, 1978. The recovery of all radionuclides except radio-strontium in these samples was always quite good. Strontium ions adsorbed in the resin could be eluted by a batch method with 3 M nitric acid; the overall recovery measured by atomic absorption spectrometry ranged between 75% and 90%, and was 82% on average. The relative error in the determination is estimated to be below 2%.

When a counting vial of 48-mm diameter was used, the mixture of the resin and the precoating material gave a height of about 9 mm. The entire column procedure of the method 2 took about 1.5 h, when 10 l of rain water was treated, and it is faster and easier than the common evaporation method.

Grateful acknowledgement is made to Mr. K. Kinebuchi of Japan Organo Co. Ltd. and Mr. T. Watari of Japan Atomic Power Co. Ltd. for their useful suggestions and encouragement.

REFERENCES

1 Pretreatment Procedures for Gamma-ray Spectrometry of Environmental Samples using a Ge(Li) Detector, Science and Techniques Agency, Japan, in preparation.
2 J. H. Harley, EML Procedures Manual HASL-300, U.S. Department of Energy, 1972, Section B-06-04.
3 T. Kimura and T. Hamada, Radioisotopes, 27 (1978) 348.
4 Analytical Procedures for Radiostrontium, Science and Techniques Agency, Japan, 1974, Ch. 3 (in Japanese).

Analytica Chimica Acta, 120 (1980) 423—425

Short Communication

A SIMPLE METHOD USING A DISPOSABLE SYRINGE TO PREPARE SAMPLES FOR $\delta^{18}O$ MEASUREMENTS IN WATER SAMPLES

EIICHI MATSUI

Centro de Energia Nuclear na Agricultura, 13400 Piracicaba, S. Paulo (Brasil)

(Received 14th April 1980)

Summary. Use of commercial 10-ml disposable syringes for $H_2{}^{18}O + C^{16}O^{16}O \rightleftharpoons H_2{}^{16}O + C^{16}O^{18}O$ equilibration in $\delta^{18}O$ measurements is described.

The capacity of many laboratories for measurements of $\delta^{18}O$ in water samples is limited by the sample preparation. The current procedure involves freezing the water samples and requires high-vacuum stopcocks and joints which take time to clean, regrease and reassemble. The isotopic equilibration of $H_2{}^{18}O + C^{16}O^{16}O \rightleftharpoons H_2{}^{16}O + C^{16}O^{18}O$ for $\delta^{18}O$ measurements in water samples by mass spectrometry can be achieved in a much simpler way through the use of 10-ml disposable syringes. The sequence of operation for mixing sulphuric acid, the water sample and carbon dioxide for equilibration is shown in Fig. 1.

Experimental

The syringes used were made of polypropylene (B-D Plastipak, Becton—Dickinson Ind. Cirurgicas, Sao Paulo). Apart from the syringes, latex stoppers (s) were required. In Fig. 1 (1) p is the place where the concentrated sulphuric acid is placed; Fig. 1 (2) shows the special pipette (d) used to add sulphuric acid without contaminating the upper internal surface of the cylinder (b). The piston is then placed in the cylinder without touching the acid (3). The water sample (3.2 ml) is then taken from the sample bottle (4) and air is ejected (5). The sample is placed under vacuum by putting the needle tip into the stopper (s) and pulling down the piston (6). After gentle shaking, the piston is pushed back to the normal position (7) and after removal of the stopper, the accumulated air is pushed out of the syringe (8) while at the same time the water volume is adjusted to 3.0 ml. Then the needle is inserted through the wall of a latex tube in which pure carbon dioxide is kept at a pressure slightly higher (ca. 0.5 bar) than outside (9). This CO_2 pressure pushes out the piston which is controlled to stop at the 10-ml position. The needle is removed from the latex tube and immediately inserted into a stopper (s) to which a piece of lead has been attached in order to keep it upright under water in a heated water bath at 28°C (10). It is then shaken overnight (15—16 h).

TABLE 1

Values of $\delta^{18}O$ (all as $^{o}/_{oo}$) obtained for working standards CENA I and CENA II on 3 different days analytical work. (The nominal values of $\delta^{18}O$ referred to Vienna Standard Mean Ocean Water are $-(7.1 \pm 0.05)\,^{o}/_{oo}$ for CENA I and $-(0.07 \pm 0.05)\,^{o}/_{oo}$ for CENA II.)

Date	22-1-80	29-1-80	19-3-80	22-1-80	29-1-80	19-3-80
Sample	CENA I	CENA I	CENA I	CENA II	CENA II	CENA II
x^a	−7.01	−7.01	−7.01	0.073	0.08	0.053
s^a	0.05	0.07	0.13	0.05	0.04	0.06

[a] x is the mean of 4 determinations; $s = [\Sigma(\Delta x_i)^2/(n-1)]^{1/2}$.

The CO_2 is extracted from the syringe by pushing out the water and immediately injecting the CO_2 into the usual extraction line through a serum cap, keeping the needle in an upwards position in order to prevent residual water entering the system. About 50 samples can be prepared by one technician in 2 h, ready for equilibration. The system for extraction and purification of the CO_2 for mass spectrometry followed the conventional design [1].

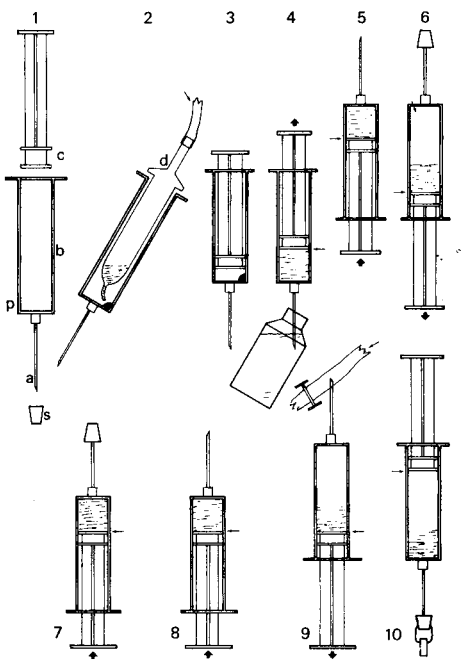

Fig. 1. Syringe and sequence of operation.

Results

The reproducibility of working standards for 3 sets of measurements is illustrated in Table 1. This new methodology was developed so that a large number of $\delta^{18}O$ determinations could be carried out for various environmental studies.

REFERENCE

1 See, e.g., W. G. Mook, Doctoral Thesis, Groningen Rijks Universiteit, 1968.

ANALYTICA CHIMICA ACTA, Vol. 120 (1980)

AUTHOR INDEX

AUTHOR INDEX

VOLUMES 111–120

The volume number is placed in parentheses before the page number

SUBJECT INDEX

VOLUMES 111—120

The volume number is placed in parentheses before the page number

A

B

C

D

E

F

G

H

I

K

L

M

N

NADH
Voltammetry; Flow system; Amperometry; Ascorbic acid; Hexacyanoferrate; Flow-through cell; Rotating glassy carbon disk electrode; Hydrodynamic modulation (116) 315

Nickel
At. abs. spectrometry; Pulse nebulization; Cadmium; Cobalt; Copper; Lead; Extraction; Chloroform and carbon tetrachloride extracts (111) 155

At. abs. spectrometry; Spectrophotometry; Dioxime-loaded open-pore polyurethane foams; α-Benzildioxime (113) 383

At. abs. spectrometry; Electrotherm. atomization; Copper; Vanadium; Coal; Direct solid sampling (115) 365

At. abs. spectrometry; Electrotherm. atomization; Chromium; Cobalt; Fish; Solid-sampling; Protein; Dried solubles (118) 307

D.c. polarography; Diffl. pulse polarography; Extraction; Cobalt; 2,2'-Bipyridine complexes in acetonitrile (115) 81

Emission spectrometry; Plasmas; Steels; Inter-element effects; U.H.F.; Spectroscopic buffers (119) 341

Kinetic analysis; Spectrophotometry; Cadmium; Manganese; Zinc; Lead; Copper; Cobalt; Ligand substitution reaction; EDTA; CDTA; Stopped-flow; SPADNS complex (111) 177

Spectrophotometry; Extraction; Cadmium; Copper; Zinc; Sea water; Dithizone-chloroform (113) 39

Nickel alloys
Activ. analysis; Sulphur; Aluminium alloys; Copper alloys; 13-MeV protons; Separation by precipitation (119) 121

Nickel-base alloys
At. abs. spectrometry; Electrotherm. atomization; Silver; Thallium; Solid samples; Induction furnace (113) 47

Niobium
Spectrophotometry; Rocks; With sulphochlorophenol S; Extraction (116) 185

Nitrate
Flow system; Spectrophotometry; Chloride; Ammonium; Waters; Computer-controlled multichannel; Small samples; Rain (113) 331

Flow system; Spectrophotometry; Nitrite; Reduction and diazotization (114) 191

Nitric oxide
Gas chromatography; Air; Reaction with copper; Presence of aromatic amines (119) 291

Nitrite
Cyclic voltammetry; Electrocatalytic determination (119) 277

Flow system; Spectrophotometry; Nitrate; Reduction and diazotization (114) 191

Flow system; Spectrophotometry; Waters; Using intermittent flows (120) 399

Spectrophotometry; Waters; 8-Quinolinol (111) 311

Spectrophotometry; Gas phase absorption spectrometry (120) 163

Nitrogen
Coulometry; Coal; Oil, heavy residual; Organic materials; Hydrogenation-micro method; Glass electrode (118) 277

Flow system; Spectrophotometry; Phosphorus; Plants; Merging zones; Flow injection analysis; Molybdophosphate reaction; Berthelot reaction (119) 305

Flow system; Spectrophotometry; Phosphorus; Waters; Kjeldahl method (119) 313

Nitrogen isotope ratios
Emission spectrometry; Soils; Plants; Ammonia-filled discharge tubes; Microwave excitation (118) 11

Nuclear fuels
Diffl. pulse polarography; Plutonium; Pyrophosphate medium (117) 225

Nucleic acids
Chromatography; Spectrophotometry; Waters; Sea water; Iron(III)-orcinol method (116) 137

O

Oil
Gas chromatography; Amines; Glow-discharge detector; Element-selective; Derivatized with trifluoroacetic anhydride (119) 283

Oil, heavy residual
Coulometry; Nitrogen; Coal; Organic materials; Hydrogenation-micro method; Glass electrode (118) 277

On-line monitor
At. fluor. spectrometry; Magnesium; Boiler feedwater (117) 241

P

R

S

T

U

V

W

Water
Flow system; Potentiometry; In organic solvents; Karl Fischer reagent (114) 199

Waters
Activ. analysis; Uranium; Urine (119) 405

Anod. stripping voltammetry; Mercury; Preconcentration in potassium permanganate (117) 165

Anod. stripping voltammetry; Thallium; Differential pulse; Hanging mercury drop electrode; Mercury film electrode (118) 243

At. abs. spectrometry; Electrotherm. atomization; Aluminium; Sewage sludge; Aluminosilicate (111) 291

At. abs. spectrometry; Trace metals; Freeze-drying; Concentration (113) 369

At. abs. spectrometry; Ion exchange; Mercury; Cold-vapor; Preconcentration; Dithiocarbamate-treated resin (115) 103

At. abs. spectrometry; Mercury; Chemical speciation; Cold-vapour (120) 129

Chromatography; Spectrophotometry; Nucleic acids; Sea water; Iron(III)-orcinol method (116) 137

Coulometry; Heavy metals; Continuous monitoring; Industrial effluents (114) 303

Diffl. pulse polarography; Anthraquinone; Black liquor (119) 243

Electrotherm. atomization; At. abs. spectrometry; Arsenic; Antimony; Bismuth; Sorption on gel containing thiol groups (117) 293

Electrotherm. atomization; At. abs. spectrometry; Arsenic; Sea water; Graphite furnace; Arsenite and arsenate; Extraction (120) 121

Emission spectrometry; Molecular emission cavity analysis; Fluoride; Toothpaste; Conversion to silicon tetrafluoride; Oxycavity (117) 247

Emission spectrometry; Phenol; Molecular emission cavity analysis (120) 371

Emission spectrometry; Molecular emission cavity analysis; Sulphate; Dusts; Soils (120) 383

Flow system; Spectrophotometry; Nitrate; Chloride; Ammonium; Computer-controlled multichannel; Small samples; Rain (113) 331

Flow system; Spectrophotometry; Phosphorus; Nitrogen; Kjeldahl method (119) 313

Flow system; Spectrophotometry; Nitrite; Using intermittent flows (120) 399

Fluorimetry; Spectrophotometry; Aluminium; 3-Hydroxypyridine-2-aldehyde 2-pyridylhydrazone (117) 319

Gas chromatography; Sediments; Phenols; Continuous liquid-liquid extractors; Evaporative concentration (115) 373

Gas chromatography; Herbicide; 3,4-Dichloroaniline metabolite; Neburon; Acetylation (116) 145

Ion exchange; X-ray fluores. spectrometry; Trace metals; Preconcentration; Chelating resin; Precipitation; Adsorption (111) 215

Ion exchange; Flow system; Spectrophotometry; Ammonium; Pulsed Nessler reagent (117) 81

Ion exchange; Fluorimetry; Spectrophotometry; Uranium; Chelex-100 resin (120) 289

Ion exchange; Radionuclide collection; Rain; γ-Spectrometry (120) 419

Isotope dilut. analysis; Disposable syringe; $\delta^{18}O$ measurements (120) 423

Kinetic analysis; Fluoride; Rocks; Soils; Air particulates; Rain (111) 89

Potentiometry; Cyanide; Cyanide-selective electrode; Presence of mercaptans (120) 367

Raman spectrometry; Phenylamide pesticides; Argon ion laser source; Azo dye derivatives (116) 1

Spectrophotometry; Nitrite; 8-Quinolinol (111) 311

Spectrophotometry; Chromium; Coprecipitation with barium sulphate; Diphenylcarbazide (113) 131

Spectrophotometry; Formic acid; Formaldehyde; Chromotropic acid (113) 189

Spectrophotometry; Extraction; Water-soluble acid dyes; Ion-pair formation; Trioctylamine (113) 307

Spectrophotometry; Anionic surfactants; 1-(2-Pyridylazo)-2-naphthol and diethylamine (116) 191

Spectrophotometry; Cobalt; Preconcentration on reagent-loaded polyurethane foams; PAN (119) 113

Spectrophotometry; Carbon, inorganic; Automated; Gas dialysis (120) 305

Spectrophotometry; Extraction; Boric acid; With 1,8-dihydroxynaphthalene-4-sulphonic acid (120) 321

T.l.c.; Sediments; Biological materials; Chloroparaffins (111) 201

Selenium; Preservation and stability (113) 237

Trace organic materials; Adsorption; Continuous extraction; Resin (113) 393

Z

TECHNIQUE INDEX

VOLUMES 111—120

The volume number is placed in parentheses before the page number

Atomic absorption spectrometry

Cobalt; Elimination of the interfering effects; Addition of cyanide (115) 155

Electrotherm. atomization; Cadmium; Sea water; Addition of EDTA (115) 163

Arsenic; Bismuth; Lead; Antimony; Selenium; Tin; Hydride generation; Flame-heated silica T-tube (115) 355

Electrotherm. atomization; Copper; Nickel; Vanadium; Coal; Direct solid sampling (115) 365

Chromium; Blood; Serum; Solid sampling; Distribution among proteins; Gel filtration (116) 105

Mercury; Air; Cold-vapour; Particulate and volatile; Sampling (116) 111

Extraction; Iron; Heavy metals; 1-Phenyl-3-methyl-4-benzoylpyrazol-5-one (116) 153

Emission spectrometry; Discrete nebulization; Trace metals; Bovine liver; Biological standards (116) 205

Voigt effect filter; Sodium (116) 365

Copper; Zinc; Continuous sampling; Hemodialysis treatment (116) 375

Palladium; Extraction; Anode sludge; Tri-n-octylmethylammonium tetrabromopalladate (116) 383

Lithium isotope abundance; Measurement of absorbance ratio (116) 427

Electrotherm. atomization; Atom-trapping; Water-cooled silica trap (117) 257

Electrotherm. atomization; Temperature variation; Contoured tube (117) 267

Electrotherm. atomization; Cobalt; Steels; Corrosion products; Extraction (117) 275

Titrimetry; Vanadium pentoxide catalysts; Vanadium; Alkali metals; Free acidity (117) 285

Electrotherm. atomization; Arsenic; Antimony; Bismuth; Waters; Sorption on gel containing thiol groups (117) 293

Electrotherm. atomization; Copper; Iron; Manganese; Sea water; Effects of ammonium nitrate (117) 397

Emission spectrometry; Soil extracts; Plant ash; Three channel spectrometer; Calcium; Magnesium; Sodium; Simultaneous determination (118) 1

Gas chromatography; Arsenic; Selenium; Germanium; Tin; Hydride generation (118) 115

Copper; Bovine serum; Semi-automatic dilution (118) 153

Electrotherm. atomization; Lithium; Sodium; Potassium; Copper; Uranium (118) 163

Sample droplet acceleration; In an air-acetylene flame; Mathematical model; Stroboscopic photography (118) 293

Electrotherm. atomization; Manganese; Constant temperature; Tungsten wire introduction; Interferences (118) 301

Electrotherm. atomization; Chromium; Cobalt; Nickel; Fish; Solid-sampling; Protein; Dried solubles (118) 307

Aerosols; Trace elements; Acid digestion; Ambient (118) 377

Mercury; Standard reference materials; Environmental materials; By pyrolysis; Cold-vapour; Two-stage amalgamation (118) 381

Electrotherm. atomization; Lead; Sea water; Tantalum-coated tube (119) 67

Electrotherm. atomization; Phosphorus; Investigation of reactions; High-temperature equilibrium calculations (119) 75

Chromium; Extraction of thiosemicarbazide (119) 157

Electrotherm. atomization; Barium; Lanthanum; Magnesium; Pancreatic islets; Biological materials; Direct injection (119) 161

Mercury; Cold-vapour; Magnesium perchlorate desiccant (119) 167

Arsenic; Selenium; Soils; Sediments; Hydride generation; Quartz-tube (119) 323

Electrotherm. atomization; Arsenic; Biological materials; Direct determination; Matrix stabilization (119) 331

Background monitoring circuit (119) 379

Flow system; Flow injection with an organic solvent (119) 383

Electrotherm. atomization; Arsenic; Waters; Sea water; Graphite furnace; Arsenite and arsenate; Extraction (120) 121

Mercury; Waters; Chemical speciation; Cold-vapour (120) 129

Hydride generation; Selenium; Reduction of chemical interference; Speciation (120) 141

Electrotherm. atomization; Iron; Serum; Graphite furnace; No sample pretreatment (120) 155

Gas chromatography; Electrotherm. atomization; Methylcyclopentadienylmanganesetricarbonyl; Air; Manganese (120) 171

Electrotherm. atomization; Selenium; Urine; Blood; Thermal stabilization; Tracer technique; Organoselenium compounds (120) 377

Emission spectrometry

Flow system

Spectrophotometry; Dispersion phenomena; Phosphate; Reactors; Optimal design; Vanadomolybdate reagent (114) 91

Theoretical aspects of flow injection analysis; Sample injection (114) 105

Microprocessor control system; Automated multiple flow injection (114) 119

Fluorimetry; Thiamine; Pharmaceuticals; Thiochrome method; Vitamin B_1 (114) 129

H.p.l.c.; Fluorimetry; Photochemical reaction detectors; Pharmaceuticals; Clobazam; Desmethylclobazam; Phenothiazines; Irradiation time (114) 137

Fluorimetry; H.p.l.c.; Solvent segmentation; Amines; Continuous-flow dansylation (114) 147

Spectrophotometry; Corticosteroids; Pharmaceuticals; Reduction of blue tetrazolium (114) 155

Spectrophotometry; Enzymatic analysis; Mixed indicator-buffer system; Wide pH range; Continuous; Stopped flow; Microcomputer (114) 165

Immunoassay; Fluorimetry; Serum albumin; Homogeneous; Energy-transfer; Merging-zone; Stopped-flow (114) 183

Spectrophotometry; Nitrate; Nitrite; Reduction and diazotization (114) 191

Potentiometry; Water; In organic solvents; Karl Fischer reagent (114) 199

Emission spectrometry; Cobalt; Sulphide; Chemiluminescence; Catalyzed oxidation of luminol; Sensitized oxidation of sulphide (114) 209

Spectrophotometry; Extraction constants; Determination (114) 215

Kinetic analysis; Strontium; Magnesium; Calcium; Differential; Cryptand (2.2.2) complexes (114) 227

Titrimetry; Modelling approach; Optical detection (114) 235

Titrimetry; Automatic titrator; Time-proportional sample flow (114) 247

Amperometry; H.p.l.c.; Hexacyanoferrate; Rotating disk electrode; Response surface; Wall-jet detector (114) 257

Amperometry; Iron; Rocks; Glassy carbon electrode (114) 267

Amperometry; Cyanides; Continuous distillation; Cylindrical silver electrode (114) 275

Voltammetry; Flow-through cell; Organic compounds; On-line analysis; Glassy carbon electrode; Mercury film electrode (114) 283

Potentiometry; Sulphate; Lead-selective electrode; Continuous monitoring; Differential system (114) 293

Curve regeneration; Fast analysis rates (114) 311

Turbidimetry; Sulphate; pH gradients; EDTA; Barium (114) 319

Fluorimetry; Gallium; Lumogallion (114) 325

Potentiometry; Proteins; Ammonia sensor; Bovine serum albumin; Human blood sera; Protease; Immobilized; L-amino acid oxidase (114) 329

H.p.l.c.; Polyphosphates (115) 269

Amperometry; H.p.l.c.; Flow-through wire detector; Iodide; Arsenic; Platinum electrode (116) 33

Amperometry; Arsenic; Platinum electrode (116) 41

Potentiometry; Microbial sensor; Glutamic acid; Carbon dioxide gas-sensor; Fermentation broths; Immobilized *Escherichia coli* (116) 61

Voltammetry; Amperometry; Ascorbic acid; NADH; Hexacyanoferrate; Flow-through cell; Rotating glassy carbon disk electrode; Hydrodynamic modulation (116) 315

Ion exchange; Spectrophotometry; Ammonium; Waters; Pulsed Nessler reagent (117) 81

Potentiometry; Ion-selective electrodes; Fluoride-selective electrode; Manual control; Computer control (117) 91

Kinetic analysis; Temperature effects in stopped-flow mixing systems (117) 99

Spectrophotometry; Amyloglucosidase activity; Fermentation samples; Glucose dehydrogenase reagent (117) 359

Purification of electrolyte solutions; Mercury cathode electrolysis (117) 367

Potentiometry; Miniaturization; Ion-sensitive field effect transistors; pH; Potassium; Calcium; Multi-ion analysis (118) 45

Pulse polarography; Flow-through detector; Potential-controlled drop synchronization (118) 73

Polarography; Electrochemical scrubber; Flow-through detection; Porous silver electrodes; Reduction of the background current and noise (118) 81

Amperometry; Chromatography; Ion exchange; Metal ions; Reverse pulse; Mercury electrode without deaeration; Polarographic detector (118) 233

Extraction; Membrane phase separator; Flow-injection principle (118) 285

Fluorimetry

Gas chromatography

ACA announcements

NEW BOOKS

Physics of Modern Materials

Publication Date: Vol. I, February 1980
Vol. II, April 1980
Price: Vol. I, Austrian Schillings 760.00
Vol. II, Austrian Schillings 980.00

Based on lectures presented at the Spring College on the Physics of Modern Materials held at the International Centre for Theoretical Physics, Trieste, 29 March to 24 June 1978.

Molybdenum: Physico-Chemical Properties of its Compounds and Alloys

Atomic Energy Review: Special issue No. 7, 1980, edited by L. Brewer

Publication Date: April 1980
Price: Austrian Schillings 1000,00

This, the seventh monograph in the International Atomic Energy Agency's Atomic Energy Review series on the physico-chemical properties of the compounds and alloys of metals for reactor engineers, deals with molybdenum.

Uranium in the Pine Creek Geosyncline

Publication Date: April 1980
Price: Austrian Schillings 1080.00

Proceedings of the International Symposium on Uranium in the Pine Creek Geosyncline, held in Sydney, Australia, 4–8 June, 1979.

International Nuclear Fuel Cycle Evaluation (INFCE)

Publication Date: Vols. 1 to 8 and Summary Vol. (Vol. 9): April 1980
Price: Complete Set: Austrian Schillings 2900.00
Individual volumes also available.

The International Nuclear Fuel Cycle Evaluation (INFCE) conference, held in Washington, U.S.A., October 1977.

Manpower Requirements and Development for Nuclear Power Programmes

Publication Date: June 1980
Price: Austrian Schillings 900.00

Proceedings of Symposium on Manpower Requirements and Development for Nuclear Power Programmes, held in Saclay, France, 2–6 April, 1979.

Occupational Radiation Exposure in Nuclear Fuel Cycle Facilities

Publication Date: July 1980
Price: Austrian Schillings 920.00

Proceedings of a symposium on Occupational Radiation Exposure in Nuclear Fuel Cycle Facilities, held in Los Angeles, California, 18–22 June 1979.

Further details of above publications from: International Atomic Energy Agency, Division of Publications, P.O. Box 100, A-1400 Vienna, Austria.

NNOUNCEMENTS OF MEETINGS

RTICLE SIZE ANALYSIS CONFERENCE, LOUGHBOROUGH UNIVERSITY, ENGLAND, –24 SEPTEMBER, 1981

The fourth Conference to be held under the auspices of the Analytical Division of the Chemical ciety will be held at the University of Loughborough on 21–24 September 1981.

All aspects of particle size analysis and powder characterisation will be covered including sampling, e preparation of samples for analysis, experience with and improvements to existing methods, parti- shape, on-line analysis, application of analyses to problems in industry. Past Conferences have oved beneficial as a forum for analysts, equipment manufacturers, designers of new equipment and earchers developing new methods or exploring the validity of existing methods. The proceedings ll be published and will be available to all those registering for the Conference. Papers will be pub- hed in English. An exhibition of equipment will be held simultaneously with the Conference in an jacent hall. A wide range of available instruments will be exhibited by the manufacturers.

Further information: P.J. Lloyd, PSA 81 Conference, Particle Technology Group, Chemical Engi- ering Department, University of Technology, Loughborough, Leics. LE11 3TU, Great Britain.

h INTERNATIONAL MASS SPECTROMETRY CONFERENCE

igust 30–September 3, 1982, Vienna, Austria.

The conference is organized by the Austrian Mass Spectrometry Group, the Austrian Society for crochemistry and Analytical Chemistry, the Austrian Chemical Society and the Institute of alytical Chemistry of the University of Vienna in co-operation with an International Scientific mmittee. The scientific programme will cover all aspects of Mass Spectrometry. The programme ll consist of invited lectures, submitted papers and posters. An extensive commercial exhibition ll be included.

Further information from Interconvention, P.O. Box 105, A-1014 Vienna, Austria.

ALENDAR OF FORTHCOMING MEETINGS

c. 8–12, 1980 rte de Versailles, ris, France	**2ème Congrès de Chimie Analytique – 34ème Congrès du G.A.M.S.** Contact: Secrétriat du G.A.M.S. (Congrès), 88, Boulevard Malesherbes, 75008 Paris, France. (Further details published in Vol. 117)
c. 16–17, 1980 ighton, Great Britain	**Chromatography, Equilibria and Kinetics** Contact: Mrs. Y.A. Fish, The Chemical Society, Burlington House, London W1V 0BN, Great Britain. Tel. 01-7349971.
b. 17–20, 1981 enna, Austria	**EURO FOOD CHEM I** Contact: Verein Osterreichischer Chemiker Dr. Werner Pfannhauser, FECS – WPFC – Secretary, Eschenbachgasse 9, A – 1010 Wien, Austria. Tel: 0 22 2/ 57 42 49
irch 9–13, 1981 lantic City, U.S.A.	**1981 Pittsburgh Conference** Contact: John A. Queiser, Programme Chairman, 1981 Pittsburgh Conference, 2523 Greenboro Lane, Pittsburgh, PA 15220, U.S.A. Tel: 412 795–7110.

March 23–June 5, 1981 Uppsala, Sweden	**Course: Biochemical Separation Methods** Contact: Secretary, Eva Linder, Institute of Biochemistry, University of Uppsala, Box 576, S–751 23 Uppsala, Sweden.
Apr. 13–16, 1981 Cardiff, Wales United Kingdom	**International Symposium on Electroanalysis in Clinical Environmental and Pharmaceutical Chemistry** Contact: Short Courses Section (Electroanalysis Symposium), UWIST, Cardiff CF1 3NU, Wales, United Kingdom. (Further details published in Vol. 116, No
April 22–24, 1981 Noordwijkerhout, The Netherlands	**Joint NL – UK Symposium on Quantitative Organic Analysis** Contact: Dr. B. Griepink, Secretary of Analytical Chemistry Section of the Royal Netherlands Chemical Society, c/o Analytical Chemistry Laboratory, Croesestraat 77A, 3522 AD Utrecht, The Netherlands. (Further details published in Vol. 118, No. 2)
May 3–7, 1981 Hindenlang, (Bavarian Alps), F.R.G.	**4th International Symposium on Capillary Chromatography** Contact: Dr. J. Rijks, Laboratory of Instrumental Analysis, University of Technology, P.O. Box 513, NL–5600 MB Eindhoven, The Netherlands.
May 5–8, 1981 Gatlinburg, TN, U.S.A.	**Separation Science and Technology for Energy Applications** Contact: A.P. Malinauskas, Oak Ridge National Laboratory, P.O. Box X, Oak Ridge, TN 37830, U.S.A.
May 11–15, 1981 Avignon, France	**Vth International Symposium on Column Liquid Chromatography** Contact: Prof. G. Guiochon, Ecole Polytechnique, Laboratoire de Chimie Analytique Physique, Route de Saclay, 91128 Palaiseau Cedex, France. (Further details published in Vol. 118, No. 1)
May 18–20, 1981 Jekyll Island, Georgia, U.S.A.	**11th Annual Symposium on the Analytical Chemistry of Pollutants** Contact: Prof. Dr. Roland W. Frei, The Free University, De Boelelaan 1083, 1081 HV Amsterdam, The Netherlands.
May 20–22, 1981 Eger, Hungary	**Symposium on the Analysis of Steroids** Contact: Prof. S. Görög, c/o Hungarian Chemical Society, 1061 Budapest VI Anker köz 1, Hungary.
June 1–5, 1981 Stresa, Lago Maggiore, Italy	**2nd European Symposium on Organic Chemistry** Contact: Prof. Giorgio Modena, Istituto di Chimica Organica, Via Marzolo, 1 35100 Padova, Italy.
June 16–17, 1981 Venice, Italy	**1st International Symposium on Chromatography in Biochemistry, Medicine and Environmental Research** Contact: Dr. A. Frigerio, Italian Group for Mass Spectrometry in Biochemist and Medicine, c/o Istituto di Ricerche Farmacologiche "Mario Negri", Via Eritrea 62, 20157 Milan, Italy. Tel: 35.54.546.
June 18–19, 1981 Venice, Italy	**8th International Symposium on Mass Spectrometry in Biochemistry, Medicine and Environmental Research** Contact: Dr. A. Frigerio, Italian Group for Mass Spectrometry in Biochemist and Medicine, c/o Istituto di Ricerche Farmacologiche "Mario Negri" Via Eritrea 62 20157 Milan, Italy. Tel: 35.54.546.
June 22–26, 1981 Nijmegen, The Netherlands	**4th International Symposium on Affinity Chromatography and Related Techniques** Contact: Dr. T.C.J. Gribnau, Organon Scientific Development Group, P.O. Box 20, 5340 BH Oss, The Netherlands. (Further details published in Vol. 118, No. 1)

ne 23–27, 1981 rl–Marx–Stadt, D.D.R.	**Tagung Festkorperanalytik** Contact: Dr. K. Danzer, Technische Hochschule, Karl–Marx–Stadt, Sektion Chemie und Werkstofftechnik, PSF 964, 9010 Karl–Marx–Stadt, D.D.R. (Further details published in Vol. 118, No. 2)
ly 5–10, 1981 vansea, Wales	**The Third Swansea Summer School of Automatic Chemical Analysis** Contact: Prof. D. Betteridge, Department of Chemistry, University College of Swansea, Singleton Park, Swansea SA2 8PP, Great Britain.
ly 6–9, 1981 rasbourg, France	**27th IUPAC Symposium on Macromolecules** Contact: Secretariat, Macro 1981, Société de Chimie Industrielle, 28, rue Saint-Dominique, 75007 Paris, France.
ig. 16–22, 1981 ncouver, Canada	**28th Congress International Union of Pure and Applied Chemistry** Contact: Congress Secretariat, 28th IUPAC Congress, c/o The Chemical Institute of Canada, 151, Slater Street, Suite 906, Ottawa, Ontario, Canada K1P 5H3.
ig. 23–28, 1981 iversity of Auckland, w Zealand	**Golden Jubilee Conference "Chemistry in the Service of Man"** Contact: Dr. D.J. McLennan, Chemistry Dept., Univ. of Auckland, Auckland, New Zealand.
ig. 23–28, 1981 poo, Finland	**Euroanalysis IV – Triennal Conference of the Federation of European Chemical Societies** Contact: Professor L. Niinistoe, Department of Chemistry, Helsinki University of Technology, SF–02150 Espoo 15, Finland. (Further details published in Vol. 109, No. 1)
ig. 23–28, 1981 nberra, Australia	**Sixth Australian Symposium on Analytical Chemistry** Contact: Hon. Secretary, Miss B.J. Stevenson, P.O. Box 1397, Canberra City, A.C.T. 2601, Australia.
ig. 30–Sep. 5, 1981 enna, Austria	**XI International Congress of Clinical Chemistry – IV European Congress of Clinical Chemistry** Contact: Congress Secretariat, Interconvention, P.O. Box 35, A-1095 Vienna, Austria. Tel. (0222) 42 13 52.
p. 1–4, 1981 ofok, Hungary	**3rd Danube Symposium on Chromatography** Contact: Hungarian Chemical Society, H–1368 Budapest, P.O.B. 240, Hungary. Tel: Budapest 427–343. (Further details published in Vol. 115)
p. 1–4, 1981 erdeen, Scotland	**ESTA 2 – The Second European Symposium on Thermal Analysis** Contact: Dr. F.P. Glasser, Chairman of the Organising Committee, ESTA 2, Department of Chemistry, University of Aberdeen, Meston Walk, Old Aberdeen, AB9 2UE, Scotland.
p. 4–8, 1981 kyo, Japan	**9th International Conference on Atomic Spectroscopy and XXII Colloquium Spectroscopicum Internationale** Contact: The Japan Society for Analytical Chemistry, 9th ICAS/XXII CSI, Gotanda Sanhaitsu, 26-2 Nishigotanda 1-chome, Shinagawa-ku, Tokyo 141, Japan. (Further details published in Vol. 118, No. 1)
p. 21–24, 1981 ughborough, England	**Particle Size Analysis Conference** Contact: P.J. Lloyd, PSA 81 Conference, Particle Technology Group, Chemical Engineering Department, University of Technology, Loughborough, Leics. LE11 3TU, Great Britain.

Sep. 28–Oct. 1, 1980	**16th International Symposium on Advances in Chromatography** Contact: Professor A. Zlatkis, Chemistry Department, University of Houston, Houston, Texas 77004, U.S.A.
April 14–16, 1982 Amsterdam, The Netherlands	**12th Annual Symposium on the Analytical Chemistry of Pollutants** Contact: Prof. Dr. Roland W. Frei, The Free University, De Boelelaan 1083, 1081 HV Amsterdam, The Netherlands.
Aug. 30–Sep. 3, 1982 Vienna, Austria	**9th International Mass Spectrometry Conference** Contact: Interconvention, P.O. Box 105, A–1014 Vienna, Austria.
Sep. 6–9, 1982 Bath, Great Britain	**4th European Symposium on Chemical Structure – Biological Activity: Quantitative Approaches** Contact: Dr. J.C. Dearden, School of Pharmacy, Liverpool Polytechnic, Byrom Street, Liverpool L3 3AF, Great Britain.
Aug. 28–Sep. 2, 1983 Amsterdam, The Netherlands	**9th International Symposium on Microchemical Techniques** Contact: Symposium Secretariat, c/o Municipal Congress Bureau, Oudezijds Achterburgwal 199, 1012 DK Amsterdam, The Netherlands. Tel: (020) 552 3459

Printed in The Netherlands.

(continued from outside of cover)

Short Communications

CONTENTS

(continued on inside page of the cover)